Durham University

Durham E-Theses

A theoretical study of the mechanism of palladium-diphosphine catalysed copolymerisation of olefins and carbon monoxide

Christopher Neville-Smith

How to cite:

Neville-Smith, Christopher (2005) A theoretical study of the mechanism of palladium-diphosphine catalysed copolymerisation of olefins and carbon monoxide. Doctoral thesis, Durham University.

Use policy

The full-text may be used and/or reproduced, and given to third parties in any format or medium, without prior permission or charge, for personal research or study, educational, or not-for-profit purposes provided that:

- a full bibliographic reference is made to the original source
- a https://etheses.durham.ac.uk/id/eprint/1762/ is made to the metadata record in Durham E-Theses
- the full-text is not changed in any way

The full-text must not be sold in any format or medium without the formal permission of the copyright holders.

Please consult the full Durham E-Theses policy for further details.

Academic Support Office, The Palatine Centre, Durham University, Stockton Road, Durham, DH1 3LE
e-mail: e-theses.admin@durham.ac.uk Tel: +44 0191 334 6107
https://etheses.durham.ac.uk

A theoretical study of the mechanism of palladium-diphosphine catalysed copolymerisation of olefins and carbon monoxide

Christopher Neville-Smith

University of Durham (Trevelyan College)

Department of Chemistry

Supervised by Mel Kilner

A copyright of this thesis rests with the author. No quotation from it should be published without his prior written consent and information derived from it should be acknowledged.



2 1 JUN 2005

Abstract

The copolymerisation of olefins and carbon monoxide using a palladium-diphosphine catalyst has been simulated by optimising the stationary points in the reaction pathway using *ab-initio* chemistry, using SDD basis sets (augmented by polarisation functions on selected chemically active atoms) and the B3-LYP method. Further information about the reaction pathways was obtained using the Intrinsic Reaction Co-ordinate process.

The mechanism of the propagation cycle was fully analysed and the results agreed with earlier findings that there were no energy barriers in the reaction cycle that cannot be overcome at temperatures as low as 50°C. It also supported the theory that the olefin insertion step was the rate-determining step, with CO insertion as the next slowest step. A number of new findings were also made; in particular, reaction pathways were determined for the addition of new CO and olefin ligands to equatorial sites.

Supplementary work carried out included considering two possible mechanisms for initiation of the copolymerisation process, where olefin insertion into a palladium-hydride bond was thought to dominate over carbon monoxide insertion into a palladium-methoxy bond. Double insertion was also tested, and the findings agreed with earlier research and theory that the double CO step is thermodynamically forbidden, whilst double olefin insertion is possible but uncompetitive with the CO insertion step. However, additional findings suggested that the strong Pd-O co-ordinate bond contributes towards lack of double olefin insertion, and addition of CO to an equatorial site competes with olefin addition after CO insertion, possibly hindering the following olefin insertion step. Termination was not investigated, but a pattern was observed where a four co-ordinate structure was maintained whenever possible, which suggested that termination by methanolysis would dominate. Therefore, one would expect a keto-end group to be formed on initiation and an ester-end group to be formed on termination.

Finally, this thesis considers how some of the properties the these reaction mechanisms can be accounted for in terms of electronic structure

Contents:

Abstract i

1 Carbon monoxide and olefin copolymerisation 1

1.1 Introduction 1

1.2 Fundamental aspects of the propagation cycle 2

1.3 Double insertion 6

1.4 Initiation and termination steps 9

1.5 Effect of diphosphine ligand 12

1.6 Use of olefins other than ethene 15

1.7 Conclusions 21

2 Ab-initio optimisation of geometries 22

2.1 Introduction 22

2.2 Single-point energy calculations 23

2.3 Optimisation of molecular structure from electronic structure 32

2.4 Frequency tests and reaction mechanisms 38

2.5 Special considerations for large systems 42

2.6 Rates of reaction 47

2.7 Ab-initio programs and alternative methods of optimisation 49

2.8 Conclusions 52

3: Mechanism of ethene/CO propagation cycle 54

3.1 Introduction 54

3.2 Technical details 55

3.3 Olefin insertion step 58

3.3.1 Introduction 58

3.3.2 Reactant and product structures 59

3.3.3 Transition state structure 62

3.3.4 Reaction path 65

3.3.5 Inclusion of second carbonyl group in optimisations of minima 69

3.3.6 Inclusion of second carbonyl group in transition state optimisation 71

3.3.7 Inclusion of second carbonyl group in reaction path 74

3.3.8 Summary of findings of olefin insertion analysis 76

3.4 Carbon monoxide insertion step 80

3.4.1 Introduction 80

3.4.2 Reactant and product structures neglecting second carbonyl group 81

3.4.3 Transition state structure neglecting second carbonyl group 82

3.4.4 Reaction path neglecting second carbonyl group 84

3.4.5 Optimisation of reactant and product including second carbonyl group 88

3.4.6 Inclusion of second carbonyl group in transition state optimisations 91

3.4.7 Inclusion of second carbonyl group in reaction path 92

3.4.8 Summary of findings of carbon monoxide insertion analysis 94

3.5 Carbon monoxide addition stage 97
3.5.1 Introduction 97
3.5.2 Early attempts to find reaction path 97
3.5.3 Final optimisation of transition state 101
3.5.4 Reaction path 102
3.5.5 Approach of carbon monoxide ligand 104
3.5.6 Summary of findings of carbon monoxide addition analysis 105
3.6 Olefin addition stage 107
3.6.1 Introduction 107
3.6.2 Early attempts to find transition state 107
3.6.3 Final optimisation of transition state of direct addition 109
3.6.4 Reaction path of direct addition 110
3.6.5 Approach of olefin ligand 113
3.6.6 Summary of findings of olefin addition analysis 113
3.7 Summary of propagation mechanism 115

4: Other aspects of copolymerisation of ethene and carbon monoxide 118
4.1 Initiation processes 118
4.1.1 Introduction 118
4.1.2 Insertion of olefin into Pd-H bond 119
4.1.3 Other initiation steps arising from insertion of olefin into Pd-H bond 122
4.1.4 Insertion of carbon monoxide into Pd-methoxy bond 126
4.1.5 Other initiation steps arising from insertion of carbon monoxide into Pd-methoxy bond 131
4.1.6 Conclusions 134
4.2 Double insertion 139
4.2.1 Introduction 139
4.2.2 Double olefin insertion, neglecting axial Pd-carbonyl bond 141
4.2.3 Double olefin insertion including axial Pd-carbonyl bond 144
4.2.4 Olefin addition prior to double insertion 145
4.2.5 Double CO insertion, neglecting axial Pd-carbonyl bond 148
4.2.6 Double CO insertion, including axial Pd-carbonyl bond 151
4.2.7 CO addition prior to insertion 153
4.2.8 Summary 155
4.3 Termination processes 160
4.4 Larger systems 164
4.4.1 Regioselectivity in propene insertion 164
4.4.2 Ab-initio optimisation of full complex 171
4.5 Overall summary 176

5: Electronic influences on geometry and reaction mechanisms 178
5.1 Introduction and basic framework 178
5.2 Bonding of individual ligands 181
5.2.1 Palladium-phosphine 181
5.2.2 Palladium-alkyl 184
5.2.3 Palladium-carbon monoxide 184
5.2.4 Palladium-olefin 185

5.2.5 Palladium-acyl/ketone 187
5.3 Effects of electronic structure on reaction parameters 191
5.3.1 Intermediate in olefin insertion stage 191
5.3.2 Axial Pd-O coordinate interactions 193
5.3.3 Palladium-carbonyl interactions without fourth ligand 196
5.3.4 Agostic Pd···H-C interactions 199
5.3.5 Length of Pd-P bonds 200
5.4 Summary 203

6 Summary 204
6.1 Overall conclusions 204
6.2 Further work 207

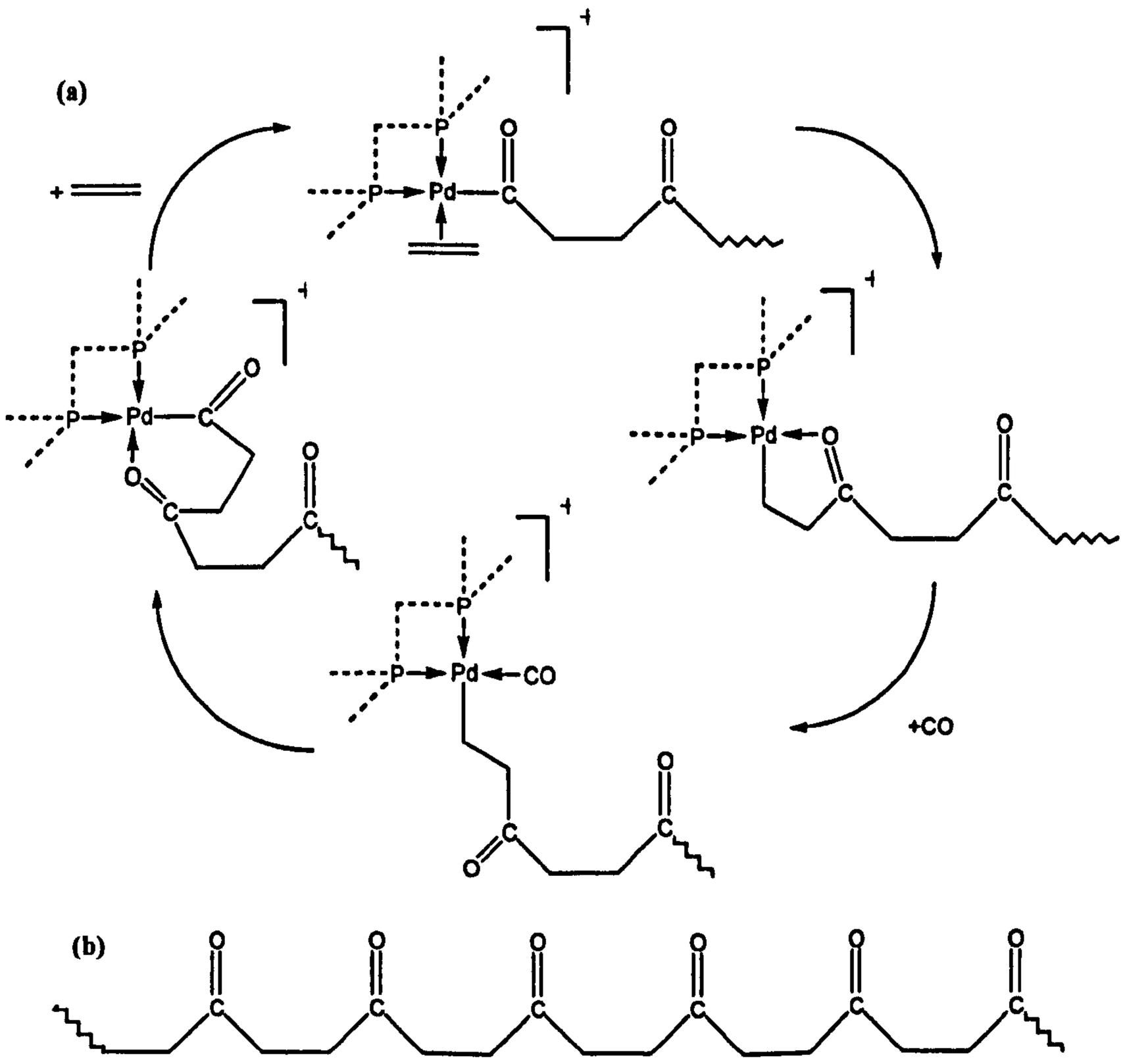
References 210

1 Carbon monoxide and olefin copolymerisation

1.1 Introduction

This project has concentrated on simulating the copolymerisation of carbon monoxide and olefins using a palladium-diphosphine catalyst. In recent years, the carbon monoxide / olefin copolymer has attracted a significant amount of interest, in particular as a biodegradable alternative to conventional polymers. A patent is currently held by Shell under the trade name CARILON.[1] The polymer has also been the subject of several review papers over the last decade.[2,3,4,5].

The fundamental aspect of copolymerisation is for an olefin to bond to a transition metal centre and undergo migratory insertion into a palladium-acyl bond, followed by a carbon monoxide molecule bonding to the palladium centre and undergoing migratory insertion into the newly-formed palladium-alkyl bond. This forms a copolymer chain of three-carbon units $(-CH_2CH_2CO-)_n$. The basic cycle and product are shown in **scheme 1.1.** With the right choice of catalyst, copolymers of very high molecular weights can be formed, and, with only one known exception, the



Scheme 1.1: (a) Basic process of CO/ethene copolymerisation; and **(b)** structure of copolymer formed

copolymers are invariably formed in perfect alternation.

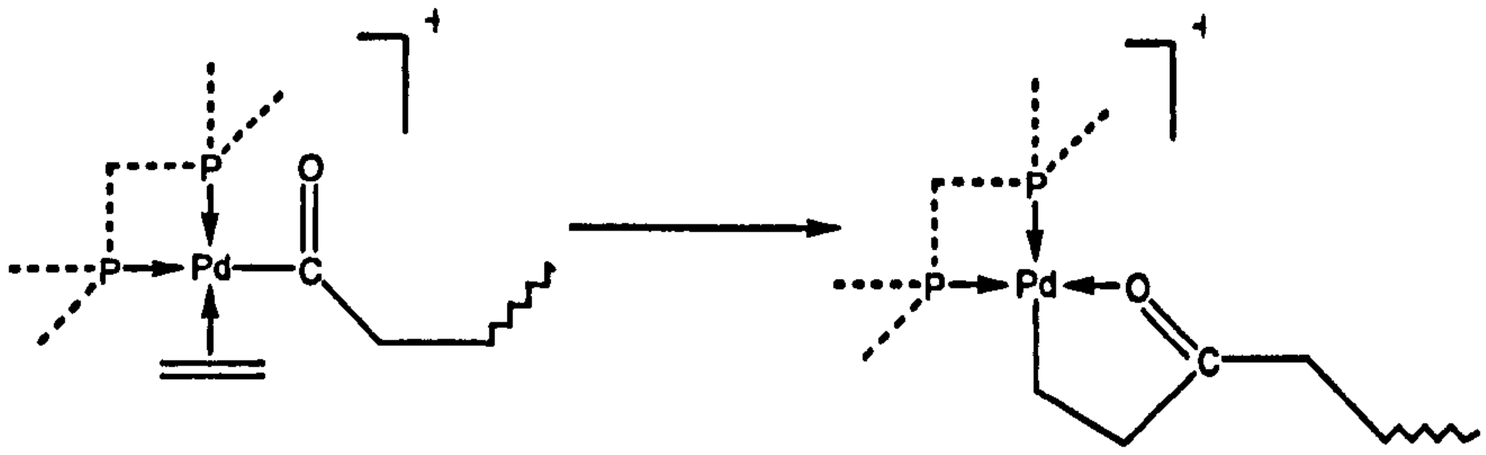
The earliest copolymerisation catalysts were nickel complexes[6], but it has since been established that the most effective catalysts are palladium diphosphine complexes. Out of these complexes, the most effective ligand of all to stabilise palladium is thought to be 1,3-bis(diphenylphosphino)propane (dppp), which forms a 6-membered ring when bonded to palladium. The most popular olefin to copolymerise with carbon monoxide is ethene, but there is also interest in using other olefins, in particular propene and styrene, owing to the different products formed and their specific properties.

The mechanism of this copolymerisation process is a matter of considerable interest, in particular to explain why there is no double insertion of olefins or carbon monoxide. This has been studied at both an experimental level and a theoretical level. In addition to the propagation cycle, it is also important to consider the mechanisms of several different possible initiation and termination processes, which have an important influence on both the chain length and the end-groups of the copolymer. There is also scope for considering how changing the diphosphine ligand affects the rate of copolymerisation and, in the case of propene or styrene insertion, the regioregularity and stereoregularity of the copolymer formed.

1.2 Fundamental aspects of the propagation cycle

This project's research has concentrated on the propagation cycle, an area given comparatively little attention in review papers, with the most consideration going to the mechanism of the initiation and termination steps. There has, however, been some research and speculation of the mechanism of the propagation steps. Possibly the most useful published research to date was undertaken in 1996 by Margl and Ziegler, which optimised some simplified structures and transition states using the ADF program.[7,8]

Drent[5] and others propose that the palladium complex maintains a d^8 square-planar arrangement throughout the copolymerisation process, and where a co-ordination site is vacant, this may be filled by a solvent molecule or other monomer, by a counter-ion, or internally by a co-ordinate bond from a carbonyl group in the copolymer chain. This evidence is backed up by observations that the most effective catalysts are those with weak anions such as tosylate and a protic acid, to minimise

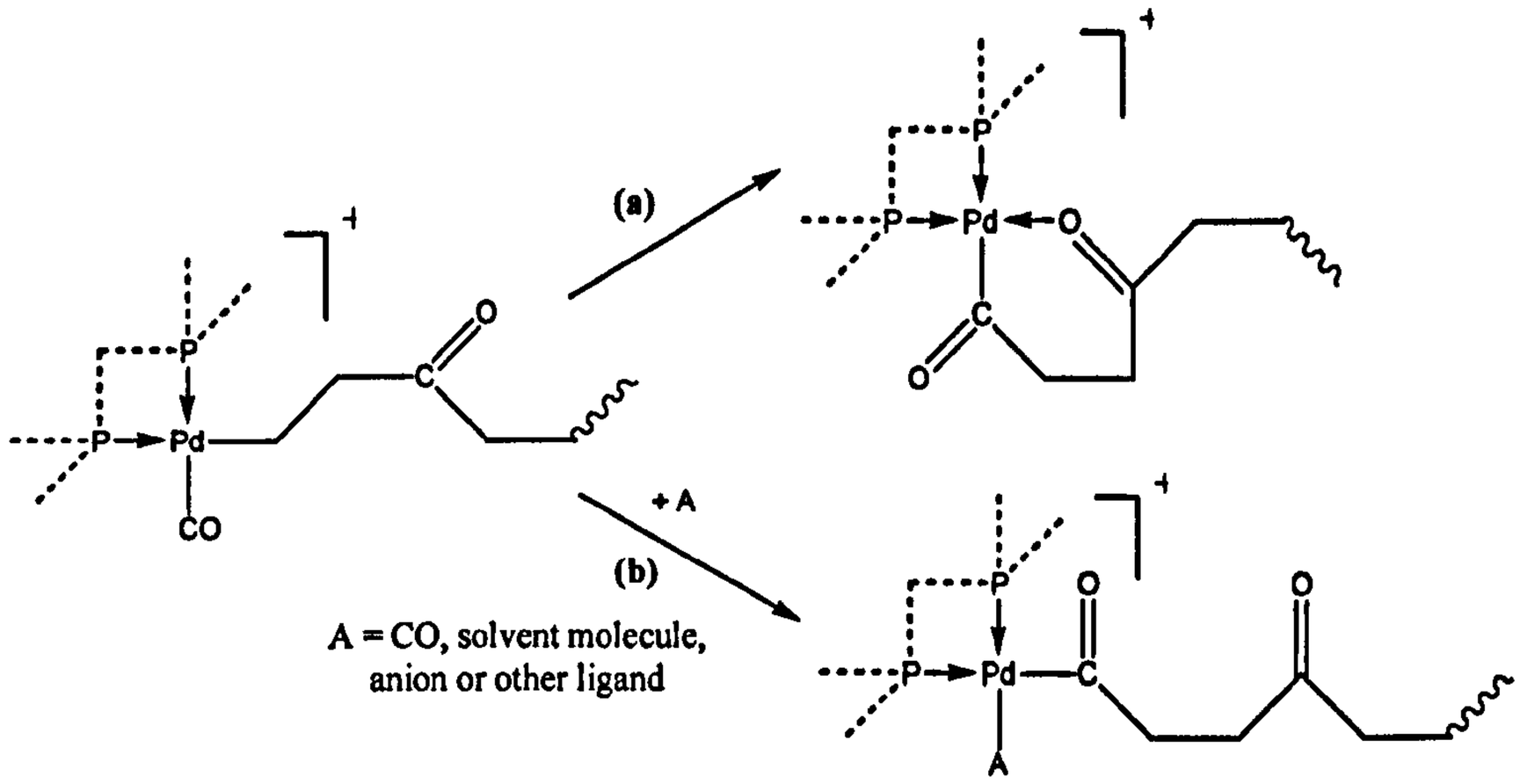


Scheme 1.2.1: Accepted mechanism of the olefin insertion step.

the time that the anion spends bound to palladium and inhibiting the reaction.[2,5,9] However, Ziegler and Margl's theoretical work found that five-co-ordinate square pyramidal complexes could also be formed by the second carbonyl group interacting with palladium above the square plane[8], but this did not cause the four-coordinate structure to be broken.

The insertion step agreed upon by most sources is the olefin insertion step. It is widely believed that after olefin insertion, a co-ordinate bond is formed between the oxygen atom on the carbonyl and the palladium centre, creating a five-membered ring as shown in **scheme 1.2.1**. There is much evidence to support this, including that: (i) Margl and Ziegler's optimised structure formed the co-ordinate bond (when the Pd-C_α-C_β-C_γ torsion angle was fixed at 180°, the energy of the complex was 24.9 kcal/mol higher);[7,8] (ii) various infrared studies have identified the C=O stretching frequency as characteristic of a carbonyl group with a co-ordinate bond on the oxygen;[9,10,11] (these studies also helped intercept intermediates thought to be present in the propagation cycle) (iii) ^1H and ^{13}C NMR have also identified nuclei characteristic of a chelated carbonyl group;[9] and (iv) the structure of closely-related species have been characterised by X-ray crystallography[12]. There are two important effects that chelation has on the cycle. Firstly, it stabilises the product, lowering the energy barrier and making the insertion harder to reverse. Secondly, this affects the following addition step, which will be discussed later.

The mechanism of the carbon monoxide insertion, however, is a matter of less consensus. Most sources agree that the square planar arrangement around palladium is maintained somehow, but they differ in suggesting how this is achieved. Out of the various mechanisms proposed, the most likely one is that after CO insertion, the Pd-O co-ordinate bond is reformed to give a six-membered ring. This structure has again been detected by infrared studies giving the right stretching frequency, though not by as many sources[11]. This structure was also favoured by Margl and Ziegler when they included a second CO group in their models[8]. Margl and Ziegler also notably

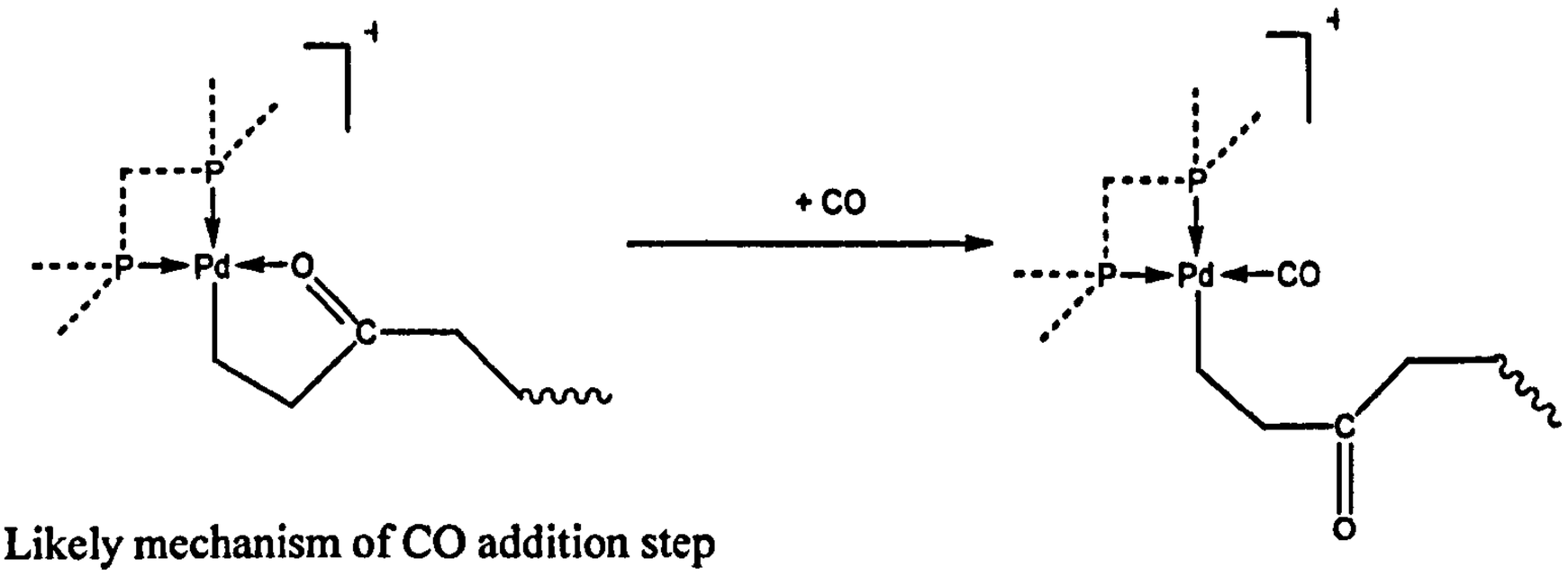


Scheme 1.2.2: Proposed mechanisms of CO insertion step **(a)** by formation of a new Pd-O bond and **(b)** with the addition of a new ligand to maintain the four-coordinate structure.

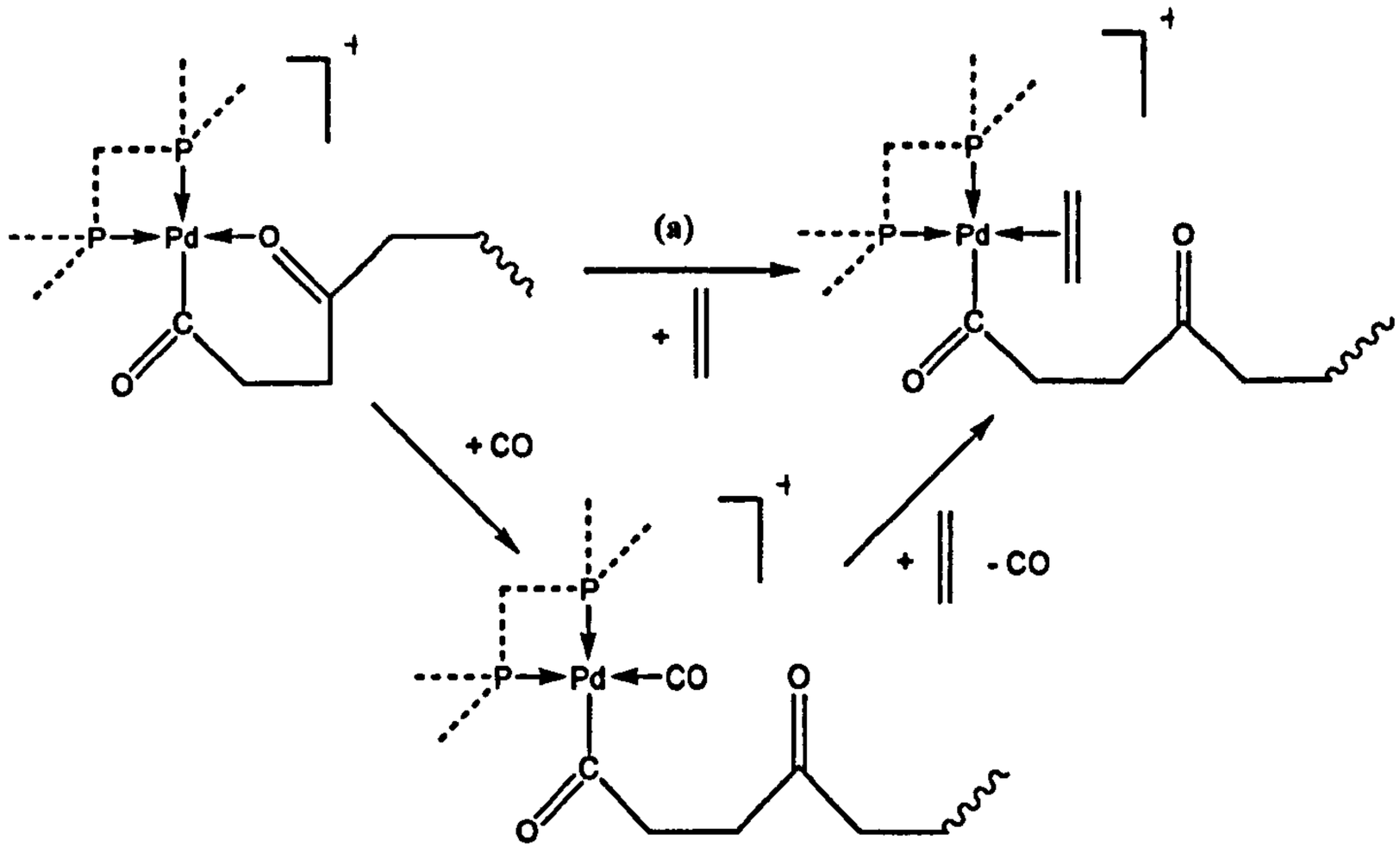
proposed that during and before insertion, the second CO group interacts *above* the CO plane in an axial site to give a square-pyramidal arrangement. There is one other theory suggested in one review paper[3], that the CO insertion is simultaneously accompanied by the addition of another CO molecule to retain the four co-ordinate structure. If this is the case, it could also be possible that other ligands (including solvent molecules and anions) could also act as a temporary fourth ligand. These two theories are shown in **scheme 1.2.2.**

The two addition stages have received the least attention of all, with many sources simply clumping ligand addition into the following insertion step. However, as it is likely that a ligand cannot be added into the Pd plane without displacing another ligand, these steps have perhaps not received the attention they should have been given. Bianchi and Meli[2] speculate that the Pd-O co-ordinate bonding contributes towards alternation of CO/olefin insertion, suggesting that in a five-membered ring, carbon monoxide is a strong enough ligand to break the Pd-O bond but olefins are not. They also speculated that this did not apply to six-membered rings which are less stable and whose Pd-O bonds can be broken by either ligand. However, it has also been shown that the presence of carbon monoxide can assist the olefin insertion stage, prompting speculation that olefins cannot displace Pd-O bonds in either the five- or six-membered ring, and instead can only bond to Pd after the Pd-O bond has been displaced by CO.[11]

The path proposed for CO addition is shown in **scheme 1.2.3,** and the paths proposed for olefin addition are shown in **scheme 1.2.4.** It has been suggested that the incoming ligands first interact directly above the palladium-ligand plane before



Scheme 1.2.3: Likely mechanism of CO addition step



Scheme 1.2.4: Proposed mechanisms of olefin addition step by **(a)** direct displacement of the Pd-O bond by the olefin and **(b)** addition after Pd-O bond is displaced by CO.

displacing the current ligands,[11] but this is speculation and there is no experimental evidence to support or oppose this.

Finally, the energy barriers associated with olefin and carbon monoxide insertion have been estimated both experimentally and computationally. Brookhart *et al* performed a kinetic study on migratory insertion of some simplified palladium diphosphine structures, two of which could be considered as analogous to CO and olefin insertion in the propagation cycle of the copolymerisation reaction, estimating activation energies.[13] Similarly, Ziegler and Margl's work also calculated thermodynamic parameters for the two insertion stages, as well as the enthalpies (but not energy barriers) of the two addition stages.[7] The thermodynamic parameters and the reactions associated with them are shown in **table 1.2.1** and **table 1.2.2** respectively.

By comparing experimental research of CO insertion[14] and olefin insertion[15] in various palladium systems, it has been proposed[5] that the olefin insertion step is likely to be the rate-determining step, but olefin insertion also plays the biggest part in

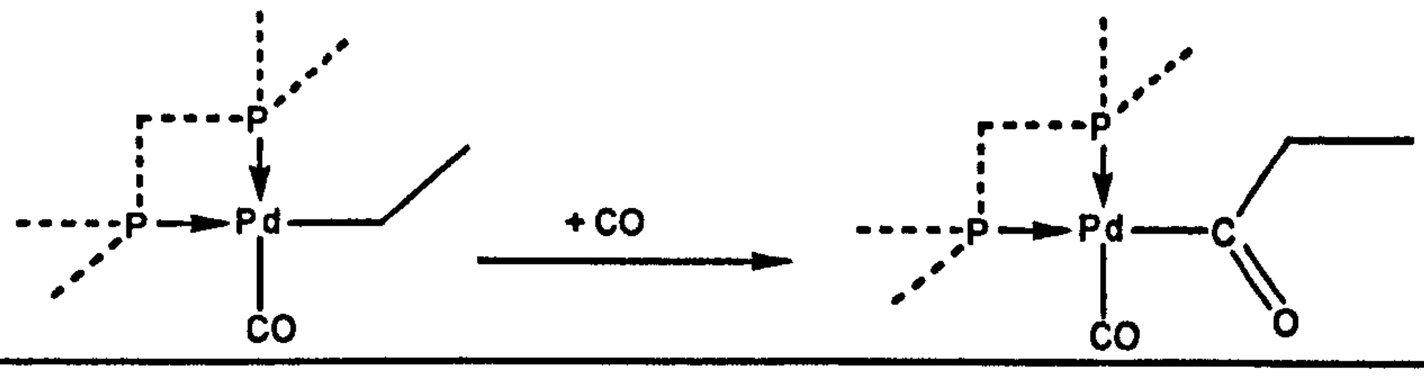
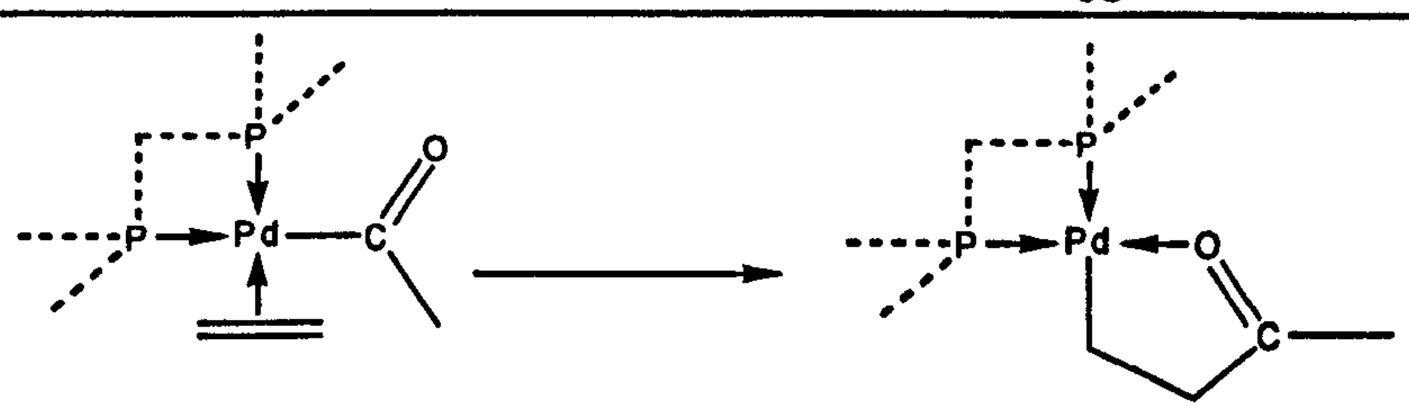
Reaction Analysed	$\Delta G^{\ddagger}$ / kcal/mol at c. -100°C
	13.4 ± 0.01
	12.3 ± 0.01

Table 1.2.1: Energy barriers of analogous CO and olefin insertion from kinetic studies by Brookhart *et al*

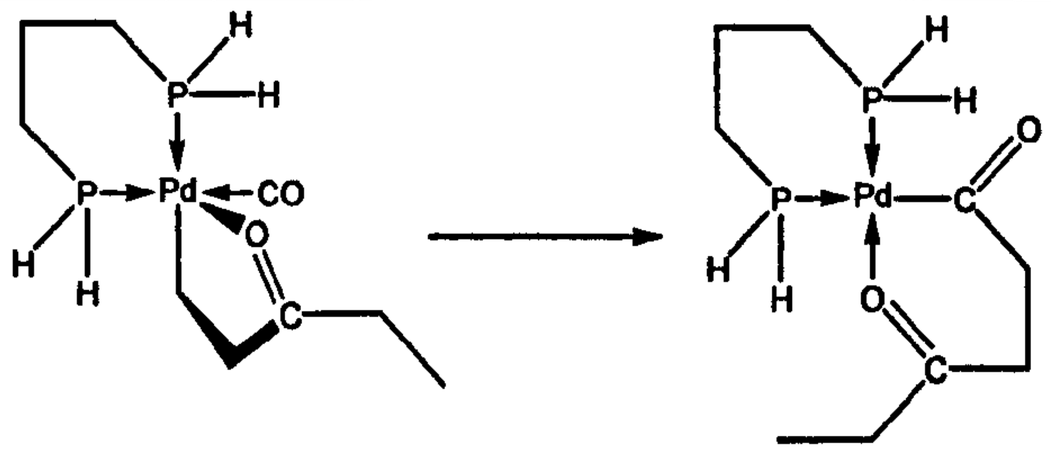
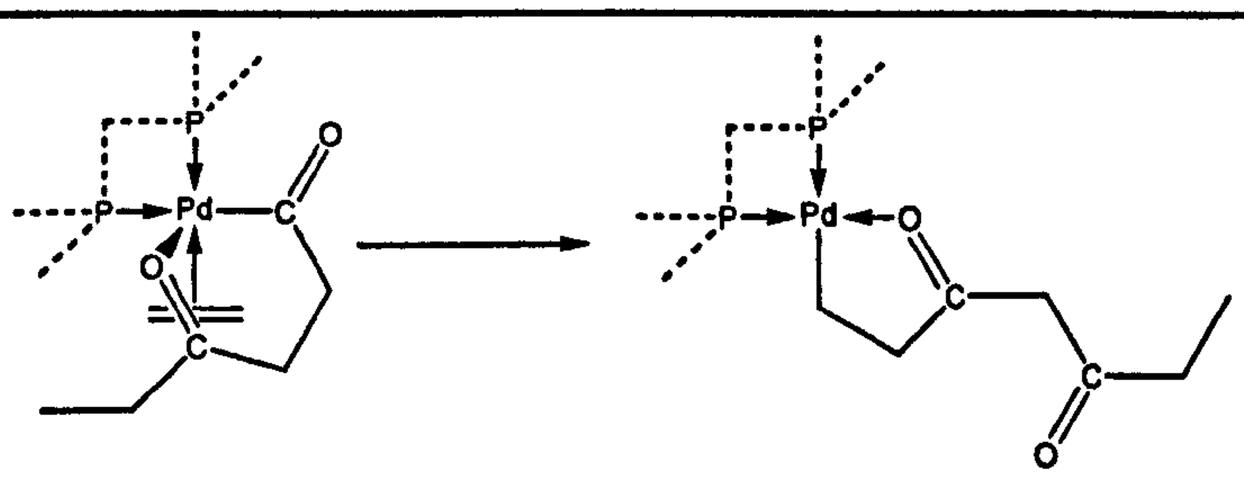
Reaction Analysed	E_a / kcal/mol	ΔH / kcal/mol
	11.7	-7.6
	15.3*	-11.5*

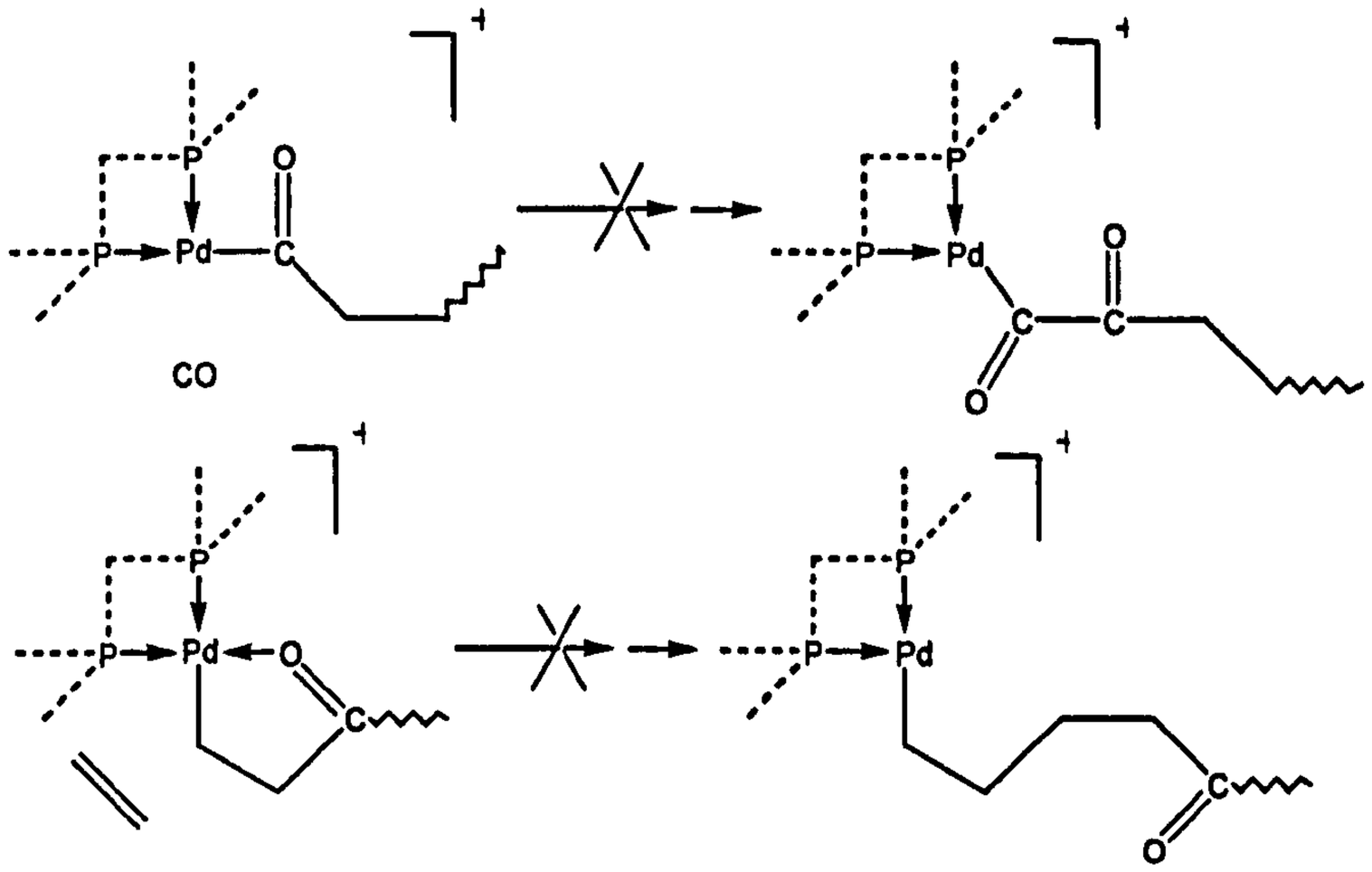
Table 1.2.2: Energy barriers of CO and olefin insertion using theoretical studies by Ziegler and Margl. Diphosphine ligand was $PH_2CH{=}CHPH_2$.

*: If the second CO ligand was neglected, the activation energy dropped to 13.9 kcal/mol, and enthalpy changed to -17.7 kcal/mol

promoting the reaction in the forward direction as it is the most difficult step to reverse. Although this experimental evidence did not directly examine the CO/olefin copolymerisation, by adding the above evidence from Brookhart *et al* and Ziegler and Margl, it is likely that this conclusion is correct.

1.3 Double insertion

Perhaps of the most interest in the mechanism of olefin / CO copolymerisation is the complete absence of consecutive insertions of two olefin or two carbon monoxide ligands into the copolymer chain. The disallowed reactions are shown in **scheme 1.3.1.** There is much speculation as to why this is the case.



Scheme 1.3.1: Double insertion of CO or olefins, not observed in copolymerisation.

It is thought, beyond reasonable doubt, that double insertion of carbon monoxide does not occur because insertion of CO into a Pd-acyl bond is thermodynamically unfeasible. This has been concluded by many different authors in both experimental[16,17,18] and computational[7,8] work, although the reverse reaction is possible[16]. The only way that two successive carbonyl groups can be formed is by reductive elimination, which is incompatible with a copolymerisation mechanism.[16]

With double insertion of olefins, however, there are different possible reasons why insertion of olefins into a Pd-alkyl bond is not observed. This kind of insertion is not thermodynamically unfavourable, and in the complete absence of carbon monoxide double insertion does occur (although one gets dimerisation to form butene rather than polymerisation.)[19] It is generally thought that CO insertion is so fast it dominates the reaction if it is present, and this has been backed up both theoretically[7,8], and through kinetic studies on small complexes.[13,20] It has been reported that even with an excess of olefins in a 10:1 ratio, alternating copolymers are still formed until CO is exhausted, and only then does double olefin insertion occur,[5] but this was not confirmed from examination of the cited reference.[21]

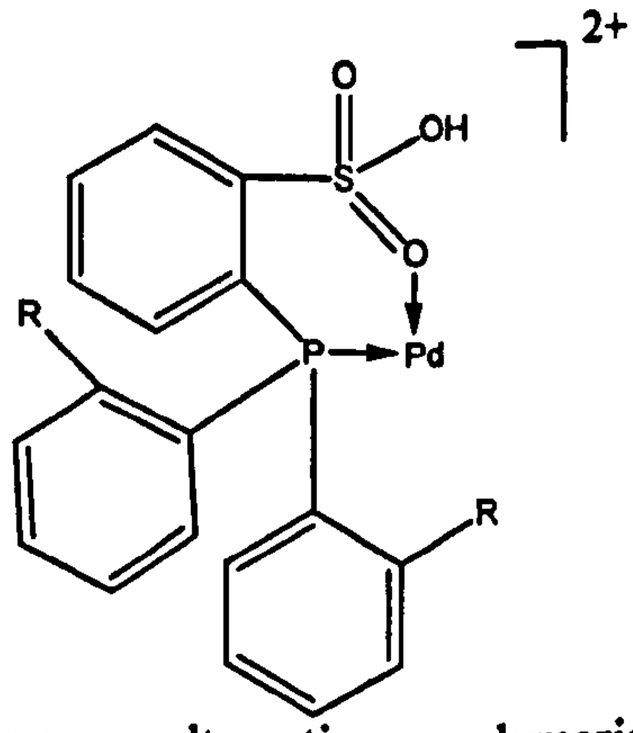
There is less agreement as to exactly what slows down the rate of olefin insertion. The olefin insertion step itself is thought to have a higher activation energy barrier than CO insertion.[7,8] However, the review papers have suggested that CO insertion is further favoured by the ease of addition of a new CO ligand to palladium prior to insertion compared to olefin addition prior to olefin insertion, due to the stronger bonding between CO and transition metals.[2,5] There is also the possible effect

of the Pd-O co-ordinate bond inhibiting the olefin addition step needed prior to olefin double insertion, as discussed in the previous section.

In both of these cases, however, one must also consider the effect the difficultly of displacing a Pd-O bond with an olefin would have on the regular olefin insertion step, when both of these factors would promote CO addition instead of olefin addition. Although CO double insertion cannot follow CO addition, if a Pd-CO bond is more stable than a Pd-olefin bond this would slow down the rate of copolymerisation, as olefin insertion could not occur whilst CO is bonded to palladium, blocking the site the olefin needs. As stated in the previous section, should Pd-O bonds be formed after CO insertion, olefin insertion could be explained either on the assumption that the Pd-O bond is weaker in a six-membered ring and easier for olefins to displace, or that a carbon monoxide ligand must displace the Pd-O bond first. It should be noted from here that increasing the pressure of carbon monoxide could either slow copolymerisation down (if CO occupies sites needed by olefins to bond to) or speed the reaction up (if CO displaces bonds to free up sites that olefins need).

Finally, one should consider that after double-insertion of either carbon monoxide or olefins, the product cannot form a Pd-O bond to form a stable 5- or 6-membered ring. 4-, 7- or 8-membered rings are unlikely to be as stable, if they form at all.[9] It is unclear whether the stability of the product affects the activation energy of insertion, but if it does then the lack of stable Pd-O bonding would raise the activation energy of both double insertion steps.

There is some commercial interest in producing copolymers with more olefin molecules than carbon monoxide molecules in the copolymer chain. There are currently no palladium-diphosphine complexes known to be capable of producing this copolymer. However, Drent *et al* recently discovered that by using a P-O ligand



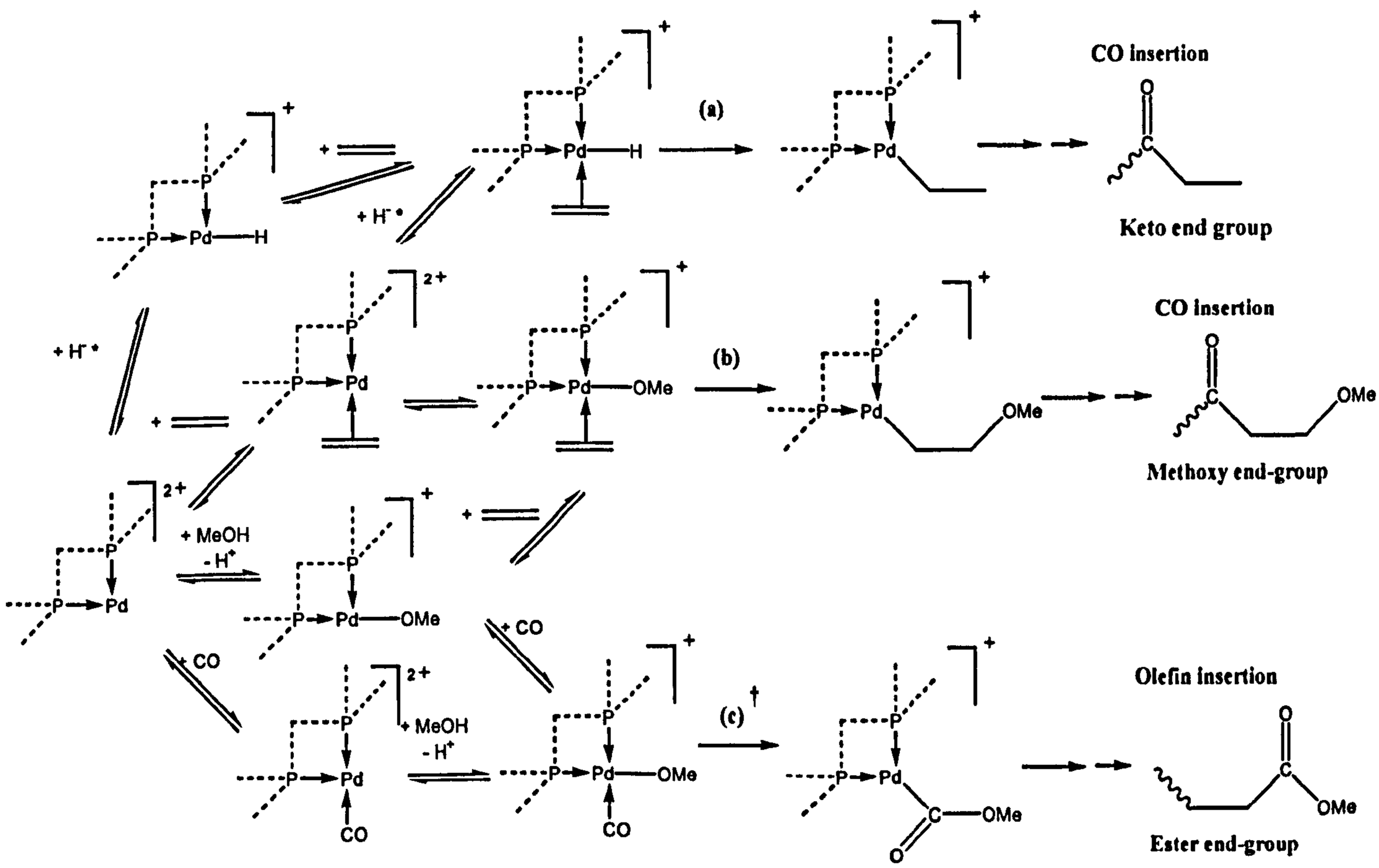
Scheme 1.3.2: Catalyst that allows non-alternating copolymerisation.

instead of a P-P ligand (shown in **scheme 1.3.2**), about 5-10% more olefins than carbon monoxide molecules were inserted into the copolymer. The reason they propose is that the oxygen ligand destabilises the Pd-O bond, making it easier for olefins to bond to the complex.[22]

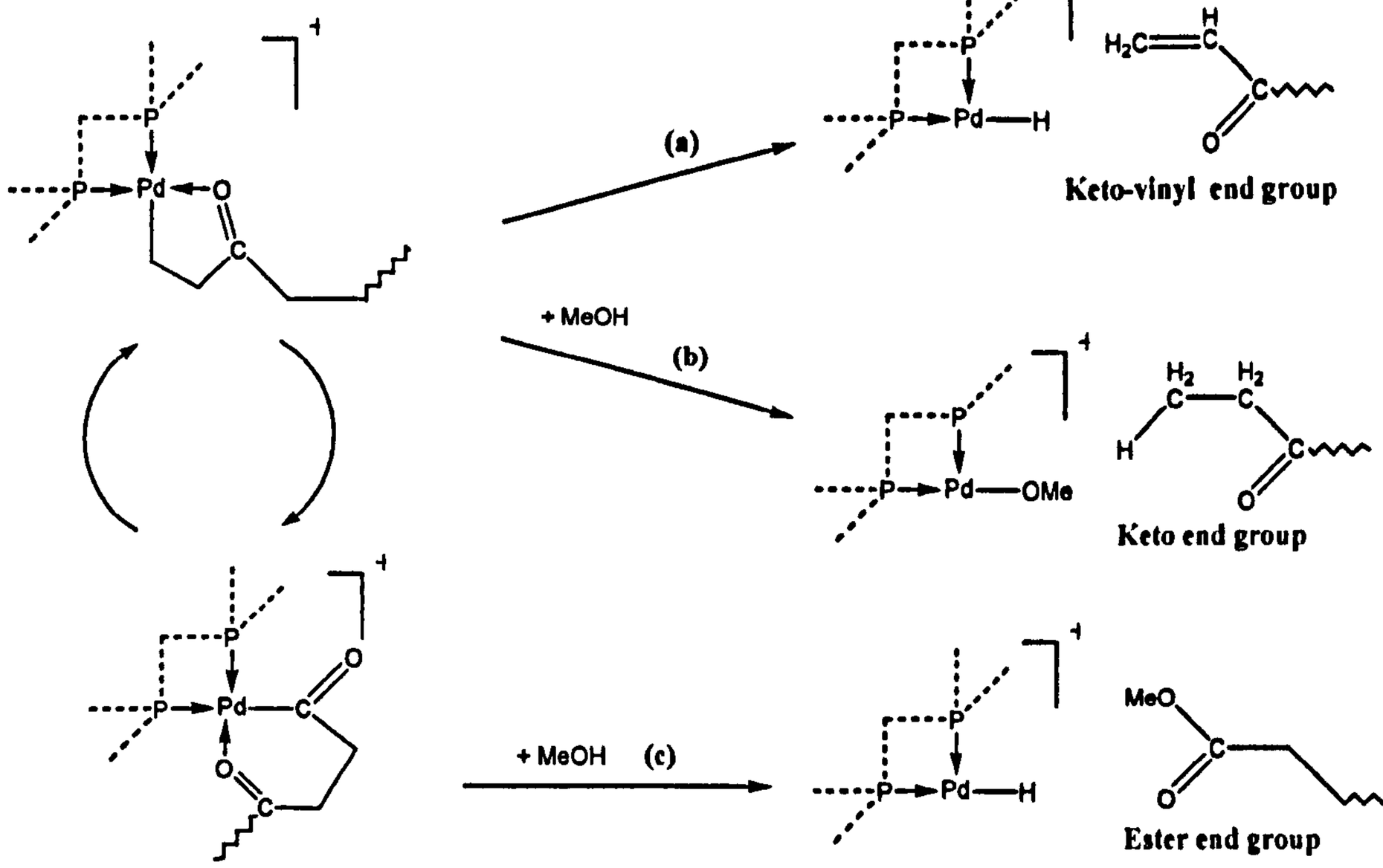
Finally, it should be noted that although the transition metal-catalysed reaction is by far the superior method of synthesising copolymers, it is possible to synthesise *random* non-alternating copolymers using a free-radical mechanism instead.[3,23] Even so, it is thought that double CO insertion is still impossible, and whilst the proportions of CO and olefins in the chain can be varied, the proportion of CO inserted is never higher than 50%. Although this has some commercial interest in its own right, the main item of interest here is that it can be shown that the melting point falls significantly as the CO content of a non-alternating copolymer falls.

1.4 Initiation and termination steps

Of just as much importance are the initiation and termination steps either side



Scheme 1.4.1: Proposed initiation steps of olefin copolymerisation by **(a)** olefin insertion into palladium-hydride bond (ref. 2, 4, 5, 21 & references therein); **(b)** olefin insertion into palladium-methoxy bond (ref. 4 & 24); and **(c)** CO insertion into palladium-methoxy bond (ref. 2, 4, 5, 21 & 25).
**: Method of generating palladium-hydride initiator unclear; six methods are suggested in ref. 5.*
†: CO insertion has also been observed into a Pd-Me bond to give a -CH_2CH_2OMe end-group (ref.26). However, this requires a starting catalyst of (P-P)PdMeX, and no mechanism has been proposed for regenerating the Pd-Me bond after the first copolymer chain is terminated, so that is not strictly part of a catalytic cycle.

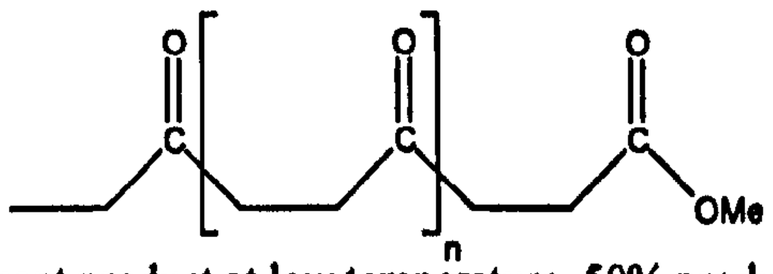


Scheme 1.4.2: Proposed termination steps of olefin copolymerisation by **(a)** β-hydride abstraction (ref. 28); **(b)** protonolysis after olefin insertion (ref. 24, 28); and **(c)** methanolysis after CO insertion (ref. 24, 28). Note that it is hypothetically possible to also have termination by methanolysis after olefin insertions (to give a $-CH_2CH_2OH$ end group) or protonolysis after CO insertion (to give a $-CH_2CH_2CHO$ end group), but these end-groups are unheard of.

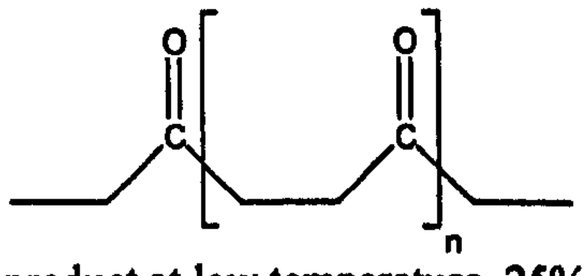
of the propagation cycle. These determine the end groups present on the copolymer chain and, in conjunction with the kinetics of the propagation cycle, the rate of copolymerisation and chain length of the copolymers.

There are several different mechanisms proposed for the initiation and termination steps, shown in **scheme 1.4.1** and **scheme 1.4.2** respectively, giving rise to different end groups.[2,4,5,21,24-28] However, most of these processes require a solvent capable of proton donation to occur. This means there are significant differences depending on whether the reaction is carried out in protic or aprotic conditions.

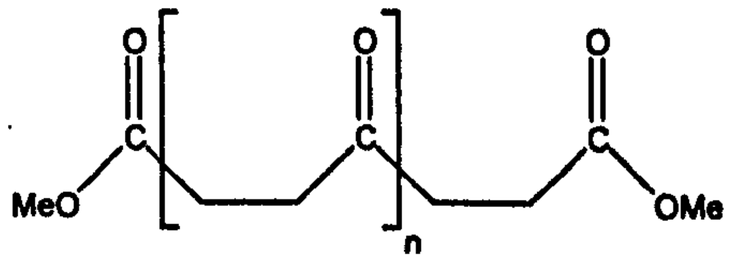
In protic conditions, where a solvent such as methanol is used (although water is also popular), the initiation and termination steps that occur in practice can be narrowed down by gas chromatography – mass spectrometry (GC-MS) of the smaller oligomers formed. It shows that all copolymers have keto- and ester-end groups, meaning that the initiation and termination steps that give rise to methoxy- and keto-vinyl-end groups can be eliminated from the possibilities. Furthermore, keto-ester oligomers, with one end group of *each* type, are the dominant copolymer formed at lower temperatures (but with the products approaching 2:1:1 keto-ester:diketo:diester at high temperatures). These copolymers are shown in **scheme 1.4.3.**[21] This strongly



Keto-ester: Dominant product at low temperature, 50% product at high temperature



Diketone: Trace product at low temperature, 25% product at high temperature

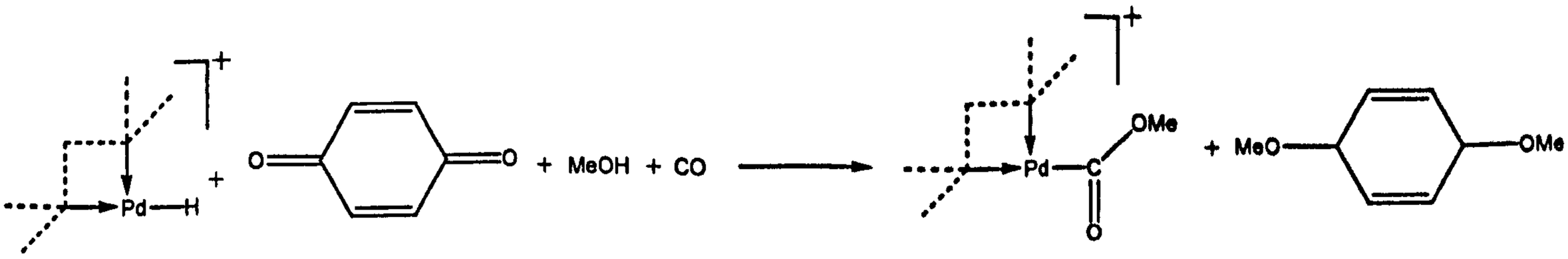


Diester: Trace product at low temperature, 25% product at high temperature

Scheme 1.4.3: Copolymers (with end groups) produced from initiation and termination steps.

suggests that there is one initiation step and one termination step that dominates at lower temperatures, and leaves two possibilities: *either* the dominant initiation process is olefin insertion into the Pd-H bond and the dominant termination process is methanolysis of a Pd-acyl bond; *or* the dominant initiation process is the formation of an ester end-group and the dominant termination process is protolysis of a Pd-alkyl bond.

There are differing opinions on which of the above two possibilities is the case. Drent and Budzelaar favoured initiation by olefin insertion into the palladium-hydride bond as the initiation step, and consequently methanolysis as the termination step, because when quinone oxidants were added to the system, the proportion of diesters were increased. They proposed that the quinones inhibited the formation of palladium-hydride bond and instead promoted initiation by ester groups using the reaction shown in **Scheme 1.4.4.**[5,21] Abu-Surrah and Rieger, on the other hand, did not favour insertion into a palladium-hydride bond because of the lack of a known chemically consistent pathway, and so favoured initiation by CO insertion into a Pd-OMe bond (which would consequently favour termination by protonolysis in order to



Scheme 1.4.4: Proposed mechanism for quinones to inhibit initiation by insertion of olefins into a Pd-H bond.

form keto-esters).[2,24]

To date, there is no clear consensus on which pathway is correct, only that it has to be one or the other.

As both possible termination processes require methanol or another protic solvent to proceed, it has been speculated that reducing the amount of methanol present causes the chain length of copolymers to be increased[4], and such observations have been made[29]. The lack of termination by β-hydride abstraction is believed to arise due to the difficulty in breaking the strong Pd-O bond present prior to termination.[5]

Copolymerisation is possible under aprotic conditions, but the initiation and termination steps are different.[27] Initiation is restricted to olefin insertion into a palladium-hydride bond, apart from the copolymerisation of the first chain, where CO insertion into a Pd-Me bond could be the initiating step if the starting catalyst is (P-P)PdMeX.[26,27] Even this process is more difficult as there are fewer ways of generating a palladium-hydride bond without methanol (although termination by β-hydride abstraction leaves the palladium with a hydride bond ready). Similarly, it is not possible for the copolymerisation to be terminated by methanolysis or protolysis from methanol, possibly leaving termination by β-hydride abstraction as the only viable method of termination.[27] However, it has also been proposed that termination by protonolysis without methanol is also possible.[2] Unfortunately, the copolymers produced have such a high chain length, presumably due to the difficulty of terminating the process, that there is no end-group analysis data available to indicate which process is more likely.

1.5 Effect of diphosphine ligand

Although the diphosphine ligand is thought to remain bonded to the palladium centre throughout the copolymerisation process, it has been seen on many occasions that altering or replacing the diphosphine backbone changes the productivity of the copolymerisation process.

Starting with the smallest changes, altering the length of the carbon backbone between the two phosphorus atoms is known to affect both the chain length of the copolymer and the rate of copolymerisation. In both cases, 1,3-

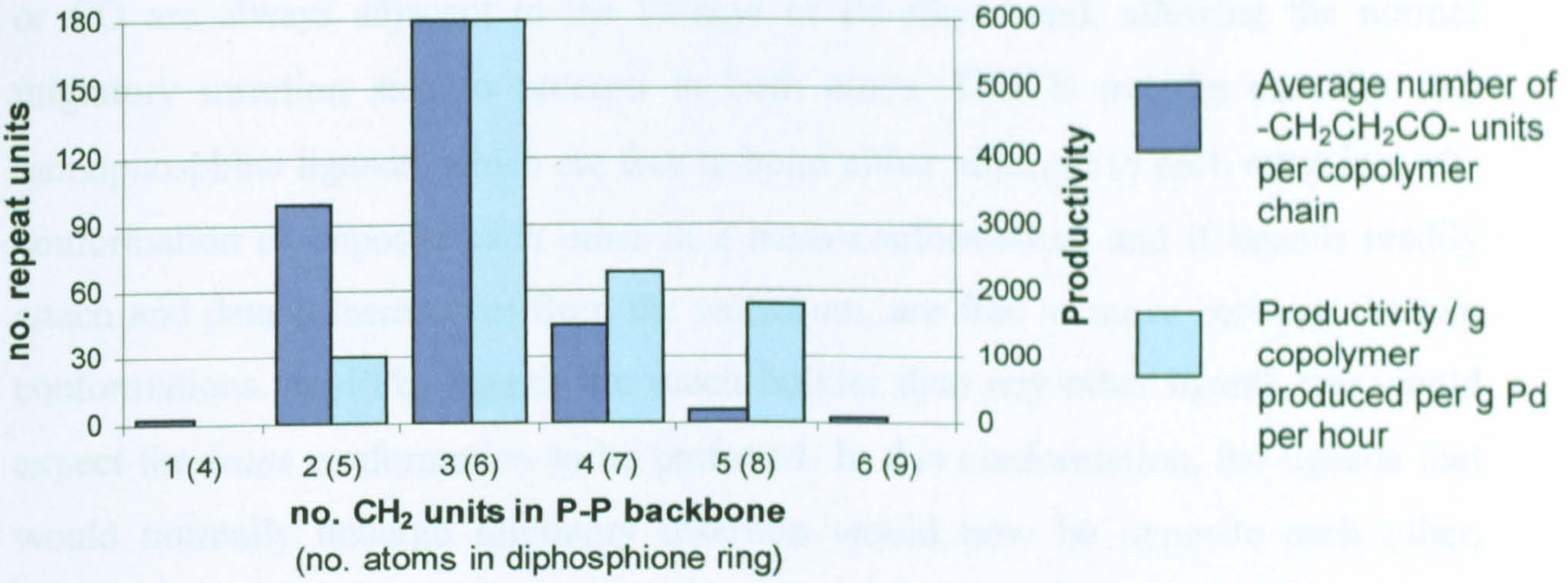
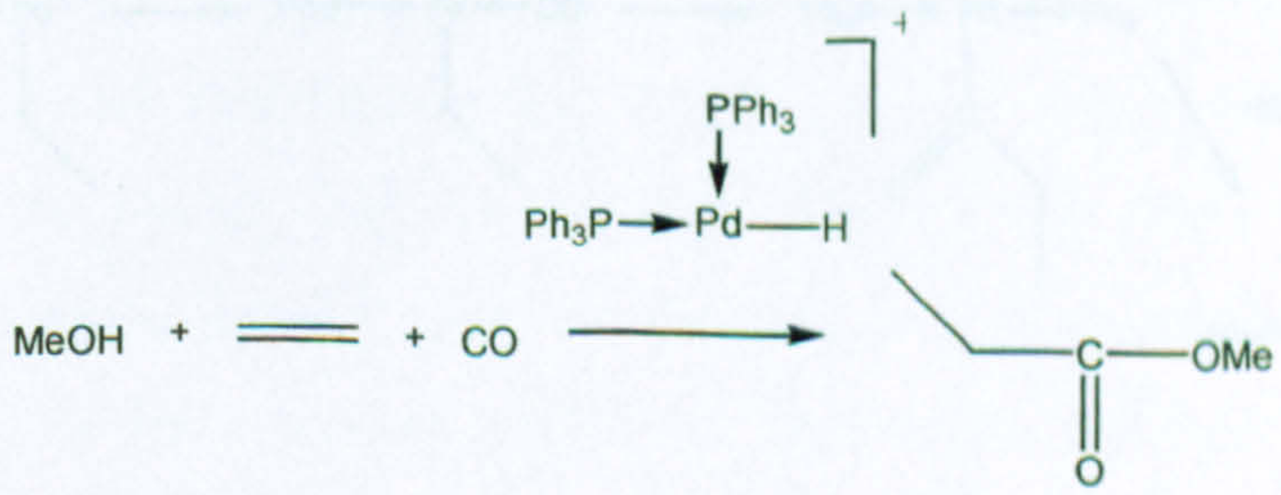


Figure 1.5: Effect of chain length of carbon backbone on diphosphine ligand on chain length and productivity. Reaction carried out in 150 ml MeOH and 0.1 mmol $Pd(NCMe)_2(TsO)_2$, with equimolar C_2H_4:CO, 84°C and 45 bar pressure.

bis(diphenylphosphino)propane is the most effective ligand in both respects. Increasing the chain length above three, or decreasing the chain length below three, decreases both the rate of copolymerisation and chain length, as shown in **figure 1.5**.[21] There is no clear explanation as to why the six-membered ring is the most effective, although a number of hypotheses have been suggested.[21,30,31] Other variations of the diphosphine ligand have also been used, including ligands with added branches on to the carbon backbone, ligands with rings or double bonds in carbon backbone to increase rigidity, and ligands with groups on the phosphorus atoms other than four phenyl groups.[2,27,32,33]

The most important difference, however, is that a *di*phosphine backbone must be used to achieve copolymerisation. If two monophosphine ligands, such as PPh_3, are used instead, there is no copolymerisation and a monomer, methyl propanoate, is formed instead, as shown in **scheme 1.5.1**.[21] Although it has not been shown with certainty why this is the case, there is one obvious likely explanation.[5,28] All diphosphine ligands are physically restricted to the *cis*-conformation, where the two

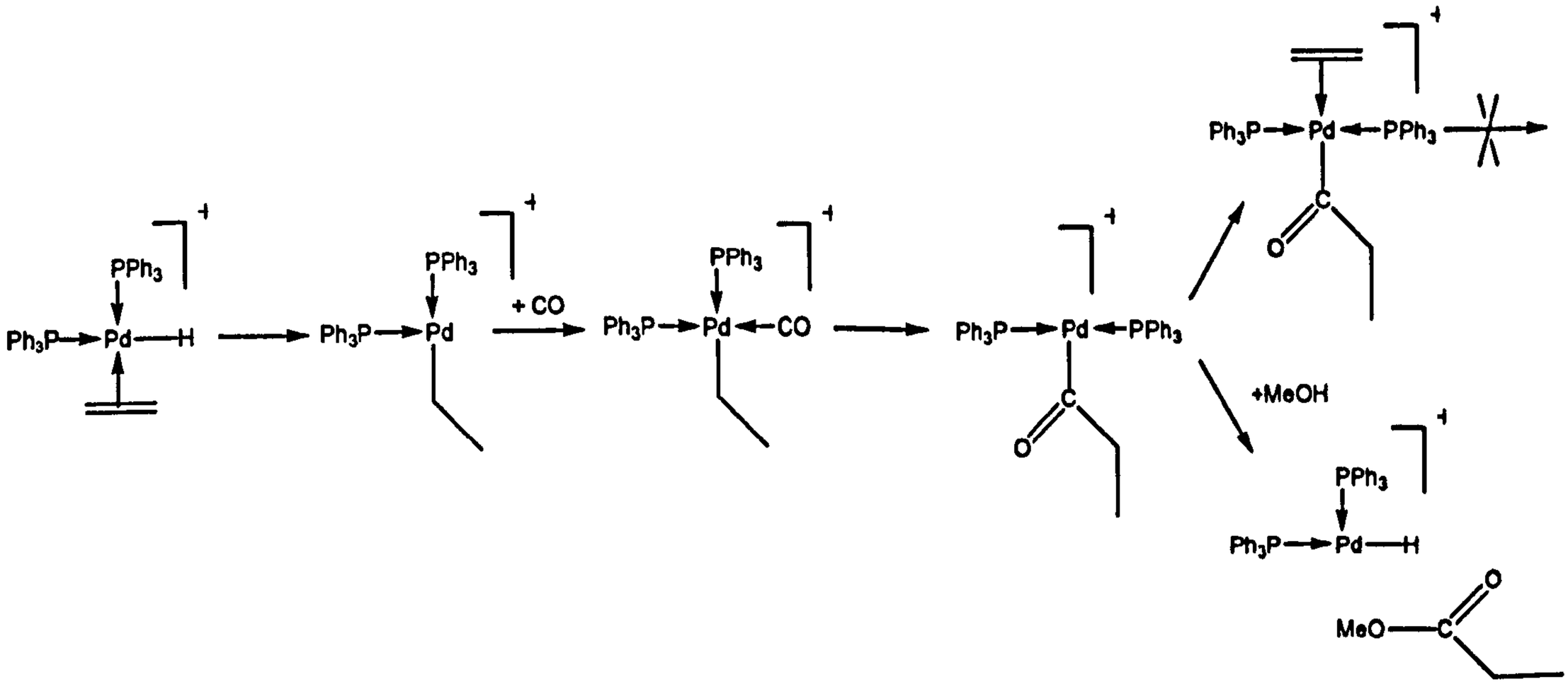


Scheme 1.5.1: Formation of methyl propanoate when monophosphine ligands are used instead of a diphosphine ligand.

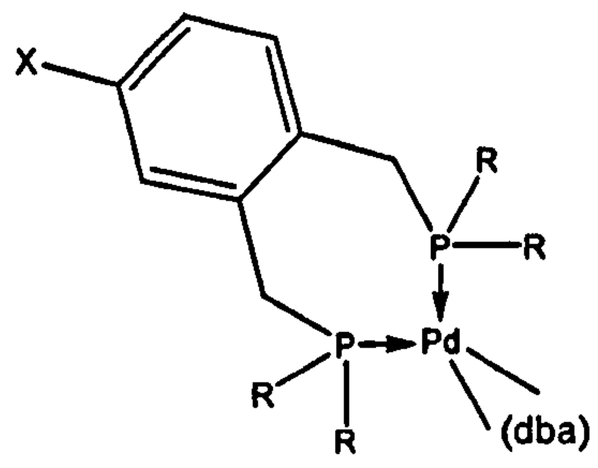
phosphorus atoms occupy adjacent sites of the square plane. This means that olefins or CO are always adjacent to the Pd-acyl or Pd-alkyl bond, allowing the normal migratory insertion step to proceed in both cases. This is not the case for two monophosphine ligands, which are free to bond either adjacent to each other in a *cis*-conformation or opposite each other in a *trans*-conformation, and if ligands readily attach and detach themselves from the palladium, are free to move between the two conformations. As PPh_3 ligands are much bulkier than any other ligand, one would expect the *trans* conformation to be preferred. In this conformation, the ligands that would normally undergo migratory insertion would now be opposite each other, unable to proceed with their normal reaction. One would expect isomerisation between the *cis*- and *trans*-states to proceed more readily with excess PPh_3 ligands or at higher temperatures, and it has indeed been observed that at lower temperatures and with a little excess PPh_3, copolymers can still be formed in aprotic solvents.[34]

A possible reaction pathway for methyl propanonate is shown in **scheme 1.5.2.**[5,28] However, there is one question still unanswered from this mechanism, which is why only olefin insertion in the Pd-acyl bond is prevented by the phosphine ligands adopting the *trans*-conformation. The monophosphine ligands have to adopt the *cis*-conformation for both the CO insertion step and the original step of olefin insertion into the Pd-H bond, so why are these steps allowed when olefin insertion is not?

The formation of monomers and low molecular weight oligomers is an extensive field in its own right, and has been reviewed in considerable depth, beyond the scope of this review[28]. Obviously, with the much shorter chains, the end-groups



Scheme 1.5.2: Proposed mechanism for the formation of methyl propionate (lower branch), plus formation of structure that prohibits further copolymerisation (upper branch).



R = t-Bu, i-Pr, Cy or Ph

X = H, NO_2 or OMe

(dba) = *trans*-,*trans*dibenzyldieneacetone

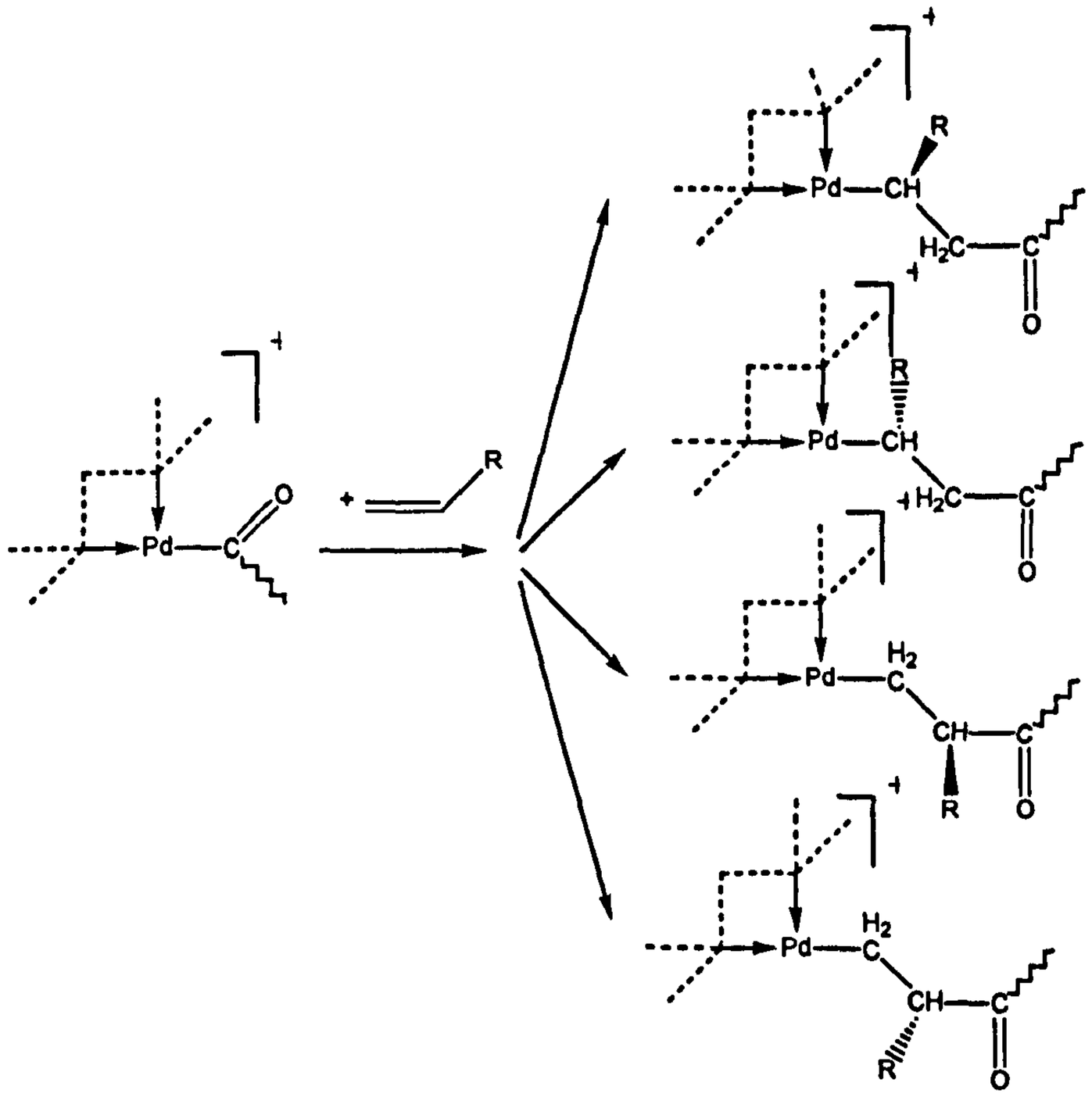
Scheme 1.5.3: Palladium-diphosphine catalyst that forms monomers or oligomers instead of copolymers.

start to have a much greater effect on the properties of the product, and so considerably more attention has been directed to controlling the initiation and termination steps to obtain the desired end-groups. One point of note is that although palladium-diphosphine catalysts nearly always produce copolymers or cooligomers, there are known exceptions. The diphosphine compounds shown in **scheme 1.5.3** predominately produce methyl propanoate instead of the usual copolymer.[33] Why this is so is the subject of continuing industrial research.

Diamine (N-N) ligands and diimine ligands (N-N ligands with double bonds between the nitrogen atoms and the end carbons in the bridging carbon backbone) are frequently used instead of diphosphine ligands for copolymerisation.[35] It is thought that the mechanism of copolymerisation is the same as with diphosphine ligands, and that it is easier to experimentally study the copolymerisation mechanism using diamine ligands instead of diphosphine ligands. Copolymerisation with diimine ligands has been studied computationally by Svensson *et al* with similar results to Ziegler and Margl's work.[36] Copolymerisation has also been observed experimentally using P-O, N-O and P-S ligands, but it is thought that these mechanisms involve additional intermediates.[2]

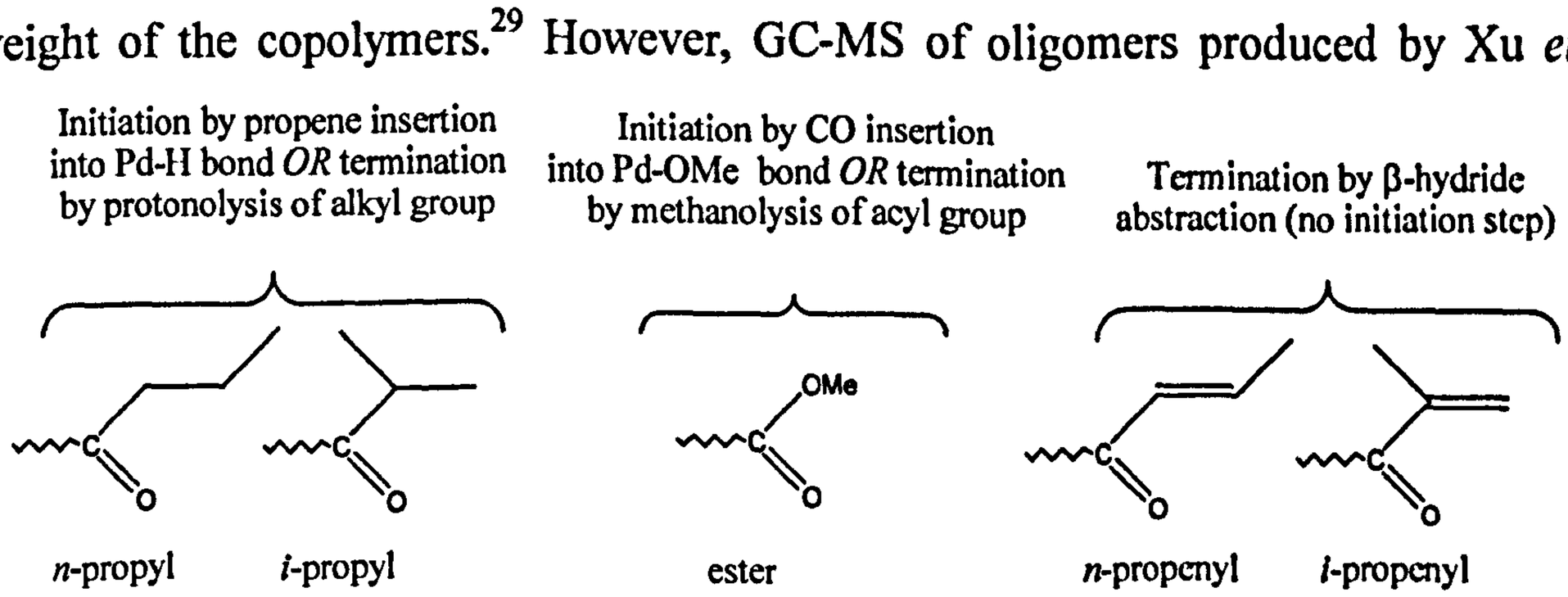
1.6 Use of olefins other than ethene

Although ethene is the most popular olefin to use for olefin/CO copolymer synthesis, this is by no means the only olefin that can be used, and copolymers have been synthesised using many other olefins, some more effectively than others. In most cases, in addition to rate of copolymerisation and molecular weight variations, two further variables are introduced that can be controlled by the choice of ligands: regioselectivity and stereoselectivity. Both of these factors arise from the fact that there are now four different ways in which an olefin can be inserted into the copolymer chain, as shown in **scheme 1.6.1.**



Scheme 1.6.1: Different products possible from insertion of 1-olefins into a Pd-acyl bond. Top two modes of insertion are 2,1-insertion, bottom two modes are 1,2-insertion. (Geometry around Pd centre is arbitrary – in practice, most likely conformation is with a Pd-O coordinate bond.)

One of the most popular olefins to study after ethene is propene. Propene and carbon monoxide have been copolymerised by several groups and studied in depth. Like CO/ethene copolymerisation, CO/propene copolymerisation proceeds in perfect alternation between the two groups, and the mechanism is believed to be the same.[2,4,5,30] The only significant difference is that in the distribution of the end-groups, shown in **scheme 1.6.2**, the keto-vinyl end-group is present.[4,30] The means that in CO/propene polymerisation, termination by β-hydride abstraction is a viable mechanism, unlike CO/ethene copolymerisation where keto-vinyl end-groups are rare. However, there are conflicting papers written on which termination process, if any, is dominant. Abu-Surrah and Rieger propose that termination by methanol remains the dominant process as increasing the amount of methanol decreased the molecular weight of the copolymers.[29] However, GC-MS of oligomers produced by Xu *et al*



Scheme 1.6.2: End-groups formed in propene/CO copolymerisation.

showed that most of their copolymers were terminated by β-hydride abstraction, even with methanol present (albeit at a higher temperature to promote the formation of short chains).[30] Sen also showed that a significant number of copolymers with keto-groups on *both* ends of the copolymer are formed, showing that termination by protonolysis is also competitive.[17] So far, there is no consensus as to why β-hydride abstraction is feasible with propene but not ethene, but the methyl group is likely to influence the chemically active atoms during this stage.

The regioregularity of the copolymer can be measured by using ^{13}C NMR on the carbonyl carbons in the final product. The chemical shift of the signal is mainly governed by the number of methyl groups on the two adjoining carbon atoms, as shown in **figure 1.6.1.**[30,37] In a perfectly regioselective copolymer, all carbonyl groups would be in a head-tail environment, whilst in a totally non-regioselective copolymer, there would be a 1:2:1 ratio of head-head:head-tail:tail-tail configurations. On its own, however, this does not indicate whether the olefin insertion step was regioselective to 1,2- or 2,1-insertion; only how regioselective it is one way or the other. There are two factors that could influence regioselectivity, shown in **figure 1.6.2.** One is that the methyl group would induce a weak dipole across the double bond that would favour 2,1-insertion, owing to the negatively-charged end of the olefin being close to the

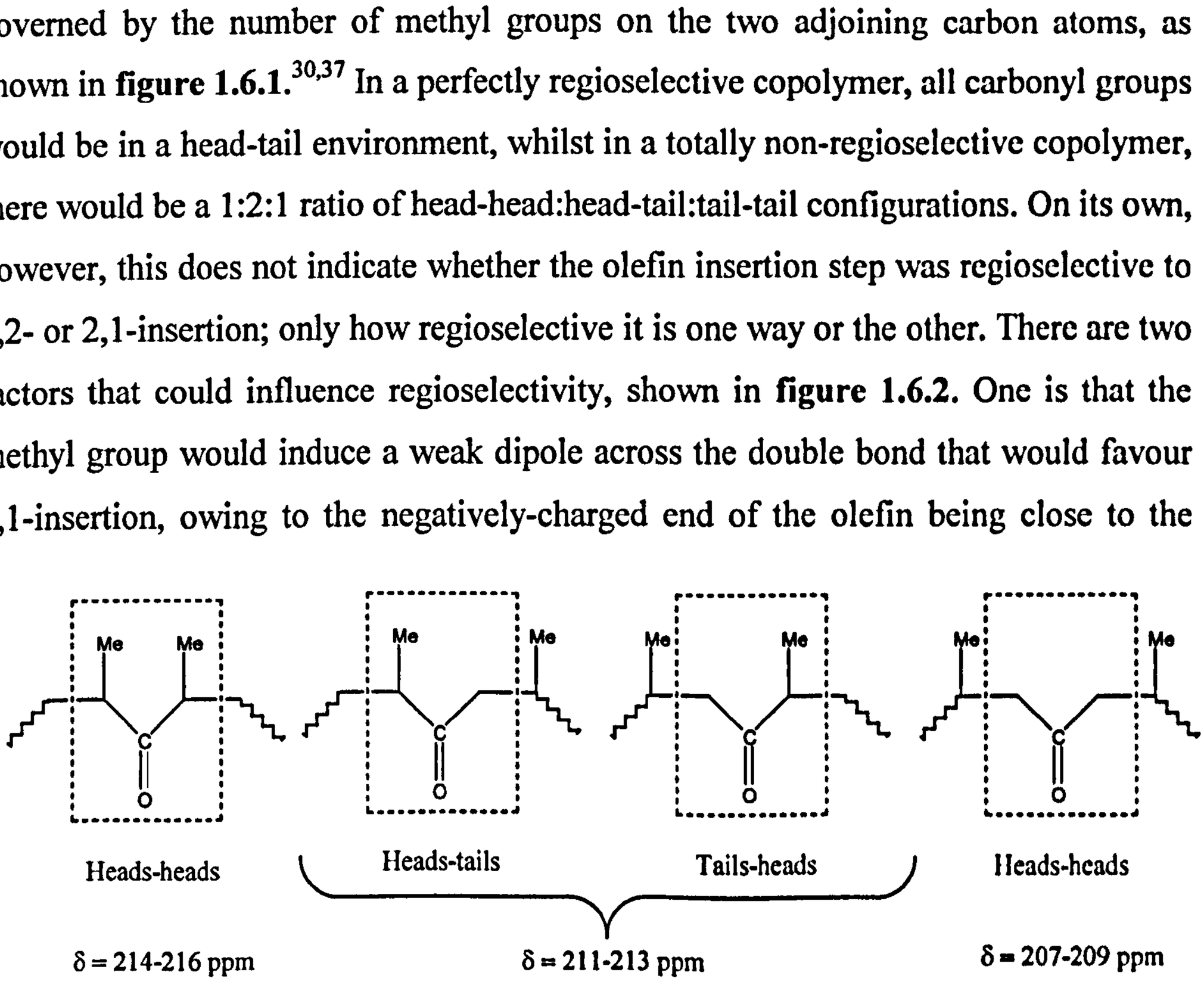


Figure 1.6.1: NMR signals to determine the regioselectivity of CO/propene copolymers

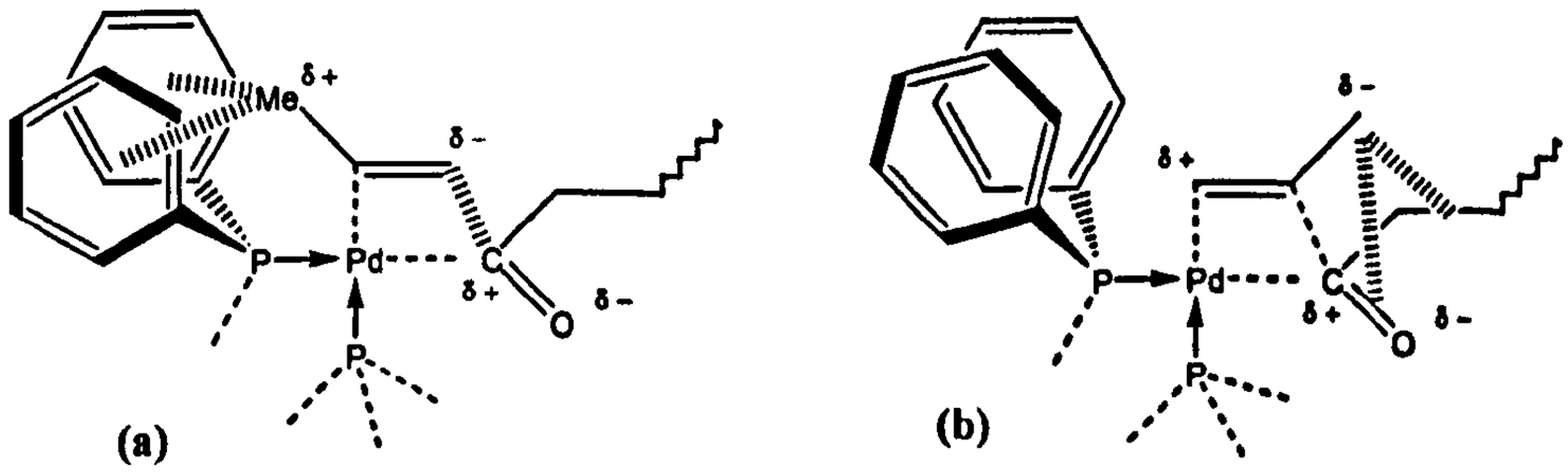


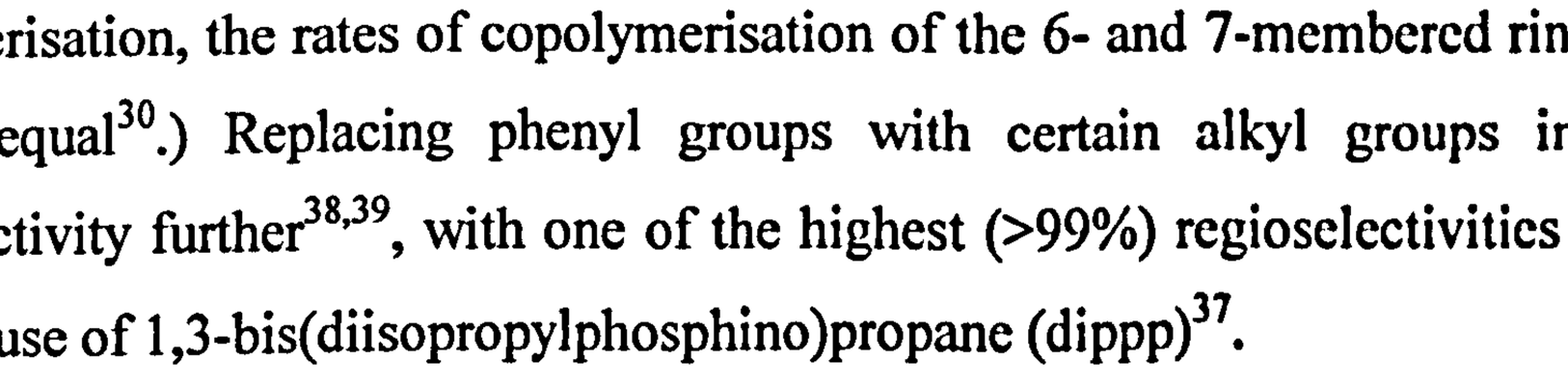
Figure 1.6.2: Diagram of steric and dipolar influences in **(a)** 2,1-insertion and **(b)** 1,2-insertion. In **(a)**, insertion is promoted by a favourable interaction between dipoles but hindered by steric interactions between the methyl group and phenyl groups. In **(b)**, the reaction is possibly hindered by steric interactions between the methyl group and copolymer chain.

positively-charged carbon on the carbonyl group (but whether this would make any significant difference is unclear). The other is that in 2,1-insertion there is steric interference between the methyl group on propene and the phenyl groups on the diphosphine, whilst in 1,2-insertion there is steric interference between the methyl group and the copolymer chain coming off the carbonyl group, which could influence regioselectivity either way.

Most evidence, however, suggests that olefin insertion always favours 1,2-insertion to some extent, ranging from 70% to near 100% depending on the diphosphine catalyst used.[5,30] Small oligomers analysed by GC-MS showed that 1,2-insertion was favoured, and the fact that regioselectivity increased when more bulky ligands were used also suggests this (otherwise, if it was 2,1-insertion regioselective, one would expect regioselectivity to *decrease*).[30] End-group analysis also shows that the initiation step nearly always forms *i*-propyl instead of *n*-propyl groups[25], also going in favour of 1,2-insertion, but it should be noted that this is insertion into a Pd-H bond rather than a Pd-acyl bond.

In general, regioselective copolymers are preferred as they have better-defined melting points[5,37]. Out of the basic $PPh_2(CH_2)_nPPh_2$ ligands, that with a seven-membered ring was found to be the most regioselective catalyst (88% to 1,2-insertion) that still gave an acceptable rate of copolymerisation. (Unlike CO/ethene copolymerisation, the rates of copolymerisation of the 6- and 7-membered rings were roughly equal[30].) Replacing phenyl groups with certain alkyl groups increased regioselectivity further[38,39], with one of the highest (>99%) regioselectivities coming from the use of 1,3-bis(diisopropylphosphino)propane (dippp)[37].

There is also interest in stereochemical control of the olefin insertion, in order to form iso-tactic or syndiotactic copolymers. Most catalysts have no stereochemical control, but there are certain catalysts that do give stereoregular copolymers[39,40,41] (but, unlike regioselectivity, it is very difficult to produce a completely stereoregular copolymer). Stereoregularity can also be measured using ^{13}C NMR from the sub-

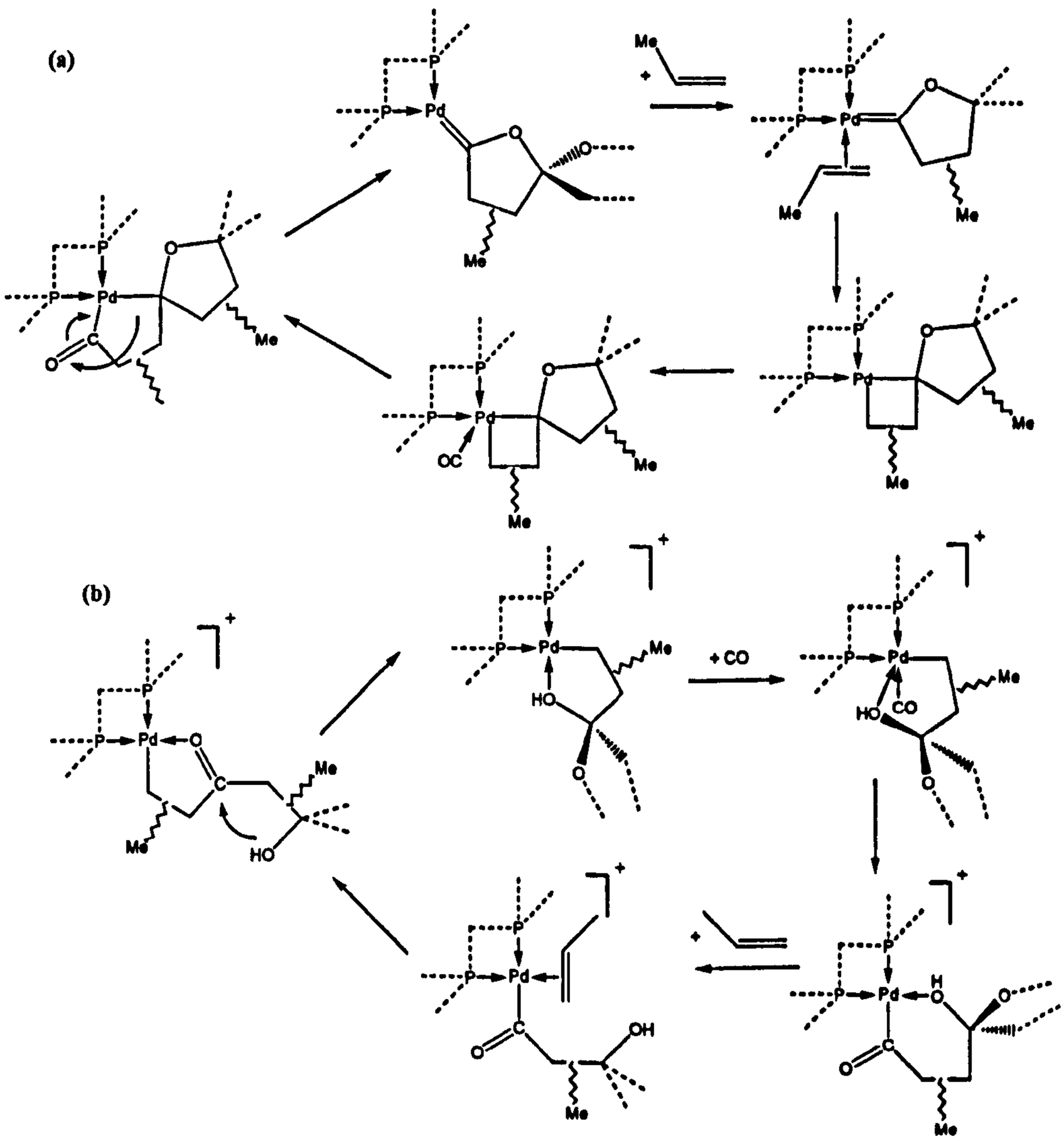


Scheme 1.6.3: Polyspiroketal in **(a)** non/partially-regioselective and **(b)** fully-regioselective structure.

peaks of the H-H, H-T and T-T groups provided that the NMR spectrometer has sufficient precision.

There is an alternative reaction to copolymerisation that occurs under certain conditions, which is the formation of polyspiroketals instead of polyketones, as shown in **scheme 1.6.3.**[42] What is surprising is that this only occurs with propene (or higher olefins) and never ethene. Polyspiroketals are easily distinguished from polyketones using ^{13}C NMR, but ^{13}C NMR also shows that the polyspiroketal can be irreversibly transformed to a polyketone through either heating or dissolving in hexafluoryl-isopropyl alcohol (HFIPA). This means it is likely that polyspiroketals are formed during the copolymerisation process. Two different mechanisms have been proposed, as shown in **scheme 1.6.4.**[5,42] However, others continue to argue that polyketones are converted to polyspiroketals after copolymerisation.[17]

The other olefin frequently used for copolymerisation is styrene, which is as popular as propene for copolymerisation with carbon monoxide, but owing to the



Scheme 1.6.4: Propagation cycles of spiroketal copolymerisation as proposed by **(a)** Consiglio *et. al* (ref. 42); and **(b)** Drent and Budzelaar (ref. 5).

impracticality of simulating reactions where a large phenyl group is involved in the reaction, the discussion here shall be brief. Unlike ethene and propene, diphosphine ligands are not ideal for styrene / CO copolymerisation, producing, at the best, low-weight oligomers. Diimine ligands are far more effective at copolymerisation. Like propene copolymerisation, termination by β-hydride abstraction is commonly observed.[43]

There is thought to be one significant difference in the mechanism of the propagation cycle compared to ethene and propene. Styrene insertion is 100% regioselective, but it is not regioselective to 1,2-insertion, as one might have expected from considering steric hindrance. Styrene insertion is always 2,1-insertion, and attention to choice of ligands is therefore focused on what gives the most stereoselective copolymer. The most likely explanation is that in 2,1-insertion, the structure is stabilised through resonance effects, which are not possible in the transition state or product of 1,2-insertion.[5,44]

Higher 1-olefins than propene can also be used for copolymerisation, and 1-hexene or longer olefins are sometimes used to change the properties of the copolymer. In particular, whilst in copolymers using ethene or propene the polar carbonyl groups dominate the copolymer's properties, when high 1-olefins are used, the apolar side arms dominate the properties. However, the molecular weights of these copolymers are usually much lower.[45]

Norbornene is also frequently used for copolymerisation. It can form copolymers, spiroketal structures, or undergo a number of other reactions. Although copolymerisation by norbornene and other strained olefins is not very efficient, it is possible to isolate certain intermediates to give indications of structures present during copolymerisation.[2,17]

Finally, it is possible to mix olefins present in the same copolymer, in particular ethane and propene.[46] CARILON uses ethene with a small amount of propene which reduces the melting point of the copolymer and makes it easier to blow-mold.[1] It is also possible, by controlling the supply of olefins, to form a copolymer with a block of $-(CH_2CH_2CO)-$ units followed by a block of $-(CH_2CH(C_nH_{2n+1})CO)-$ units, in order to form a copolymer with polar and non-polar ends.[4,45]

1.7 Conclusions

Copolymerisation of olefins and carbon monoxide with palladium-diphosphine catalysts is not only a promising reaction of commercial value but also a challenge for the computational chemist to account for the many aspects of the reaction. There are four distinct steps of olefin addition (to an equatorial site of palladium), olefin insertion, carbon monoxide addition and carbon monoxide insertion. The entire process can easily be accomplished at temperatures as low as 50°C, so an accurate computational system should be able to identify a low-energy pathway throughout the entire process.

The initiation and termination steps have a few more unanswered questions, as there are two possible mechanisms each of initiation and termination that could account for the experimentally observed end-groups, and it has never been certain which of the processes take place, only that in both cases, the 50:50 ratio of end-groups suggest it is either one process or the other that solely takes place. The complete lack of double-insertion is something else to account for, along with explanations for why certain ligands other than diphosphines allow a trace of double olefin insertion.

There are many other characteristics of the copolymerisation process that provide scope for further investigation, such as the switch to monomer insertion when two monodentate ligands or certain bidentate ligands are used, the poorer performance when chelate rings other than the 6-membered ring are present in the catalyst, and the regioregularity that is introduced when higher 1-olefins are used instead of ethene. Altogether, there are many traits to this reaction where computational chemistry has the opportunity to offer explanations.

2: Ab-initio optimisation of geometries

2.1 Introduction

The structure of any system, and the thermodynamic properties of reactions, can, in principle, be determined by solving Schrödinger's equation, or an approximation, for the entire system. The principles behind ab-initio calculations have been known since the 1970s. However, it has only been within the last decade that computers have become powerful enough to obtain useful information on any sizeable system. One of the most recent comprehensive reviews of the techniques used in ab-initio chemistry for transition-metal systems was given by Tom Ziegler[47]. The subject has also been reviewed by Niu and Hall (but with a much larger emphasis on examples of reaction systems studied by ab-initio chemistry)[48], and, more specifically, applications to palladium and platinum chemistry have been reviewed by Dedieu[49].

In computational chemistry, (and often in experimental chemistry too), it is common practice for complex multi-step reactions to be treated as a series of elementary steps of the form A + B → C + D, as shown in **figure 2.1**. In the case of most of the reactions studied in this project, they were unimolecular and the form simplified to A → C. The key points on the energy profile are: the structure of the reactant(s), product(s), and transition state; the energy barrier between the reactant and transition state (and the product and transition state if the possibility of a reverse reaction is being considered); the energy difference between the reactant and product; and sometimes, the structures of points on the lowest-energy path between the reactant, transition state and product. Occasionally, a stage originally thought to be a

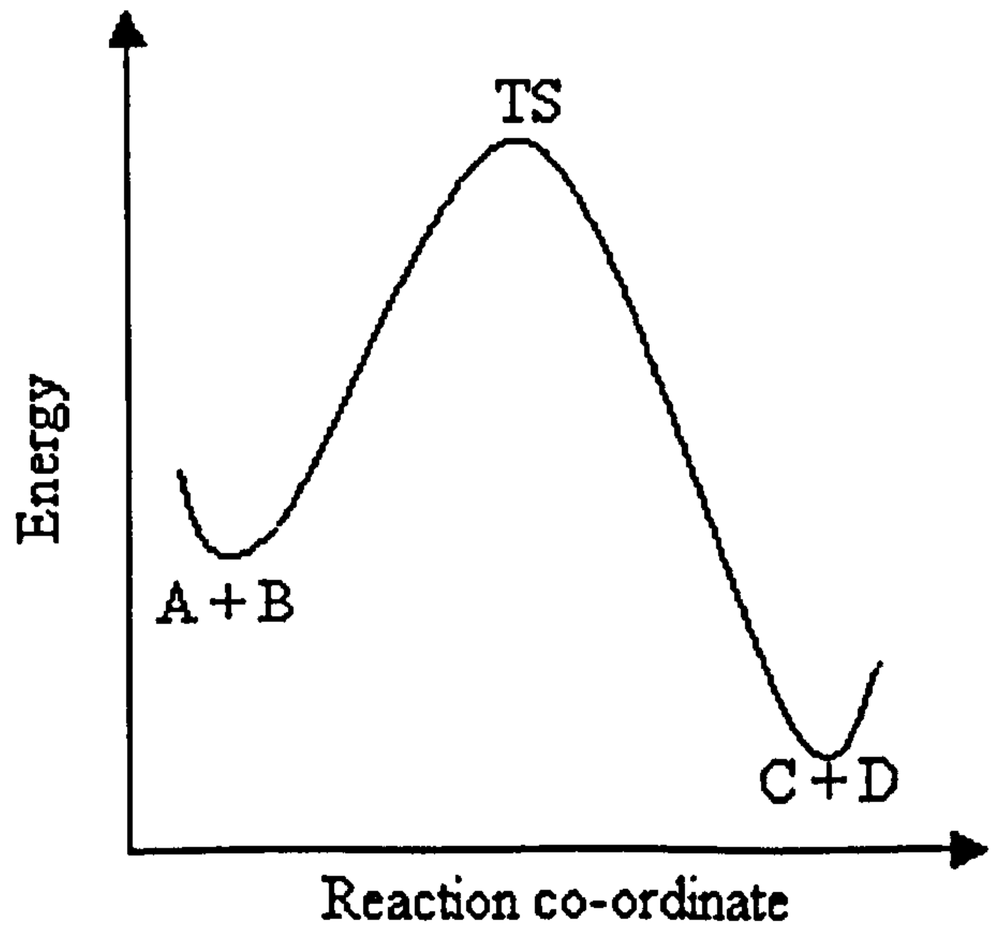


Figure 2.1: Universal shape of reaction profile for a single step A + B → C + D (TS = transition state)

single step can turn out to be two (or more) steps with an intermediate (or intermediates) between the reactant and product at a local minimum (or minima).

This chapter begins by discussing the two distinguishable processes that the optimisation of any stationary points can be broken down into: the first and fundamental process is the calculation of the energy of any given structure; and the other process is the determination of the geometry of the stationary point in question once the energies and forces of any structures are known. Next, special difficulties that are faced when dealing with transition metal complexes are discussed, along with ways to overcome these problems. Once these stationary points have been found, further tests can then be done to ascertain that they are indeed the stationary points one was looking for, and gain more information about the reaction mechanism. Finally, this chapter considers some of the alternative methods of evaluating reaction mechanisms, in particular for larger systems.

2.2 Single-point energy calculations

In order to optimise the structure of any molecule, no matter how big or small, one needs to be able to evaluate the energy of a structure, the force acting on every atom (or the first derivatives of the energy) and, to a lesser extent, the force constants on every atom (or the first derivatives of the forces, or the second derivative of the energy). All of these can be obtained from calculating the electronic structure of a complex, although, in complexes as large as transition metal complexes, the shape of the electronic structure itself is of limited interest.

This project applies the techniques described here to transition metal complexes and does not attempt to redevelop any methods itself. Therefore, this chapter does not attempt to outline every single step involved in applying quantum mechanics to optimisation of transition metals, which would involve rewriting page after page of lengthly derivations. Instead, this chapter aims to qualitatively describe the process and draw attention to any aspects of practical consequence in this project.

The first rule of all computational chemistry is that any electronic structure calculation is a series of approximations, and one must always pay caution to how much error the approximations cause. The exact solution of the electronic structure is governed by the Schrödinger equation:[47,50]

$$\hat{H}_T\Theta = E_T\Theta$$

where H_T is the Hamiltonian Operator of the entire system, E_T is the *total* energy of the system, and Θ is the wavefunction that depends on all of the electronic and nuclear coordinates. However, there is only one system where the Schrödinger equation can be solved mathematically, and that is the hydrogen atom (or any other hypothetical ion with any nucleus and one electron) – any other system cannot be solved because a three-body system has been proven impossible to solve.

Nevertheless, the results are very useful as they describe the shapes and energies of not only the ground-state 1*s* orbital that the ground-state electron occupies, but also the orbitals in all of the other shells that the electron could occupy.

The first approximation applied to practically every electronic structure calculation is the *Born-Oppenheimer approximation*, which assumes that the position of every nucleus in a system is fixed relative to each other, and only the electron(s) are free to move.[47,50] As the mass of any nucleus is always thousands of times greater than that of the electron, one would not expect the nucleus to move much anyway, and this approximation has been found to be very reliable for ground-state molecules. It is not always as reliable for molecules in excited states, but it is thought there are no stages in the CO/olefin copolymerisation process where it is necessary to pass through an excited state. (There are, in fact, a number of other problems presented by excited states, such as the difficulty of Density Functional Theory calculations and identifying the reaction mechanism between a single and triplet state.)

Even so, there is only one additional structure that the Born-Oppenheimer approximation allows to be solved, which is the H_2^+ ion – all other species involve three bodies making the Schrödinger equation impossible to solve again. However, the orbitals and their energies present in the H_2^+ ion are again useful, because they show the shapes of the σ- and π-bonding and antibonding orbitals that are found between any two atoms.[50]

Moving on to finding approximate solutions for systems with more than one electron, atoms shall be considered first. At this level of complexity, the first significant approximation must be made, by using the **Self-Consistent Field (SCF) method.** In this method, one begins with an estimate of the shapes of the orbitals surrounding an atom (this could be the orbitals of a hydrogenic atom of the relevant

nucleus, or the orbitals of a similar atom whose electronic structure has already been calculated). Then, going through each electron in turn, one solves the Schrödinger equation for that electron whilst assuming that *all other electrons have their charge distributed throughout the orbital to which they have been assigned.* Once all of the electrons have had an orbital calculated for them, a new cycle is started going through all of the electrons and considering their interactions with the revised orbitals of the other elections, and this process is continued until the changes in the shapes of the wavefunctions are negligible.[50]

However, in most cases one needs to determine the electronic structure of a molecule. In theory, a similar approach could be used by deriving the orbitals of the H_2^+ ion to determine the shapes and energies of the σ- and π-orbitals in any diatomic molecule, but this would be useless for any molecules with more than two atoms. Instead, the approach used in practically every case is to construct the σ- and π-bonding and antibonding molecular orbitals, along with any other possible kind of orbital over any number of atoms, by overlapping the appropriate atomic orbitals from different atoms in phase or antiphase as needed.[50]

It is normal for the entire electronic structure of a complex to be calculated this way, but there is one alternative (and semi-qualitative) approach of building the molecular orbitals manually by overlapping the relevant atomic and molecular orbitals in bonding and anti-bonding combinations. Hypothetically, it is possible to account qualitatively for the entire electronic structure of a complex this way, but the method is certainly not competitive with ab-initio optimisation in terms of accuracy and time. However, the molecular orbital theory can be used in conjunction with ab-initio optimisation to explain some of the more unusual structures found. This is covered in Chapter 5.

The simplest method of calculating the electronic structure of a molecule is the **Hartree-Fock method**. This is similar to the SCF method for a single atom, except that in a single cycle one goes through every electron in the molecule instead of just a single atom. (However, the solving the Schrödinger equation in this situation is a lot more difficult than solving the equations for an atom because molecules lack the spherical symmetry of atoms.) A slight problem with this method is that it sometimes fails to lead to the lowest-energy wavefunctions. This normally happens when one attempts to find the electronic structure of a complex in a geometry that is nowhere

near a stable molecular structure (usually because of a poor guess of a starting structure in a geometry optimisation). However, there is also occasionally the odd reasonable molecular structure whose electronic structure fails to converge because the Hartree-Fock method causes the electronic structure to oscillate through the same few conformations.[47,50]

It is at this point that **basis sets** also start to become a factor that limits the accuracy of the electronic structure calculations (and, ultimately, goes on to limit the accuracy of the energy differences and optimised structures). In any sort of SCF calculation, it is impossible to go through every possible shape of the wavefunction of a single electron, so the shape of the wavefunction must be limited to a combination of pre-conceived orbitals. This is not much of a problem in individual atoms, when one can have a very good idea of the shape of the orbitals anyway, but this can be a problem in molecules, where the shapes of orbitals can be very difficult to guess and – in the case of molecules larger than a few atoms – there are usually limited resources to allow for every possible orbital shape.

Optimisations requiring any significant degree of accuracy normally use basis sets with *Gaussian-type orbitals*, where all orbitals are a linear combination of Gaussian distributions in *s*-, *p*- *d*- or *f*- shape, known as *primitive Gaussians*. (There are also *Slater-type* orbitals, although these are less popular because they are difficult to integrate. Indeed, in Gaussian, the closest available basis set to Slater-type orbitals is the STO-3G basis set, which approximates a Slater-type orbital from three Gaussian-type functions.) Some primitive Gaussians are grouped together in a fixed linear combination to form a fixed *basis function*, and this is usually the way that core orbitals are represented, as the shape of core orbitals of particular atoms are not subject to much change from interactions with other atom. A basis function consisting of two or more primitive Gaussians obviously takes more time to process than a basis function with only one Gaussian.[50]

However, the quantity normally used to estimate the amount of computer run-time needed is the number of different basis functions. Different basis functions are added to each other in a linear fashion, but in a variable linear combination to allow the optimum energy of the wavefunction. Valence electrons are usually represented by two basis functions, to allow an optimum shape to be found, but some larger basis sets add further basis functions. As there are more variables to adjust in this situation,

a higher number of basis functions significantly increases the run-time needed to converge the energy calculations. (It is partly for this reason that when a calculation is performed on a complex with a very large basis set, it is often advisable to proceed in stages, firstly using a smaller basis set first to both optimise the structure and, then using the optimised wavefunction as the initial guess for the higher basis set.)[50,51]

The effect of combining primitive Gaussian and different basis functions is illustrated in **figure 2.1**.

(The *s*-, *p*- *d*- and *f*- shaped Gaussians all differ from each other in terms of

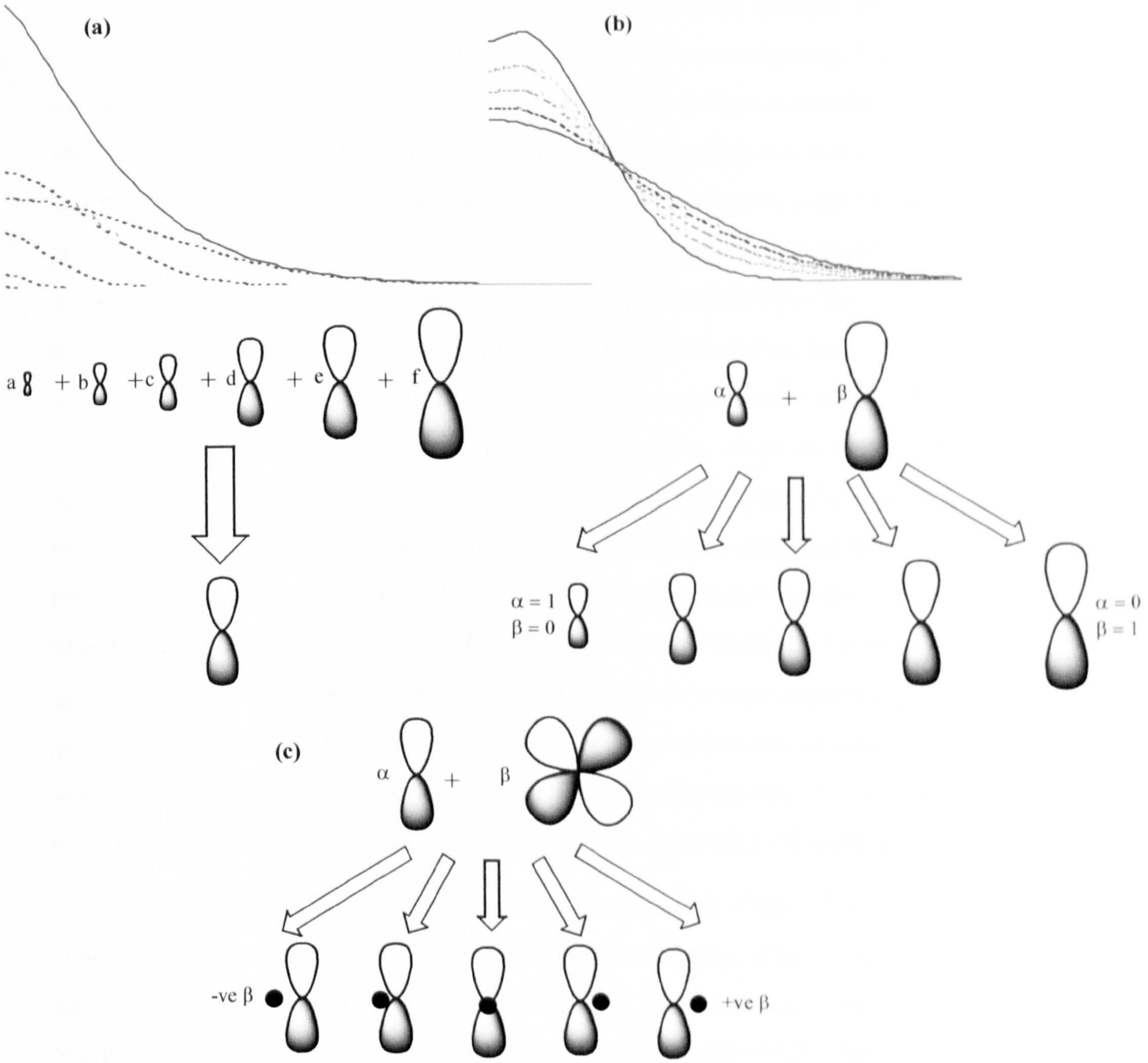


Figure 2.1: Illustrative examples of the effects of **(a)** combining primitive Gaussians to form a single basis function; **(b)** wavefunctions that can be obtained from combining two basis functions in a basis set (same principle applies to adding a diffuse function, except second wavefunction in diffuse function should be *much* more diffuse); and **(c)** effect of adding a polarisation function to a basis function (dot indicates positions of nucleus). (All diagrams not to scale.)

their angular distribution functions in the same way that the orbitals are shaped. This means that to include a *p*-orbital in the basis set, three separate basis functions are needed to allow for the *p*-orbitals in all three dimensions. The *d*-basis functions are sometimes arranged into six identical orbitals instead of the five normally used in molecular orbital theory because it is often easier to perform calculations on six identical orbitals than five orbitals where one is a different shape to the others. In this case, the extra basis function, in effect, amounts to an extra *s*-orbital-shaped wavefunction. A similar arrangement exists that increases the seven *f*-shaped wavefunctions to ten.[52])

There are two other kinds of basis functions that can be added to improve results. *Polarisation functions* allow a wavefunction to be centred away from the nucleus, by adding a Gaussian wavefunction one spin-state higher than the highest spin-state currently in the basis set. (e.g. In the Li-Ne row of atoms, one would need to add a set of *d*-shaped basis functions as polarisation function in order to allow polarisation. The *p*-shaped Gaussians already present would serve to polarise the *s*-shaped basis function.) Polarisation functions are often donated by adding a * symbol to the basis function (or ** if polarisation functions are included on hydrogen atoms too), such as the 6-31G* basis set. Such basis sets have proven to be popular. Less commonly used, but also in existence, are *diffuse functions,* which are simply a set of one very diffuse function per each shape used (so in the Li-Ne row of atoms, one would need one *s*-shaped diffuse function and a set of three *p*-shaped diffuse functions). They increase the range that electrons may interact with other electrons beyond the limits of the most diffuse function in a standard basis set. However, some people are sceptical about using diffuse functions without a large supporting basis set, and suggest that diffuse functions with the wrong basis set can actually make results worse. Diffuse functions typically add a + or ++ symbol to the basis set, such as 6-31G+. The effect of these functions is illustrated in **figure 2.1 (b)** and **(c)**.[50,51]

As a rule of the thumb, one needs a basis set the size of the 6-31G basis set or thereabouts to produce a solution that has a reasonable degree of quantitative accuracy. (6-31G means that, for atoms in the Li-Ne row, there will be one basis function of six primitive Gaussians for the 1*s* electrons, and two basis functions of three primitive Gaussians and one primitive Gaussians respectively are used to represent the 2*s* and 2*p* electrons.) In the case of atoms bonded to a transition metal as

a ligand, it is increasingly expected that there should be a polarisation function in the basis set too (the basis set of the transition metal atom itself will be discussed in section 2.5). (Smaller basis sets such as the 3-21G basis set can be used for qualitative results for minima, but as this project shows, in the transition state of a transition metal complex the result was not even qualitatively accurate.) Unfortunately, this is also near the limits of feasibility for transition metal complexes, and should a basis set of this size not be accurate enough for a geometry optimisation, a larger basis set may necessitate a very long wait. (However, the accuracy of an energy calculation can often be improved by re-calculating the single-point energy of the optimised structure with a larger basis set.)[48]

The parameters of basis sets are a study in their own right, as poorly chosen basis functions can lead to inaccurate results. However, no matter how many basis functions are included in a basis set and how well-chosen the basis functions are, the calculated electronic structure is not the exact answer because the Hartree-Fock method assumes that the interaction of electrons with each other is averaged out over time over the whole wavefunction.[48] This, of course, is not the case, and at any instantaneous moment electrons will be in different positions interacting with each other in different ways. The most common method of addressing the problem within the Hartree-Fock method is to use Møller-Plesset methods such as MP2, which adds to the Hartree-Fock method a perturbation theory that addresses the configuration interactions between different electronic states.[50] Unfortunately, this method is much more computationally demanding than Hartree-Fock, especially for larger systems, and is not normally an option for systems as large as transition metal complexes. (But again, it is feasible to improve the accuracy of an energy calculation by re-calculating the single-point energy of the optimised structure at a higher level as well as with a larger basis set.[48])

For transition metal complexes, the most efficient way of obtaining accurate energies is to use **Density Functional Theory (DFT)** instead of Hartree-Fock.[47,48,49] Unlike the Møller-Plesset methods that are effectively Hartree-Fock with additional procedures to take into account configuration interaction between different electronic states, DFT is fundamentally different because it considers the electron density instead of wavefunctions when calculating electronic structure. Most codes are based on the *Kohn-Sham* approach,[53] where the electrons are considered to behave as

uncharged particles with no Coulombic repulsion when kinetic energy is calculated. Unlike Hartree-Fock, the effect of exchange (that no two electrons may have the same quantum state) must be calculated as a separate term. However, this is compensated by the ability of DFT to take into account the effects of configuration interactions far more efficiently than Hartree-Fock-derived methods such as Møller-Plesset.

Another disadvantage of DFT is that it generally cannot be used to calculate the electron structure of excited states other than constraining the system to, say, a triplet instead of a singlet state,[47] although a few recent methods have been designed to overcome this feature. This problem is not important in this project as the entire reaction process is thought to take place in the ground state.

The ground-state energy of a complex has a basic equation in Kohn-Shan-modelled DFT of the form:

E = [kinetic energy of non-interacting electrons] +[electron-nucleus attraction energy]+ [coulombic electron-electron repulsion energy]+ [exchange-correlation energy]

The first three terms are very easy to calculate, but the last term, which represents all of the non-classical interactions between the electrons including the correlation between different states and the exchange effects, is difficult to evaluate.[47,50] The many different kinds of Density Functional methods available vary largely on their method of estimating this final term. One of the most popular simple schemes is the **Local Density Approximation (LDA)**, which obtains the exchange-correlation functional from the energy per electron in a homogenous electron gas, although this method tends to be more popular with physicists than chemists as this method is best suited to the solid state.[50]

However, one very popular method with chemists that usually gives accurate results in a relatively short amount of time is the **Becke's Three-parameter / Lee-Yang-Parr (B3-LYP)** method.[47,54] This is one of a range of hybrid methods that calculates the exchange-correlation energy from a fractional combination of different methods, and in the case of B3-LYP, one of the terms used to calculate the exchange energy is the Hartree-Fock exchange energy. This method is able to improve the accuracy of the calculations to a level comparable to Hartree-Fock-based methods of directly calculating the configuration interactions, but requiring far less computational time. This is especially important in transition metal complexes as the amount of run-

time needed for Møller-Plesset methods scales up with an increase in electrons much faster than Hartree-Fock or B3LYP scales up.

Although the method of calculating the energy of a given electronic structure is fundamentally different to Hartree-Fock, the process of finding the lowest-energy electronic structure is very similar. The orbitals used in DFT are *Kohn-Sham* orbitals, which are based on electron density rather than a wavefunction, but the basis sets used in Hartree-Fock methods can be derived to form an equivalent set of available Kohn-Sham orbitals. Also, as with Hartree-Fock, in DFT one must begin with a set of guessed Kohn-Sham orbitals, and use these orbitals to calculate an improved set of orbitals until the energy has converged.[47,50]

Not all computational chemists endorse B3-LYP, and in particular there are reservations about the use of parameters in B3-LYP to correlate results with data sets of energies of certain structures obtained from higher-accuracy methods, and examples have been cited of cases where B3-LYP-generated results have a significant error.[55] Nevertheless, B3-LYP remains a popular and reliable method in most cases, and has been shown to produce much better estimates in bond-lengths and energies than the Hartree-Fock method (along with the Møller-Plesset methods and higher methods). It is thought that the inaccuracy of Hartree-Fock is greater for first-row transition metals[56] than second-row transition metals[57] because the top row has 4*s* and 3*d* orbitals that are very close in energy,[47,48] but there was still a case for believing that in second-row transition metal complexes such as the palladium complexes examined in this project, the extra time spent using B3-LYP instead of Hartree-Fock would be worth the extra accuracy achieved. Nevertheless, the results should be treated with caution, (as indeed the results of any computational calculation at any level should be,) and any results obtained should be compared to experimental results or other computational results where such comparable results are available.

Whatever method of calculation is used, in addition to the energy of this point, other characteristics of the structure intrinsic to the process are also calculated. These include charge distribution over the complex, electron distribution at all energy levels, the dipole, quadrupole and octopole of the structure, and the moments of inertia (and from this rotational energy levels), although normally only energy is normally of interest in studying reaction mechanisms of large systems. Certain characteristics,

such as NMR spectra or vibrational frequencies, require additional calculations and are normally only performed on points known to be stationary points.[51]

In theory, a method that used both a large enough basis set and an intensive enough method of calculating electron structure would give a result that would be almost identical to the result one would obtain from solving the exact Schrödinger Equation for that structure, but in practice, a method such as B3-LYP and a basis set of the size of 6-31G** are the best compromise one can expect for systems as large as transition metal complexes. However, the electronic structure of any molecular structure, and the calculated energy, is nearly meaningless unless it is the optimised structure of the complex, which, in many cases, is not known. Determining the optimised structure of a complex from electronic structure calculations is the other half of the optimisation process, which will be discussed next.

2.3 Optimisation of molecular structure from electronic structure

In order to optimise a minimum from any estimated starting structure, one needs to move the structure to a lower energy conformation until the minimum-energy structure has been released. As it happens, it is a simple matter to calculate the first derivatives of the energy (i.e. the force on each atom) once the electronic structure of the system is known, which determines the direction the atoms need to move in. Once the atoms have been moved in the direction of the forces acting on them, a fresh electronic structure calculation can be made on the new structure to determine the revised forces, and these steps can be continued until a minimum energy structure is found.

The difficultly in optimising a minimum arises from the uncertainty in how far the atoms should be moved in the direction of the forces acting on them. Close to the optimised structure, the steps need to be very small to avoid overstepping the minimum, but away from the structure, larger steps must be used otherwise there would be a huge number of steps requiring electronic structure calculations and the total run-time needed would be many times longer than necessary.

In theory, one could attempt to estimate how far away a structure is from the minimum by quantifying the magnitude of the forces acting on the atoms. However,

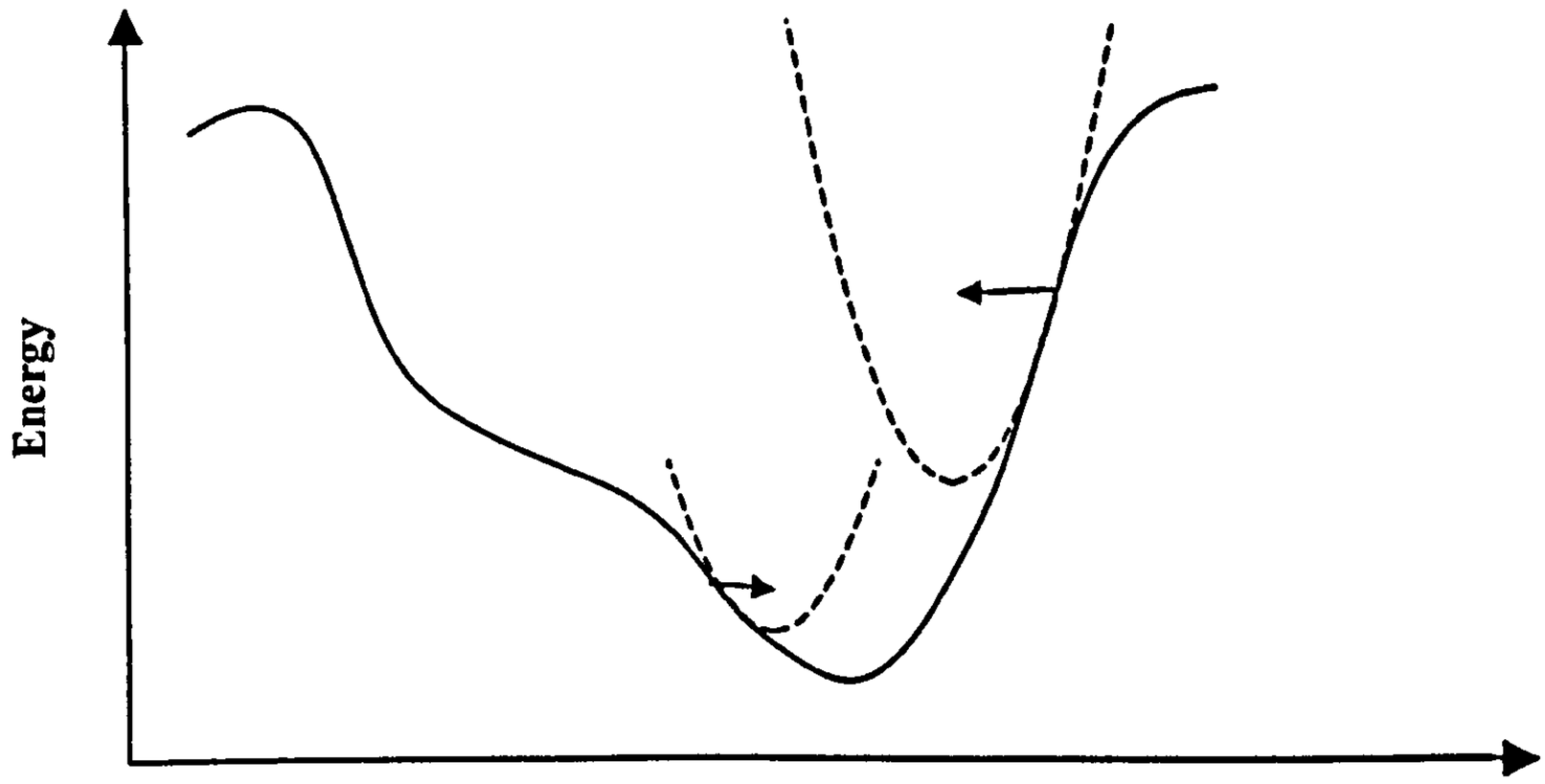


Figure 2.3: Schematic diagram of effect of DIIS optimisation on a point near to the minimum (left) and far from the minimum (right) from consideration of second derivatives. (Note that in a real system, the energy surface would not be a one-dimensional line illustrated here but a surface with 3N-6 dimensions, where N is the number of atoms in the system: one dimension (distance) for the second atom, two dimensions (distance + bond angle) for the third, and three dimensions (distance, bond angle and dihedral angle) for the fourth atom onwards.)

this would only be reliable if the magnitude of the forces as a function of the distance the atoms are away from their minimum were consistent for different complexes, and this is not the case. In some complexes, the force increases very sharply away from the minimum, whilst other complexes have minima away from the "flat" regions where the forces acting on the atoms around the minima are low.

Instead, the method most commonly used is to estimate the location of the minimum from a given point by considering the second derivatives (force constants) acting on the atoms in a particular step. If both the forces and force constants acting on the atoms are known for a step, one can imagine the energy surface around this point to be parabolic. From this model, a location of the energy minimum can be estimated and provide an indication as to whether the next energy step should be a large step or small step in the direction of the force, as illustrated in **figure 2.3**. The problem with this approach is that, unlike first derivatives, second derivates, although they can be solved analytically, take far longer to calculate than either electronic structure or first derivatives.[58]

The normal solution is to use a method like the DIIS method, which builds up a map of second derivatives from the forces acting on previously calculated structures. Optimisation usually commences with no knowledge of second derivatives, and as more and more points have their forces and energies calculated, increasingly accurate estimates of the second derivatives can be made. This method is normally very

reliable and dramatically reduces the number of steps one would need to optimise a structure, the only slight pitfall being that should a starting structure be estimated that is very close to the optimised structure, the minimum may be overshot a few times before enough information is obtained about the second derivatives for the cut-off requirements to be met.

In some cases this method is assisted by analytically calculating the force constants for the first step only, in order to start with some reliable information from which the force constants at other points can be derived. Analytically calculating the force constants in every single step is possible, but it is very computationally intensive and is normally only used as a last resort.[51,52]

Typically, when this method is used, the structure will be deemed to have reached a minimum when forces (both root-mean-squared and maximum forces) fall below a cut-off point deemed to be accepted as close enough to zero, *and* the displacement of the structure between one step and the next as required by consideration of the force constants (again both root-mean-squared and maximum forces) also fall below cut-off points. Forces below cut-off points are not normally used on their own, because forces can be very near zero but exist in an unusually flat region of the complex (i.e. a large region where the force is near-zero), where there can be a considerable distance between the point where the forces have been calculated to be below the zero cut-off point and the point where the forces truly are zero. (*Gaussian* does, however, deem a structure to have converged anyway if forces have fallen below one hundredth of their cut-off values, to allow structures with a minimum with a very flat surface to converge. This happened frequently during the project, usually, but not always, when a structure was being optimised with an incoming ligand at a distance.)[51]

The only major weakness of obtaining a minimum by moving a structure in the direction of the forces acting on its atoms is that this does not indicate whether the minimum reached was the minimum that one intended to reach. The most common scenario is when one was intending to optimise the global energy minimum of a complex (the lowest energy conformation of all), but instead a local minimum (where the energy of the complex is increased if any atom is displaced, but the energy remains above that of the global minimum) is optimised. Unfortunately, there is no analytical method capable of determining whether or not the minimum optimised is a

global minimum, let alone determine the structure at a global minimum from any starting point. Quite often, one must examine an optimised structure and use common sense to decide whether or not a lower-energy minimum is likely to exist.[51]

If in doubt, one recognised method of maximising the chance of finding the global minimum is to search though different conformations of the complex (normally specifying dihedral angles of various groups to vary) with a relaxed potential energy scan (normally at a lower level than the *ab-initio* calculations normally employed), noting which points go to the lowest energy. These lowest-energy points can then be fully optimised, and the structure that is optimised at the lowest energy can be declared with reasonable confidence to be the global minimum.[58]

The difference in energies of two structures on either side of a single step (provided that they used the same basis set and same method for the same set of atoms) gives the enthalpy of the reaction, which serves as an indication on whether a step is more likely to proceed in a forward or reverse direction. (Strictly speaking, the energy calculation of both stationary points should include adjustments for zero-point and thermal energy – see next section.) However, this does not give many clues about the energy barrier between the two states, and for any indication more accurate than a guess based on the likely chemical properties of such a reaction, one must optimise the transition state between the two states.

Transition states are harder to optimise, and computational experiments that are not directly concerned with a step-by-step reaction mechanism often leave out transition state optimisations altogether. In terms of energy surfaces, a transition state is a first-order saddle-point (i.e. the energy is at a minimum in every dimension but one) and this makes the search much harder to do. Moving the atoms of a system in the direction of the forces acting on them is a foolproof way of finding a minimum, but this obviously does not work for a transition state search as not all points surrounding the stationary point have a higher energy.

One of the earlier methods used to locate a transition state was the **Linear Synchronous Transit** method. This method worked by plotting an estimated path between the reactant and product structures (the LST2 method guessing a path from the reactant and product structures alone, and the LST3 method plotting the path through a specified estimated transition state), and then searching along this path for

the highest-energy point. However, the weakness of this method is that it is only as accurate as the estimated reaction path, and unless the path happens to pass through the exact transition state, the point obtained from an LST method is not the true transition state at all, but rather the maximum point from any path, right or wrong, between the reactant and product.[52] It has certainly been observed in this project that the highest energy point found in the first cycle of the Opt=Path methods (which is, in effect, the LST method of finding the energies along a predetermined pathway) is *not* a reliable indicator of where the transition state is, especially if (as was sometimes thought to be the case during this project when the Opt=Path method was used) the estimated reaction path was later found to be wrong. The best information the LST method can really give is an over-estimate of the energy barrier between the reactant and product. It has also been used as a means of estimating a transition state as a starting structure for more reliable methods.

It is hypothetically possible to locate a transition state by calculating the energy of the points surrounding the transition state and literally finding the transition state once the energy map is formed. However this would require a *very* good guess of where the transition state is likely to be and which variables (e.g. bond lengths, bond angles and dihedral angles) vary as the structure passes through the transition state in order to choose which geometric parameters to vary for the search. Adding an extra dimension to the energy map and searching through only five points will quintuple the run-time needed, and a poor guess of the location of the transition state will produce an energy map that misses the transition state completely, wasting a lot of run-time. Therefore, this method is not really feasible and it is really only useful to obtain supplementary information about a reaction mechanism once the transition state has been located and there is a good idea of the reaction mechanism already.[48,59]

Therefore, it is normal for transition states to be located by optimising the stationary point itself. Although algorithms exist that attempt to locate it from a single starting point,[52] the most popular methods use the reactant and product structures (meaning the minima each side of the transition state for the step in question) in the search for the transition state. One such method is the **Quadratic Synchronous Transit** method (QST).[51,52,60] Starting from either an estimated structure part-way between the reactant and product (QST2) or an estimated transition state chosen manually (QST3), the energies and forces on the structure are calculated as normal.

However, instead of moving the atoms in the direction of the forces acting on them, the direction in which the atoms are moved is determined by a complicated arrangement of eigenvectors calculated from the geometry of the current structure under optimisation, the forces and force constants (if available) acting on this structure, and the reactant and product structures. The steps used are a mixture of climbing steps, and steps calculated to be in the likely direction of the transition state. As with the optimisation of minima, the QST method does not normally calculate force constants, relying instead on approximate force constants estimated from the forces of the points optimised so far.

The greatest limitation of the QST methods is that they only work if the estimated starting structure of the transition state is a good estimate, otherwise, the QST method often ends up mistaking a minimum for a transition state and endlessly searching for a saddle-point in that region. For this reason, in large systems the QST2 method usually does not work as there are too many variables for the estimated starting structure to be sufficiently close. Even the QST3 method is fallible if it is difficult to guess manually where the transition state is likely to exist. For this reason, it is often necessary to derive the estimated transition state from a transition state structure previously optimised, or use an LST-related method to get a good estimate of a transition state (by taking the highest point along an estimated reaction path), if a transition-state search is to succeed.[48,61] Even so, this method is not always successful, in particular in energy barriers where the activation energy is expected to be high.[59] There is no systematic method that guarantees the successful optimisation of a transition state, and it may sometimes be necessary to abandon the search if this proposed step is likely to be uncompetitive with an alternative mechanism.

The great advantage of the QST methods, however, is that if it successfully locates a transition state, it is a stationary point, as opposed to methods such as the LST methods that can, at best, only locate an estimated transition state somewhere near a stationary point.

The difference in energy between the transition state and the reactant is, of course, the activation energy, which is chiefly responsible for determining the rate of reaction in the forward the direction. (Again, one should consider the zero-point and thermal energy for the exact answer.) In the case of a step where the enthalpy of the reaction is not strongly negative, the energy barrier between the transition state and

product can also be equally as important to consider, as this determines the rate of a possible reverse reaction.

But whilst a little caution is recommended for stationary points optimised in a minimum search, a much greater amount of scepticism is needed when considering points optimised by a transition state search. The stationary point optimised often turns out to be not a first-order saddle point but a minimum, or second- or higher-order saddle point. Even if the stationary point is proven to be a first-order saddle point, it is not necessarily the transition state one was looking for – quite often it can turn out to be the wrong transition state and instead be the saddle point for, say, the rotation of a $-CH_3$ group between two minima, or the inversion of a ring between two conformations. It is at this point where the importance of frequency testing becomes important.

2.4 Frequency tests and reaction mechanisms

An important final stage normally performed with most optimisations is to perform a frequency test on an optimised structure. This involves calculating the force constants on the optimised structure, but it normally takes a relatively short amount of time compared to that usually required to optimise a structure. From the force constants, the vibrational frequencies are easily calculated. The only rule one must remember is that the algorithms used to calculate frequencies are only valid when the point is a stationary point. For this reason, frequency tests should only ever be performed on previously optimised structures, using the same method and basis set used for the optimisation.[51,52]

The vibrational frequencies themselves are not normally of much interest when considering reaction mechanisms (although there is scope for comparing these frequencies to the infra-red and Raman spectra of the real molecules). What is of the most interest is the number of modes of vibration calculated to have *imaginary* frequencies (often reported as negative frequencies). A true minimum should have no imaginary frequencies at all, although it is unusual for a saddle point to be accidentally optimised in a search for a minimum. A transition state, on the other hand, as a first-order saddle point, should have one imaginary frequency, and the direction of this vibration should be in the direction of the reaction one was expecting. It is at this stage that many second-order saddle points and transition states of the

wrong step mistakenly optimised by the QST methods are exposed.[51] The magnitude of the imaginary frequency is also of interest as this provides an indication of the potential energy surface surrounding the transition state.

The other important value calculated from a frequency test is the **Zero-point energy** (ZPE), which is the total energy of all of the ground-state vibrations over the minimum overall energy of the complex. This should ideally be added to the energies of the reactant, product and transition state to get more accurate calculations of the enthalpy and activation energy. (Some experiments omit vibrational calculations and neglect ZPE when it has been shown that similar structures are the intended structures and the difference the ZPE introduces is negligible). There is a systematic error observed for Zero-point energies (and vibrational frequencies) and correction factors have been quoted for many methods / basis set combinations (although for a system as large as B3-LYP/6-31G, the correction factor is only around 5%). For a very accurate energy calculation, one should consider the thermal energy, normally quoted as energy per unit temperature (to take into account that above 0K, not all of the vibrational modes of a molecule will be in the ground state). These latter two factors were not considered in this project as the margin of error from the basis set was expected to be higher than the adjustments from either of these two factors.[51]

Niu and Hall suggest that there are fewer basis sets and methods suitable for frequency calculations than geometry optimisations, and in particular suggests that the double-zeta polarised basis sets are too large for frequency calculations[48]. However, it was noticed during this project that the extra run-time needed to do a frequency calculation was substantially lower than the amount of run-time needed to optimise the structure in the first place. They also rule out worthwhile frequency calculations at levels of MP2 or higher, although this matter is not too important as these levels are generally not used for optimisations in transition metal complexes anyway, and performing a frequency test on a structure with a different basis set or method to the ones used to optimise it would not be valid.

In many projects, the structures of the reactant, product and transition state are taken as enough information to consider the reaction mechanism of the single step. Other projects also consider the direction of the imaginary frequency in the transition state. However, this does not necessarily give all of the information obtainable about the reaction mechanism, and it can potentially fail to give information such as aspects

of the reaction mechanism between the reactant and transition state or transition state and product, or whether any local minima exist along the reaction path, or even whether a path exists between the perceived reactant, transition state and product at all!

The **Intrinsic Reaction Co-ordinate** job is a method that is designed to determine the lowest-energy reaction path between the reactant, transition state and product. Starting from the transition state structure (and using both forces and force constants on the atoms, the latter normally taken from a preceding frequency calculation), successive points are optimised in both directions in the path of the imaginary frequency, such that the energy of each point optimised increases in every direction orthogonal to the direction of reaction.[48,51]

In theory, the reaction path continues until either the set limit of points have been optimised or a point is reached that is considered to be a supposed minimum. (As the set limit of the number of points was always increased up to the program maximum of 200 in this project, the former case never applied. There were also occasions when the IRC simply terminated due to convergence failure or other errors, or a region was reached where a point along the path could not be found at all.) However, in the experience of this project, what was declared by the IRC job to be a minimum was rarely an actual minimum, and when these final points were optimised, the structure usually underwent a fair amount of further rearrangement before a true minimum was optimised. Nevertheless, the step-by-step path travelled between the final point of the IRC job and the minimum usually gave a good indication of what the later parts of the reaction path away from the transition state would look like.

Should the final minimum reached on either side of the transition state *not* be the same structure as the reactant or product, this would normally be a sign that an additional local step existed between the transition state and reactant/product. In such cases, the transition state between the reactant/product and this local intermediate, and the reaction path either side of this local transition state, would need to be optimised in order to complete the reaction path. Alternatively, if this minimum is of a lower energy than the reactant/product, it could be the case that the original perceived reactant/product is not on the reaction pathway at all and a true lower-energy reactant/product has been found.

There are two other approaches that can be used for determining a reaction pathway. One is to perform a relaxed energy scan (i.e. where every point is optimised to its lower energy conformation except for the parameters being varied to form the energy map) to form a map of energy against the molecular parameters that vary during the reaction, and trace a lowest-energy path manually. The other method is the Opt-Path job, which is like a QST optimisation except that several points along a reaction path are optimised simultaneously, with the highest-energy point going to the transition state and the other points going to points along the reaction path. However, both of these methods are too computationally intensive to be practical normally for systems the size of transition metal complexes, although the latter method is useful for going through 10-20 cycles to find a suitable starting transition state in a QST3 optimisation.

The description of the steps needed to determine the reaction pathway of a single step is now complete, but there are two final notes of caution that one should consider, which apply irrespective of how accurate the basis set and DFT / Hartree-Fock method is. The first note is that the reaction path found, even a reaction path that is proven to connect up the reactant and product, is not necessarily the lowest energy reaction path, and there is always the possibility that a lower-energy transition state may exist and provide a faster pathway. Unfortunately, there is no systematic method that can prove that the transition state optimised is the lowest-energy transition state that exists, and one must normally use common sense to decide if a lower energy route could exist. The second note is that the reaction pathway found is a theoretical model of the *lowest energy* pathway. In a real molecule, the atoms will never travel along the lowest energy pathway, but instead, will travel in random directions in the reactant structure until, if the thermal energy is high enough to overcome the activation energy barrier, the atoms happen to travel in the general direction of the transition state, cross the energy barrier, and then travel in random directions around the product structure. This is especially important in steps where the energy barrier is low, as if the thermal energy of the system is in great excess to the energy barrier, there will be much scope for deviation from the minimum energy pathway.

2.5 Special considerations for large systems

So far, the methods discussed in this chapter have been applicable to systems of any size, save that discussion has been largely restricted to techniques that can be used in larger systems. However, for larger systems, a number of special considerations must be made.

The first and most obvious problem is the large number of electrons whose properties must be calculated in transition metal systems. The time needed to calculate the electronic structure depends on a factor of n^4 (n = number of electrons) for methods such as Hartree-Fock and B3-LYP. In larger systems when most electron-electron interactions are zero, it effectively reduces to n^2. Other methods can scale to higher factors, which is why methods such as MP2 are normally considered unfeasible for transition metal compounds, but even with Hartree-Fock and B3-LYP the number of electrons push most computers to the limit.[52] Then there is the additional problem that larger compounds usually have more degrees of freedom (such as freely rotating methyl or phenyl groups), which means that more optimisation steps are required to find a stationary point.

Therefore, the first step normally taken for any large system is to remove any unnecessary groups and replace them with hydrogen atoms. The only care that needs to be taken is with the decision over which groups are and are not necessary to include in an optimisation. The most obvious example, which is usually an open-and-shut case, is to reduce phenyl groups to hydrogen atoms, instantly taking 40 electrons out of the system per phenyl group replaced, and phenyl groups are rarely expected to influence the reaction mechanism. Aromatic rings within indispensable carbon chains can also sometimes be eliminated by replacing them with two double-bonded carbon

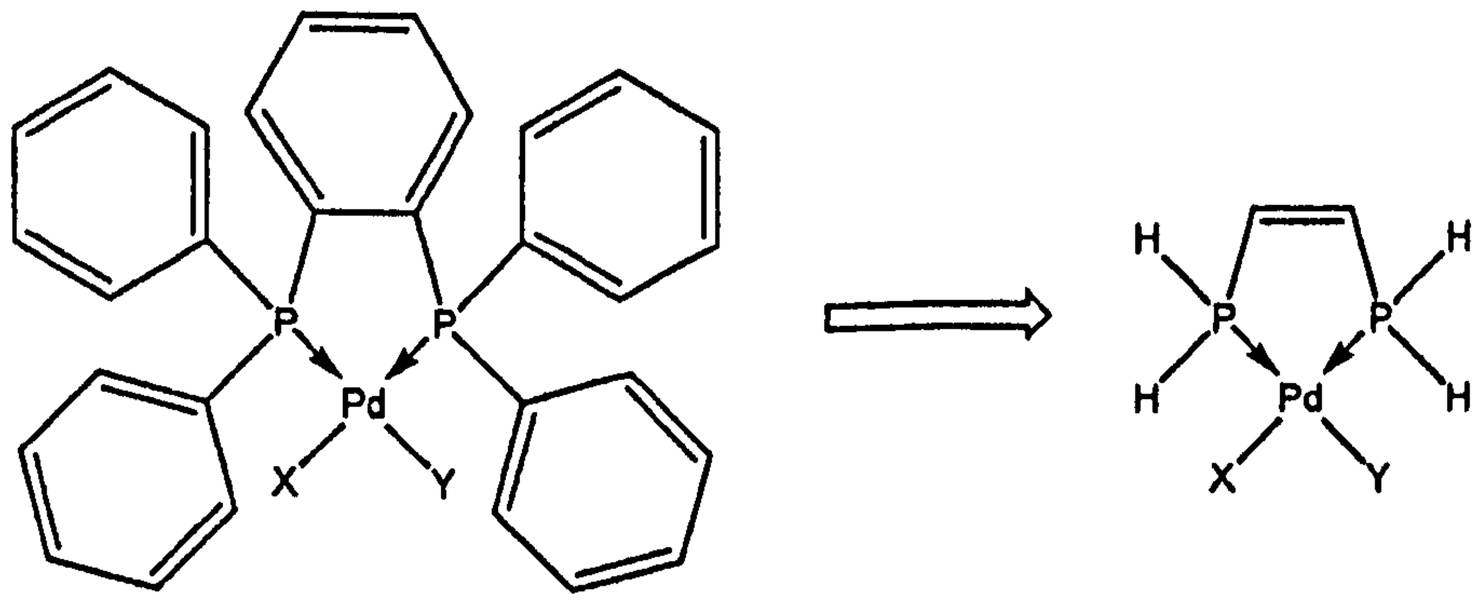


Figure 2.5.1: Example of how real complexes are simplified to reduce systems to a size feasible to optimise, in this case removing 188 electrons from the system. (Example from ref. 7; X and Y are chemically active ligands that vary throughout the reaction.)

atoms. Methyl groups are more of a borderline case, as replacing a methyl group with a hydrogen atom only takes 14 electrons out of the system, and methyl groups have a positive inductive effect that could affect the reaction mechanism.

An example of how a structure can be simplified is shown in **figure 2.5.1**. Should a full structure be subsequently required, the omitted groups can be restored at the end of the optimisation and be optimised with a lower-level calculation such as molecular mechanics or a semi-empirical method (making sure that the positions of all of the atoms optimised as ab-initio level are frozen). The only real problem with this method arises when large bulky groups *do* affect the reaction mechanism, usually through steric hindrance. This scenario will be discussed later.

The next matter to consider is the transition metal atom itself (which also mostly applies to other atoms from the 4*s* region of the periodic table onwards). The first general problem is that basis sets and methods are normally developed for smaller atoms. Most of the popular basis sets have only been developed up to the 3*p* elements,[52] and methods are normally developed and tested using small atoms only (and, in the case of methods such as B3-LYP, parameterised on small atoms). There is little one can do about this other than make use of the methods and basis sets available, and (as one should be doing anyway) paying caution to the results produced and compare them, where possible, to the results of experimental tests and other calculations of similar systems.

There are two more specific problems, both of increasing concern with the increasing mass of the atom. Firstly, even when a complex is simplified by removing groups such as phenyl groups, there are a substantial number of electrons contributing to the system from the many core orbitals of the transition metal, which are capable of

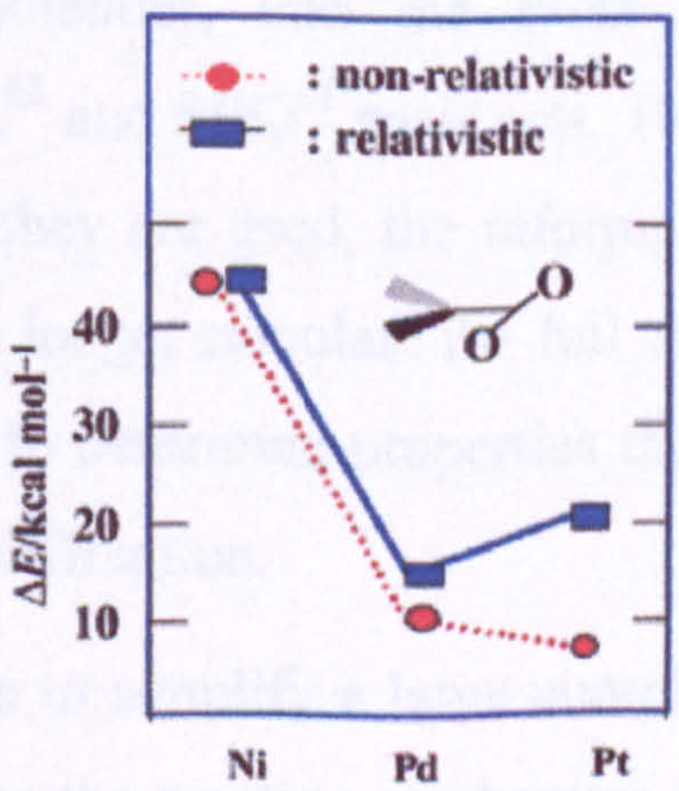


Figure 2.5.2: Variation of relativistic effects of transition metal nuclei moving down the periodic table (example given for M-O_2 bond energies in $(PH_3)_2$ M–O_2 (M =Ni, Pd, Pt).

decreasing the computational speed significantly. Secondly, as the charge of the nucleus increases, electrons close to the nucleus start to approach the speed of light, meaning that relativistic effects start to affect the structure and reaction mechanism. It is really only for third-row transition metals that relativistic effects start to make a serious difference (as shown as an example in **figure 2.5.2**)[47,62], but nevertheless, it is one more source of error even for second-row transition metals.

It is possible to adapt the calculations to consider relativistic effects using Dirac-Fock methods.[61] However, a solution that addresses both the large number of core electrons and the relativistic effects is the use of **pseudopotentials**. Normally, the potential at a particular point in an atom has hyperbolic dependence on the distance from the centre, and the effects of all of the core and valence electrons on any electron at this point are considered separately. When a pseudopotential is used, the nucleus and core electrons are replaced with a single potential surface that takes into account the effect of both the nucleus and all of the core electrons – and a further advantage is that this potential can be adapted to have a similar effect on electrons close to the nucleus as relativistic effects do. The potential in the area normally occupied by valence electrons is virtually unchanged, but any valence electrons in the core region are placed under a potential reflecting the influence of both the nucleus and the core electrons instead of considering their effects separately.[47,48]

The calculation of pseudopotentials is a very complicated process that is not considered here. The only note that is made here is that simply collapsing the core electrons to the nuclear centre is not valid as this would simply change a heavy atom into a lighter atom, with the valence electrons forming a new set of 1*s*, 2*s*, 2*p* orbitals and so on.[58] Atoms using pseudopotentials normally have their own basis sets customised for the pseudopotential, and the most common basis sets using pseudopotentials are LanL2DZ[63] and SDD[64] basis sets. The most obvious drawback to pseudopotentials is that once they are used, the information about the core electron orbitals is lost, and one can no longer calculate the full electronic structure. This may be a problem if it is intended to determine properties that depend on core electrons, such a XPS spectra and X-ray diffraction.

Should it be impossible to simplify a large complex to a smaller one without the loss of groups that influence the reaction mechanism (e.g. there are phenyl groups that cause steric interference), there are three basic strategies that can be used to deal

with this. The crudest strategy is to optimise a simplified structure at ab-initio level, then optimise the remainder of the structure at semi-empirical or molecular mechanics level, and consider the difference in energies between different conformations of the full complex. This method is by far the fastest method but is also subject to the wildest errors and is really restricted to comparing the energies of different isomers of the same complex undergoing different amounts of steric hindrance.

At the other end of the scale, another option, if enough run-time on a supercomputer is available, is to attempt to optimise an entire complex at ab-initio level. As was discovered during this project, the large amount of run-time needed is not the only problem and there are further obstacles that need to be overcome when dealing with systems of this size (see section 4.4.2). However, it is often the case that keeping the entire complex in ab-initio calculations is preferable to the other two options in spite of the additional run-time needed to do it this way.

The third option, which lies between the two, is to optimise the full structure using Quantum Mechanics / Molecular Mechanics methods (QM/MM).[47,65] These methods split the complex into two or more different layers, calculated at different levels. Normally, this will involve the chemically active region being treated with an ab-initio method, and the other regions using a lower level of calculation such as molecular mechanics or semiemperical methods. After the forces on the atom are calculated at each step, the step-by-step optimisation can then proceed as normal. This allows for steric interference to be calculated at a molecular mechanics level without losing ab-initio treatment of the chemically active region itself.

The problem with QM/MM methods lies in the border between different regions. QM/MM methods normally calculate the QM region electronic structure by replacing all of the groups in the MM regions by hydrogen atoms, and then making corrections for the effects of the groups in the MM region represented by hydrogen atoms. However, QM/MM methods are a relatively new technique and a lot of caution must be given to the accuracy of the corrections in the borderline region. It is possible to research structures using QM/MM,[66] but it is advisable to compare some structures with ab-initio structures, and one should never rely on a program to automatically calculate the parameters without understanding the limitations.

One of the more popular QM/MM methods is the ONIOM method, which allows up to three layers of method to be used. In addition to mixing *ab-initio* and non-*ab-initio* methods, ONIOM is also sometimes used to mix DFT and Hartree-Fock methods for the same complex.[67]

One final factor to consider is that all of the calculations described so far have assumed that the molecule(s) is/are in a vacuum, with no interaction from other molecules. In practice, this is not the case and real reactions will usually take place in a solvent. In specific cases, one could expect individual solvent molecules to interact with the system to the extent of forming co-ordinate bonds at available sites, but these can be treated as side-steps in a reaction. The main question is whether the presence of solvent molecules affects the overall energy and geometry of the complex.

There are two recognised method of modelling the effect of a solvent. The most obvious model is to surround the complex with the appropriate solvent molecules. Unfortunately, at ab-initio level it is generally only possible to add a few solvent molecules before the optimisation becomes unfeasible, and usually a few solvent molecules is not enough to adequately model the solvent. However, it is reported that methods are under development that use the QM/MM system, where the MM force fields are chosen to reflect the solvating properties of the solvent molecules.[47]

The other method is to surround the molecules with a region of dielectric continuum to represent the solvent molecules, which affects the polarisation of the complex. This is generally a much more efficient way of modelling the effect of solvent molecules, although this does not allow any individual solvent molecules to explicitly interact with the complex.[47,50,68] The shape of the cavity in the dielectric continuum is normally ellipsoidal, centred over the solute molecule, but the study of optimising the shape of this cavity, whether as a sphere, an ellipsoid, or a more complicated shape such as a cluster of spheres centred on each of the atoms, is a subject warranting its own research.[69] The solvation effects have been neglected from calculations, partly because it was one more thing that could slow down calculations or be wrongly assessed and reduce accuracy, and partly because this is generally applied to chemical reactions that involve charge transfer[68]. Nevertheless, it should be remembered that all results are subject to influences of a solvent.

2.6 Rates of reaction

Having calculated the structures and energies of the stationary points, one might have thought it would be a simple matter to derive the rate of reaction from the energy barrier. However, this is not as simple as one might expect, because there are factors other than the activation energy that are needed to fully calculate the rate of reaction.

The rate constant for a reaction, k, can be expressed as:[47]

$$k = \kappa \frac{k_B T}{h} e^{\frac{-\Delta G_a}{RT}}$$

k_B, h and R are the Boltzmann's, Planck's and the gas constants respectively, and T is the absolute temperature. All of these values are known. The difference in Gibbs free energy, $-\Delta G_a$, however, is not completely known. The enthalpy part is the activation energy, but the entropy of the reactant and transition state are unknown. Finally, κ is a constant encompassing the quantum effects of the system, the probability of recrossing the transition state to go back to the reactant, and non-equilibrium effects. This is very difficult to calculate.

This leaves two options. One option is to approximate the system to assume that the entropy remains unchanged between the reactant and transition state (so that ΔG_a reduces to E_a) and reduce κ to 1, if only a qualitative solution is desired (and given all of the approximations that are normally made to get the activation energy, a qualitative result is normally the best one could expect anyway). The other option, which is probably more applicable if high-accuracy energy calculations are used beforehand, is to consider all of the statistical factors governing the rate of reaction, which is beyond the scope of this project to cover.

An alternative method of determining the rate of reaction is to abandon optimisation of stationary points altogether and instead use a dynamical method to estimate the rate of reaction. The general principle of molecular dynamics is that all atoms in a system are given a random velocity to reflect the thermal energy at a certain temperature, and instead of moving atoms in the direction of the calculated forces at each step, the velocities of the atoms are altered. Alternatively, the Monte Carlo method can be used, where atoms are displaced in random directions in every

step, but if the new position is a higher energy than an old position, there is probability (increasing with higher energy differences) to move the atom back to its old position.

The advantages of these methods, especially the molecular dynamics method, is that the movements of the atoms are far more reflective of real systems than the minimum energy IRC paths found from the optimisation of stationary points. Furthermore, they are not restricted to predetermined directions of reaction and, as a result, may find a low-energy path that would otherwise not be known to exist. However, the disadvantage is that the random nature of these methods means that many different runs have to be taken to get any meaningful statistical distribution on the outcome of the dynamical approaches.

In practice, dynamical methods alone are not suitable for evaluating reaction paths in systems as large and complex as transition metal complexes. Some 10,000 steps can be needed on a single trajectory, and although there are short-cuts that make calculations quicker, they cannot compete with optimisation of the reactant and transition state as the most efficient method of determining the reaction rate. Dynamical methods are, in general, better suited to determining the rates of processes like diffusion in a solid or liquid where a step-by-step consideration of the energy barriers would be impossible due to hundreds or thousands of possible steps existing. However, molecular dynamics is sometimes used in conjunction with optimisation of the stationary points in some organometallic systems to obtain more information about the reaction mechanism, such as the dynamics of atoms moving downhill from a transition state.

In this project, only the energy barriers are considered in estimating rates of reaction. At 50°C (the typical temperature that copolymerisation reactions are carried out), almost all of the energy barriers are low enough for the rate to be considered instantaneous. The rate constant for a step with an energy barrier of 10 kcal/mol is of the order of 10^6 s^{-1}, and it is only when the energy barrier approaches 20 kcal/mol that the rate constant starts to fall below 1 s^{-1}. Therefore, in practical terms, the only factors likely to limit the rate of copolymerisation will be the rate at which monomers can be fed into the reactor and the speed in which they can diffuse towards the catalysts. (It also means that it would be near-impossible to experimentally obtain the structures of any intermediates or the energy barriers of any particular step, which is a

problem as it seriously limits the data to which theoretical results can be compared, apart from other theoretical results.) Of more importance is how the energy barriers of alternative steps compare to each other, such as the probability of double insertion or termination instead of propagation. An increase of 1 kcal/mol in an energy barrier was estimated to decrease that rate of reaction by approximately 80%, so an increase of only a few kcal/mol will ensure practically 100% selectivity to the lower-energy pathway.

2.7 *Ab-initio* programs and alternative methods of optimisation

There are many computer programs that have been written to handle the intense number crunching necessitated by ab-initio calculations. By far the most popular program[58] is the *Gaussian* software package[70,71], which owes much of its popularity from the ease of its use. Provided one is aware of the limitations of accuracy offered by different basis sets and methods, it is usually easy to optimise a structure to the desired level of accuracy with little previous experience of *ab-initio* optimisations.

Out of the other software packages, two of them are notable. The *GAMESS* program performs many of the operations that Gaussian does, but has the added advantage of being free.[72] The other notable program is the *Amsterdam Density Functional* program (ADF)[61,73]. The main difference between the two packages is that ADF requires a much more detailed input than Gaussian, as Gaussian automatically chooses a number of parameters for which ADF requires a manual input. ADF is therefore generally more suited to those who understand DFT in considerable detail, but it does avoid the trap that Gaussian sometimes falls into of automatically choosing some parameters that turn out to be unsuitable for the process in question. (This is especially true of the characteristics of the boundaries between the QM and MM regions in ONIOM, the QM/MM method used in Gaussian.) One minor but important difference is that ADF has its own techniques for locating transition states,[61] which some people find preferable to those used in Gaussian.

A fundamentally different method of optimising structures at DFT level is used in the *Cambridge Serial Total Energy Package* (CASTEP).[74] Instead of constructing the electron density from orbitals around individual atoms, CASTEP

works by placing the structure in a periodic cell and constructing the electron density from plane waves in all three dimensions. In this case, pseudopotentials are essential for *every* atom because plane waves cannot accurately account for core electrons. Other than this it is possible to calculate the energy and forces of atoms in the system in the same manner, and use this for optimisation if needed, as well as produce useful information such as the conduction and valence bands in semiconductors.

Not surprisingly, CASTEP is mainly used by solid-state physicists dealing with solids, where it is natural to consider atoms in a periodically recurring cell. It is possible to adapt CASTEP's methods to single complexes by placing the complex in a "supercell", which is a unit cell of large enough dimensions such that identical complexes in the neighbouring unit cells are too far away to interact. It is claimed by some people (many of them CASTEP developers) that this is a more efficient method of optimising complexes than methods using basis sets. However, as plane waves cover the entire supercell and the complex only occupies a small part of this cell, time is needed to optimise an electronic structure where the plane waves cancel out over the rest of the cell where the electron density is obviously zero. As basis sets never add electron density away from the atoms they are centred on, this problem does not apply to programs such as Gaussian and ADF. Most computational chemists recommend that although optimisation using supercells and plane waves is possible, this method should only be used if the properties of a molecule need to be compared with those of a solid or liquid.

Moving away from *ab-initio* chemistry altogether, the two main alternatives to this method are available in *CAChe*.[75] Both methods are computationally much simpler than any form of *ab-initio* calculations, and so are suited to much bigger systems, or smaller systems where a few days on a supercomputer are not available to get a result needed.

In *molecular mechanics*, all atoms, in various configurations, are given optimum bond lengths to other atoms, bond angles and dihedral angles. Any deviation from these optimum parameters, or any non-bonding atoms moving too close to each other to cause steric interference, increases the energy of the system by a set formula. In effect, this reduces the system to a "balls on springs" model. This method can easily handle hundreds of atoms, and it can be used to optimise structures and compare energies between different conformations of the same structure, so it is

particularly useful for searching through hundreds of conformations to find a lowest-energy conformation.[76]

However, the very nature of the balls-on-springs model makes molecular mechanics useless for reaction mechanisms, as all of the bonds between atoms need to be defined, and one cannot use molecular mechanics for a partially-formed bond present in most transition states. And unlike other methods, where energy calculations can be used to calculate enthalpies to any other structure containing the same atoms, energies may only be compared in molecular mechanics between structures with both the same atoms and *the same bonds connecting the atoms*. Molecular mechanics is therefore restricted to comparing different conformations of the same molecule(s). Even in this case, the balls-on-springs approach, which neglects quantum effects completely, is a very crude approach and it is not generally reliable to use as a source of quantitative information for either structures or energies.

The *Molecular Orbital Package* (MOPAC) is a package based on a semi-empirical method, which is a compromise between the accuracy and versatility of quantum mechanics and the speediness of parameterised calculations. MOPAC solves the Schrödinger equation for a system using fixed Hamiltonians for different atoms. The Hamiltonians and orbitals of these atoms are determined from a set of parameters, the most common ones used in CAChe being the AM1, PM3 and PM5 parameter sets. MOPAC is capable of solving optimised geometries, transition states, vibrational frequencies and many other properties that can be solved by *ab-initio* methods for a fraction of the run-time, to a much greater degree of accuracy than molecular mechanics methods.[75]

The limitation of MOPAC is that it can only be as accurate as the parameters for the different atoms allow it to be, and this is where transition metal chemists lose out. Until recently, no parameter sets included *d*-electrons at all, making optimisation of transition metal compounds impossible. The latest version of CAChe does include parameters for a few transition metal atoms, but these were tested during research in the project and found to be very unreliable – in particular, it never succeeded in producing a plausible optimised structure for a transition state. Whilst it is unlikely that MOPAC could ever equal *ab-initio* chemistry for accuracy, it would be extremely useful if reliable parameters existed for transition metals, so that provisional transition states could be optimised in a matter of minutes before being used as the starting

structure for a B3-LYP optimisation, thereby cutting the run-time by starting with a structure close to the actual transition state. Unfortunately, MOPAC is currently not reliable for transition metal atoms so this project has to use the time-consuming ab-initio techniques alone.

In general, molecular mechanics and semi-empirical methods such as MOPAC are more commonly used in larger systems, beyond the limits of *ab-initio* calculations, that are not concerned with chemical reactions. These methods are often suitable for large molecular dynamics or Monte Carlo calculations, as they are for the low-level region of QM/MM optimisations, and for searches through hundreds of different conformations to identify local minima. This is not to say that molecular mechanics or MOPAC methods are never used for optimisation, as the use of molecular mechanics has been tested on large systems with the intention of obtaining accurate results[77]. In this project, although no structures' energies quoted here were calculated using MOPAC or molecular mechanics (apart from the propene insertion regioselectivity calculations described in section 4.4.1), CAChe was often used to help choose a starting structure for an *ab-initio* optimisation.

(Note: The other advantage of CAChe is that its in-built molecular building and viewing program is much better than any other program available in the Durham Chemistry Department, and all of the structures optimised by Gaussian shown in this project are displayed as shown in CAChe, after converting the file to the appropriate format. Gaussian only reports the positions of the atoms – the bonds drawn between the atoms are arbitrary and only shown for purposes of clarity. The only scale diagrams that are not taken from CAChe are the modes of vibration diagrams, which are taken from Jmol.[78])

2.8 Conclusions

Advances in both *ab-initio* methods and computational techniques have, between them, made it possible, within the last decade, to model the reaction mechanism of transition metal-catalysed systems to a semi-quantitative degree of accuracy, and interest in this area is growing swiftly. By optimising the stationary points, both minima and transition states, it is normally possible to determine the mechanism of the entire process, and judge from energy barriers whether a reaction is feasible and which of two or more competing steps is more likely to take place.

The main limitation of optimising transition metal complexes is the accuracy at which electronic structure can be calculated in a reasonable amount of time. An optimisation at a DFT level using a basis set the size of, say, 6-31G* will normally be near the limits of the capabilities of most high-performance computers, and although this allows for a reasonable degree of confidence, caution should always by paid to any results and the results should, where possible, be compared to experimental and theoretical results of similar complexes. Run-time can be saved by using pseudopotentials for transition metal atoms, and replacing any large groups that are not chemically active with hydrogen atoms.

Energies and forces on atoms can be calculated analytically from the electronic structure. From this, minima are relatively easy to optimise by moving the atoms in the direction of the force, with estimates of second derivatives used to calculate how far the atoms should be moved between steps. Transition states are more difficult to optimise, and normally require the QST3 method, where the structure of the reactant, and product and an estimated transition state are all considered in locating the transition state. Even so, the starting structure for a QST3 optimisation usually needs to be a fairly good one for the optimisation to succeed.

Stationary points should always have their frequencies calculated in order to ensure that they are the intended minima or first-order saddle points. The zero-point energy corrections can also be added to energies for greater accuracy of enthalpies and activation energies. Care should also be taken to ensure that an optimised minimum is not a local minimum when the global minimum was intended, and that the transition state did not miss a lower-energy reaction path. Unfortunately, there are no systematic methods that can guarantee that either of these will be avoided.

Once transition states have been optimised, the reaction path can be completed by running IRC jobs from the transition state, which sometimes gives rise to further local intermediates and transition states. The complete reaction mechanism can then give a valuable insight into why certain reactions do and do not occur in situations where the compounds cannot be isolated by experimental means.

3: Mechanism of ethene/CO propagation cycle.

3.1 Introduction

The original reason for optimising a step of the propagation cycle was as part of a process to predict the regioselectivity of propene insertion in propene/CO copolymers. Since then, the scope of the research expanded to take in the entire propagation cycle, with the intention of expanding it to determine the mechanisms of the initiation or termination processes, and the reasons for lack of double insertion.

Study of the cycle was broken down into the four steps shown in scheme 1.1: olefin addition, olefin insertion, carbon monoxide addition, and carbon monoxide insertion. It was normally convenient to consider each step as a separate reaction. However, there was the occasional exception, where an unexpected product structure from one step determined the reactant structure of the next step, or where an unexpected reactant structure determined the product structure of the previous step. The mechanisms of the two insertion steps have already been studied in some details by Ziegler and Margl[7,8] and Svensson *et al*[36], but neither group gave much consideration to the mechanism of the two addition steps, assuming, as have many other researchers, that the addition steps are not important.

Note: Throughout this thesis, the terms "reactant" and "product" are always used to refer to the starting and finishing structures of the stage in question. It does NOT mean the reactant and product of the entire reaction (i.e. the feed gases and the copolymer produced).

The basic approach for each step was straightforward. Firstly, the reactant and product structures of each step were optimised. These two structures were then used to try to optimise the transition state. Once that was optimised, the validity of the stationary point obtained for the reactant, product or (most importantly) transition state structure was verified with a frequency test. If this was valid, the reaction path was analysed from the transition state both ways using the IRC method. When the limit was reached, the path was completed by optimising the structure from the final point. If either of these structures optimised to an intermediate instead of the reactant/product structure, the path between this intermediate and the reactant/product was then considered.

There were, however, numerous deviations from this approach employed as necessary, all of which are described at the appropriate point in the following account of the research.

The diphosphine ligand chosen for this research was 1,3-bisdiphenylphosphinopropane (dppp), partly because it made sense to choose the most active catalyst and partly because less feasible reaction paths are generally more difficult to optimise. Ethene was chosen as the olefin to minimise the number of variables to control in the project.

3.2 Technical details

Most of the project was run on the High Performance Computing Service at the University of Durham. Gaussian was used, as it was the only ab-initio program available at Durham suitable for dealing with transition metal complexes.

Throughout the project, it was necessary to simplify the structures by reducing the phenyl groups and copolymer chain to smaller groups. The phenyl groups were originally simplified to methyl groups, and then later further simplified to hydrogen atoms on advice that hydrogen atoms were generally a better approximation for phenyl groups than methyl groups were. The copolymer chain was also truncated by replacing the chain with a hydrogen atom after a point where it was assumed that the copolymer chain would play no further part in the reaction. However, it later turned out that the assumptions were sometimes wrong.

At the start of the project, the computer available, marvin, was a relatively low-performance computer. Therefore, every measure possible had to be taken to use as little run-time as possible. The earliest optimisation jobs run on marvin used the Hartree-Fock method and the 3-21G basis set on Gaussian-94[70]. Although the reactant and product structures obtained were plausible, the transition state structure was found to be unrealistic and it was realised that this basis set was too small to give any reliable information.

The QST3[60] method was always used for optimising the transition state, which meant that the reactant and product structure either side of the transition state always had to be optimised first. It was found that simply using the Opt=TS method, where only an estimated structure of the transition state was inputted, was never able to

locate the transition state in a structure of this size. However, even with the QST3 method, it was often difficult to choose a starting structure of the transition state close enough to be successfully optimised. The information used to choose the starting structure is described in each individual case.

After several attempts to upgrade the method and/or transition state, it was found that by upgrading the chemically active atoms to the 6-31G** basis set[79,80] (DZDP basis set for palladium[79,81]), an acceptable structure of a transition state could be found. However, the rate of optimisation was ridiculously slow, and attempts to upgrade the method from Hartree-Fock to the more reliable B3-LYP method made the rate unacceptably slow. (B3-LYP was preferred owing to the questionable accuracy of Hartree-Fock-optimised bond lengths from transition metals to ligands.) Attempts were made to speed up the rate by removing the carbon bridge in the diphosphine group, but this introduced two extra degrees of freedom in the rotation of the $-PH_3$ groups. This was more trouble than it was worth, and the plan was abandoned.

Then it was suggested that a basis set with pseudopotentials should be used, to cut out all of the unnecessary run-time spent on the core electrons of palladium. The basis set chosen for this was the Stuttgart/Dresden (SDD)[79,64] basis set. This was attempted and the increase in speed was enormous. This coincided with the replacement of marvin with hal, a new much faster high performance computer (which also introduced Gaussian-98[71]). This enabled the method to be upgraded to B3-LYP without slowing the jobs down too much.

One disadvantage of using SDD was that although it covered elements over the entire Periodic Table, it did not include any diffuse or polarisation functions, and there were no known papers that investigated adding such functions to this basis set.[52,64] Arbitrary diffuse and polarisation functions were added to the chemically active atoms (it was found that adding them to all the atoms slowed down the optimisation too much), but the diffuse functions were later dropped when it was advised that without a large basis set supporting them, diffuse functions can sometimes make the results worse.

The polarisation functions added to the SDD basis set for carbon, oxygen and phosphorus were the same polarisation functions used in the 6-31G** basis set[79,80] (*d*-shaped functions with contraction coefficients of 0.8, 0.8 and 0.55 respectively). The

polarisation function added to palladium was an *f*-shaped function with a contraction coefficient chosen to be 0.4. Diffuse functions, when used, were calculated using the step-down method (where the contraction coefficient was that of the most diffuse function divided by the quotient of the coefficients of the second most diffuse function divided by the most diffuse function: $\alpha_{dif} = \alpha_N$ / (contraction coefficent) = α_N / (α_{N-1} / α_N) = α_N^2 / (α_{N-1})).

Hal is an 8-node Sun Ultra Grid with each node having 4 x 450 MHz Ultra II processors and 2 Gb memory.

Therefore, unless otherwise specified, all results described in this thesis were obtained using Gaussian-98, the B3-LYP method, and the SDD basis set augmented with the polarisation functions described above. Transition states were optimised using the QST3 method. All minima and transition states were verified with frequency tests. Reaction profiles between minima and saddle points were calculated using the IRC method, with the stepsize set to 25, for as many points as the program would run, and completed by optimising the final points to the minima. All other parameters not described were set to the Gaussian-98 defaults.

All energies were reported in Gaussian in Hartrees, using a SCF energy that could only be compared to other structures with the same atoms, method and basis set. Only the relevant energy differences are reported here, and all energies are converted to kcal/mol using the conversion factor of 1 Hartree = 627.5095 kcal/mol.

3.3 Olefin insertion step

3.3.1 Introduction

The olefin insertion step of the propagation cycle is perhaps the most thoroughly analysed stage of the reaction. The step has been previously investigated by Ziegler and Margl[7,8], and Svensson *et al,*[36] and their proposed structures are shown in **figure 3.3.1.**

This step was the most interesting step to monitor for two reasons. Firstly, the structure of the olefin insertion transition state in propene/CO copolymerisation would be most likely to determine the regioselectivity between 1,2- and 2,1-insertion.

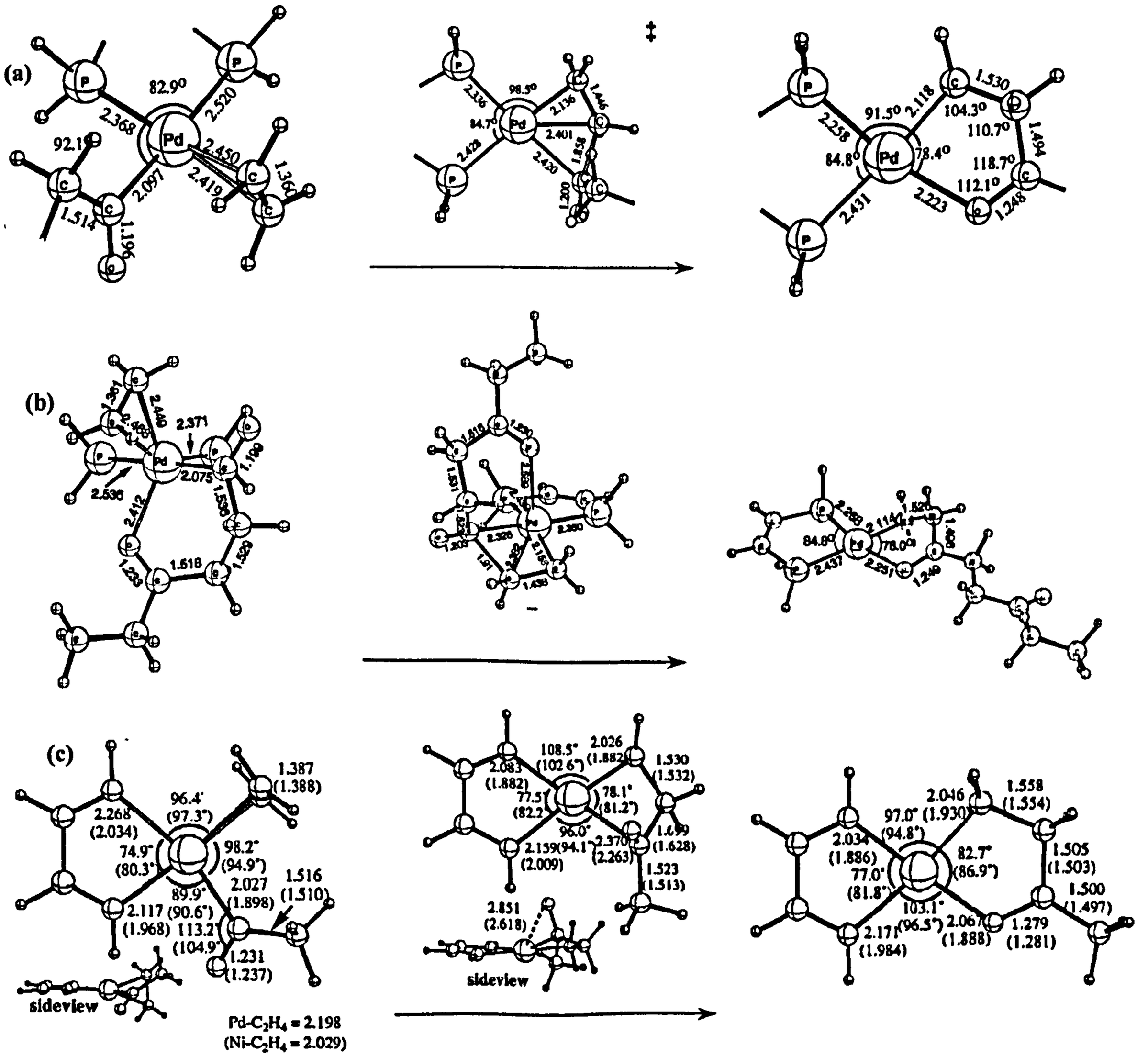


Figure 3.3.1: Structures of reactant, transition state and product of olefin insertion step previously optimised by **(a)** Ziegler and Margl (ref. 7); **(b)** Ziegler and Margl including interaction from second CO group (ref. 8); and **(c)** Svensson *et al* using diimine ligands instead of diphosphine (ref. 36 – figures in brackets are using nickel instead of palladium).

Secondly, if it was correct that olefin insertion was the slowest step, the dynamics of this step would play a major part in governing the speed of the whole reaction.

All of the previous work agreed with the speculation that, after olefin insertion, a strong Pd-O co-ordinate bond was formed, and the structure of the transition state predictably demonstrated the lengthening and shortening of the bonds one would expect to be broken and formed. The only item of note is that when a second carbonyl group was taken into consideration (as in figure 3.3.1 (b)), this interacted above the square plane in the reactant and transition state structures. Although there was some scope to examine the reaction mechanism between the stationary points, the main purpose of examining this step was to ascertain whether the method used in this project was reliable.

3.3.2 Reactant and product structures

These structures were the first structures in this propagation cycle to be optimised using Gaussian, and optimisation turned out to be relatively easy. Even using basis sets as small as 3-21G (this stage was originally optimised with this basis set before it was realised how unsuitable the basis set was), the same qualitative structures were always formed. The structures of the reactant and product optimised using the augmented SDD basis set and B3-LYP are shown in **figure 3.3.2.1** and **figure 3.3.2.2** respectively.

There were no major surprises in either of these structures. In the reactant

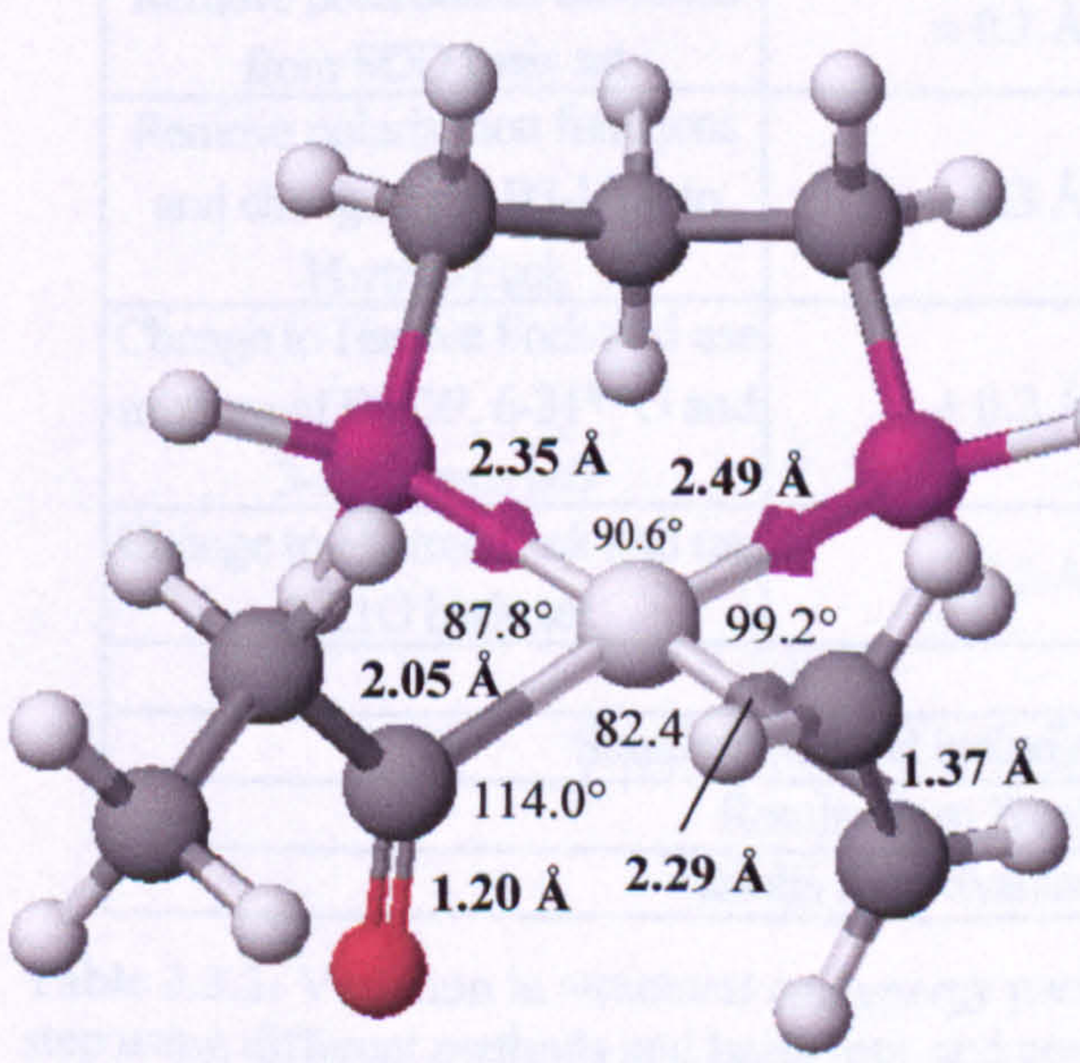


Figure 3.3.2.1: Optimised structure of reactant prior to olefin insertion, neglecting second carbonyl group.

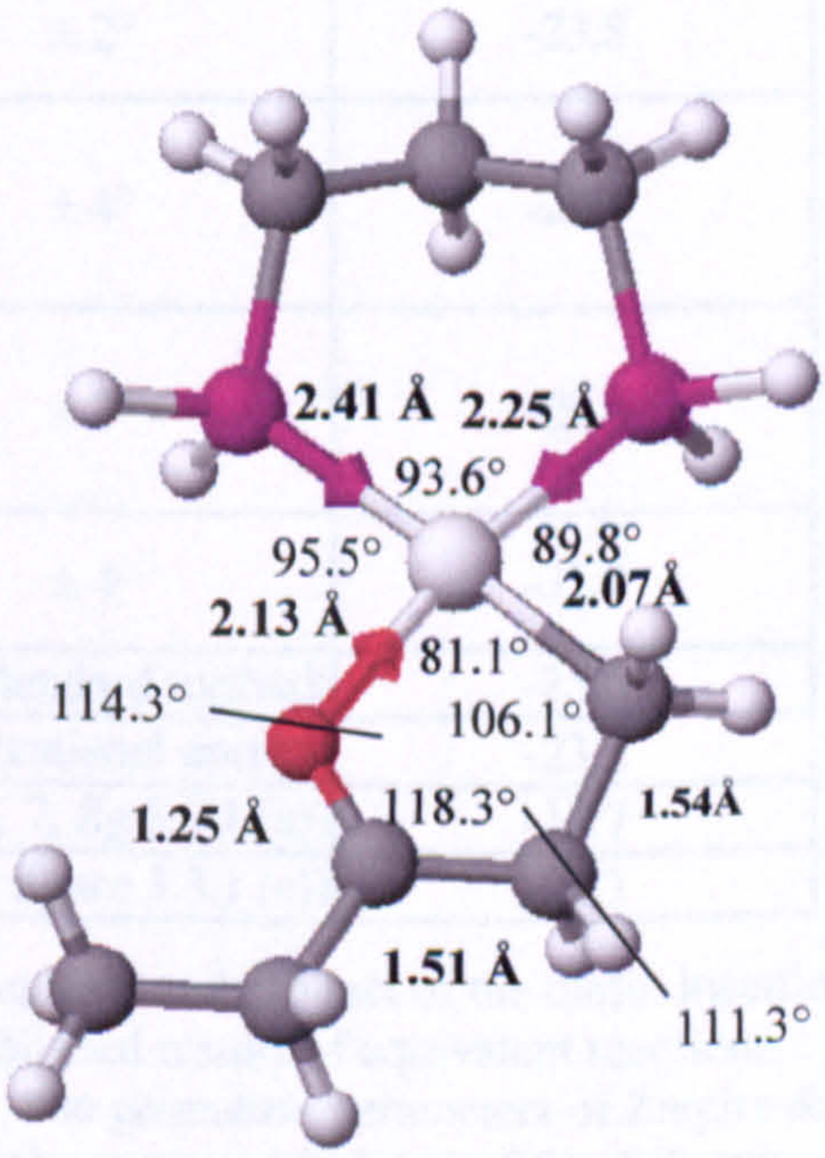


Figure 3.3.2.2: Optimised structure of product after olefin insertion, neglecting second carbonyl group.

structure, the olefin was π-coordinate bonded to the palladium centre with the olefin perpendicular to the square plane. This, on its own, could be explained as the least sterically hindered structure, although later work suggested that bonding from the olefin's π/π*-orbitals had an effect (see section 3.3.4 and 5.3.1). In the product structure, almost any starting structure optimised a structure with a definite co-ordinate bond between palladium and oxygen, which supported all of the earlier theories advocating this interaction.

The enthalpy of this insertion process was -25.6 kcal/mol, with the formation of the Pd-O co-ordinate bond presumably contributing to such a large negative enthalpy. When zero-point vibrational energies were included from frequency tests, the difference fell to –23.2 kcal/mol. However, as with all zero-point corrections, it should be noted that there were many degrees of freedom for the program to consider and it was possible that the correction made for zero-point energy could be outweighed by a significant margin of error.

These two structures were also optimised using several different methods and/or basis sets. When diffuse functions were added to the atoms, the difference to the geometry of the structure was slight. Removing the polarisation functions or switching to Hartree-Fock introduced larger changes (the most obvious change in

Change to basis set/method	Variation of bond lengths	Variation of bond angles	Enthalpy of insertion / kcal/mol
Add diffuse functions to SDD basis set	± 0.03 Å	± 0.5°	-24.9
Remove polarisation functions from SDD basis set	± 0.1 Å	± 2°	-23.8
Remove polarisation functions and change from B3-LYP to Hartree-Fock	± 0.3 Å	± 4°	-25.4
Change to Hartree Fock and use mixture of DZDP, 6-31**G and 3-21G basis sets	± 0.2 Å	± 3°	-29.0
Change to Hartree Fock and use 3-21G basis set	± 0.3 Å	± 4°	-31.8
		Standard method:	-25.6
		Standard method including zero-point vibrational energy:	-23.2
		Results from Ziegler & Margl (ref. 7, fig 3.3.1 (a))	-17.7
		Results from Svensson et al (ref. 36, figure 3.3.1 (c))	-22.3

Table 3.3.2: Variation in structural and energy parameters of the reactant and product of the olefin insertion step using different methods and basis sets, and comparisons to published results of equivalent reactions. Unless otherwise noted, zero-point vibrational energy is neglected. The geometric parameters of Ziegler & Margl's structure and Svensson *et al's* structures could not be directly compared because of the different diphosphine/diimine backbone used, but where parameters could be compared (i.e. not related to the bidentate bite angle), a correlation was observed to within 0.1Å or 2°.

Hartree-Fock being a sharp increase in the Pd-P bond lengths). A summary of the changes induced by the different methods and basis sets is given in **table 3.3.2**. However, whilst differences in bond angles and bond lengths could be measured, all of these structures were qualitatively close enough to each other to appear near-identical at a first glance, even when using the relatively small 3-21G basis set.

In this project, one major weakness apparent throughout the propagation cycle was the lack of non-theoretical data for purposes of comparison. Apart from the experimentally-obtained energy barriers of reactions of similar steps shown in table 1.2.1, there was little experimental evidence that could back up the theoretically-obtained parameters, simply because of the difficultly in isolating any of the intermediates in the process. In fact, there was only one structure found in the Cambridge Structural Database[83] that bore a reasonable similarity to any intermediate in the propagation cycle, and this is shown in **figure 3.3.2.3**.[31]

The parameters that could be compared showed a variation in bond lengths of ±0.1 Å, but notably, the largest variations were observed in the Pd-P bond lengths. Crucially, the variation in bond length of the Pd-acyl bond was only ±0.02 Å. The variation in bond angles was not so encouraging, with some angles varying by up to ±4° (including the Pd-C-O bond angle), but again, it is unclear how much of the variation could have been down to the presence of the chlorine atom.

In the case of the product, the closest structure that could be compared was a

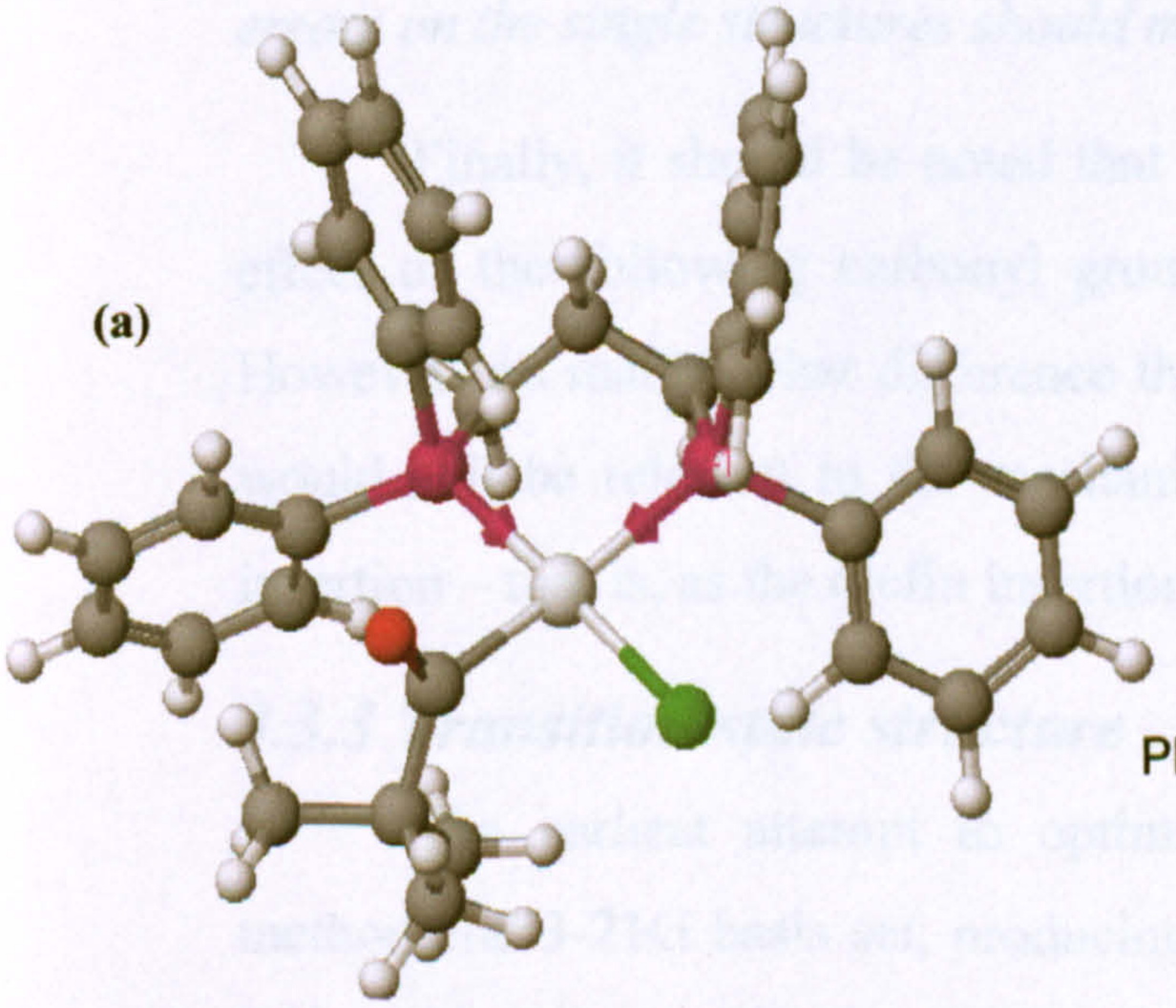


Figure 3.3.2.3: (a) 3D and **(b)** Schematic diagram of the TEXPER structure from the Cambridge Structural Database for comparison with the structure obtained in **figure 3.3.2.1**. (Positions of hydrogen atoms are arbitrary.)

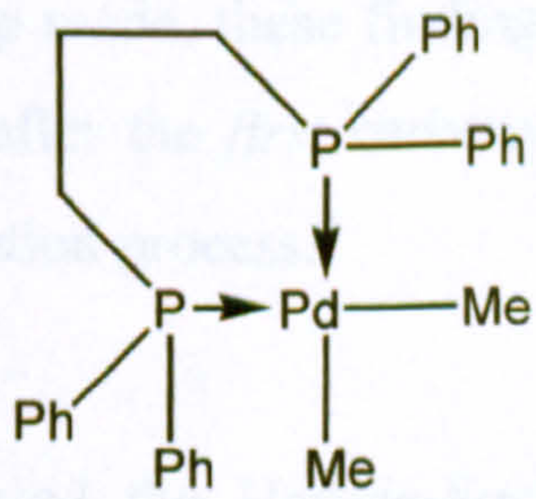


Figure 3.3.2.4: Schematic diagram of the CAKXER structure from the Cambridge Structural Database for comparison with the Pd-acyl bond lengths.

fragment shown in **figure 3.3.2.4**. The length of the Pd-methyl bond was compared to the length of the Pd-acyl bond in the product structure and was again found to vary by only ±0.02 Å.[83]

On the whole, the most reliable parameters obtained by Gaussian appear to be the palladium-ligand parameters other than the Pd-P bond lengths. The accuracy of the Pd-P bond lengths was less certain from these comparisons, but as is explained later in section 5.3.5, it is much more likely that the variation in Pd-P bond lengths was caused by the electronic influence of the other ligands rather than any errors arising from theoretical approximations. The only parameters that were found to have a possible significant margin of error were the bond angles, where errors of up to ±4° could not be ruled out.

Based on the variation in results using different basis sets/methods, the usual margin of error for energy differences seems appropriate here. However, the smaller enthalpy difference (by 7.9 kcal/mol) calculated in Ziegler and Margl's work should be noted. It was assumed (but not proven) that the different diphosphine backbone used in Ziegler and Margl's work would be responsible for such a high difference. Other than that, the results appeared to be reasonably consistent with this work.

Note: It is usual for SCF energies of theoretically optimised structures to be allowed a margin of error of ± 5 kcal/mol. However, the margins of error for enthalpies and energy barriers are likely to be much less than this, because the structures of the reactant, product and transition state are similar enough that the errors on the single structures should mostly cancel each other out.

Finally, it should be noted that both of the optimised structures neglected the effect of the following carbonyl group on the reaction. This was examined later. However, no matter what difference the second carbonyl group made, these findings would still be relevant to the mechanism of olefin insertion after the *first* carbonyl insertion – that is, as the olefin insertion component of the initiation process.

3.3.3 Transition state structure

The earliest attempt to optimise a transition state used the Hartree-Fock method and 3-21G basis set, producing the structure shown in **figure 3.3.3.1.** Whilst this structure looked interesting, the possibility of the transition state being in a final step where a Pd-C (acyl) bond is broken and a Pd-O bond is formed seemed unlikely.

When an IRC job was applied to this transition state, and no plausible reaction path found was to either the reactant or the product, it was decided this structure was meaningless. Furthermore, the energy of the transition state was 6.5 kcal/mol *lower* than the energy of the reactant. In fact, this was chiefly responsible for the decision not to use the 3-21G basis set in future.

At the time, computational resources were limited and so it was necessary to upgrade the basis set no more than necessary. Starting from the transition state structure proposed by Ziegler and Margl, and either upgrading to the 3-21++G basis set or the B3-LYP method, Gaussian failed to converge on a transition state at all. It was only when a mixed basis set of 6-31G++ for chemically active atoms (or DZDP for palladium, as 6-31G was not available for palladium) and 3-21G for the rest of the structure that a plausible transition state was found, after a job that ran for 47 days. (It was necessary to shorten the distance between the olefin and acyl group to prevent the structure moving away from the transition state. The job was later re-run using 6-31G** instead of 6-31G++.)

Later, the SDD basis set was also found to give good results in less time, and when computational resources became available, upgrading the method to B3-LYP using this method also gave a transition state. The structure optimised using B3-LYP, and the SDD basis set augmented by polarisation functions, is given in **figure 3.3.3.2**.

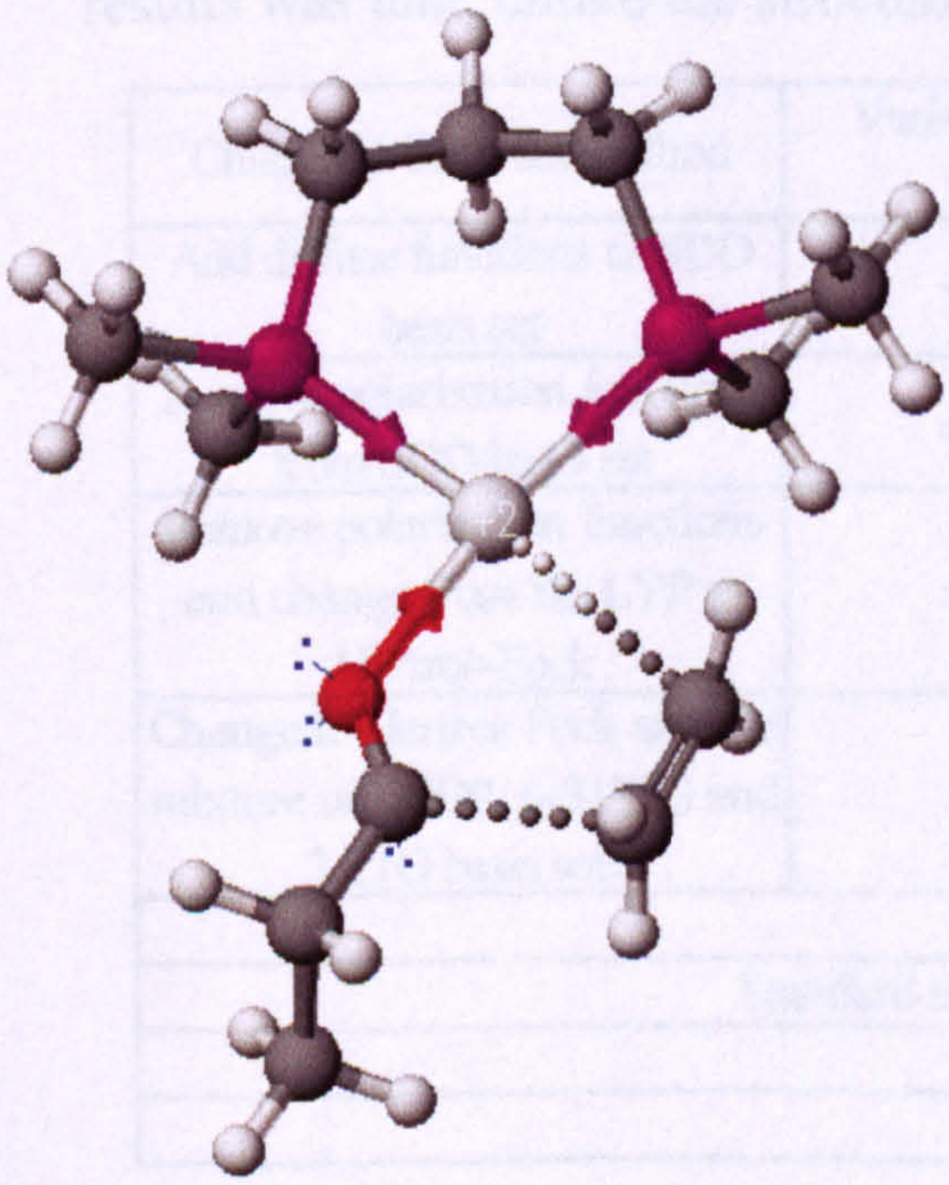


Figure 3.3.3.1: Transition state structure optimised using HF/3-21G.

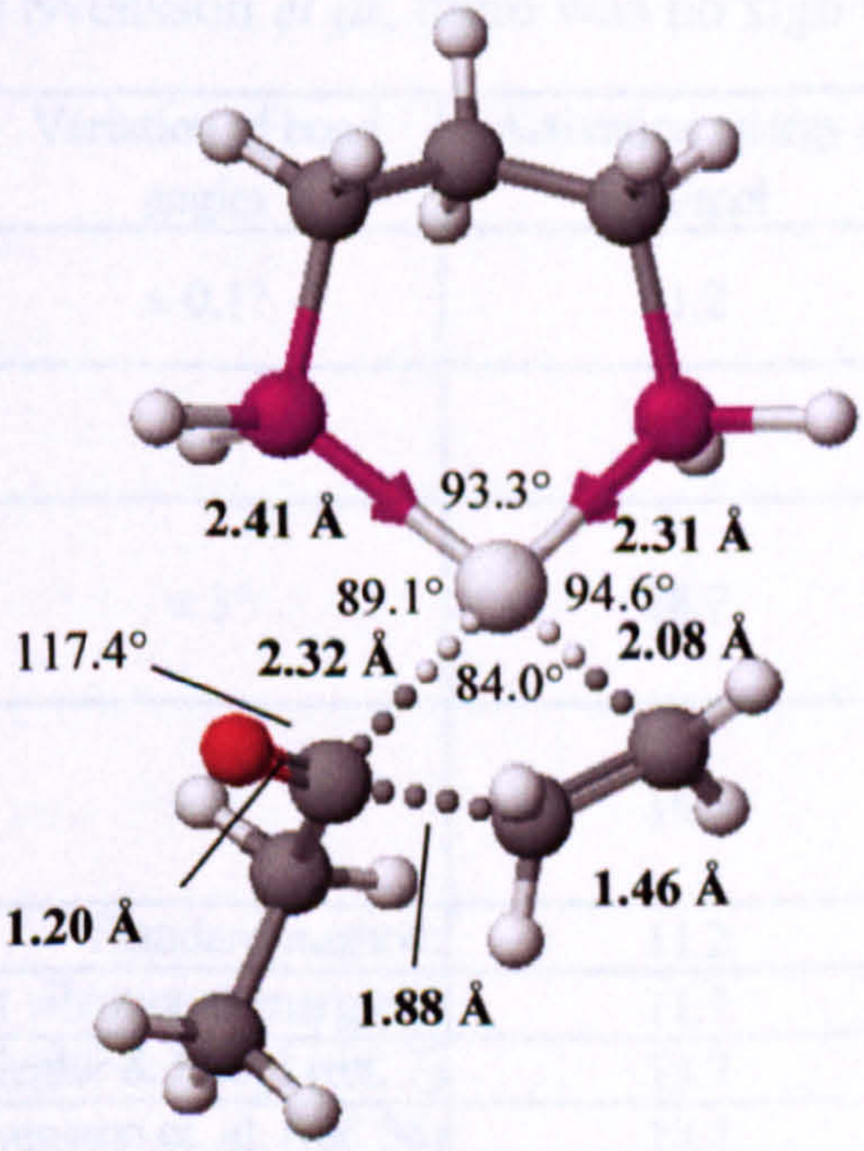


Figure 3.3.3.2: Transition state structure optimised using B3-LYP/aug-SDD.

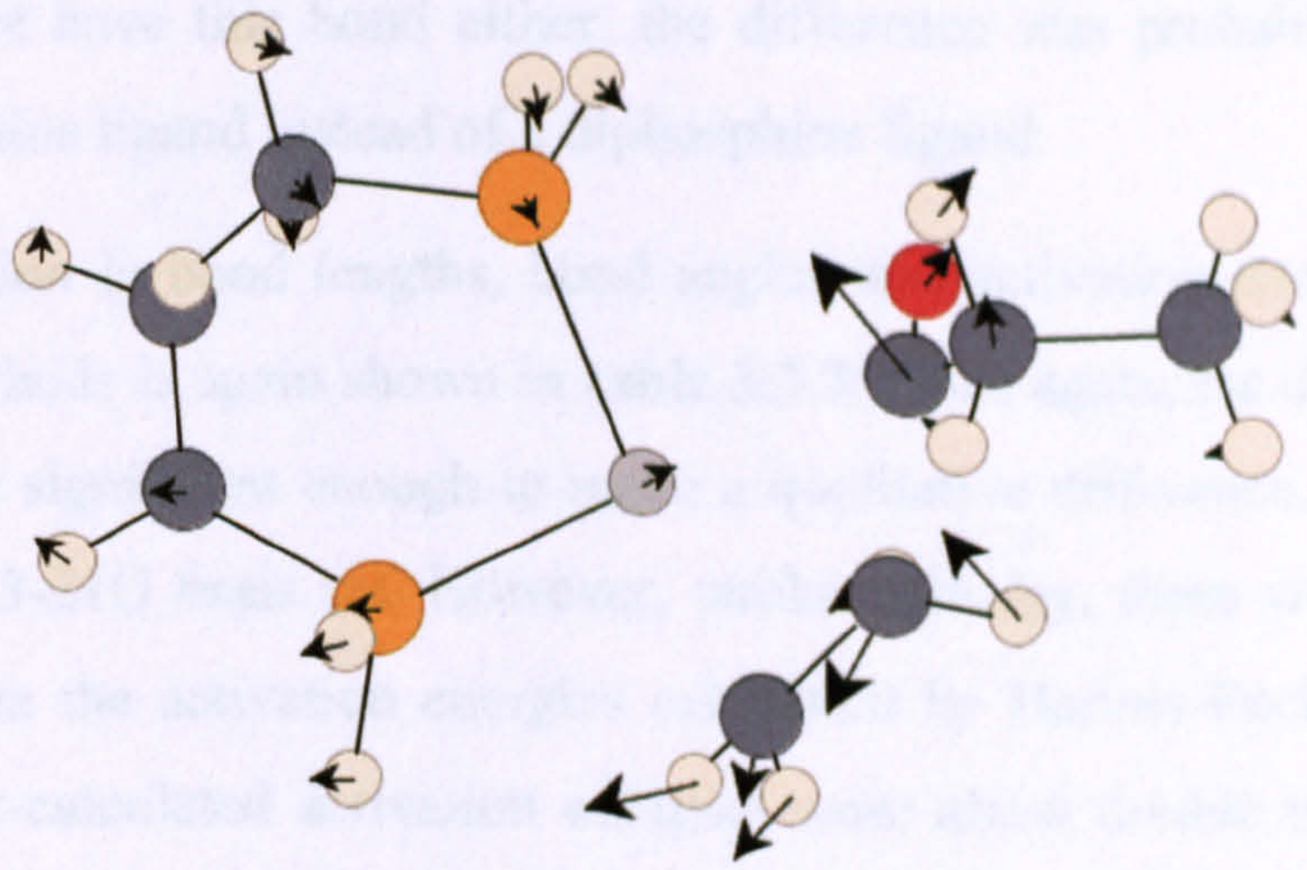


Figure 3.3.3.3: Vibrational mode of imaginary frequency. (Imaginary frequency = -311.9 cm^{-1})

The validity of this structure was verified using a frequency test, and the mode of vibration of the imaginary frequency is shown in **figure 3.3.3.3**.

This structure was much more consistent with those of other research groups, as it was shown that the transition state was reached part-way through the insertion of the olefin into the Pd-acyl bond itself, and not just during the consequential re-arrangement of other bonds after insertion as suggested by the original optimisation using the 3-21G basis set. The energy barrier calculated between the reactant and transition state was 11.2 kcal/mol, or 11.7 kcal/mol including zero-point vibrational energies, which was consistent with earlier experimental and theoretical results, and well within the range for this step to be feasible. The only slight differences to earlier results was that, unlike the structure optimised by Svensson *et al*, there was no sign of

Change to basis set/method	Variation of bond lengths	Variation of bond angles	Activation energy / kcal/mol
Add diffuse functions to SDD basis set	< 0.01 Å	± 0.1°	11.2
Remove polarisation functions from SDD basis set	± 0.08 Å	± 2°	13.3
Remove polarisation functions and change from B3-LYP to Hartree-Fock	± 0.15 Å	± 3°	28.7
Change to Hartree Fock and use mixture of DZDP, 6-31**G and 3-21G basis sets	± 0.2 Å	± 4°	18.7
		Standard method:	11.2
		Standard method (zero-point vibrational energies):	11.7
		Results from Ziegler & Margl (ref. 7)	13.7
		Results from Svensson et. al. (ref. 36)	18.2

Table 3.3.3: Variation in structural and energy parameters of olefin insertion transition state using different methods and basis sets, and comparisons to published results of analogous reactions. HF/3-21G was excluded from this table as the structure was too different to compare parameters.

any bonding between palladium and oxygen at this point. As the structure by Ziegler and Margl did not have this bond either, the difference was probably down to the presence of a diimine ligand instead of a diphosphine ligand.

The variation in bond lengths, bond angles and activation energy from other basis sets and methods is again shown in **table 3.3.3**. Once again, the difference in the geometry was not significant enough to make a qualitative difference, apart from the results using the 3-21G basis set. However, unlike enthalpy, there was a significant difference between the activation energies calculated by Hartree-Fock and B3-LYP. The Hartree-Fock-calculated activation energies were about double those calculated by B3-LYP, and with the B3-LYP energies closer to previous experimental and theoretical results, it was decided that B3-LYP would be significantly more reliable than Hartree-Fock when considering the relative feasibility of two or more competing steps.

Once again, it should be noted that the effect of the second carbonyl group had been neglected.

3.3.4 Reaction path

The transition state structure still left unanswered the question of the reaction path between the reactant, transition state and product, and it was unclear from the structure of the transition state alone whether there would be any intermediates during olefin insertion.

By applying an IRC job to the structure from the transition state in both directions, and completing the path by optimising the furthest point optimised in each direction, a reaction profile was obtained, as shown in **figure 3.3.4.1**. Some of the structures passed through are shown in **figure 3.3.4.2.**

(Note: Throughout this project, the IRC curves reported here have been slightly smoothed. Individual points were liable to be sporadically high or low. There was no smoothing introduced to the sections obtained from optimising the final points from IRC runs, but some points were omitted when the step proceeded up in energy instead of down.)

The olefin insertion step was perhaps the most complicated stage in the whole propagation cycle. One small simplification was to break this stage down into two steps with their own energy barriers and an intermediate separating the two. The

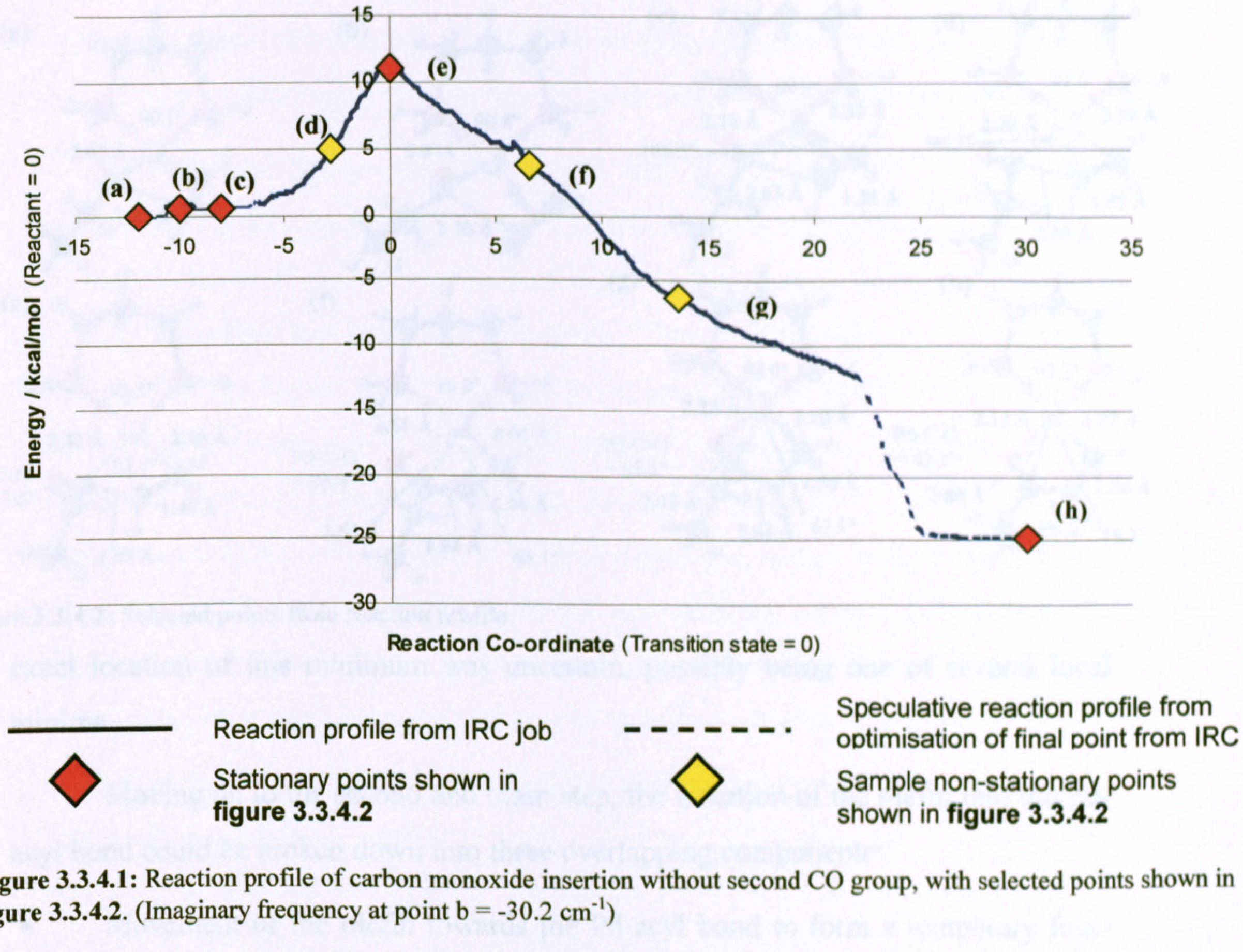


Figure 3.3.4.1: Reaction profile of carbon monoxide insertion without second CO group, with selected points shown in **figure 3.3.4.2**. (Imaginary frequency at point b = -30.2 cm^{-1})

second and main step was the (still complicated) insertion of the olefin into the Pd-acyl bond.

The first step, on the other hand, was a simple step involving the rotation of the olefin, about the π-coordinate bond, from the more stable conformation where the olefin double bond is perpendicular to the palladium-ligand plane (shown in **figure 3.3.4.2 (a)**) to the slightly less stable conformation (0.5 kcal/mol higher, or 0.6 kcal/mol including zero-point corrections) where the olefin double bond is parallel to the plane (shown in **figure 3.3.4.2 (c)**). The energy barrier to this local transition state (shown in **figure 3.3.4.2 (b)**), however, was only 0.8 kcal/mol (1.2 kcal/mol including zero-point corrections), so it is highly unlikely that this local step would have any significant effect on the rate of reaction. (The reasons for this step are considered in section 5.3.1.) There were some small discrepancies in the structure of the intermediate, depending on whether the structure was reached from the olefin rotation step (point b) or from the olefin insertion step (point d), but the difference in energies was tiny, less than 0.01 kcal/mol. Nevertheless, it could be deduced from this that the

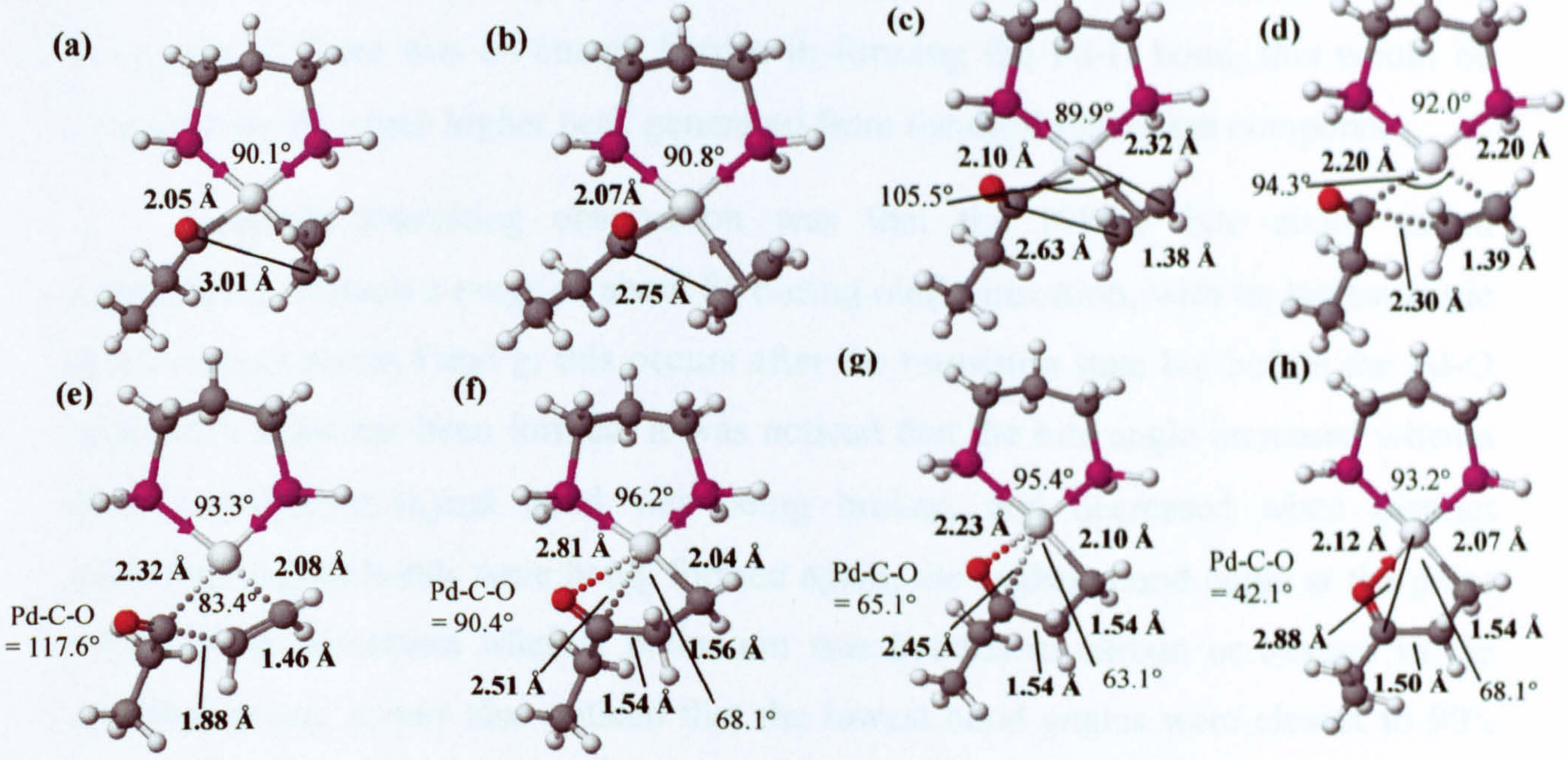


Figure 3.3.4.2: Selected points from reaction profile.

exact location of this minimum was uncertain, possibly being one of several local minima.

Moving on to the second and main step, the insertion of the olefin into the Pd-acyl bond could be broken down into three overlapping components:

- Movement of the olefin towards the Pd-acyl bond to form a temporary four-membered Pd-C-C-C- ring (points c-e);
- Lengthening of the C=C bond as it loses its double bond character, and the shortening of the distance of the new C-C bond being formed (points d-f); and
- Transfer of the old Pd-C (acyl) bond to a new Pd-O co-ordinate bond (points e-h);

This reaction profile was the first real piece of evidence that palladium-II complexes have a strong preference to square-planar four-coordinate structures – not just maintaining this structure at each minimum, but *keeping a four-coordinate structure as closely as possible throughout each step.* As a consequence of this, the most significant finding was that the formation of the Pd-O coordinate bond was not, as one might have assumed, a separate step after olefin insertion, but an inseparable component to the olefin insertion step. This may partly be due to a very strong attraction between the palladium and oxygen atoms, but the likelier contributing factors are that: one would expect a five-membered ring present once the Pd-O bond has been formed to be far more stable than any four-membered ring; and that after the

olefin insertion, there are arguably an unstable five bonds to the carbon atom bonded to oxygen. If there was an energy barrier in forming the Pd-O bond, this would be swamped by the much higher peak generated from the olefin insertion component.

Another interesting observation was that the P-Pd-P bite angle varied significantly through a range of about 8° during olefin insertion, with its largest angle reach around points f and g; this occurs after the transition state but before the Pd-O coordinate bond has been formed. It was noticed that the bite angle increased when a distinct palladium-ligand bond was being broken, and decreased when distinct palladium-ligand bonds were being formed again; the highest bond angle at the point where it was uncertain whether palladium was bonded to carbon or oxygen in the carbonyl group. It was also noticed that the lowest bond angles were closest to 90°, the bond angle one would expect in a perfect square-planar complex. It could be that the flexible diphosphine ligand adjusts its bite angle to form the most stable geometry relative to the other ligands on palladium. It is therefore possible that the flexibility of the positions of phosphorus atom may be able to stabilise some of the transition states. It would take a considerable amount of extra work to test this theory, but it might well explain why the less flexible dppe ligand, with its 5-membered palladium-diphosphine ring, is a less efficient catalyst. One small piece of supporting evidence was that the less flexible ligand studied by Ziegler and Margl had an energy barrier that was 2.5 kcal/mol higher, but as they used a different basis set and method, no reliable conclusions can be drawn from this.

The P-Pd-P bite angle has previously been studied by analysing the relevant structures available in the Cambridge Structural Database.[84] It was found that diphosphine ligands that were sufficiently flexible could bond at the bite angle appropriate to the geometry of the complex (i.e. 90° for square planar and octahedral complexes, 114° for tetrahedral complexes), but those that were unable to adjust to these angles did not bond as a bidentate ligand at all. These findings seem to add further weight to the theory that the P-Pd-P bite angle is *very* sensitive to adopting the conformation that will bring maximum stability to the complex.

Finally, it was during optimisation of the reaction path that it was noticed that the acyl group could be optimised in two different conformations, by rotation of the dihedral angle around the Pd-acyl bond (O-C-Pd-P) by 180°. The difference to the energies of stationary points was very slight (no more than 0.3 kcal/mol), so there was

little point in duplicating all of the results for this different conformation. It should, however, be noted that in all the reaction schemes proposed in this thesis, there would be two parallel reaction schemes whilst there is a Pd-acyl bond, one for each of the Pd-acyl bond environments.

3.3.5 Inclusion of second carbonyl group in optimisations of minima

It was later decided to re-run all of the optimisations of the olefin insertion stage with the next carbonyl group added to the copolymer chain. There were several reasons for doing this: firstly, during optimisation of the carbon monoxide insertion transition state, it had been discovered that the second carbonyl group along the chain was playing a part in the reaction (see section 3.4); secondly, earlier work by Ziegler and Margl had found that the second carbonyl group of the chain did interact with the chemically active atoms; and thirdly, this was a factor that had to be considered when attempting to optimise the full complex.

Starting by adding the second carbonyl group to the reactant structure, a structure similar to the structure optimised by Ziegler and Margl was optimised, as shown in **figure 3.3.5.1**. In this case, there was quite clearly a Pd-O axial interaction above the square plane, creating a five-co-ordinate square pyramidal structure. However, if, instead, the carbonyl group started away from the palladium centre, the optimisation converged instead on a structure where the oxygen atom was drawn towards the positively-charged carbon atom on the next carbonyl group, as illustrated

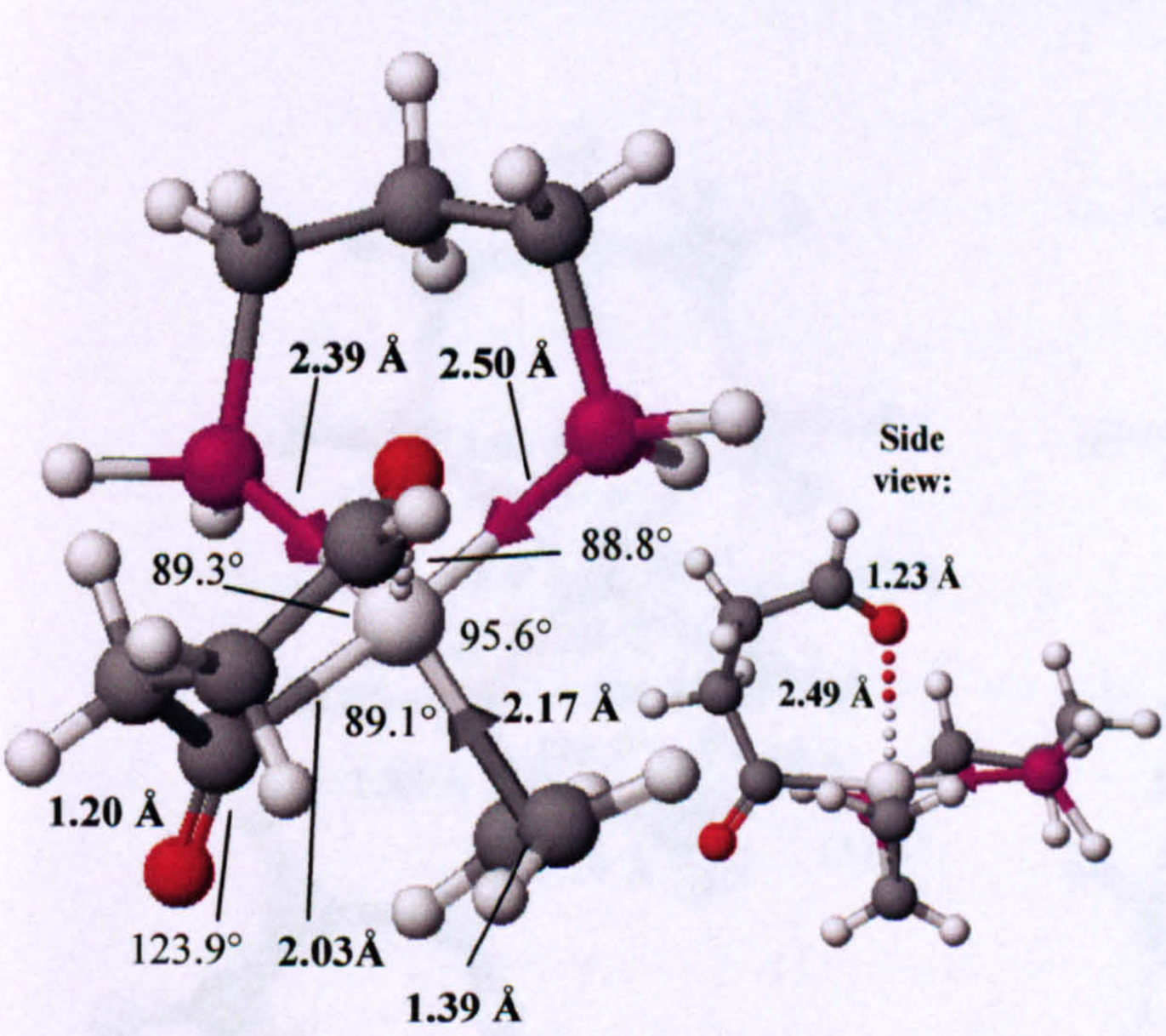


Figure 3.3.5.1: Olefin insertion reactant optimised with second CO group interacting with palladium centre.

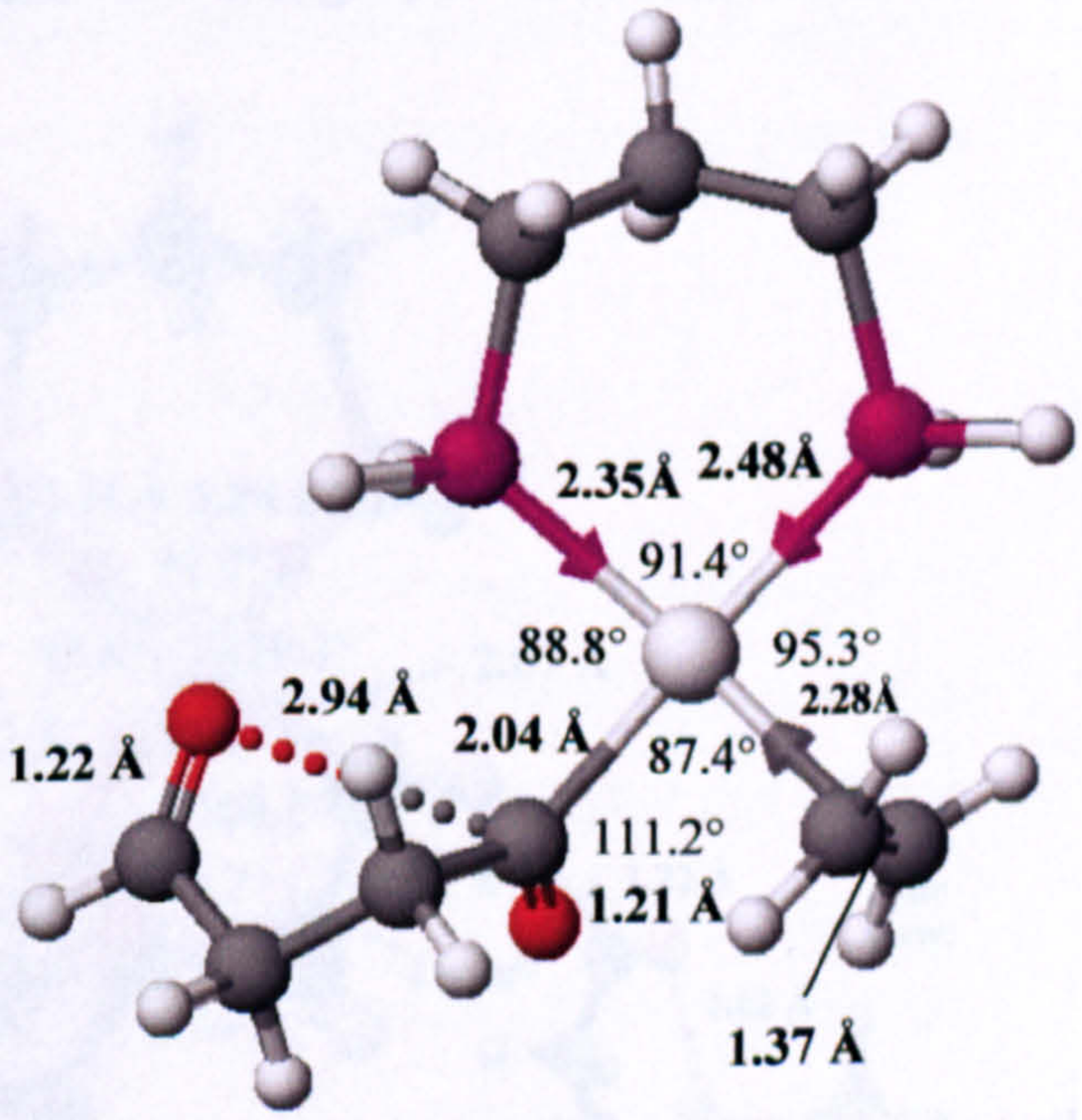


Figure 3.3.5.2: Olefin insertion reactant optimised w second CO group interacting with first CO group.

in **figure 3.3.5.2**. Unexpectedly, the energy of this structure was 0.7 kcal/mol *lower* (unchanged when including zero-point corrections) than the structure optimised by Ziegler and Margl. It was also noted that, in both cases, the structural parameters of the rest of the complex were barely altered by the presence of the new carbonyl group. The structure of the remainder of the reactant, however, remained unchanged whether or not there was any sort of interaction from this carbonyl group.

This difference was too small to be certain which of the two structures is more stable. According to both the preceding step in Ziegler and Margl's paper and this project, the former structure (in figure 3.3.5.1) is formed by the olefin addition step (see section 3.6), so a propagation cycle path exists without going through the latter structure (in figure 3.3.5.2). However, the latter structure could well allow olefin insertion with the second carbonyl group of the chain still bonded to the first carbonyl group instead of the palladium atom. This raised a new question: if there was a transition state with the second carbonyl group bonded to the first carbonyl group instead of the palladium, would this provide a lower energy reaction path?

The product structure proposed by Ziegler and Margl was also re-optimised in this project, producing the structure shown **figure 3.3.5.3**. However, an alternative structure, with the second carbonyl group in the chain experiencing dipolar attraction towards the first, was also optimised, as shown in **figure 3.3.5.4**. This latter structure had an energy 3.9 kcal/mol lower (3.3 kcal/mol lower when including zero-point corrections) than the structure proposed by Ziegler and Margl. (It was assumed that an

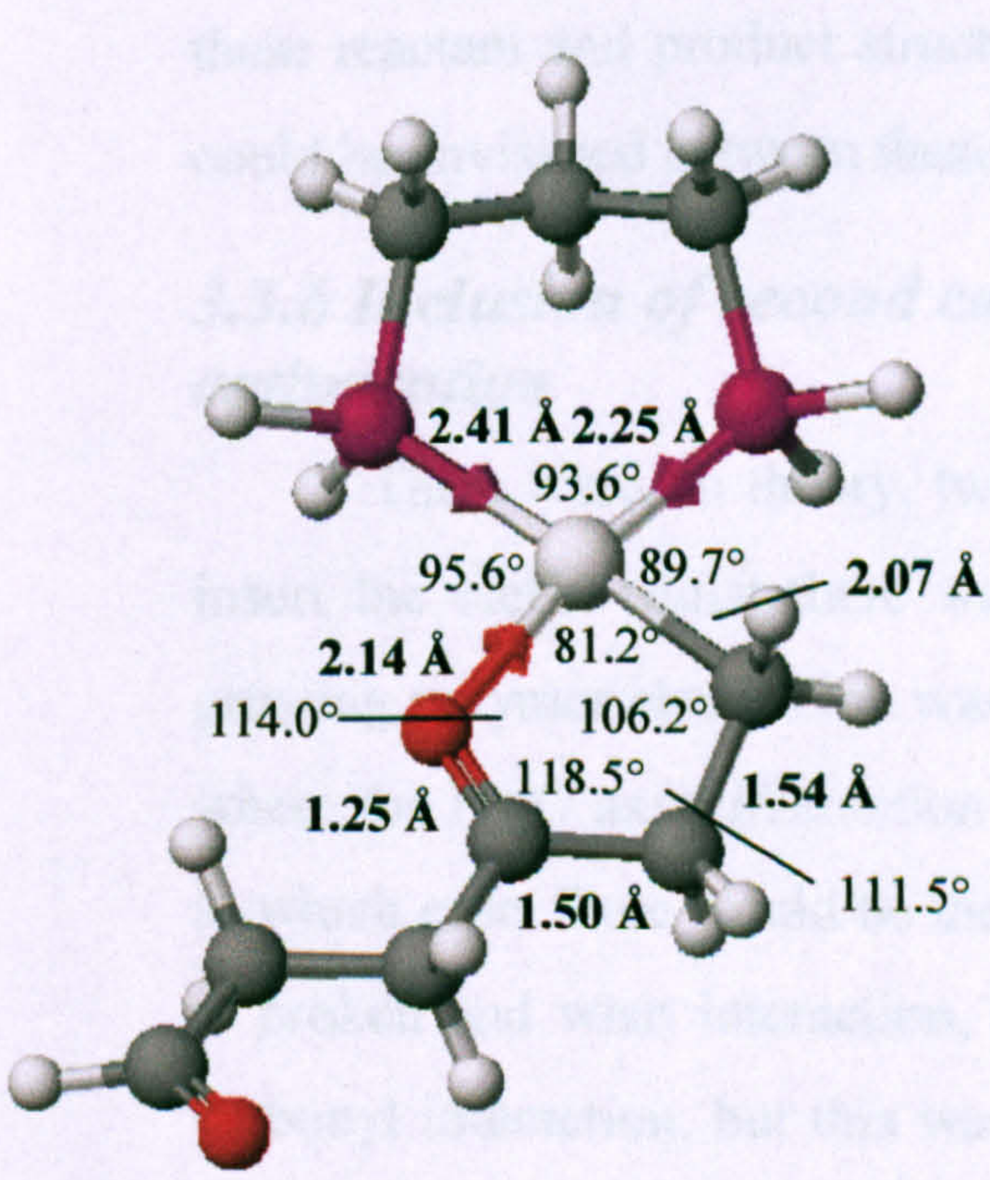


Figure 3.3.5.3: Olefin insertion product with no interaction from second carbonyl group.

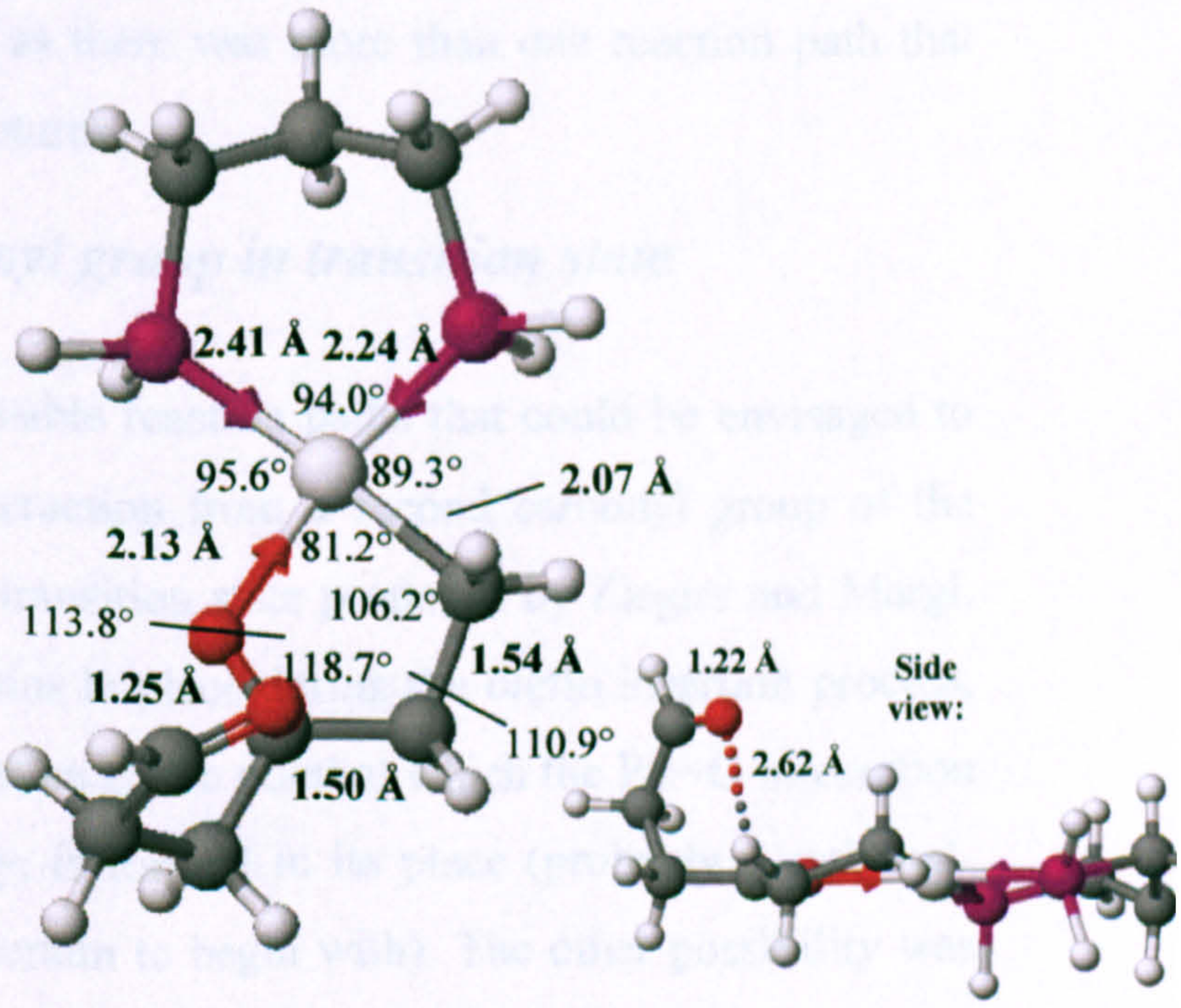


Figure 3.3.5.4: Olefin insertion product with second carbonyl group interacting with first carbonyl group.

Reactant structure \ Product structure	With no interaction from 2nd carbonyl to 1st carbonyl (figure 3.3.5.3)	With weak interaction from 2nd carbonyl to 1st carbonyl (figure 3.3.5.4)
With axial interaction from 2nd carbonyl to palladium (figure 3.3.5.1)	-20.5 (-18.7)	-24.4 (-22.0)
With weak interaction from 2nd carbonyl to 1st carbonyl (figure 3.3.5.2)	-19.8 (-18.0)	-23.7 (-21.3)

Table 3.3.5: Energy changes of olefin insertion from different conformation of reactant and product structures of olefin insertion. (All energies in kcal/mol.)

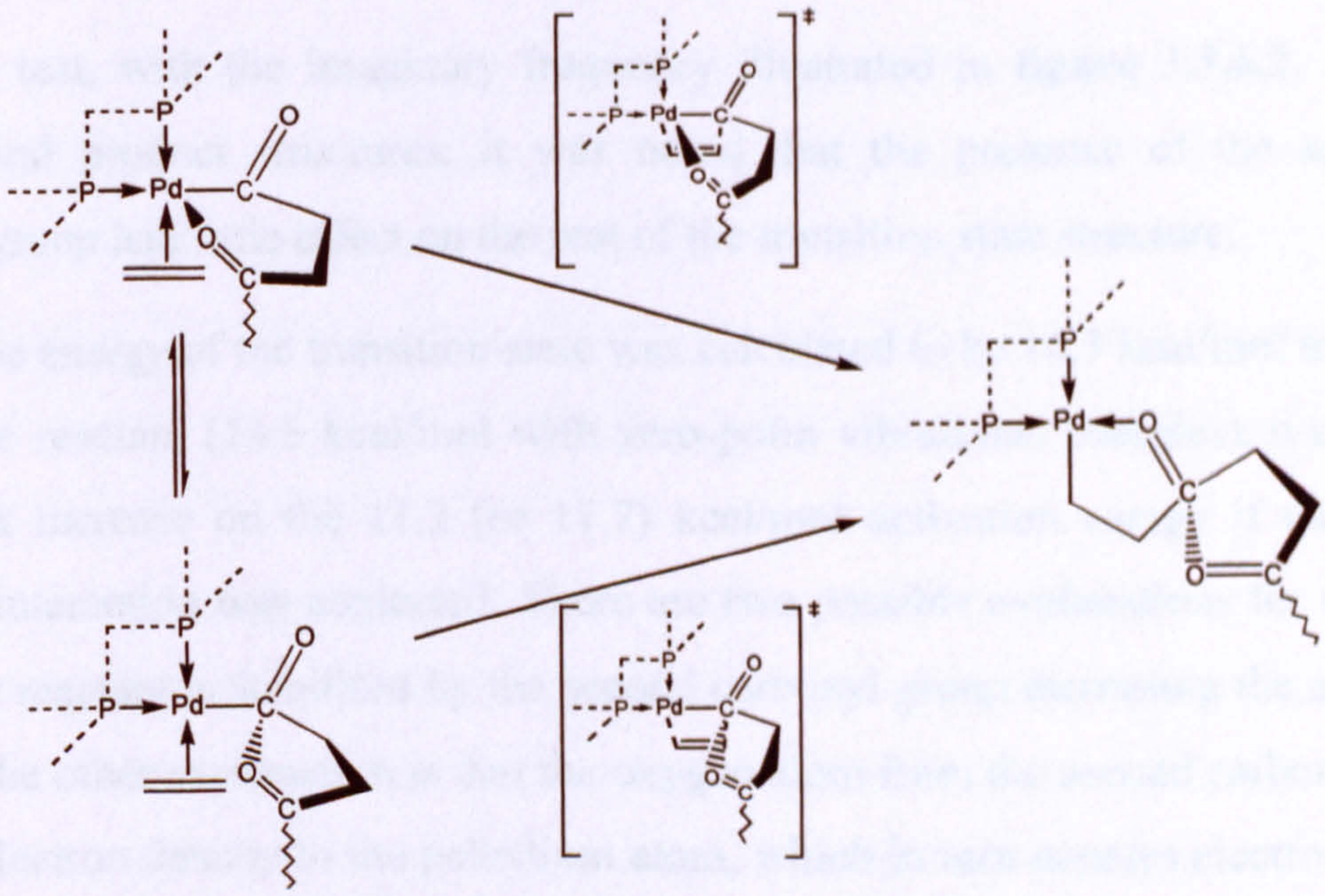
axial interaction between palladium and oxygen in the second carbonyl group of the chain would be geometrically impossible). Once again, it was noted that the presence of a second carbonyl group made little difference to the structure of the rest of the complex.

The enthalpy of the olefin insertion, depending on what reactant and product structures are used, was calculated to be between –19.1 kcal/mol and –24.4 kcal/mol, (or -17.3 kcal/mol and -24.4 kcal/mol including ZPE – details given in **table 3.3.5**), compared to –11.5 kcal/mol calculated by Ziegler and Margl. Once again, it was assumed that the fact that they examined a different complex contributed to the difference in energies, but there was one important additional contributing factor to consider: the effect of the weak interaction between carbonyl groups in the product structure. Ziegler and Margl proposed that the reduction in the energy difference was due to the stabilisation of the reactant structure by the Pd-O axial interaction; in this project, the effect seems to have been cancelled out by the stabilisation of the product structure by the carbonyl-carbonyl weak bond in the chain.

The next task was to establish what transition states could be formed between these reactant and product structures, as there was more than one reaction path that could be envisaged between these structures.

3.3.6 Inclusion of second carbonyl group in transition state optimisation

There were, in theory, two possible reaction paths that could be envisaged to insert the olefin whilst there was interaction from a second carbonyl group of the growing polymer chain. One was the transition state proposed by Ziegler and Margl, where the Pd-O axial interaction remains in place during the olefin insertion process, in which case, there would be the question of the point at which the Pd···O interaction is broken and what interaction, if any, is formed in its place (probably a carbonyl-carbonyl interaction, but this was uncertain to begin with). The other possibility was



Scheme 3.3.6: Possible transition states of olefin insertion with interaction from second carbonyl group.

that the second carbonyl group of the chain remained interacting with the first throughout the olefin insertion stage. The two possibilities are shown in **scheme 3.3.6**.

Starting with the former path, it was difficult to optimise the transition state using the QST3 method because of the number of parameters involved that had to be optimised: all of the variable parameters in olefin insertion without the second CO group, plus the position of the second carbonyl group relative to the palladium group. However, when the position of the olefin and second carbonyl group were initially set to the positions optimised by Ziegler and Margl in their work, a transition state was optimised, as shown in **figure 3.3.6.1**. The validity of the structure was verified by a

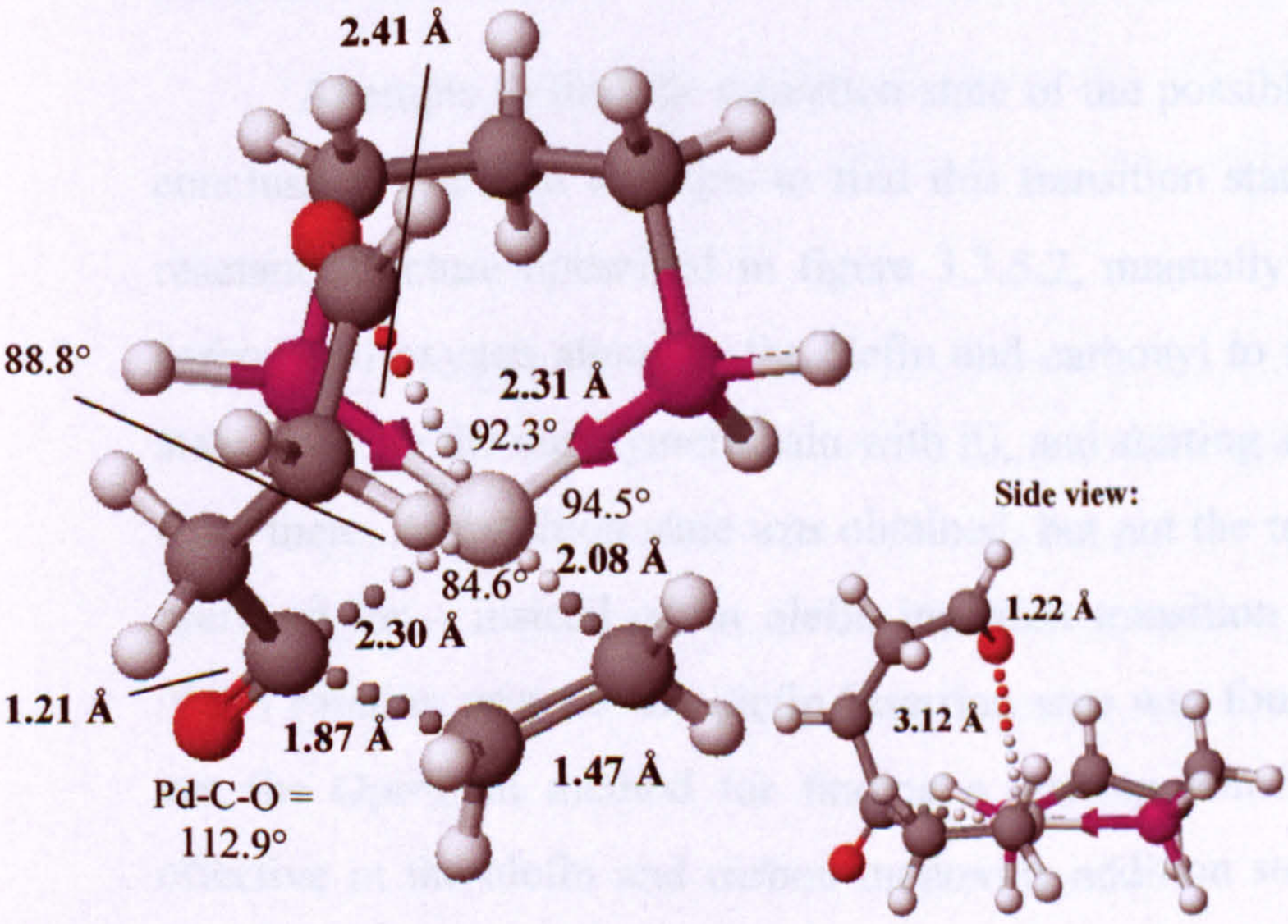


Figure 3.3.6.1: Optimised transition state of olefin insertion with axial Pd-carbonyl bond,

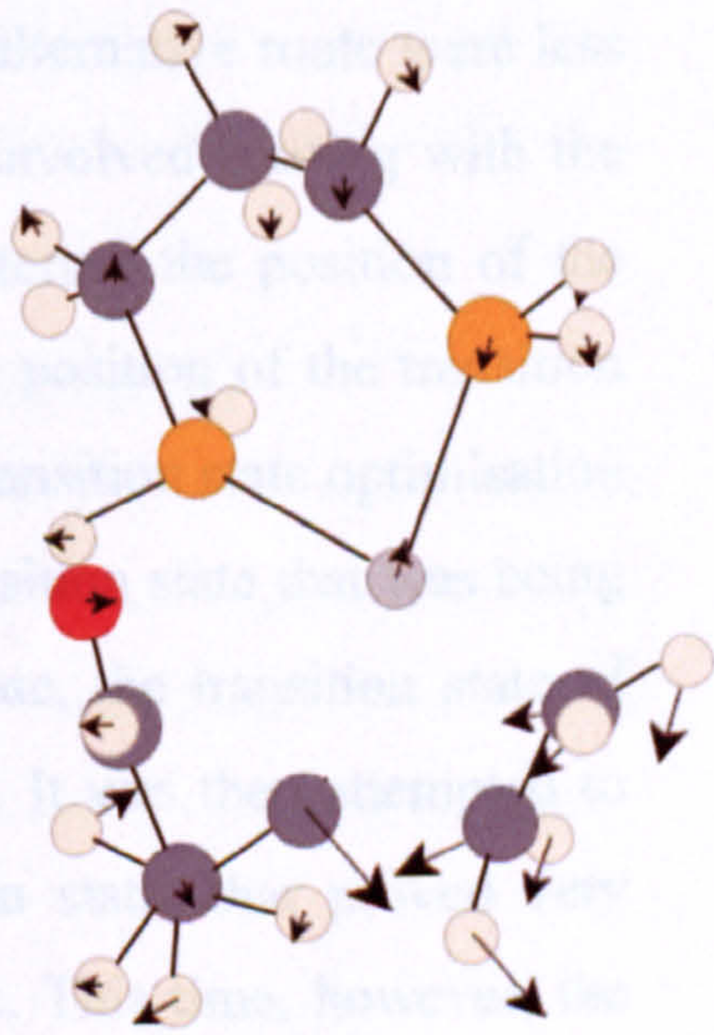


Figure 3.3.6.2: Vibrational mode of imaginary frequency (-326.1 cm^{-1})

frequency test, with the imaginary frequency illustrated in **figure 3.3.6.2.** Like the reactant and product structures, it was noted that the presence of the additional carbonyl group had little effect on the rest of the transition state structure.

The energy of the transition state was calculated to be 14.3 kcal/mol more than that of the reactant (14.5 kcal/mol with zero-point vibrational energies), a small but significant increase on the 11.2 (or 11.7) kcal/mol activation energy if the second carbonyl interaction was neglected. There are two possible explanations for this. One is that the reactant is stabilised by the second carbonyl group increasing the activation energy. The other explanation is that the oxygen atom from the second carbonyl group donates electron density to the palladium atom, which in turn donates electron density to the carbon atom in the first carbonyl group, reducing the positive charge on this carbon atom and making it less susceptible to electrophilic attack. Out of the two possibilities, the former seems more likely. Between the reactant and transition state, the Pd-O distance increased from 2.50 Å to 3.12 Å, suggesting the Pd···O interaction weakened (but see section 5.3.2), whilst on examining the charge density of the carbon atom in the first carbonyl group, the presence of the second carbonyl group was found to make little difference to its charge density.

The activation energy of olefin insertion with interaction by a second carbonyl group calculated by Ziegler and Margl was 15.3 kcal/mol, again slightly higher than the energy barrier calculated in this project, but both works were in agreement with an increase in activation energy arising from presence of a second carbonyl group in an axial interaction to Pd.

Attempts to find the transition state of the possible alternative route were less conclusive. The first attempts to find this transition state involved starting with the reactant structure optimised in figure 3.3.5.2, manually altering the position of the carbon and oxygen atoms in the olefin and carbonyl to the position of the transition state (moving the copolymer chain with it), and starting a transition state optimisation from there. A transition state *was* obtained, but not the transition state that was being searched for – instead of an olefin insertion transition state, the transition state of olefin rotation prior to the olefin insertion step was found. It was then attempted to use the Opt=Path method for finding a starting transition state, that proved very effective in the olefin and carbon monoxide addition steps. This time, however, the job did not even start, because Gaussian was unable to find a path between the two

structures. All attempts to simplify the path – including using an estimated transition state; using the post-olefin rotation intermediate as the reactant structure; ensuring that hydrogen atoms in the estimated transition state were not in the way on the reaction path; and using the original estimated transition state structure as the product structure (as this structure was most likely on the reactant side of the transition state) – all failed to get the path optimisation started.

Compared to the original path, where a transition state was found, it was possible, without knowing the structure of the transition state, to begin an Opt=(QST2, Path=5) job. Unfortunately, the fact that Gaussian was unable to find a path between the two structures to begin with did not necessarily mean that there was no reaction path – the method used to find the reaction path was ultimately a "balls and sticks" approach which did not have much regard for chemical properties at this stage. However, one piece of evidence against this second reaction path was that one might expect the carbonyl-carbonyl bond to lead to the positive charge on the carbon being negated by lone pair donation from the oxygen in the next carbonyl group, which in turn would weaken the attraction of that carbon to the electron-rich olefin. Also, when estimated transition states were being created, it was observed that it was difficult to produce a structure that was distinguishable from the transition state of the standard mechanism.

There are still some other methods for finding the transition state that have not yet been attempted, but none of these ideas show much promise in being any more successful. Furthermore, there is no method that can easily prove that a transition state does *not* exist. Therefore, it was assumed (but not proven) that the reaction path proposed by Ziegler and Margl with a second carbonyl group in the axial position is the only reaction path possible.

3.3.7 Inclusion of second carbonyl group in reaction path

With the transition state obtained, the next question to be answered was at what point does axial Pd···O interaction transfer to a weak carbonyl-carbonyl interaction. By performing an IRC job on the transition state, the reaction profile shown in **figure 3.3.7.1** was obtained, with selected points along the reaction profile shown in **figure 3.3.7.2.**

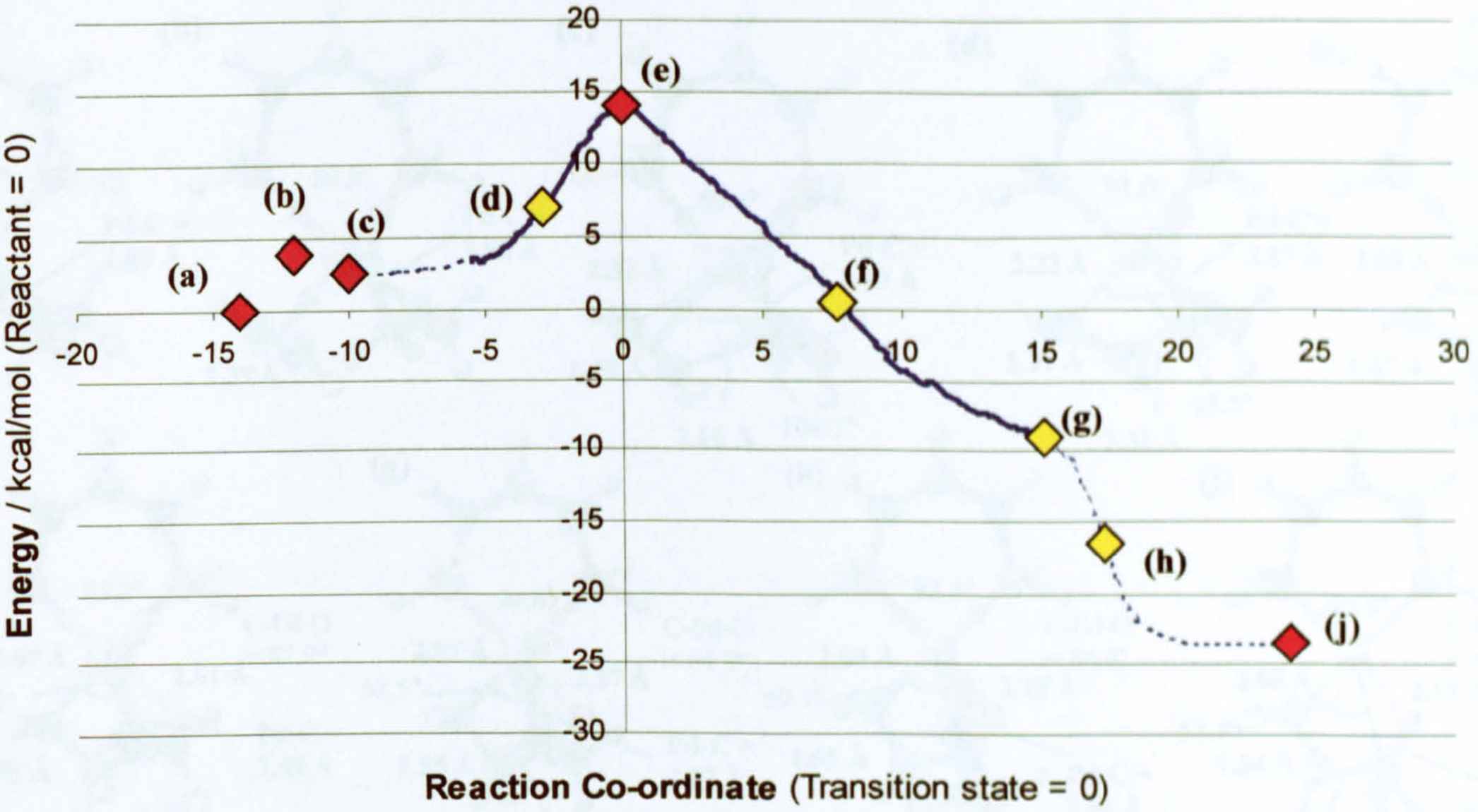


Figure 3.3.7.1: Reaction profile of carbon monoxide insertion with second CO group forming axial interaction to palladium, with selected points shown in **figure 3.3.7.2**.

This reaction profile appeared to give very little new information about the reaction mechanism of the olefin insertion stage, other than that, apart from the increase in the activation energy barrier, the presence of the axial Pd···O interaction has very little effect on the reaction mechanism during this stage. The only feature of significant interest was what happens to the axial Pd···O interaction itself. From examining the structures along the reaction path, it was observed that there was no significant difference in the geometry of the Pd-O bond throughout most of the reaction. There are just two points of interest:

- At the very beginning of the reaction (points a-b), during the olefin rotation stage, the geometry of the Pd-O axial interaction changes significantly. Why this was so is unclear. However, this does seem to increase the energy of the system, as the activation energy of rotation is 4.1 kcal/mol and the energy of the intermediate is 2.6 kcal/mol higher than the reactant (or 3.9 kcal/mol and 2.9 kcal/mol respectively including zero-point corrections). This is considered in section 5.3.2.
- After the olefin has clearly been inserted and the co-ordinate Pd-O bond has clearly been formed (point g), where the C-Pd-O bond angle adjusts to a slightly more stable geometry for a 5-membered ring, the second carbonyl group is pulled away from the palladium atom to form the carbonyl-carbonyl interaction (points h-j).

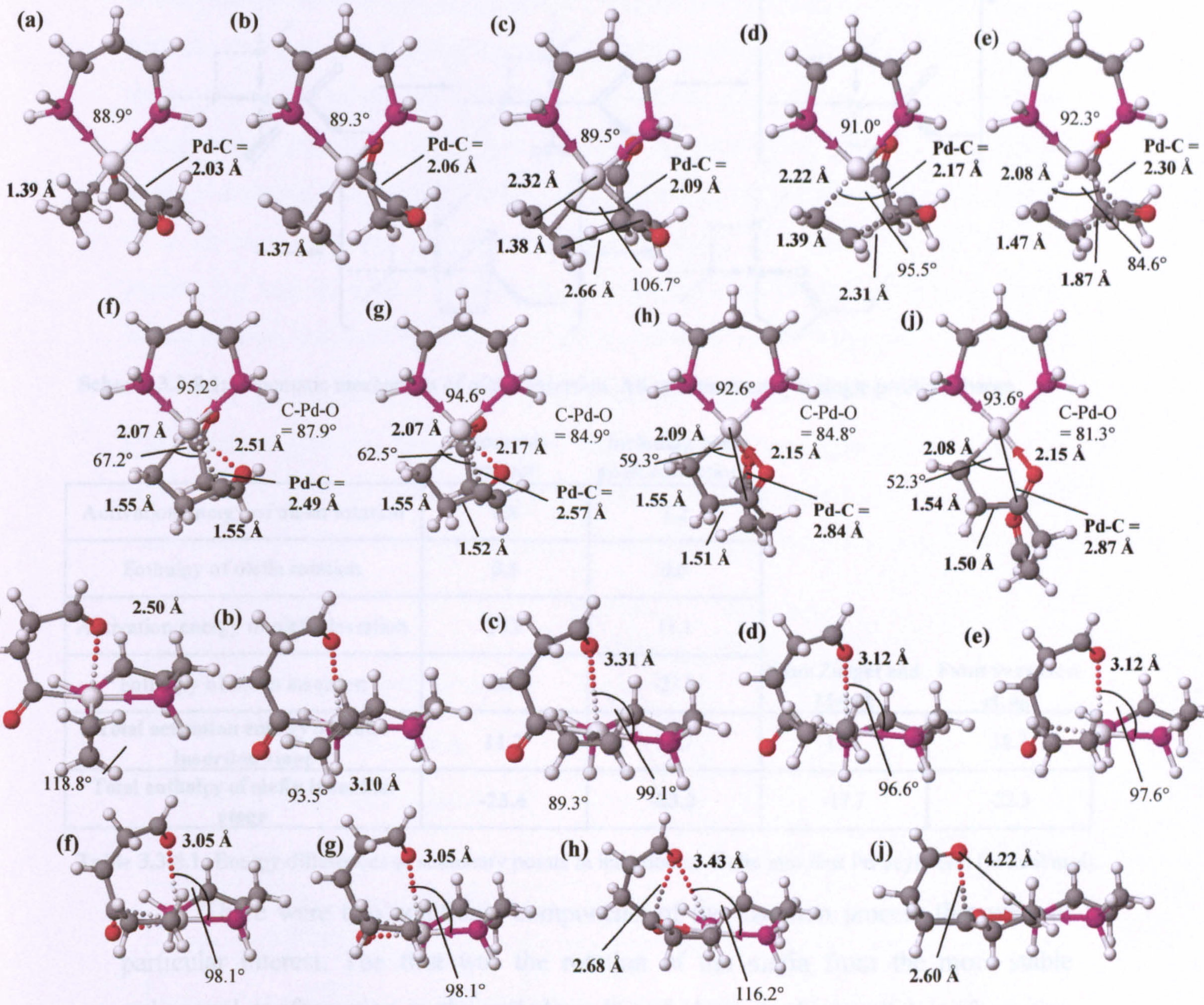
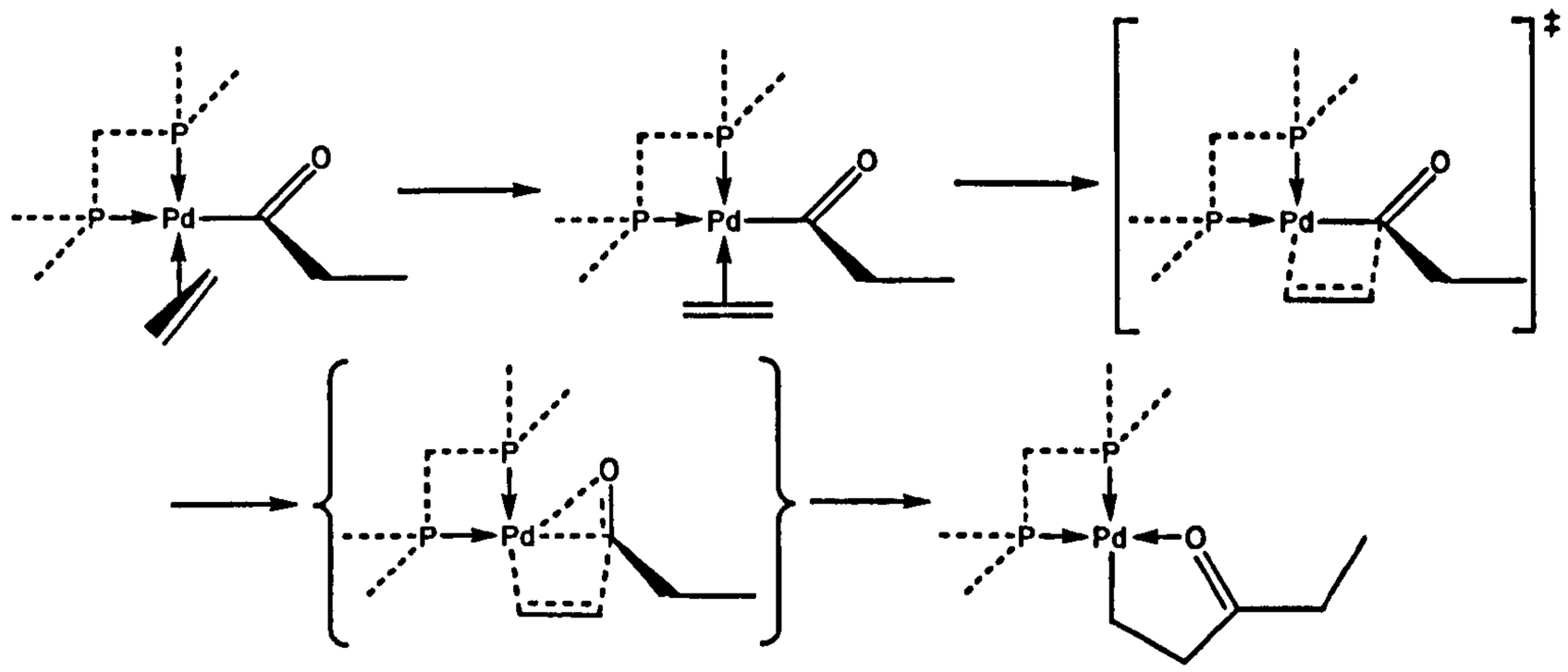


Figure 3.3.7.2: Selected points from reaction profile. (Imaginary frequency of point b = -96.9 cm^{-1})

Given the uncertainty in the bonding geometry of the axial interaction, it can be concluded that the axial interactions from oxygen to palladium are relatively weak compared to the equatorial bonds and have no influence over the reaction mechanism, and the geometry of the axial interaction is solely governed by the bonding environment of the surrounding atoms in the equatorial sites.

3.3.8 Summary of findings of olefin insertion analysis

The studies of olefin insertion into a palladium-acyl bond produced straightforward results that were consistent with the previous work carried out in this area. The rate-limiting component of this stage was indeed the olefin insertion itself, but the activation energy was low enough for olefin insertion to be a feasible stage.



Scheme 3.3.8.1: Schematic mechanism of olefin insertion. All structures carry a single positive charge.

	From this project:	Including zero-point corrections		
Activation energy of olefin rotation	0.8	1.2		
Enthalpy of olefin rotation	0.5	0.6		
Activation energy of olefin insertion	10.7	11.1		
Enthalpy of olefin insertion	-26.1	-23.8		
			From Zielger and Margl:	From Svensson et. al.:
Total activation energy of olefin insertion stage	**11.2**	**11.7**	13.7	18.2
Total enthalpy of olefin insertion stage	**-25.6**	**-23.2**	-17.7	-22.3

Table 3.3.8.1: Energy differences of stationary points in insertion of olefin into *first* Pd-acyl bond (in kcal/mol).

There were two additional components of the insertion process that were of particular interest. The first was the rotation of the olefin from the more stable orthogonal conformation to the palladium-ligand plane, to the parallel conformation needed to begin the insertion process. This was found to be a separate step in its own right with its own energy barrier and intermediate, although the differences in energy were too small to make any significant difference to the reaction dynamics. The other component was, after insertion of the olefin, the transfer of the Pd-acyl bond to a Pd-O co-ordinate bond. This stage was part of a concerted process with olefin insertion, and was not a step in its own right, but the formation of this stable Pd-O bond meant that the reverse reaction would be unlikely.

The other notable feature of the insertion was that the complex retained, as far as possible, a square planar conformation throughout the insertion process.

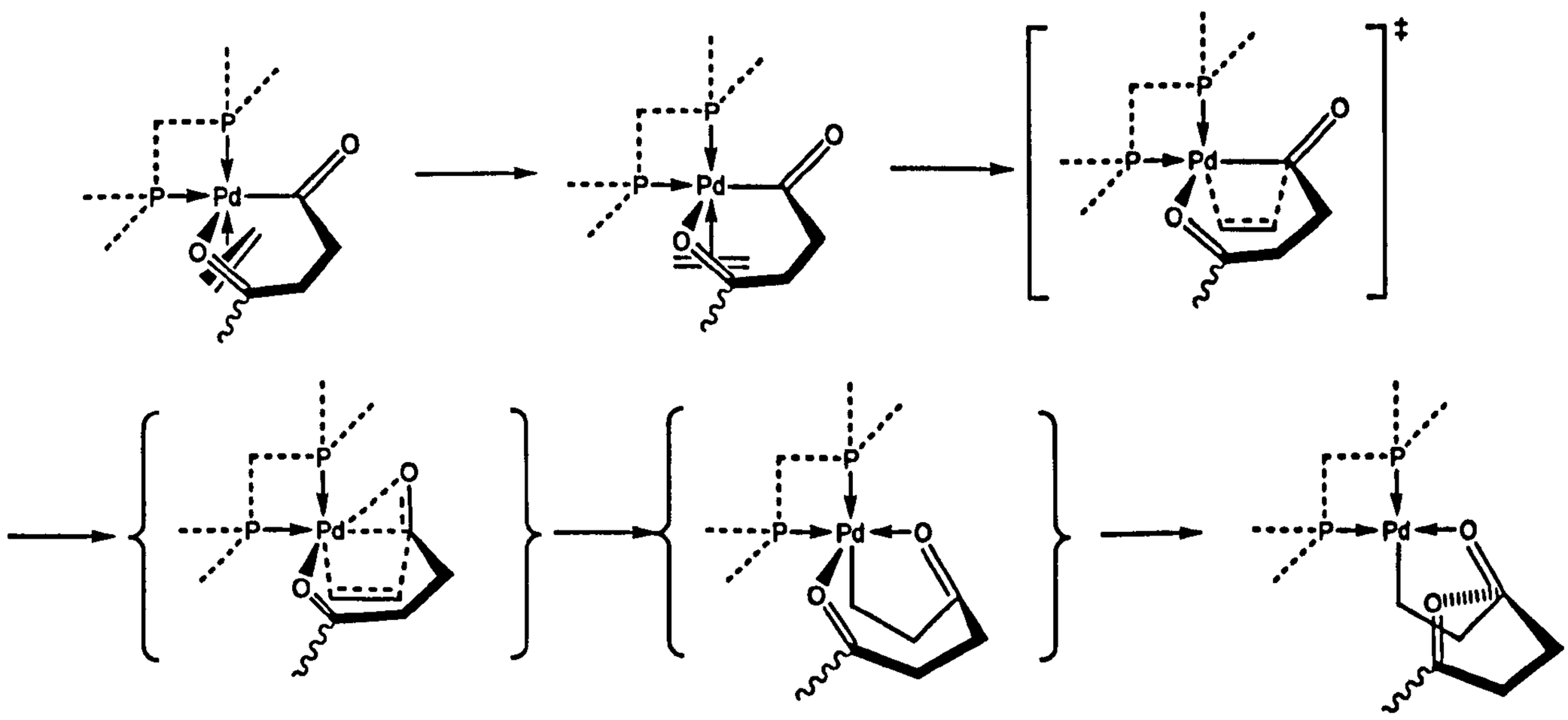
After insertion of an olefin into the *first* Pd-acyl bond, the previously-formed carbonyl group also had an effect on the reaction by forming an axial Pd···O

interaction to create a square pyramidal complex (transferring to a weak interaction with the carbonyl group at the end of the insertion process). This had little effect on the reaction mechanism, but it stabilised the reactant structure enough to increase the energy barrier somewhat, and lessen the fall in the enthalpy of insertion (although not to the extent that Ziegler and Margl had suggested, as they overlooked the possibility of a carbonyl-carbonyl interaction in the product). The possibility of insertion proceeding instead with a permanent carbonyl-carbonyl interaction throughout the insertion stage was considered to be unlikely, but could not be ruled out.

For the insertion of the olefin into the first Pd-acyl bond, the final proposed mechanism is given in **scheme 3.3.8.1**, and the key energy differences are given in **table 3.3.8.1**. With a second carbonyl group present, as would be the case for all subsequent insertions, the final proposed mechanism is given in **scheme 3.3.8.2**, and

	From this project:	Including zero-point corrections	
Activation energy of olefin rotation	4.1	3.9	
Enthalpy of olefin rotation	2.6	2.9	
Activation energy of olefin insertion	11.7	11.6	
Enthalpy of olefin insertion	-27	-24.9	From Zielger and Margl:
Total activation energy of olefin insertion stage	**14.3**	**14.5**	**15.3**
Total enthalpy of olefin insertion stage	**-24.4**	**-22.0**	**-11.5**

Table 3.3.8.2: Energy differences (in kcal/mol) of stationary points in insertion of olefin with interaction from second carbonyl group (i.e. olefin insertion into the second and subsequent Pd-acyl bonds onwards).



Scheme 3.3.8.2: Schematic mechanism of olefin insertion with interaction from second carbonyl group. All structures carry a single positive charge.

the key energy differences are given in **table 3.3.8.2.**

The final question to answer was whether olefin insertion was, as was commonly thought to be, the rate determining step. To find out, the energy barriers of carbon monoxide insertion would need to be considered next.

3.4 Carbon monoxide insertion step

3.4.1 Introduction

The other step that was studied in detail by previous workers[7,8,36] was the carbon monoxide insertion step. The mechanisms proposed by Ziegler and Margl, and Svensson *et al* are shown in **figure 3.4.1.** This was the second step whose reaction path was optimised in this project, although the attempted analysis of the olefin and carbon monoxide addition steps *started* earlier. (For details of why the addition steps took longer to analyse, see sections 3.5-3.6.)

The structures of the reactant and transition state of this migratory insertion process were nothing surprising: simply a lengthening of the Pd-alkyl bond and the insertion of the CO ligand. The product structure, however, was more ambiguous. Without the second carbonyl group intervening, the minimum that was most likely to be formed after passing through the transition state had the four-coordinate structure

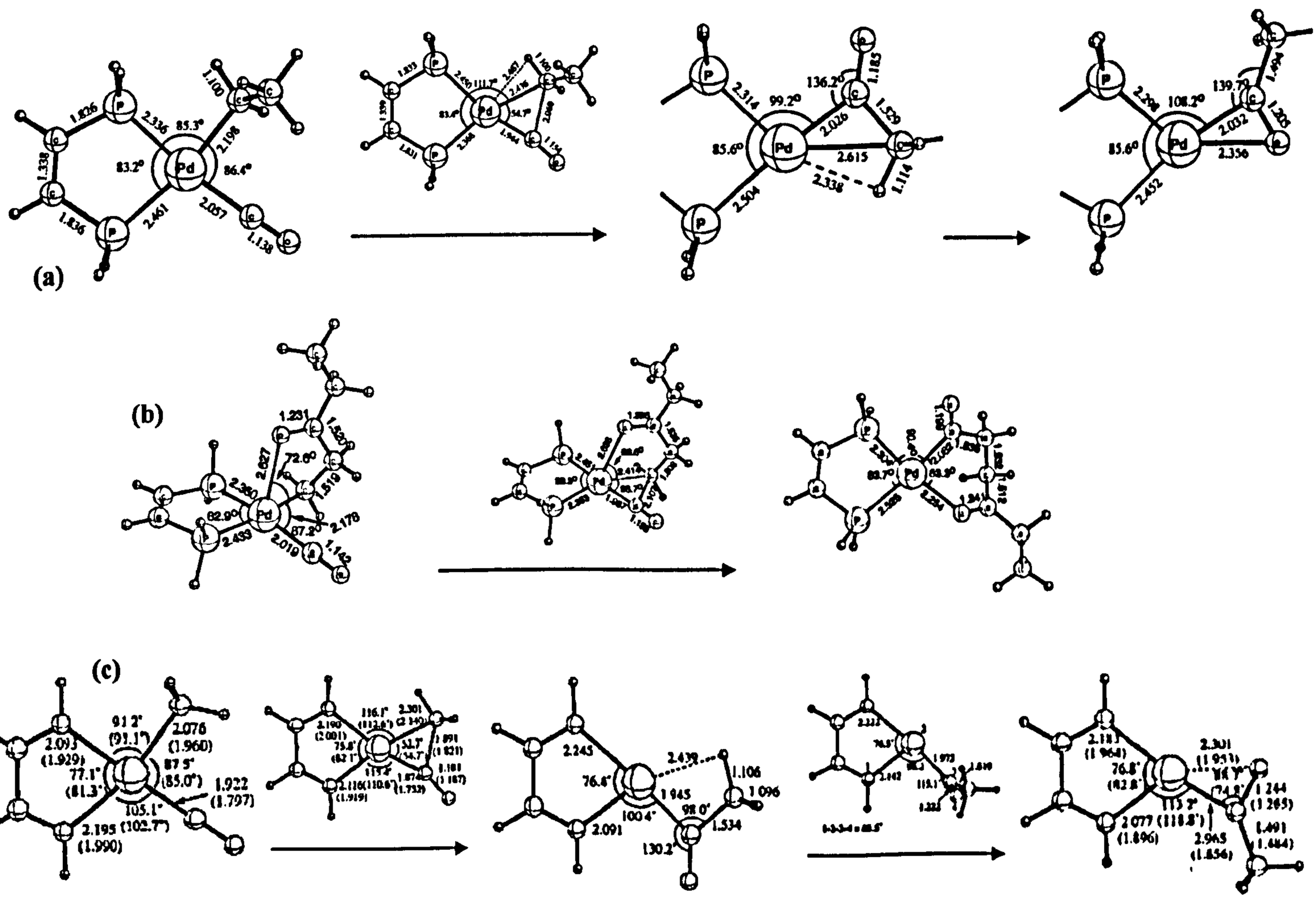


Figure 3.4.1: Structures of reactant, transition state and product of carbon monoxide insertion step previously optimised by **(a)** Ziegler and Margl (ref. 7); **(b)** Ziegler and Margl including interaction from second CO group (ref. 8); and **(c)** Svensson *et al* using diimine ligand instead of diphosphine (ref. 36 – figures in brackets are using nickel instead of palladium).

completed by a β-agostic Pd···H-C interaction. However, the lowest energy conformation of the post-CO insertion product had a bond between the Pd centre and the C=O double bond instead. Svensson *et al* also proposed a transition state to get between these two conformations.

If, on the other hand, the second carbonyl group was included, the mechanism of the reaction changed significantly. In the reactant and transition state, the structure remained unchanged apart from the second carbonyl group forming an axial interaction above the plane. However, a completely different product was formed, as instead of the β-agostic Pd···H-C interaction or bond to the C=O double bond, a far more stable Pd-O co-ordinate bond was formed with the second carbonyl group, to create a six-membered ring. What was unclear was whether either of the other two product structures would have been passed through in order to reach this product, and at what point the Pd-O co-ordinate bond moved from the axial position to the equatorial position.

3.4.2 Reactant and product structures neglecting second carbonyl group

Optimising the minima either side of the carbon monoxide insertion process, in the absence of the second carbonyl group, was a straightforward process. By optimising the reactant, the minimum structure shown in **figure 3.4.2.1** was found. Assuming that the final product was a structure with bonding the Pd to the CO bond and not the structure with the agostic Pd···H-C interaction, the product structure shown in **figure 3.4.2.2** was optimised. It should be noted that it was not possible to optimise a structure with only a bond from palladium to the carbon in the carbonyl

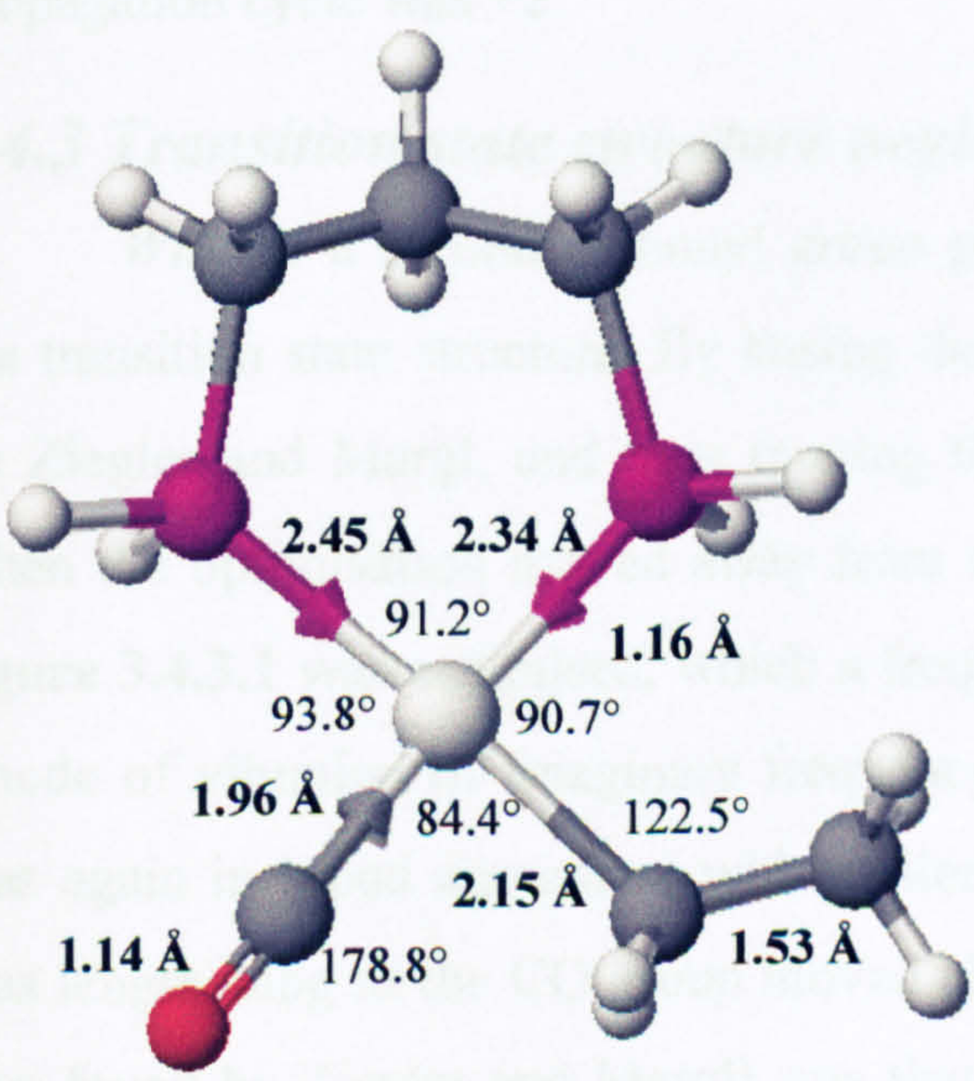


Figure 3.4.2.1: CO insertion reactant neglecting second carbonyl group.

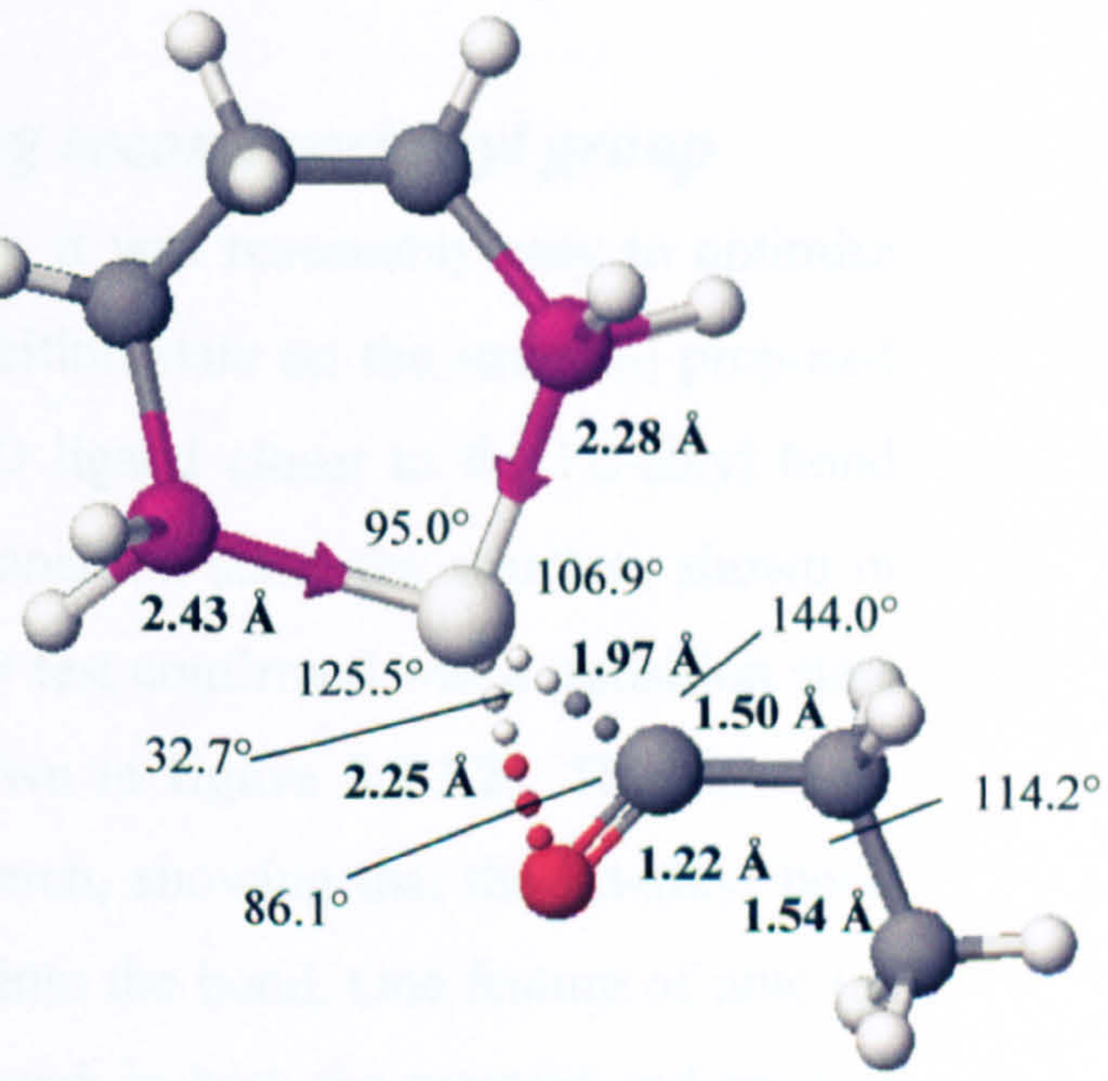


Figure 3.4.2.2: CO insertion product neglecting second carbonyl group.

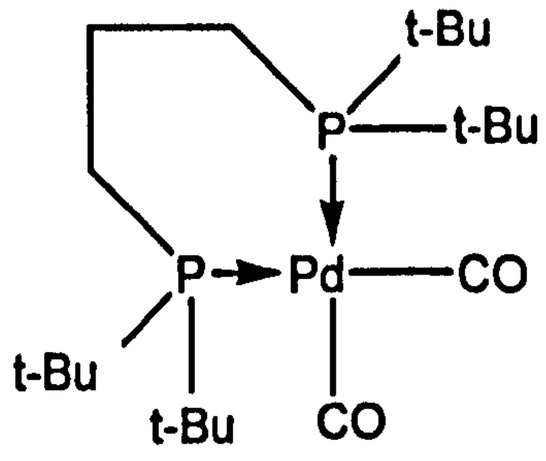


Figure 3.4.2.3: Schematic diagram of the XAJPIH structure from the Cambridge Structural Database for comparison with the theoretically-determined Pd-CO bond lengths.

group – starting an optimisation from this structure resulted in either failure to proceed beyond the first step or optimisation towards the same product structure as before. This further backed up the pattern observed from the olefin optimisation, that the palladium complexes would always arrange themselves to get a four-coordinate planar structure if at all possible. Other than that, there were no unexpected aspects to the reactant and product structures.

The energy difference between the two structures was –7.6 kcal/mol (-6.5 kcal/mol with zero-point corrections). This compared to -2.9 kcal/mol in Ziegler and Margl's work and, interestingly, +2 kcal/mol in the work of Svensson *et al* (but this used a diimine ligand instead of a diphosphine ligand).

The Pd-CO bond length was a parameter that could be compared to a fragment found in the Cambridge structural database (see **figure 3.4.2.3**).[82,85] The variation between the bond lengths was small (±0.02 Å). However, this was not a fully reliable comparison as the oxidation state was 0 (there were no equivalent fragments found with only one CO ligand), whilst the oxidation state of palladium throughout the propagation cycle was +2.

3.4.3 Transition state structure neglecting second carbonyl group

Without a second carbonyl group present, it was reasonably easy to optimise the transition state structure. By basing the transition state on the structure proposed by Ziegler and Margl, and then moving the CO ligand closer to the Pd-alkyl bond when the optimisation moved away from the transition state, the structure shown in **figure 3.4.3.1** was optimised, which a frequency test confirmed was a transition state (mode of vibration of imaginary frequency shown in **figure 3.4.3.2**). This structure was again in broad agreement with earlier research, showing that the Pd-alkyl bond was lengthening as the CO group moved closer into the bond. One feature of note (as also found by Ziegler and Margl) was that although in both the reactant and product

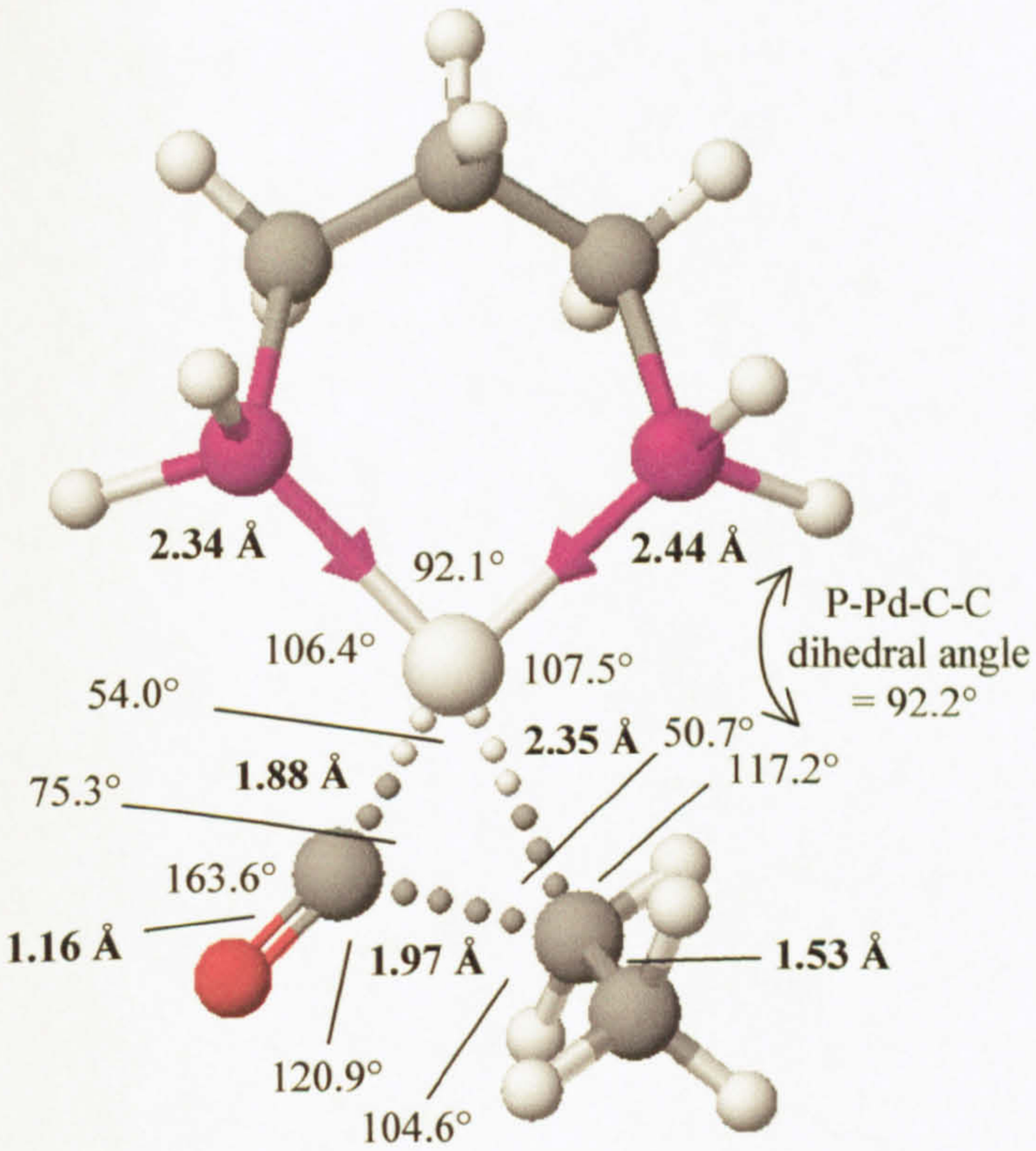


Figure 3.4.3.1: CO insertion transition state neglecting second carbonyl group.

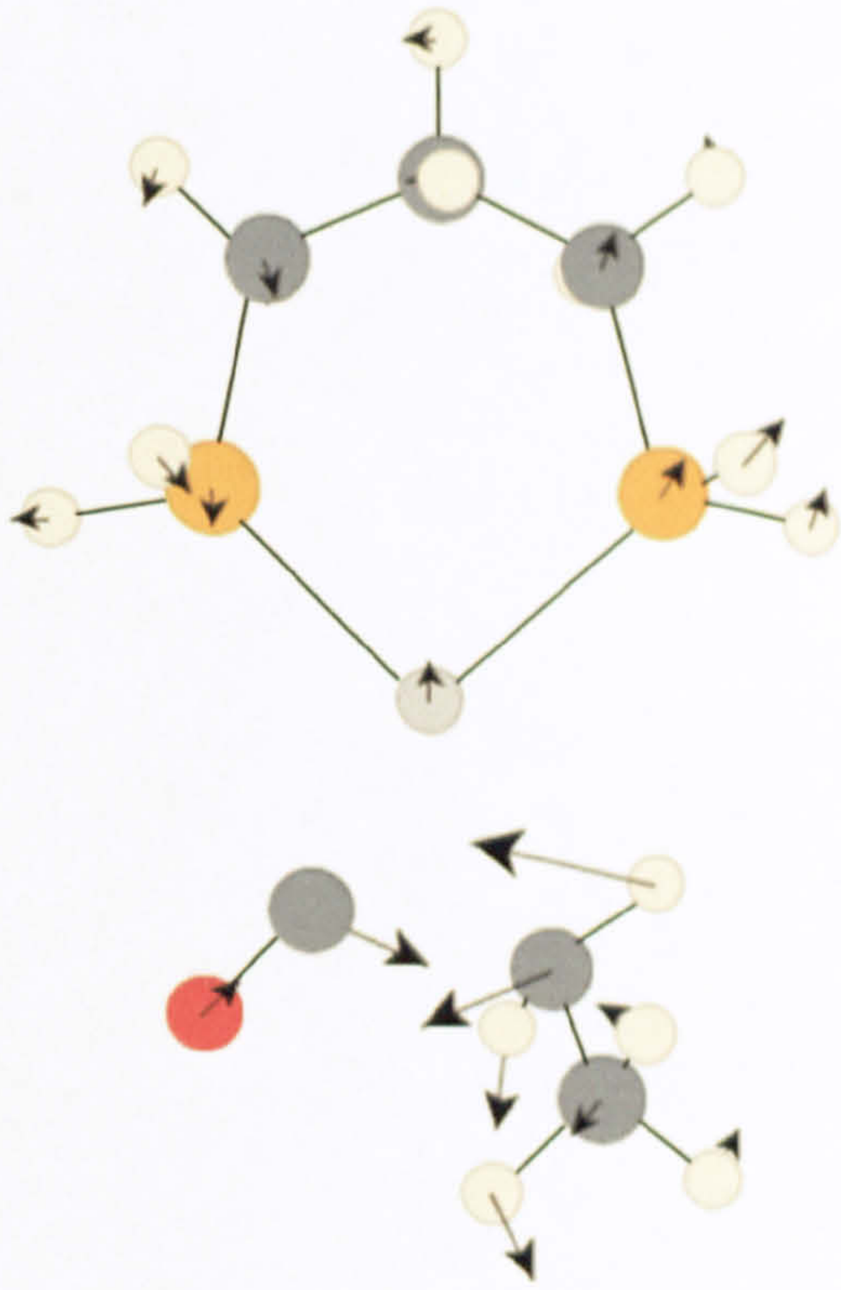


Figure 3.4.3.2: Vibrational mode of imaginary frequency (-304.7 cm^{-1})

structures the alkyl group was in the plane of the palladium ligands, in the transition state the C-C bond in the alkyl group moved out of the plane.

The energy barrier from the reactant was calculated to be 9.2 kcal/mol (8.9 kcal/mol with zero-point corrections), which was slightly less (by 2.0 kcal/mol or 2.8 kcal/mol with ZPE) than the olefin insertion energy barrier, suggesting that the carbon monoxide insertion was probably the faster step, though the margins of error were too high to be certain. This energy compares to 11.5 kcal/mol in Ziegler and Margl's work, and 15.0 kcal/mol in Svensson's work, and made an interesting comparison to the increases in energy barriers observed in the olefin insertion step. By comparing

	This project	Ziegler and Margl (5-membered diphosphine ring)	Svennson *et al* (diimine ligand)
Energy barrier of olefin insertion	11.2 (11.7)	13.7	18.2
Difference from this project	-	2.5 (2.0)	7.0 (6.5)
Energy barrier of CO insertion	9.2 (8.9)	11.5	15.0
Difference from this project	-	2.3 (2.6)	5.8 (6.1)

Table 3.4.3: Comparison of activation energies (in kcal/mol) of olefin and CO insertion stages calculated by different groups researching catalysis using different ligands. (Figures in brackets include zero-point corrections.)

the differences in **table 3.4.3**, it was observed that the increase in the height of the energy barrier found in this work over that of other researchers was roughly equal for both CO and olefin insertion processes. Whilst it cannot be ruled out that the change in method was responsible, it could be that changing the ligand to a less favourable ligand (the dppp ligand used in this project being the most efficient for copolymerisation) hinders both insertion steps roughly equally.

3.4.4 Reaction path neglecting second carbonyl group

With the force constants calculated from the frequency test, the next step was to perform an IRC calculation in both forward and reverse directions. By starting with an IRC calculation and completing the pathway with an optimisation of the final point to the minimum, a path between the reactant and transition state was obtained. However, in the forward direction, the minimum reached was not the product structure but, instead, the structure with an agostic Pd···H-C interaction, as both Ziegler and Margl and Svensson *et al* speculated would be formed. This structure is shown in **figure 3.4.4.1**.

In line with the previous work, this structure was quite clearly not the lowest energy product. The energy was 2.4 kcal/mol *above* the reactant structure (3.0 kcal/mol with zero-point vibrational energies included), compared to –7.6 kcal/mol for the product structure calculated earlier. (Ziegler and Margl calculated +4.5 kcal/mol, Svensson *et al* calculated +8.4 kcal/mol.) It was not clear at this stage whether a further step would be necessary to reach the product structure, or whether

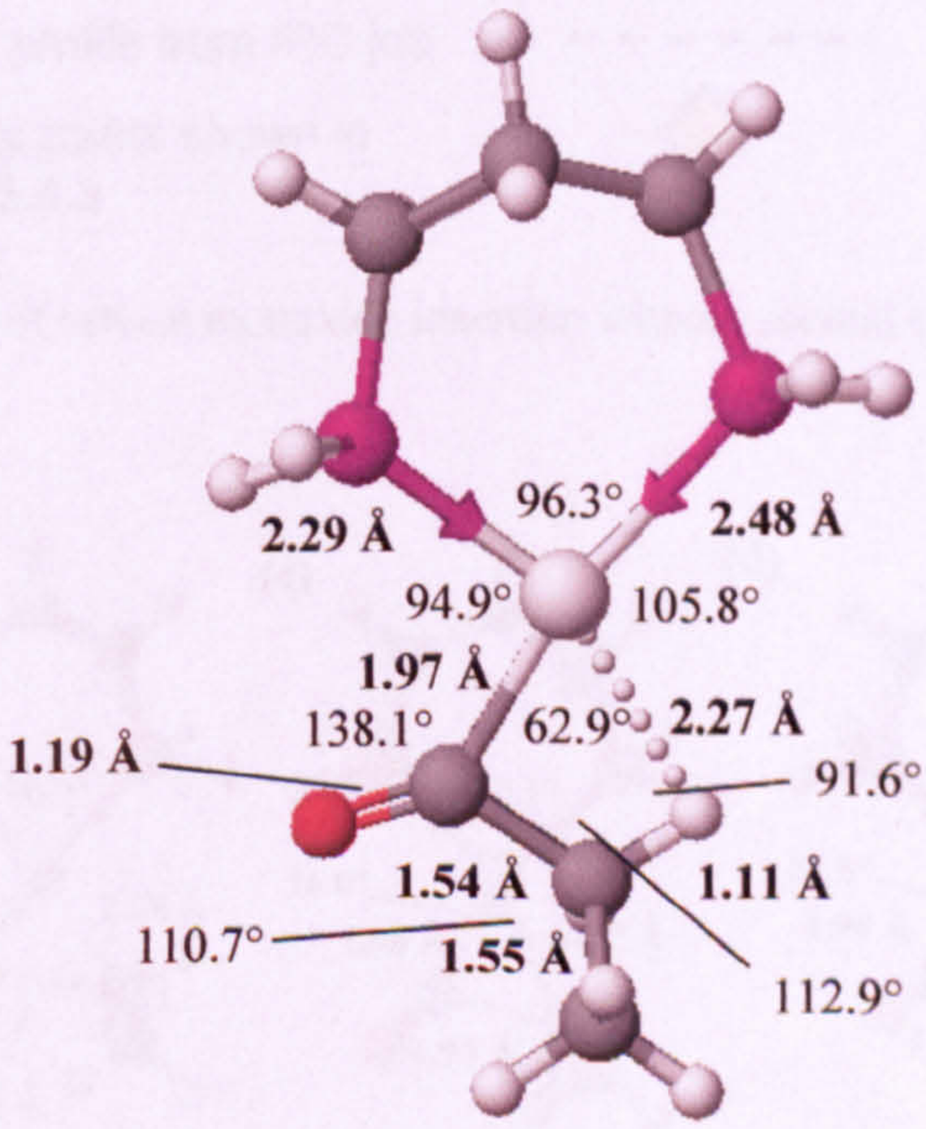


Figure 3.4.4.1: β-agostic Pd···H-C interacting intermediate reached after transition state of CO insertion step (without second carbonyl group).

that step could be by-passed by the Pd···H-C interaction being displaced by an olefin or other ligand.

This turned out to be the first of several complexes (and indeed the occasional non-stationary point in an insertion reaction) to be stabilised by an agostic Pd···H-C interaction. As well as this activity being noted in the previous work relating to this project[7,36], agostic metal···H-C interactions have already been documented to influence other transition metal reactions, particularly in olefin polymerisation.[86]

The reaction profile is shown in **figure 3.4.4.2**, with structures on the route of

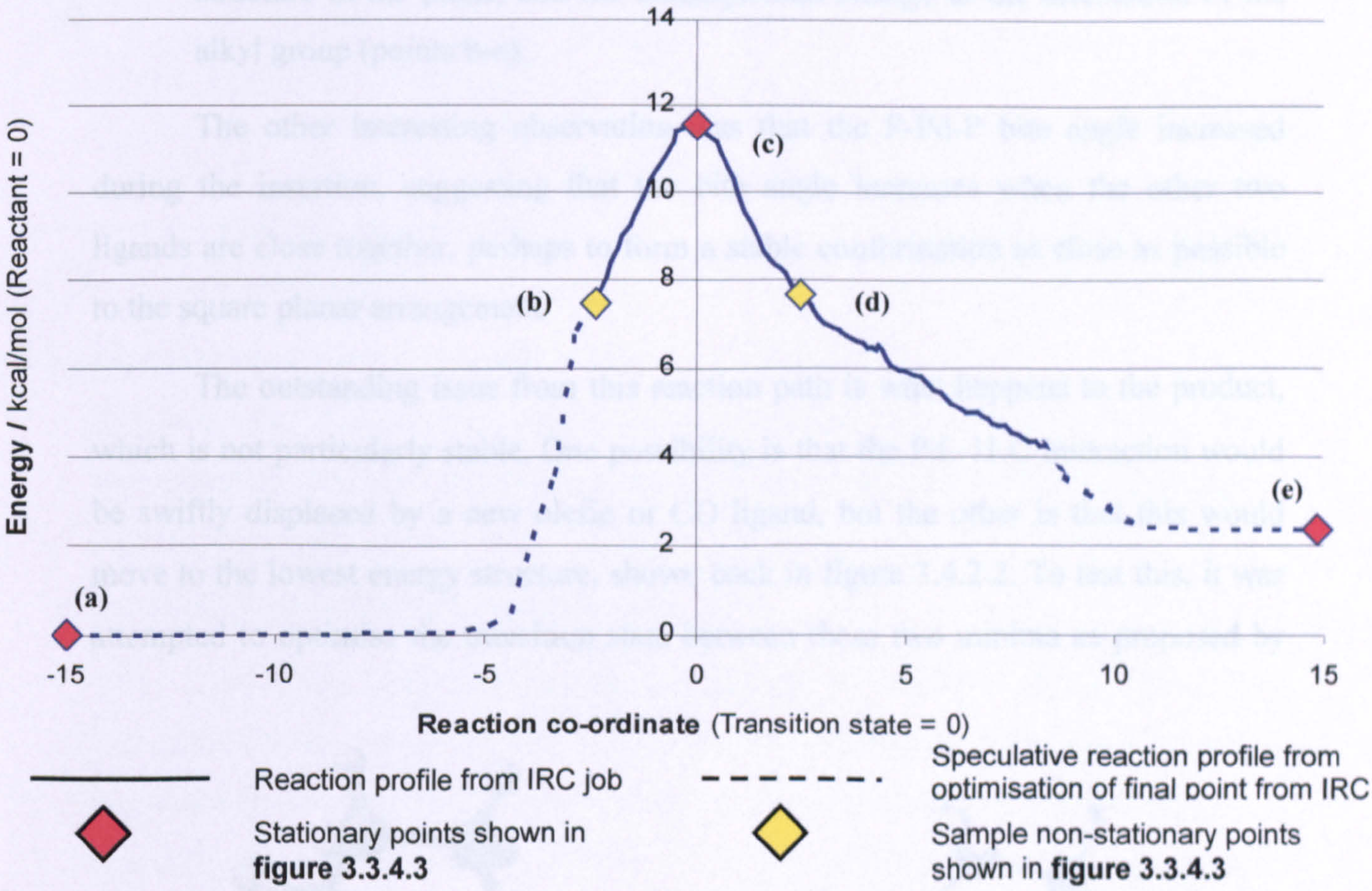


Figure 3.4.4.2: Reaction profile of carbon monoxide insertion without second CO group, with selected points shown in **figure 3.3.4.3**.

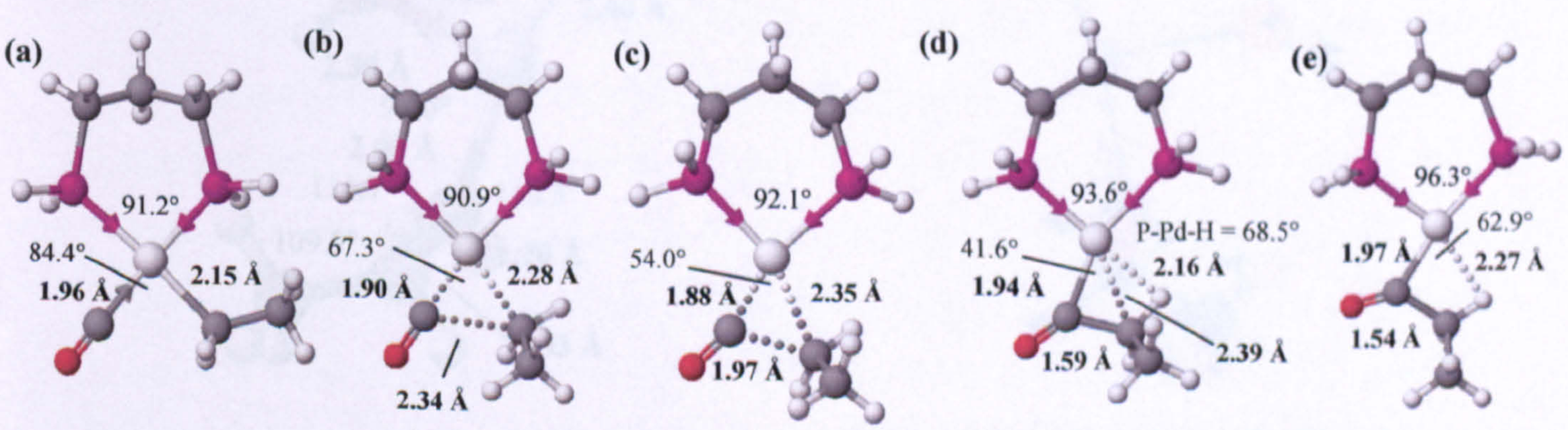


Figure 3.4.4.3: Selected points from reaction profile of carbon monoxide insertion.

the minimum energy path shown in **figure 3.4.4.3**. Observing these structures, there appeared to be three partly overlapping processes involved in CO insertion:

- Rotation of the alkyl group to bring the bonding site to CO into the right position (points a-b);
- The migration of the alkyl group to the carbonyl, observed through the shortening of the new C-C bond, the lengthening of the old Pd-alkyl bond, and the decrease in the C-Pd-C bond angle (points a-d); and
- The formation of a Pd···H-C interaction to maintain a four co-ordinate structure in the plane, and the consequential change to the orientation of the alkyl group (points b-e).

The other interesting observation was that the P-Pd-P bite angle increased during the insertion, suggesting that the bite angle increases when the other two ligands are close together, perhaps to form a stable conformation as close as possible to the square planar arrangement.

The outstanding issue from this reaction path is what happens to the product, which is not particularly stable. One possibility is that the Pd···H-C interaction would be swiftly displaced by a new olefin or CO ligand, but the other is that this would move to the lowest energy structure, shown back in figure 3.4.2.2. To test this, it was attempted to optimise the transition state between these two minima as proposed by

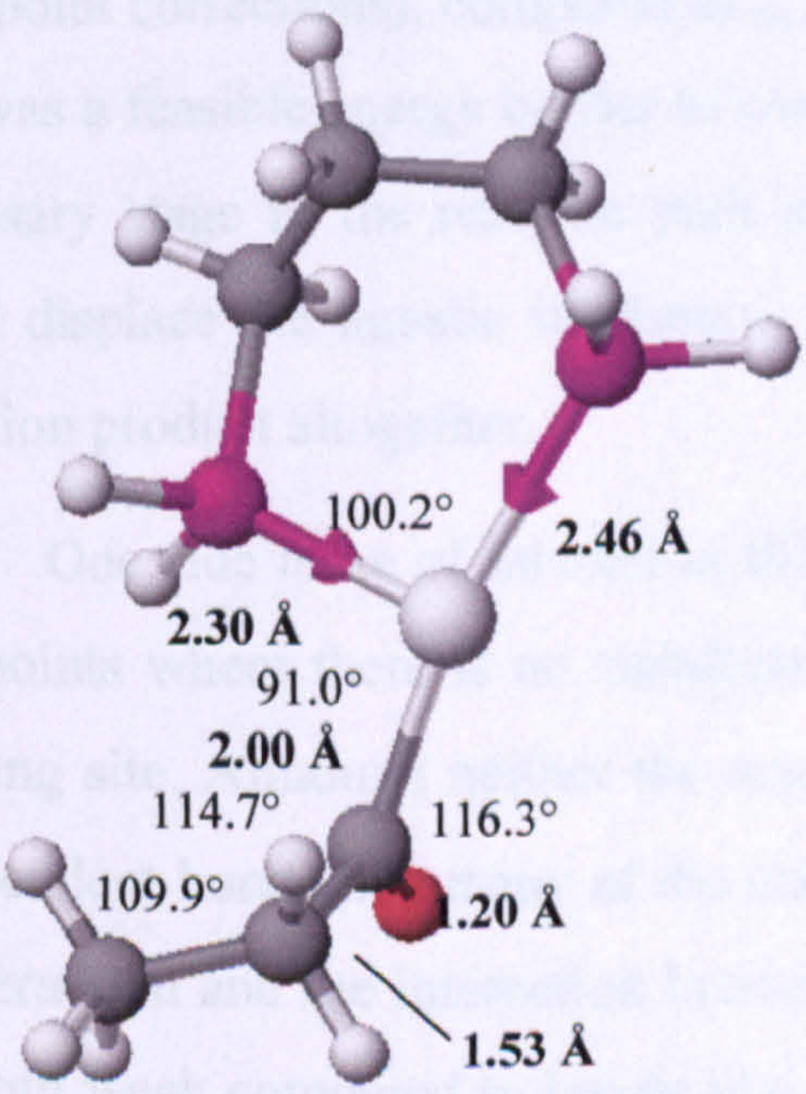


Figure 3.4.4.4: Transition state between two conformations of post-CO-insertion product.

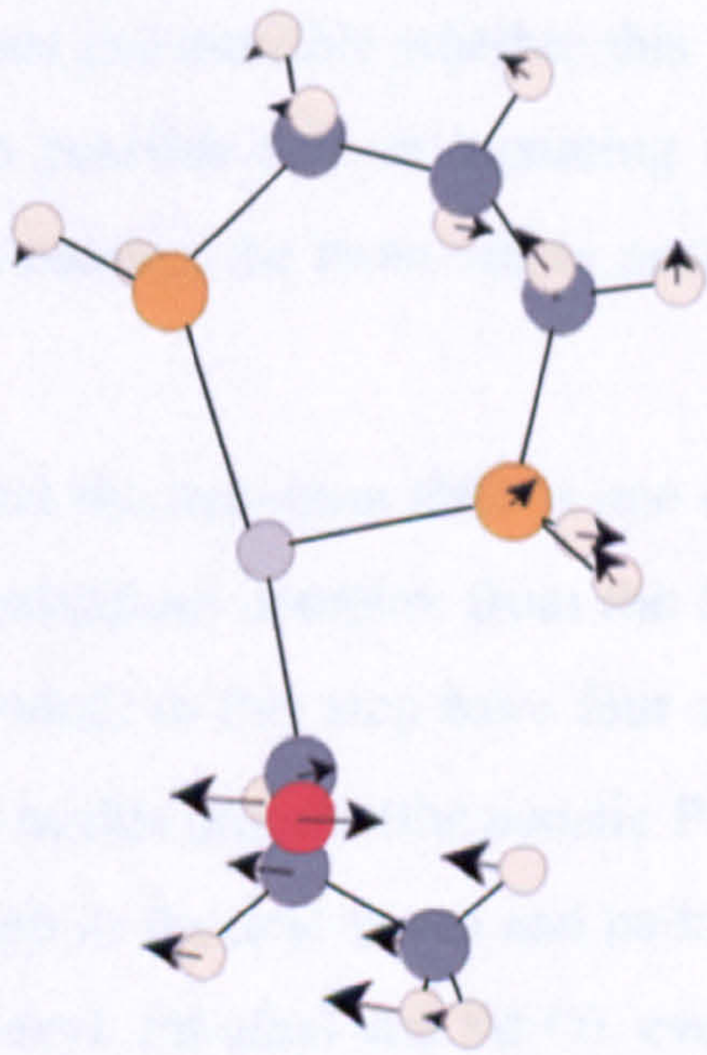


Figure 3.4.4.5: Vibrational mode of imaginary frequency (-33.3 cm^{-1})

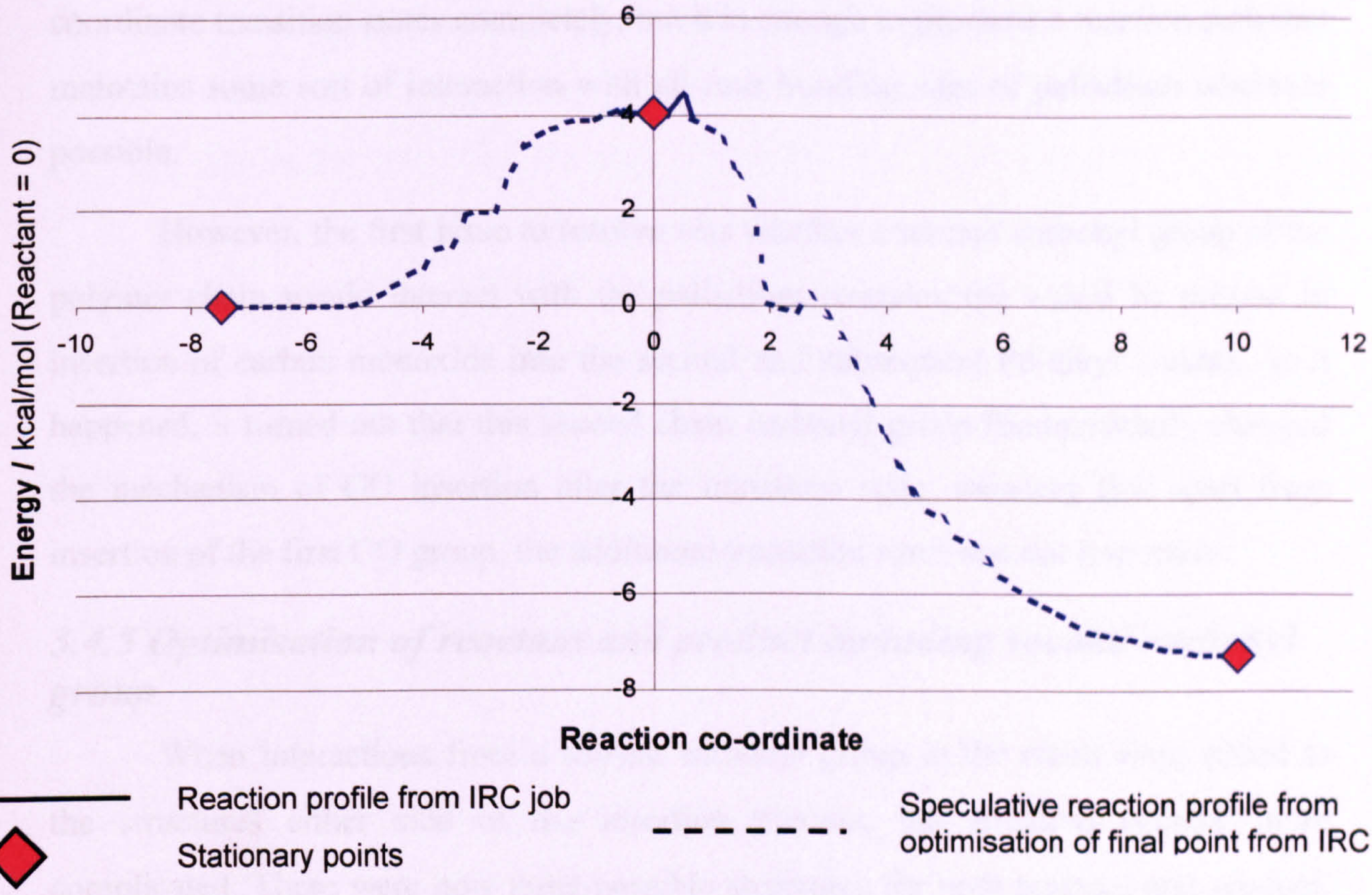


Figure 3.4.4.6: Reaction profile between two product states.

Svensson *et al.* This was successful, and the transition state shown in **figure 3.4.4.4** was obtained, with the vibrational mode of the imaginary frequency shown in **figure 3.4.4.5**. It was possible to trace a full reaction path between the two minima, and this reaction profile is shown in **figure 3.4.4.6**.

The energy barrier for this final stage was 4.1 kcal/mol (4.9 kcal/mol with zero-point corrections), compared to 2.2 kcal/mol calculated by Svensson *et al.* Whilst this was a feasible energy barrier to overcome, it was questionable whether this was a necessary stage in the reaction path at all. It was possible that an incoming olefin could displace the agostic interaction directly, by-passing the most stable post-CO-insertion product altogether.

One side issue of interest in this stage is that the transition state is one of the few points where there is no stabilisation of the palladium complex from the fourth bonding site. Although neither the reactant nor product in this step have four strong independent bonds like many of the mimina found in this process (the agostic Pd···H-C interaction and the interaction between the oxygen in the acyl group and palladium are both weak compared to bonds like Pd-CO, Pd-acyl, Pd-alkyl and Pd-O), even the weakest interaction to the fourth site is 4.1 kcal/mol more stable than the structure

with no interaction to the fourth site at all. This is not enough to rule out three-coordinate transition states completely, but it is enough to promote a reaction path that maintains some sort of interaction with all four bonding sites of palladium wherever possible.

However, the first issue to resolve was whether a second carbonyl group of the polymer chain would interact with the palladium complex (as would be present in insertion of carbon monoxide into the second and subsequent Pd-alkyl bonds). As it happened, it turned out that this second chain carbonyl group fundamentally changed the mechanism of CO insertion after the transition state, meaning that apart from insertion of the first CO group, the additional transition state was not important.

3.4.5 Optimisation of reactant and product including second carbonyl group

When interactions from a second carbonyl group in the chain were added to the structures either side of the insertion process, the situation became more complicated. There were now three possible structures for both reactant and product, and it was not immediately clear which structures would be part of the reaction cycle. In line with Ziegler and Margl's findings, a minimum was optimised as shown

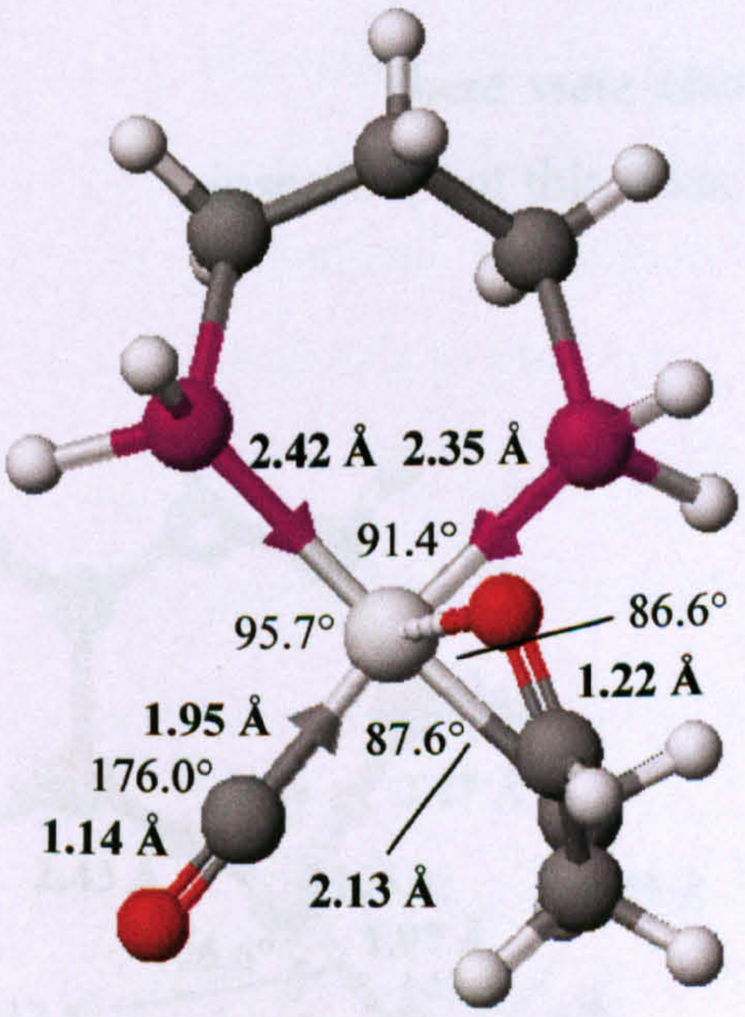


Figure 3.4.5.1: Reactant before CO insertion with Pd-O axial interaction from second carbonyl group

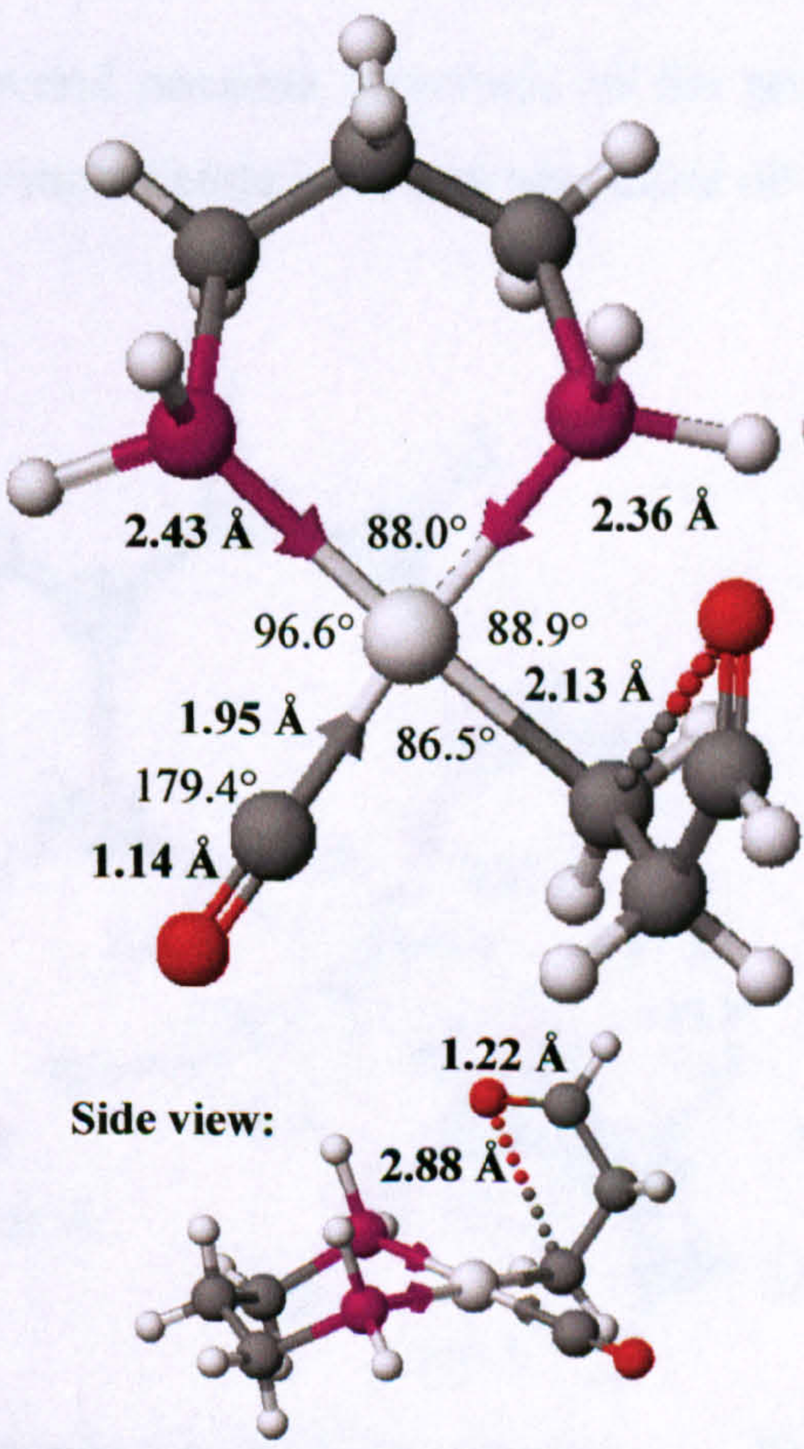


Figure 3.4.5.2: Reactant before CO insertion with attraction between second carbonyl and carbon bonded to Pd.

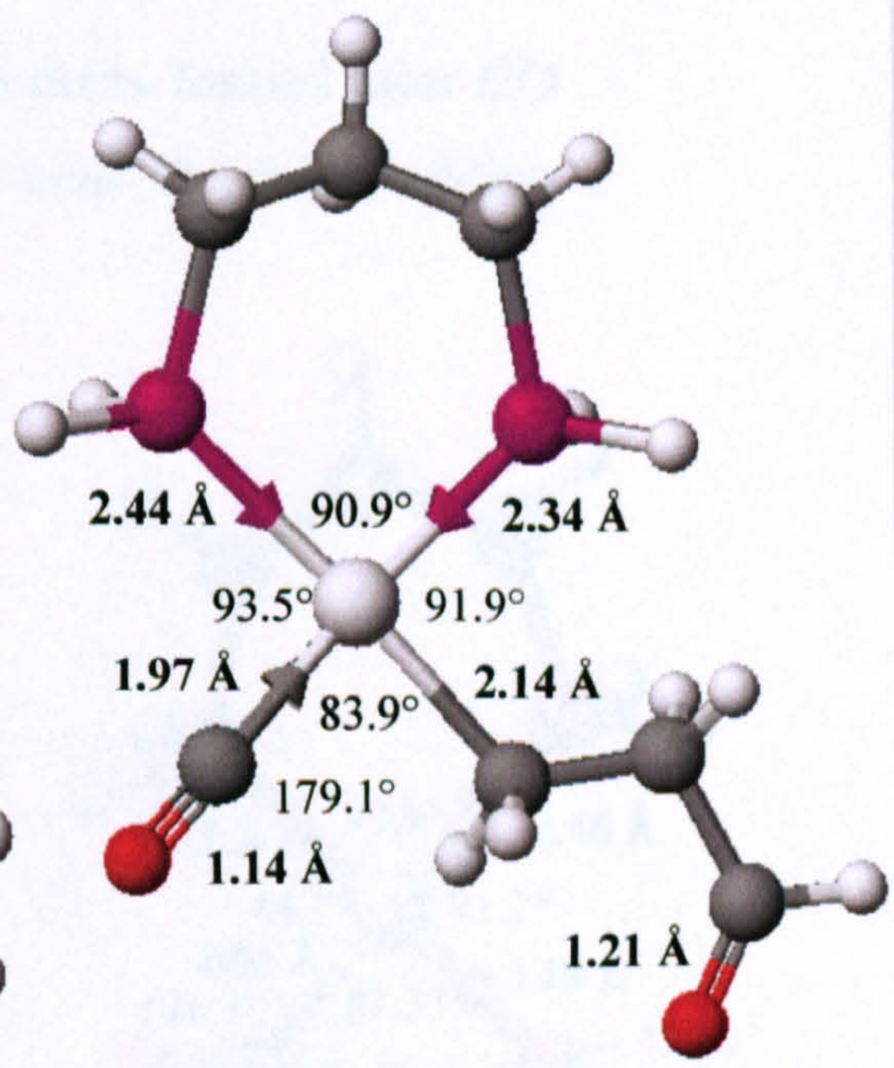


Figure 3.4.5.3: Reactant before CO insertion with no interaction from second carbonyl.

in **figure 3.4.5.1**, where the second carbonyl group formed an axial Pd···O interaction to give a square pyramidal complex. However, two other possible minima were also optimised and verified by frequency tests, shown in **figure 3.4.5.2**, where the oxygen was attracted to the carbon on the alkyl group bonding to palladium (although it is uncertain whether this minimum was real or just a product of theoretical error), and in **figure 3.4.5.3**, where the carbonyl group did not interact with any other part of the complex at all. The existence of the a minimum for the latter structure was uncertain – although this structure could be optimised when diffuse functions were included in the basis set, without them the complex optimised to the structure shown in figure 3.4.5.2.

The energies of the first two structures were very close, with the structure shown in figure 3.4.5.2 being 0.4 kcal/mol lower in energy than the structure proposed by Ziegler and Margl shown in figure 3.4.5.1 (with the difference reduced to 0.2 kcal/mol when considering ZPE). This was far too close within the margin of error to tell which of the two structures was more stable. The energy of the last structure, in figure 3.4.5.3, was *estimated* to be 5.2 kcal/mol higher, by comparing the energies for the structures shown in figures 3.4.5.1 and 3.4.5.3 using the energies calculated with diffuse basis functions included. This was high enough to rule the structure shown in figure 3.4.5.3 out of any likely part in the propagation cycle.

There were also several possible structures of the products formed after CO insertion, but this time, the most stable structure was more obvious. By simply adding

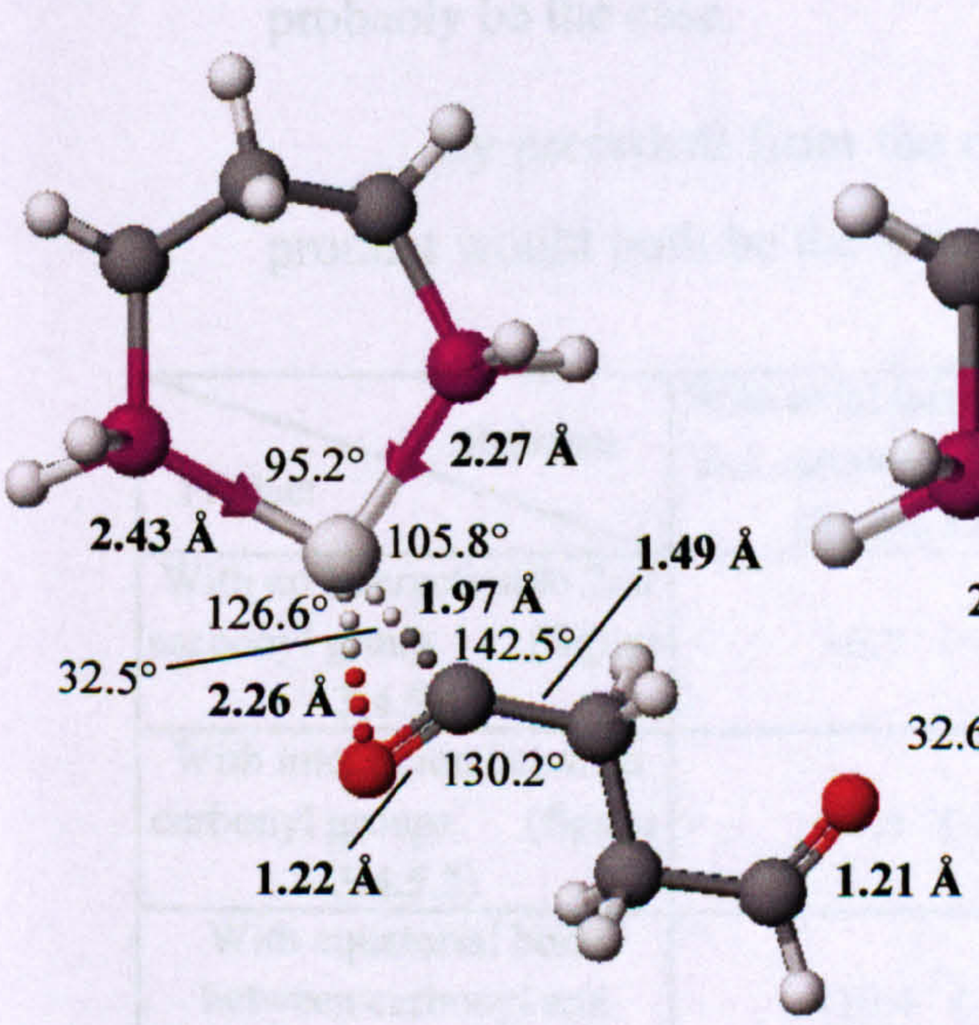


Figure 3.4.5.4: Product after CO insertion with no interaction from second carbonyl.

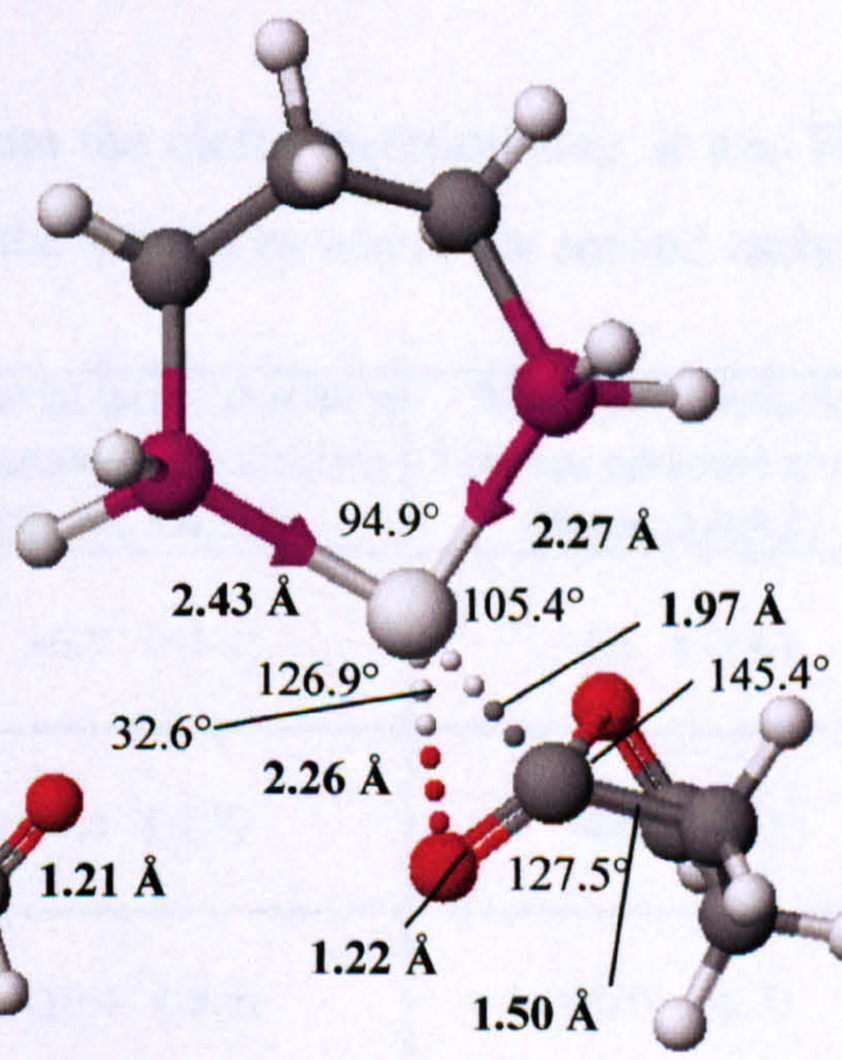


Figure 3.4.5.5: Product after CO insertion with carbonyl-carbonyl interaction.

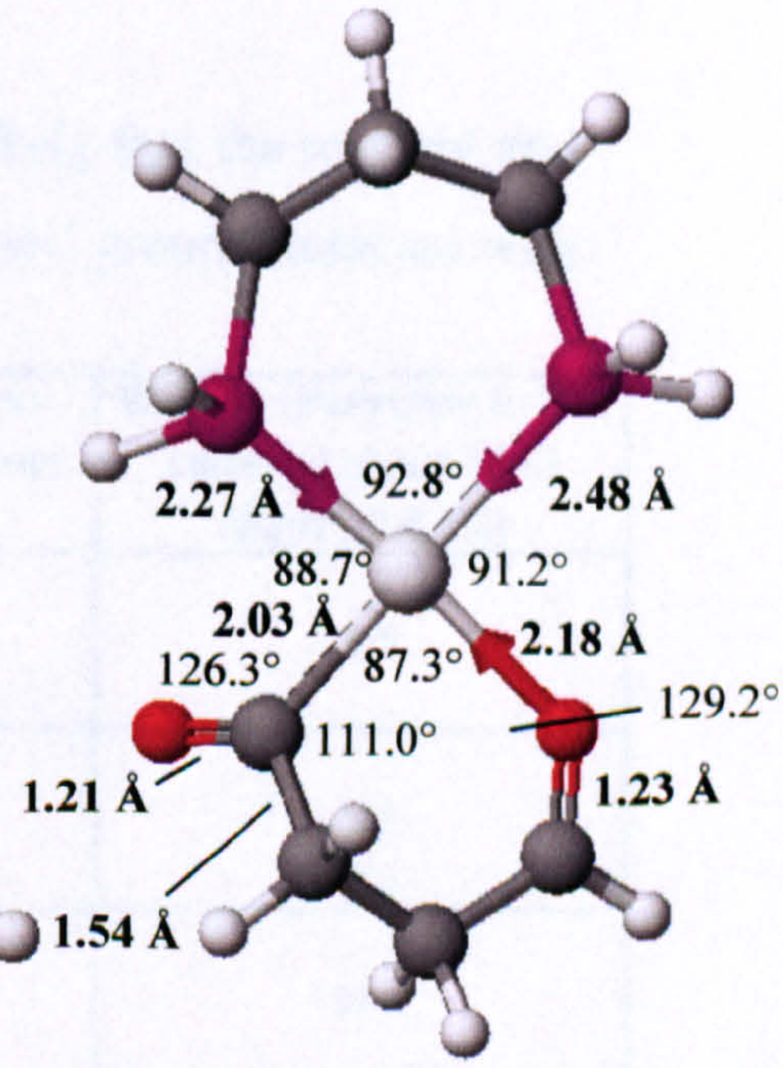


Figure 3.4.5.6: Product after CO insertion with Pd-O bond formed to produce 6-membered ring.

a carbonyl group on to the end of the ethyl group, the structure shown in **figure 3.4.5.4** was optimised. By moving the second carbonyl group to form a weak interaction with the newly-inserted carbonyl group, the structure shown in **figure 3.4.5.5** was optimised, with an energy 3.7 kcal/mol lower (3.2 kcal/mol including ZPE) – a fall in energy roughly equal to that produced when forming a carbonyl-carbonyl interaction in the product after olefin insertion. Apart from the interaction involving the second carbonyl group in the chain, both structures were very similar to the product structure having no second carbonyl group. The most stable structure of all, however, was where the second carbonyl group formed a Pd-O co-ordinate bond to form a six-membered ring, shown in **figure 3.4.5.6,** whose energy was a clear 11.1 kcal/mol lower than the first structure (10.3 kcal/mol with ZPE). This showed that the formation of a Pd-O co-ordinate bond greatly stabilised the complex having 6-membered rings, although the effect of stabilisation in 5-membered rings was greater.

It was not immediately clear which of the reactant and product structures would form part of the propagation cycle, so the enthalpies of all of possible reactions are calculated, shown in **table 3.4.5**. Comparing these possible enthalpies to the enthalpy of –7.6 kcal/mol (-6.5 kcal/mol with ZPE) for insertion neglecting the effect of the second carbonyl group, showed that the second carbonyl group would promote the reaction in the forward direction – but only if there was a clear path to the product structure with the Pd-O coordinate bond to form the six-membered ring. The enthalpy calculated by Ziegler and Margl was –7.6 kcal/mol, which suggested this would probably be the case.

By precedent from the olefin insertion step, it was likely that the reactant and product would both be the structures where the second carbonyl group interacted with

Product \ Reactant	With axial interaction from 2nd carbonyl to palladium **(figure 3.4.5.1)**	With weak interaction between carbonyl groups **(figure 3.4.5.2)**	With no interaction to 2nd carbonyl group (est.) **(figure 3.4.5.3)**
With no interaction to 2nd carbonyl group **(figure 3.4.5.4)**	+0.7 (+1.4)	+1.1 (+1.6)	-4.5
With interaction between carbonyl groups **(figure 3.4.5.5)**	-3.0 (-1.8)	-2.6 (-1.6)	-8.2
With equatorial bond between carbonyl and palladium **(figure 3.4.5.6)**	-10.4 (-8.9)	-10.0 (-8.7)	-15.6

Table 3.4.5: Energy changes (in kcal/mol) of olefin insertion from different conformation of reactant and product structures of carbon monoxide insertion. (Zero-point correction energies shown in brackets.)

palladium to give maximum stabilisation, making *–10.4 kcal/mol (-8.9 with ZPE)* the most likely enthalpy for this step. However, it would be necessary to optimise the transition state and find the reaction path before it could be ascertained that this was the case.

3.4.6 Inclusion of second carbonyl group in transition state optimisations

As with olefin insertion, there were three hypothetical reaction paths for carbon monoxide insertion. One path, as proposed by Ziegler and Margl, would proceed via a transition state where the second carbonyl group was still bonded to palladium through an axial Pd-O interaction, although Ziegler and Margl did not consider whether there was a feasible path between the transition state and product. Another path would involve retaining a weak interaction between oxygen and the carbon directly bonded to the palladium, as in the structure shown in figure 3.4.5.2. The final possibility was for insertion to proceed with no interaction from the second carbonyl group at all. The first path was more likely for two reasons: firstly, the transition state had already been found by Ziegler and Margl, and secondly, a similar position of the second carbonyl group had been found in the olefin insertion stage.

When simply guessing the starting structure of the transition state, it was not possible to optimise the stationary point, probably because there were too many variables to adjust to the minimum. The only thing that was indicated by the

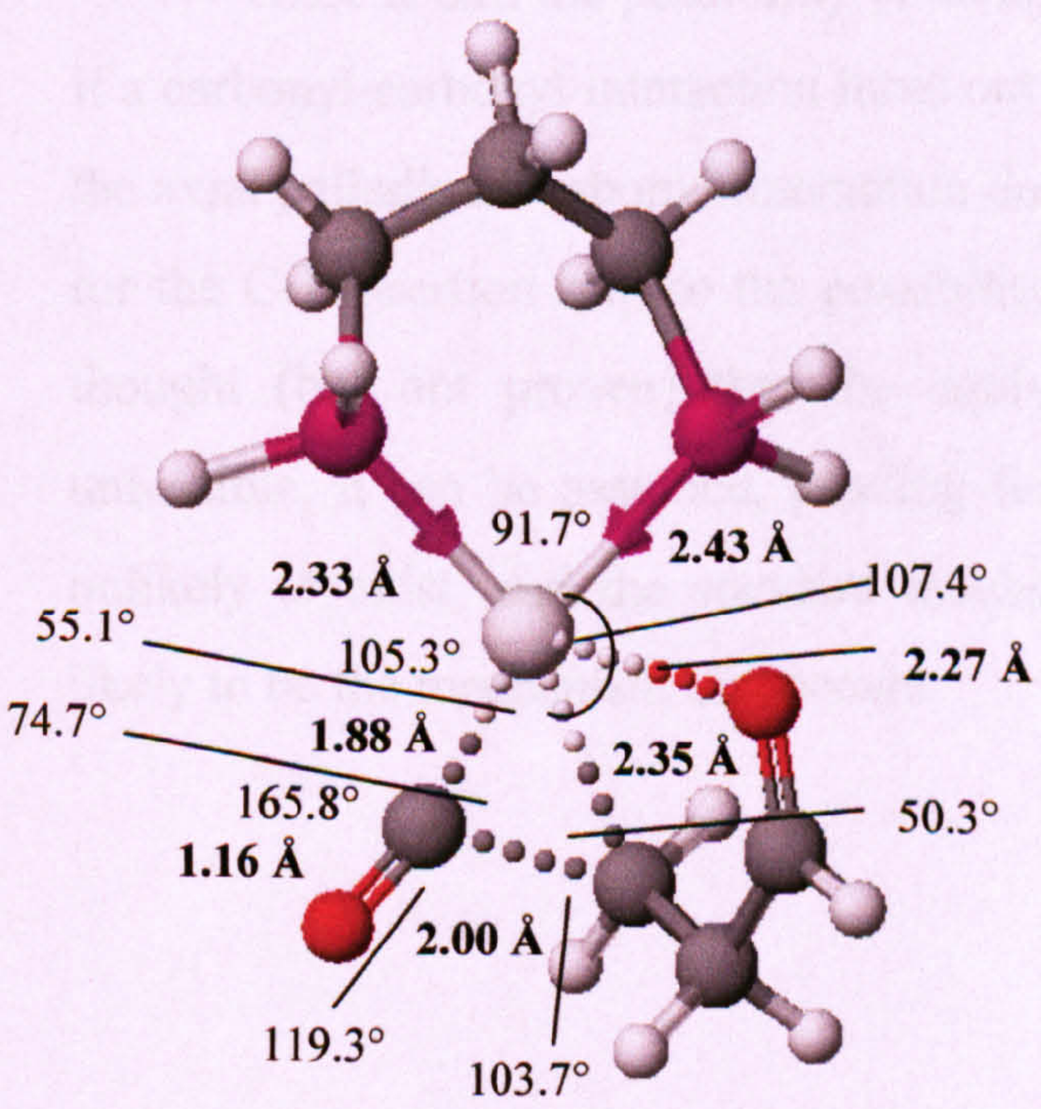


Figure 3.4.6.1: Transition state of CO insertion with axial Pd-O bond from second carbonyl group.

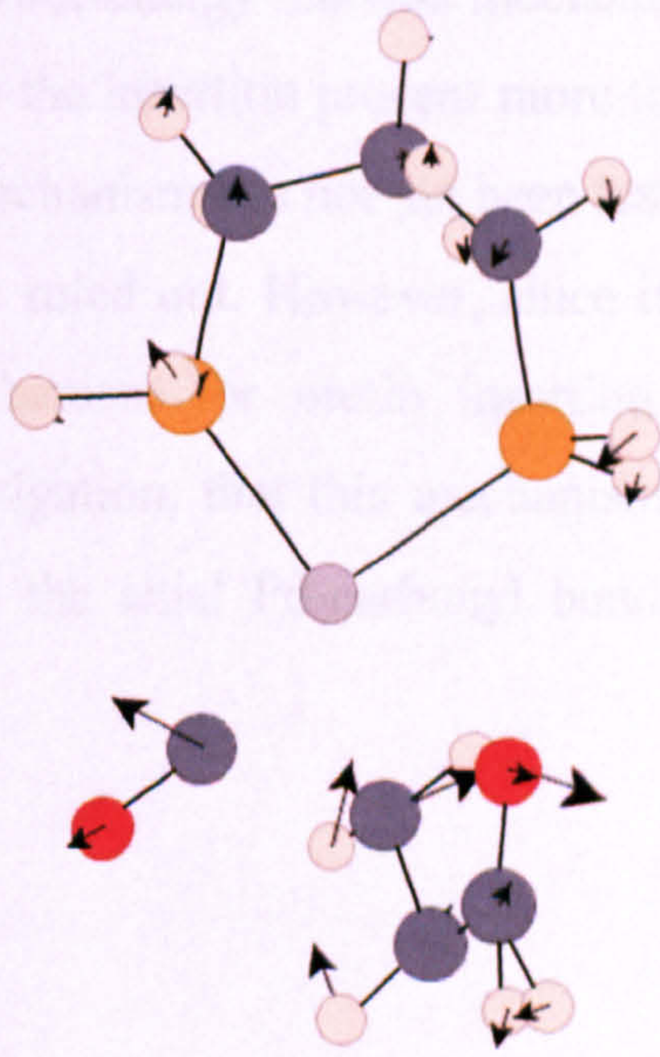


Table 3.4.6.2: Vibrational mode of imaginary frequency (-300.6 cm^{-1})

optimisation was, even if the second carbonyl group started at the furthest possible distance away from the palladium atom, the carbonyl group always moved towards palladium during the optimisation. If one optimised the transition state of CO insertion without the second carbonyl group first, and then the second carbonyl was added, the structure of the transition state was optimised easily, as shown in **figure 3.4.6.1** (mode of vibration of imaginary frequency shown in **figure 3.4.6.2**). Yet again, the presence of a Pd-O axial interaction made very little difference to the geometry of the rest of the complex.

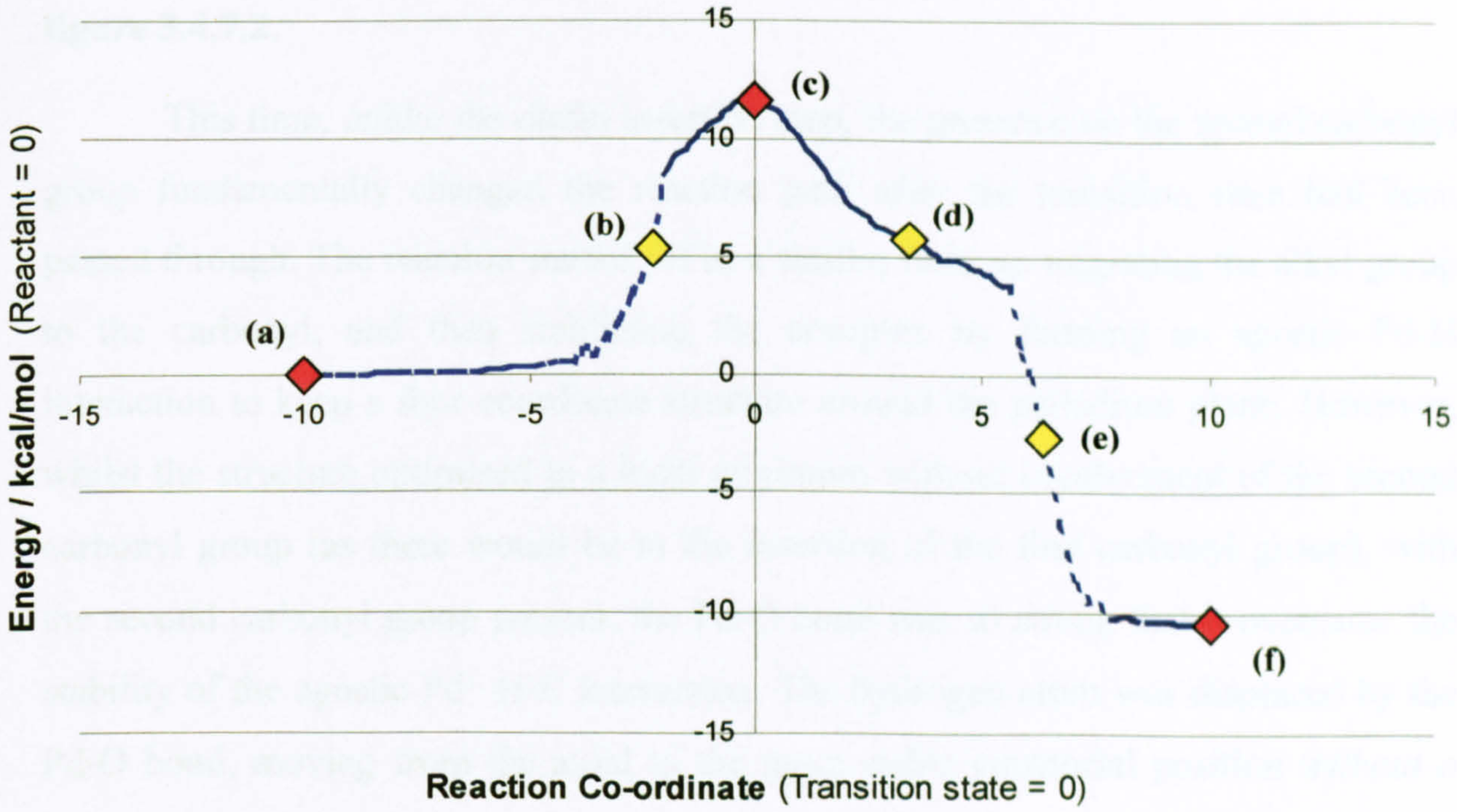
The activation energy between the reactant and product was calculated to be 11.9 kcal/mol (11.5 kcal/mol including zero-point energies), a small increase over the activation energy without the second carbonyl group present, but not as high an increase as a second carbonyl group caused in olefin insertion. This may have partly been because the theory given in section 5.3.2 as to why the reactant of olefin insertion is stabilised does not apply to the CO insertion.

This energy barrier was 2.4 kcal/mol lower than the activation energy for olefin insertion (-3.0 kcal/mol including zero-point energies), so this backed up the accepted consensus that olefin insertion is the rate-determining step, but only just, and the margins of error were too high to be certain of this for the ab-initio calculations alone. The energy barrier proposed by Ziegler and Margl was very close, at 11.7 kcal/mol.

There is still the possibility of an alternative lower-energy reaction mechanism if a carbonyl-carbonyl interaction turns out to stabilise the insertion process more than the axial palladium-carbonyl interaction does. This mechanism has not yet been tested for the CO insertion step so the possibility cannot be ruled out. However, since it is thought (but not proven) that the equivalent mechanism for olefin insertion is unfeasible, it can be assumed, pending further investigation, that this mechanism is unlikely to exist, and the standard mechanism with the axial Pd-carbonyl bond is likely to be the mechanism that occurs.

3.4.7 Inclusion of second carbonyl group in reaction path

The second carbonyl group meant that there were a number of possible minima that could be reached beyond the transition state. If the reaction proceeded in the same manner as the migratory insertion of the first CO, the next minimum could



Reaction profile from IRC job

Stationary points shown in **figure 3.4.7.2**

Speculative reaction profile from optimisation of final point from IRC

Sample non-stationary points shown in **figure 3.4.7.2**

Figure 3.4.7.1: Reaction profile of carbon monoxide insertion with second CO group, with selected points shown in **figure 3.4.7.2**.

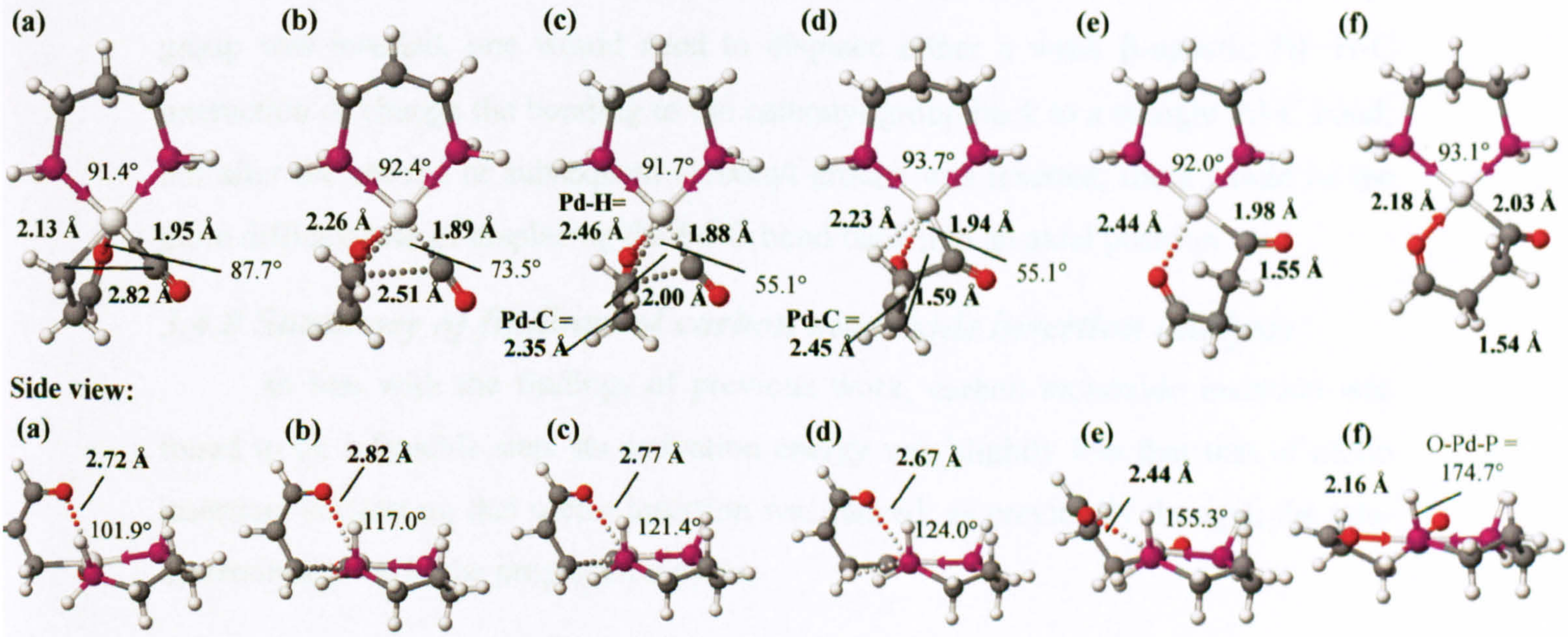


Figure 3.4.7.2: Selected points from reaction profile.

be similar to the intermediate and product structures in figures 3.4.2.2 and 3.4.4.1, but with an additional carbonyl group in an axial site to palladium. Alternatively, the next minimum could be a six-membered ring formed by the Pd···O interaction migrating to the equatorial site. The reaction profile of the transition state was therefore taken, with the energy barrier shown in **figure 3.4.7.1**, and points on the reaction path shown in **figure 3.4.7.2**.

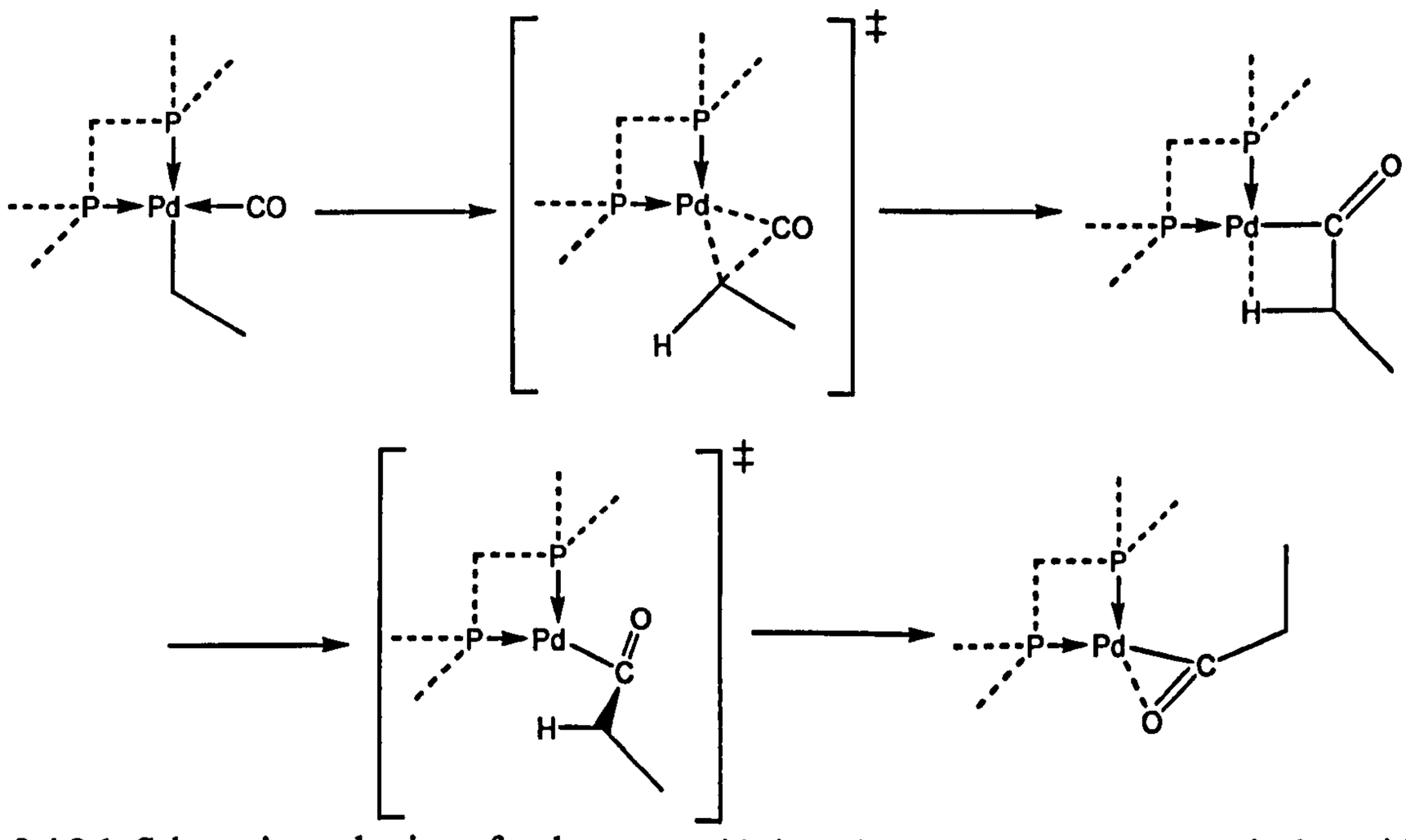
This time, unlike the olefin insertion step, the presence on the second carbonyl group fundamentally changed the reaction path after the transition state had been passed through. The reaction started off in a similar fashion, migrating the alkyl group to the carbonyl, and then stabilising the complex by forming an agostic Pd-H interaction to keep a four-coordinate structure around the palladium plane. However, whilst the structure optimised to a local minimum without involvement of the second carbonyl group (as there would be in the insertion of the first carbonyl group), with the second carbonyl group present, the Pd-O bond was so strong that it overcame the stability of the agostic Pd···H-C interaction. The hydrogen atom was displaced by the Pd-O bond, moving from the axial to the more stable equatorial position *without a further energy barrier to overcome*.

It could therefore be concluded, beyond reasonable doubt, that the most stable product structure, with the Pd-O bond in the square plane, was indeed the structure that formed after CO insertion, with no need to overcome any local energy barriers. This would mean that the following olefin addition step would be completely different after insertion of the first and subsequent carbonyl groups: after the first carbonyl group was inserted, one would need to displace either a weak β-agostic Pd···H-C interaction or change the bonding to the carbonyl group back to a straight Pd-C bond; but after the second or subsequent carbonyl groups was inserted, there would be the more difficult task of displacing the Pd-O bond back into an axial position.

3.4.8 Summary of findings of carbon monoxide insertion analysis

In line with the findings of previous work, carbon monoxide insertion was found to be a feasible step. Its activation energy was slightly less that that of olefin insertion, suggesting that olefin insertion was indeed, as previously thought, the rate-determining step in the propagation cycle.

Without the interaction of a second carbonyl group, the mechanism of CO insertion was not as complicated as that of olefin insertion. There were three components to insertion, but the dominant component was insertion of the carbonyl into the Pd-alkyl bond itself (the other two components being re-arranging parts of the complex away from the minimum energy conformation in the reactant and towards a minimum energy conformation for the product). The only thing that was unclear was which product structure would be formed. The local minimum reached after the transition state achieved a four-coordinate structure by forming an agostic H-interaction, but the most stable structure of all had bonds to carbon and oxygen of the carbonyl group. The energy barrier between the two states was significant (possibly as a result of having to pass through a structure with only three obvious metal ligand-bonds), so it was unclear at this stage whether the most stable structure would be



Scheme 3.4.8.1: Schematic mechanism of carbon monoxide insertion. All structures carry a single positive charge.

	From this project:	Including zero-point corrections	From Zielger and Margl:	From Svensson et. al.:
Activation energy of CO insertion	9.2	8.9	11.5	15.0
Enthalpy of CO insertion	2.4	3.0	4.5	8.4
Activation energy of product re-arrangement	4.1	4.9	Not calculated	2.2
Activation energy of product re-arrangement	-10.0	-9.5	-7.4	-6.4
Total activation energy of CO insertion stage	**9.2**	**8.9**	11.5	15.0
Total enthalpy of CO insertion stage	**-7.6**	**-6.5**	-2.9	2.0

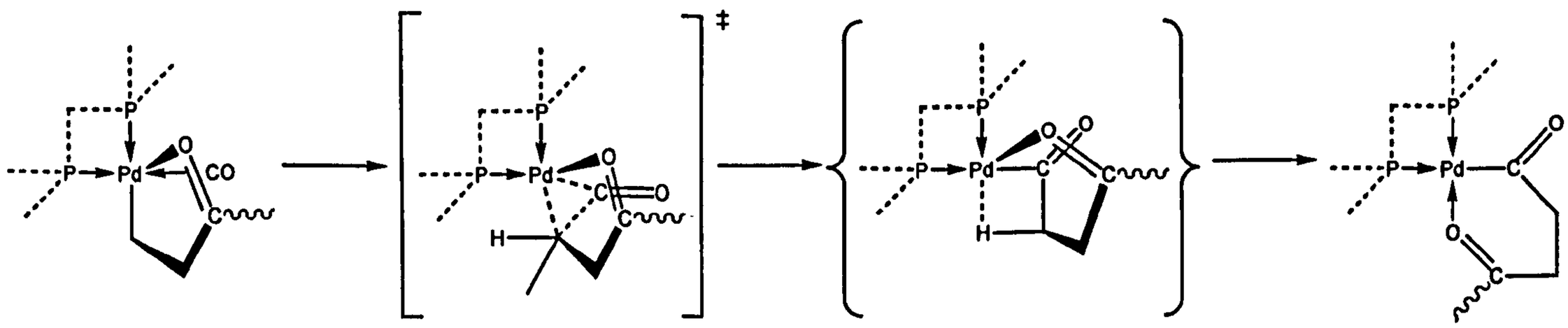
Table 3.4.8.1: Energy differences (in kcal/mol) of stationary points in insertion of first carbon monoxide ligand.

formed at all, or whether the H-interaction would be displaced by a new incoming ligand first, bypassing the other structure.

The insertion mechanism beyond the transition state changed fundamentally with a second carbonyl group interacting with the complex – which there would be on insertion of the second and subsequent carbonyls into the chain. With a second carbonyl group present, although the H-interacting structure was passed through in the reaction path, the strong Pd-O axial interaction would displace the β-agostic Pd···H-C interaction to move into its equatorial site, without any intermediate being formed, to form a very stable 6-membered ring through the Pd-O bond.

For the insertion of CO into the first Pd-alkyl bond, the final proposed mechanism is given in **scheme 3.4.8.1,** and the key energy differences are given in **table 3.4.8.1**. With a second carbonyl group present, as would be the case for all subsequent insertions, final proposed mechanism is given in **scheme 3.4.8.2,** and the key energy differences are given in **table 3.4.8.2**. In both cases, the energy barrier to CO insertion is a few kcal/mol less than olefin insertion with the same number of interacting carbonyl groups. It is therefore reasonable to conclude that olefin insertion is the rate-determining step. The drop in energy also suggests that the insertion step is unlikely to be easily reversible, but given the much lower changes in energy in the work of Ziegler and Margl, and Svensson *et al,* it is uncertain whether that conclusion is correct in the case of insertion of the first CO.

The structure of the reactant and product, with the second carbonyl group present, acted as a good point of reference for the addition steps.



Scheme 3.4.8.2: Schematic mechanism of carbon monoxide insertion with second carbonyl group. All structures carry a single positive charge.

	From this project:	Including zero-point corrections	From Zielger and Margl:
Total activation energy of CO insertion stage	**11.9**	**11.5**	11.7
Total enthalpy of CO insertion stage	**-10.4**	**-8.6**	-7.6

Table 3.4.8.2: Energy differences (in kcal/mol) of stationary points in insertion of second and subsequent carbon monoxide ligand.

3.5 Carbon monoxide addition stage

3.5.1 Introduction

Unlike the two insertion stages, there had previously been little consideration of the mechanisms of the two addition stages. Both Ziegler and Margl's papers and Svensson *et al*'s paper simply optimised the structures before and after addition, with no real consideration given to what energy barrier, if any, may need to be overcome for addition to take place. However, there has been a fair amount of speculation from experimental chemists (see chapter 1) over the effect the addition mechanisms may have on the overall reaction.

In the case of carbon monoxide addition, the question left unanswered was whether the Pd-O co-ordinate bond, formed during the previous olefin insertion step, hindered the addition of the next molecule to be inserted. Pd-O was a strong bond that would need to be displaced before a new molecule could bond in the Pd-ligand plane for insertion. It was possible that this contributed towards the lack of double insertion, as the energy barrier for CO addition could be a lot lower than the energy barrier for addition of a second olefin.

It was therefore attempted to find the unknown transition state of olefin addition. Throughout the process, the copolymer chain was truncated after the carbonyl group inserted in the last cycle.

3.5.2 Early attempts to find reaction path

The very first attempt to find a reaction path for carbon monoxide addition took into account that there might not be an energy barrier at all. Optimisation of a complex after olefin insertion was commenced with a carbon monoxide molecule at a distance. At a distance of around 10 Å, the carbon monoxide molecule was attracted towards the palladium complex. (At larger distances, the forces were too small for Gaussian to detect.) However, rather than simply fall into place in an axial site, displacing the Pd-O ligand (which is what one would have expected to happen if there was no energy barrier), the carbon monoxide molecule always came to rest at some point above or below the palladium coordination plane. Exactly where the CO molecule came to rest varied significantly depending on what basis set was used and from what direction the CO molecule approached the complex. However, most attempts to optimise such a complex caused the CO to drift off and find a minimum

somewhere else. It was therefore most likely that the potential surface of an incoming molecule to the palladium system was a complicated surface with several different local minima to be found.

The earliest attempts to identify some of transition states involved attempting a QST3 optimisation using: the complex described above as the reactant, the complex with CO bonded to palladium in an equatorial site as the product, and a guessed transition state. The problem was that without any prior research in this area, there were no published structures to use as a starting structure of the transition state. All attempts to arbitrarily increase the Pd-O bond length and decrease the Pd-CO distance as a starting transition state failed miserably to optimise the transition state, with the structure always moving away from any plausible transition state structure.

The next attempt was to undertake a relaxed potential energy scan of the product (i.e. the complex after CO addition to the equatorial site but before CO insertion), with the length of the Pd-CO bond being increased gradually. These results were interesting, but not helpful for obtaining the transition state. When the Pd-CO bond length was increased up to 3.477 Å, the structure remained the same apart from the increased bond length, and the energy of the system increased. However, when the bond length was increased to 3.940 Å or higher, the complex re-arranged itself so that the CO molecule ceased to bond to Pd in the plane, to be replaced with an agostic Pd···H-C interaction. The energy profile of the scan in shown in **figure 3.5.2.1**.

For a while, it was wondered if the CO addition process was a two-stage process, with the Pd-O bond changed to the weaker Pd···H-C interaction before being displaced by the incoming CO molecule (although the sharp increase in energy to get

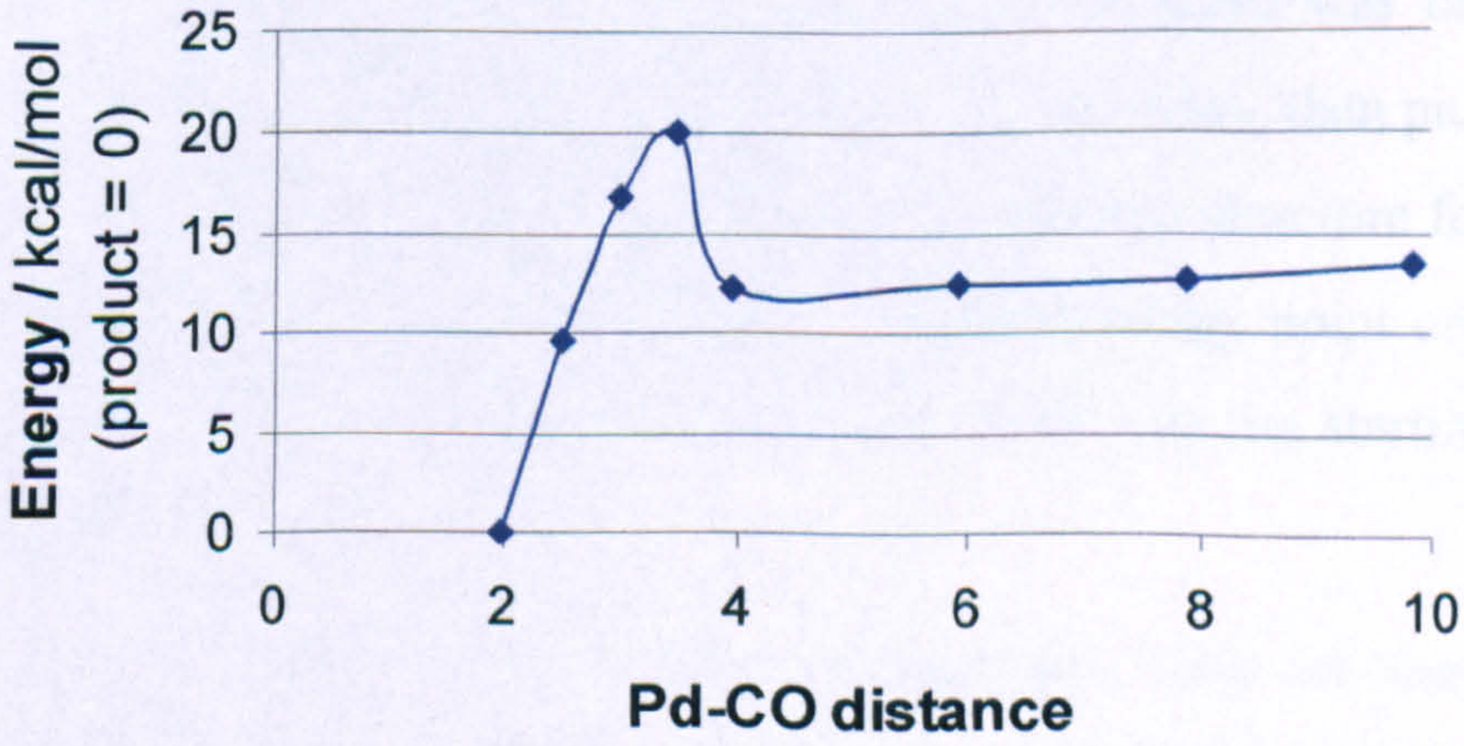


Figure 3.5.2.1: Energy profile of relaxed potential energy scan of Pd-CO distance for addition of new carbon monoxide ligand.

the agostic H-interaction made this process doubtful). Unfortunately, attempts to optimise a transition state of CO addition displacing a Pd···H-C bond instead of a Pd-O bond proved to be equally fruitless. However, this did strongly suggest that there was an energy barrier involved in CO addition itself, and instead the energy barrier was caused by the need to displace a ligand from a stable square-planar complex in order to allow a new ligand in.

Attempts were then made to try to identify the region of the transition state by starting a standard optimisation with an increased Pd-CO distance, and observe in which direction the CO molecule moves in the first few steps (which would be in the direction of the forces acting on it), and starting a transition state search in the area where the direction changed from towards the Pd centre to away from the Pd centre. Again, however, this approach did not work.

Around this time, it had been established that the product of this stage, being the reactant of the CO insertion stage, would probably have an axial interaction from the second CO group, so attention switched to trying to find an addition reaction that displaced the oxygen atom from an equatorial position to an axial position, rather than remove the palladium-oxygen interaction completely. Yet again, however, all attempts to guess the transition state failed.

A new approach was then adopted to find the transition state, using the Opt=(Path=M,QST2/3) option available in Gaussian. The Path=M option, used in conjunction with QST2 or QST3, instead of attempting to optimise a single transition state, optimises M points simultaneously (where M is a chosen integer) between the reactant and product structures, with the highest energy point optimising towards the transition state. Unfortunately, it was not practical to use this job for its intended purpose in complexes of this size, because the run-time required was far too long, even on hal. It could, however, be used to go through a few cycles, then pick the point on the path with the highest energy and use this as the starting structure for a normal QST3 job. In effect, this amounted to picking the highest-energy point on a reaction path – but not necessarily the lowest energy reaction path – as the starting structure for a QST3 optimisation.

To minimise the amount of run-time required, the basis set was originally reduced back to 3-21G. With the carbon monoxide molecule starting at a distance

from the palladium complex as the reactant structure (c. 10Å), and the CO molecule in an equatorial position as the product structure, and an estimated transition state to start the job, (a Path/QST2 job was unable to find a starting reaction path,) a seven-point path job was started, and after twenty passes, the augmented SDD basis set was restored and the third point (with the highest energy, as shown in **figure 3.5.2.2**) was used as the starting structure for a normal QST3 optimisation. However, there were already doubts about whether there could be a transition state with CO over 5 Å away from Pd.

Once again, however, this point failed to converge on any transition state. When the second and fourth points, either side of this starting transition state, were optimised to minima, however, the reason why was discovered: both minima optimised towards the palladium centre. This clearly meant that what the region that the 3-21G basis set had identified as the region of the transition state was wrong – had it been reasonably accurate, optimising the points either side of the transition state should have moved the CO molecule in opposite directions. The minimum that was optimised is shown in **figure 3.5.2.3** – a minimum that was clearly missed when using the 3-21G basis set. This minimum was reasonably close to having a perpendicular axial Pd-CO interaction, but there was still some deviation from a rigid square pyramidal structure that might have been expected from the structures suggested by

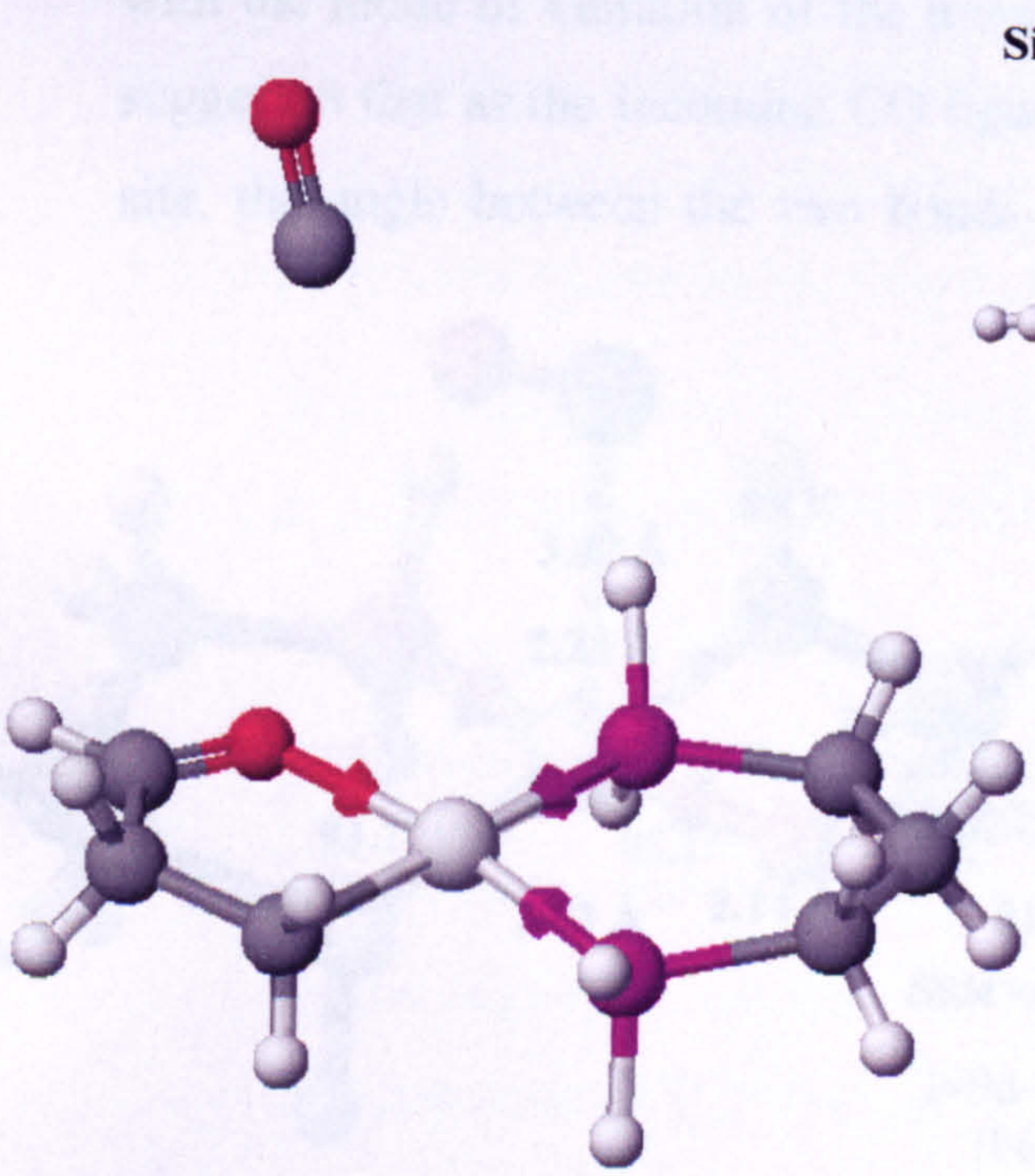


Figure 3.5.2.2: Starting structure to find CO addition transition state obtained from path job after 20 passes using 3-21G basis set.

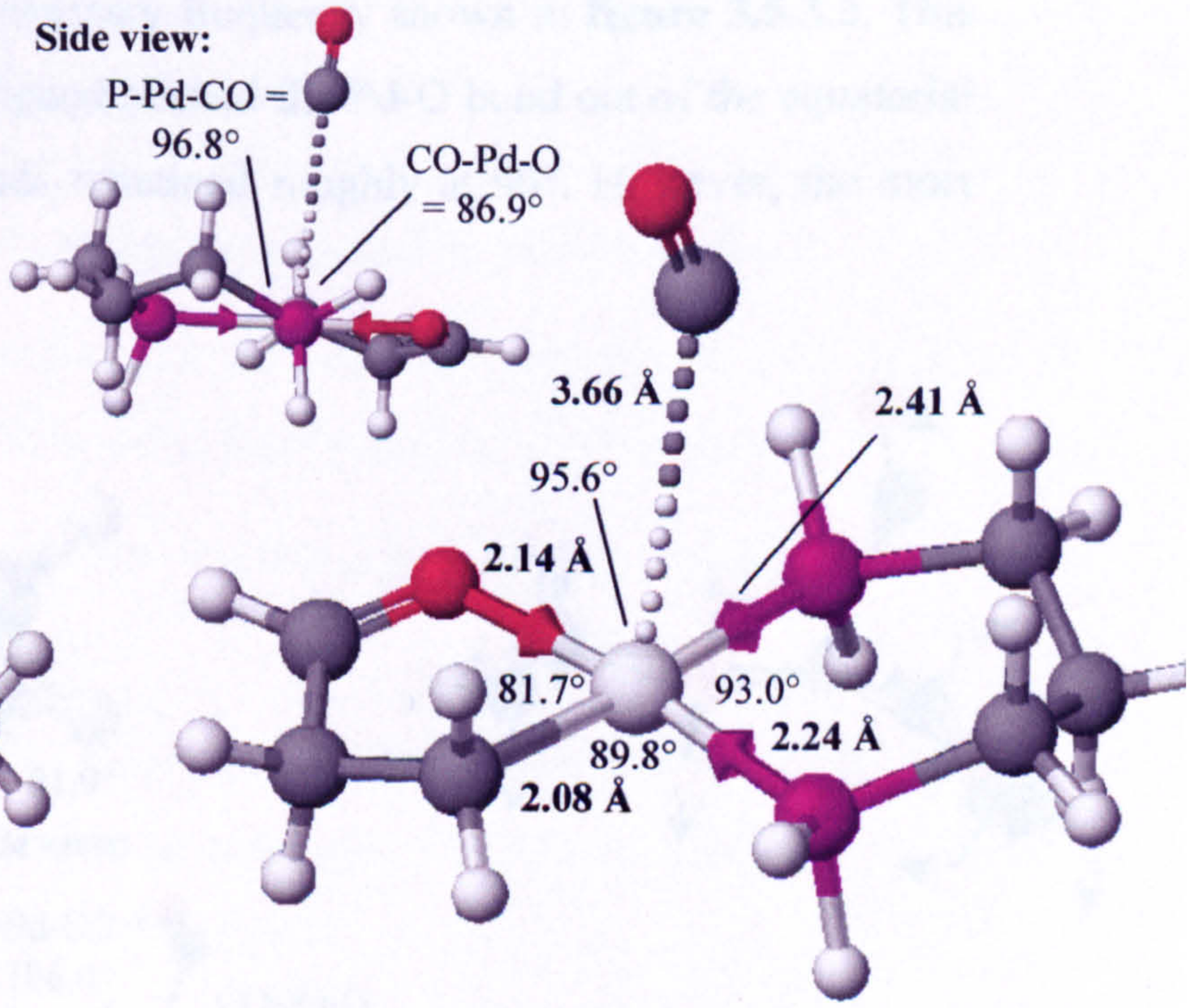


Figure 3.5.2.3: Minimum obtained using augmented SDD basis set when optimising structure given in figure 3.5.2.2 or nearby points to nearest minimum.

experimental chemists.

It was therefore concluded that in order to find the transition state using a path job, the full augmented SDD basis set would have to be used, in spite of the long run-time needed. This time, it did lead to the optimisation of the transition state.

3.5.3 Final optimisation of transition state

Having learnt all of the lessons from all of the previous failed attempts to choose a suitable starting structure to optimise a transition state, the final attempt that led to a successful search started with a new Path job between the minimum obtained in figure 3.5.2.3 as the reactant, and the product structure shown back in figure 3.4.5.1. Using a Path/QST2 job with five points (this time, the job could proceed without the need for a starting transition state between the two structures) and the usual augmented SDD basis set, the path job was allowed to run for twenty cycles before the third point (the highest energy point) was taken as the starting transition state structure for a QST3 optimisation, with the same reactant and product structures.

It looked at first like the transition state optimisation was going to fail. However, after a very large number of optimisation steps (the job had to be extended beyond the default number of steps normally allowed in the optimisation of a complex of that size) a stationary point was finally found. A frequency test confirmed this was a transition state, and the structure of the transition state is shown in **figure 3.5.3.1**, with the mode of vibration of the imaginary frequency shown in **figure 3.5.3.2**. This suggested that as the incoming CO ligand pushed the Pd-O bond out of the equatorial site, the angle between the two bonds remained roughly at 90°. However, the most

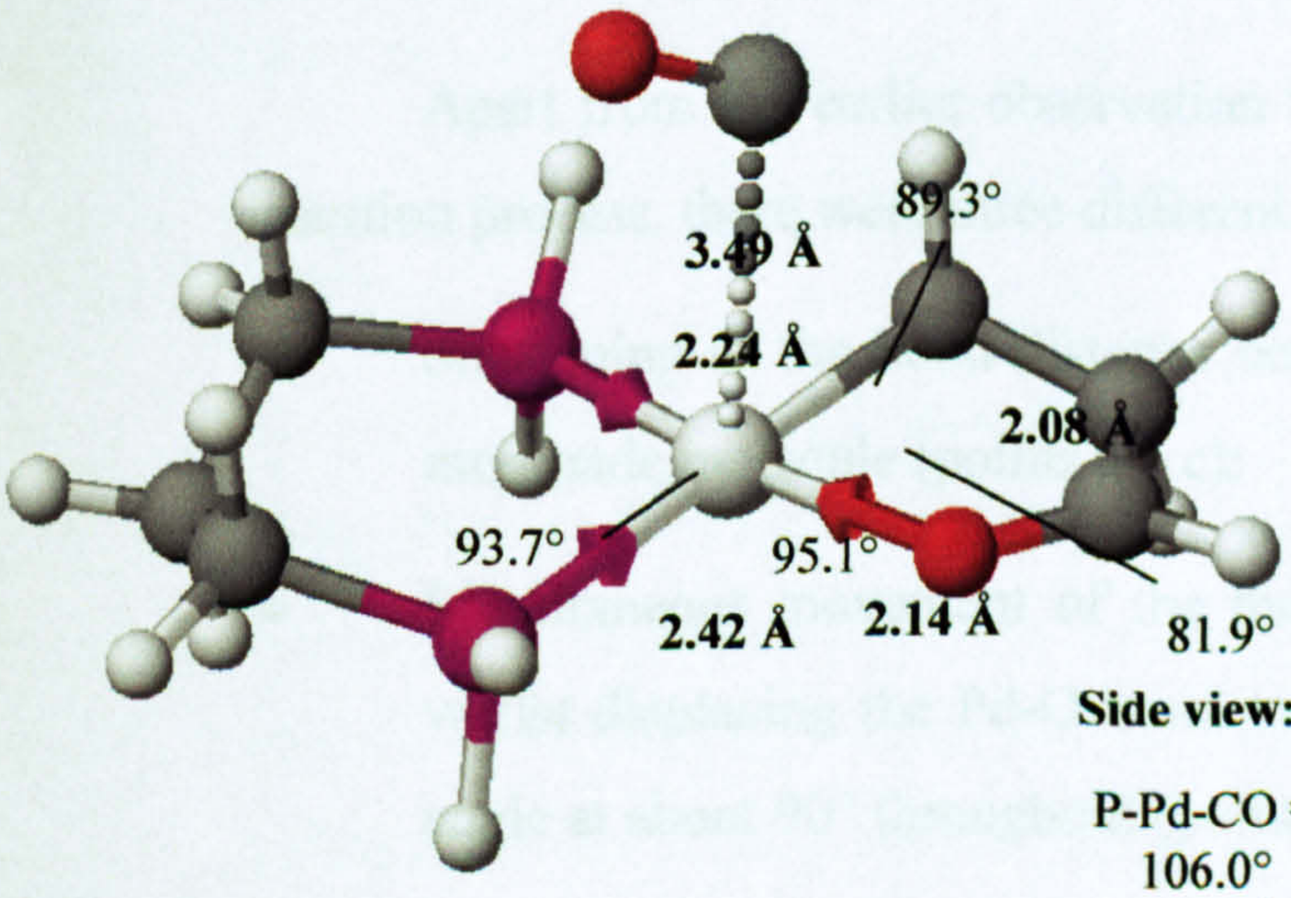


Figure 3.5.3.1: Transition state of CO addition.

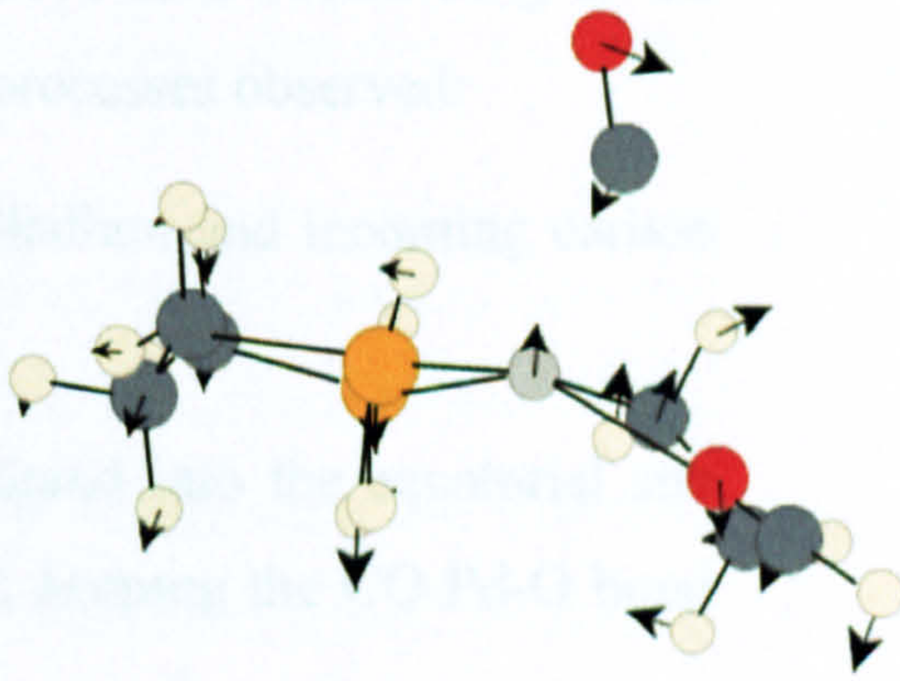


Figure 3.5.3.2: Vibrational mode of imaginary frequency (-57.3 cm^{-1})

notable feature was that the transition state was early in the reaction path, as the P-Pd-CO bond angle, increasing from 90° to 180° over the reaction path, had only increased to 117.5° at the transition state.

The early transition state could be influenced by the energetics. The energy barrier was calculated to be 2.1 kcal/mol (2.6 kcal/mol including zero-point corrections), and the overall enthalpy between the reactant and the product was -4.8 kcal/mol (-3.6 kcal/mol including zero-point corrections). This meant that the bonding force to the new CO molecule in an equatorial position was significantly stronger than the force to keep the Pd-O co-ordinate bond in an equatorial position, meaning that the force driving the addition step forwards could hypothetically overcome the force pushing it back early on in this step. The energy barrier was very small compared to the energy barrier in the two insertion steps, so there should not have been any problem proceeding through this step, although the low enthalpy would also make this step easily reversible.

3.5.4 Reaction path

Unlike the two insertion transition states, when an IRC job was run on the carbon monoxide addition transition state, only a few points either way were optimised before reporting that a minimum had been found, with the path not giving any helpful information about either the energy surface or the reaction path. However, the furthest point in each direction could then be optimised to a minimum in each direction, giving a good indication of the reaction path. There were no further intermediates discovered in the reaction path. The energy profile is shown in **figure 3.5.4.1**, and some points on the lowest energy path are shown in **figure 3.5.4.2**.

Apart from the earlier observation that the transition state occurs early in the insertion process, there were three different overlapping processes observed:

- Shortening of the bond distance between the palladium and incoming carbon monoxide molecule (points a – c);
- Simultaneous movement of the incoming CO ligand into the equatorial site whilst displacing the Pd-O bond to an axial site, keeping the CO-Pd-O bond angle at about 90° throughout (points b-d); and
- Lengthening of the Pd-O distance once it is in the axial position (points c-e).

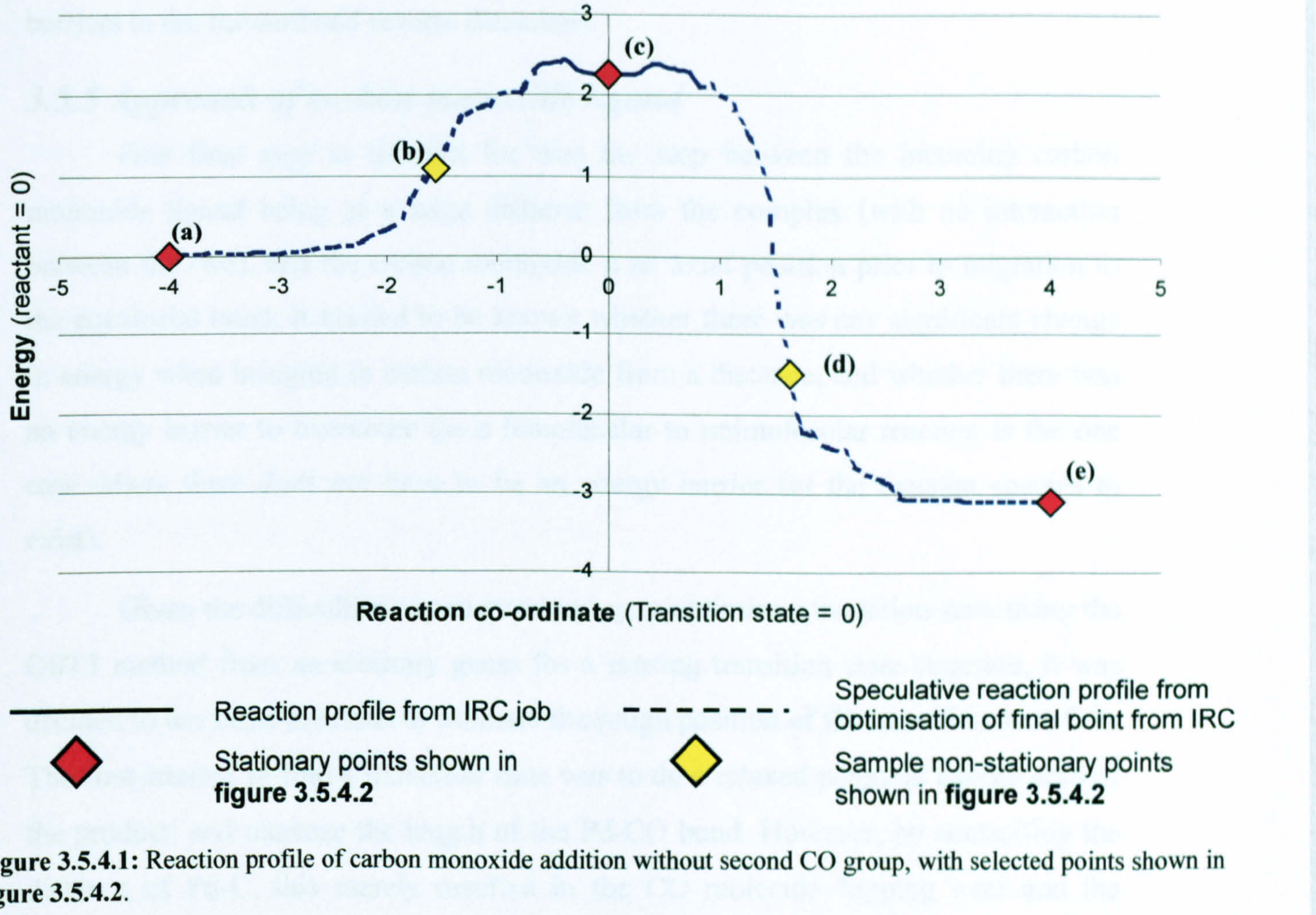


Figure 3.5.4.1: Reaction profile of carbon monoxide addition without second CO group, with selected points shown in **figure 3.5.4.2**.

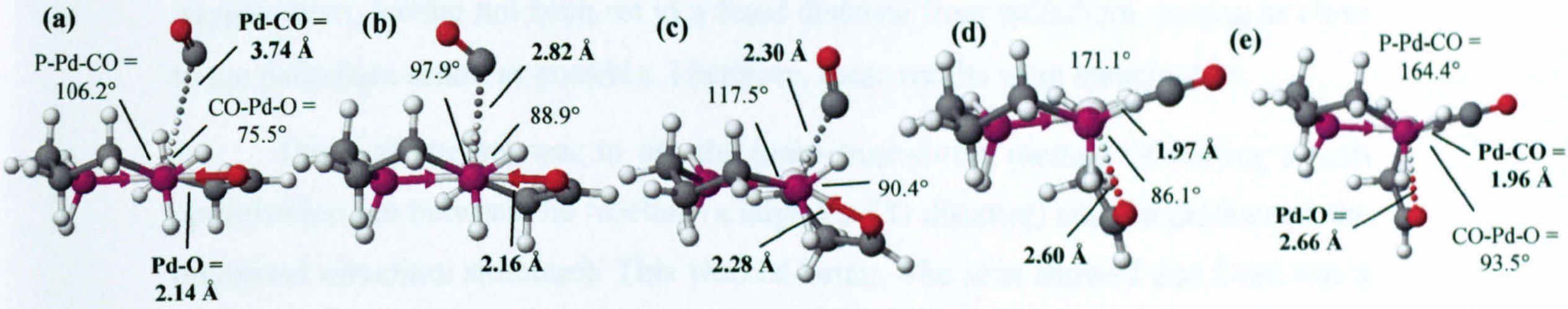


Figure 3.5.4.2: Selected points from reaction profile.

Other than this, the geometry of the rest of the complex appeared to remain the same.

Notably, the structure and energy of the product from the IRC job did not quite match the structure and energy of the reactant optimised earlier. It was suspected that the reason for this was that there was more than one local minimum of this structure, and the two runs had optimised to different minima. As there could be several pathways from CO at a large distance to an equatorial position, the structure of this point should therefore only be taken as a guide. However, this did not affect the

important factors, being the presence of energy barriers, and the magnitude of energy barriers in the forward and reverse directions.

3.5.5 Approach of carbon monoxide ligand

One final step to account for was the step between the incoming carbon monoxide ligand being at a large distance from the complex (with no interaction between the two), and the carbon monoxide n an axial position prior to migration to the equatorial bond. It needed to be known whether there was any significant change in energy when bringing in carbon monoxide from a distance, and whether there was an energy barrier to overcome (as a bimolecular to unimolecular reaction is the one case where there does not have to be an energy barrier for the reactant species to exist).

Given the difficulties experienced trying to optimise a transition state using the QST3 method from an arbitrary guess for a starting transition state structure, it was decided to use other methods to estimate the rough position of the transition state first. The first attempt to find a transition state was to do a relaxed potential energy scan of the product, and increase the length of the Pd-CO bond. However, by controlling the distance of Pd-C, this merely resulted in the CO molecule flipping over and the oxygen atom, having not been set to a fixed distance from palladium, getting as close to the palladium centre as possible. Therefore, these results were meaningless.

The next attempt was to use the more trustworthy method of starting a path optimisation job between the reactant (a large Pd-CO distance) and the product (at the optimised minimum structure). This worked better. The scan showed that there was a maximum in energy between these two points, suggesting that there probably was an energy barrier between the two. However, the method of taking the highest energy point as a starting point for a transition state search, which had proved itself to be effective elsewhere, failed to find a transition state. It was thought at this time that the potential surface would be too complicated to locate the transition state, and an estimate would have to be made of the energy barrier. However, it was discovered by accident (when trying to determine the energy of the bimolecular reactant) that when the Pd-CO distance was increased to five times its normal length to start an optimisation, the CO molecule moved straight back towards the axially-interacting site. Therefore, it was concluded that there was *no* energy barrier from the bimolecular reactant to form the Pd-O axial interaction, and that the energy barrier

suggested by the path search must have been as a result of missing the barrier-free path.

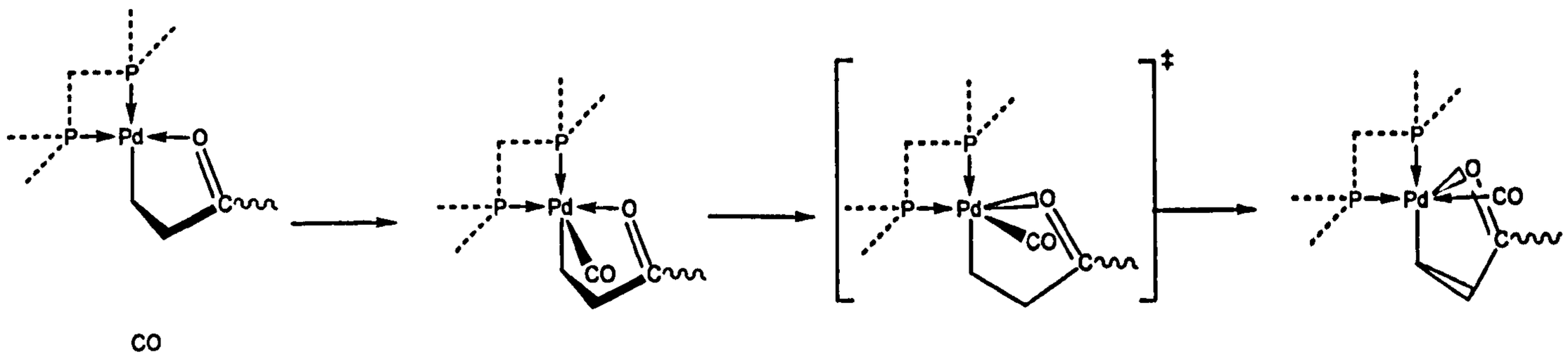
By increasing the distance between the complex and incoming CO group to such a large distance that the force between the two molecules was negligible, the energy difference from forming a Pd-CO bond from a new CO molecule was calculated to be –2.3 kcal/mol. However, a frequency test showed there to be imaginary frequencies in the system (as was found to be the case whenever there were incoming ligands at a large distance). Therefore, *throughout the project, it had to be noted that the enthalpies of bringing in ligands from large distances should be treated as estimates only*. It also meant that it would be meaningless to attempt to use zero-point correction energies in cases such as this.

3.5.6 Summary of findings of carbon monoxide addition analysis

The mechanism of adding a new carbon monoxide ligand to an equatorial site for subsequent migratory insertion was found to be more complicated than previously speculated, but the energy barriers to be overcome were very low compared to those for the two insertion stages.

The most significant finding of the mechanism was the continued use of axial palladium-ligand interactions in the mechanism. Rather than the incoming CO ligand directly displacing the oxygen atom bonded to palladium outright, the CO forms an axial interaction with palladium first. This bond then migrates to the equatorial site, displacing the Pd-O bond to the opposite axial site. The new axial Pd-O interaction, whilst not as strong as the equatorial bond, still stabilises the structure and would strongly encourage the CO insertion mechanism whilst the axial Pd···O interaction was still in place.

The mechanism of CO addition is summarised in **scheme 3.5.6**, and the energetics are summarised in **table 3.5.6**. As one can see from the energy differences, the energy barrier of the overall reverse reaction was reasonably high, at 7.1 kcal/mol. This was, however, less than the energy barrier of the next stage, CO migratory insertion, at 11.9 kcal/mol, meaning forward and reverse addition would most likely happen several times before the insertion step proceeded, but the thermodynamic favourability of CO addition would help promote the next step eventually.



Scheme 3.5.6: Schematic mechanism of carbon monoxide addition to equatorial site. All structures carry a single positive charge.

	From this project:	Including zero-point corrections	
Energy barrier of CO addition to axial site	No barrier	-	
Enthalpy of CO addition to axial site	-2.3	-	
Energy barrier of migration from axial to equatorial site	2.1	2.6	
Enthalpy of migration from axial to equatorial site	-4.8	-3.6	
Total activation energy of CO addition to equatorial site	*	*	From Ziegler and Margl:
Total enthalpy of CO addition to equatorial site	**-7.1**	**-5.9**	**-7.6**

Table 3.5.6: Energy differences (in kcal/mol) of stationary points in carbon monoxide addition.
**: The energy of the transition state is lower than the starting energy of the bimolecular reactant, therefore no energy would be required in the bimolecular product to overcome this energy barrier. If the complex loses its energy in the axially-bonded intermediate, it will need 2.1 kcal/mol of energy to overcome the barrier to reach the equatorial site.*

The final stage to analyse, to complete the cycle, was olefin addition, where the key question would be if, in that stage of the reaction, the olefin would be able to displace to Pd-O equatorial bond as easily as CO did in this stage.

3.6 Olefin addition stage

3.6.1 Introduction

As with carbon monoxide addition, there was no previous theoretical research into the mechanism of olefin addition prior to the insertion stage, which meant that work once again had to start from scratch. However, unlike carbon monoxide insertion, there were additional complications to consider. Firstly, there were two possible ways that olefins could be added to an equatorial site: either directly displacing the Pd-O bond out of the equatorial position, or a two-stage process where the Pd-O bond is first displaced by a CO molecule, which is then replaced by an olefin. Secondly, although displacement of the Pd-O bond would normally be required to add the olefin, after insertion of the *first* olefin and CO, a different bond would need displacing, depending on the product formed after CO insertion.

There was also the possibility that understanding the olefin addition mechanism could give clues as to whether excess carbon monoxide would promote copolymerisation (by assisting in removing Pd-O bonds from the equatorial sites) or hinder it (by occupying the sites that olefins need to be in for the next stage).

3.6.2 Early attempts to find transition state

Like carbon monoxide addition, it was a struggle to find the transition state of olefin addition. Until a successful method of finding the carbon monoxide addition transition state was found, fewer attempts were made at finding the olefin addition transition state, because of the additional variable of the orientation of the olefin molecule. Nevertheless, a few attempts were made to find the transition state before the path method was found to work for carbon monoxide addition.

Initially, research started with the product of CO insertion neglecting the second carbonyl ligand. (This was before it was found that the second carbonyl ligand made an important difference to the structure.) One of the first attempts to evaluate the energy surface was to do a rigid potential energy scan of the distance between palladium and one of the carbon atoms on the olefin, back from the structure after the olefin has been added (shown in figure 3.3.2.1). (A relaxed potential energy scan was more difficult as simply fixing only one Pd-C distance caused the other carbon to move closer towards palladium and lose the π-coordinate bond structure.) The rigid map is shown in **figure 3.6.2.**

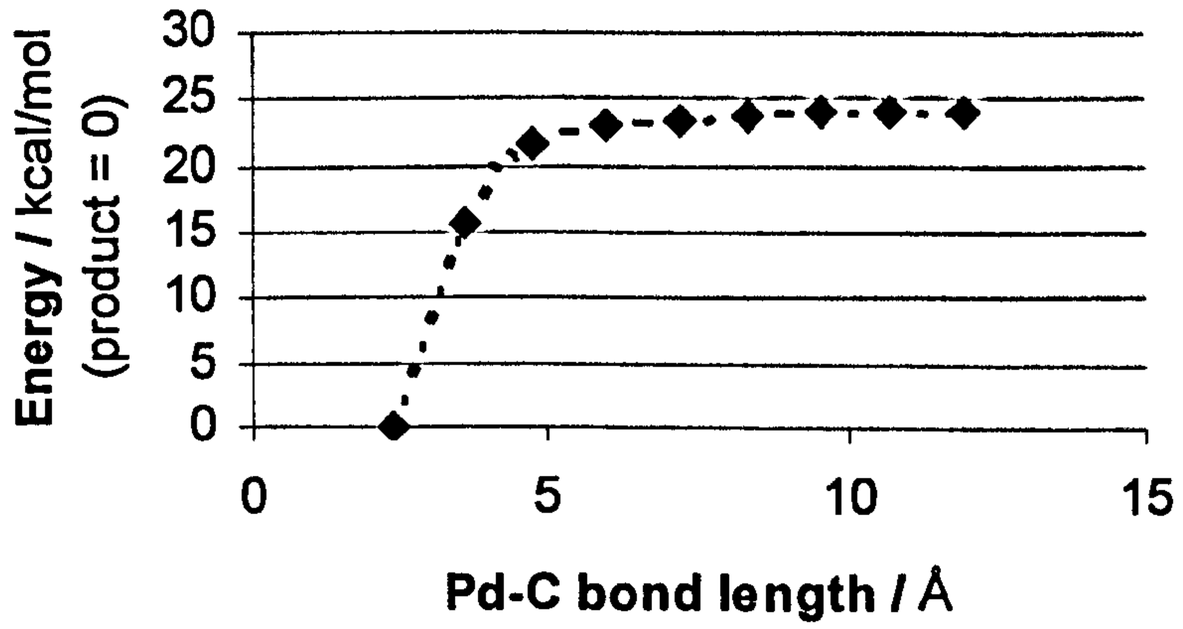


Figure 3.6.2: Rigid potential energy scan of energy at controlled distance of olefin from palladium centre.

As this was a rigid map and not a relaxed map, it was not surprising that the energy increased as the olefin was moved away from the palladium centre, as the rest of the complex did not have the chance to rearrange itself as the olefin moved away. However, when a quasi-relaxed scan was managed instead (a manual series of optimisations fixing the distances between palladium and *both* carbon atoms), this gave little useful information about where a transition state might be. Increasing the Pd-C distance by any significant amount caused the arrangement of the Pd-carbonyl bonding to change from an obvious bond from palladium to carbon to the bonding to both palladium and oxygen (as in the post-CO insertion structure shown in figure 3.4.2.2). However, there was no sign of any peak in energy, unlike the relaxed scan that increased the Pd-CO bond length during the carbon monoxide addition analysis.

Attempts were made to find a starting transition state by setting the Pd-C-O bond angle in the carbonyl group to halfway between those found in the pre-addition and post-addition structures and positioning the olefin a slightly longer distance away from the palladium than the distance in the product structure, to reflect the carbonyl group being re-arranged as the new ligand comes in. It was also attempted to assist finding the transition state by optimising a structure close to a possible transition state. It was hoped that optimisation for a few steps would show which direction forces were acting in, and would help to find the point when the direction of the forces changes (as was also tried for carbon monoxide addition). Unfortuantely, this failed to help find the transition state.

After this point, further attempts to find the transition state were put on hold whilst alternative approaches were attempted for carbon monoxide addition. It was

only when the carbon monoxide addition transition state was finally located with the assistance of a path job that the search for the olefin transition state was resumed, by applying the same method that had proved itself to be successful.

3.6.3 Final optimisation of transition state of direct addition

By the time the path method had been shown to work, it had been concluded that after the insertion of the second carbonyl, there would be a Pd-O co-ordinate bond that would need displacing rather than just a rearrangement of a carbonyl group. To begin with, a structure of the post-CO insertion product with an incoming olefin molecule above the palladium-ligand plane was optimised, with the stationary point shown in **figure 3.6.3.1**. However, a frequency test later showed that this was not, as had been assumed, a minimum, but a saddle point with an imaginary frequency centred on the rotation of the olefin. By the time this was realised, this structure had already been used for optimisation of the transition state, but fortunately this did not prevent a transition state being found. This error was noticed in the reaction path analysis and the corrected structure is shown in the next section.

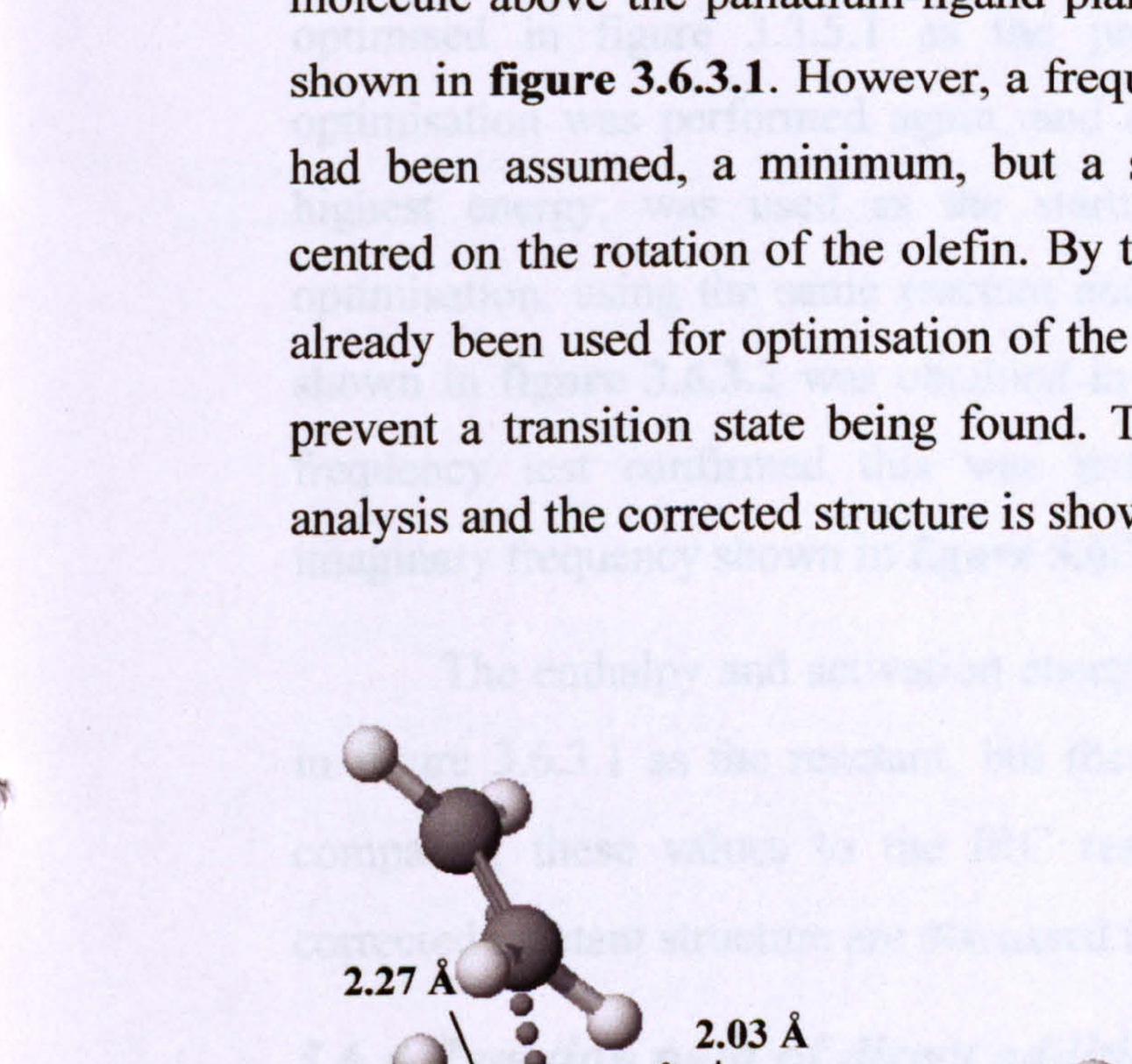


Figure 3.6.3.1: Optimised stationary point used as reactant for location of transition state.

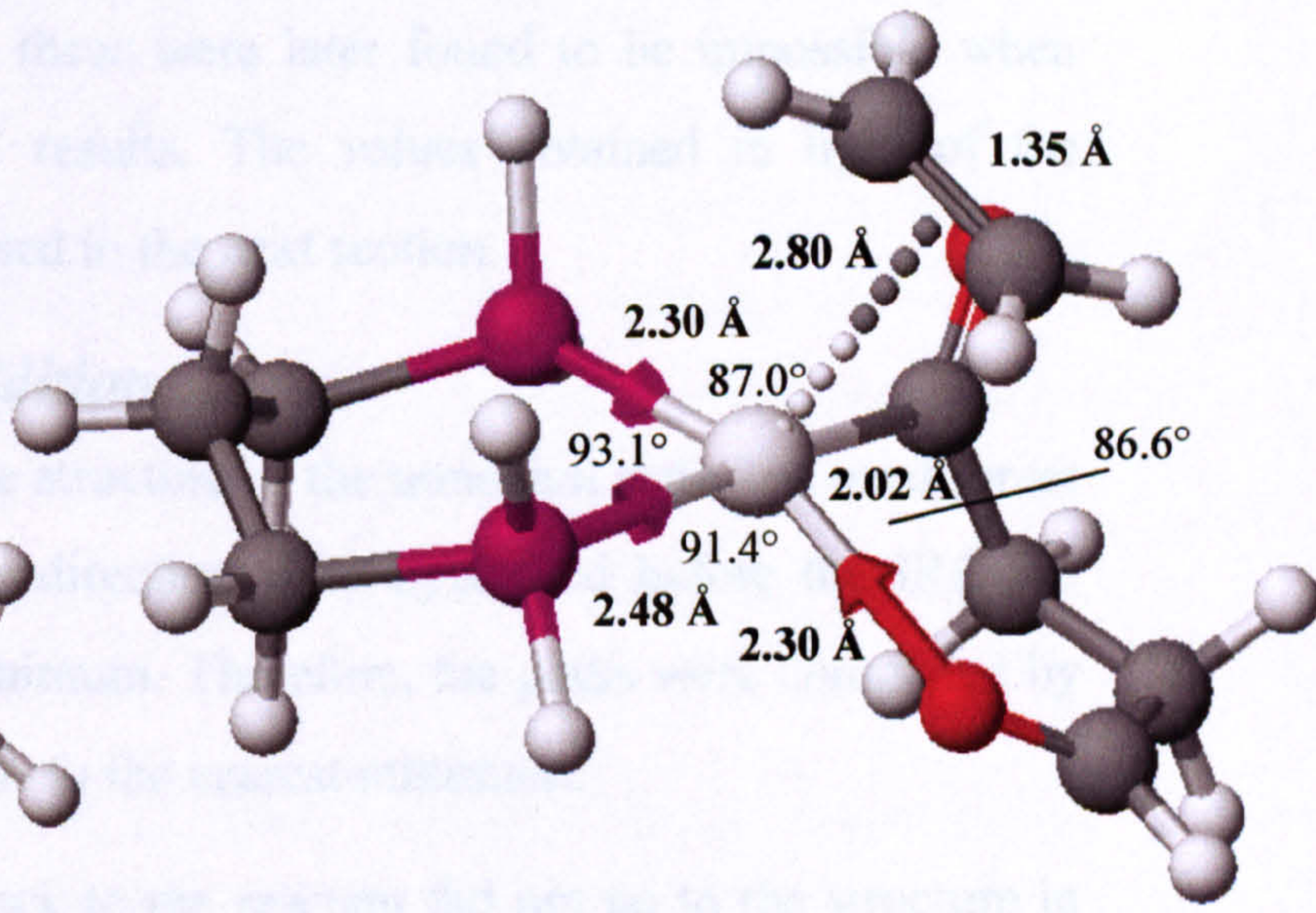


Figure 3.6.3.2: Optimised transition state of olefin addition.

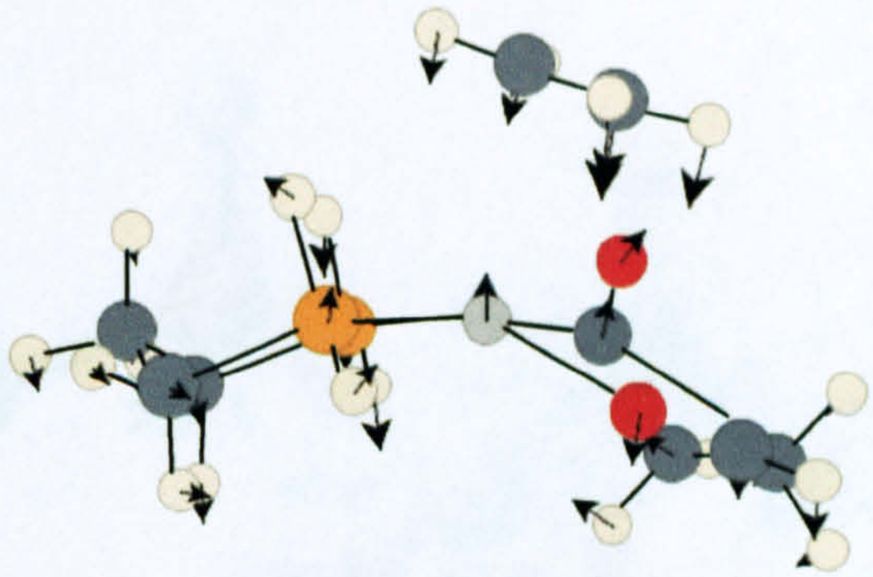


Figure 3.6.3.3: Vibrational mode of imaginary frequency of transition state (-51.6 cm^{-1})

Using this structure in figure 3.6.3.1 as the reactant structure, and the structure optimised in figure 3.3.5.1 as the product structure, a five-point QST2 path optimisation was performed again, and after 23 passes, the middle point, with the highest energy, was used as the starting structure for a QST3 transition state optimisation, using the same reactant and product structure. An optimised structure, shown in **figure 3.6.3.2** was obtained in a surprisingly short amount of time, and a frequency test confirmed this was indeed a saddle-point (vibrational mode of imaginary frequency shown in **figure 3.6.3.3**).

The enthalpy and activation energy were calculated using the structure shown in figure 3.6.3.1 as the reactant, but these were later found to be impossible when comparing these values to the IRC results. The values obtained in light of the corrected reactant structure are discussed in the next section.

3.6.4 Reaction path of direct addition

As with CO addition, when the structure of the transition state was used for an IRC job, only a few points in either direction were optimised before the IRC job declared the final point to be at a minimum. Therefore, the paths were completed by optimising the final point on either side to the nearest minimum.

Most significantly, the path back to the reactant did not go to the structure in figure 3.6.3.1, originally thought to be the reactant structure, but instead went towards what was presumably the true reactant structure, shown in **figure 3.6.4.1**. Unfortunately, a frequency test showed this structure to be a first-order saddle point too, and further attempts to find a minimum were unsuccessful. Therefore, this can only be taken as an estimate of the intermediate structure. It is not immediately clear how far away from this estimated structure the actual intermediate is.

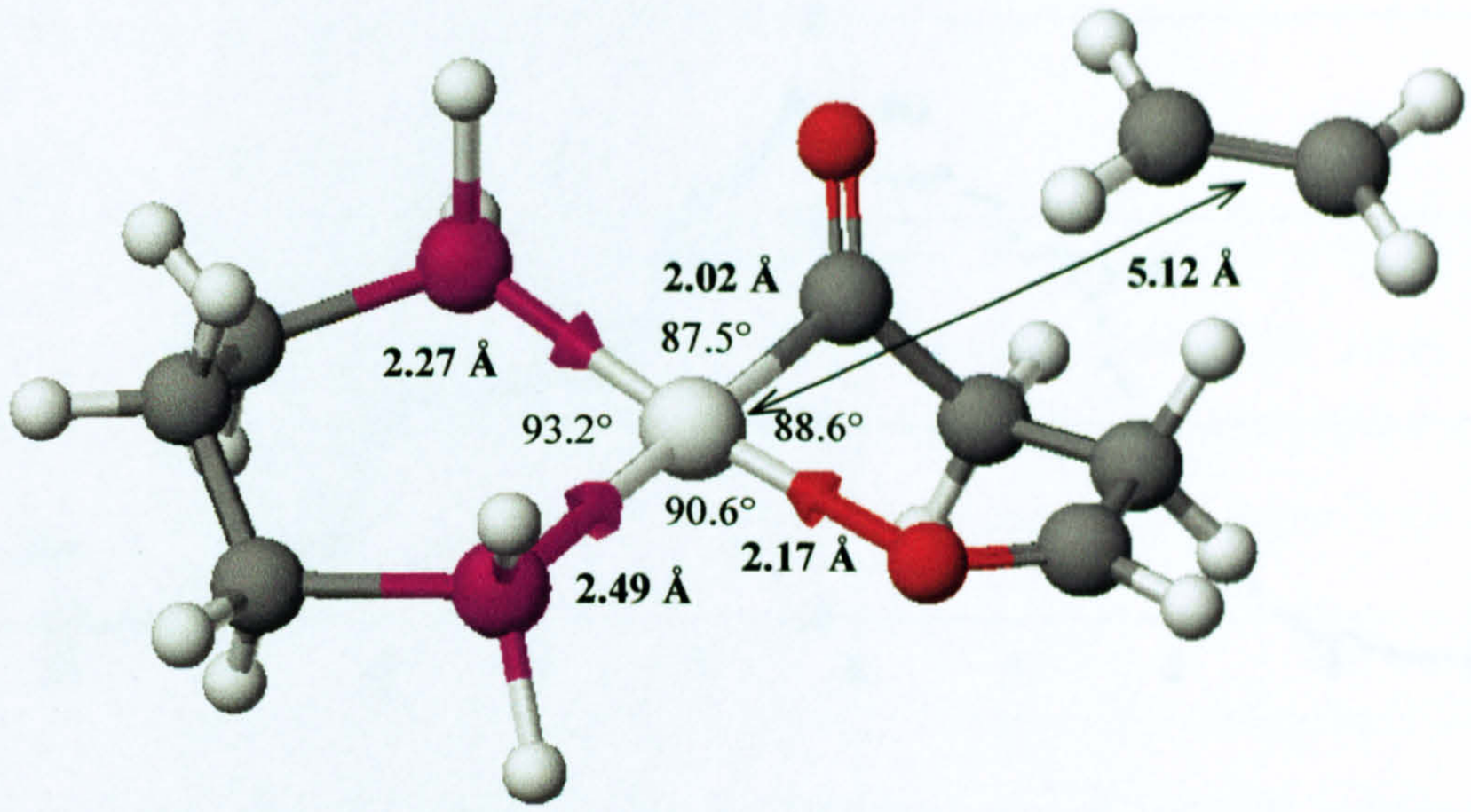


Figure 3.6.4.1: Optimised saddle-point estimated to be reactant structure of olefin addition, from backwards reaction path analysis from olefin addition transition state.

Nevertheless, if it was assumed that this saddle point was close to the structure of the minimum, an activation energy and enthalpy of this step could now be estimated; these were 2.2 kcal/mol and –0.2 kcal/mol respectively (plus whatever the energy difference was between this saddle point and the true minimum). Even allowing a margin of error for the energy of the local minimum, this directly contradicted the theory that olefin ligands are too weak to displace Pd-O bonds in six-membered rings and require CO to displace the bond for them. The relative ease of transition from a Pd-O equatorial bond to axial interaction rather than the outright breakage of the bond probably contributed to the ease of adding another ligand into its equatorial site, but this was a significant change from previous theories concerning the mechanism between insertion steps. The only remaining consideration now was whether CO addition would be faster and compete with olefin addition. (See Section 4.2.7.)

A diagram of the reaction profile is shown in **figure 3.6.4.2**, with selected points along the path being shown in **figure 3.6.4.3**. In spite of the path towards the reactant ending in a saddle-point rather than a minimum, useful information could be obtained about the reaction mechanism. The mechanism could be broken down into the following stages:

- Movement of the olefin into an axial site above palladium (points a – b – the exact mechanism is unclear owing to the uncertainty over the structure of the reactant);

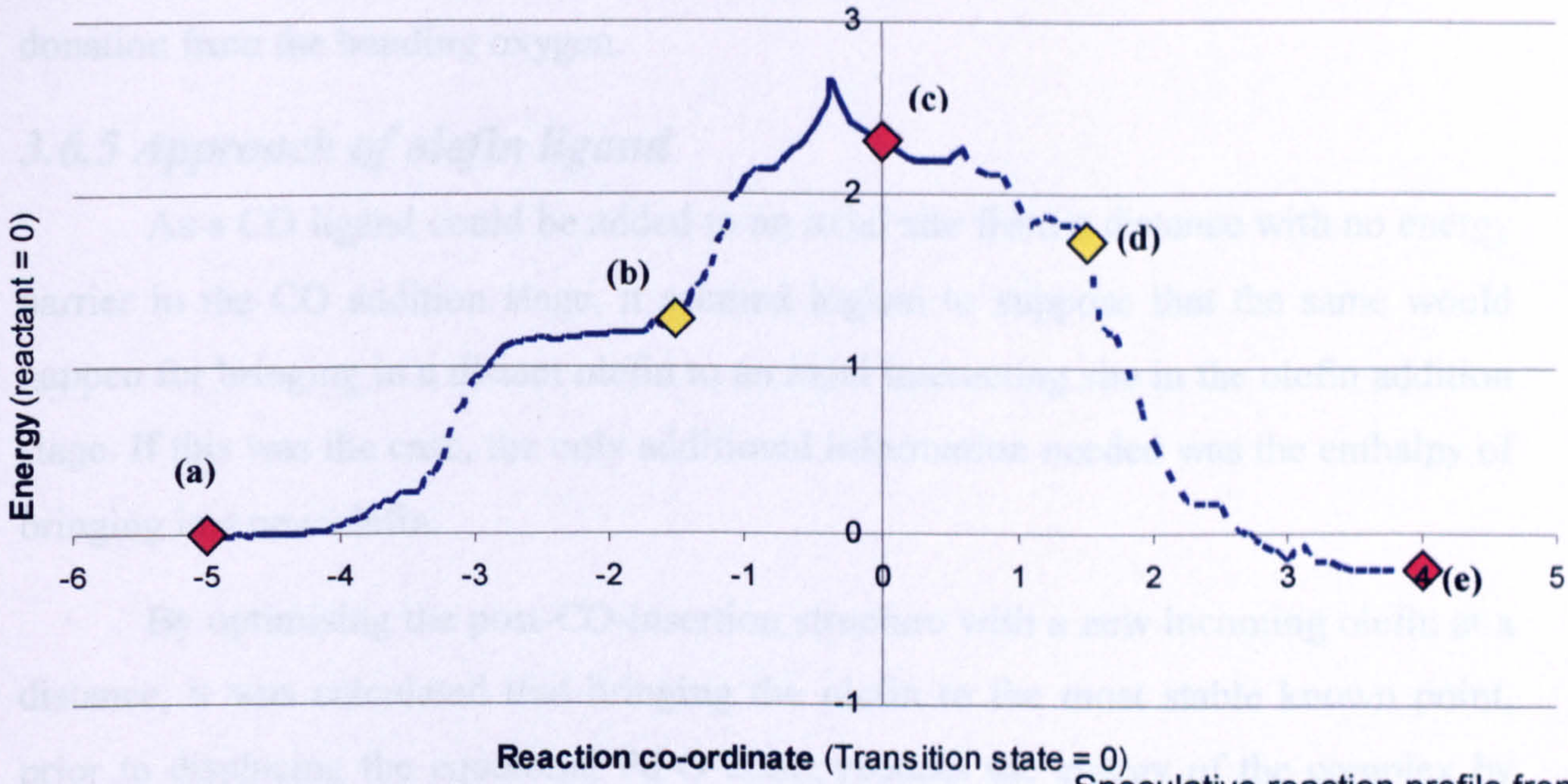


Figure 3.6.4.2: Reaction profile of olefin addition without second CO group, with selected points shown in **figure 3.6.4.3**.

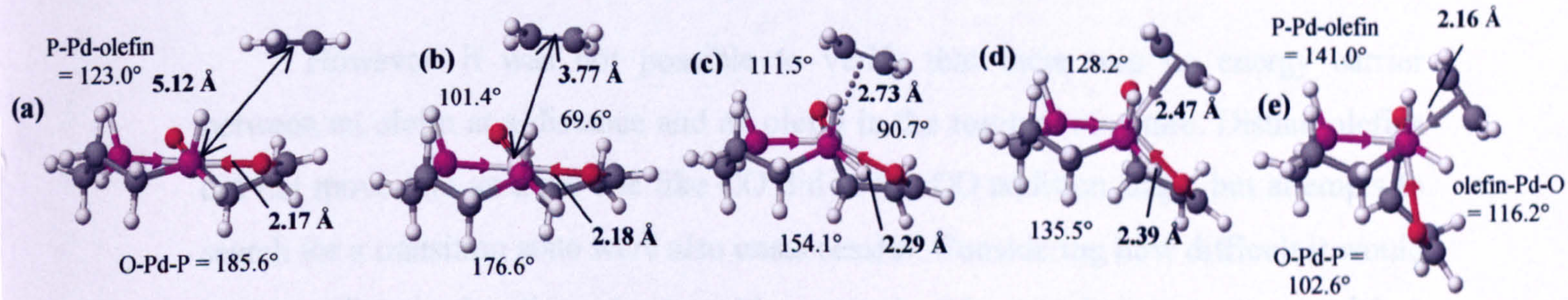


Figure 3.6.4.3: Selected points from reaction profile.

- Shortening of the π-coordinate bond between the olefin and palladium, whilst assuming a more definite structure characteristic of a bonding olefin (points b-d);
- Displacement of the Pd···O interaction from the equatorial position to the axial position the by the Pd-olefin bond moving into the equatorial site (points b-e);
- Re-arrangement of the $-CH_2CH_2CO-$ group to its lowest energy conformation (points d-e).

The product structure is almost identical to the reactant structure of the next step (olefin insertion). One notable aspect of the structure, however, is that the new olefin ligand does not quite take up an equatorial position, instead occupying a

position part-way to the equatorial site. This may be an effect arising from electron donation from the bonding oxygen.

3.6.5 Approach of olefin ligand

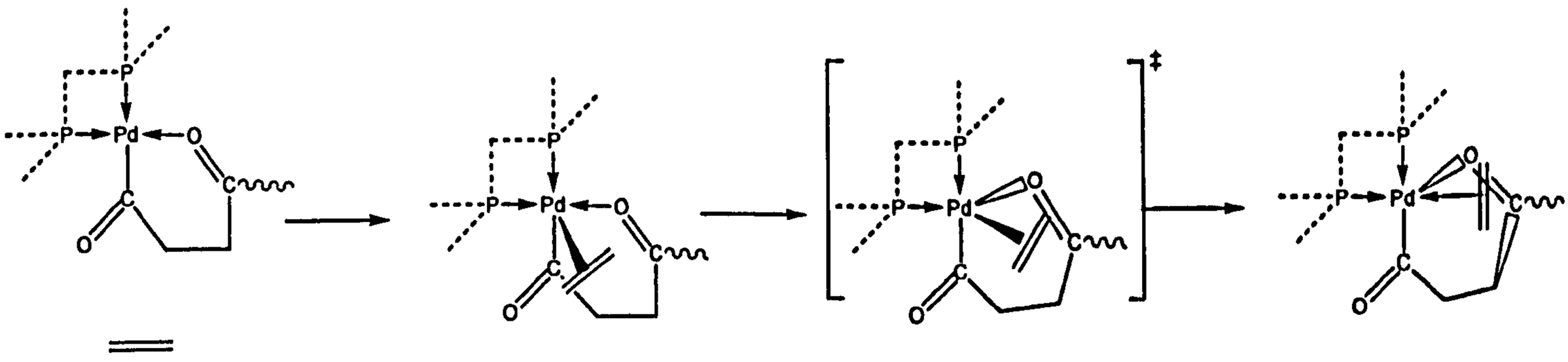
As a CO ligand could be added to an axial site from a distance with no energy barrier in the CO addition stage, it seemed logical to suppose that the same would happen for bringing in a distant olefin to an axial interacting site in the olefin addition stage. If this was the case, the only additional information needed was the enthalpy of bringing in a new olefin.

By optimising the post-CO-insertion structure with a new incoming olefin at a distance, it was calculated that bringing the olefin to the most stable known point, prior to displacing the equatorial Pd-O bond, reduces the energy of the complex by 2.5 kcal/mol, almost the same as the energy difference for bringing in a new CO molecule to an axial site in the CO addition stage. (This quantity was subject to the error of the optimised intermediate not being a minimum, but this error cancelled out with the enthalpy and activation energy of the following step.)

However, it was not possible to verify that there was no energy barrier between an olefin at a distance and an olefin in the reactant structure. Distant olefins did not move into an axial site like CO did in the CO addition stage, but attempts to search for a transition state were also unsuccessful. Considering how difficult it would be to predict the location of a transition state in this step, it is not too surprising. However, in practical terms this result is unlikely to make any difference, because if an energy barrier exists, it is likely to be tiny and not make the slightest difference to the reaction dynamics at all.

3.6.6 Summary of findings of olefin addition analysis

In spite of the doubts that previous authors have cast over the ability of an incoming olefin to directly displace a Pd-O bond, there appeared to be little difficulty in accomplishing this process. The mechanism of olefin addition seemed to proceed in a very similar fashion to the carbon monoxide addition, with the olefin displacing the Pd-O bond from an equatorial site to an axial site. The only significant difference in the mechanism was that there was no significant axial interaction between palladium and the olefin prior to displacement as there was for the Pd-CO bond in CO addition.



Scheme 3.6.7: Schematic mechanism of olefin addition to equatorial site. All structures carry a single positive charge.

Energy barrier of olefin addition to axial site	No barrier?	
Enthalpy of olefin addition to axial site	-2.5?	
Energy barrier of migration from axial to equatorial site	2.2?	
Enthalpy of migration from axial to equatorial site	-0.2?	
Total activation energy of olefin addition to equatorial site	**1.4**	From Ziegler and Margl:
Total enthalpy of olefin addition to equatorial site	**-2.7**	-6.0

Table 3.6.7: Energy differences (in kcal/mol) of stationary points in olefin addition. Figures with a question mark are estimated values in view of the fact that the structure used as the intermediate prior to the displacement of the olefin to an equatorial site was a first-order saddle-point and not a minimum. (In view of the estimate of the energy of the axially-bonded structure, all zero-point energy corrections were impractical.)

The energy barrier, estimated to be 2.2 kcal/mol (plus corrections for the reactant structure being a saddle point and not a minimum), is very similar to the 2.2 kcal/mol barrier for CO addition. Whether this was because the olefin was better at displacing Pd-O bonds than previously speculated, or because Pd-O bonds are weaker in 6-membered rings than 5-membered rings, had yet to be determined. However, the enthalpy of this step was -0.2 kcal/mol (again with the same correction), unlike CO addition where displacement significantly stabilised the complex. This meant that the energy barrier for the reverse reaction would be only 2.4 kcal/mol, meaning that this stage would be more prone to competition from other processes, such as termination by methanolysis, or inhibition by a CO molecule occupying the site the olefin needs.

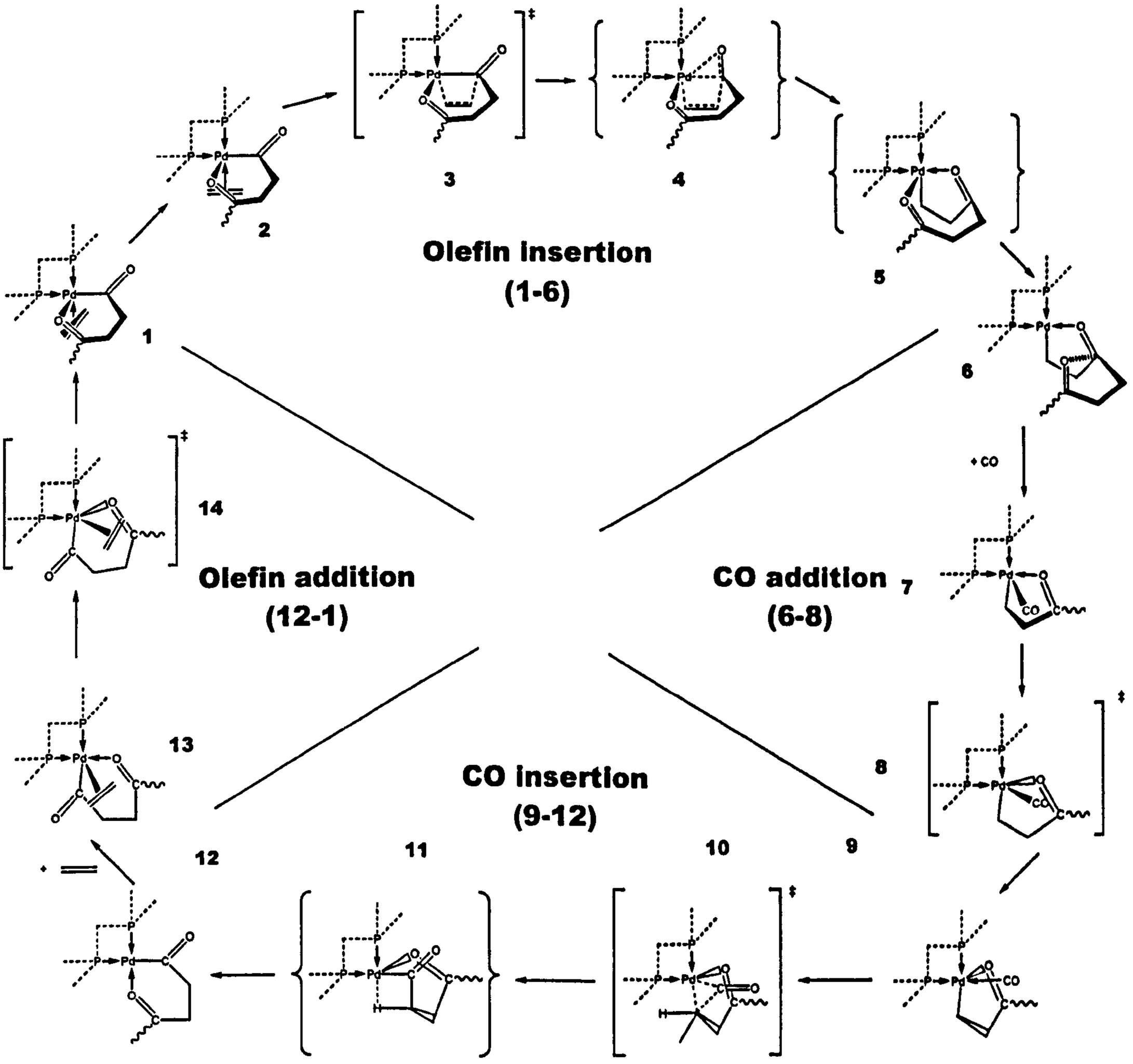
The mechanism of the olefin addition process is given in **scheme 3.6.7**, and the energy differences are given in **table 3.6.7**.

This completed the reaction cycle, showing the propagation mechanism to be a viable process, in line with experimental evidence.

3.7 Summary of propagation mechanism

The complete propagation cycle for alternating copolymerisation of olefins and carbon monoxide was modelled using the B3-LYP method and the SDD basis set augmented by polarisation functions on the chemically active atoms. The complete mechanism of the cycle is illustrated in **scheme 3.7.** The energy changes required to get through the cycle are illustrated in **figure 3.7** and tabulated in **table 3.7.**

The mechanisms of the olefin and carbon monoxide insertion steps were both found to be consistent with previous theoretical experiments to monitor the reaction mechanism. Both stages have energy barriers in the order of 10 kcal/mol, but the olefin insertion barrier was a little higher value suggesting that the olefin insertion



Scheme 3.7: Full mechanism of propagation cycle of olefin-CO copolymerisation. Transition states are shown in square brackets, selected non-stationary points are shown in curved brackets, and other structures are minima. All structures carry a single positive charge.

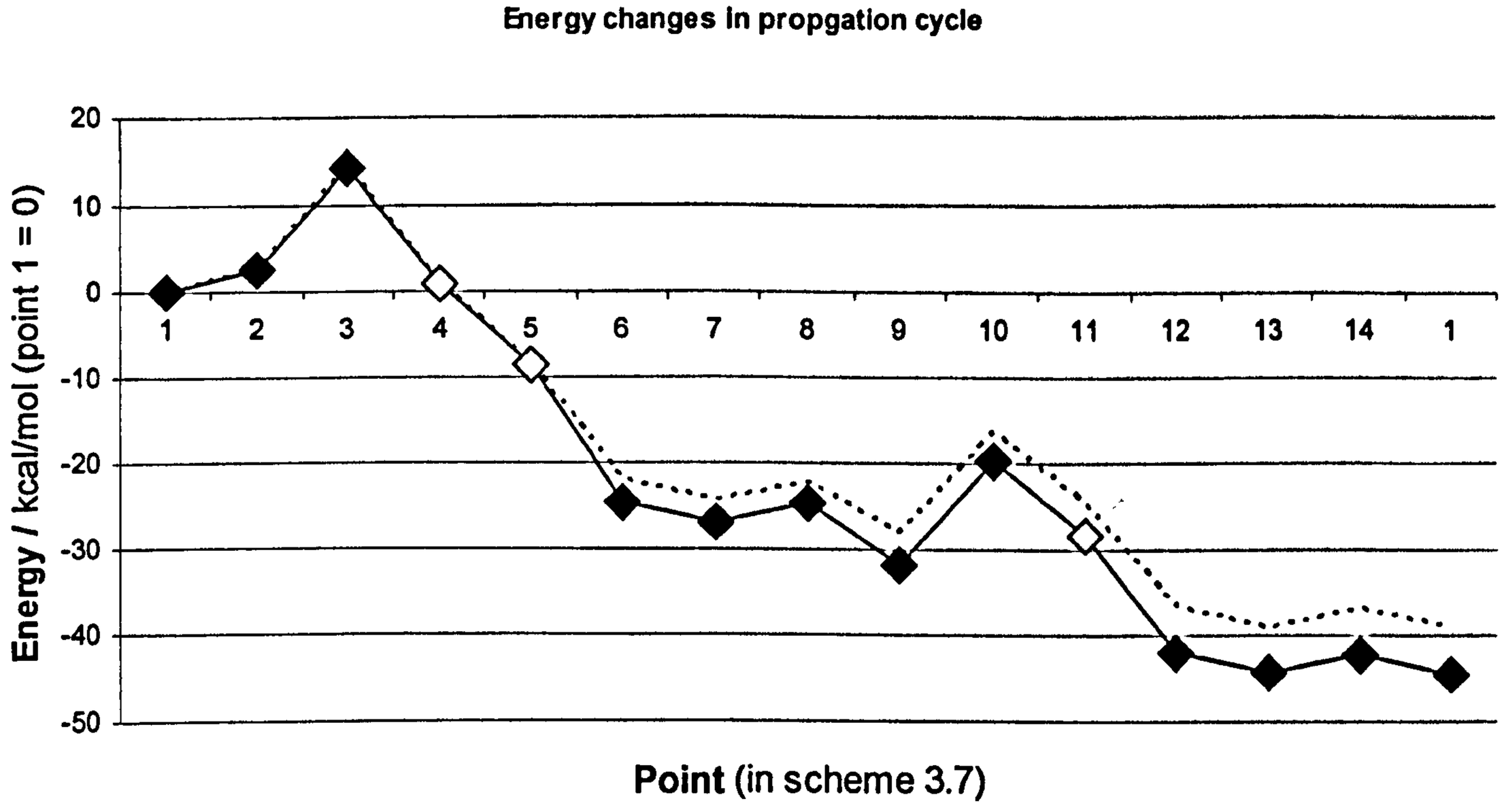


Figure 3.7: Energy changes associated with **scheme 3.7** (non-stationary points, shown in yellow, are approximations). Dotted line includes zero-point corrections.

stage is the rate-determining step. The mechanism was governed very strongly by the tendency for the palladium to maintain a four-coordinate geometry around the planar sites, in particular by Pd-O co-ordinate bonds that stabilised some of the complexes significantly and played a significant part in promoting the forward reaction and preventing the reverse reaction. However, the second carbonyl group along the chain also frequently interacted with the palladium to form a Pd-O axial interaction when no other site was available.

For the first time, the energy barriers associated with the two addition stages have been compared with the olefin and carbon monoxide insertion stages. The mechanisms of adding a new ligand turned out to be reasonably complex, involving moving the new ligand into a vacant axial site, and then displacing the Pd-O co-ordinate bond from its equatorial site into the opposite axial site. But in spite of previous speculation that there may be difficulty in displacing the Pd-O co-ordinate bonds, in particular by the weaker olefin ligand, the energy barriers of both these processes were very small compared to the insertion energy barriers, so it did not seem necessary for there to be a stronger ligand to displace the Pd-O bond first.

	From this project:	Including zero-point energies	From Ziegler & Margl (ref. 8)
Olefin rotation (1-2)	2.6	2.9	-
Energy barrier of olefin insertion (1-3)	14.3	14.5	15.3
Enthalpy of olefin insertion (1-6)	-24.4	-22.0	-11.4
Addition of CO to axial site (6-7)	-2.3	-	-
Energy barrier of migration of CO to equatorial site (7-8)	2.1	2.6	-
Enthalpy of migration of CO to equatorial site (7-9)	-4.8	-3.6	-
Total enthalpy of CO addition (6-9)	-7.1	-5.9	-7.7
Energy barrier of CO insertion (9-10)	11.9	11.5	11.7
Enthalpy of of CO insertion (9-12)	-10.4	-8.6	-7.6
Addition of olefin to axial site (12-13)	-2.5?	-	-
Energy barrier of migration of olefin to equatorial site (13-14)	2.2?	-	-
Energy change of migration of olefin to equatorial site (13-1)	-0.2?	-	-
Total energy change of olefin addition (12-1)	-2.7	-	-6.0
Total energy change of one cycle:	-44.6	-39.2	-32.7

Table 3.7: Summary of key energy changes (in kcal/mol) in propagation cycle.

There was, unfortunately, very little experimental data to which these results could be compared. However, some of the energy barriers could be compared to similar reactions whose energy barriers could be analysed experimentally, and some of the stationary points could be compared to barriers from the Cambridge Structural Database. There was a reasonable correlation between the theoretical and experimental energy barriers, and a good agreement on the lengths of the Pd-acyl, Pd-alkyl and Pd-CO bond lengths. The only parameters where there were possible grounds to doubt accuracy beyond ±4° were the bond angles.

Having completed the propagation cycle, attention could now move on to the possible initiation and termination steps, as well as consider what would happen in double insertion of olefins or carbon monoxide occurred.

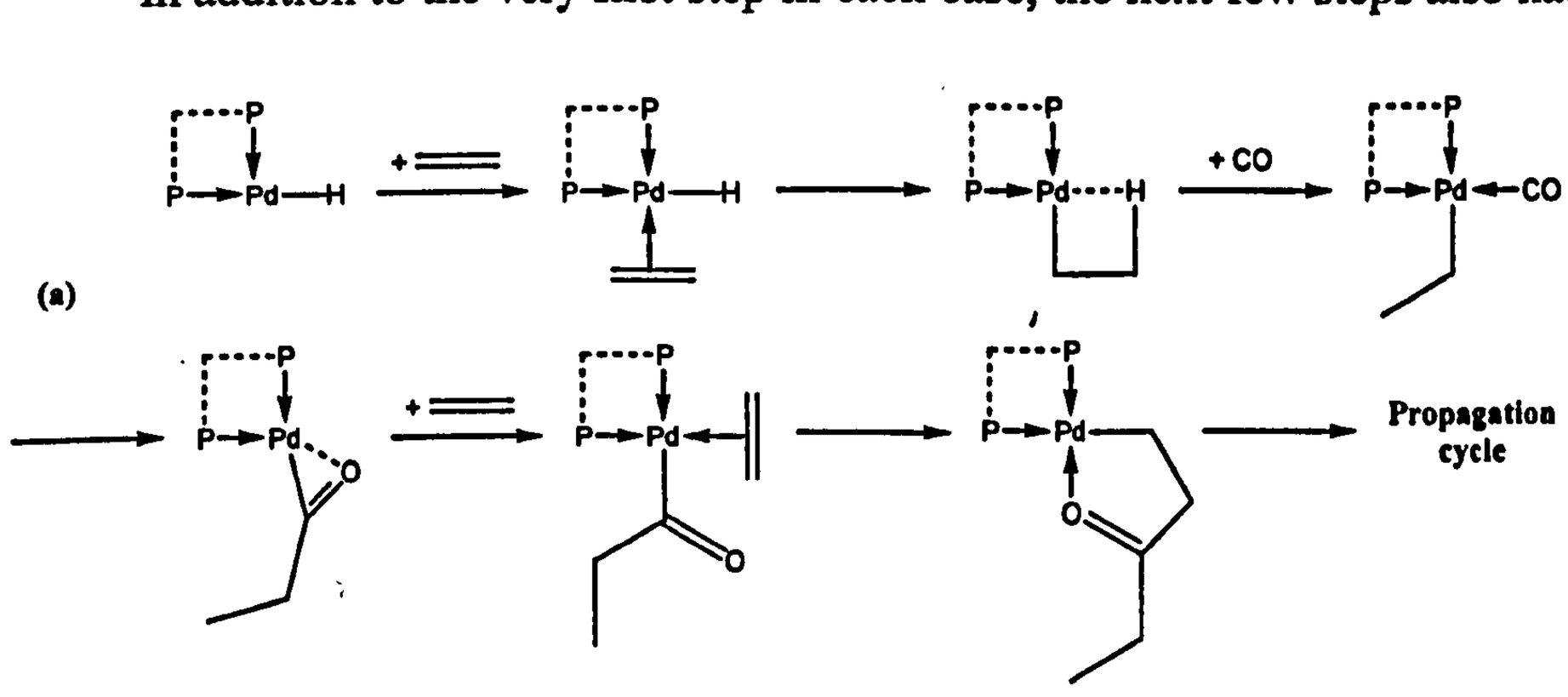
4: Other aspects of copolymerisation of ethene and carbon monoxide

4.1 Initiation processes

4.1.1 Introduction

Several different mechanisms have been hypothesised for the initiation process to start copolymerisation, but there are only two possible mechanisms that give rise to the end groups that are actually observed on copolymer chains. One method is insertion of the first olefin into a Pd-hydride bond, to produce a keto- (CH_3CH_2CO-) end group, and the other is to insert the first CO into a Pd-methoxy group to produce an ester (CH_3OCO-) end-group. Whilst it is thought that the former process is the one that actually occurs (the latter group is thought to be produced in the termination stage), it was decided to examine both proposed initiation mechanisms to determine which process was more feasible.

In addition to the very first step in each case, the next few steps also had to be



Scheme 4.1.1: Initiation steps for olefin/CO polymerisation by **(a)** inserting an olefin into a Pd-H bond to give a keto-end group; or **(b)** inserting a carbon monoxide ligand into a Pd-OMe bond to give an ester end-group.

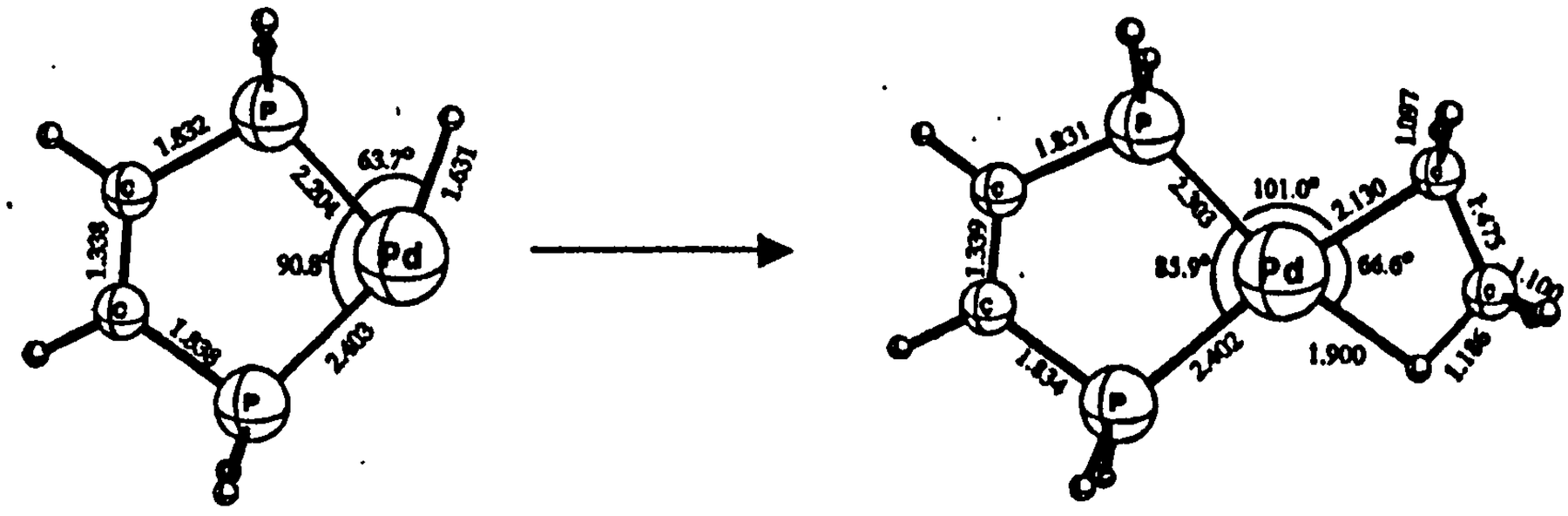


Figure 4.1.1: Initiation mechanism proposed by Ziegler and Margl. Note that they proposed that there were no intermediates or transition states in this reaction mechanism.

examined, owing to the lack of the carbonyl group to form an axial bond that is normally present in the propagation cycle. The full steps are shown in **scheme 4.1.1.** Some of the steps had already been determined during analysis of the propagation cycle, but most of the steps were new and had to be determined separately.

Only one of the initiation steps was known to have been analysed previously, and that was the initiation step, analysed by Ziegler and Margl.[7] (Svensson *et. al.* examined initiation by insertion of CO into a Pd-Me bond[36], but the Pd-Me bond could only be present in the first place by the use of a suitable Pd complex. Furthermore, there was no conceivable route for regenerating the Pd-Me bond after termination, and the nearest alternative – forming a Pd-ethyl bond – was effectively the same as Ziegler and Margl's proposed mechanism.) Their proposed mechanism is shown in **figure 4.1.1.** Even so, certain details, such as addition of the second olefin into the Pd plane for insertion (following insertion of the first CO), had not been considered. There was no known analysis of initiation by insertion of CO into a Pd-methoxy bond, so this had to be started from scratch.

Note: all of the computational details in this chapter are the same as in Chapter 3.

4.1.2 Insertion of olefin into Pd-H bond

Although there were several steps in the initiation process, starting from insertion of an olefin into a Pd-H bond, before this became indistinguishable from the propagation cycle, there was only one significant step that needed to be determined, which was the migratory insertion of the olefin into the Pd-H bond itself. The insertion of CO into the Pd-alkyl bond and an olefin into the Pd-acyl bond, both without the influence of another CO group forming an axial bond, are already covered in Chapter 3 in the process of determining the mechanism of the propagation cycle.

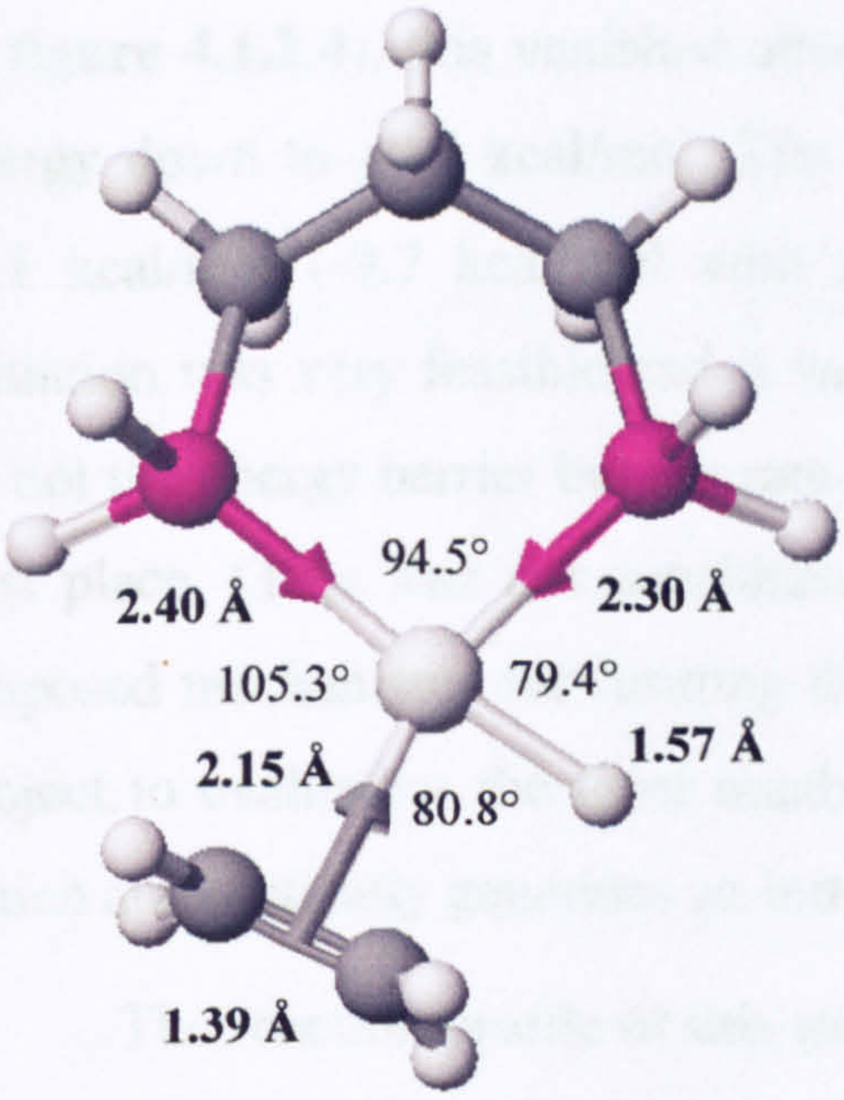


Figure 4.1.2.1: Optimised structure of reactant for olefin insertion into Pd-H bond.

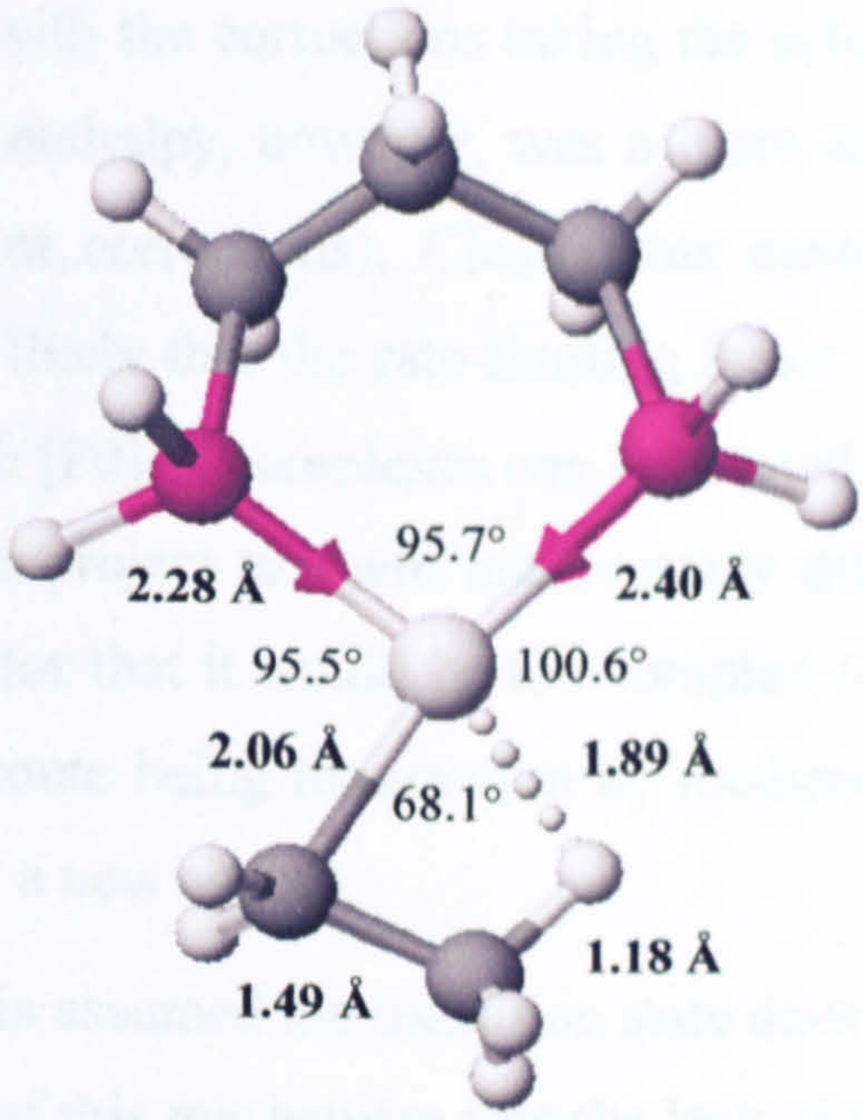


Figure 4.1.2.2: Optimised structure of product for olefin insertion into Pd-H bond.

The reactant and product structures were optimised first, as shown in **figure 4.1.2.1** and **4.1.2.2** respectively. Notably, but as expected from earlier optimisations, in the product the four-co-ordinate structure was completed by forming an agostic Pd···H-C interaction with a hydrogen on the second carbon atom. Optimisation of the transition state, as it happened, succeeded on the first attempt using the QST2 method – there was not even any need to guess a transition state structure. The optimised structure is shown in **figure 4.1.2.3**. However, it was doubtful as to whether there was a transition state at all. This structure was practically identical to the structure of the reactant, and the energy barrier was almost nonexistent, at just 0.2 kcal/mol, but when

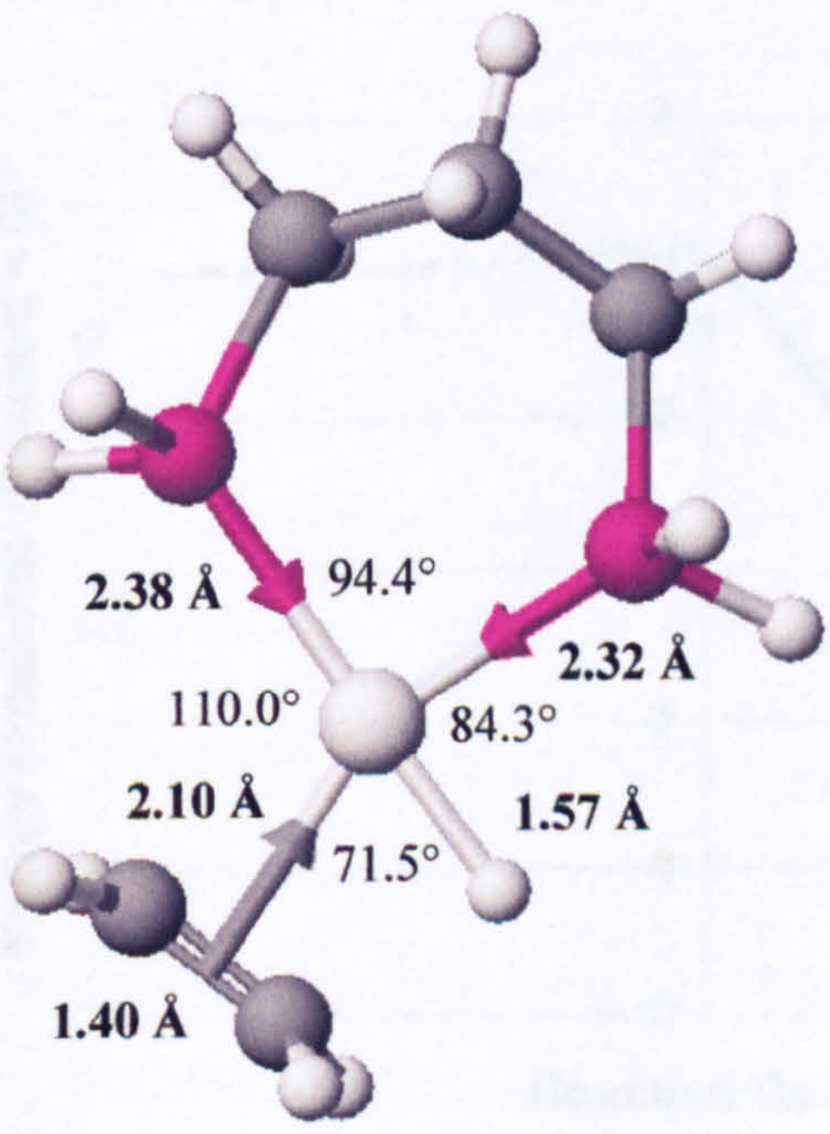


Figure 4.1.2.3: Optimised structure of transition state for olefin insertion into Pd-H bond.

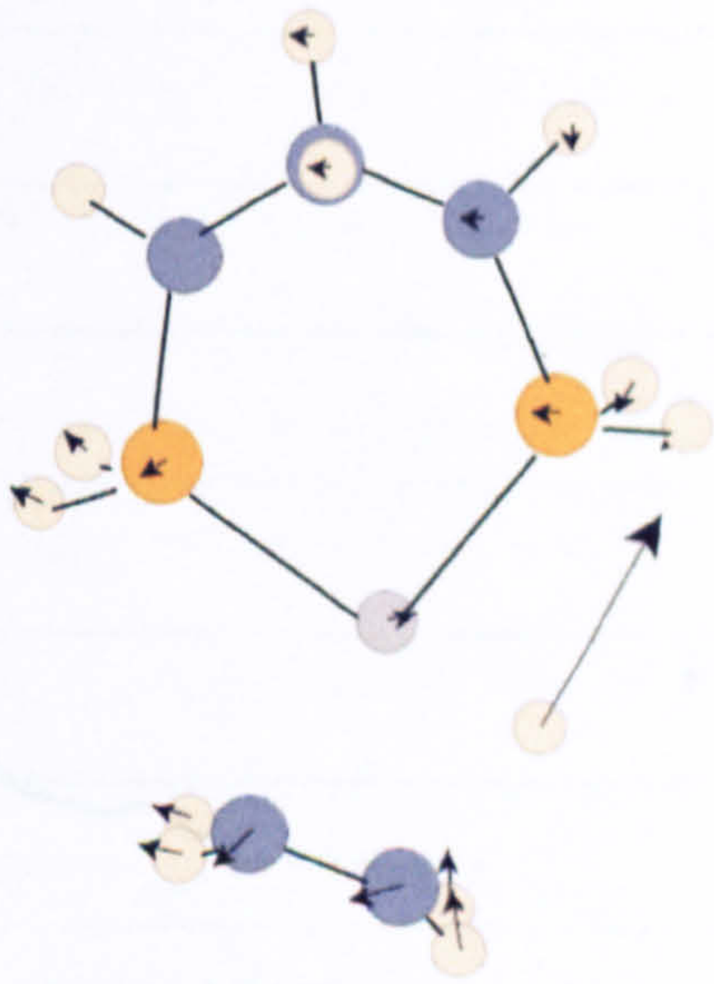


Figure 4.1.2.4: Mode of vibration of imaginary frequency (-321.1 cm^{-1}).

zero-point energies were included (mode of vibration of imaginary frequency shown in **figure 4.1.2.4**), this vanished altogether, with the corrections taking the activation energy down to –0.7 kcal/mol. The overall enthalpy, however, was a more definite -9.1 kcal/mol (-9.7 kcal/mol with zero-point corrections). Clearly this method of initiation was very feasible and it was most likely that the rate-limiting factor would be not the energy barrier but the rate at which [Pd]-H complexes can be formed in the first place. (This was not considered in this project as there are so many different proposed mechanisms for forming this initiator that it would be too complex for this project to evaluate – the most notable one route being termination by methanolysis, which automatically generates an initiator for a new chain.)

The reaction profile of this step (if it is assumed the transition state does exist) is given in **figure 4.1.2.5**. A notable feature of this mechanism was the lack of a local energy barrier to rotate the olefin, as there is for olefin insertion into a Pd-acyl bond. In this case, the most stable conformation of the reactant was with the olefin C-C axis in the Pd-ligand plane. (Possible reasons for this change in geometry will be discussed in Chapter 5.) Therefore, the need to rotate the olefin out of its most stable conformation would be eliminated.

Compared to the results obtained by Ziegler and Margl, the difference was that they proposed that there was no energy barrier to olefin insertion at all, and any optimisation of the starting structure with an olefin nearby led to insertion into the complex. This difference, however, was of little consequence, because an energy barrier of the magnitude of 0.2 kcal/mol would have virtually no effect in hindering

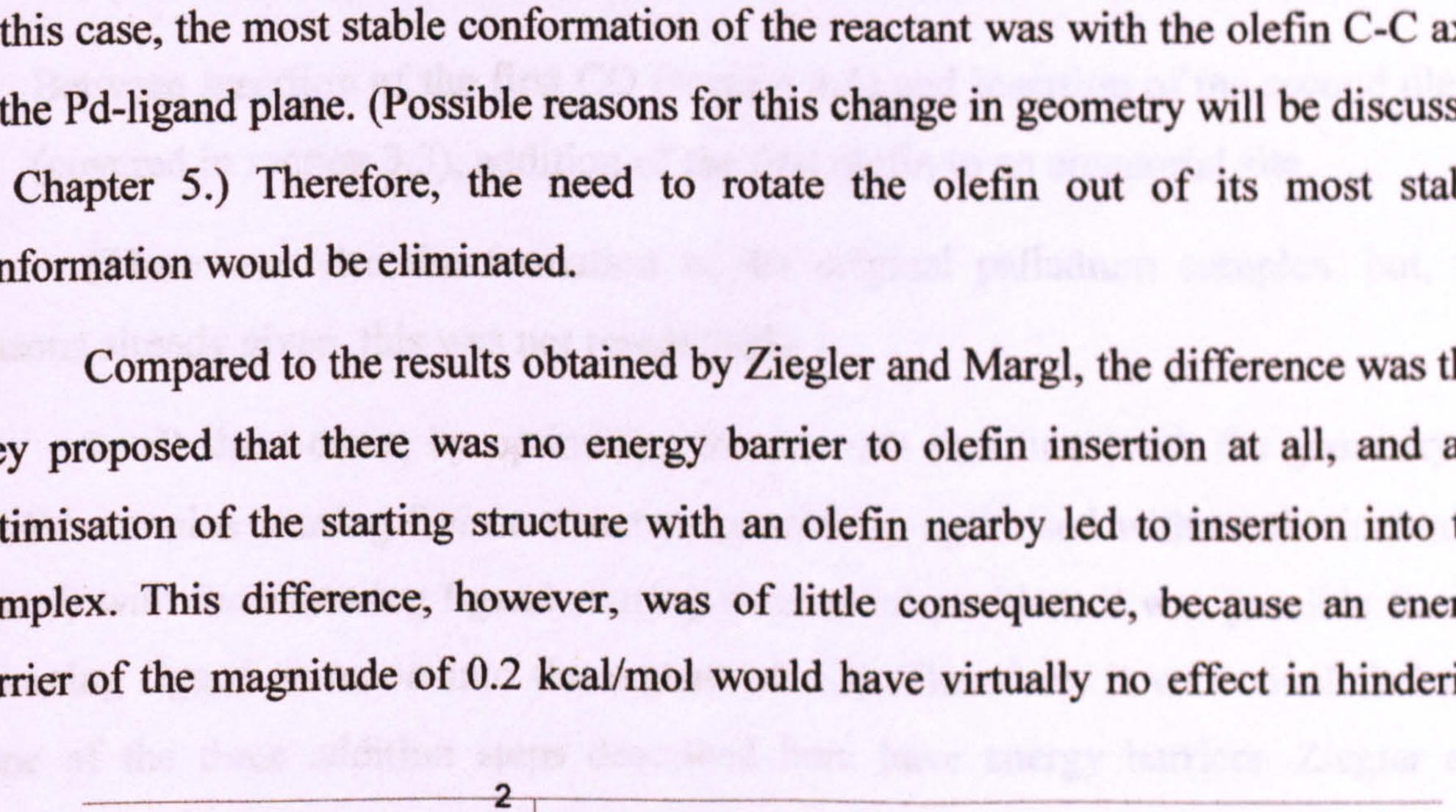


Figure 4.1.2.5: Reaction profile of olefin insertion into Pd-H bond.

the reaction. On the other hand, both this project and Ziegler and Margl agreed on the existence of the β-agostic Pd···H-C interaction in the product structure, and, most importantly, agreed that there were no obstacles to undergoing this initiation step.

4.1.3 Other initiation steps arising from insertion of olefin into Pd-H bond

The CO insertion into the Pd-alkyl bond and the second olefin insertion into the Pd-acyl bond are covered in sections 3.4 and 3.3 respectively. The remaining steps in the initiation process were all addition steps, as follows:

- Prior to insertion of the olefin into the Pd-H bond (described above), addition of the first olefin to an equatorial site.
- Between insertion of the first olefin (described above) and insertion of the first CO (covered in section 3.4), addition of the first CO to an equatorial site.
- Between insertion of the first CO (section 3.4) and insertion of the second olefin (covered in section 3.3), addition of the first olefin to an equatorial site.

(There was also the formation of the original palladium complex, but, for reasons already given, this was not researched.)

In all three cases, by optimising the reactant structure (with the geometry of the Pd complex starting from a structure previously optimised without the incoming ligand) with the incoming ligand starting in an axial position, it was possible for the incoming ligand to move into the equatorial site. Therefore, it was concluded that none of the three addition steps described here have energy barriers. Ziegler and Margl's research also agreed that there was no energy barrier in these steps.

Note: Throughout these steps, it should be remembered that the stationary points of complexes with distant ligands were not necessarily minima, therefore the energy calculations for these addition steps should be treated as estimates, and zero-point energy corrections would be meaningless.

The enthalpy from adding the first olefin to an equatorial site of a [Pd]H complex ([Pd] = palladium and the diphosphine ligand) from a distance was a total of -32.0 kcal/mol, a huge drop in energy that could be attributed to changing the Pd complex from á 3-coordinate structure to a much more stable 4-coordinate structure.

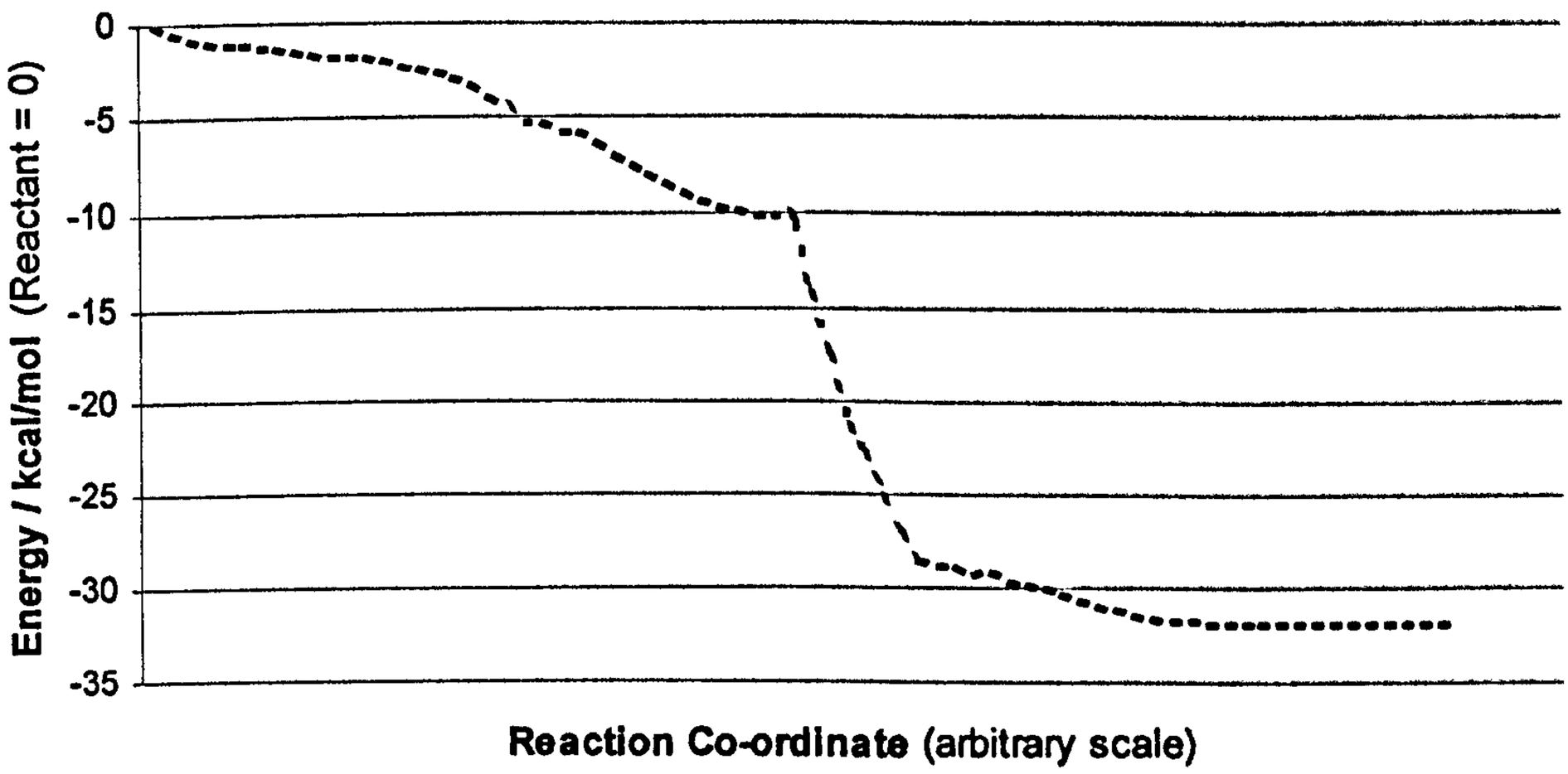


Figure 4.1.3.1: Speculative energy profile of addition of an olefin into a vacant site of [Pd]-H to form [Pd]H(C_2H_4).

An energy profile is shown in **figure 4.1.3.1.** (It is not meaningful to plot structures along the reaction path as the starting structure was chosen arbitrarily. However, it could be noted that the fall of the last 5 kcal/mol or so could be attributed to rotating the olefin to its most stable position.) Thus, the total enthalpy of olefin insertion into a Pd···H-C agostic interaction from a distant olefin a huge -41.1 kcal/mol (-41.7 . including the zero-point correction in the olefin insertion step).

After olefin insertion into the Pd-H bond, the addition of the next CO ligand into an equatorial site proceeded smoothly, with the CO ligand cleanly displacing the weak Pd···H-C agostic interaction. This addition caused the energy of the complex to fall by a further -18.6 kcal/mol – not as much as the addition of the first olefin when the reactant was in the unfavourable 3-coordinate geometry, but still a big difference brought on by the displacement of a weak ligand by a far stronger ligand. The speculative energy profile is shown in **figure 4.1.3.2.**

After this CO ligand is inserted into the chain, one is left with either a Pd···H-C agostic interaction or an acyl group bonding to palladium from both C and O. In the former case, the Pd···H-C agostic interaction is again easily displaced by an incoming olefin, causing a change in energy of a further -16.7 kcal/mol. Again, the huge change in energy appears to be brought about by the displacement of such a weak interaction by a stronger one. The speculative energy profile is shown in **figure 4.1.3.3.**

Figure 4.1.3.2: Speculative energy profile of addition of CO to displace Pd···H-C agostic interaction of $[Pd]C_2H_5$ after insertion of first olefin.

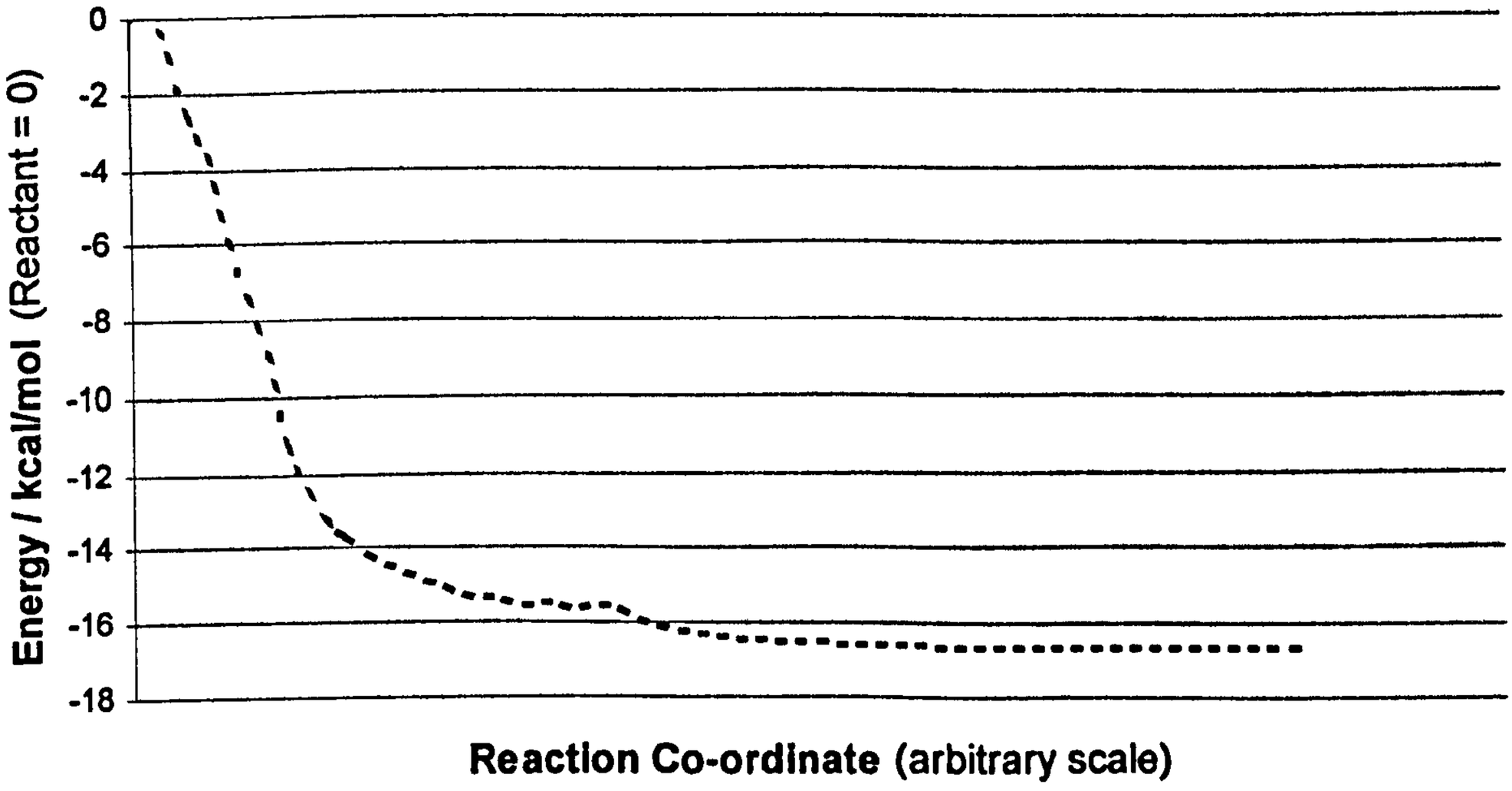


Figure 4.1.3.3: Speculative energy profile of addition of second olefin to displace Pd···H-C agostic interaction of $[Pd]COC_2H_5$ after insertion of first CO.

Addition of an incoming olefin in the latter case, in which the acyl oxygen atom occupies the fourth co-ordination site, was more difficult, as, depending on the starting position, the olefin was just as likely to drift away from the complex as towards one of the sites depending on the starting position of the olefin – this suggested that the path of the incoming ligand was critical. When it did move into an equatorial site, the process was accompanied by a rotation of the acyl group about the Pd-C bond so that the carbonyl was perpendicular to the palladium-ligand plane by

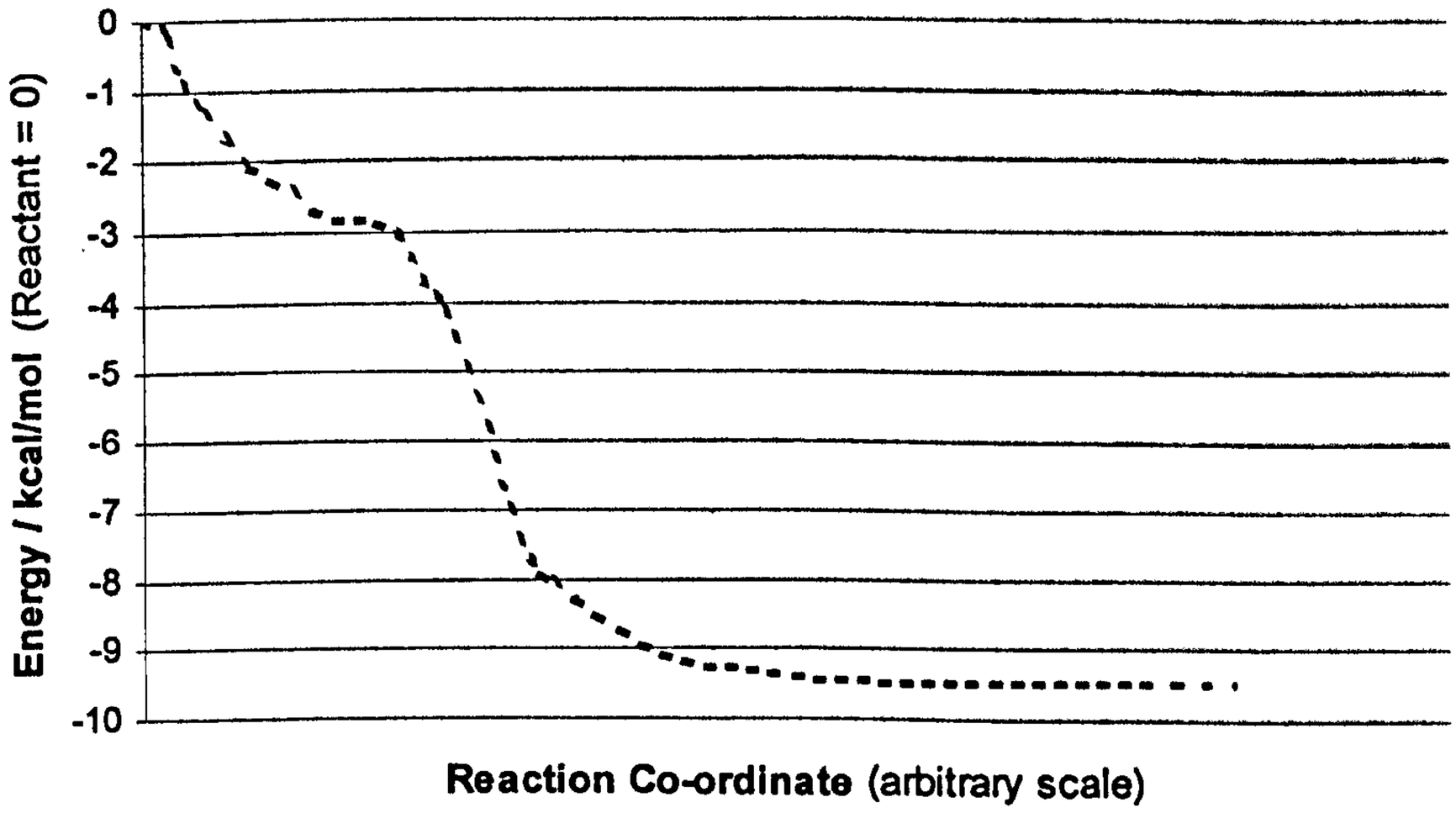


Figure 4.1.3.4: Speculative energy profile of addition of second olefin to displace Pd···O interaction in [Pd]COC_2H_4 and relaxation to most stable structure.

the time the olefin reached its equatorial position. The total energy change was –9.5 kcal/mol, and the speculative energy profile is shown in **figure 4.1.3.4.**

The flatter area to the left of the figure 4.1.3.4 was the region where the carbonyl group was being rotated from parallel to the palladium-ligand plane to its orthogonal position, stopping the carbonyl from donating electrons at two sites, but essential to allow the olefin to occupy an equatorial site. If the same exercise was done with a metal centre that bonded more strongly to the carbonyl or more weakly to the olefin (or even if the calculation was repeated with a different method or basis set), it is possible that a minimum and energy barrier could arise here.

There was a slight discrepancy in the energy calculations, as the enthalpy to reach the reactant in this step from the β-agostic Pd···H-C interacting conformation was –7.6 kcal/mol, making the total of these two steps –17.1 kcal/mol, slightly overstepping the -16.7 kcal/mol enthalpy calculated for direct displacement of the β-agostic Pd···H-C interaction by an olefin. However, a difference of 0.5 kcal/mol in steps of this magnitude was not significant, and this was well under the margin of error one should expect from computational calculations of energy differences. The most likely reason for the discrepancy was that at one structure was optimised to slightly different local minima (probably with one of the ligands at a large distance) in different runs.

Together with the insertion steps considered in sections 3.3, 3.4 and 4.1.2, this completes analysis of all of the steps in the initiation process. After insertion of the second olefin, all the subsequent steps (starting with addition of another CO ligand) are part of the main propagation cycle. All of the steps and their associated energy changes are summarised in section 4.1.6.

The initiation steps from insertion of an olefin into the Pd-H bond could therefore be shown to be a very thermodynamically favourable process, more favourable than even the propagation cycle itself. However, the question remained over whether the alternative method of initiation, through insertion of CO into a Pd-methoxy bond, would be faster.

4.1.4 Insertion of carbon monoxide into Pd-methoxy bond

The alternative mechanism of initiation was a less well-explored route. The insertion of CO into the Pd-OMe bond itself was originally thought to be analogous to CO insertion into a Pd-alkyl bond, but it turned out there was an important difference.

There were two local minima found for the reactant structure, and the lower energy structure (and the structure later found to connect to the reaction path) is shown in **figure 4.1.4.1**. (The other structure had a slightly lower C-Pd-O bond angle, but otherwise was similar.) The single product structure optimised is shown in **figure 4.1.4.2** respectively. Both structures were similar to the structures for CO insertion

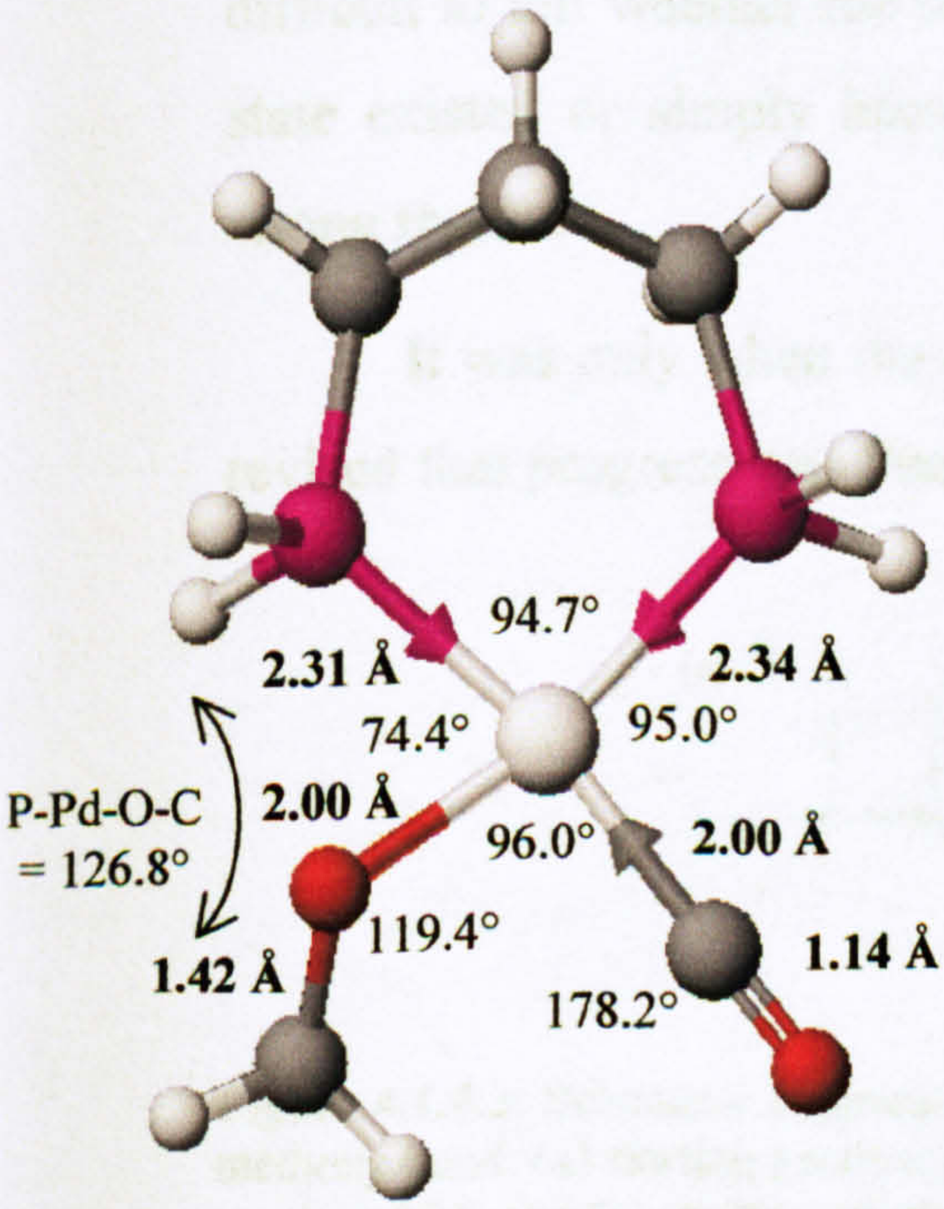


Figure 4.1.4.1: Structure of reactant of CO insertion into Pd-methoxy bond.

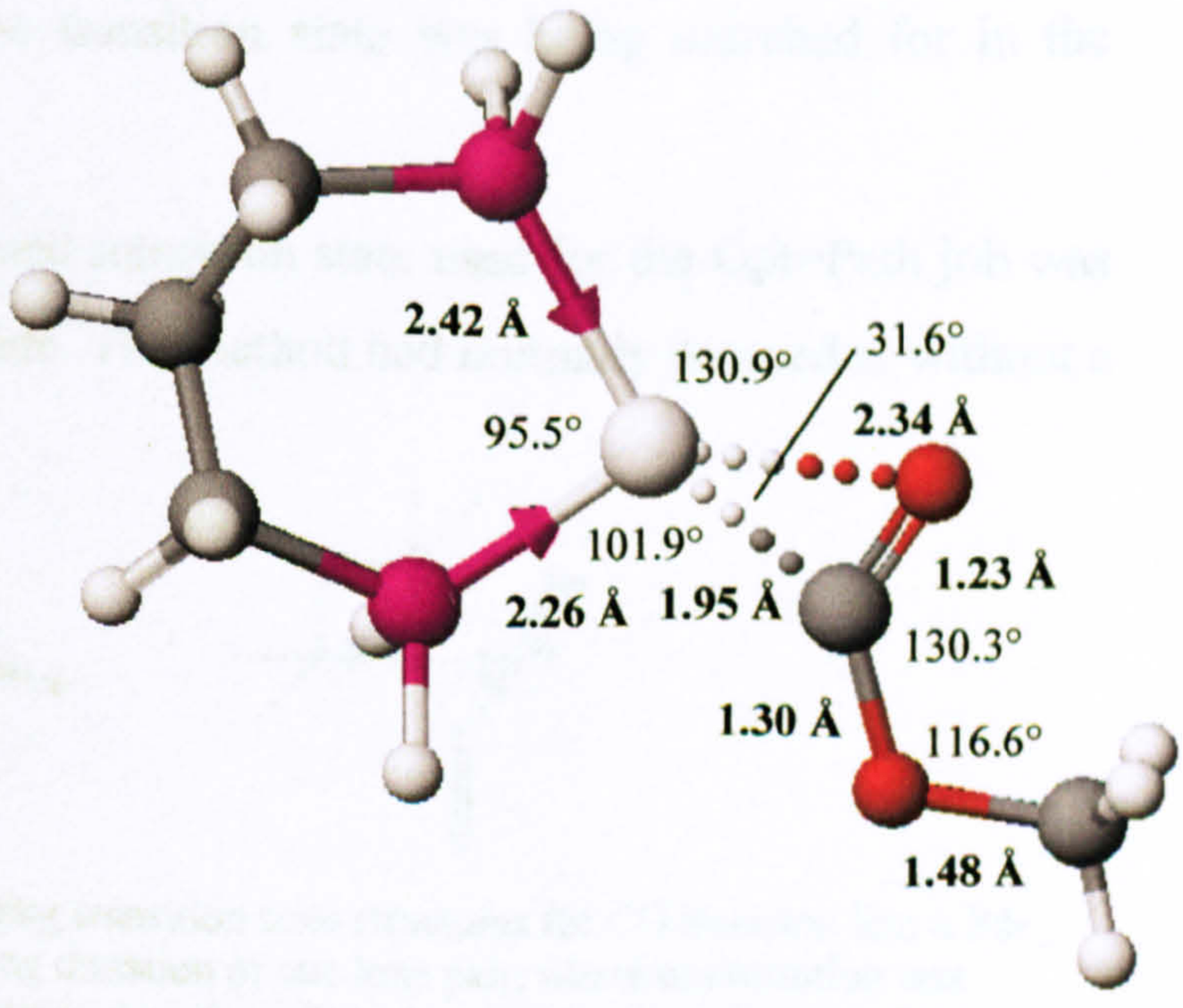


Figure 4.1.4.2: Structure of product of CO insertion into Pd-methoxy bond.

into a Pd-ethyl group, the only difference being the replacement of one CH_2 in the ethyl group with an O atom. The energy difference between the reactant and product structures was –12.1 kcal/mol (-10.7 kcal/mol including ZPE), a slightly greater difference than insertion of an olefin into a Pd-H bond. The structures were qualitatively similar to the reactant and product of CO insertion into a [Pd]-ethyl bond as optimised in section 3.4, but there were some differences in bond lengths and angles, and the drop in enthalpy was not as great for CO insertion into a Pd-alkyl bond.

The search for a transition state, however, turned out to be far more difficult than any transition state search described so far in this thesis. The previously foolproof method of finding a path between the reactant and product using the Opt=Path method, at first, was unsuccessful in finding a suitable starting structure for a QST3 transition state search. After several cycles, all of the points on the supposed reaction path were clustered around either the reactant or product structure, and any attempt to use one of these points as a starting structure caused a saddle point to be optimised, but with the mode of vibration of the imaginary frequency bearing no resemblance to CO insertion (usually with a vibration centred on inversion of the palladium-diphosphine ring as the imaginary frequency). At this stage, it did not appear possible to complete this step without breaking the four co-ordinate geometry, because unlike CO insertion into a Pd-alkyl bond, there was no H atom that could form a temporary Pd···H-C agostic interaction to stabilise the structure, but it was difficult to tell whether the failure to find a transition state was because no transition state existed or simply because the transition state was being searched for in the wrong region.

It was only when the estimated transition state used for the Opt=Path job was revised that progress was finally made. The method had normally proceeded without a

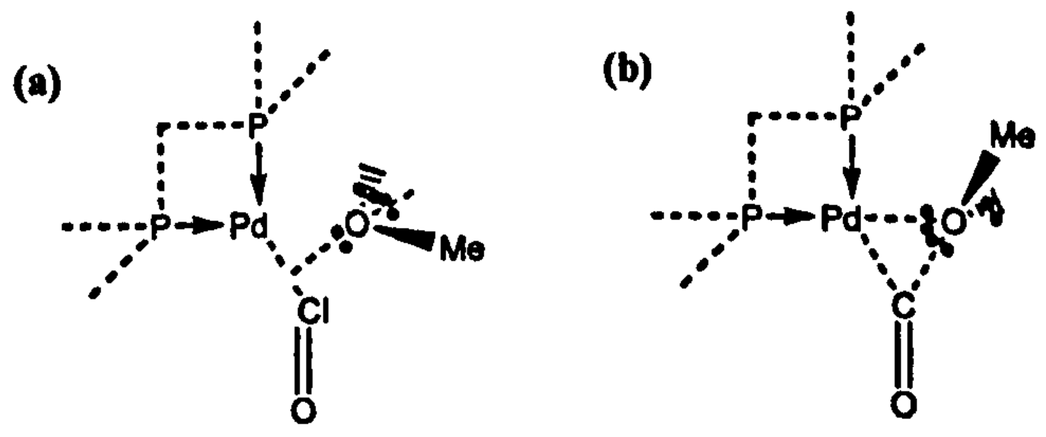


Figure 4.1.4.3: Schematic diagrams of starting transition state structures for CO insertion into a Pd-methoxy bond: **(a)** starting geometry allowing donation of one lone pair, where optimisation was unsuccessful; and **(b)** starting geometry allowing donation of two lone pairs, where optimisation was unsuccessful. (Dotted/hashed lines on oxygen atom indicate direction of lone pairs.)

manually entered starting transition state because the Opt=(QST2,Path) method had been capable of plotting a plausible-looking path on its own. However, it was questioned whether the orientation of the alkyl group during insertion was the most stable one, and the estimated transition state structure was revised, as shown in **figure 4.1.4.3**, using a theory of lone pair stabilisation first suggested by Dockter, Fanwick and Kubler[87]. The crucial difference was that in **figure 4.1.4.3 (b)**, the transition state structure could be stabilised by two lone pairs on the OMe^- group instead of one (something that is not possible in insertion of CO into a Pd-alkyl bond because of the absence of a second lone pair on a CH_2R^- group). A transition state of this shape had already been optimised for similar nickel, palladium and platinum complexes by Neave and Macgregor[88].

Even so, to start with the results were not encouraging. When a nine-point path was plotted, the program only got as far as completing the first cycle before a point on the second cycle failed to converge and the run terminated. Altering the number of points failed to produce any improvement. However, when the highest-energy point from this single cycle was used as the starting structure for a normal QST3 optimisation, the correct transition state was obtained at last, as shown in **figure 4.1.4.4**. A frequency test further confirmed that not only was this indeed a saddle-point, but the mode of vibration of the imaginary frequency, shown in **figure 4.1.4.5**,

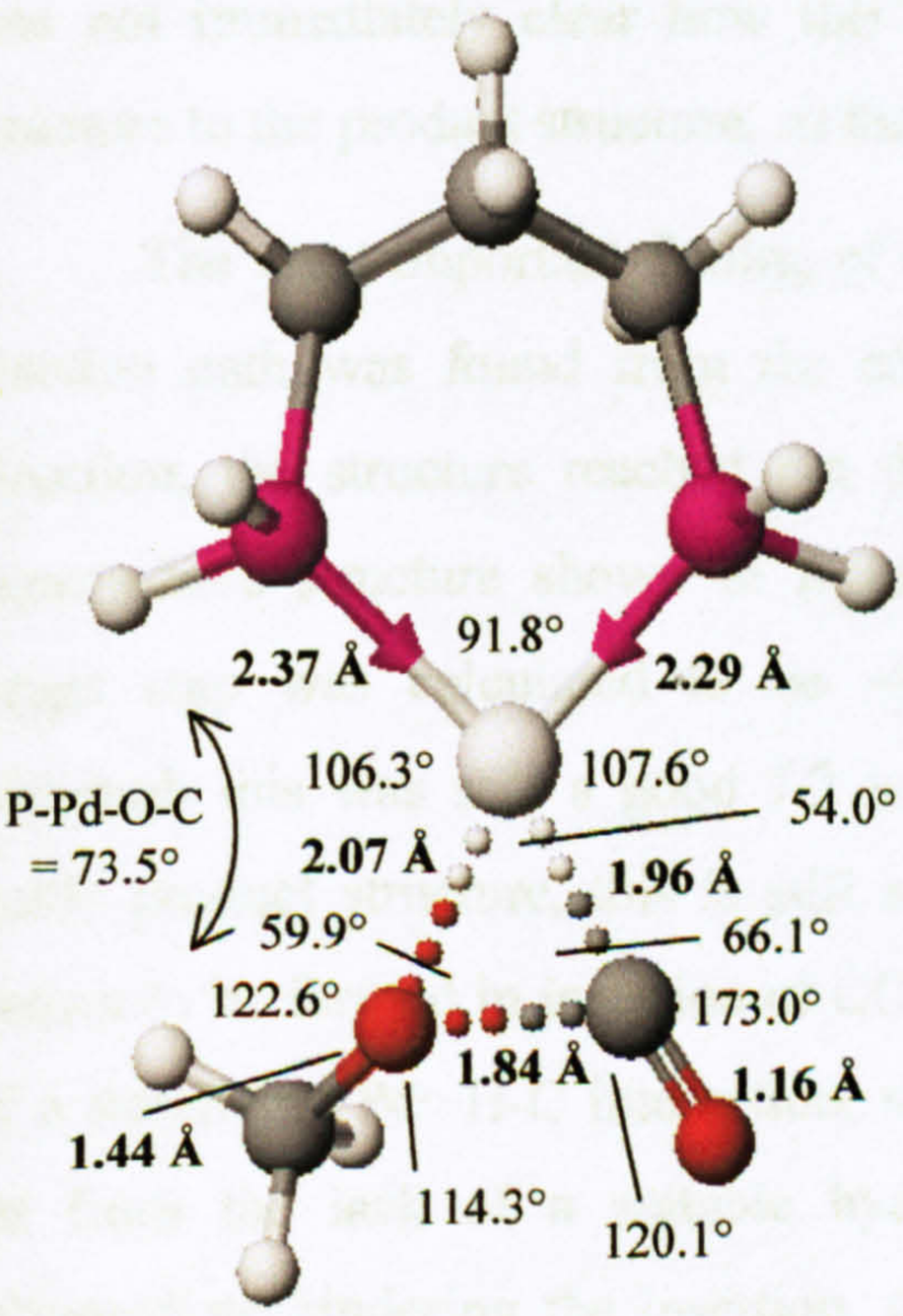


Figure 4.1.4.4: Optimised structure of transition state for CO insertion into Pd-methoxy bond.

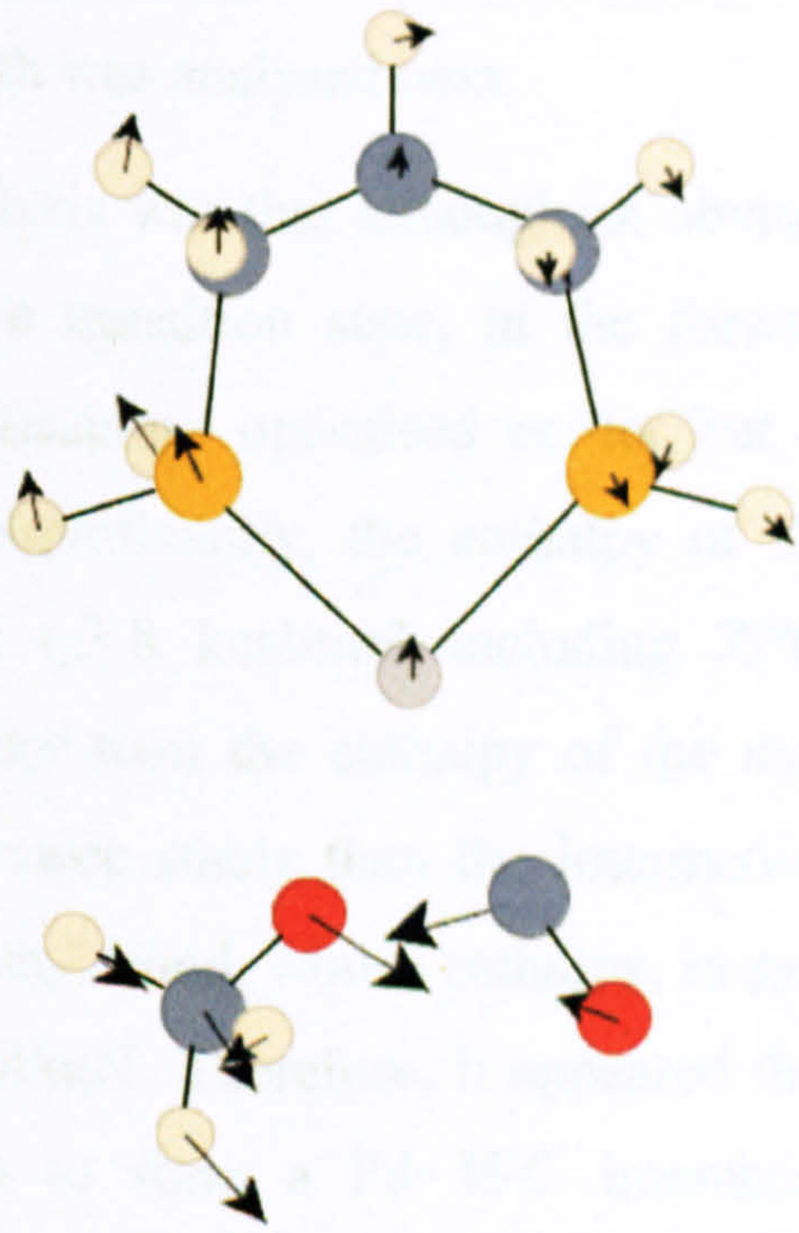


Figure 4.1.4.5: Mode of vibration of imaginary frequency (-205.4 cm^{-1}).

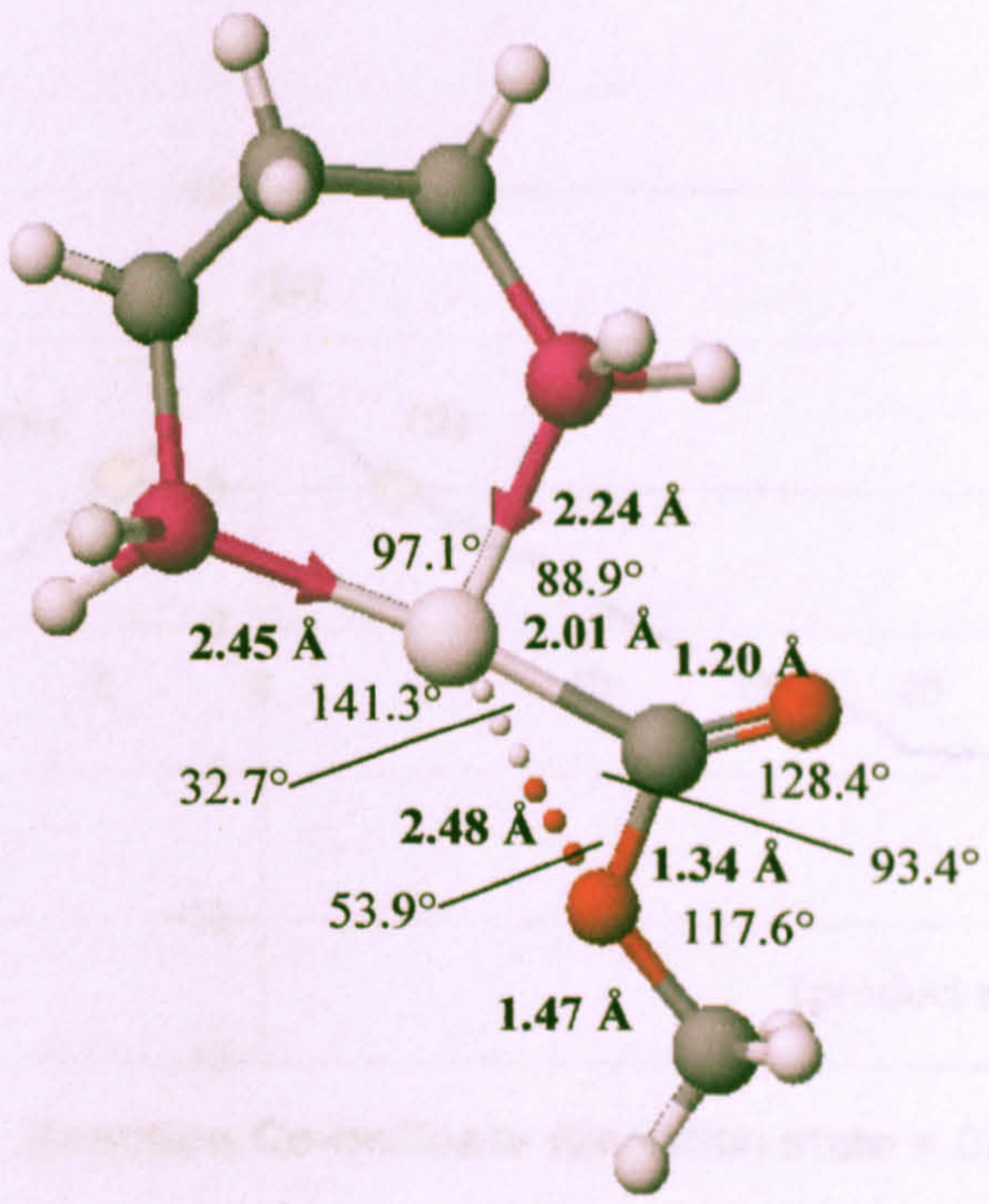


Figure 4.1.4.6: Intermediate formed after insertion of CO into a Pd-methoxy bond.

was in the direction one would expect for an insertion step.

Once the transition state had been located, the activation energy found was not that high: only 9.1 kcal/mol (8.9 kal/mol with zero-point corrections), slightly lower than the equivalent barrier for CO insertion into a Pd-alkyl group. The most likely reason for this lower activation energy is that two lone pairs on the oxygen could stabilise the structure (as opposed to only one in CH_2R^- group). Also, it was observed that at this stage, the four co-ordinate structure had not yet been broken. However, it was not immediately clear how this step could proceed from the transition state structure to the product structure, so the reaction path was analysed next.

The most important finding of the IRC analysis was that although an obvious reaction path was found from the reactant to the transition state, in the forward direction, the structure reached not the product structure optimised earlier but an intermediate structure shown in **figure 4.1.4.6**. Significantly, the enthalpy of this single step was calculated to be -4.9 kcal/mol (-3.8 kcal/mol including ZPE). Although this was still a good 7.2 kcal/mol greater than the enthalpy of the most stable product structure, this is still a good deal more stable than the intermediate known to be formed in insertion of CO into a Pd-ethyl bond, whose enthalpy, in spite of a stabilising Pd···H-C interaction, was +2.4 kcal/mol. Therefore, it appeared that, far from the lack of a suitable hydrogen atom to form a Pd···H-C interacting intermediate hindering the insertion, the presence of the additional O atom does in fact enable a more stable intermediate to be formed, promoting this step.

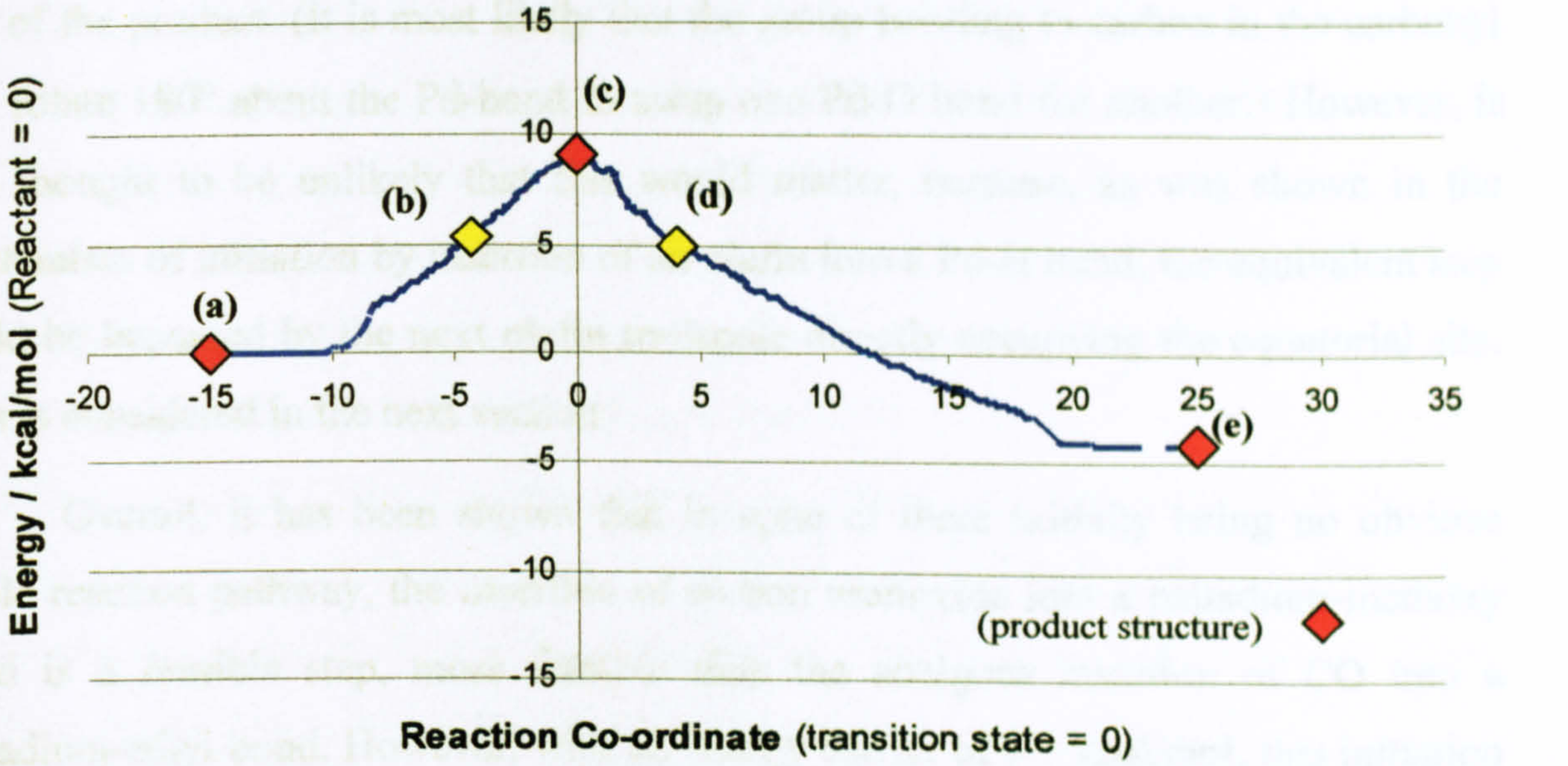


Figure 4.1.4.7: Reaction profile of CO insertion into Pd-methoxy bond.

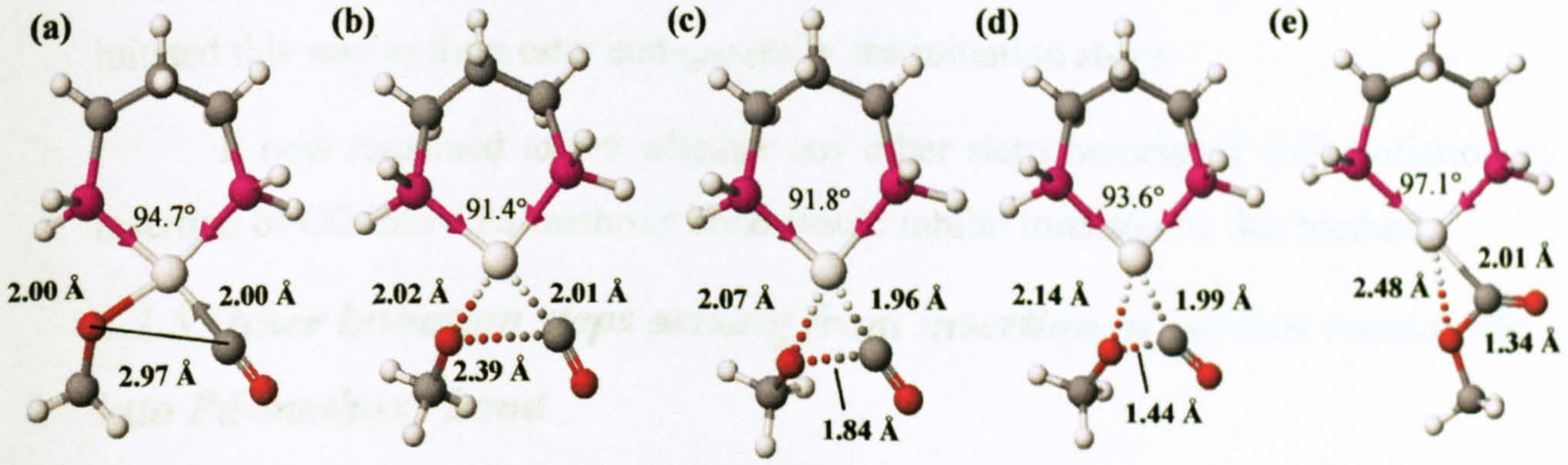


Figure 4.1.4.8: Selected points from reaction profile.

The remainder of the reaction mechanism is shown in the reaction profile in **figure 4.1.4.7**, with selected points shown in **figure 4.1.4.8**. The mechanism turned out to be similar to that for CO insertion into a Pd-ethyl bond, with the mechanism starting with rotation of the methoxy group into its optimum orientation for its migration to the carbonyl group (except that the optimum orientation of the methoxy group would allow two lone pairs to stabilise the structure instead of one). The only major difference was that the end of the process involved stabilising the structure with the formation of a Pd···O interaction instead of a Pd···H-C interaction.

Whilst the structure of an intermediate of this stability was unexpected, possible reasons for its stability are speculated upon in Chapter 5. There was not time

to investigate which mechanism, if one exists, converts this intermediate structure into that of the product. (It is most likely that the group bonding to carbon in the carbonyl will rotate 180° about the Pd-bond to swap one Pd-O bond for another.) However, it was thought to be unlikely that this would matter, because, as was shown in the mechanism of initiation by insertion of an olefin into a Pd-H bond, the equivalent step could be bypassed by the next olefin molecule directly occupying the equatorial site. This is considered in the next section.

Overall, it has been shown that in spite of there initially being no obvious stable reaction pathway, the insertion of carbon monoxide into a palladium-methoxy bond is a feasible step, more feasible than the analgous insertion of CO into a palladium-ethyl bond. However, with an energy barrier of 9.1 kcal/mol, this initiation step is still clearly uncompetitive with the insertion of an olefin into a Pd-H bond, whose energy barrier was only 0.2 kcal/mol. Therefore, it is likely that the methoxy-mechanism is not the dominant method of initiation and that most copolymers are initiated by the hydrido-method to form keto-end groups. However, at higher temperatures, it is conceivable that a significant minority of copolymers could be initated this way to form ester end-groups in the initiation stage.

It now remained to see whether any other steps associated with initiation by insertion of CO into a Pd-methoxy bond would inhibit initation by this method.

4.1.5 Other initiation steps arising from insertion of carbon monoxide into Pd-methoxy bond

First of all, the very first step, preceding the CO insertion into [Pd]-OMe, was considered. By optimising a structure of [Pd] -OMe with an incoming CO ligand nearby, the CO ligand moved into an equatorial site with no need to cross any energy barrier, but the enthalpy of bringing in a CO ligand from a large distance was calculated to be only –3.6 kcal/mol. This was partly due to the pre-addition structure stabilising itself by forming an β-agostic Pd···H-C interaction between palladium and the methyl group. This compared to the –32.0 kcal/mol enthalpy for addition of an olefin to the [Pd]-H complex.

However, this is not the fairest of comparisons and it does not necessarily make this method of initiation any less competitive, and the rates of these steps would also be influenced by the formation of the [Pd]-H and [Pd]-OMe complexes in the

first place. Since [Pd]-H is a three co-ordinate complex, this structure would be very difficult to form in the first place. Furthermore, the reactant structures for either initiation step would not necessarily need to be formed this way at all. They could just as conceivably be formed from the displacement of, say, a solvent molecule from the fourth site (in which case, addition of the olefin for initiation by insertion of an olefin into a Pd-H bond would become *much* less exothermic because it would no longer be going from a 3-coordinate to 4-coordinate structure). Alternatively, the step may not be necessary at all if the structure needed is formed by termination of a previous copolymer chain. Determining which initiation process is favoured from the formation of the reactant structure for the first insertion step is likely to be a very complicated business that would be beyond the scope of this project.

After insertion of a carbonyl group into a Pd-OMe bond was achieved, there were no problems with the remaining steps of the initiation process. Starting with the step immediately following insertion of the first CO, there were, once again, two ways to add the next monomer (in this case, the first olefin) to an equatorial site: either by waiting until the final product structure of CO insertion is formed and then displacing the Pd···O interaction with the incoming olefin (where O is the oxygen in the carbonyl group); or by directly displacing the Pd···O interaction when the complex is still in the intermediate structure of CO insertion (where O is the oxygen in the methoxy group), by-passing the step between the intermediate and product altogether. Both of these mechanisms turned out to be feasible, although, once again, in the former mechanism,

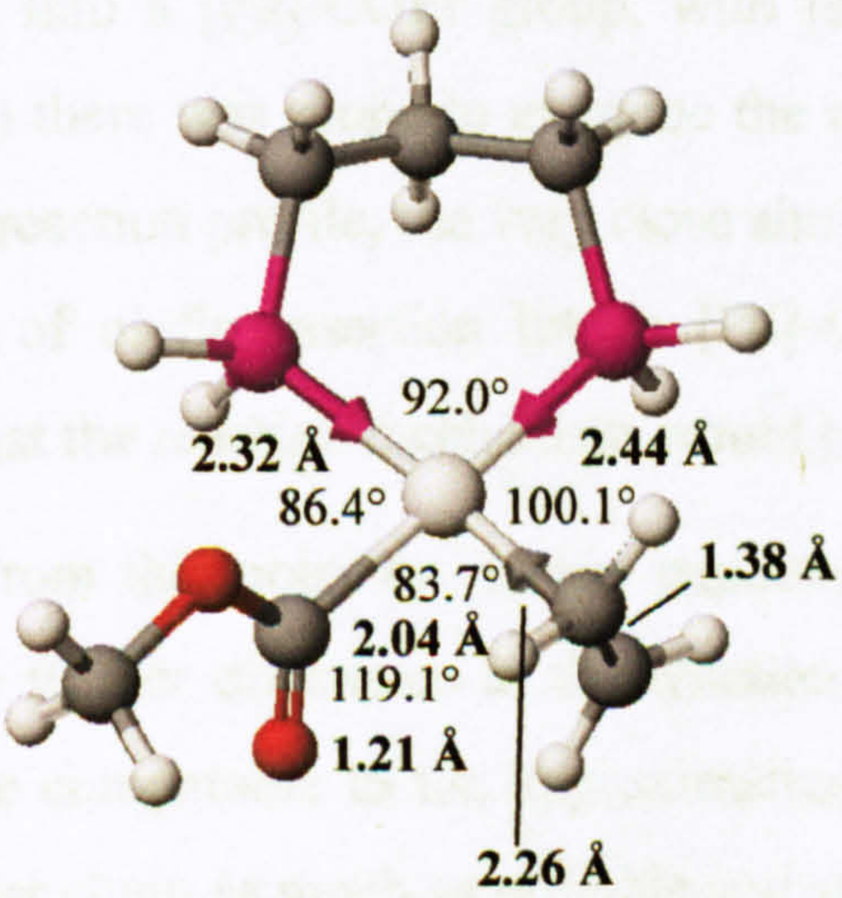


Figure 4.1.5.1: Reactant structure in olefin insertion step following initiation by insertion of CO into Pd-OMe bond.

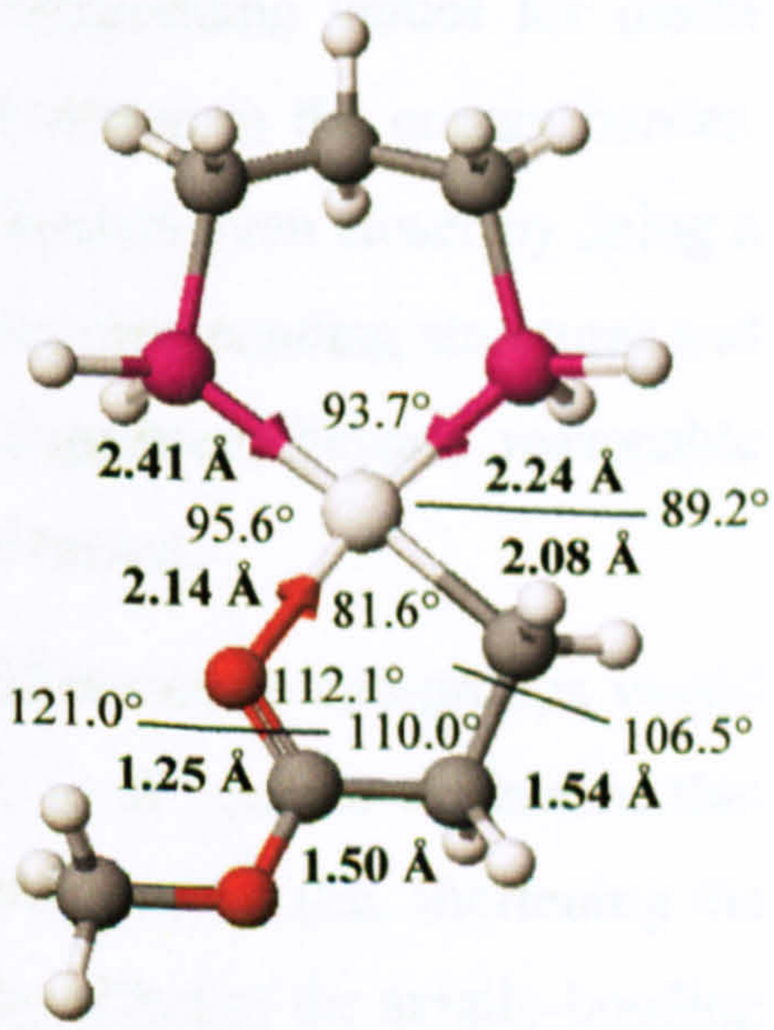


Figure 4.1.5.2: Product structure in olefin insertion step following initiation by insertion of CO into Pd-OMe bond.

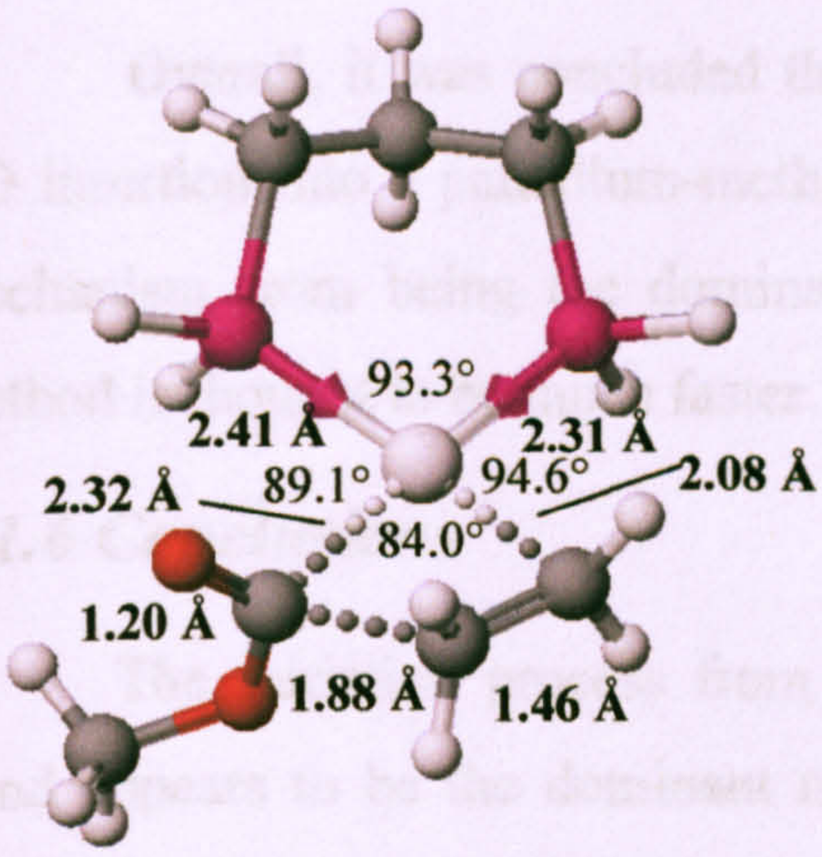


Figure 4.1.5.3: Transition state structure in olefin insertion step following initiation by insertion of CO into Pd-OMe bond.

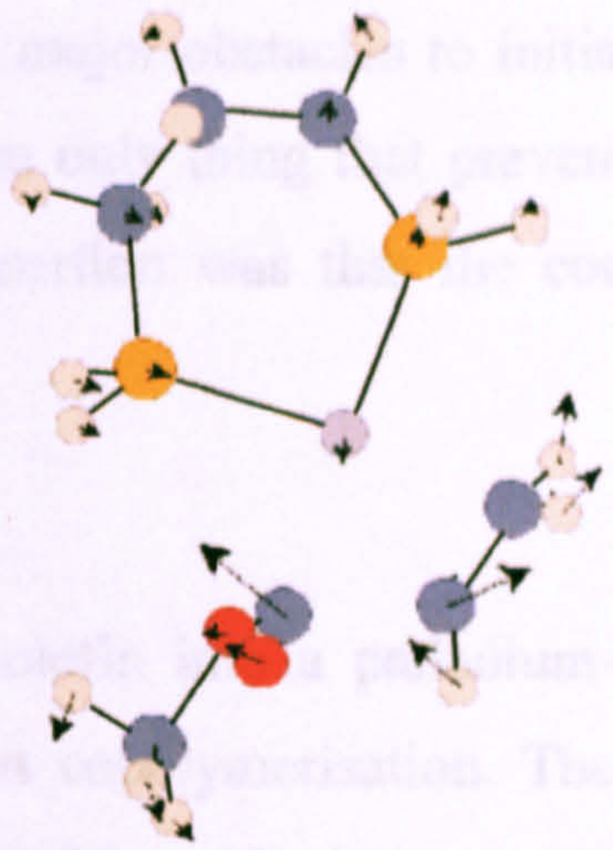


Figure 4.1.5.4: Mode of vibration of imaginary frequency (-341.6 cm^{-1}).

olefin addition only occurred when the olefin approached the complex from the right direction. The enthalpy of adding the olefin to the product structure was –15.5 kcal/mol, whilst the enthalpy of adding the olefin to the intermediate structure was -23.0 kcal/mol.

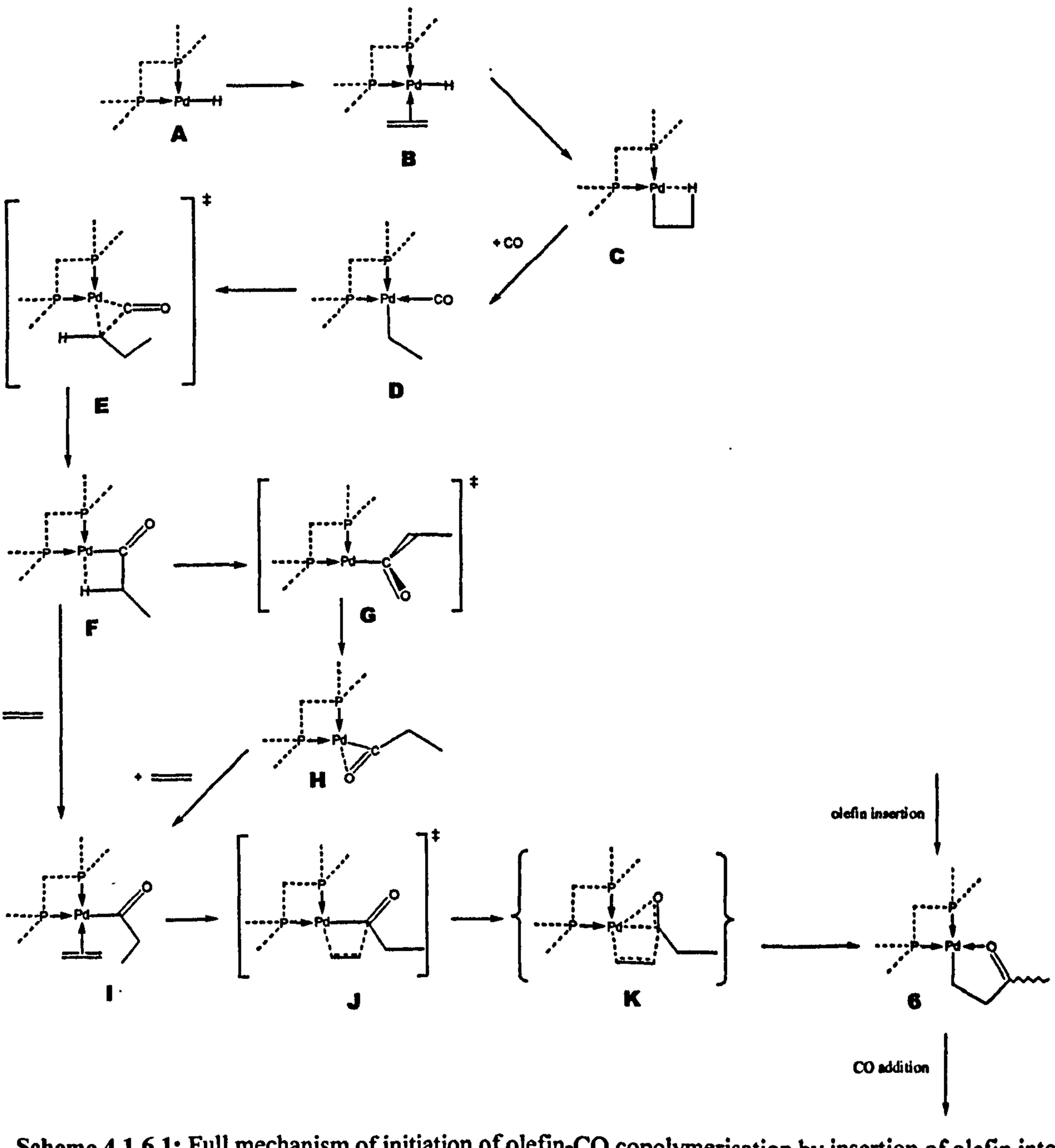
The next stage was the first olefin insertion step, where all the structures were optimised by replacing the relevant CH_2 group from insertion into the Pd-COEt bond with an oxygen atom to reflect insertion into the Pd-COOMe bond. The optimised structures are shown in **figure 4.1.5.1**, **figure 4.1.5.2** and **figure 4.1.5.3** respectively, with the mode of vibration of the imaginary frequency of the transition state shown in **figure 4.1.5.4**. The enthalpy change was calculated to be –25.5 kcal/mol (-23.1 kcal/mol with ZPE), and the energy barrier was calculated to be 12.5 kcal/mol (12.7 kcal/mol with ZPE). This was quite close to the corresponding values for olefin insertion into a [Pd]-COEt group, with just a small increase in the energy barrier. Although there was scope to examine the reaction mechanism even closer by doing a detailed reaction profile, the very close similarities to the corresponding structures and energies of olefin insertion into a [Pd]-COEt bond suggested, beyond reasonable doubt, that the reaction mechanism would be virtually identical.

From this point on, it was expected that the difference in end-groups would make no further difference to the reaction mechanism, or at least no difference that would be comparable to the approximations made in this project (i.e. shortening the copolymer chain as much as possible and still include the effect of the axially-bonding carbonyl group).

Overall, it was concluded that there were no major obstacles to initiation by CO insertion into a palladium-methoxy bond, and the only thing that prevented this mechanism from being the dominant method of insertion was that the competing method is thought to be much faster.

4.1.6 Conclusions

The initiation process from insertion of an olefin into a palladium-hydride bond appears to be the dominant mechanism to start copolymerisation. The master diagram of the mechanism is shown in **scheme 4.1.6.1,** with the energy changes illustrated in **figure 4.1.6.1** and tabulated in **table 4.1.6.1.** These take into account the mechanisms of the CO and olefin insertion with a second carbonyl group as



Scheme 4.1.6.1: Full mechanism of initiation of olefin-CO copolymerisation by insertion of olefin into palladium-hydride. Transition states are shown in square brackets, selected non-stationary points are shown in curved brackets, and other structures are minima. All structures carry a single positive charge.

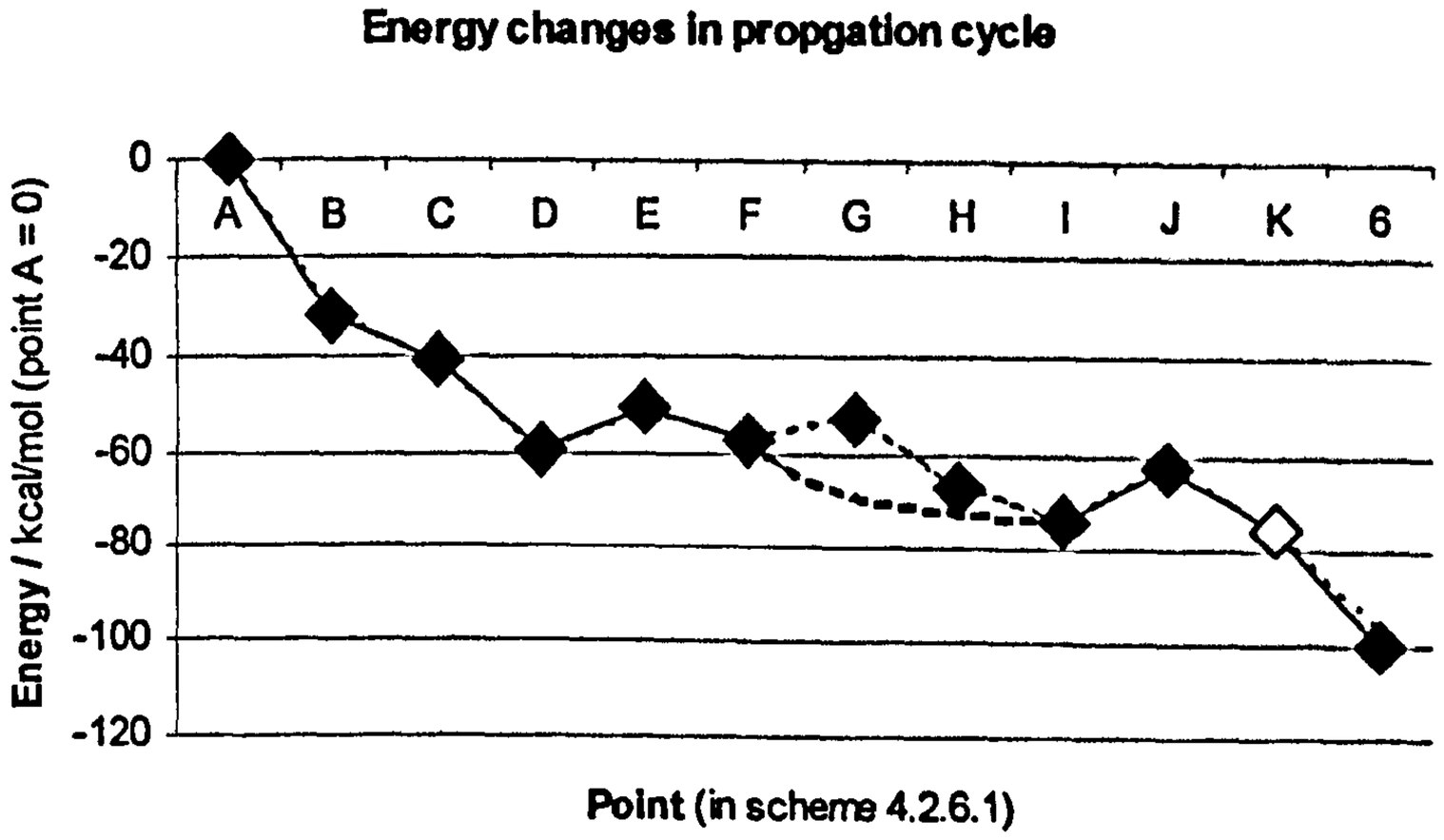


Figure 4.1.6.1: Energy changes associated with **scheme 4.1.6.1** (non-stationary points, shown in yellow, are approximations; dotted line in points I-K is with zero-point energy corrections).

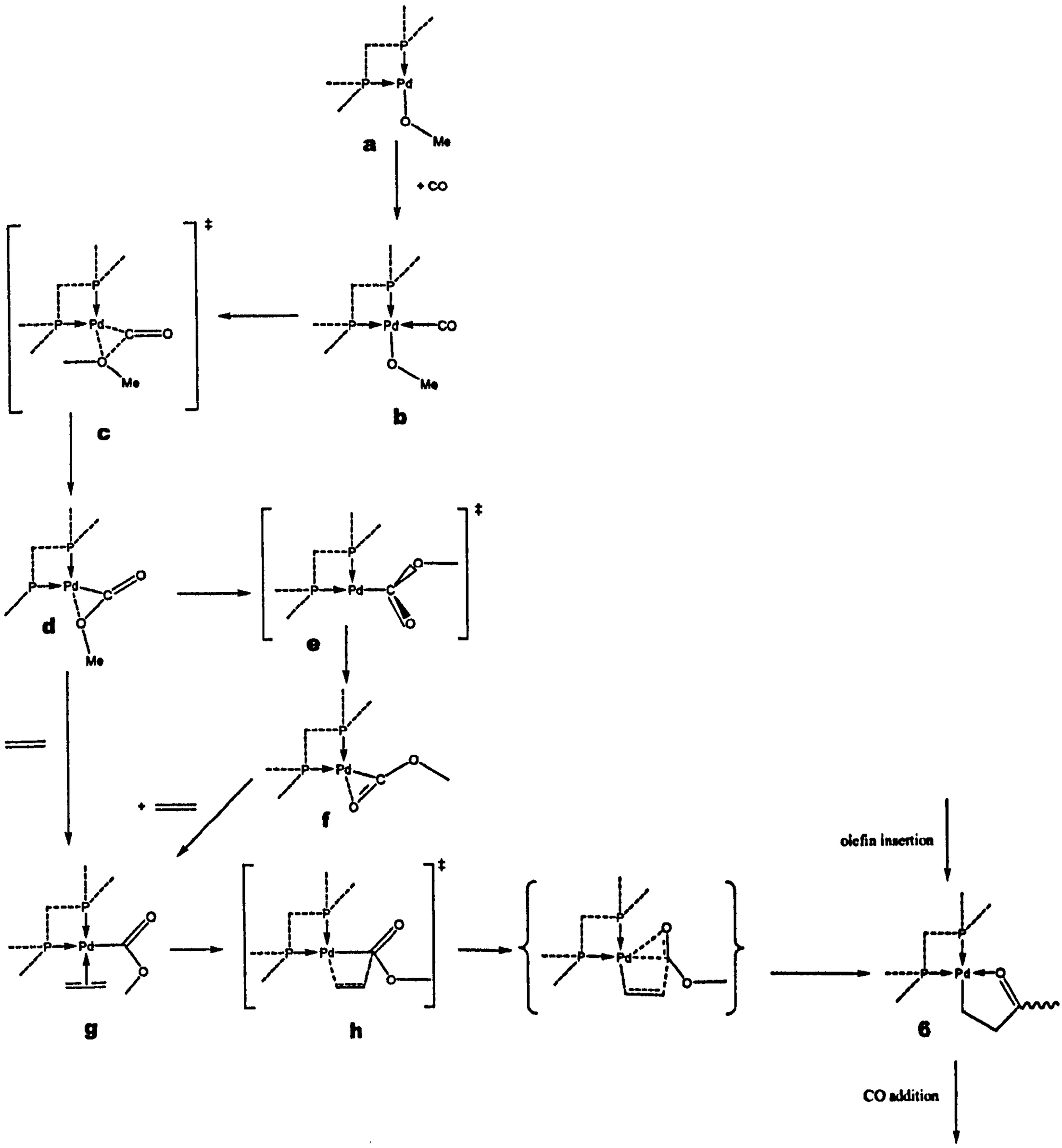
	From this project:	Including zero-point corrections	From Ziegler & Margl (ref. 7)
Olefin addition (A-B)	-32.0	-	N/A
Olefin insertion to Pd-H (B-C)	-9.1	-9.7	N/A
Total enthalpy of [Pd]-H to [Pd]-ethyl (A-C)	-41.1	-41.7	-42.3
CO addition (C-D)	-18.6	-	-18.6
Energy barrier of CO insertion to [Pd]-Et (D-E)	9.2	8.9	11.5
Enthalpy of CO insertion to forming H-bonded product (D-F)	2.4	3.0	4.5
Energy barrier between CO insertion products (F-G)	4.1	4.9	-
Enthalpy from H-bonded product to carbonyl-bonded product (F-H)	-10.0	-9.5	-2.9
Olefin addition displacing Pd-H bond (F-I)	-16.7	-	-20.6
Olefin addition displacing Pd-acyl bond (H-I)	-6.7	-	-13.1
Energy barrier of olefin insertion to [Pd]-COEt (I-J)	11.2	11.7	13.9
Enthalpy of olefin insertion (I-6)	-25.6	-23.2	-17.6
Total energy change initiation (A-6)	**-99.6**	**-97.2**	**-94.6**

Table 4.1.6.1: Summary of key energy changes in initiation process by insertion of olefin into Pd-H bond.

previously optimised in sections 3.3-3.4. These two steps have energy barriers

comparable to the corresponding steps in the propagation cycle with the second CO groups interacting, but the other steps have small or no energy barriers and are very strongly exothermic.

An alternative reaction mechanism of insertion from insertion of CO into a Pd-OMe bond to form an ester end-group was also found to be feasible. The reaction mechanism is shown in **scheme 4.1.6.2**, with the energies associated with this process shown in **figure 4.1.6.2** and **table 4.1.6.2**. There were doubts that it would be possible to accomplish CO insertion into a Pd-methoxy bond because of the lack of an



Scheme 4.1.6.2: Full mechanism of initiation of olefin-CO copolymerisation by insertion of CO into palladium-methoxy. Transition states are shown in square brackets, selected non-stationary points are shown in curved brackets, and other structures are minima. All structures carry a single positive charge.

	From this project:	Including zero-point energies
CO addition (a-b)	-3.6	-
Activation energy of CO insertion to Pd-OMe (b-c)	9.1	8.9
Enthalpy of CO insertion to Pd-OMe intermediate (b-d)	-4.9	-3.8
Ethalpy from intermediate to product (d-e)	7.2	6.9
Enthalpy of CO insertion to Pd-OMe (b-f)	-12.1	-10.7
Olefin addition to CO insertion intermediate (d-g)	-23.0	-
Olefin addition to CO insertion product (f-g)	-15.5	-
Energy barrier of olefin insertion to [Pd]-COEt (g-h)	12.5	12.7
Enthalpy of olefin insertion (g-6)	-25.5	-23.1
Total energy change of initiation (a-6)	**-57.0**	**-53.5**

Table 4.1.6.2: Summary of key energy changes in initiation process by insertion of CO into Pd-methoxy bond.

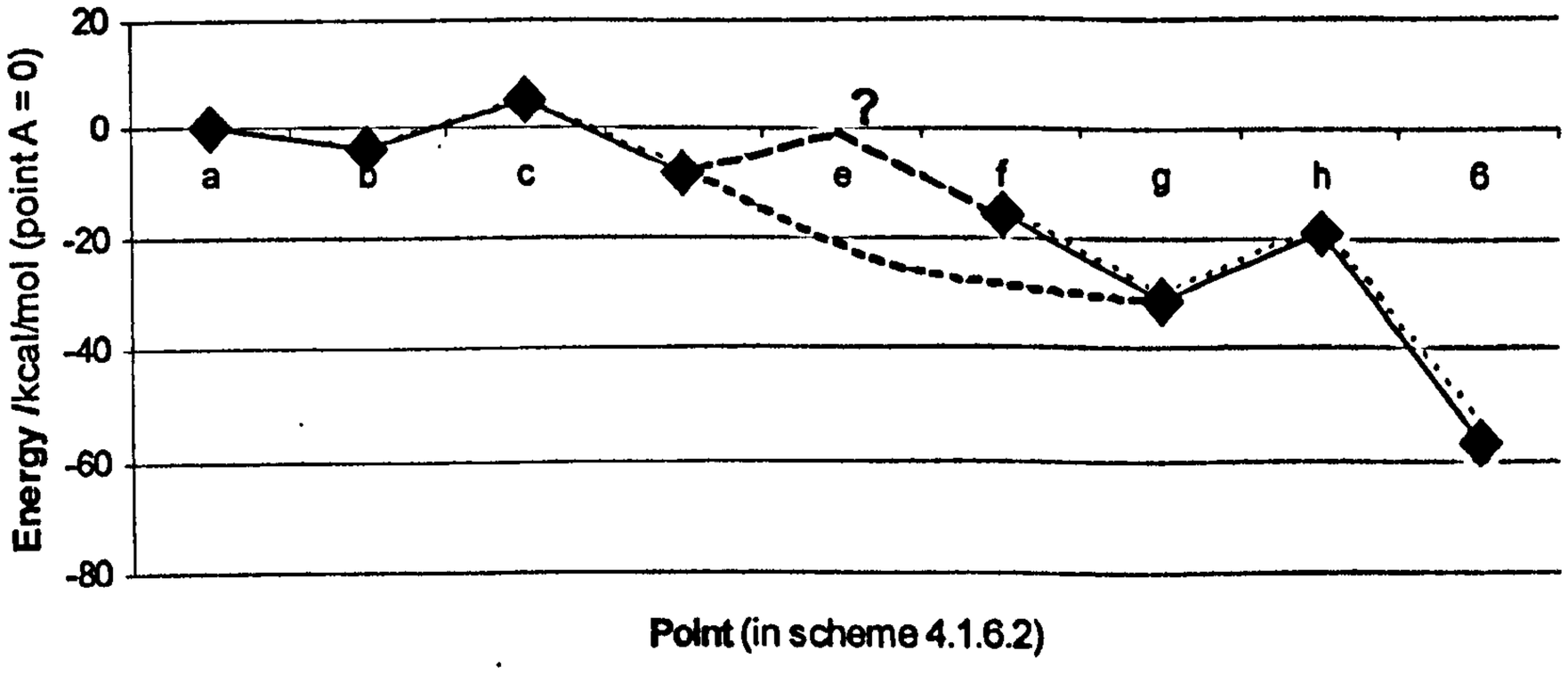


Figure 4.1.6.2: Energy changes associated with **scheme 4.1.6.2** (dotted line is including zero-point corrections).

appropriately positioned hydrogen atom to form an agostic Pd···H-C interaction, but it turned out that the oxygen atom in the methoxy group in fact stabilised the transition state more than the $-CH_2-$ group does in the analogous step of CO insertion into an ethyl group. However, in spite of this stability, the energy barrier still remains higher than the (almost nonexistent) energy barrier of the competing initiation mechanism of olefin insertion into a Pd-hydride bond.

Having summarised the mechanisms of both possible initiation processes, one can now consider whether either of the mechanisms dominates the initiation process, and if so, which one.

Overall, it is likely that initiation by insertion of an olefin into the Pd-H bond is the dominant method of initiation because this step is a very fast process. It appears that the alternative method, insertion of a CO molecule into a Pd-OMe bond, would not normally occur because this step, although feasible, is uncompetitive owing to the higher energy barrier of the key step. Therefore, it can be further concluded that initiation of this copolymerisation process should be responsible for the keto-end groups, rather than termination. Since copolymers are known to have 50% keto-end groups and 50% ester end-groups at lower temperatures, it must follow that the dominant termination process must by methanolysis, although analysis of the termination steps themselves would be needed to confirm this.

However, the energy barrier of CO insertion into a Pd-OMe bond is not high enough to rule out this mechanism completely. At higher temperatures, it is conceivable that the selectivity between the two initiation mechanisms will be reduced.

There is one alternative theory governing the selectivity between the two initiation processes that cannot yet be ruled out. Since both initiation processes were found to be valid mechanisms in their own right, the selectivity between the initiation process may be influenced by how easy it is to form the starting structures: [Pd](olefin)H and [Pd](CO)OMe. As these structures are formed automatically by termination, it is still possible that the selectivity towards the initiation process may be determined by the selectivity of the termination process. It will therefore be necessary to consider the feasibility of the termination processes before any final conclusions can be drawn about what is responsible for determining which mechanism is used for initiation.

4.2 Double insertion

4.2.1 Introduction

The copolymerisation of olefins and carbon monoxide is known to proceed in perfect alternation using any palladium-diphosphine complex as long as there are both kinds of reactor molecules available for addition and insertion. The absence of both kinds of double insertion has been accounted for by both experimental and theoretical analysis of insertion steps, but there has, so far, been little attention to the actual mechanism of double insertion or the addition of the ligand to an equatorial site needed for double insertion.

Double insertion of carbon monoxide is now widely thought to be impossible due to its unfeasibly high energy barrier, and has already been considered by Ziegler and Margl and Svensson *et al,* with their optimised structures shown in **figure 4.2.1.1.**[7,8,36] There are still a few unanswered questions such as whether it would make a difference if there was an axial Pd-carbonyl bond present, or whether there would be difficulty in getting a CO ligand into an equatorial site in the first place, but it is unlikely that either of these would be the case. As part of the project the structures in this project were re-optimised to analyse the full mechanism between the reactant and

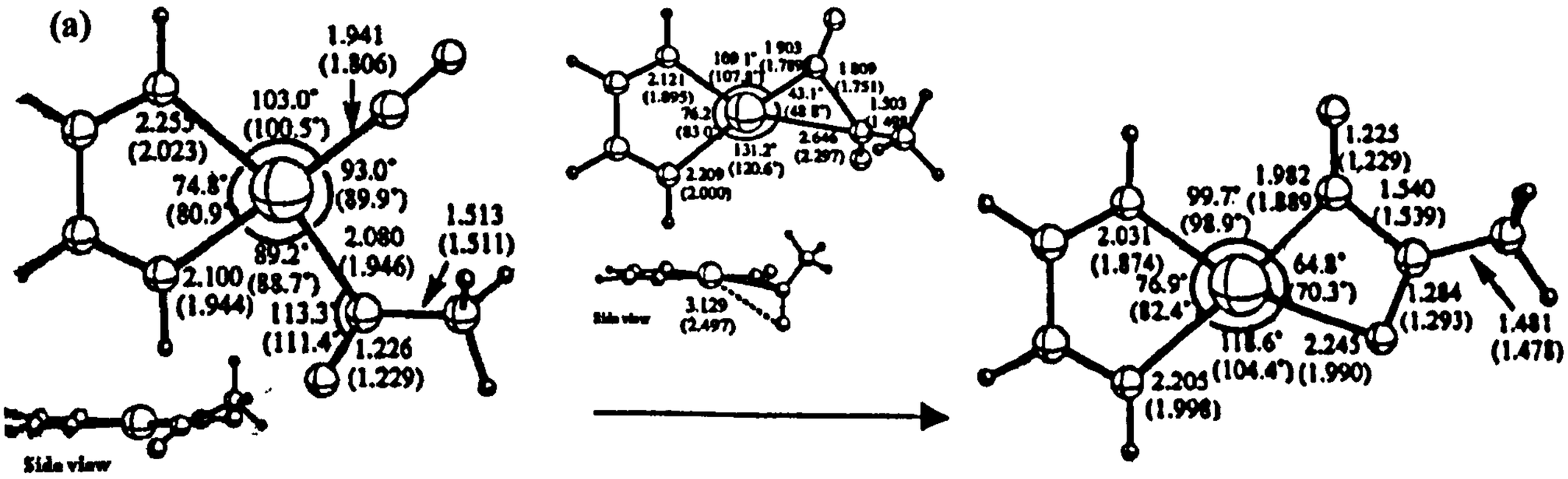


Figure 4.2.1.1: Mechanism of double CO insertion proposed by **(a)** Svensson *et. al.* and **(b)** Ziegler and Margl.

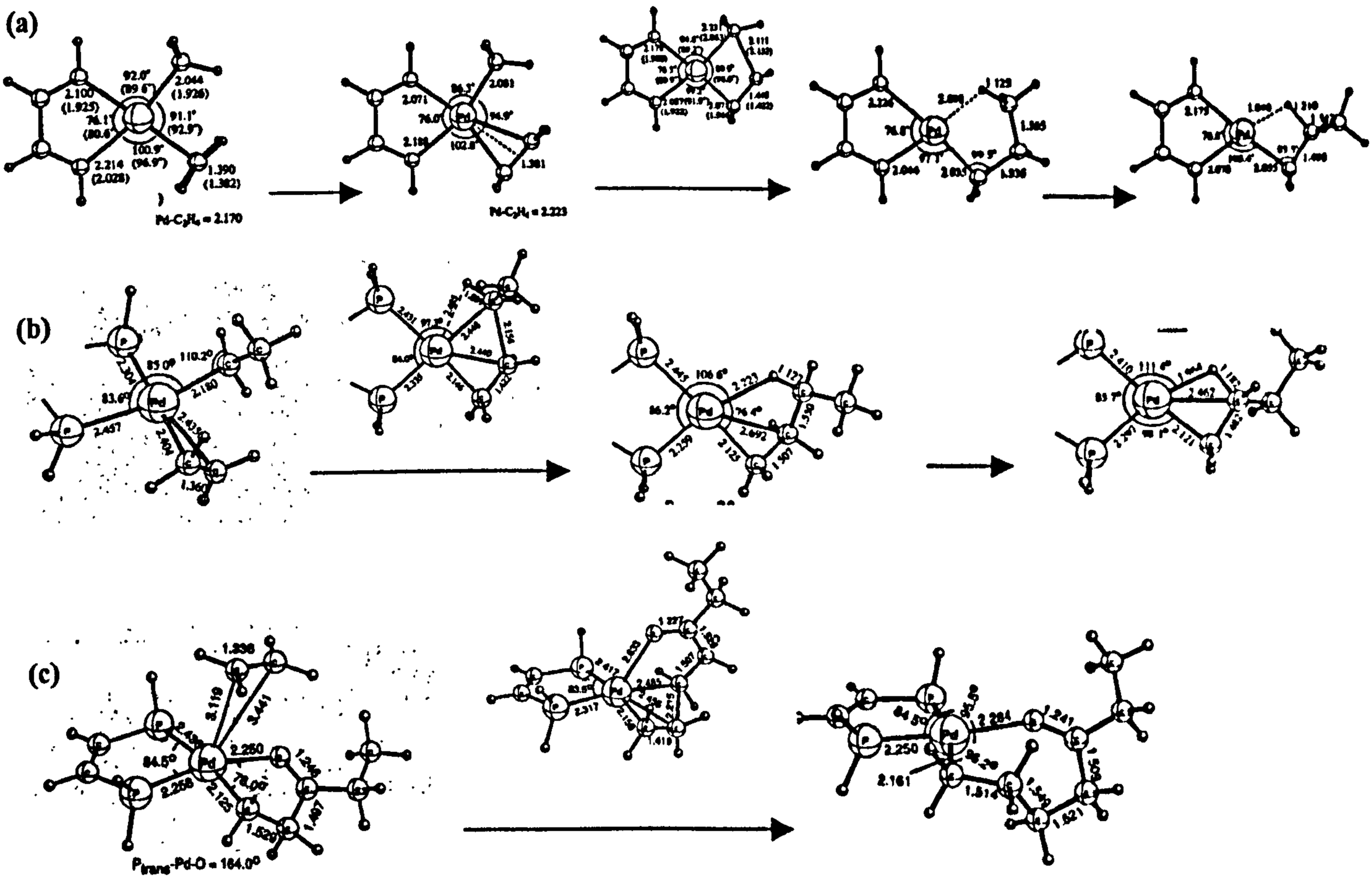


Figure 4.2.1.2: Mechanism of double olefin insertion proposed by **(a)** Svensson *et al*; and Ziegler and Margl **(b)** without and **(c)** with interaction from a carbonyl group in the copolymer chain.

product, in an attempt to account for high energy barrier.

The reasons for lack of double olefin insertion, however, were more ambiguous. It is thought that although double olefin insertion is possible on its own, or where the partial pressure of CO is very low, but under normal conditions insertion of CO is so much quicker that double olefin insertion cannot compete. The optimised structures obtained by Ziegler and Margl and Svensson *et. al.*, are shown in **figure 4.2.1.2.** However, it was unclear whether rapid CO insertion was the *only* reason for no double insertion, as it had been speculated that the previous step, where a strong Pd-O coordinate bond must be displaced by a comparatively weak olefin, also contributed towards the lack of double insertion. This was potentially important, as palladium complexes have recently been developed that allow a little olefin double insertion, and it has been suggested that weakening the Pd-O coordinate bond contributed to this. There was also some other outstanding issues, such as there being a variety of possible products of double insertion (bonding through different Pd···H-C

agostic interactions) and the uncertainty of which structure the transition state relaxes to.

It was therefore decided to attempt to optimise both of the double insertion processes, and the preceding ligand addition steps, to try to get further information on the double insertion processes, and try to identify both the reasons for lack of double insertion and ways that double insertion of olefins might be promoted.

4.2.2 Double olefin insertion, neglecting axial Pd-carbonyl bond

It was originally attempted to optimise the transition state of double olefin insertion from the structure proposed by Ziegler and Margl, which included co-ordination by the second carbonyl group. However, this structure did not converge on a saddle point, so, to reduce the number of variables that Gaussian had to deal with, it was decided to begin by neglecting the carbonyl group forming the axial Pd-O co-ordinate bond.

To begin with, reactant and product structures of double olefin insertion were optimised. The optimised structure of the reactant was easily obtained and is shown in **figure 4.2.2.1**. For the product, the structure in **figure 4.2.2.2** was obtained, but it was noted that this was only one of several possible minima suggested as possible products, and a reaction path would be needed to identify what role, if any, this structure had. Then, using Ziegler and Margl's proposed structure of a transition state as a starting point, the transition state as shown in **figure 4.2.2.3** was optimised (mode

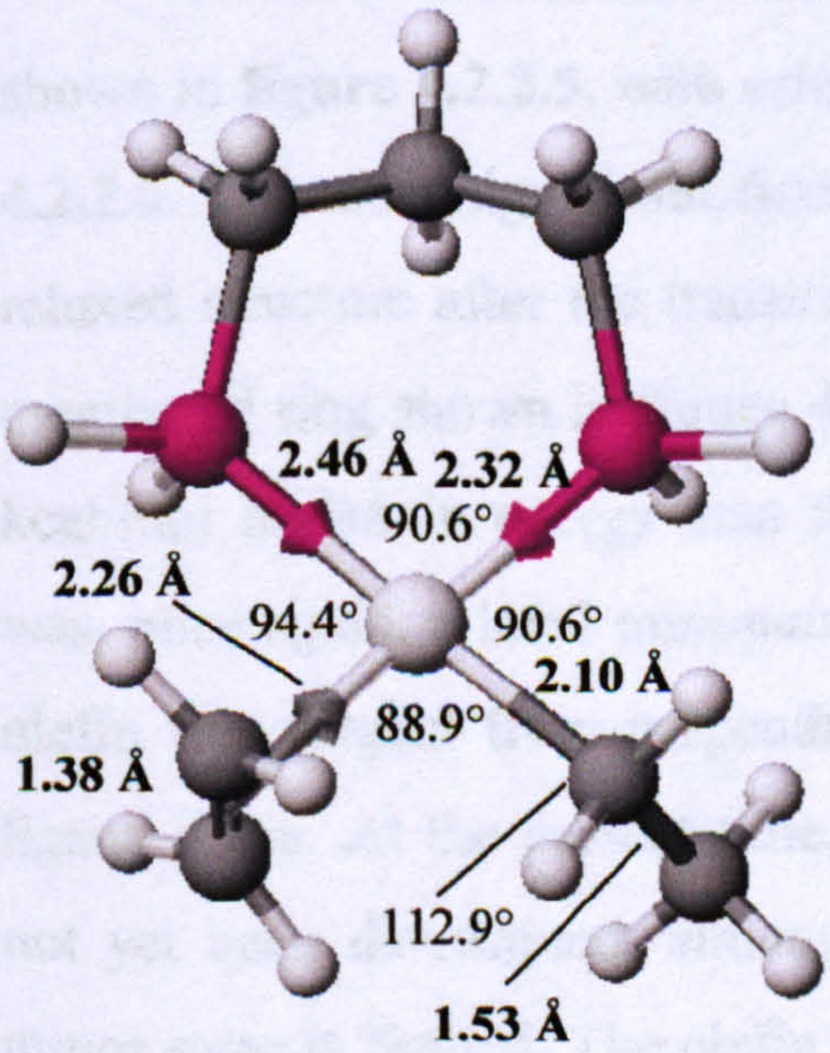


Figure 4.2.2.1: Reactant of double olefin migratory insertion neglecting axial Pd-carbonyl bond.

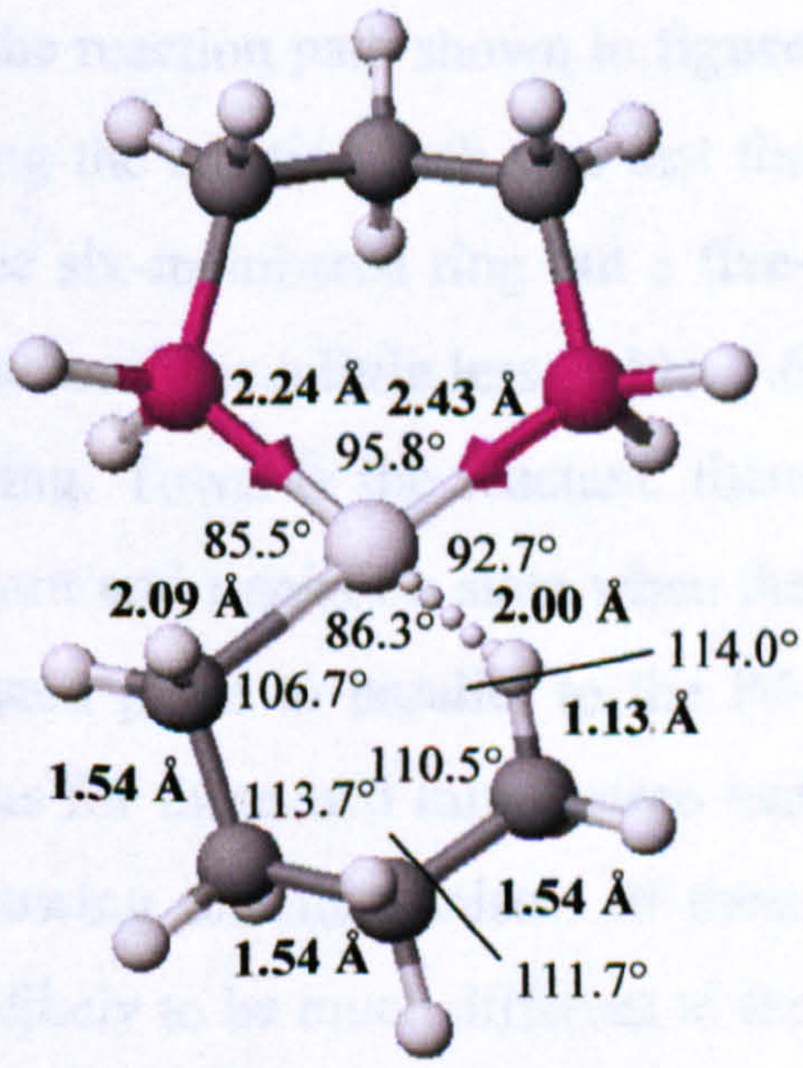


Figure 4.2.2.2: Product of double olefin migratory insertion neglecting axial Pd-carbonyl bond.

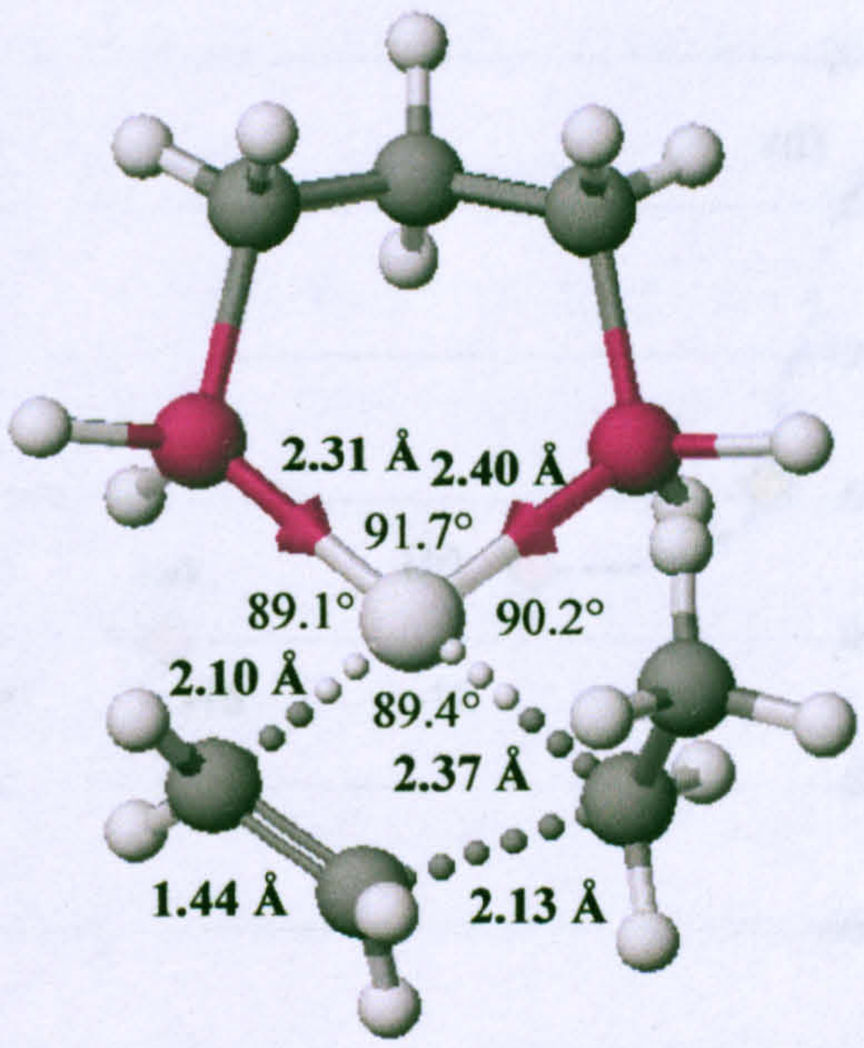


Figure 4.2.2.3: Transition state of double olefin migratory insertion neglecting axial Pd-carbonyl bond.

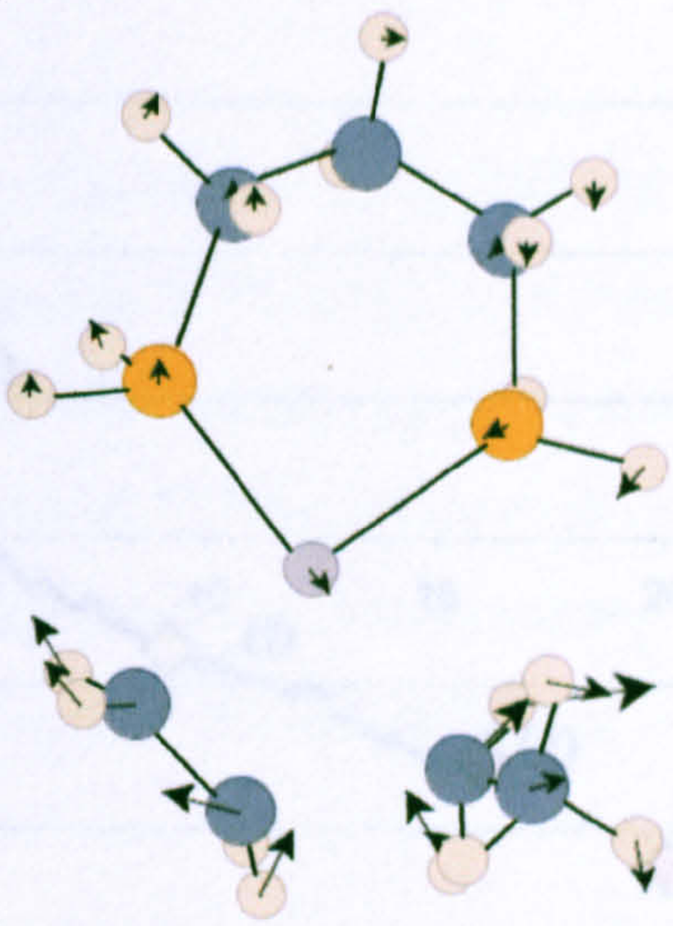


Figure 4.2.2.4: Mode of vibration of imaginary frequency (-367.3 cm^{-1}).

of vibration of imaginary frequency shown in **figure 4.2.2.4**).

The energy barrier of this step was calculated to be 16.4 kcal/mol (17.0 kcal/mol including ZPE). This compared to an energy barrier of 9.2 kcal/mol in the competing CO insertion step, so this was a definite increase. It was also a significant increase over the 11.2 kcal/mol energy barrier for insertion of an olefin into a Pd-acyl bond. However, the enthalpy calculation showed a *larger* drop in the energy of the complex: -11.2 kcal/mol (-9.6 kcal/mol including ZPE) compared to –7.6 kcal/mol in the competing CO insertion step. The analogous step of olefin insertion to a Pd-acyl bond, however, remained as the largest drop in energy, with an energy difference of -25.6 kcal/mol.

The IRC mechanism was considered next, and energies for this process are shown in **figure 4.2.2.5**, with selected structures on the reaction path shown in **figure 4.2.2.6**. The most significant finding from considering the reaction path was that the relaxed structure after the transition state was not the six-membered ring but a five-membered ring shown in **figure 4.2.2.6 (g)**. This structure was a little less stable, 3.6 kcal/mol higher in energy than the six-membered ring. Towards the reactant, there was, once again, a local minimum between the reactant and transition state when the olefin was rotated from perpendicular to the Pd-ligand plane to parallel to the Pd-ligand plane. At the present time, the transition states for these two minor steps had not yet been determined, although the value in knowing the mechanisms of these minor steps is limited. The olefin rotation stage is unlikely to be much different to the

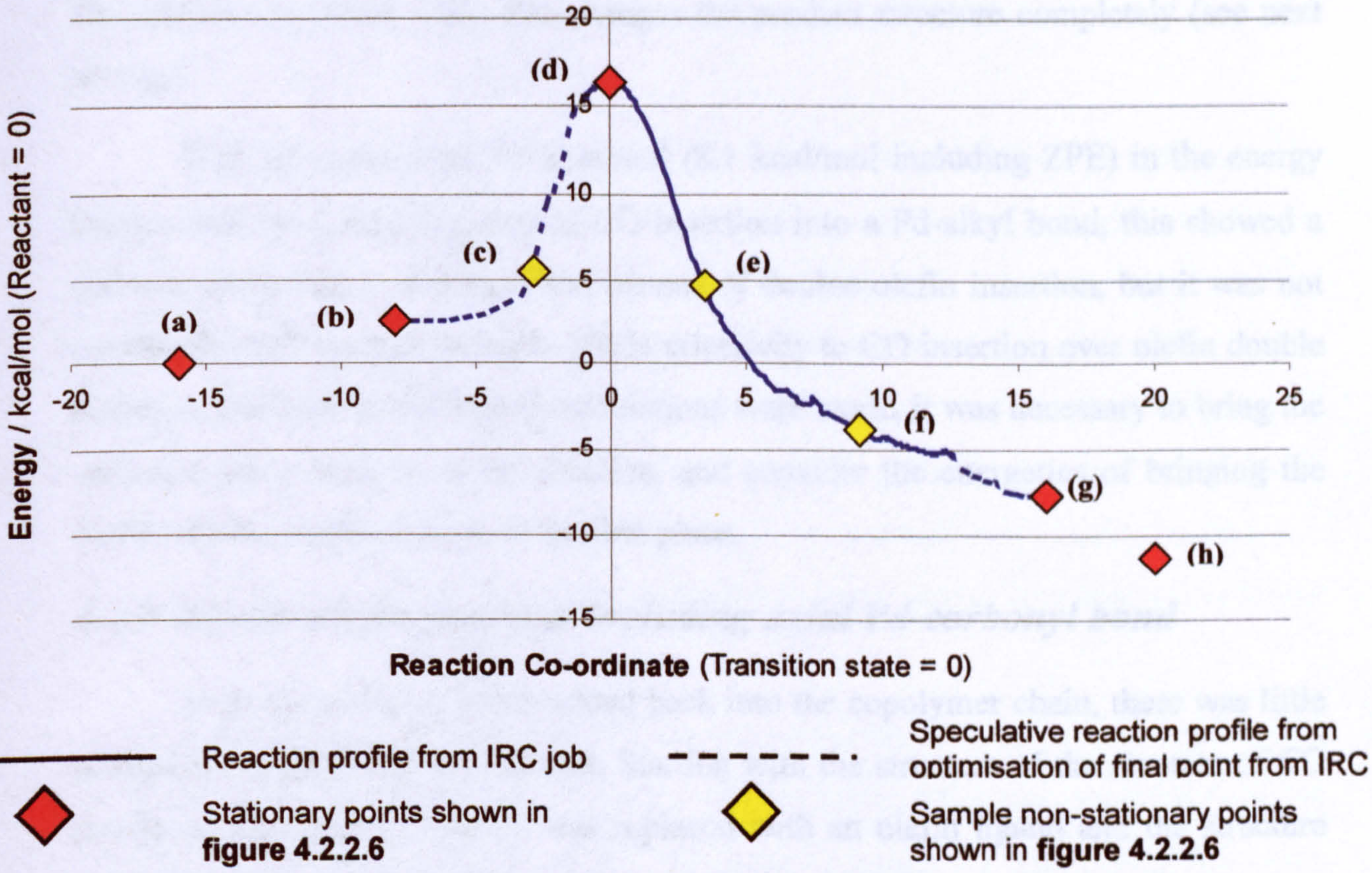


Figure 4.2.2.5: Reaction profile of double olefin insertion without second CO group, with selected points shown in **figure 4.2.2.6**.

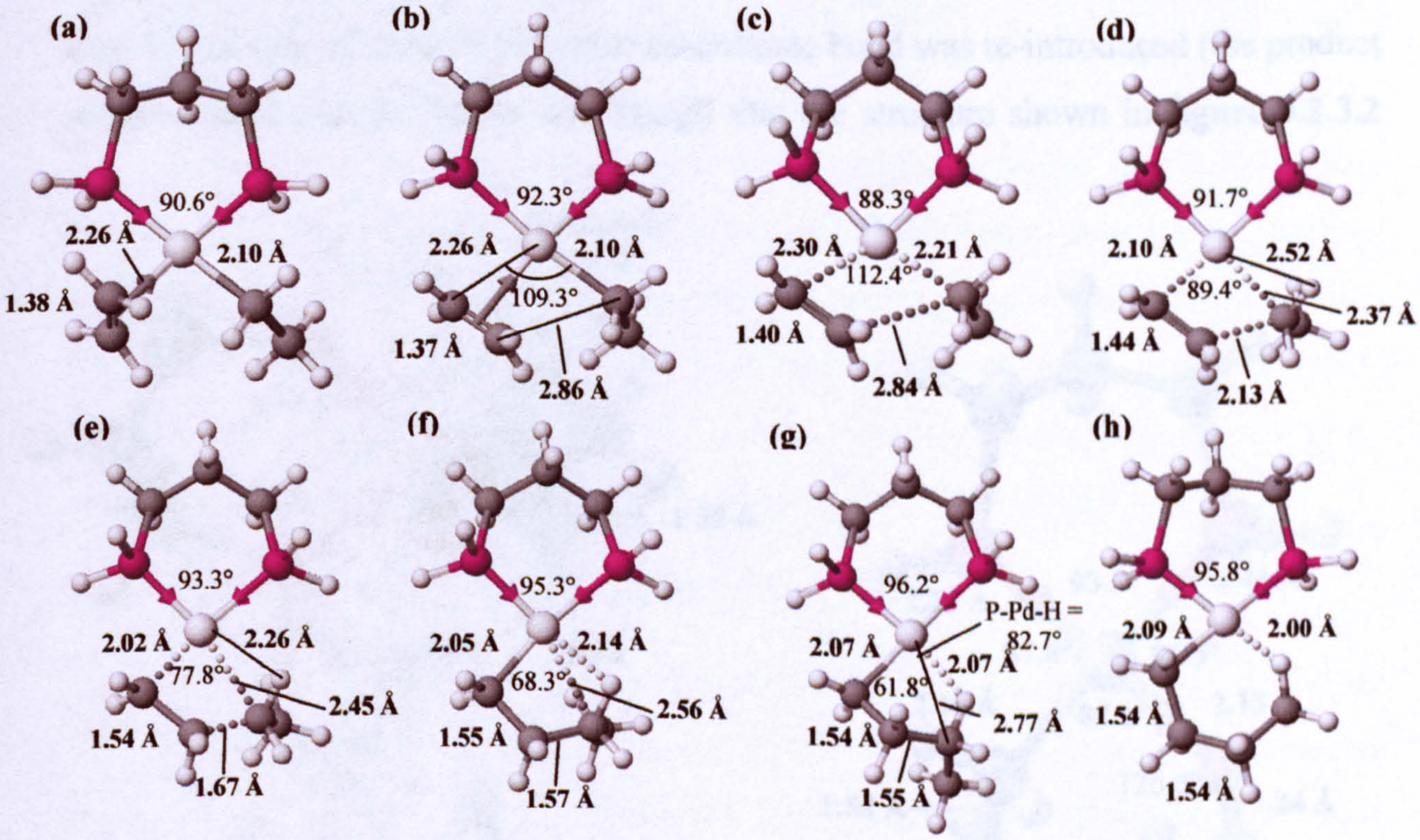


Figure 4.2.2.6: Selected points from reaction profile.

similar process in normal olefin insertion, and switching from 5-membered rings to 6- or 4-membered rings after double olefin insertion is unlikely to explain anything further about the high energy barrier, and would not be applicable after insertion of

the first CO molecule when this changes the product structure completely (see next section).

With an increase of 7.2 kcal/mol (8.1 kcal/mol including ZPE) in the energy barrier over the competing step of CO insertion into a Pd-alkyl bond, this showed a definite preference to CO insertion instead of double olefin insertion, but it was not necessarily high enough to imply 100% selectivity to CO insertion over olefin double insertion. But before any further calculations were made, it was necessary to bring the carbonyl group back in to the reaction, and consider the energetics of bringing the olefin into the equatorial site in the first place.

4.2.3 Double olefin insertion including axial Pd-carbonyl bond

With the carbonyl group added back into the copolymer chain, there was little difficulty in optimising the reactant. Starting with the structure of the reactant of CO insertion, when the CO ligand was replaced with an olefin ligand and the structure was re-optimised, the structure shown in **figure 4.2.3.1** was obtained. The product structure was more difficult to optimise, and when several structures were inputted without any definite fourth ligand, the optimisation failed to proceed beyond the first step. It was only when a Pd-O ketone co-ordinate bond was re-introduced (the product structure proposed by Ziegler and Margl) that the structure shown in **figure 4.2.3.2**

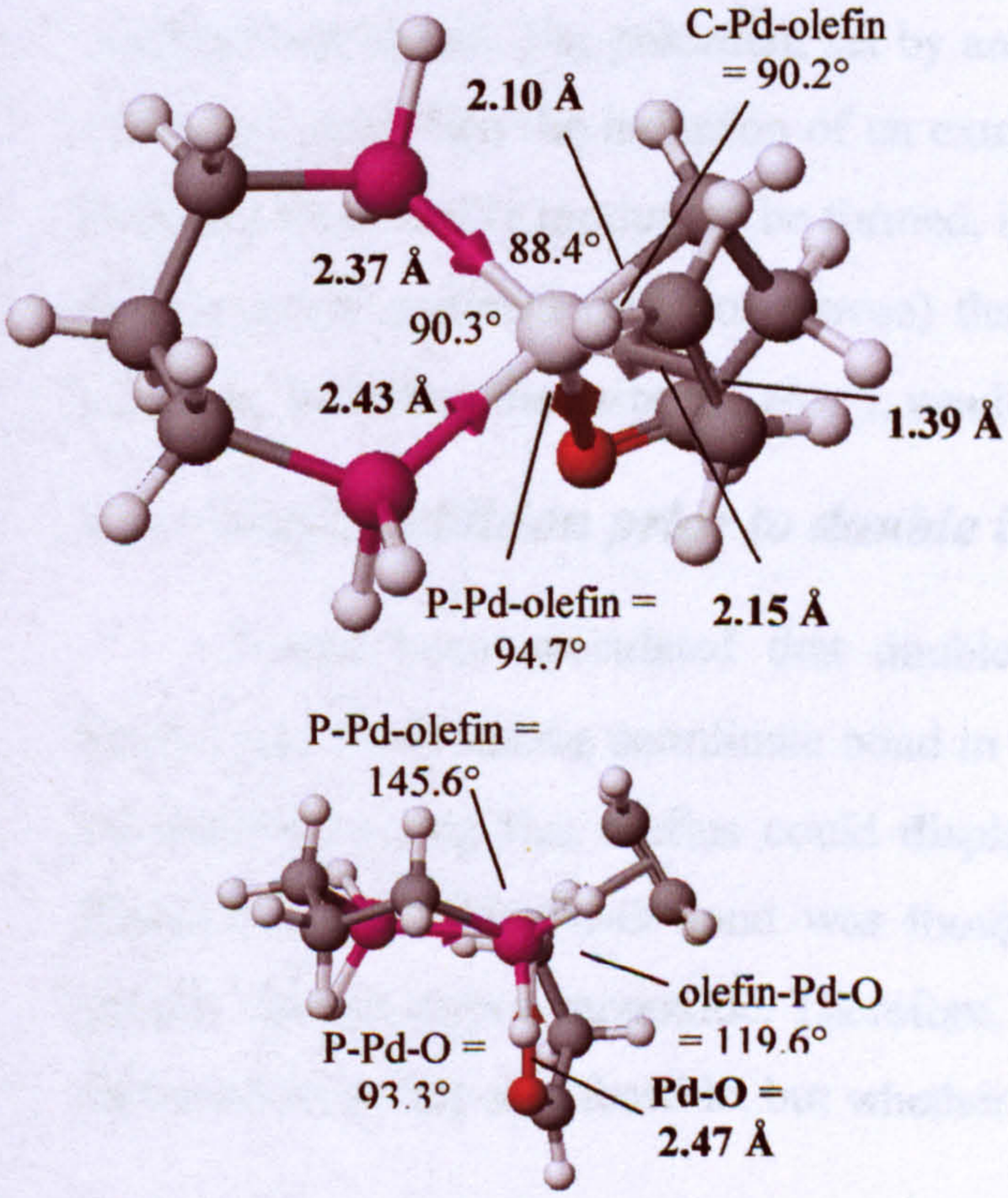


Figure 4.2.3.1: Optimised structure of reactant for double olefin insertion.

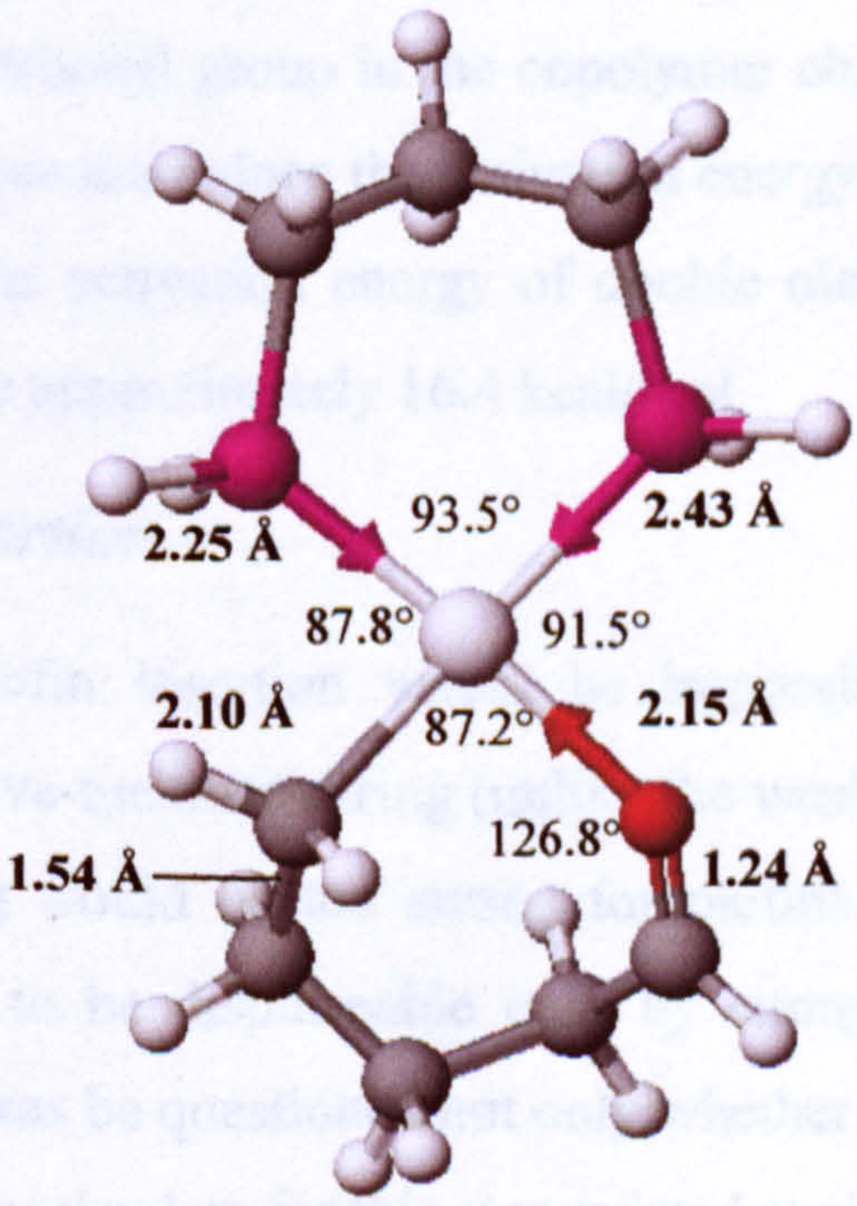


Figure 4.2.3.2: Optimised structure of product for double olefin insertion.

was obtained. Even so, it had yet to be confirmed that this was the product that was reached from the transition state.

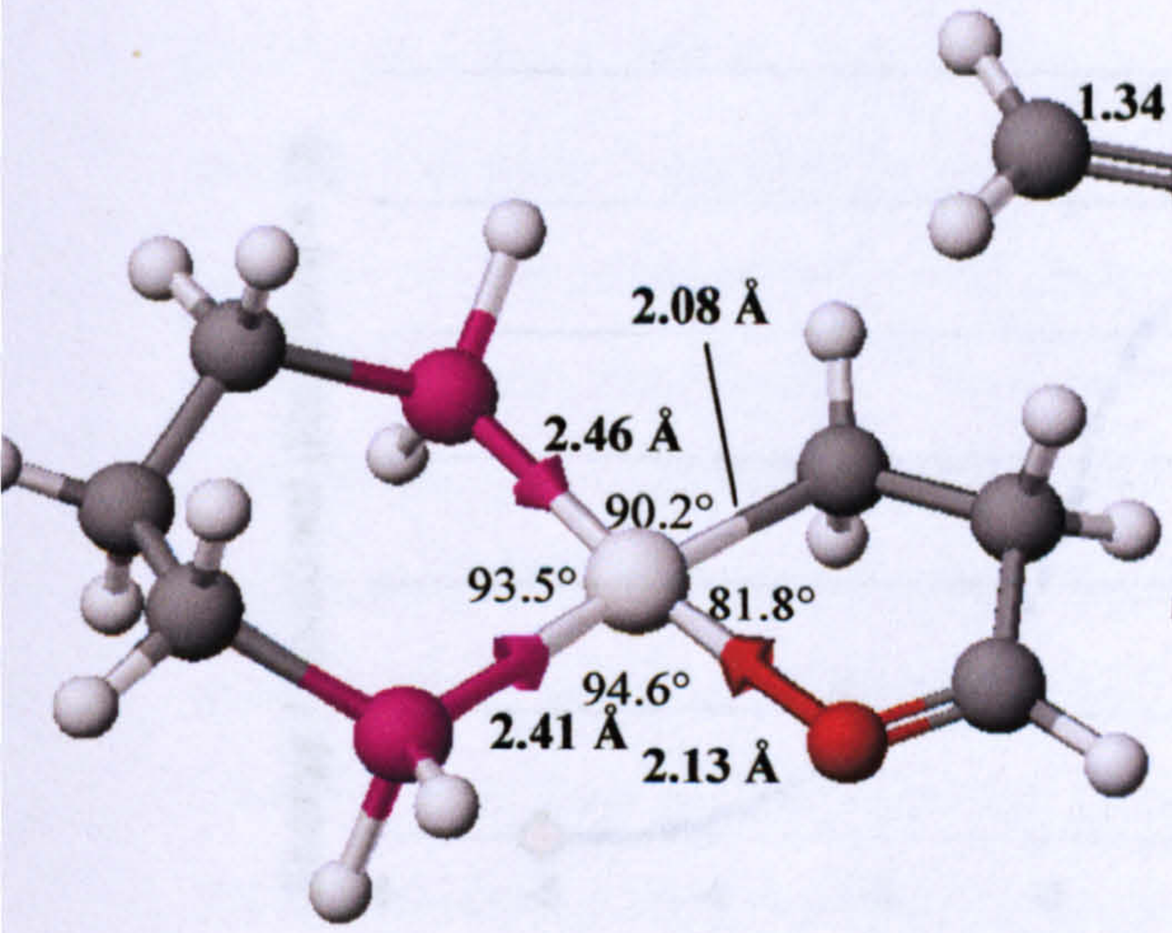
The transition state, however, proved to be far more difficult to optimise. The normally reliable Opt=Path method failed to produce any plausible path between the reactant and product at all, making this useless for finding a starting structure. The next attempt was to base a starting transition state structure using parameters from the structure proposed by Ziegler and Margl, but for one reason on another (which could have been the difference in methods, basis sets, diphosphine backbones, or simply the lack of information in the paper to pinpoint the exact position of every atom), this structure failed to optimise to any region that could have conceivably been the transition state.

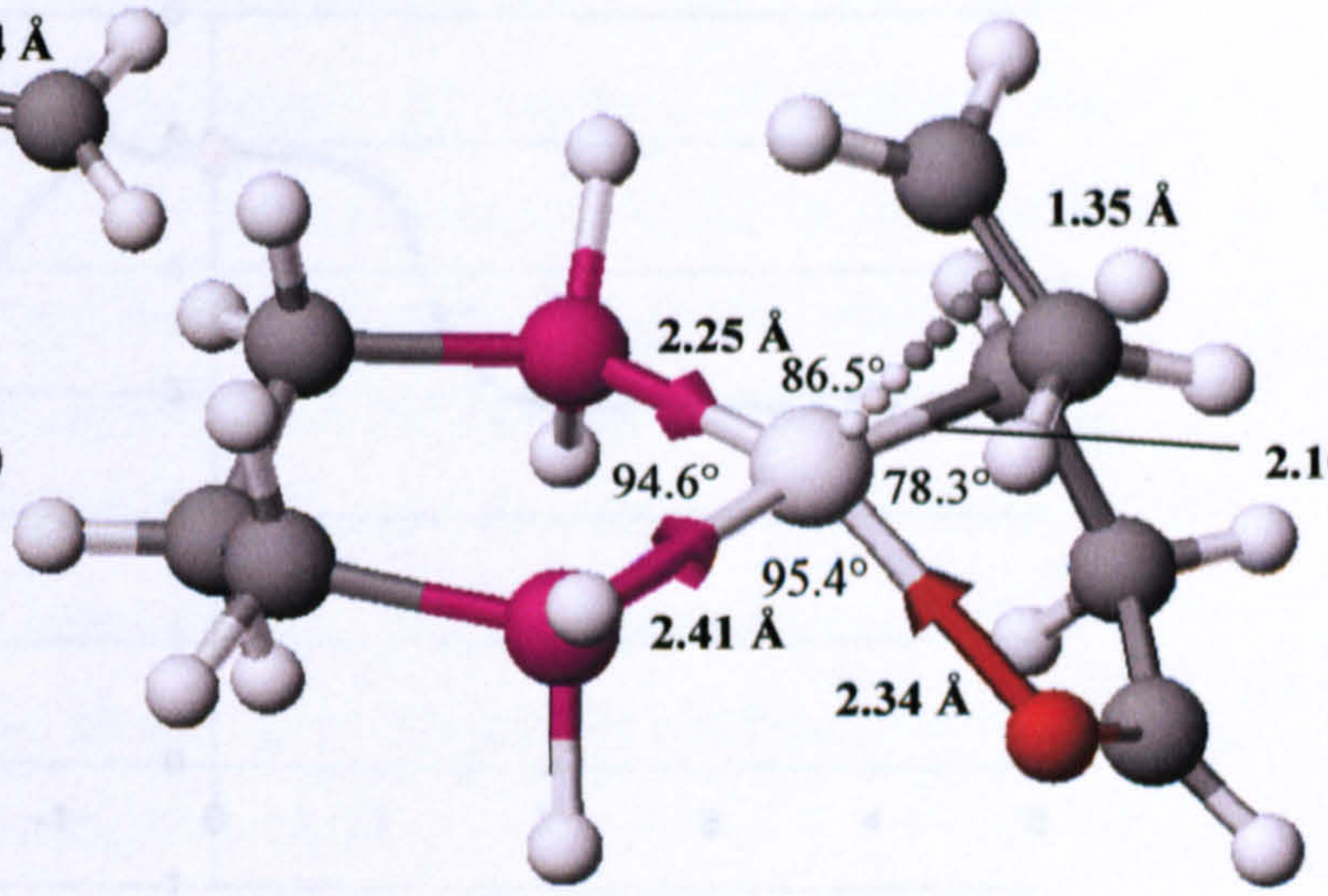
Nevertheless, the enthalpy of this step was calculated to be very exothermic: -22.6 kcal/mol (19.8 kcal/mol including ZPE), showing that the availability of an oxygen atom to stabilise the product once again makes the enthalpy much more negative. This value is about the same as the enthalpy of olefin insertion into a Pd-alkyl bond (-24.9 kcal/mol, or –22.0 kcal/mol with ZPE), but, significantly, it was a lot larger than the enthalpy of CO insertion (-10.4 kcal/mol, or –8.6 kcal/mol with ZPE).

However, it is unlikely that this highly negative enthalpy will make double insertion any easier. The precedent set by analysis of CO insertion in the propagation cycle was that when the inclusion of an extra carbonyl group in the copolymer chain enables a more stable product to be formed, it does *not* reduce the activation energy. It was therefore assumed (but not proven) that the activation energy of double olefin insertion, including the carbonyl group, would be approximately 16.4 kcal/mol.

4.2.4 Olefin addition prior to double insertion

It had been speculated that double olefin insertion would be impossible because the Pd-O ketone coordinate bond in a five-membered ring (unlike the weaker six-membered ring that olefins could displace) would be too strong for olefins to displace Instead this Pd-O bond was thought to be displaceable only by stronger ligands such as carbon monoxide. Therefore, it was be questioned not only whether an olefin addition step was feasible, but whether a mechanism for this step existed at all.





Side view:

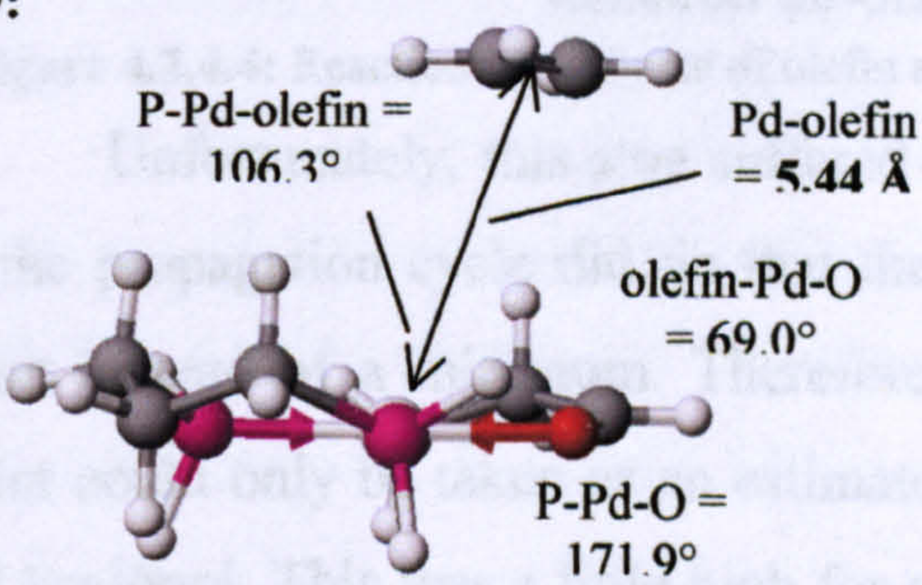


Figure 4.2.4.1: *Estimated* structure of reactant for olefin addition prior to double olefin insertion based on optimised structure of saddle point.

Side view:

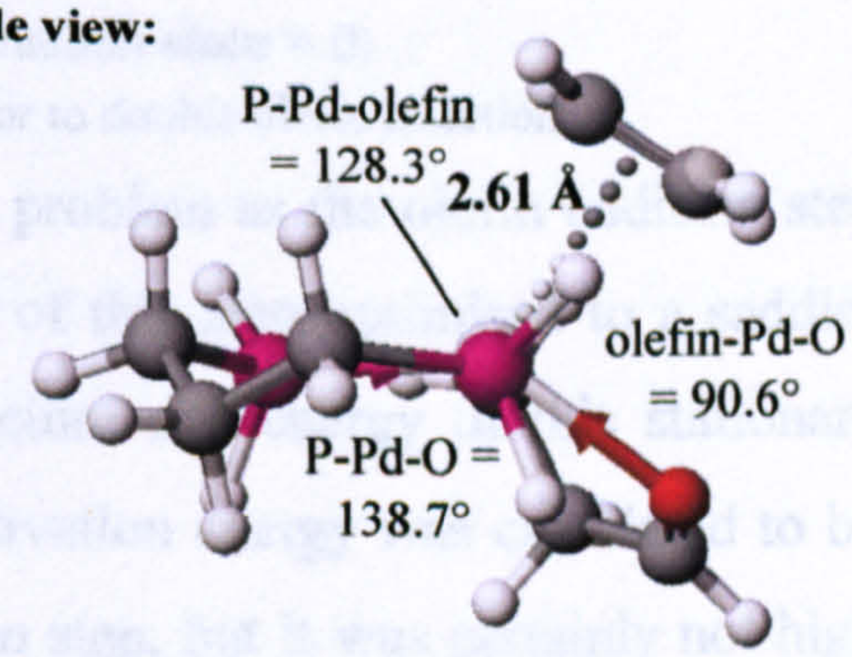


Figure 4.2.4.2: Optimised structure of transition state for olefin addition prior to double olefin

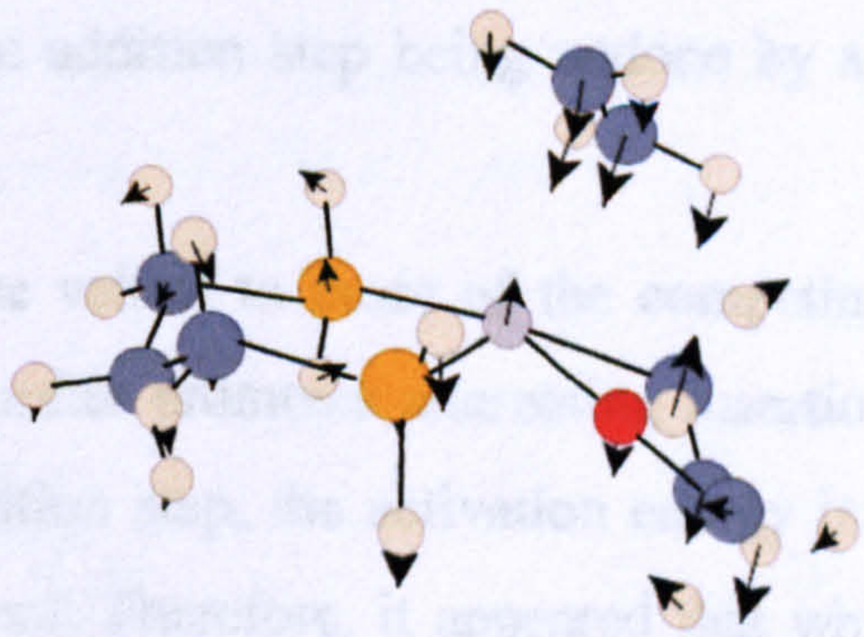


Figure 4.2.4.3: Mode of vibration of imaginary frequency (-66.1 cm^{-1})

However, it turned out that a reaction mechanism did exist. The product structure is shown in figure 4.2.3.1. The reactant of this step was optimised as shown in **figure 4.2.4.1**. By using the Opt=Path method, a suitable estimated transition state was chosen as a starting structure for a transition state optimisation, and the transition state optimised was shown in **figure 4.2.4.2** (mode of vibration of imaginary frequency shown in **figure 4.2.4.3**).

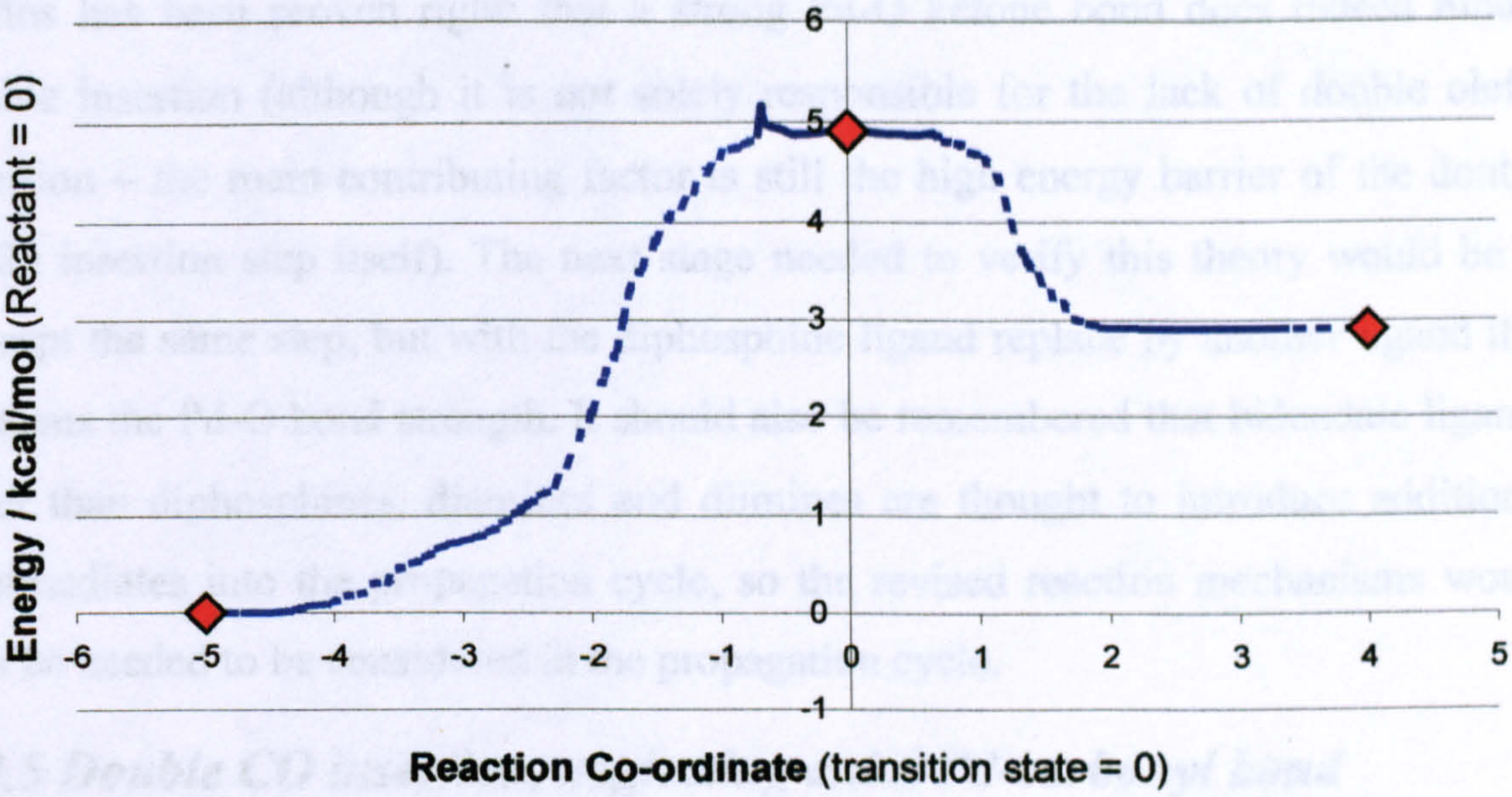


Figure 4.2.4.4: Reaction co-ordinate of olefin addition prior to double olefin insertion.

Unfortunately, this step suffered the same problem as the olefin addition step in the propagation cycle did, in that the reactant of this step optimised to a saddle-point instead of a minimum. Therefore the structure and energy of this stationary point could only be taken as an estimate. The activation energy was calculated to be 4.8 kcal/mol. This was a little high for an addition step, but it was certainly not high enough to make this step impossible as some theories suggested. The enthalpy, however, was +3.1 kcal/mol. This would make double olefin insertion more difficult, as the likelihood of the addition step being undone by a reverse reaction would be high.

Comparing these values to those of the competing step, CO addition in the propagation cycle, it further promotes alternating insertion over double insertion. In the competing CO addition step, the activation energy is only 2.2 kcal/mol, and the enthalpy is –3.1 kcal/mol. Therefore, it appeared that whilst the olefin addition step prior to double olefin insertion is not impossible, the unfavourable activation energy and enthalpy make double insertion even less likely.

The reaction profile of this step is shown in **figure 4.2.4.4**. (The reaction mechanism was similar to that of olefin addition in the propagation cycle, shown in figure 3.6.4.3.) The enthalpy of bringing in a distant olefin to the axial position was calculated to be –1.9 kcal/mol. Comparing this to the competing step of CO addition, the enthalpy of bringing in a distant CO to the axial position was -2.3 kcal/mol.

Overall, it seems that part of Drent's theory on promoting double insertion of olefins has been proven right: that a strong Pd-O ketone bond does indeed hinder double insertion (although it is not solely responsible for the lack of double olefin insertion – the main contributing factor is still the high energy barrier of the double olefin insertion step itself). The next stage needed to verify this theory would be to attempt the same step, but with the diphosphine ligand replace by another ligand that weakens the Pd-O bond strength. It should also be remembered that bidendate ligands other than diphosphines, diamines and diimines are thought to introduce additional intermediates into the propagation cycle, so the revised reaction mechanisms would also be needed to be considered in the propagation cycle.

4.2.5 Double CO insertion, neglecting axial Pd-carbonyl bond

In view of the difficulties of optimising a transition state of double olefin insertion with the additional variable of an axial Pd-carbonyl bond, it was decided to start this step by omitting this group. The simplest structure to optimise was the reactant, as shown in **figure 4.2.5.1**.

The product structure, however, was more complicated. The first structure to be optimised is shown in **figure 4.2.5.2**, but the enthalpy of this step, at +21.1 kcal/mol, was very high, even for a step thought to be thermodynamically forbidden. By rotating the O=C-C=O dihedral angle by 90°, it was possible (although difficult, requiring careful positioning of a Pd-H bond) to optimise a very slightly more stable

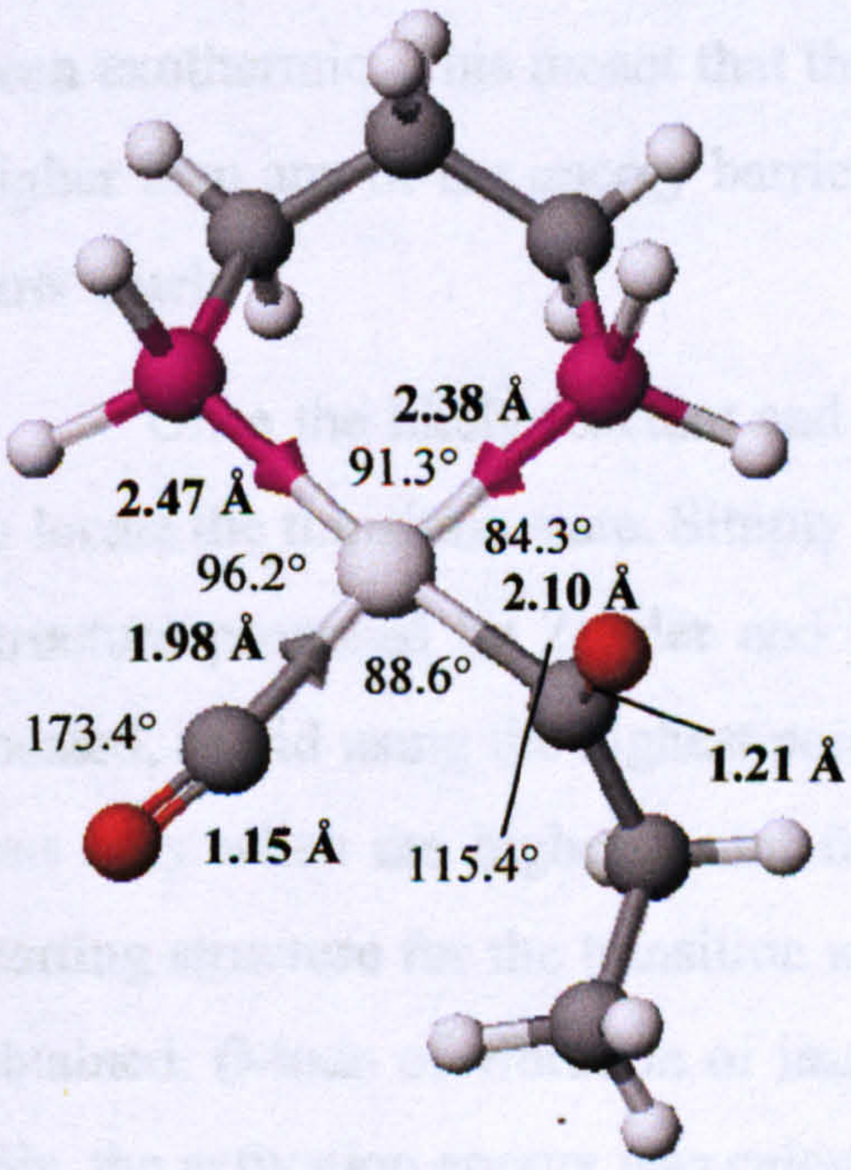


Figure 4.2.5.1: Reactant of double CO insertion neglecting axial Pd-carbonyl bond.

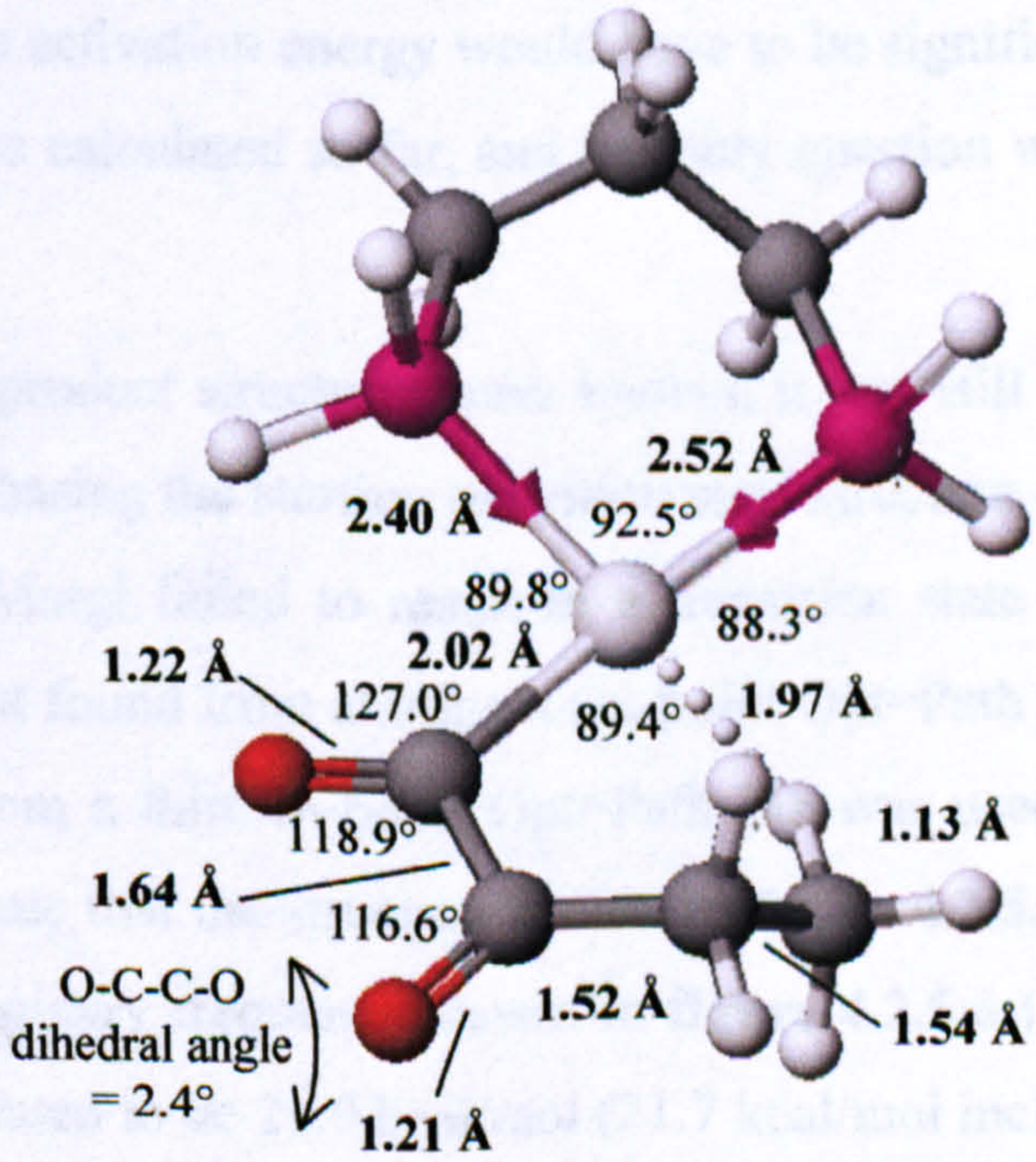


Figure 4.2.5.2: First product structure of double CO insertion neglecting axial Pd-carbonyl bond.

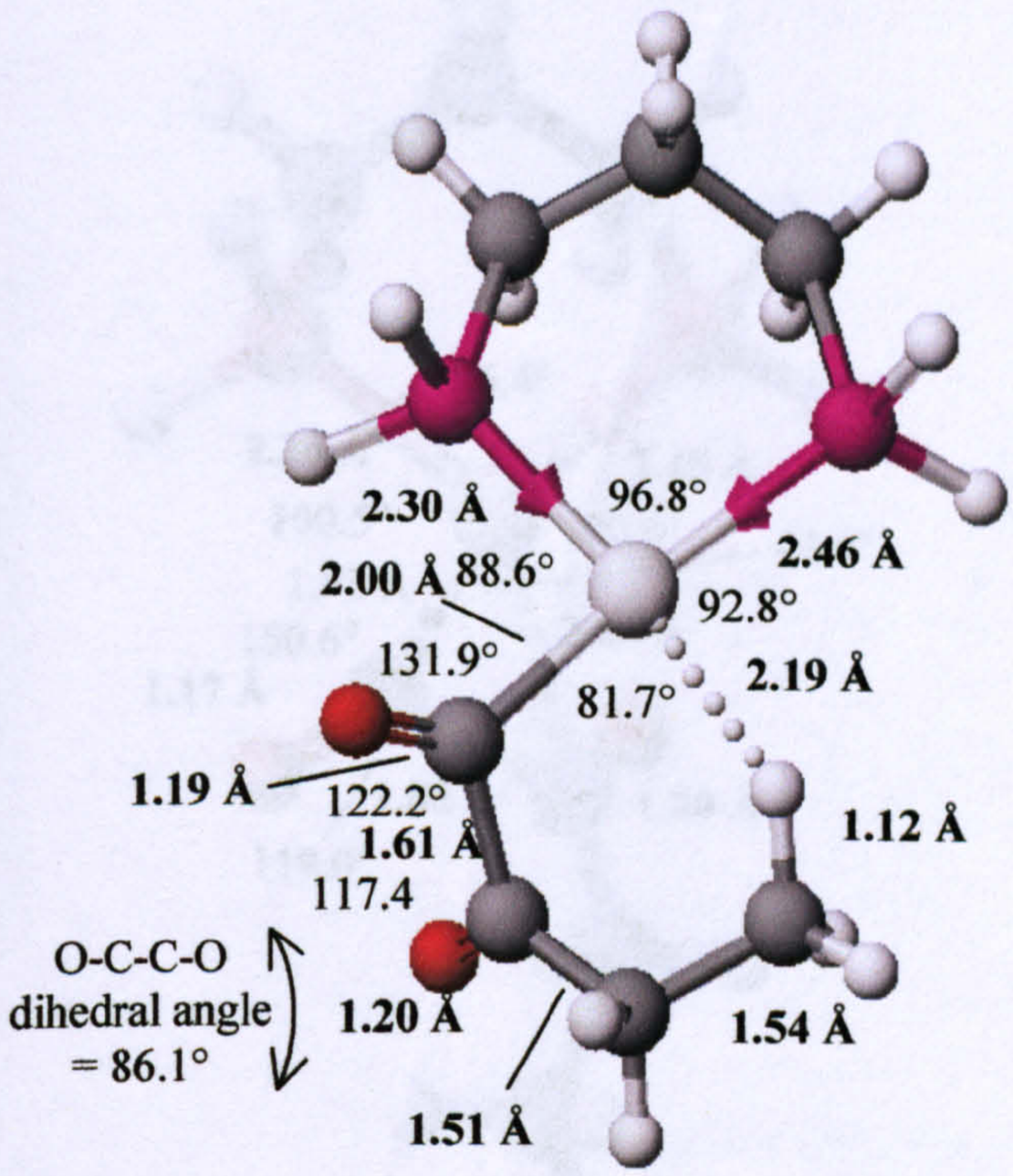


Figure 4.2.5.3: Second product structure of double CO insertion neglecting axial Pd-carbonyl bond.

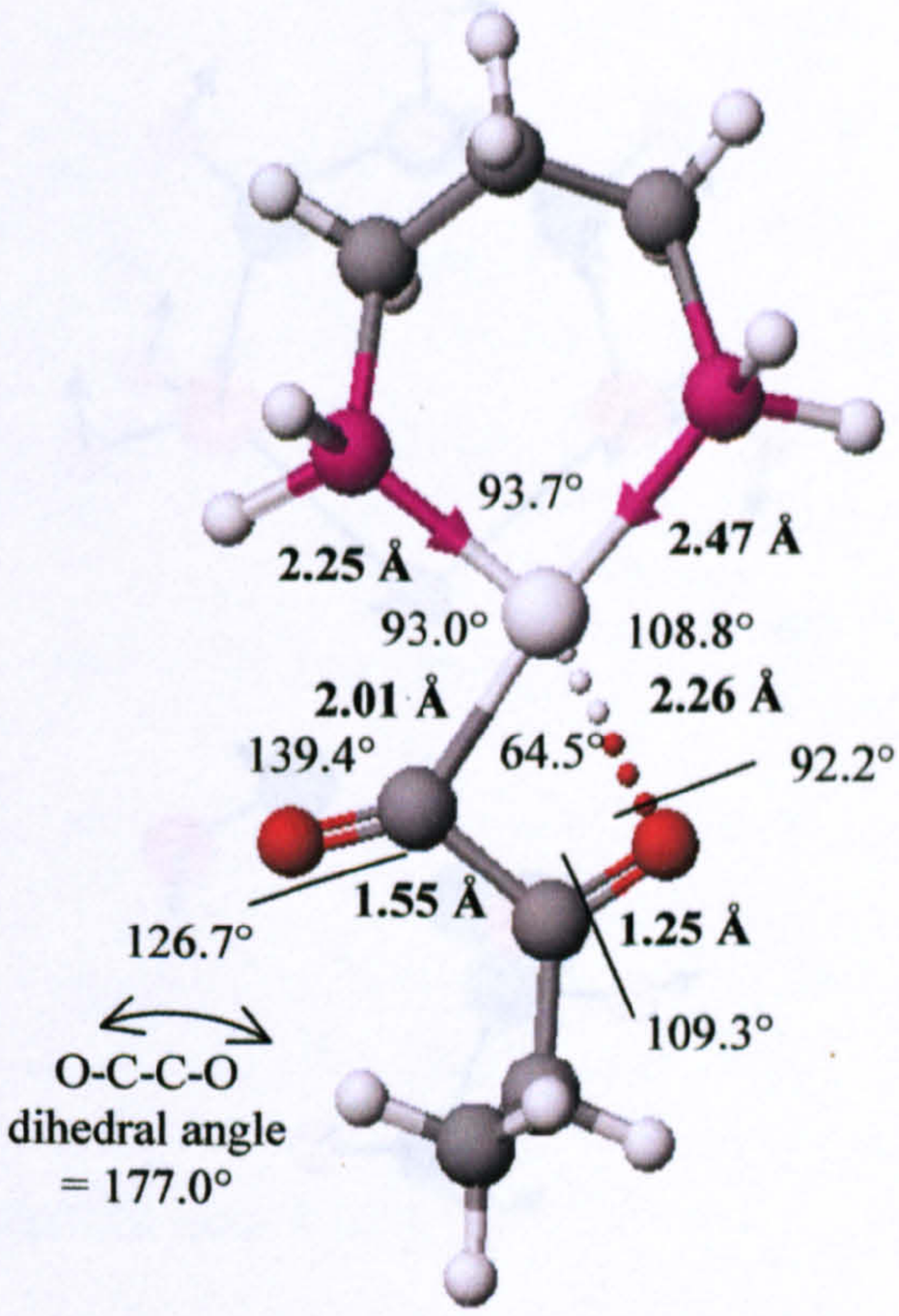


Figure 4.2.5.4: Third product structure of double CO insertion neglecting axial Pd-carbonyl bond.

structure, shown in **figure 4.2.5.3**, reducing the enthalpy to +20.6 kcal/mol. By far the most stable structure, however, was by rotating this dihedral angle another 90° to give the structure shown in **figure 4.2.5.4** (as proposed by Ziegler and Margl). This reduced the enthalpy to +13.0 kcal/mol. (With zero-point corrections, the enthalpies for the structures in figures 4.2.5.2, 4.2.5.3 and 4.2.5.4 become 21.3 kcal/mol, 20.8 kcal/mol and 14.4 kcal/mol respectively.) Even so, this last enthalpy was still very highly positive, considering practically all of the insertion steps considered so far had been exothermic. This meant that the activation energy would have to be significantly higher than any of the energy barriers calculated so far, and the only question was by how much.

Once the likely reactant and product structures were known, it was still tricky to locate the transition state. Simply basing the starting transition state structure on the structure proposed by Ziegler and Margl failed to result in a transition state being located, as did using the highest point found from starting a six-point Opt=Path job. It was only when the highest point from a thirteen-point Opt=Path job was used as a starting structure for the transition state that the structure shown in **figure 4.2.5.5** was obtained. (Mode of vibration of imaginary frequency shown in **figure 4.2.5.6**.) From this, the activation energy was calculated to be 21.9 kcal/mol (21.7 kcal/mol including ZPE), only slightly higher than some of the less stable product structures. This

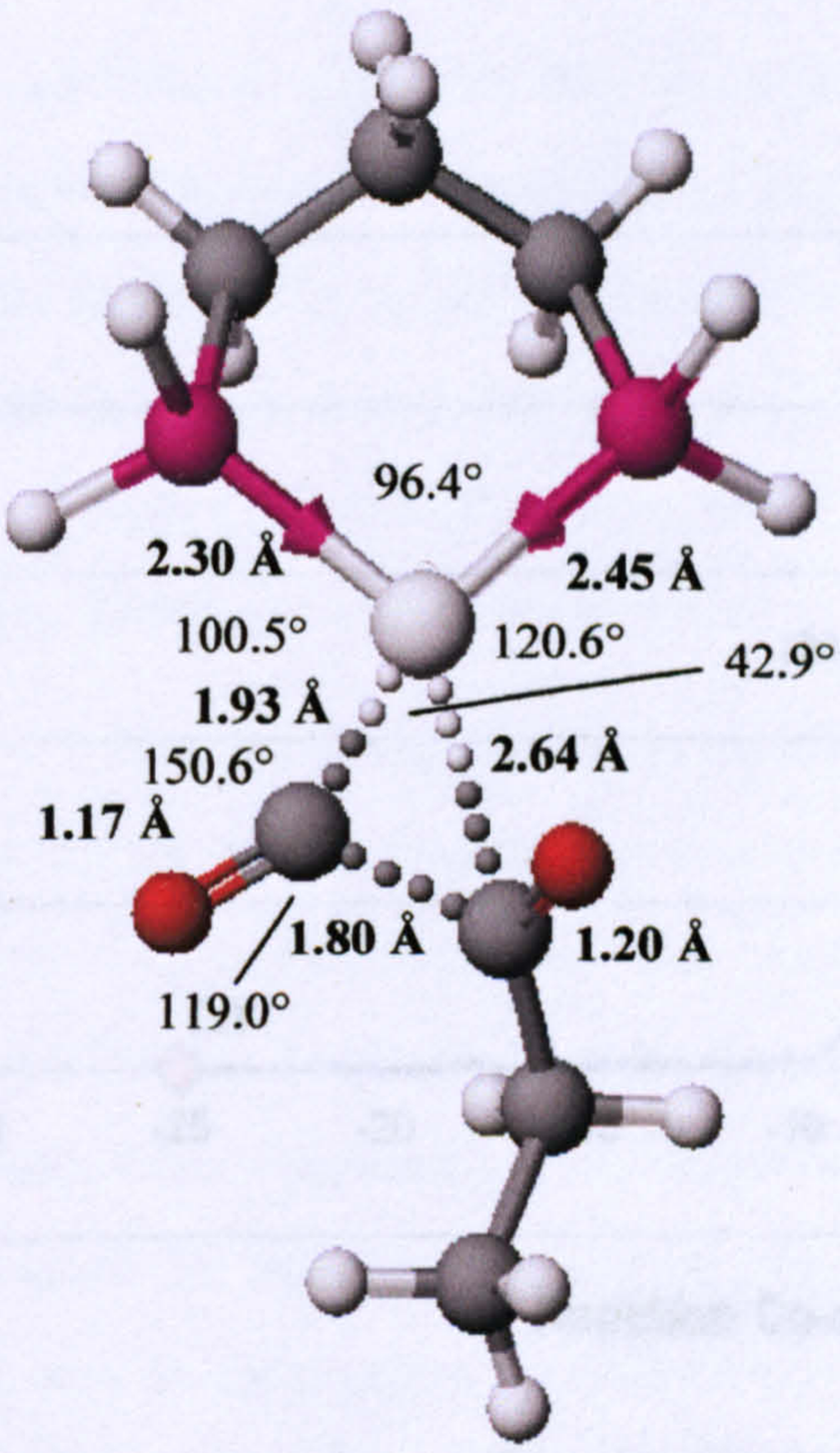


Figure 4.2.5.5: Transition state of double CO insertion.

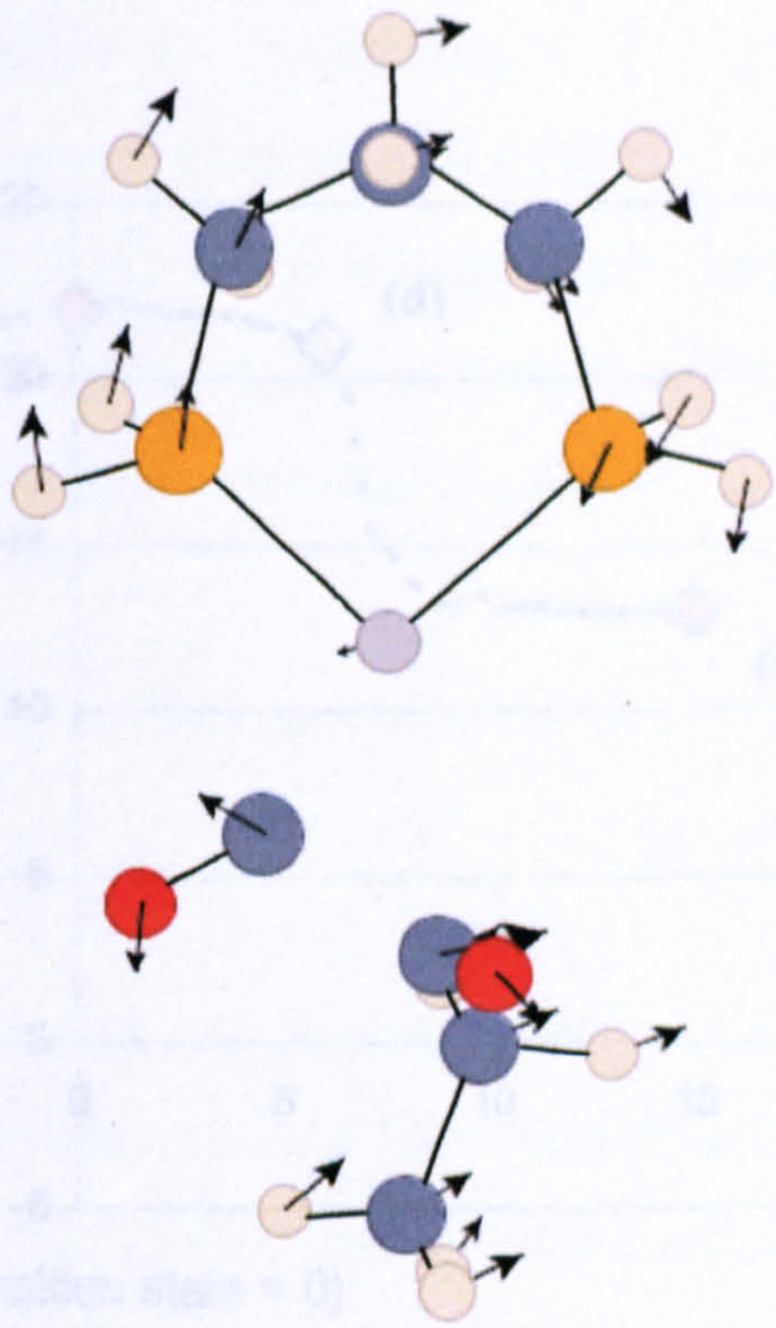


Figure 4.2.5.6: Mode of vibration of imaginary frequency (-86.1 cm^{-1})

activation energy was much higher than those for both the competing olefin insertion step, 11.2 kcal/mol, and the CO insertion into a Pd-acyl bond, 9.2 kcal/mol, and therefore heavily supported earlier conclusions that double CO insertion is ruled out on thermodynamic grounds.

Nevertheless, the reaction mechanism of this hypothetical step was examined, with the reaction profile shown in **figure 4.2.5.7**, and selected points shown in **figure 4.2.5.8**. The main component of this mechanism was the migration of the acyl group to the CO ligand (points a-d), and this was followed by the formation of a palladium-oxygen ketone interaction to stabilise the structure.

Overall, as expected, the energy barrier rules out any double CO insertion, and should any double CO insertion occur, it could easily be immediately followed by the reverse reaction. It appears that the instability of adjacent carbonyl groups is chiefly responsible for lack of double insertion rather than a high energy barrier between two stable structures, for the energy of the structure rises very sharply as the carbonyl-carbonyl bond is formed and only falls a little when the structure stabilises. The distance between the carbon atoms in the adjacent carbonyl groups certainly appears to be on the high side compared to the usual distance between two carbon atoms in sp^2 environments (and higher still in the less stable conformations of the product) – in

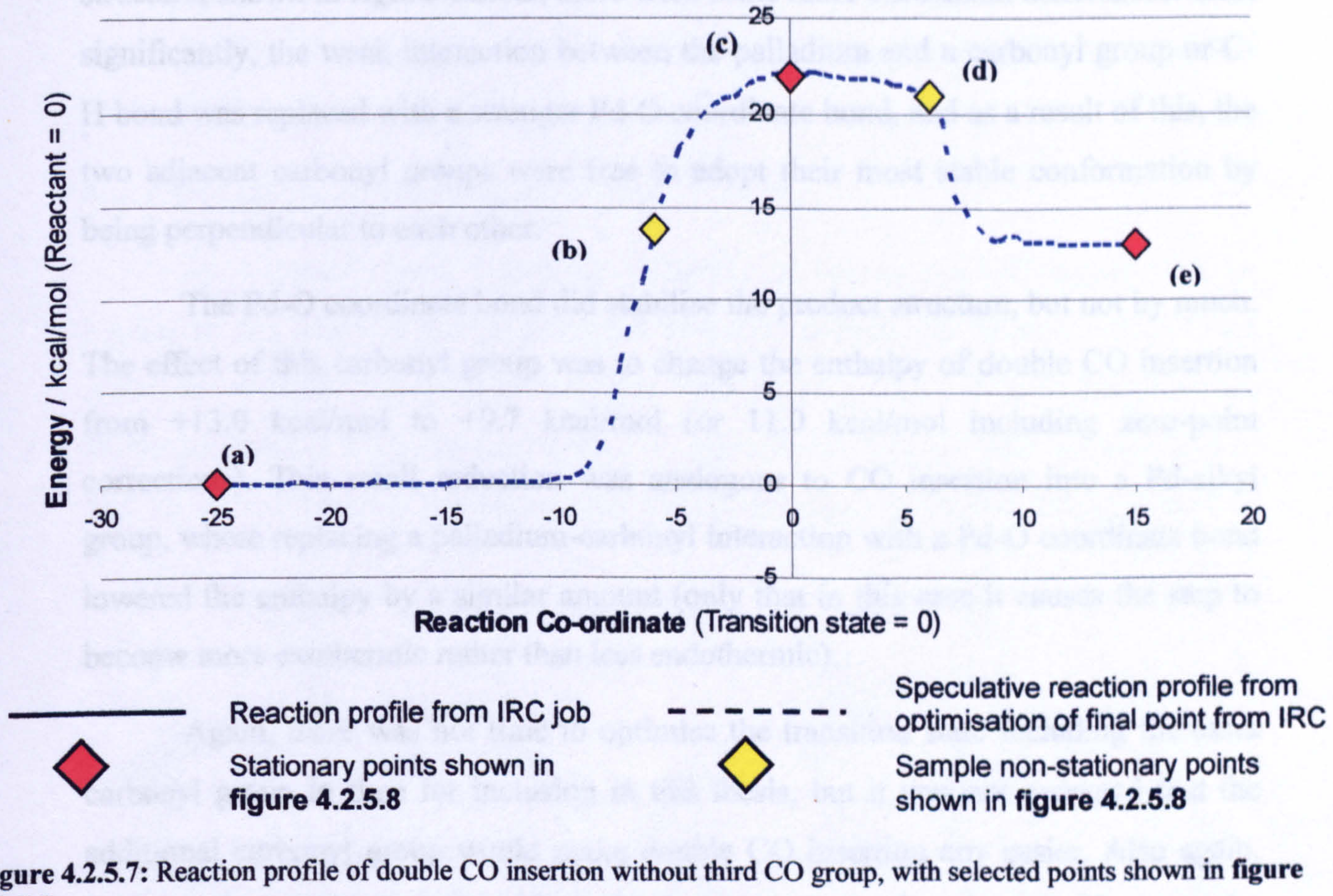


Figure 4.2.5.7: Reaction profile of double CO insertion without third CO group, with selected points shown in **figure 4.2.5.8.**

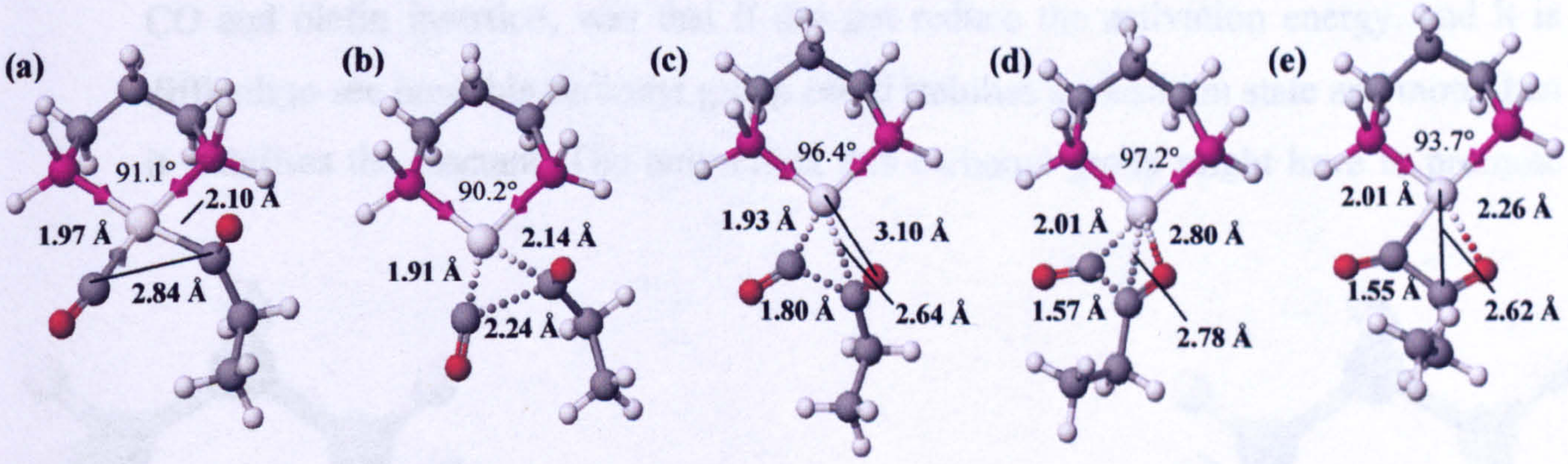


Figure 4.2.5.8: Selected points from reaction profile.

olefins the distance is normally about 1.4 Å. However, these calculations neglect the effect of the next carbonyl group interacting with the palladium atom, so this is considered next.

4.2.6 Double CO insertion, including axial Pd-carbonyl bond

The reactant and product structures for double CO insertion, including the effects of the axial Pd-carbonyl double bond, were optimised. There was little difference to the reactant structure, shown in **figure 4.2.6.1**, other than the presence of

an additional palladium-carbonyl bond in an axial site. However, in the product structure, shown in **figure 4.2.6.2**, there were some more substantial differences: most significantly, the weak interaction between the palladium and a carbonyl group or C-H bond was replaced with a stronger Pd-O coordinate bond, and as a result of this, the two adjacent carbonyl groups were free to adopt their most stable conformation by being perpendicular to each other.

The Pd-O coordinate bond did stabilise the product structure, but not by much. The effect of this carbonyl group was to change the enthalpy of double CO insertion from +13.0 kcal/mol to +9.7 kcal/mol (or 11.0 kcal/mol including zero-point corrections). This small reduction was analogous to CO insertion into a Pd-alkyl group, where replacing a palladium-carbonyl interaction with a Pd-O coordinate bond lowered the enthalpy by a similar amount (only that in this case it causes the step to become more exothermic rather than less endothermic).

Again, there was not time to optimise the transition state including the extra carbonyl group in time for inclusion in this thesis, but it was not expected that the additional carbonyl group would make double CO insertion any easier. Also again, the precedent set by inclusion of an axially-interacting carbonyl group, from regular CO and olefin insertion, was that it did not reduce the activation energy, and it is difficult to see how this carbonyl group could stabilise a transition state any more than it stabilises the reactant. The only effect this carbonyl group might have to promote

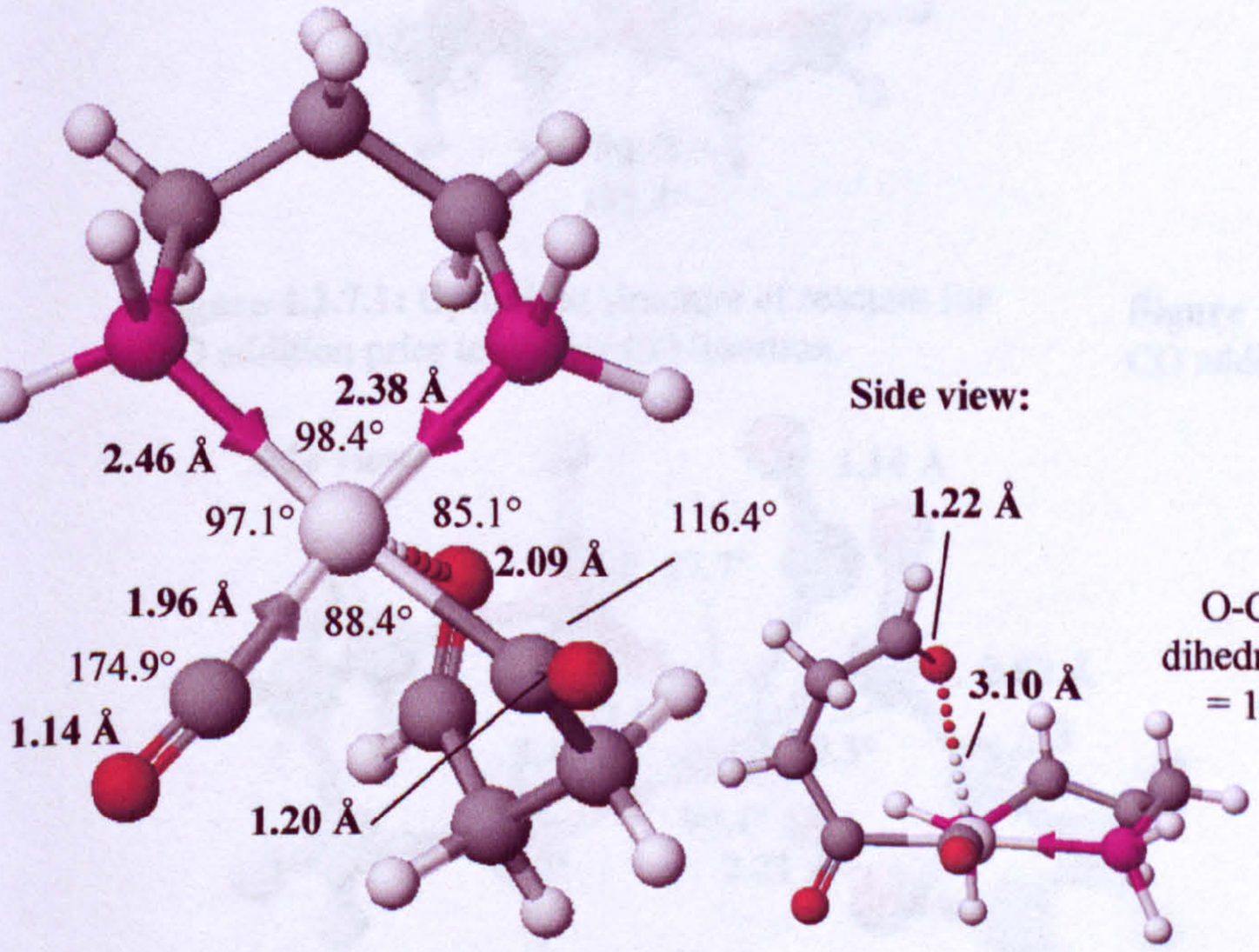


Figure 4.2.6.1: Reactant of double CO insertion including axial Pd-carbonyl bond.

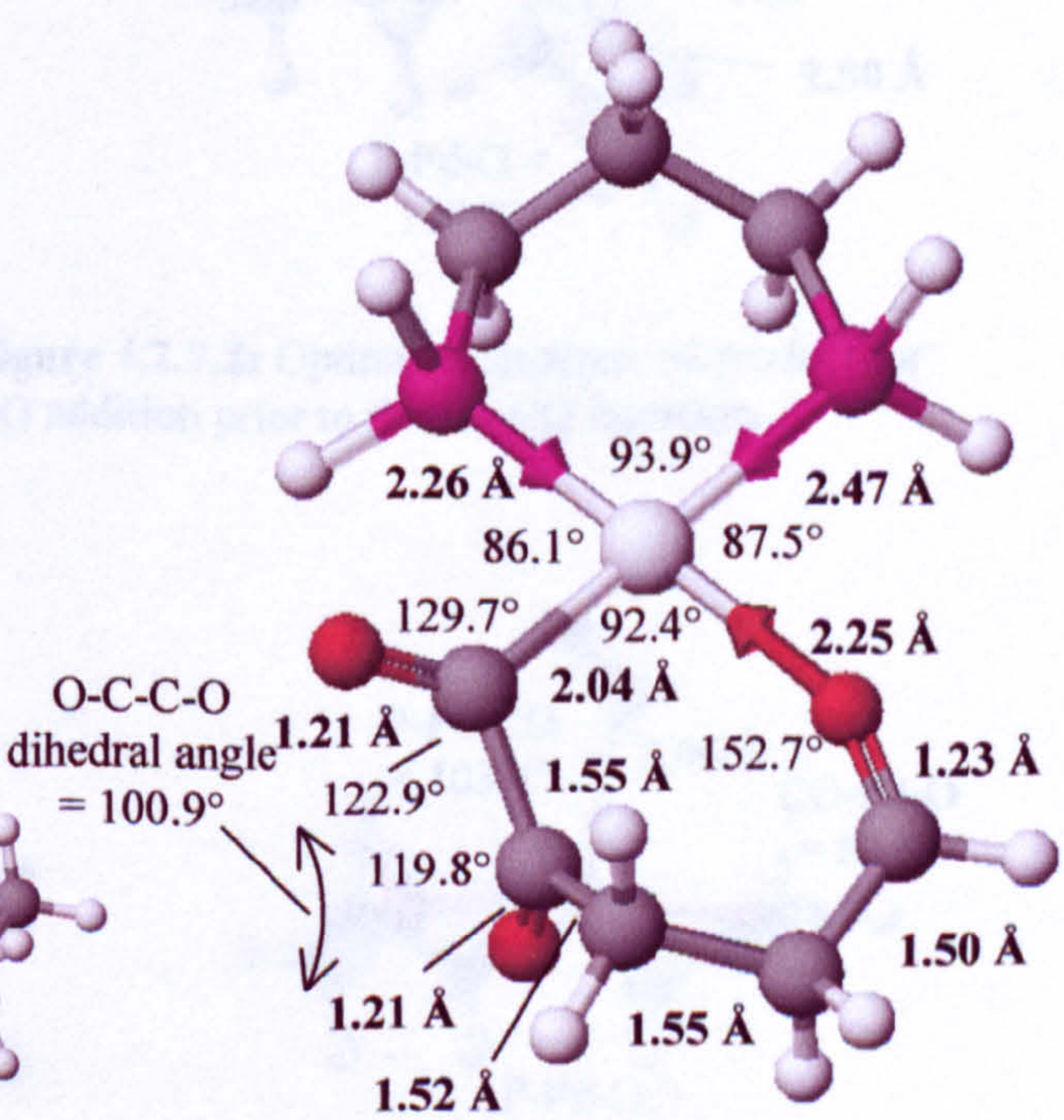


Figure 4.2.6.2: Product of double CO insertion including axial Pd-carbonyl bond.

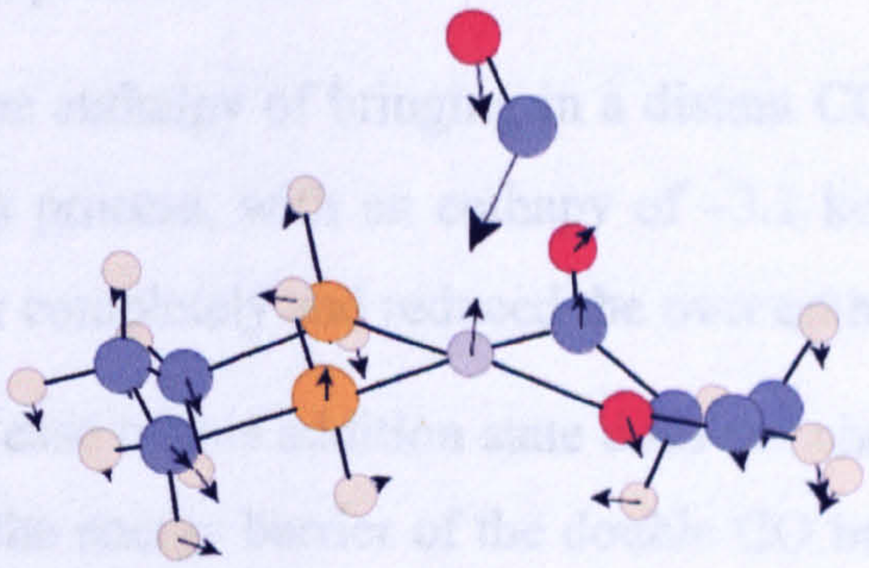


Figure 4.2.7.4: Mode of vibration of imaginary frequency (-42.8 cm^{-1}).

optimised the transition state structure shown in **figure 4.2.7.3** (mode of vibration of imaginary frequency shown in **figure 4.2.7.4**).

Unlike olefin addition prior to double olefin insertion, there did not seem to be any thermodynamic obstacles to accomplishing this step. The enthalpy of the step was –5.9 kcal/mol (-5.2 kcal/mol with zero-point corrections), and the activation energy was only 0.5 kcal/mol (no change with ZPE). The reaction profile of this step is shown in **figure 4.2.7.5**. Although there were similarities to the CO addition step in the propagation cycle, there was a small difference in that, towards the reactant structure, the transition state relaxed to a stationary point 0.3 kcal/mol above the energy of the minimum, with its energy barely below the transition state energy. Comparing this point to the reactant structure, the incoming CO molecule was closer to the reactant. This is not particularly important as the only energy values that were important to compare were the energy of the complex with CO at a large distance, and

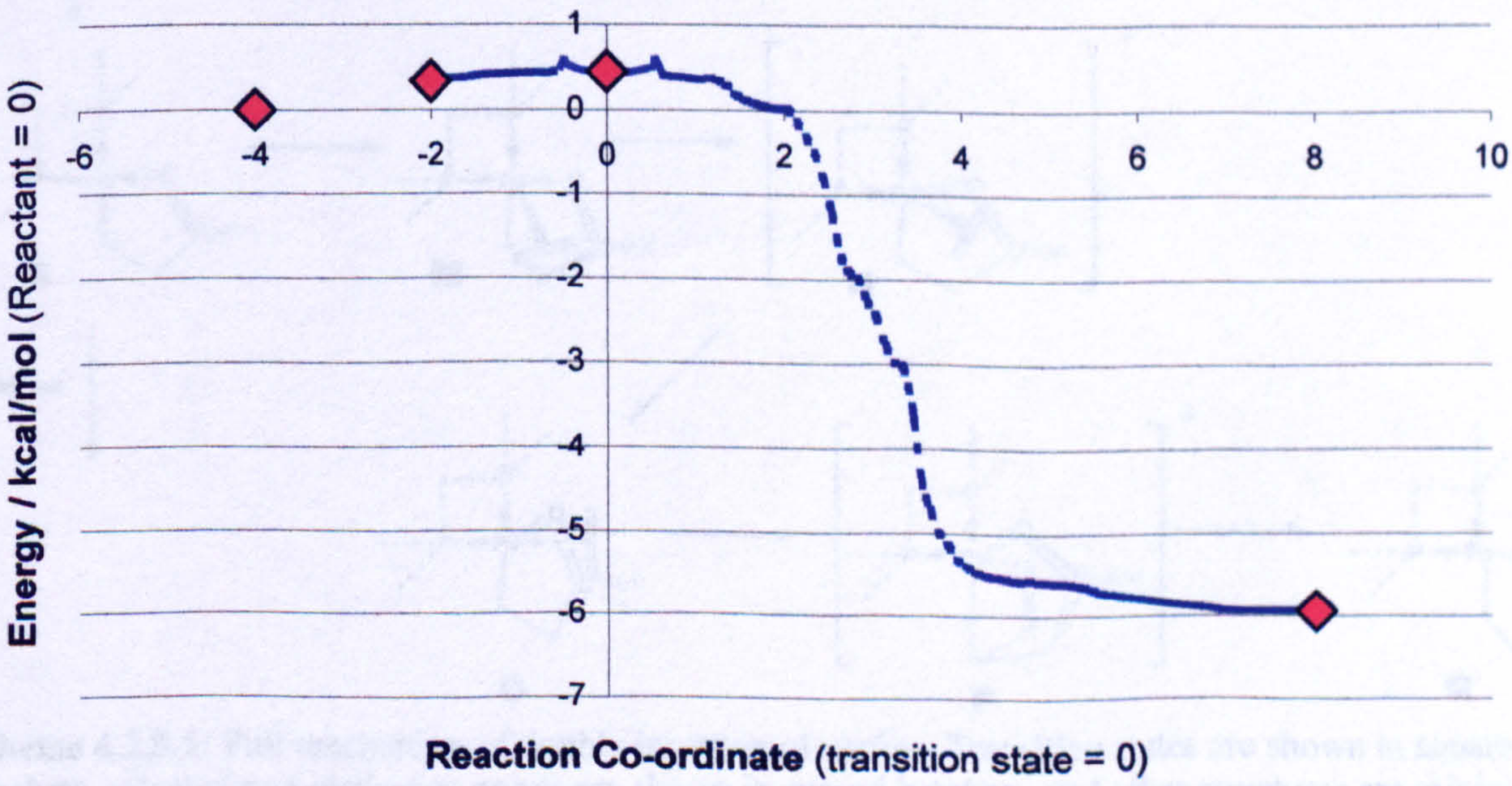


Figure 4.2.7.5: Reaction co-ordinate of CO addition prior to double CO insertion.

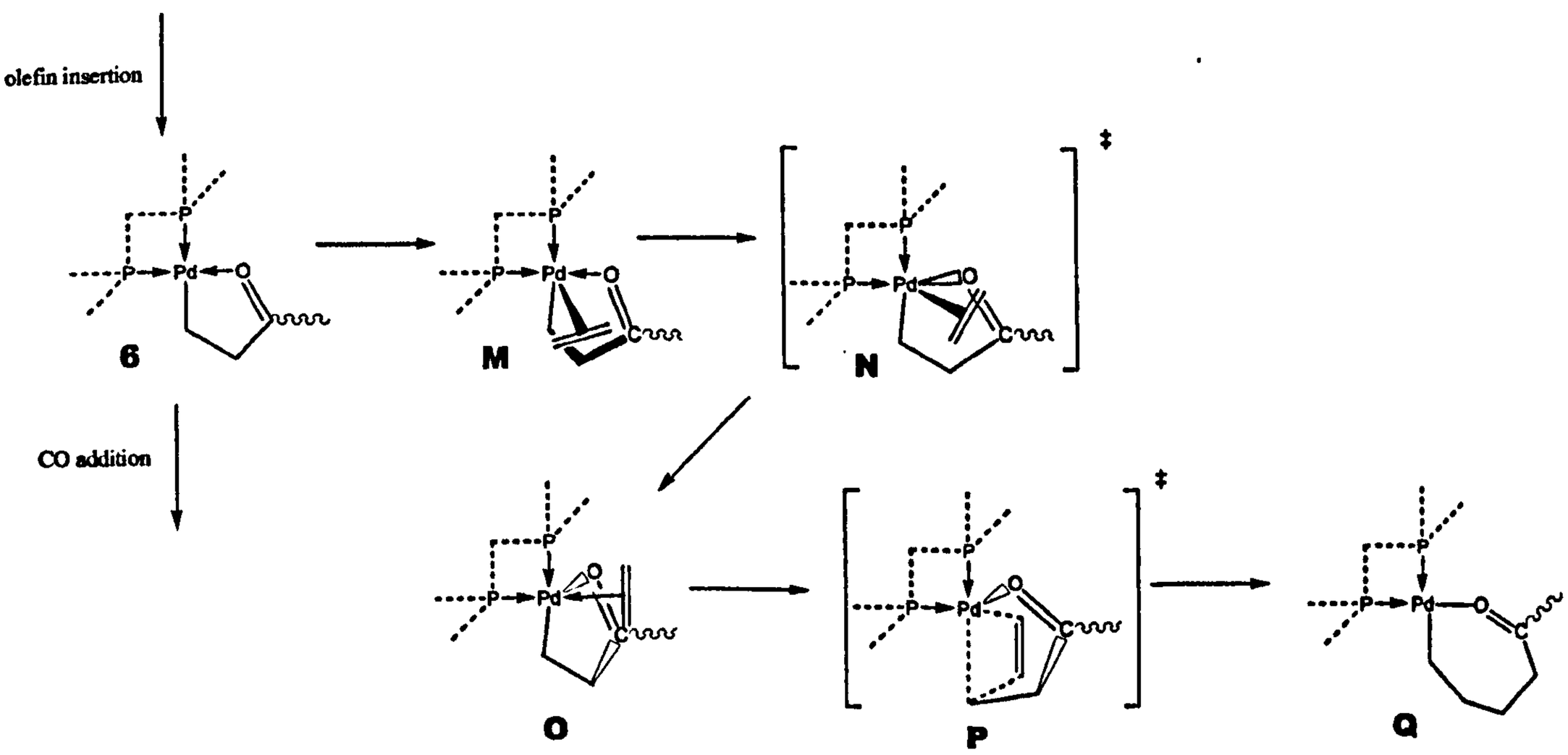
the energy of the final product.

Calculating the enthalpy of bringing in a distant CO molecule to the axial site further promoted this process, with an enthapy of –3.1 kcal/mol. This eliminated an overall energy barrier completely and reduced the over enthalpy to –9.0 kcal/mol.

Although the ease of this addition state does not change the conclusion of lack of double insertion (the energy barrier of the double CO insertion step is high enough to rule it out irrespective of the feasibility of the preceding step), these calculations present a new problem to address. Whilst it was previously calculated that there was no thermodynamic reason why Pd-O ketone co-ordinate bonds shouldn't be displaced by an olefin, it is clear that displacement by CO is a far more competitive alternative step. Therefore, the possibility of the Pd-O bond being displaced first by CO, and for this ligand to then be displaced by an olefin will need to be considered after all. On the other hand, it may well be the case that CO could act as an *inhibitor* in this stage of the copolymerisation, by occupying an equatorial site that an olefin needs for copolymerisation to proceed at all.

4.2.8 Summary

Although calculations on both double olefin insertion and double CO insertion have yet to be completed, it appears that from the results obtained so far, both processes can be ruled out, in line with experimental results.



Scheme 4.2.8.1: Full mechanism of double insertion of olefins. Transition states are shown in square brackets, selected non-stationary points are shown in curved brackets, and other structures are minima. All structures carry a single positive charge.

The mechanism and energies of double olefin insertion is currently awaiting a successful optimisation of a transition state that takes into account the effect of an axial palladium-carbonyl interaction, but the activation energy can already be estimated from the transition state neglecting this group.

Using this estimate for the activation energy, the mechanism of double olefin insertion is shown in **scheme 4.2.8.1**, and the energies of each step, compared to the energy of the competing CO addition / insertion step, are illustrated in **figure 4.2.8.1** and tabulated in **table 4.2.8.1**. Although the activation energy of the double olefin

		Including ZPE
Enthalpy of olefin addition to axial site (6-M)	-1.9	-
Energy barrier of migration from axial to equatorial site (M-N)	4.8	5.5
Enthalpy of migration from axial to equatorial site (M-O)	3.1	2.0
Energy barrier of olefin insertion step (O-P)	16.4*	17.0*
Enthalpy of olefin insertion step (O-Q)	-22.6	-19.8
Total activation energy of double olefin insertion (6-P)	**17.6***	**17.1***
Total enthalpy of double olfein insertion (6-Q)	**-19.5**	**-17.8**
Total activation energy of alternating CO insertion	**4.8**	**5.6**
Total enthalpy of CO addition to equatorial site	**-17.5**	**-14.5**

Table 4.2.8.1: Table of energy changes associated with double insertion of olefins.
**: Estimate based on activation energy with carbonyl group neglected.*

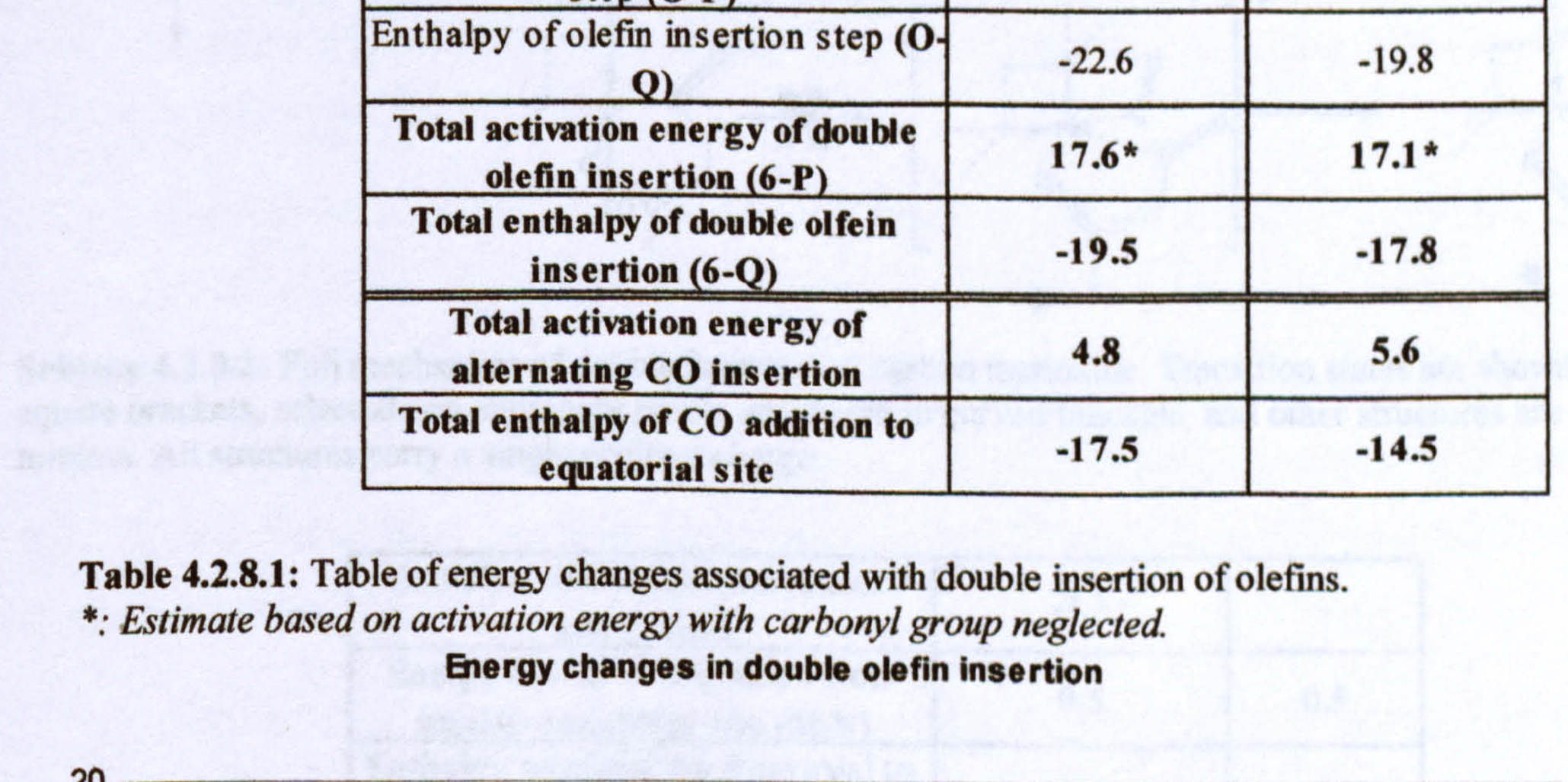
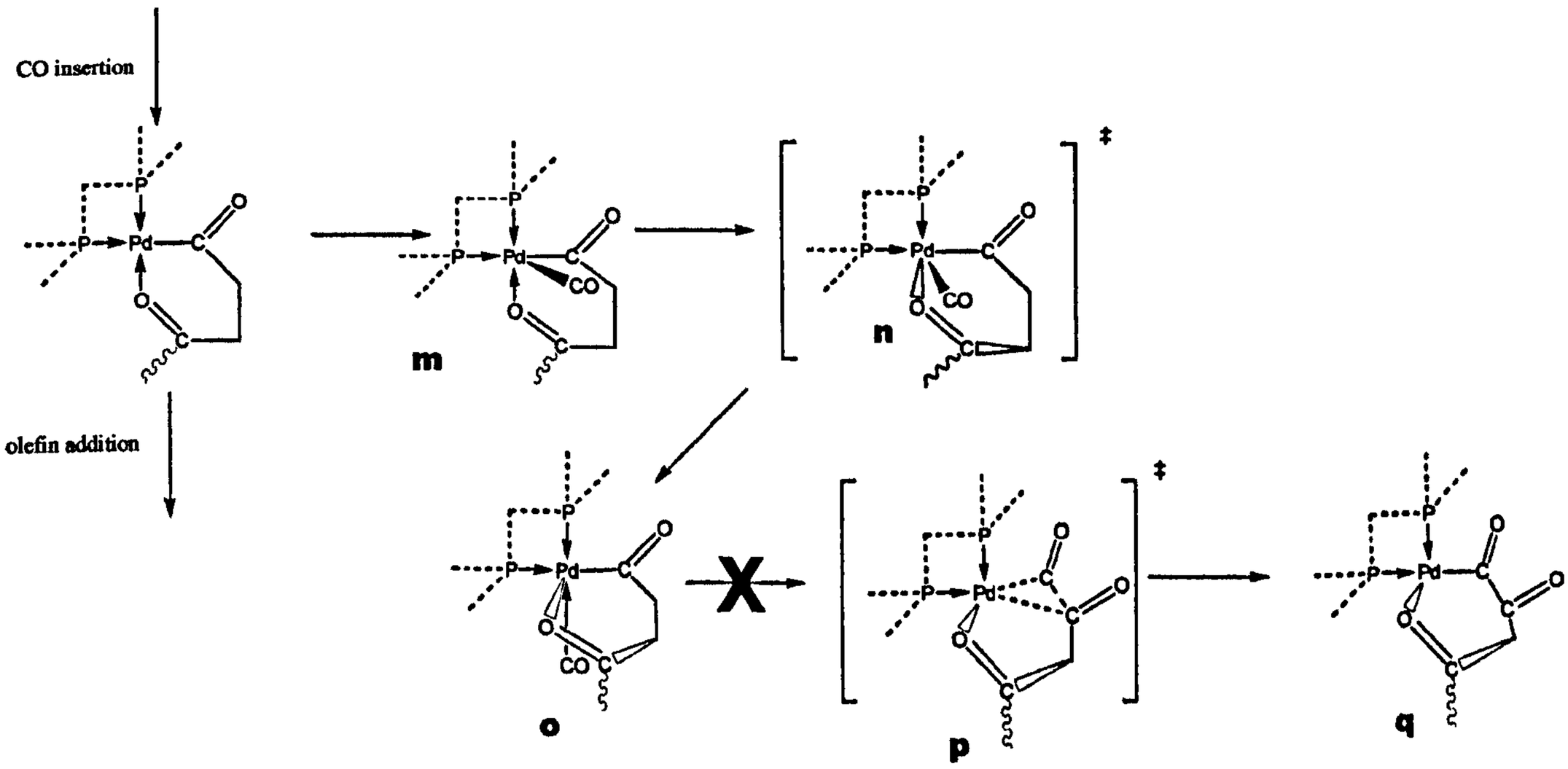


Figure 4.2.8.1: Diagram of energy changes associated with double insertion of olefins compared to energy changes associated with competing CO insertion (magenta dashed line). (Blue dashed line is estimated barrier of olefin insertion step.)

insertion step (16.4 kcal/mol) itself is only moderately higher than the CO insertion step (11.9 kcal/mol), when combined with the enthalpy of bringing the molecule into the equatorial site for insertion to be possible, the difference in activation energies gets as high as 12.8 kcal/mol, which is enough to ensure exclusive selectivity to alternating insertion. The only residual question is whether, if olefin addition step plays such an important role in preventing double insertion, changing the diphosphine ligand for a ligand that weakens the Pd-O bond and promotes the olefin insertion step



Scheme 4.2.8.2: Full mechanism of double insertion of carbon monoxide. Transition states are shown in square brackets, selected non-stationary points are shown in curved brackets, and other structures are minima. All structures carry a single positive charge.

Enthalpy of CO addition to axial site (12-m)	-3.1	-
Energy barrier of migration from axial to equatorial site (M-N)	0.5	0.5
Enthalpy of migration from axial to equatorial site (m-o)	-5.9	-5.2
Energy barrier of CO insertion step (o-p)	21.9*	21.7*
Enthalpy of CO insertion step (o-p)	9.7	11.0
Total activation energy of double CO insertion (12-p)	**16.0***	**15.8***
Total enthalpy of double CO insertion (12-q)	**0.7**	**2.0**
Total activation energy of olefin insertion (12-p)	**11.6**	**11.8**
Total enthalpy of olefin insertion (12-q)	**-27.1?**	**-22.0**

Table 4.2.8.2: Table of energy changes associated with double insertion of CO.
**: Estimate based on transition state neglecting axially-interacting carbonyl group.*

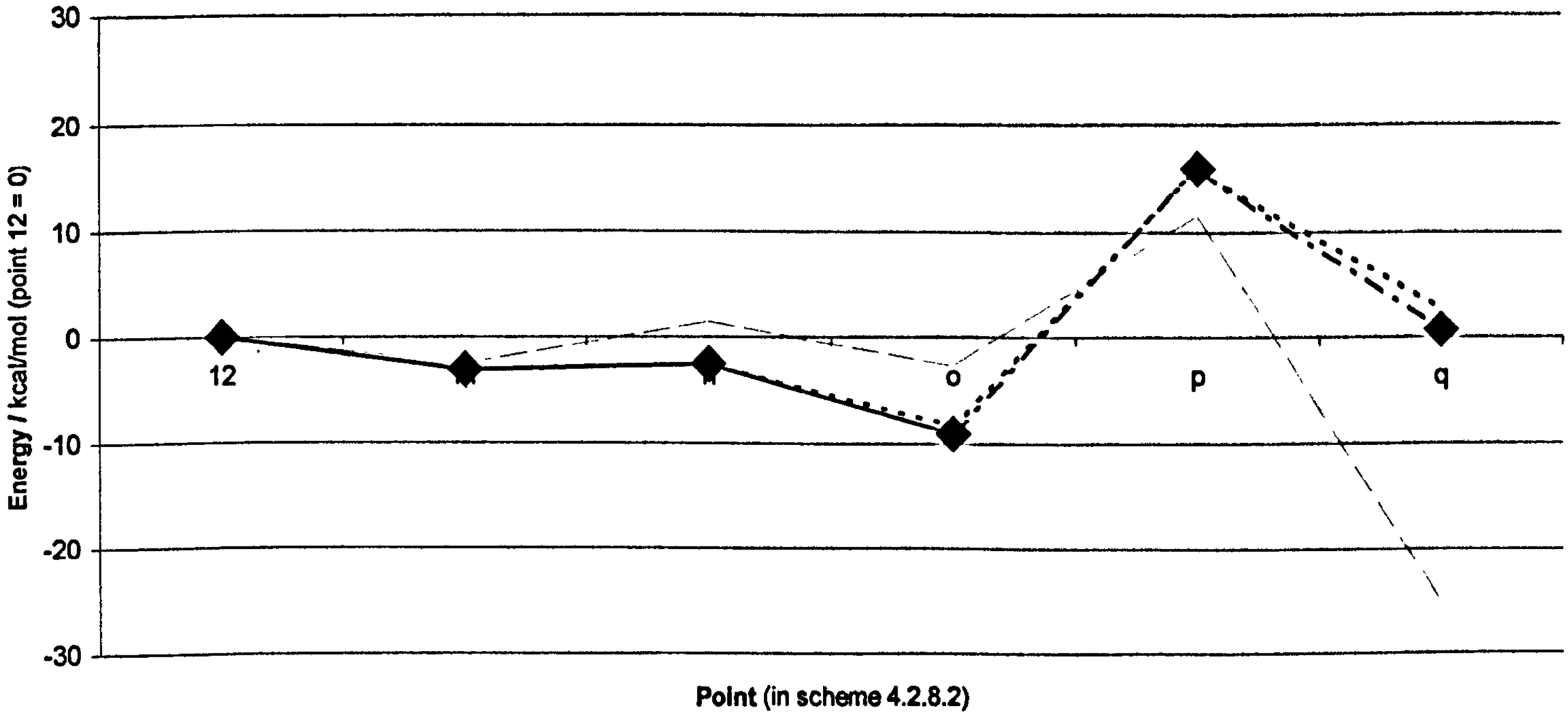


Figure 4.2.8.2: Diagram of energy changes associated with double insertion of CO compared to energy changes associated with competing olefin insertion (magenta dashed line). (Dotted line includes zero-point corrections, dashed line is estimate based on transition state neglecting axially-interacting carbonyl group.)

allows double insertion to occur.

Moving on to double CO insertion, it is again not yet possible to evaluate the final activation energy, as a transition state including the axial ketone carbonyl group would need to be optimised. However, the energy barrier can again be estimated from a transition state that neglects this group. The likely mechanism is given in **scheme 4.2.8.2**, and the known energies of the process are illustrated in **figure 4.2.8.2** and tabulated in **table 4.2.8.2.**

Although the overall energy change from the structure prior to addition of CO to the energy of the transition state (point 12 to point p) is only 4.4 kcal/mol higher than the equivalent change of the competing olefin insertion step, the activation energy of the double CO insertion step itself (point o to point p), at 21.9 kcal/mol, is high enough to make this step highly improbable. There is also an adverse thermodynamic driving force compared to the highly exothermic olefin insertion. Therefore, double CO insertion can be ruled out. (The same conclusion was reached by Ziegler and Margl from similar data regarding a very high activation energy of the double CO step itself, in spite of ease of the preceding CO addition step.[7]) However, to make absolutely certain that double CO insertion is impossible, it may be necessary to locate the transition state including the axial P-O interaction from the next carbonyl

group in the chain, or even undertake a detailed kinetic study of the double insertion process.

Turning attention to the addition steps, one can see that when adding a new ligand to the equatorial sites, CO addition much more thermodynamically favourable than the competing olefin insertion step. Therefore, although there is no reason to believe that olefins cannot displace the Pd-O ketone bond on their own, there is a significant chance that CO will displace the ligand first – or even be the dominant mechanism over olefin addition – and it remains to the seen whether this promotes or inhibits copolymerisation.

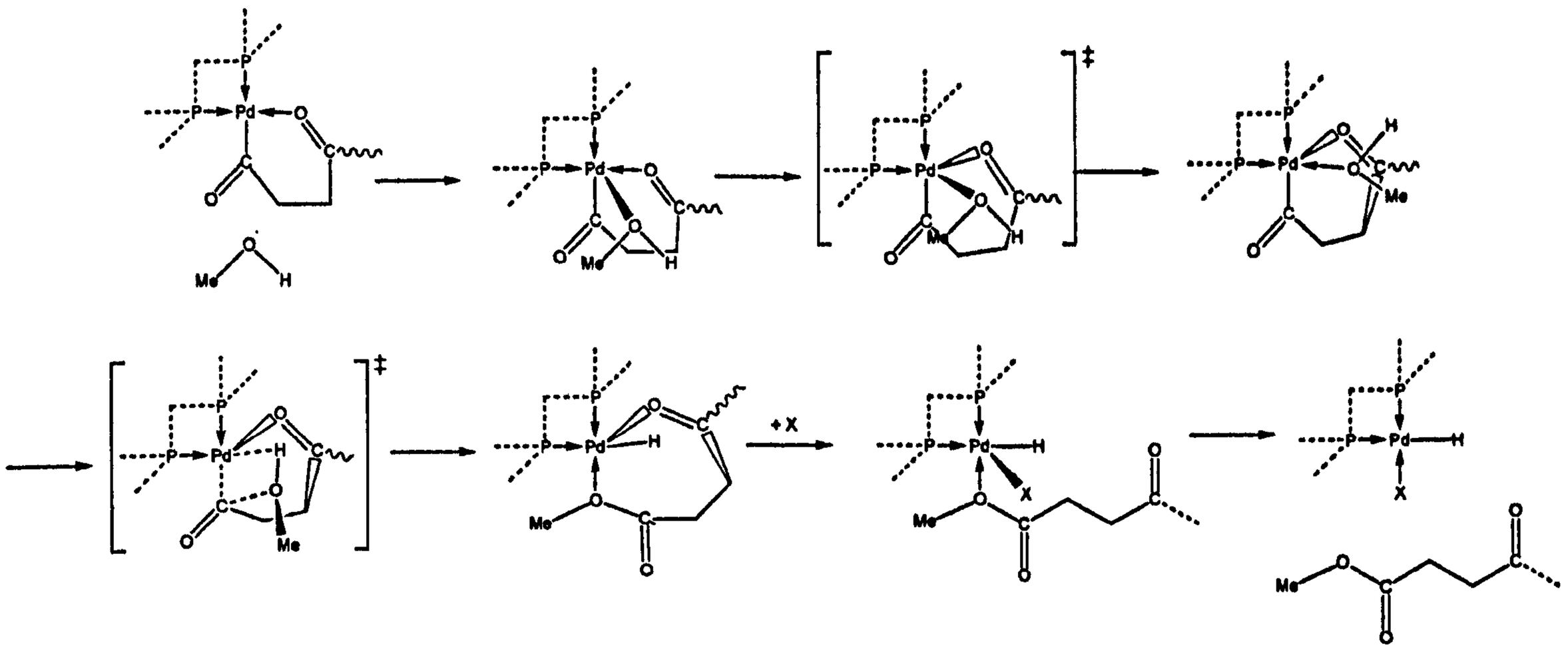
4.3 Termination processes

Although work has not yet commenced on the mechanism of the termination processes, the results obtained so far from the initiation, propagation and double insertion mechanisms can give some clues as to how the termination mechanism might proceed.

There are not yet any known works that have considered the termination process of olefin/CO copolymerisation, and it has been speculated that it would be difficult to find the mechanisms of such processes, and this may well turn out to be the case. The energy barriers are likely to be significantly higher than the energy barriers in the propagation cycle (otherwise dimers and oligomers would be formed instead of copolymers), which leaves more scope for the termination steps to proceed through transition states that are difficult to guess or locate. Combined with the lack of previously-optimised transition states to work from, this task could turn out to be more difficult than any steps considered so far.

Nevertheless, there is scope to speculate how the mechanism for the termination steps might proceed. If the mechanisms of the steps in the initiation and propagation cycles are taken as precedents, it is likely that methanol (assuming methanol is used as the terminating agent) would get close enough to the copolymer chain to cause a termination reaction by taking a position in an equatorial site, bonding to palladium though a co-ordinate bond from the oxygen atom. Given the way that all other incoming molecules have bonded to the complex, it is likely that methanol would approach the complex from an axial position, and then displace the existing Pd-O ketone bond to an axial position for the methanol to take up this equatorial position. Depending on how the energy barrier and enthalpy of these steps compares to addition of CO or olefins to an equatorial site, methanol addition may also serve as an inhibitor to both the CO insertion step and olefin insertion step, just as CO could serve as an inhibitor to the olefin insertion step.

Turning the attention to the termination step itself, the mechanism can only be guessed, but one strong precedent that has been set in this project is that four-coordinate structures around the palladium plane are maintained wherever possible, and any steps that necessitate losing the four-coordinate structure have a significant increase in their activation energy barrier. Therefore, it is likely that in the termination

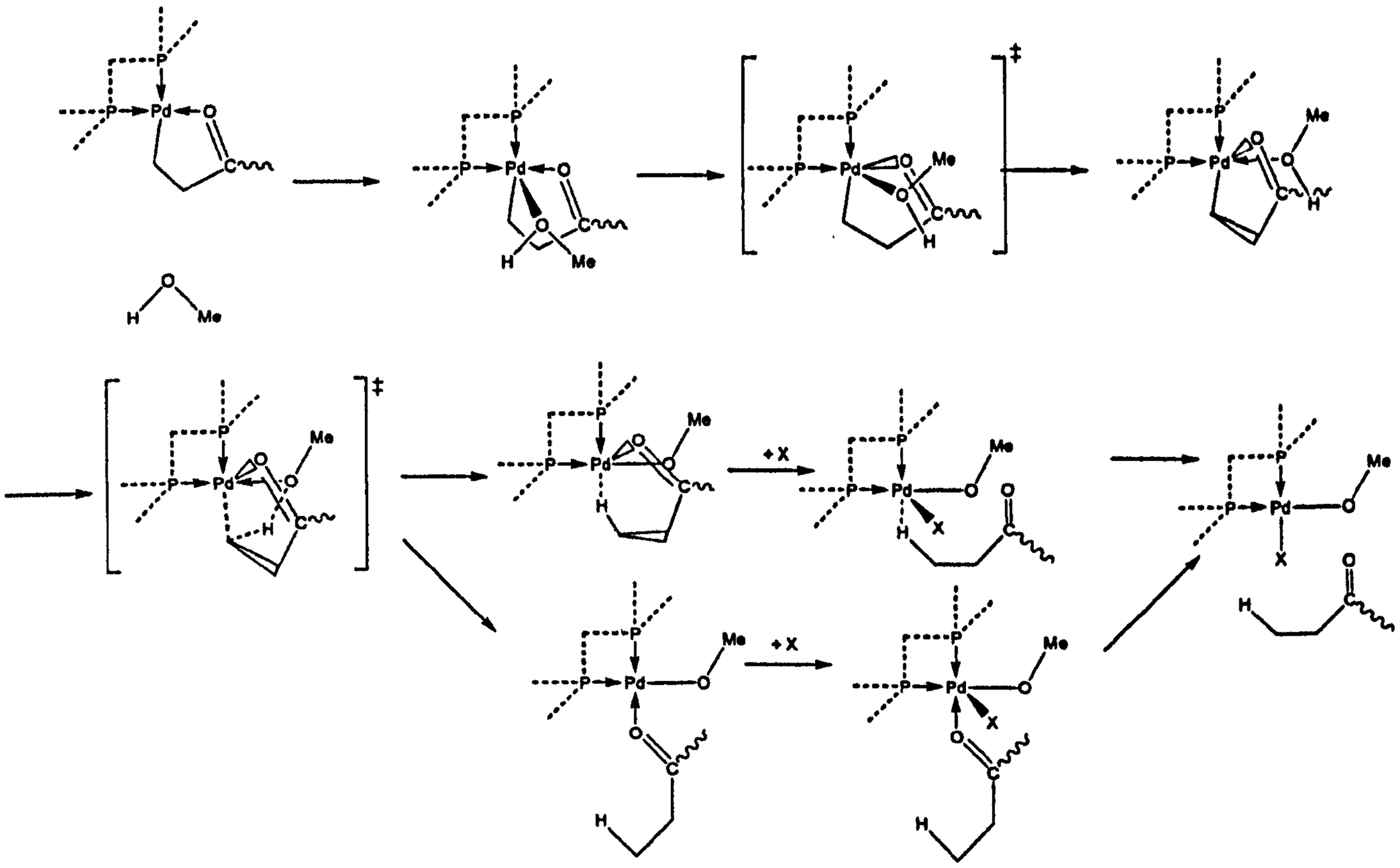


Scheme 4.3.1: Speculative mechanism of termination by methanolysis (X = any ligand molecule).

steps, the reaction mechanism would be one that does indeed keep a four-coordinate structure.

In termination by methanolysis this could be achieved by the oxygen atom displacing the coordinated carbon atom of the copolymer chain from its equatorial site (with the oxygen atom still bonding to palladium though a coordinate bond), with the hydrogen atom left over from methanol taking the place of oxygen in the site it just vacated. Exactly how the oxygen atom breaks the co-ordinate bond to form a free-standing copolymer product is less clear, as this alone would involve going back to a three co-ordinate structure with a potentially large energy barrier. It is more likely that another incoming molecule would need to displace oxygen from the equatorial site, and if this molecule was an olefin, this would take the complex straight back into the initiation stage for a new copolymer, skipping the first step of adding an olefin to a three-coordinate structure. A speculative mechanism of this process in shown in **scheme 4.3.1.**

It is harder to see how the alternative mechanism, termination by protonolysis, can maintain such a stable four-coordinate environment around the palladium atom. Whilst in termination by methanolysis the oxygen atom on the ester end-group could conceivably complete the 4 co-ordinate arrangement with a co-ordinate bond prior to substitution by another ligand, in termination by protonolysis there is no atom on the end of the keto-end group that form such a stable co-ordinate bond. There are two possible alternatives, being the formation of a less stable Pd···H-C agostic interaction, or the axial Pd-O bond moving back into the equatorial position, but neither of these alternatives seems viable to compete with the much more obvious

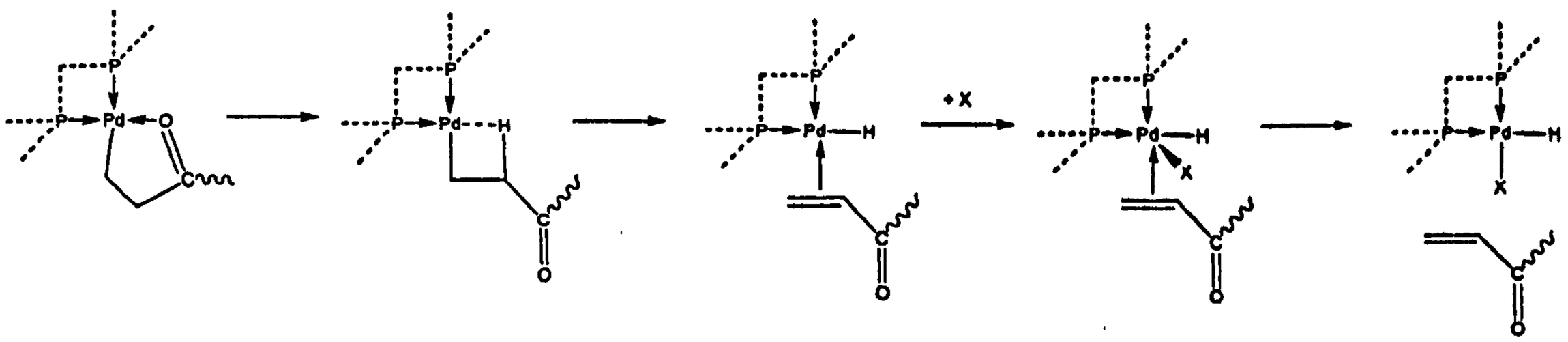


Scheme 4.3.2: Speculative mechanism of termination by protonolysis (X = any ligand molecule).

mechanism available for termination by methanolysis. Nevertheless, the mechanism of CO insertion into a palladium-methoxy bond showed that unexpected ways of stabilising the transition states and intermediates can be discovered in the process of determining the reaction mechanism. The speculative mechanisms are shown in **scheme 4.3.2,** but these mechanisms are questionable.

Since copolymers have about 50% ester end-groups and about 50% keto-end groups, and the initiation mechanism consideration came down heavily in favour of the mechanism that produces the keto-end group, it follows that mechanism favoured in the termination step should be the one that produces the ester-end groups, the methanolysis mechanism. The unanswered question is how much this mechanism is favoured, and given the possible influence the selectivity of termination has on the selectivity on the initiation of the next copolymer the complex forms, this will be an important factor to consider.

A final mechanism that should be considered is the β-hydride abstraction, which produces the keto-vinyl end-group. Although keto-vinyl end-groups are very rare in ethene/CO copolymerisation, these end-groups are observed in higher 1-olefins and so it would be useful to establish the mechanism for ethene/CO copolymerisation before using these structures to determine the mechanism (if different) and energies of termination by β-hydride abstraction in propene/CO copolymerisation.



Scheme 4.3.3: Speculative mechanism of termination by β-hydride abstraction (X = any ligand molecule).

As it happens, a likely first step to the β-hydride process was discovered by accident during early attempts to find the transition state in the CO addition step. By switching the Pd-O coordinate bond in the post-olefin insertion product for a β-agostic Pd···H-C interaction, a structure is optimised that is suitable for β-hydride abstraction (the second structure on the left in scheme 4.3.3). This work was carried out using a different method and basis set to those used for the final result in this thesis, but according to this basis set and method, the enthalpy was approximately +15 kcal/mol, and the activation energy was approximately 18 kcal/mol. Even allowing for the fact that these results cannot be directly compared with other results because of the different basis set and method, this step is definitely uncompetitive with the propagation cycle. (This competing CO addition step has an enthalpy of –7.1 kcal/mol and an energy barrier of only 2.1 kcal/mol.) However, the energy barriers of the rest of this termination process would be needed to ascertain that this process was not competitive with the other methods of termination.

How β-hydride abstraction proceeds beyond this step is pure speculation, but one would expect, if possible, a mechanism that preserves the four-coordinate geometry around palladium. The most likely way of doing this would be, instead of the keto-vinyl group directly dissociating itself from palladium in one step, to remain bonded to palladium through a π-coordinate bond between palladium and the double bond, before being replaced by another ligand to form the free-standing copolymer. A speculative mechanism is shown in **scheme 4.3.3.**

Overall, the mechanism of the termination steps looks set to be a challenging conclusion to completing the mechanism of CO/olefin copolymerisation, but it would be well worth doing to test whether the theories that favour termination by methanolysis to form the ester end-group are correct.

4.4 Larger systems

4.4.1 Regioselectivity in propene insertion

Although most of the research in this project has concentrated on CO/ethene copolymerisation, there was one other factor that was considered that only comes into effect when higher olefins are used: the regioregularity of the copolymer formed. The background to insertion of higher olefins has already been covered in section 1.6 of this thesis. It was attempted (indeed this was one of the earliest pieces of work attempted in this project and provided the inspiration to determine the mechanism of the entire copolymerisation process) to quantitatively predict the regioregularity of the copolymer formed, and at the level of considering the copolymerisation process on a step-by-step basis, this was done by considering the regioselectivity of a single propene insertion step.

The biggest problem in predicting regioselectivity was that it was not practical to calculate it using entirely ab-initio methods. Regioselectivity was influenced partly or mainly by the bulky phenyl groups attached to the phosphorus atoms and their steric hindrance with the olefin. Throughout this project, the phenyl groups had been simplified to hydrogen atoms, and the prospect of optimising many different structures with an extra 40 atoms and 160 electrons in the system looked bleak. Even if the phenyl groups were omitted, certain common olefins, such as styrene, would also have been difficult to optimise because of introducing a phenyl ring into the system (this styrene ring could not be simplified to hydrogen because of possible interactions between its π-bonds and the rest of the system).

It was for this reason that propene was chosen as the olefin to examine. Only ethene, propene and styrene have been examined in particular detail because other 1-olefins generally give poor yields. Ethene obviously gives no information about regioselectivity, and styrene insertion was impractical to model. This left propene, and it was decided to attempt to account for the steric repulsion between propene and the phenyl groups of the diphosphine by using a lower level of calculation.

The first stage was to derive the many structures of a propene insertion transition state, with various different diphosphine backbones, from a single structure of an ethene insertion transition state with a six-membered ring. (It would have been

desirable to optimise at *ab-initio* level a separate transition state for each diphosphine backbone, but there were difficulties experienced in attempting to do this and not enough time to overcome them.) This was done in three steps: firstly, by changing the hydrogen atoms on the phosphorus atoms back to phenyl groups; secondly, by adding or removing the appropriate atoms from the diphosphine backbone; and finally, by replacing the appropriate hydrogen atom on the ethene with a methyl group to get propene. The latter two steps meant that one single transition state structure would give sixteen derived structures to work with, as illustrated by **figure 4.4.1.1.** The four diphosphine backbones investigated in this project are shown in **figure 4.4.1.2.**

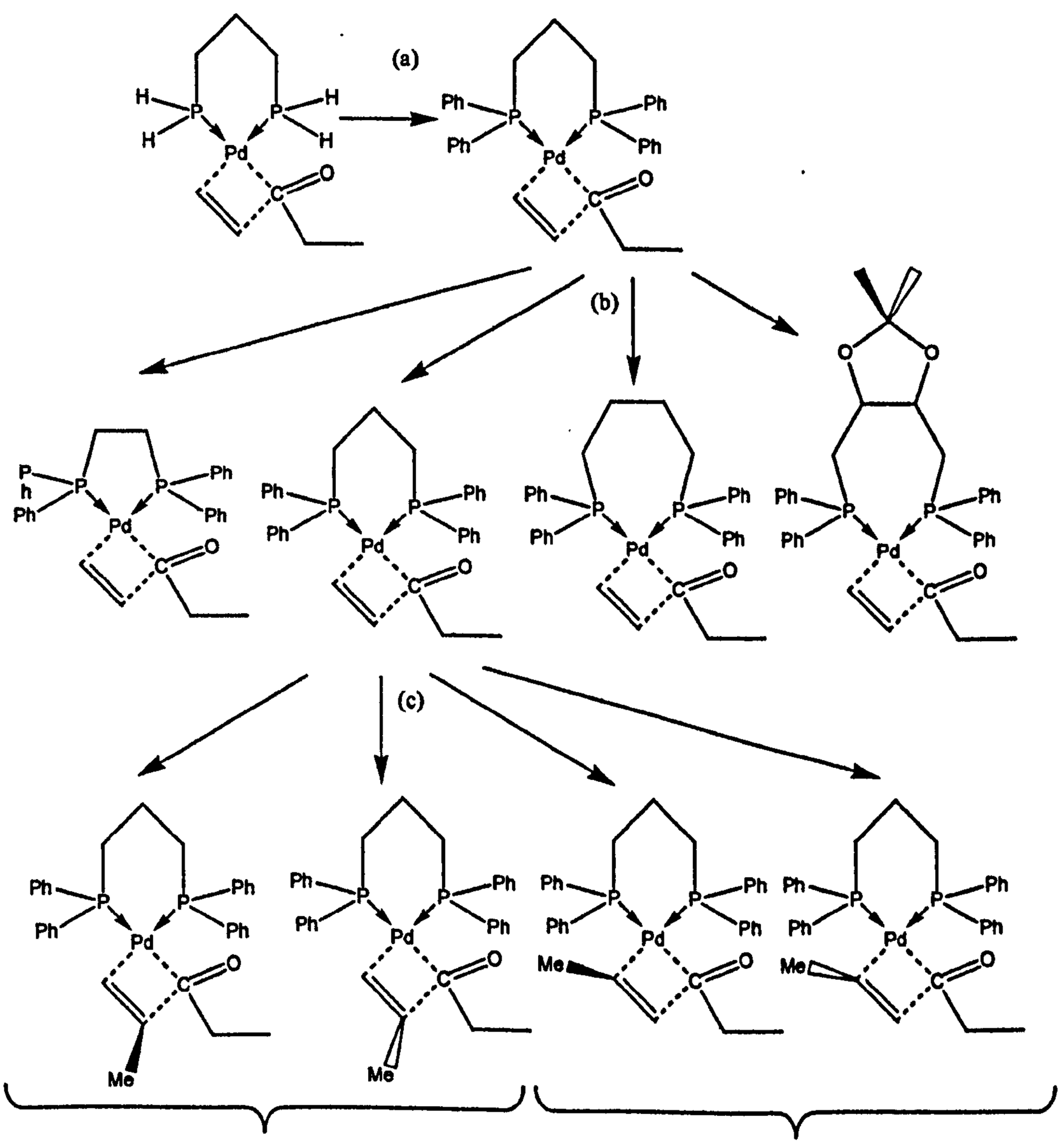
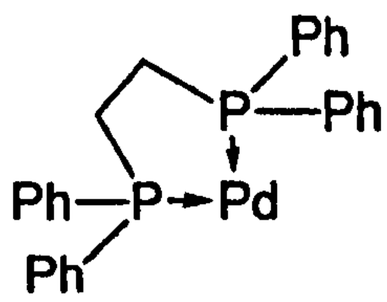
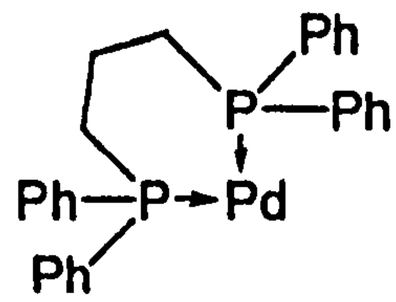


Figure 4.4.1.1: Method of obtaining pre-optimisation structures of propene insertion transition states from ab-initio optimised transition state of olefin insertion, through **(a)** conversion of hydrogen atoms back to phenyl groups; **(b)** adding or removing atoms from diphosphine group to obtain appropriate ligand; **(c)** conversion of ethene ligand to propene ligand in the appropriate orientation (for 1,2- or 2,1-insertion).

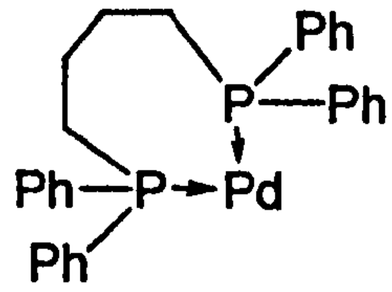
1.



2.



3.



4.

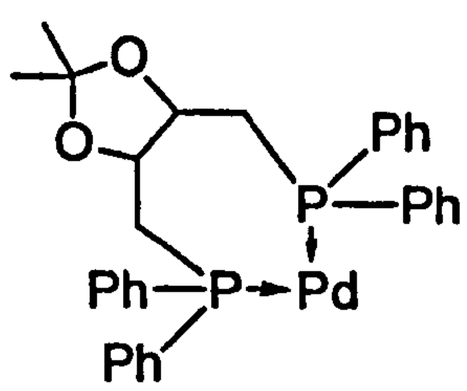


Figure 4.4.1.2: Diphosphine backbones investigated in regioselectivity calculations.

There were, however, small but important details as to how one changed the structure of the optimised complex. In particular, from considering fragments of similar structures from the Cambridge Structural Database[31,82,89], it was noted that the P-Pd-P bond angle varied depending on the diphosphine backbone used. Without the structures of olefin insertion transition states being available for every diphosphine backbone, the system (admittedly a crude system) used to take this into account was to set the P-Pd-P bond angle to the same angle as the closest matching fragment found in the Cambridge Structural Database. It was *assumed* that for every degree that the P-Pd-P bond angle increased, the two P-Pd-C bond angles (between phosphorus and the acyl group, and phosphorus and nearest carbon in the olefin undergoing insertion) would decrease by half a degree each, leaving the structure of the olefin and acyl

Complex (from **figure 4.4.1.2**)	**1**	**2**	**3**	**4**	**Ab-initio structure**
P-Pd-P bond angle (determined by CSD)	85.6°	91.6°	92.9°	96.9°	93.3°
Adjustment from ab-initio structure	-7.7°	-1.7°	-0.4°	+5.6°	-
Consquential adjustment to C-Pd-P bond angles	+3.8°	+0.8°	+0.2°	-1.8°	-
P-Pd-C (acyl) bond angle	92.9°	89.9°	89.3°	87.3°	89.1°
P-Pd-C (nearside olefin) bond angle	98.4°	95.4°	94.8°	92.8°	94.6°
C-Pd-C bond angle	83.9°	83.9°	83.9°	83.9°	83.9°

Table 4.4.1.1: Diphosphine backbones investigated in regioselectivity calculations.

group relative to each other unchanged. This effect is tabulated in **table 4.4.1.1**.

The next stage of the process was optimisation of the full complex to give the minimum energy conformation for this transition state. It was assumed that the position of all of the chemically active atoms would remain unchanged when phenyl groups were added and ethene was changed to propene, so the position of the following atoms were locked: the palladium centre, the phosphorus atoms, the carbon atoms in the carbonyl group (but not the oxygen – this was found to give more reliable results), both carbon atoms over the double bond and all four atoms leading off the double bond (but not the hydrogen atoms on the methyl group in propene – they need to be free to rotate).

The original method used to effectively optimise the transition state was to do a rigid potential energy scan of the phenyl groups and methyl group rotated through intervals of 15° and pick the points with the lowest energy. However, this method was found to be unsatisfactory as the carbon backbone was found to be very flexible and was itself able to have a significant influence on the geometry of the optimum structure. So the next method tried was to optimise the geometry of the entire structure, save those atoms specified above whose geometries were locked. This method worked better, but occasionally some sporadic results were obtained. The problem identified was that once the phenyl groups were included in the structure, the

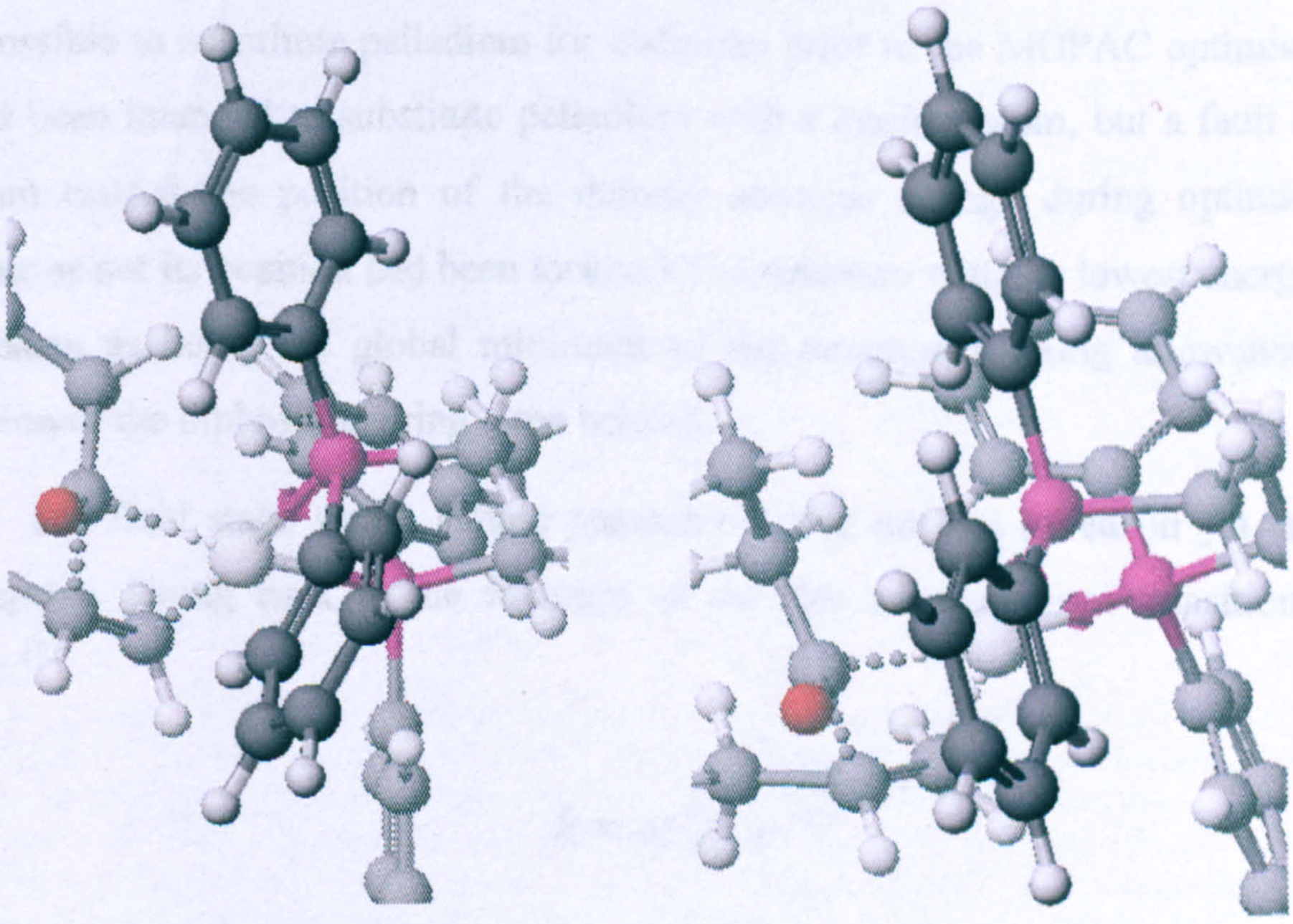


Figure 4.4.1.3: Example of different local minima found from sequence of conformations search (after points optimised to nearest minimum with MOPAC PM5 parameters).

flexible nature of the diphosphine ligand meant that there was nearly always more than one local minimum the to which structure could be optimised, making it difficult to compare energies.

The method that was finally used to locate the global minimum at the transition state was to use CAChe[75] for a sequence of conformations search with multiple passes at MM3 level, by rotating the phenyl groups and methyl group to search for the global minimum. The lowest energy points were then examined to find the different structures that existed (usually two distinguishable local minima could be identified), and these structures were then optimised to the corresponding minimum. An example of how two different local minima of the same structure could exist is illustrated in **figure 4.4.1.3.** (There were never more than two local minima that needed to be optimised – when searching through the sequence of conformations, it was always several kcal/mol above the lowest energy structure before a structure could be found that was likely to optimise to a third local minimum, and that was very unlikely to be the global minimum when optimised with MOPAC.)

For the optimisation to the local minimum, the MOPAC method with PM5 parameters was used. Molecular mechanics methods did work but were found to give more temperamental results. A disadvantage of MOPAC was that there were no parameters for palladium, but as all of the atoms bonding to palladium were locked, with their positions having already been determined by the *ab-initio* optimisation, it was possible to substitute palladium for cadmium prior to the MOPAC optimisation. (It had been intended to substitute palladium with a dummy atom, but a fault in the program caused the position of the dummy atom to change during optimisation whether or not its position had been locked.) The structure with the lowest energy was then taken as being the global minimum of the structure (barring allowances for inversion of the diphosphine ring – see below).

The final stage was a simple process to carry out but relied on yet another assumption. Going back to the equation of the rate constant from transition state theory:[47]

$$k = \kappa \frac{k_B T}{h} e^{\frac{-\Delta G_a}{RT}}$$

There were still two unknown variables in this equation: the quantum effects constant κ and the entropy component of the Gibbs free energy. If, however, it was assumed that these two variables are *unchanged* between the transition states of 1,2 and 2,1-insertion, the ratio of the rate constants could be reduced to an equation where all the terms are known

$$\frac{k_{1,2}}{k_{2,1}} = \frac{\kappa \frac{k_B T}{h} e^{\frac{-\Delta G_a(1,2)}{RT}}}{\kappa \frac{k_B T}{h} e^{\frac{-\Delta G_a(2,1)}{RT}}} = e^{\frac{-H_0(1,2)+H_0(2,1)-T(S_0(1,2)+S_0(2,1))}{k_B T}} = e^{\frac{-E_0(1,2)+E_0(2,1)}{k_B T}}$$

From this, the preference towards 1,2-insertion could be calculated as:

$$\%(1,2-\text{insertion}) = \frac{k_{1,2}}{k_{1,2}+k_{2,1}} \times 100\% = \frac{\frac{k_{1,2}}{k_{2,1}}}{\frac{k_{1,2}}{k_{2,1}}+1} \times 100\%$$

There was a complication in that there were two structures each of 1,2- and 2,1-insertion to consider for each diphosphine backbone. It was decided to use the *lower* of the two energies in each case. The reason for this was that the optimised minimum of one 1,2-insertion transition state was ultimately equivalent to the structure of the other 1,2-insertion transition state (with the methyl group and hydrogen atom switched around) if the diphosphine ring's structure was inverted, with the same applying for the 2,1-insertion structures. It was therefore assumed that no matter which site the methyl group occupied in 1,2-insertion (or 2,1-insertion), the diphosphine ring would be inverted if this was necessary to reach a lower energy

Complex (from figure 4.1.1.2)	Experimental Regio-selectivity	Lowest MOPAC/ PM5 energy of transition state of: 1,2 insertion	2,1-insertion	With no adjustment: Energy difference	Calculated regioselecitivty	With adjustment of -1.0 kcal/mol to energy differences Energy difference	Calculated regioselecitivty
1	70%	169.3	170.6	1.3	88.52%	0.3	61.88%
2	70%	160.2	161.9	1.7	93.48%	0.7	75.11%
3	88%	156.7	160.8	4.1	99.83%	3.1	99.19%
4	88%	80.8	80.5	-0.3	38.69%	-1.3	11.73%

Table 4.4.1.2: Regioselectivity to 1,2 insertion calculated from experimental evidence (ref 30) and computationally, with and without a constant adjustment to the energy differences. (The experimental values were reported in ref. 30 as regioselectivity towards Head-Tail environments, and were converted to regioselectivity to 1,2-insertion using the formula: $P(H\text{-}T) = P(1,2\text{ unit}) \times P(1,2\text{ unit}) + P(2,1\text{ unit}) \times P(2,1\text{ unit}) \Rightarrow P(1,2\text{ unit}) = \frac{1}{2}(1 \pm \sqrt{(2 \times (\%H\text{-}T\text{ units})-1)})$. It should be noted that these results alone could just as easily imply the equivalent regioselectivity towards *2,1* units, although practical considerations make this possibility unlikely.)

transition state.

The calculated regioselectivites, compared to the experimental results[30], are shown in **table 4.4.1.2.** These were all found to over-estimate the regioselectivity, but the results for three of the four complexes did at least correctly predict which of the complexes would be more regioselective than the others. Given the number of errors that could have been introduced into this process in the various stages outlines above, all making their own assumptions, there was plenty of scope to distort the results. There was an attempt made to reduce all energy differences by 1.0 kcal/mol, using a crude assumption that the sources of error affected all results equally, and the revised regioselectivity calculations obtained as a result are shown in the final two columns of **table 4.4.1.2.** This did not do much to make the results any more reliable, as this only highlighted that when introducing a constant in order to get the regioselectivity for complexes **1** and **2** into the 70% region to be consistent with results, the regioselectivity for complex **3** was still too high, and the regioselectivity for complex **4** was much too low.

However, one small success found from this method was that if the phenyl groups in the seven-membered ring were replaced by $-CH_2C_6H_4X$ (X = F or Cl), then the regioselectivity calculated was found to be near-100% regioselective to 1,2-insertion, whilst experimental results also agreed that regioselectivity was at least 97%.[30] From examination of the 3D structure, it was found that when phenyl-rings when replaced with benzyl-shaped rings, they were obviously more sterically restrictive on any diphosphine backbone.

It would have been desirable to repeat these tests on more complexes, but there were no more experimental results found that had diphosphine rings from the Cambridge Structural Database needed to calculate the bond angle. Therefore, based on the results that could be obtained, it was concluded that this method of predicting regioselectivity could only be helpful as a qualitative method. It could be used to distinguish diphosphine backbones that give rise 100% regioselectivity either way from those that only give rise to partial or no regioselectivity. However, the method is too unreliable to be used as a quantitative technique to determine the degree of regioselectivity from any particular diphosphine backbone, and it is, at best, temperamental if being used to determine if one diphosphine backbone would give rise to a more regioselective copolymer than another.

Although this conclusion was a disappointing one, it was not too surprising considering all of the steps where errors could have been introduced. Attention was therefore turned to approaches that have less scope for errors, which was the inspiration for attempting to optimise an entire complex at ab-initio level.

4.4.2 Ab-initio optimisation of full complex

In view of the numerous sources of error introduced by using molecular mechanics for regioselectivity calculations, it was decided to attempt to eliminate all of these sources of error by optimising the entire complex, including phenyl groups, at an ab-initio level, for the olefin insertion step. This also stood to serve as an indication for how reliable the geometry optimisation and energy calculations were without the phenyl groups included.

The most obvious problem in performing calculations of this size was the vast amount of run-time that would be needed for optimisation of the complex. Even without the phenyl groups, optimisations on hal took a significant length of time to run (and pushed calculations on marvin – even calculations using Hartree-Fock and the 3-21G basis set on all of the chemically inactive atoms – to the limit). Therefore, run-time was successfully applied for on columbus, the EPSRC High Performance Computing Service at Rutherford.

However, a greater problem turned out to be not the availability of run-time, but choosing a basis set and method that worked for the entire system at all. When structures were pre-optimised using and CAChe (by freezing the position of the chemically active atoms on an simplified *ab-initio* complex and optimising the rest of the structure using PM3 parameters around these atoms) as a starting structure for a calculation using the SDD basis set, the energy calculation often failed to converge on the first step, let alone make any progress in optimisation. Even when structures were optimised using a simple basis set like STO-3G, using the optimised structure as a starting structure for the next basis set up, 3-21G, also gave the same result.

A final concern was the risk of optimising to a local minimum instead of the global minimum. Whilst such a structure would not invalidate the reaction mechanism, optimising to a local minimum was liable to affect energy calculations if the minima optimised in different structures were inconsistent.

One alternative approach that was considered was to use a quantum mechanics / molecular mechanics method such as ONIOM, which would have allowed an ab-initio method such as SDD/B3LYP to be used on the chemically active atoms and molecular mechanics to be used on the phenyl rings (but, unlike the method used in the previous section, optimisation of the two regions would proceed simultaneously with the forces the two sections exert on to each other being taken into account in the calculations). However, this created a possible source of error concerning the parameters connecting the QM and MM regions.

After consultation with the EPSRC High Performance Computing Service at Rutherford, it was decided to persist with the system of optimising the entire complex with the same *ab-initio* method, using methods advised for large systems: no method lower than B3-LYP, and no basis set lower than 3-21G**. The other revision made to the method was to perform a multiple pass sequential scan in molecular mechanics on the structures before starting on any ab-initio optimisations to make sure that the lowest energy conformation was being optimised. (There was the risk that the lowest energy minimum using molecular mechanics would not be the same lowest energy minimum one would obtain using quantum mechanics, but there was little that could be done short of optimising every single local minimum that could be the global

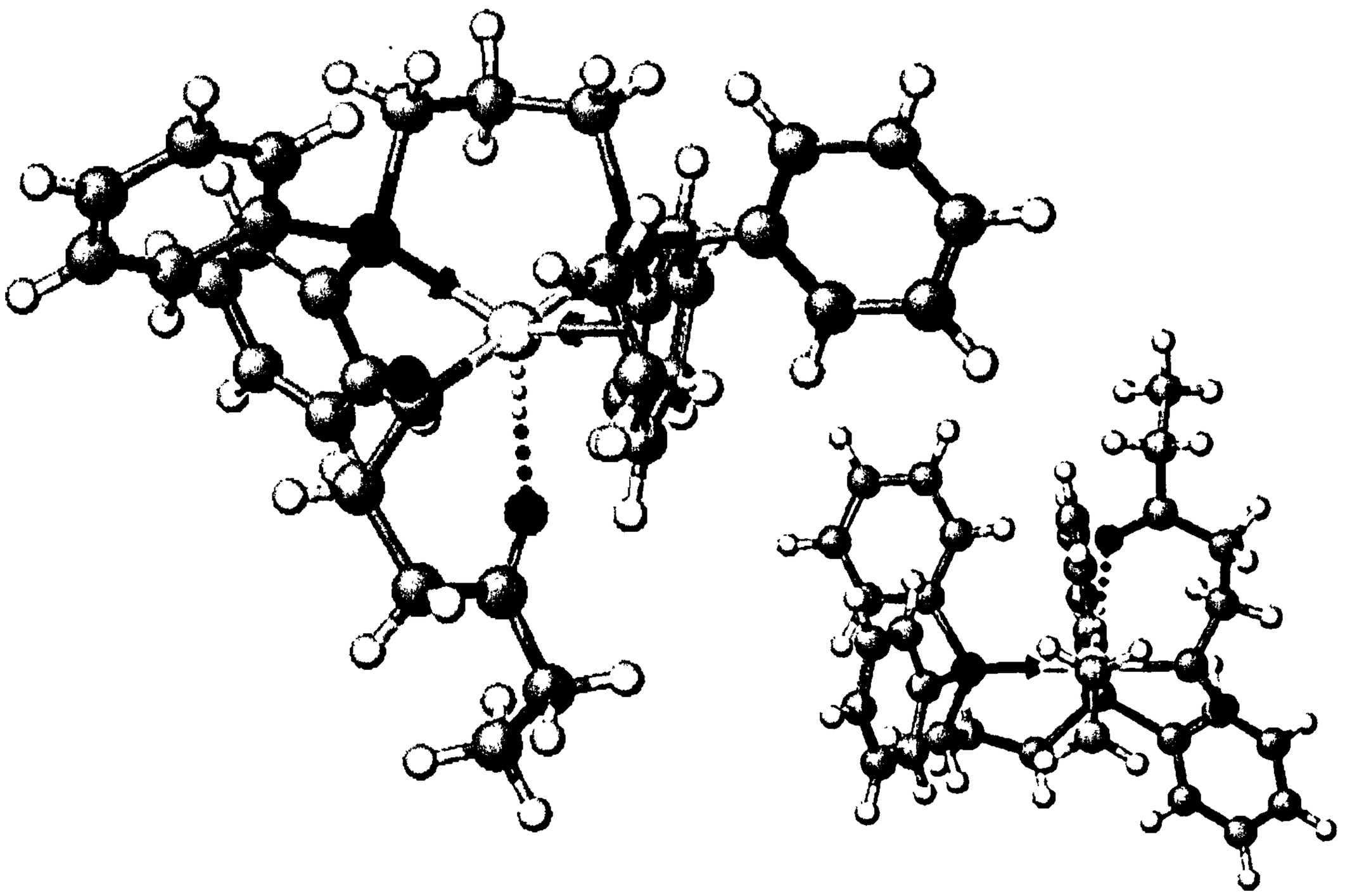


Figure 4.4.2.1: Optimised entire structure of reactant for olefin insertion.

One alternative approach that was considered was to use a quantum mechanics / molecular mechanics method such as ONIOM, which would have allowed an ab-initio method such as SDD/B3LYP to be used on the chemically active atoms and molecular mechanics to be used on the phenyl rings (but, unlike the method used in the previous section, optimisation of the two regions would proceed simultaneously with the forces the two sections exert on to each other being taken into account in the calculations). However, this created a possible source of error concerning the parameters connecting the QM and MM regions.

After consultation with the EPSRC High Performance Computing Service at Rutherford, it was decided to persist with the system of optimising the entire complex with the same *ab-initio* method, using methods advised for large systems: no method lower than B3-LYP, and no basis set lower than 3-21G**. The other revision made to the method was to perform a multiple pass sequential scan in molecular mechanics on the structures before starting on any ab-initio optimisations to make sure that the lowest energy conformation was being optimised. (There was the risk that the lowest energy minimum using molecular mechanics would not be the same lowest energy minimum one would obtain using quantum mechanics, but there was little that could be done short of optimising every single local minimum that could be the global

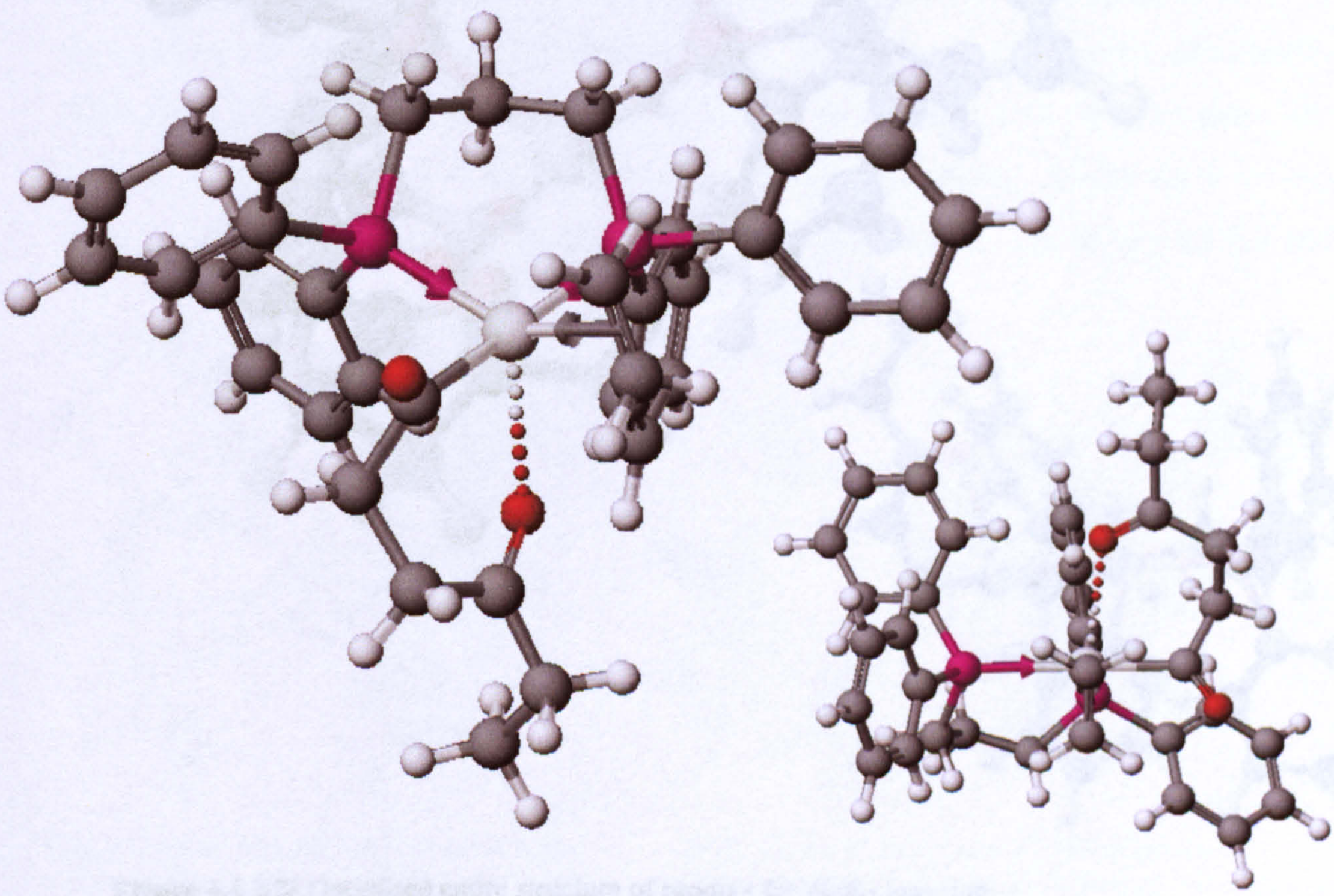


Figure 4.4.2.1: Optimised entire structure of reactant for olefin insertion.

minimum, for which there was not enough run-time.) Finally, it was advised that the GDIIS method should be used instead of the DIIS method for searching the minimum once the energy and forces of a structure had been calculated, as the GDIIS method was better at locating minima on near-flat surfaces (i.e. surfaces with very low force around the minimum) than the DIIS method. However, this was found to work only for minima and not transition state optimisations.

The final approach used for the reactant and product was to firstly lock the position of all of the chemically active atoms bonded to palladium (the acyl group, the olefin, the carbonyl group bonding from the axial position, both phosphorus atoms and the palladium atom itself), and then to find the global minimum using the multiple pass sequence of conformations search in CAChe using MM3 parameters. The lowest energy structure found was then optimised in Gaussian using the B3LYP method and the 3-21G** basis set throughout the complex. (An arbitrary polarisation function was added to palladium for this purpose. These calculations were done on hal as the

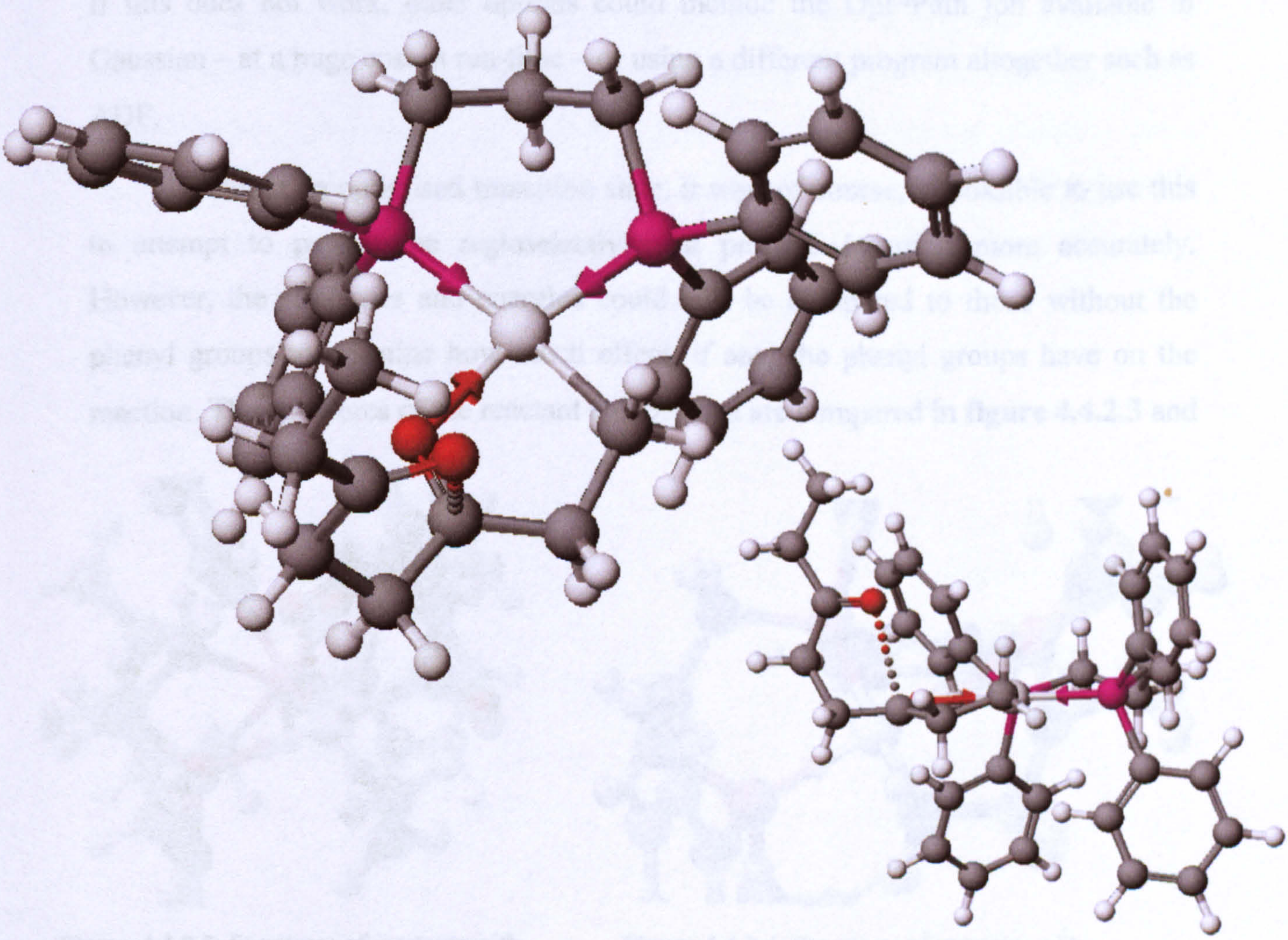


Figure 4.4.2.2: Optimised entire structure of product for olefin insertion.

calculations were small enough for hal to manage.) The resultant optimised structure was then re-optimised using the SDD basis set and the B3LYP method. Minima of the reactant and product were successfully optimised as a result, and these are shown in **figure 4.4.2.1** and **figure 4.4.2.2** respectively.

However, this approach did not work for optimisation of the transition state. Although it was possible to start optimisation and allow it to proceed beyond the first step, the structure moved away from the area where the transition state could conceivably exist. It was suspected that there were too many variables (the position of the olefin relative to the Pd-acyl bond, the position of the axially-bonding carbonyl group and the interactions from all of the phenyl groups) for Gaussian to be able to locate the transition state using the QST3 method. One method that could be attempted in the future would be to first optimise the transition state (and before that, reactant and product) without the second carbonyl group to form the axial bond, in order to remove one of the variables. This structure would then be used as the basis for the starting structure when the second ketone carbonyl group is added back again. If this does not work, other options could include the Opt=Path job available in Gaussian – at a huge cost in run-time – or using a different program altogether such as ADF.

Without an optimised transition state, it was, of course, impossible to use this to attempt to predict the regioselectivity of propene insertion more accurately. However, the structures and energies could still be compared to those without the phenyl groups to examine how much effect, if any, the phenyl groups have on the reaction. The structures of the reactant and product are compared in **figure 4.4.2.3** and

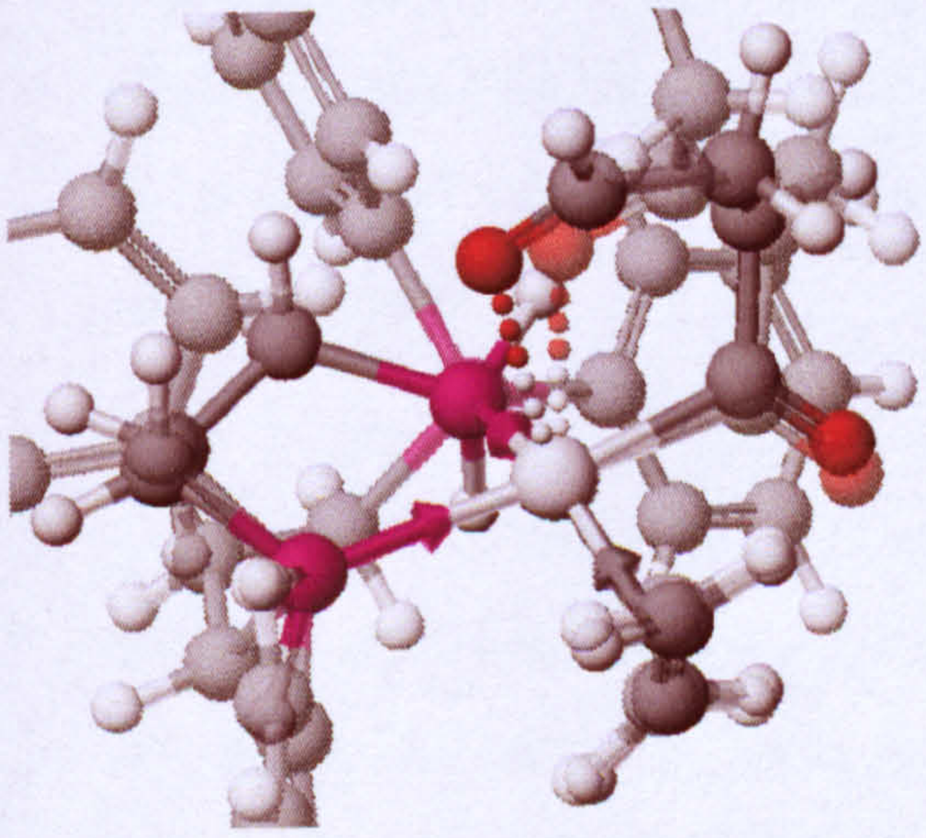


Figure 4.4.2.3: Structures of reactants with (transparent) and without (solid) phenyl groups included compared to each other.

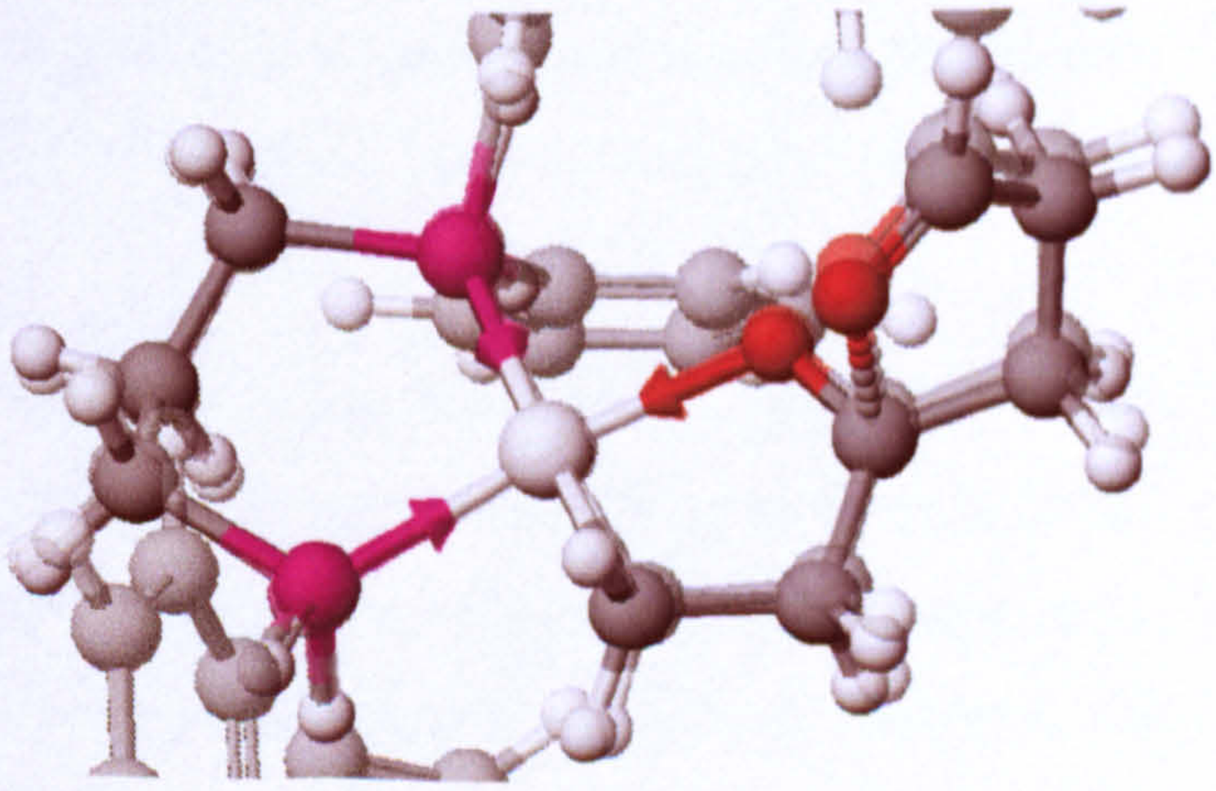


Figure 4.4.2.4: Structures of reactants with (transparent) and without (solid) phenyl groups included compared to each other.

figure 4.4.2.4 respectively. It could be seen that the differences in geometries around the equatorial sites were slight, and the only notable difference was the axial interaction in the reactant. It is unclear whether this difference was due to the phenyl groups, or the diphosphine backbone adopting a different geometry to allow the phenyl groups to assume their lowest energy conformation. As the position of the ketone carbonyl group in the axial site is already known to be very sensitive to changes in the bonding environment (see section 3.3.7), this is not much of a surprise.

The enthalpy of olefin insertion when the phenyl groups were included was calculated to be –23.1 kcal/mol. This compares to –23.8 kcal/mol when using the same basis set (i.e. SDD basis set with *no* augmented polarisation functions) and method without the phenyl groups. Again, this difference is very small and could be down to the inversion in the diphosphine backbone as much as anything else.

Overall, it can be concluded that in terms of predicting the regioselectivity of propene insertion, it may be possible to do this by optimising the entire structure, but the process will be a very difficult one, and the price in run-time to obtain these results would be a high one. However, it can also be concluded that the approximation made throughout this project of substituting phenyl groups with hydrogen atoms appears to be a safe assumption, at least for minima. It is possible that transition states (needed to calculate activation energy) might not give as close a match, but other than that, there are good reasons to be confident in the results obtained when the phenyl groups were omitted.

4.5 Overall summary

Although it has not been possible to complete the studies of all of the aspects of olefin/CO copolymerisation outside of the propagation cycle, the information provides a fair amount of evidence supporting the existing theories on initiation and termination processes and the absence of double insertion. The research also supports some theories on why some processes do and don't occur and conflicts with some theories.

Although CO insertion into a Pd-OMe bond was found to be a viable method of initiation, it is believed that, at room temperature, this method is uncompetitive with the much more thermodynamically favourable process of olefin insertion into a Pd-H bond. However, for the preferred method of initiation, olefin insertion into a Pd-H bond, the enthalpies are all very favourably exothermic and the energy barriers are usually lower than those in the propagation cycle, making this copolymerisation process very easy to start.

Although the work on double insertion is currently incomplete, the work done so far agrees with experiment that double insertion of either CO or olefins can both be ruled out. Double CO insertion, as widely suggested, was shown to be thermodynamically unfeasible by both the high positive enthalpy of the CO insertion step and the high activation energy of this step, in spite of the ease of adding a CO molecule into the necessary equatorial site. However, the latter finding raises questions about whether CO acts as an inhibitor or promoter at this stage of the propagation cycle. Double olefin insertion appears to be permissible except for the fact that the CO insertion step is faster, but the contributing effect of the difficulty of displacing the Pd-O ketone bond with an olefin at this stage was noted. It should now be considered whether weakening the Pd-O ketone bond will make double olefin insertion easier.

There was not time to consider termination mechanisms, but the reaction mechanism can be speculated on from the mechanism of the cycle optimised so far. Two possible mechanisms are proposed: termination by methanolysis to form an ester end-group and termination by protonolysis to form an keto end-group. However, the latter process proceeds through a questionable mechanism in order to maintain a four-coordinate structure, and a precedent has been set that steps outside of the four co-

ordinate structure are generally thermodynamically unfavourable. Therefore, it is expected that termination by methanolysis after CO insertion will be favoured. However, the energy barriers of termination are likely to be high and identifying a reaction mechanism could be a significant challenge.

Finally, whilst there has been some success extending the reaction mechanisms beyond the propagation cycle, there has only been limited success extending the study to take into account the effects of the phenyl groups. It has been found to be particularly difficult to optimise structures with phenyl groups present, even with sufficient run-time to perform the calculations. Attempts to find a substitute for modelling the phenyl groups without ab-initio optimisation of the entire complex have not been particularly successful. However, the phenyl groups do not appear to have much effect on the reaction mechanism apart from steric hindrance, so the approximation made of simplifying phenyl groups to hydrogen appears to be sound.

Having now discussed all of the findings of this project, the next step is to attempt to account for these properties from molecular orbital theory.

5: Electronic influences on geometry and reaction mechanisms

5.1 Introduction and basic framework

Whilst the structures and energies of the optimised complexes have all been justified in terms of SCF energies (and occasionally, similarities to X-ray-determined structures), it must be remembered that the basis set and method used approximations from the fundamental *ab-initio* level. There was always a risk that a calculated structure or reaction mechanism could be significantly inaccurate. Therefore, it was desirable to account for as many characteristics as possible in terms of the complex's electronic structure.

The electronic structure of transition metals, and the way they form bonds with ligands, is well-understood. All transition metals have three electronic sub-shells that can play a part in forming σ and π-bonds (and, occasionally, δ–bonds) with ligands: the *d*-subshell, which would be partly filled in the isolated atom (in the case of palladium, 4*d*), and the *s*- and *p*-subshells from the next shell up (5*s* and 5*p* in palladium). All of the inner *s*-, *p*- and *d*-subshells are always fully filled, forming a core of electrons that plays no part in the bonding.

Although π-bonding strengthens many metal-ligand bonds, it is nearly always the σ-bonds that are fundamental to the bonding. The most common case studied is a basic octahedral complex of $MX_6^{n\pm}$. The structure can be modelled though the 18-electron rule or by considering the σ-bonding to be formed by the σ-donating orbitals of the ligands overlapping with the *s*, *p*, and *d* valence orbitals (or a hybridised combination of these orbitals) of the metal, but the most technically accurate method is to construct an energy-level diagram with the valence orbitals of the metal overlapping with the six σ-donating orbitals of the ligands in various combinations of phase corresponding to the symmetry of metal orbitals.[90,91]

A square-planar complex bonding description is more complicated, because the interaction with palladium in the *z*-direction is different from that in the *x*- and *y*-directions. The $5p_z$ orbital and $4d_{z^2}$ orbital of palladium, both heavily involved in

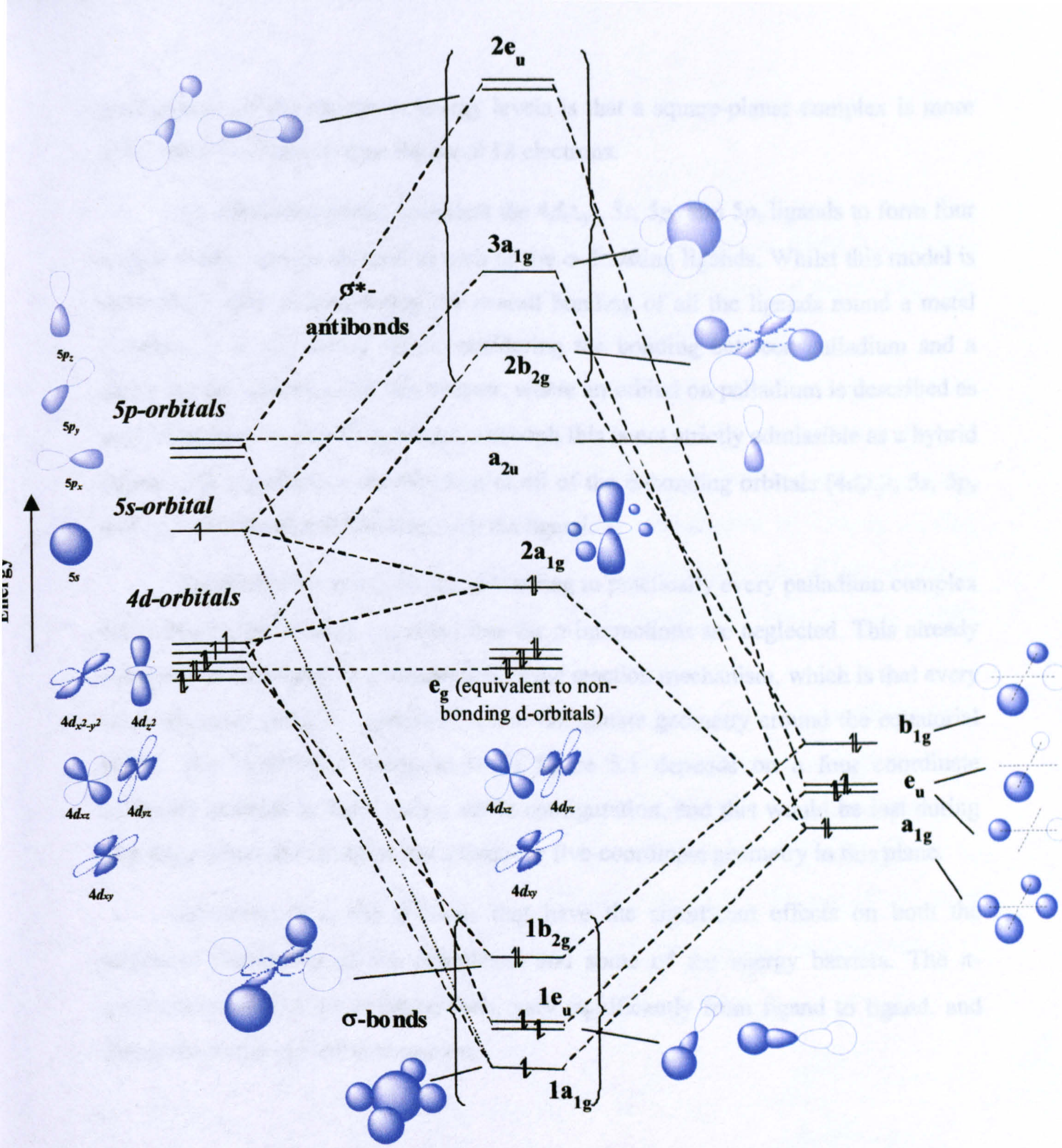


Figure 5.1: Electronic structure of a square planar complex of the form PdX_4 (not to scale), neglecting π–interactions. (Note that the above symmetry labels do not apply to asymmetrical square planar structures, and assignment of electrons to separate fragments is arbitrary.)

σ–bonding in an octahedral complex, can both no longer form σ–bonds in the *z*-direction. The $5p_z$ orbital becomes a non-bonding orbital, and the $4d_{z^2}$ orbital's effect on the electronic structure is significantly reduced. The resultant energy diagram, for a square planar complex of the form PdX_4, is shown in **figure 5.1**, and it is anticipated that a similar electronic structure would exist for other square planar structures (in this case, of the form Pd[P-P]XR) if π–interactions are neglected.. The most important

consequence of the change in energy levels is that a square-planar complex is more stable with 16 electrons than the usual 18 electrons.

An alternative model considers the $4d_{x^2-y^2}$, $5s$, $5p_x$ and $5p_y$ ligands to form four hybrid σ-type orbitals to bond to each of the σ-donating ligands. Whilst this model is now rarely used in considering the overall bonding of all the ligands round a metal complex, it is still useful when considering the bonding between palladium and a single ligand. Therefore, in this chapter, where an orbital on palladium is described as a σ-donating or σ-accepting orbital, although this is not strictly admissible as a hybrid orbital, this represents a combination of all of the σ-bonding orbitals ($4d_{x^2-y^2}$, $5s$, $5p_x$ and $5p_y$) contributing to bonding with the ligand.

This model accounts for the σ-bonding in practically every palladium complex optimised in this project, provided that the π-interactions are neglected. This already accounts for one important observation of the reaction mechanism, which is that every step, wherever possible, maintains a four-coordinate geometry around the equatorial plane. The 16-electron arrangement in figure 5.1 depends on a four coordinate geometry in order to form such a stable configuration, and this would be lost during any stage where the complex has a three- or five-coordinate geometry in this plane.

However, it is the π-bonds that have the significant effects on both the structural parameters of the complexes and some of the energy barriers. The π-interactions, unlike the σ-interactions, vary significantly from ligand to ligand, and this is the subject of the next section.

5.2 Bonding of individual ligands

5.2.1 Palladium-phosphine

Before considering the bonding between the chemically active ligands and palladium, the bonding between phosphorus and palladium shall be considered first, as these bonds are common to every complex optimised in this project.

The orbitals of phosphorus responsible for σ-bonding to the σ-type orbitals on palladium and the other atoms are the 3*s* and 3*p* orbitals (by considering them as either an sp^3 hybridisation or a combination of the σ-bonding orbitals surrounding phosphorus). However, the Pd-P bond could be strengthened by π–back-bonding between the occupied $4d_{xy}$, and $4d_{yz}$ orbitals on palladium and some of the orbitals on the phosphorus atoms. The simplest model uses the unoccupied $3d_{xy}$, and $3d_{yz}$ orbitals on phosphorus, as shown in **figure 5.2.1.1**.[92]

However, it is now thought that the dominant method of forming the π–back-bonds uses the σ*–antibonding orbitals in the phosphine groups, with the chief evidence behind this being that π–back-bonding behaviour was observed in a computational model that neglected the *d*-orbitals altogether.[92,93] (It should be considered that this considered PH_3 and not any sort of PR_3 fragment – the latter fragment may be a weaker π–acceptor, and if so, this introduces a potential source of

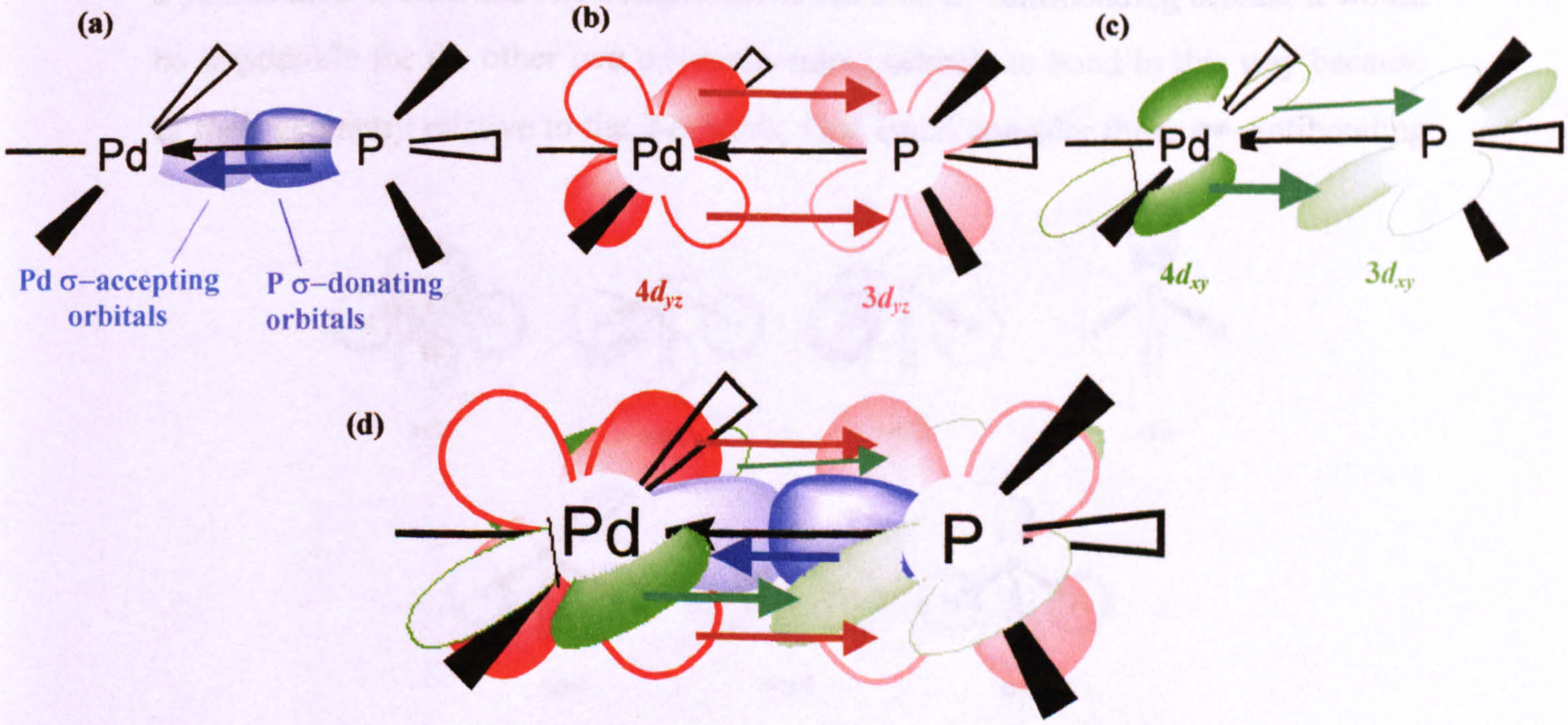


Figure 5.2.1.1: Bonding from palladium to phosphorus using *d*-orbitals on phosphorus for π–bonds as **(a)** σ-bonds; **(b-c)** π-bonds; and **(d)** combined bonding.

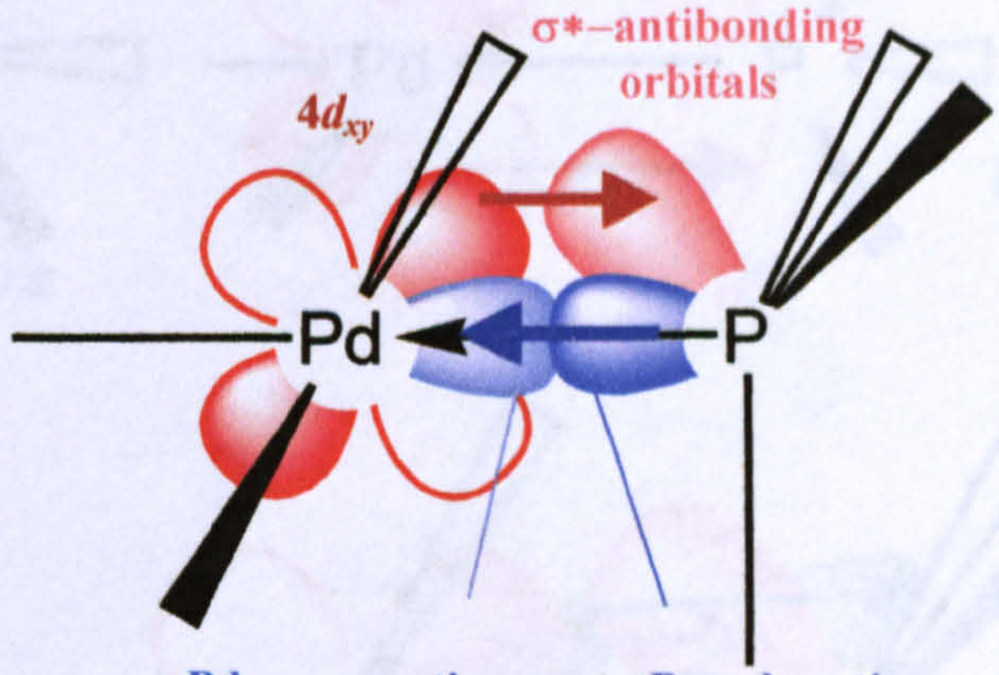


Figure 5.2.1.2: Bonding from palladium to phosphorus using σ*–antibonding orbitals on phosphorus for π–bonds, as proposed in reference 92. (Possible bonding from other P-X bonds not included.)

error into the results of this project as a result of approximating the phenyl groups to hydrogen atoms.) However, it was not considered by these researchers exactly how the orbitals overlap to form this π–bond.

One proposed model treats a σ*-antibonding orbital as a single-lobed molecular orbital that overlaps with a single lobe of one of the *d*-orbitals,[94] as shown in **figure 5.2.1.2**. Unfortunately, this treatment of bonding orbitals is a different method to the way the molecular orbitals of the other ligands in this project were considered, and it was preferred to use a universal system that applied to all of the ligands. More seriously, whilst this model adequately described the bonding between a palladium *d*-orbital and one component of one P-C σ*–antibonding orbital, it would be impossible for the other two σ*–antibonding orbitals to bond in this way because of their geometry relative to the *d*-orbitals. One could consider these σ*–antibonding

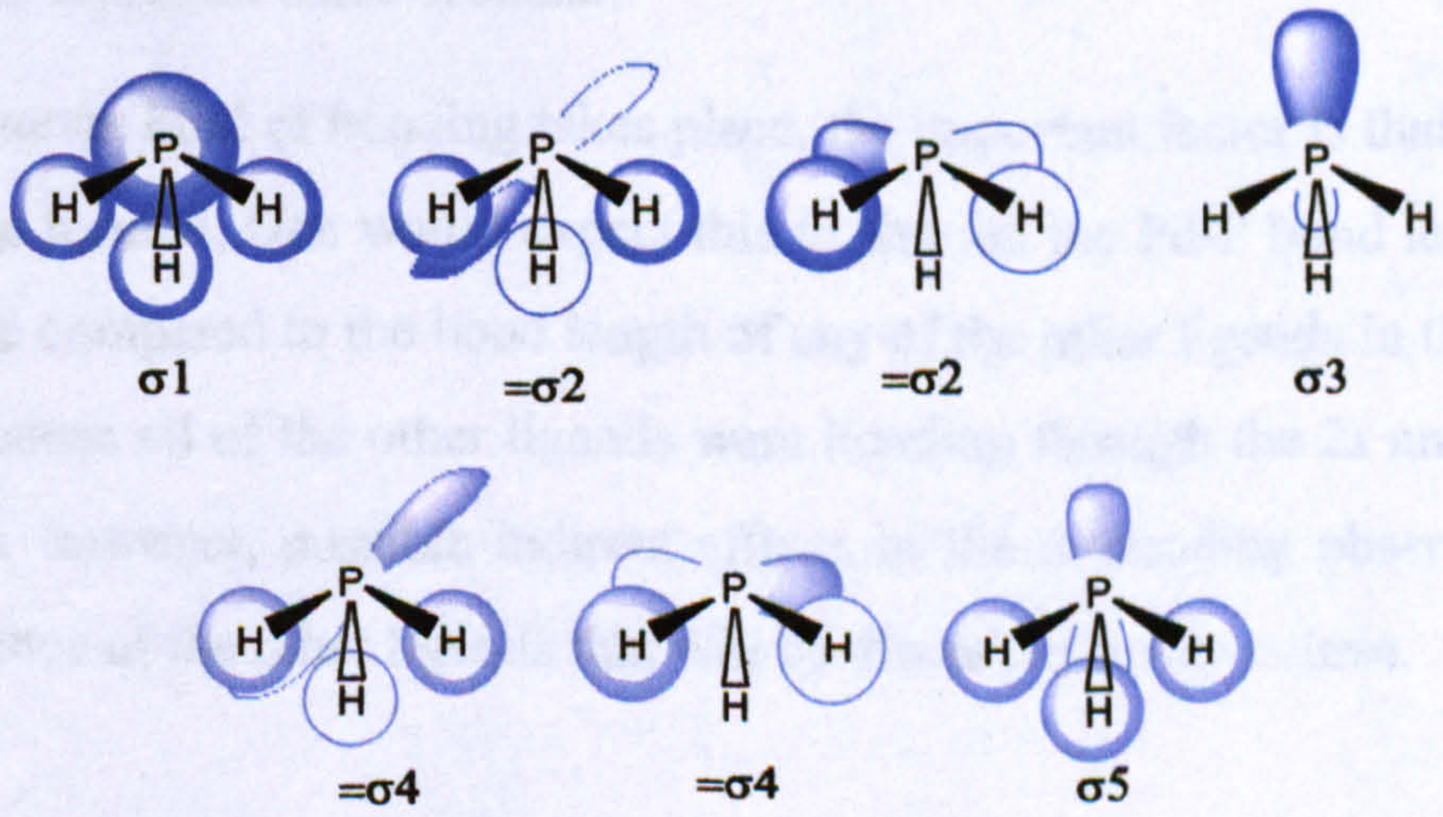


Figure 5.2.1.3: Non-hybridised molecular orbitals of PH_3 fragments. (Ordering of unoccupied molecular orbitals uncertain – labels are arbitrary.)

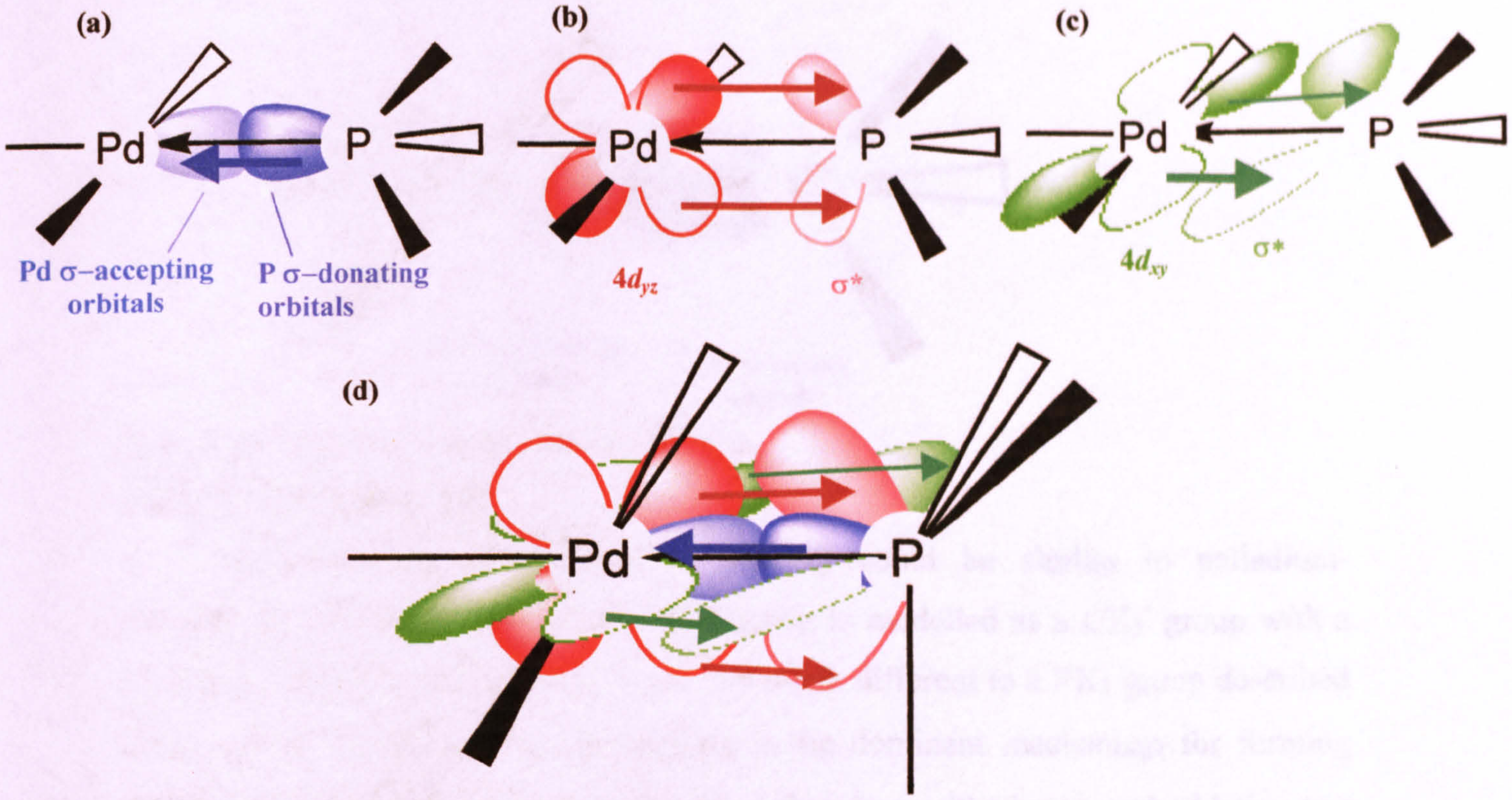


Figure 5.2.1.4: Bonding from palladium to phosphorus using σ*–antibonding orbitals on phosphorus for π–bonds as **(a)** σ-bonds; **(b-c)** π-bonds; and **(d)** combined bonding.

orbitals to bond to a linear combination of the two *d*-orbitals, but this would be complicated.

An alternative method was to consider the molecular orbitals of a PH_3 fragment, shown in **figure 5.2.1.3**. The two σ4-orbitals antibonding orbitals could π–bond to palladium as shown in **figure 5.2.1.4**, and this conveniently allows each lobe on the palladium *d*-orbitals to overlap with a different individual lobe on the PH_3 antibonding orbitals. Although this does not immediately look like bonding to P-C σ*–antibonding orbitals, the antibonding orbitals shown in this PH_3 fragment are simply an alternative representation of the σ*–antibonding orbitals, and can be hybridised to represent those orbitals.

Whatever kind of bonding takes place, the important factor is that π–bonds are known to be formed. One would expect this to shorten the Pd-P bond length, but this could not be compared to the bond length of any of the other ligands in the complexes studied, because all of the other ligands were bonding through the 2*s* and 2*p* orbitals. There were, however, possible indirect effects of the π–bonding observed from the *trans*-influence of the other ligands that will be discussed in due course.

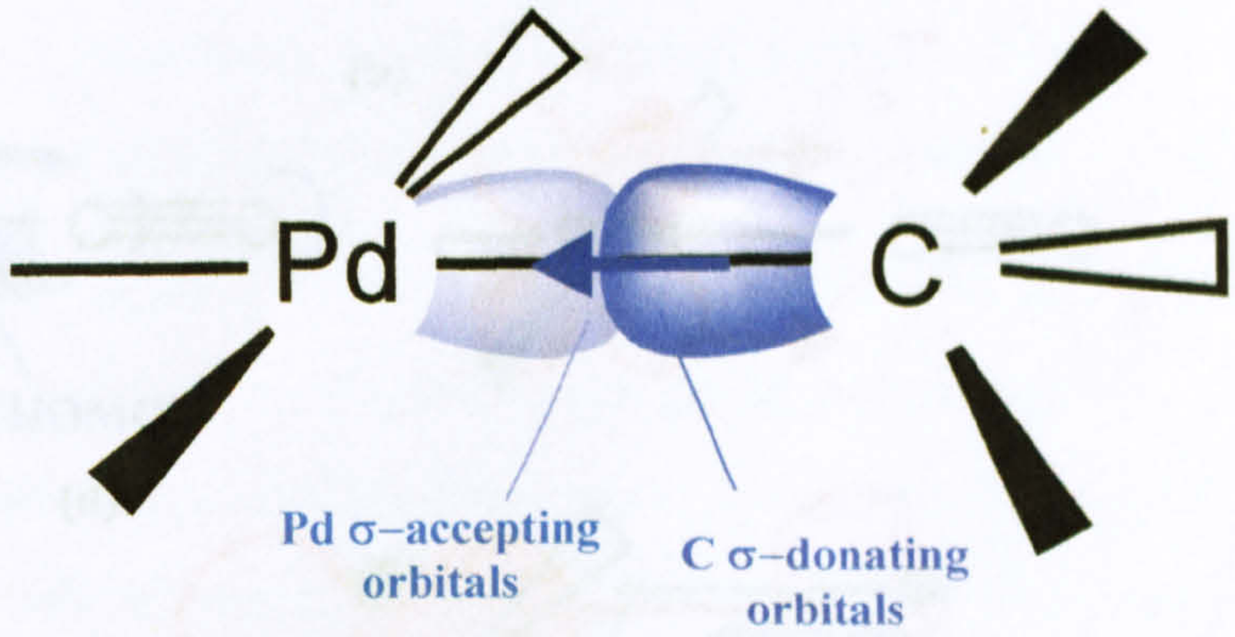


Figure 5.2.2: σ-bonding from sp^3 carbon to palladium.

5.2.2 Palladium-alkyl

Hypothetically, palladium-alkyl bonding could be similar to palladium-phosphorus bonding because, if the alkyl group is modelled as a CX_3^- group with a co-ordinate bond to palladium, it is not that much different to a PX_3 group described above. As it is believed the σ*–bonding is the dominant mechanism for forming π–bonds to palladium instead of *d*-orbital in phosphorus (the latter method being one that carbon certainly could not copy), in theory, carbon could form π–bonds to palladium in the same way. However, in practice, this is very unlikely to be the case, as when PH_3 and NH_3 were compared for formation of π–bonds to metals, only PH_3 was found to form noticeable π–bonds[92,93]. It can therefore be assumed that formation of π–bonds to metals is restricted to third-row elements downwards, and palladium carbon bonding is σ–bonding only, as shown in **figure 5.2.2**.

5.2.3 Palladium-carbon monoxide

The ligands with *sp* and sp^2 hybridisation are more complicated, as they can form π-bonds in various ways. Starting with the simplest ligand of this type, carbon

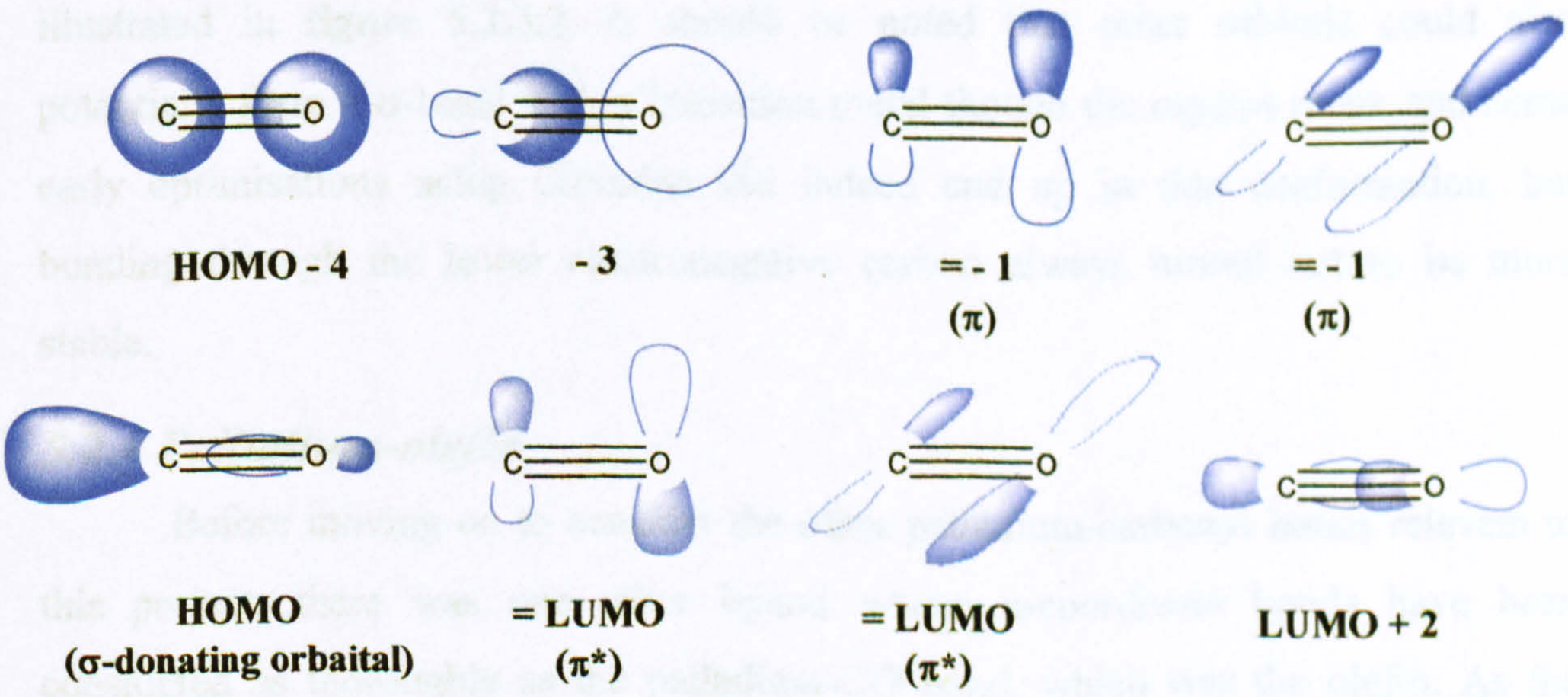


Figure 5.2.3.1: Carbon monoxide molecular orbitals (unoccupied orbitals in ground state in light blue; shapes of frontier orbitals adapted from quantitative diagrams in ref. 89).

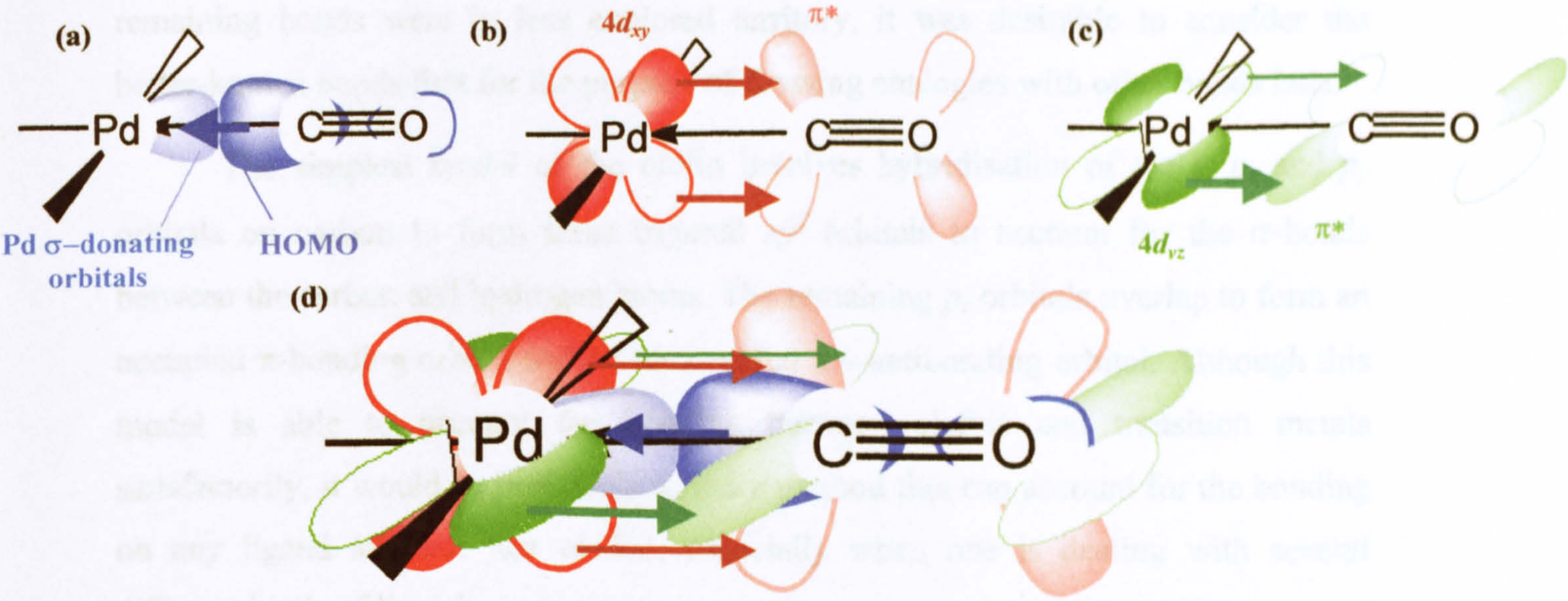


Figure 5.2.3.2: Bonding from palladium to carbon monoxide as **(a)** σ-bonds; **(b-c)** π-bonds; and **(d)** combined bonding.

monoxide, by constructing an energy-level diagram between carbon and oxygen, eight molecular orbitals (including two pairs of degenerate orbitals) are formed between carbon and oxygen, as shown in **figure 5.2.3.1**.[91] These orbitals were also obtained, in the same order of energy, from a CAChe calculation of electronic structure.[75]

There are three orbitals that matter in this project: the HOMO, with a large lobe on carbon to enable σ–bonding to other atoms; and the two degenerate π*–antibonding LUMOs. (There are also some complexes where one or both of the π–bonding orbitals form a bond to a second or third metal centre[91], but that does not apply to this system.) The HOMO is the bonding orbital that may be used to form σ-bonds with palladium or any other transition metal. Both LUMOs can then overlap with the *d*-orbitals on palladium to form π–backbonds. These bonds are illustrated in **figure 5.2.3.2**. It should be noted that other orbitals could also potentially form a σ-bond with a transition metal though the *oxygen* atom, and some early optimisations using Gaussian did indeed end up in this conformation, but bonding through the lower electronegative carbon always turned out to be more stable.

5.2.4 Palladium-olefin

Before moving on to consider the other palladium-carbonyl bonds relevant to this project, there was one other ligand whose π-coordinate bonds have been considered as thoroughly as the palladium-CO bond, which was the olefin. As the

remaining bonds were in less explored territory, it was desirable to consider the better-known bonds first for the purpose of drawing analogies with other bonds later.

The simplest model of the olefin involves hybridisation of the *s*, p_x and p_y orbitals on carbon to form three trigonal sp^2 orbitals to account for the σ-bonds between the carbon and hydrogen atoms. The remaining p_z orbitals overlap to form an occupied π-bonding orbital and an unoccupied π*–antibonding orbital. Although this model is able to account for bonding between olefins and transition metals satisfactorily, it would be preferable to use a method that can account for the bonding on any ligand and not just olefins, especially when one is dealing with several different kinds of ligand.

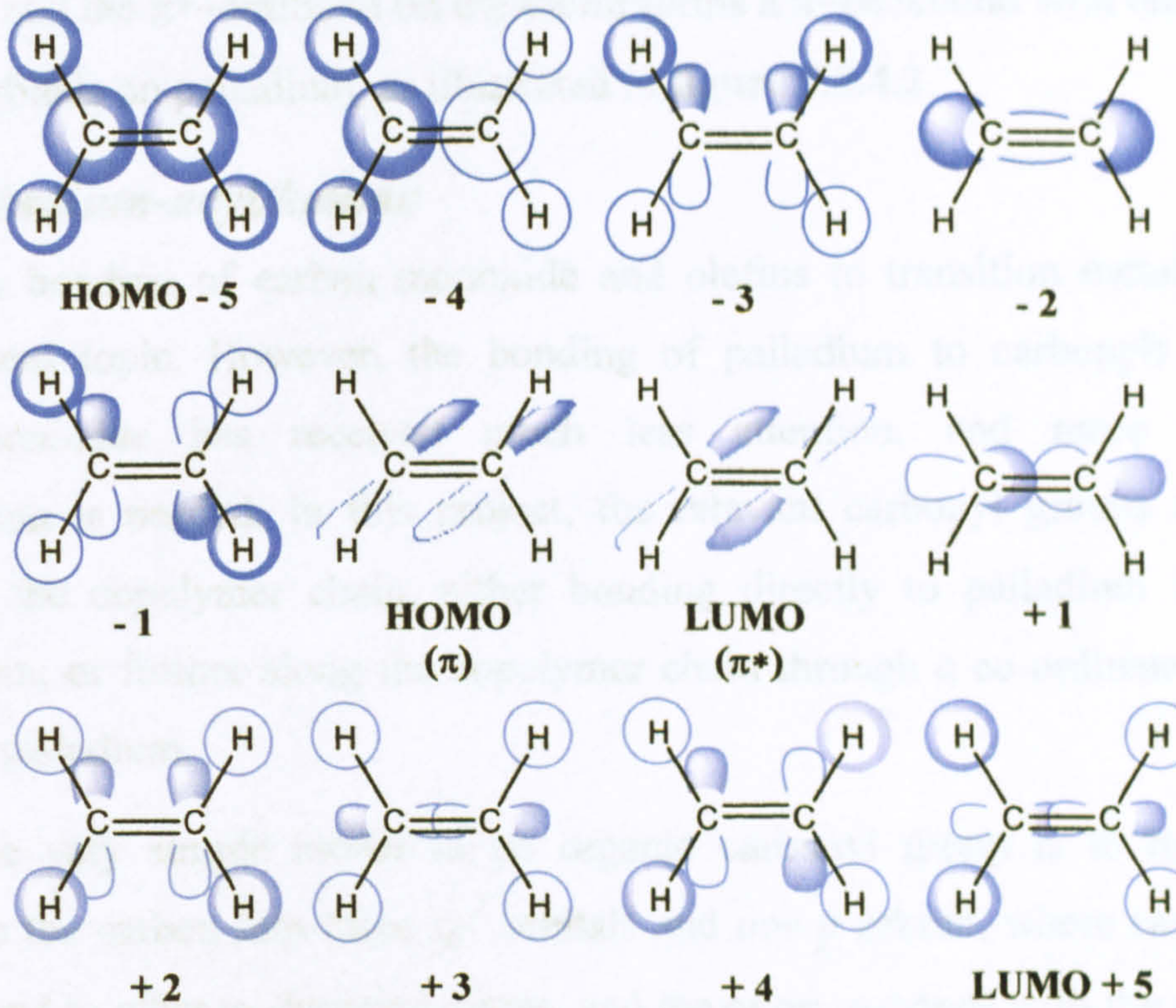


Figure 5.2.4.1: Molecular orbitals of C_2H_4 molecule.

It was possible to model *all* of the bonding orbitals between valence electrons in C_2H_4 from an energy level diagram by either pairing two fragments of bent CH_2,[90] or adding four H atoms to a C_2 molecule. The molecular orbitals could also be estimated using CAChe.[75] Whichever method was used, the results were always the same, and the molecular orbitals present in C_2H_4 are shown in **figure 5.2.4.1**. (Although there are no new orbitals able to significantly contribute to bonding to a transition metal found from this approach, there are similar orbitals in carbonyl fragments that become important in the next section.)

The π-bonding orbital on the olefin forms a σ-bond with the σ-type orbital on

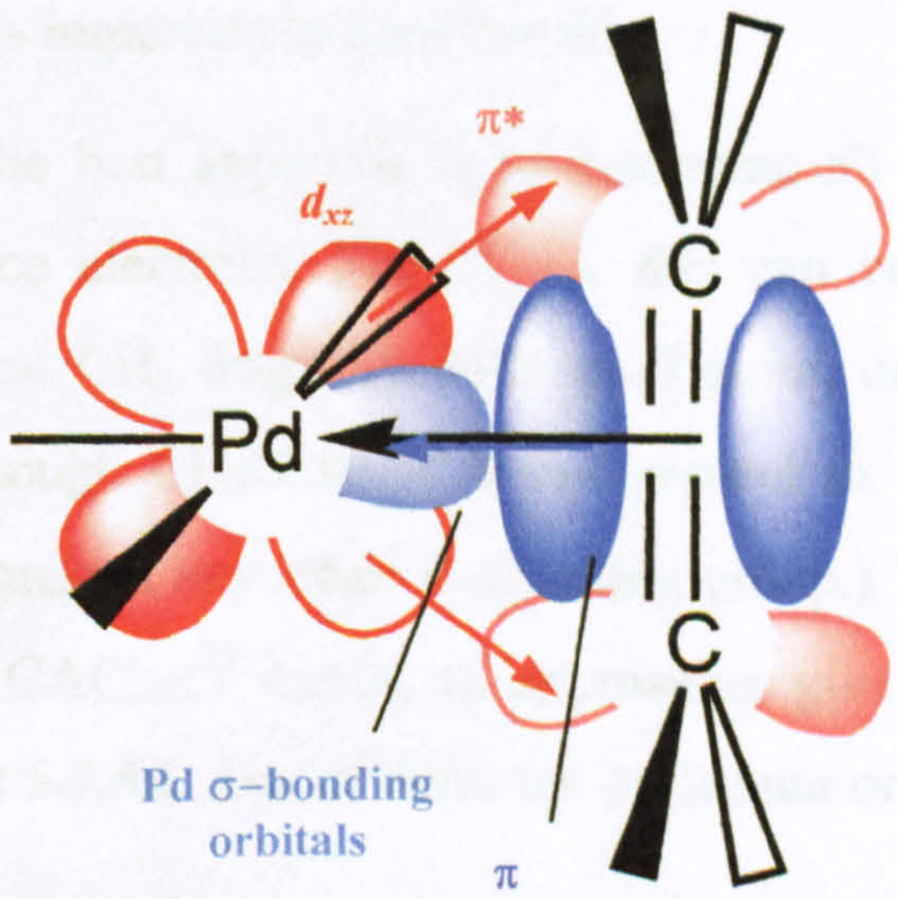


Figure 5.2.4.2: σ-bonding from olefin to palladium (blue) and π-back-bonding from Pd d-orbitals (red).

palladium, and the π*–antibond on the olefin forms a π–backbond with one of the d_{xy}, d_{xz} or d_{yz} orbitals on palladium, as illustrated in **figure 5.2.4.2.**

5.2.5 Palladium-acyl/ketone

The bonding of carbon monoxide and olefins to transition metals is a very well-explored topic. However, the bonding of palladium to carbonyls other than carbon monoxide has received much less attention, and more speculative consideration is needed. In this project, the relevant carbonyl groups are the CO groups in the copolymer chain, either bonding directly to palladium through the carbon atom, or further along the copolymer chain through a co-ordinate bond from oxygen to palladium.

One very simple model of an organic carbonyl group is to hybridise the orbitals on the carbon into three sp^2 orbitals and one p orbital, where two of the sp^2 orbitals bond to other σ–donating atoms, and the other σ–bonds with the p_z orbital on oxygen, whilst the remaining p orbital in oxygen forms a π–bond with the p_y orbital on oxygen. The remaining two orbitals on oxygen, p_x and s are suggested by the model to be occupied by electron pairs and not take part in the bonding.[95] This model is far from satisfactory because it does nothing to explain how a carbonyl group can form co-ordinate bonds from the oxygen. A better model is to treat oxygen similar to carbon and think of the oxygen orbitals as three hybrid sp^2 orbitals and one p orbital, which would form a σ-bond and π-bond in the same manner as an olefin, except that the oxygen would have two lone pairs occupying the other two sp^2 orbitals instead of two more σ-bonds. Even so, it still does not guarantee that all molecular orbitals have been accounted for, and given the number of different ways that carbonyls bond in this reaction, it is important to consider this.

Again, the best approach is to determine all of the bonding orbitals arising from the valence electrons. For CH_2O, this can be accounted for through either interacting a bent CH_2 fragment with an O atom, or adding two H atoms to a CO molecule. (Although CH_2O itself is not present in this reaction, the H atoms can equally well represent any other σ-donating group.) The molecular orbitals can also be modelled in CAChe.[75] Again, all approaches give the same molecular orbitals, as shown in **figure 5.2.5.1.** Out of these ten molecular orbitals, there are three that matter

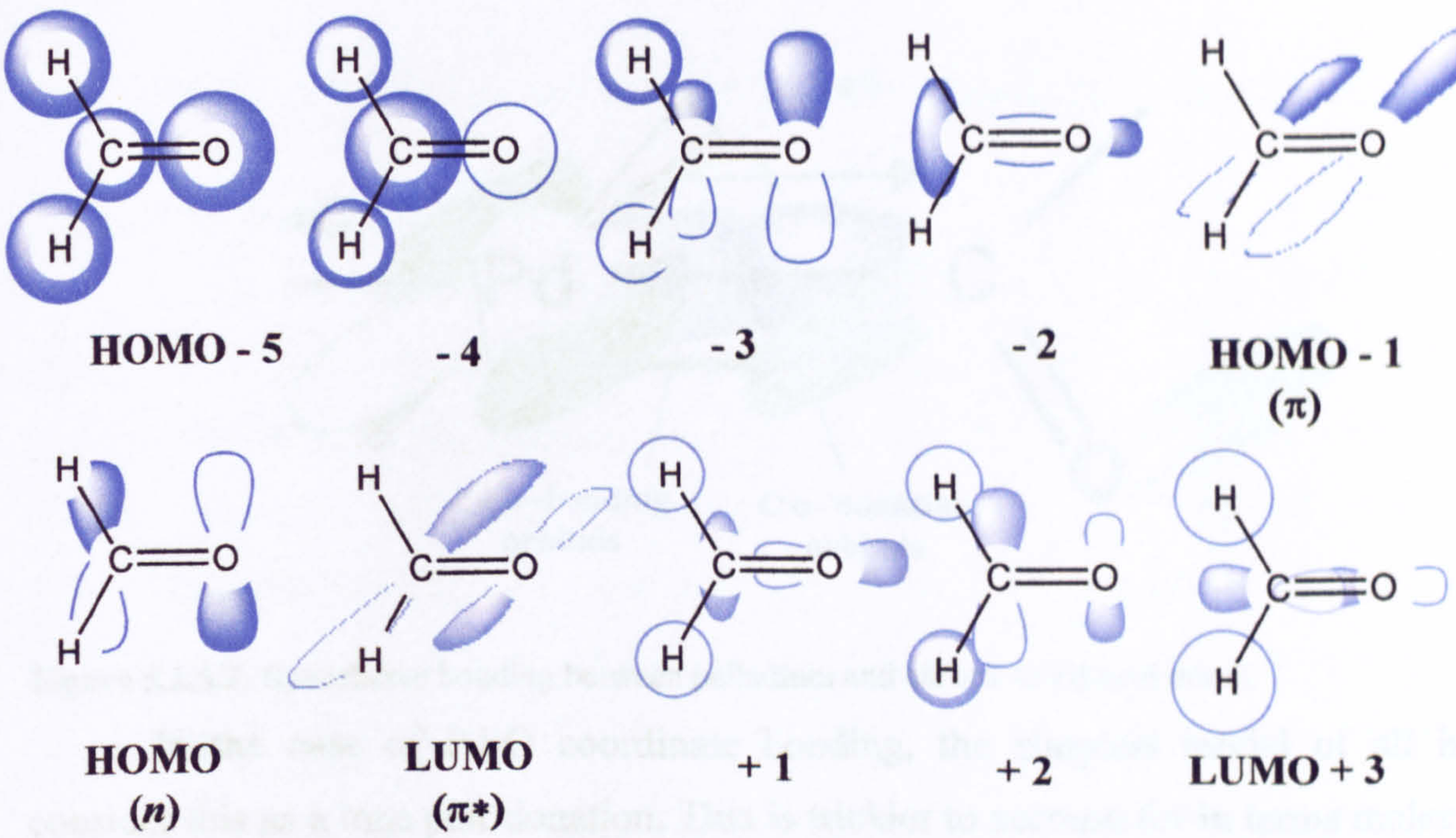


Figure 5.2.5.1: Molecular orbitals of CH_2O fragment (exact ordering uncertain, some orbitals outside of the frontier orbitals may be reversed).

in this project, being the HOMO, LUMO and the orbital immediately below the HOMO, normally labelled as the *n* (for non-bonding), π*- and π-orbitals respectively.

An important difference between this electronic structure and the electronic structure of olefins is that it is no longer possible for the HOMO of the ketone group to be the π–bonding orbital *and* for the LUMO to be the π*–antibonding orbital (in spite of one reference's claim to the contrary[96]), because it is impossible to arrange the energy level diagrams so that these two energy levels are adjacent. The existence of a molecular orbital lying between these π and π* orbitals is supported by reported UV-visible spectroscopy, which identifies both $n \rightarrow \pi^*$ transitions and $\pi \rightarrow \pi^*$ transitions in >C=O groups.[97]

Having established the molecular orbitals in a carbonyl group, one can then consider how such a group bonds to palladium. Unlike the other fragments, there are principally two ways that the carbonyl group bonds to palladium: either directly as a Pd-acyl bond or through oxygen via a Pd-O co-ordinate bond.

In a Pd-acyl bond, the σ-bond between Pd and C is already accounted for as this replaces the C-H bond in CH_2O. It seems likely that the bond would be further strengthened by back-bonding between the $4d_{yz}$ orbital on palladium and π* antibonding orbital on the carbonyl, in a similar manner to the *d*-π* bonding between palladium and carbon monoxide, although how much effect this actually has is uncertain. A diagram is given in **figure 5.2.5.2**.

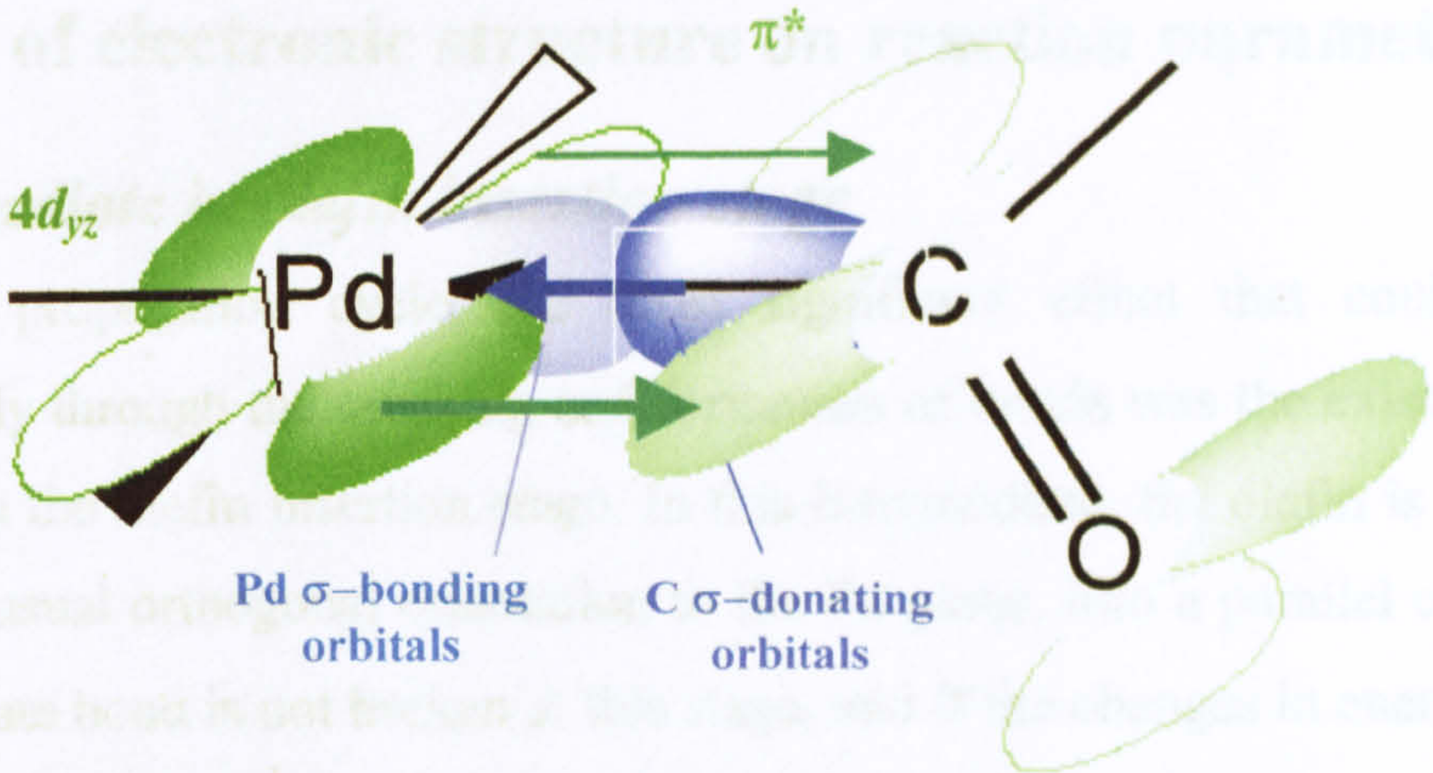


Figure 5.2.5.2: Speculative bonding between palladium and carbon in Pd-acyl bond.

In the case of Pd-O coordinate bonding, the simplest model of all is to consider this as a lone pair donation. This is trickier to account for in terms molecular orbitals of CH_2O, but if this electron donation is to be accounted for from these molecular orbitals, most of the occupied orbitals contain lobes in the direction of the palladium atom that could contribute towards the electron donation. Whichever orbitals contribute towards the Pd-O coordinate bond, the bond could conceivably be strengthened by π-back-bonding between the $4d_{xz}$ and the π* orbital on the carbonyl. A diagram is given in **figure 5.2.5.3**.

Having now considered all of the common bonding groups present in the reaction cycle, attention can now be given to several notable features of the reaction that can only be explained by the electronic structure.

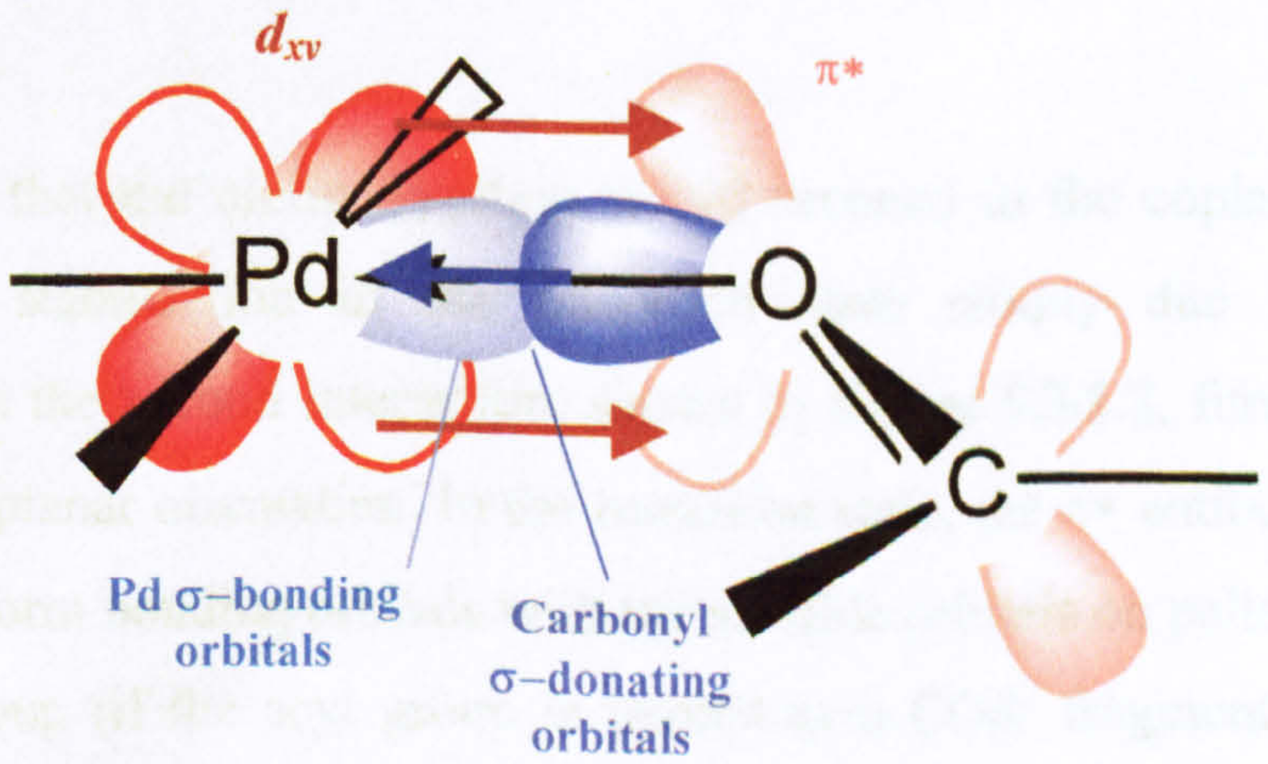


Figure 5.2.5.3: Speculative bonding between palladium and oxygen in a Pd-O co-ordinate bond.

5.3 Effects of electronic structure on reaction parameters

5.3.1 Intermediate in olefin insertion stage

In the propagation cycle, the most significant effect that could not be explained solely through the breaking and formation of bonds was the existence of an intermediate in the olefin insertion stage. In this intermediate, the olefin is rotated by 90°, from the usual orthogonal orientation to the Pd plane, into a parallel orientation. The π-coordinate bond is not broken at this stage, and if the changes in energy were to be explained in terms of steric hindrance alone, one would expect the energy to be at or near a maximum when the olefin was rotated by 90° rather than a local minimum.

This property has been previously explained, in part, through electronic structure by Roald Hoffmann.[98] There are two interactions that influence the orientation of the olefin during this stage: π–bonding to a *d*-orbital on palladium, and later a more complicated interaction with both the palladium ligand and migrating acyl group.

Starting with the first interaction, this has already been described in section 5.2.4. The π*–antibonding orbitals on the olefins overlap with the $4d_{yz}$ orbital of palladium prior to rotation (i.e. when the olefin is perpendicular to the palladium-ligand plane), and the $4d_{xy}$ orbital of palladium after rotation (if the *x*-direction is defined as the direction of the palladium-olefin bond and the *z*-direction is defined as the direction orthogonal to the palladium-ligand plane.), as shown in **figure 5.3.1.1.** Due to the symmetry of these two *d*-orbitals, an equally stable π–backbond can be formed by the π*–antibonding orbitals overlapping with any combination of the two *d*-orbitals on palladium. The only factor that may make the coplanar orientation less stable than the orthogonal orientation is the increased steric hindrance in the former structure.

It is likely that the olefin insertion would proceed in the coplanar geometry with or without stabilisation in the transition state simply due to geometric considerations, but the second interaction, shown in **figure 5.3.1.2**, further promotes insertion in the coplanar orientation. In the transition state, the π* antibonding orbital on the olefin can form bonding orbitals with the suitable orbitals on palladium and the migrating acyl group (if the acyl group is treated as a $COR^{\cdot}$ fragment). Due to the orientation of the olefin relative to these atoms, the most likely orbitals that the π*

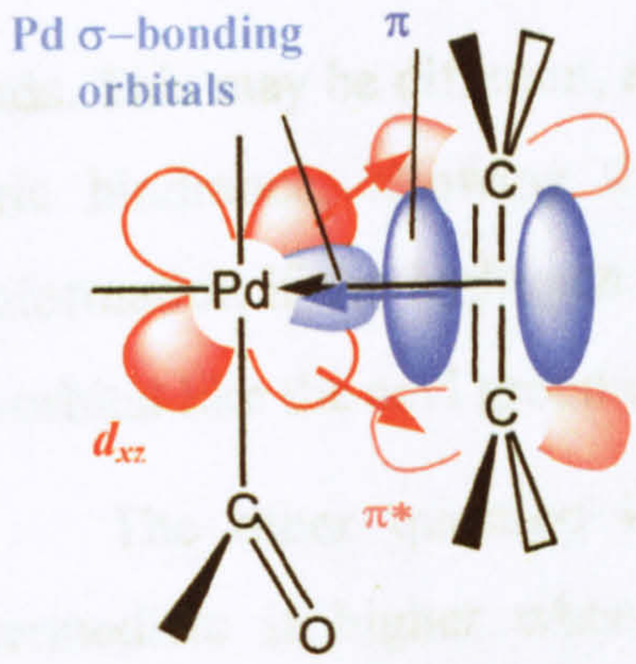


Figure 5.3.1.1: Electronic structure responsible for stabilisation of reactant of olefin insertion.

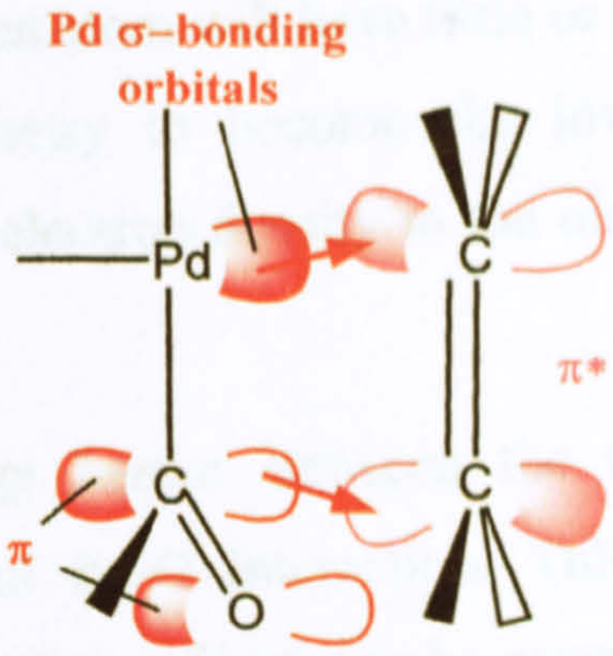


Figure 5.3.1.2: Electronic structure responsible for stabilisation of transition state of olefin insertion. (Similar interaction from π–orbitals may also be possible.)

orbitals of the olefin would interact with would be the σ–bonding orbitals on palladium (that previously formed the π–coordinate bond to the olefin), and either the π or π* orbitals from the organic carbonyl group. Although it cannot be shown whether or not this alters the reaction mechanism of the insertion step, this effect is important as it would stabilise the transition state and lower the activation energy of the slowest step in the propagation cycle, therefore promoting high chain length and greater productivity of the copolymer product.

One residual question is why there is a local minimum after the olefin is rotated through 90°, because if steric hindrance favours the orthogonal orientation, one would expect the olefin in a coplanar orientation to be either a maximum or very near a maximum rather than a local minimum. A possible explanation is that the bonds shown in figure 5.3.1.2 can actually start to be formed *before* the insertion step begins, thereby sufficiently stabilising the coplanar alkene to form a local minimum.

There are a few other minor residual questions. The first is how a local minimum is formed during double olefin insertion, as a migrating alkyl group does not have π and π* orbitals to bond as a migrating acyl group does. It is possible that the lone pair on the alkyl group (if it is treated as an anion) could donate electrons instead of these orbitals, but the orientation of the atoms bonding to this carbon atom does not give a particularly favourable geometry. However, some of the component orbitals of a CX_3^- group (see sections 5.2.1-2) could potentially act as substitutes and do have lobes in a more suitable direction for bonding.

On a similar note, in the case of olefin insertion into the Pd-H bond, the lowest energy conformation of the reaction is when the olefin is in a coplanar geometry, rather than the orthogonal geometry for olefin insertion into the Pd-acyl or Pd-alkyl

bonds. This may be different, as a single hydrogen atom will have little or no effect on steric hindrance, allowing the coplanar geometry to become the lowest energy conformation if the hydrogen atom can donate electron density to the olefin's empty π^*-orbital like the acyl group can.

The other question is why the energy barrier between the reactant and intermediate is higher when there is an axial Pd-O interaction. This is a more complicated matter, and the nature of this interaction will need to be considered first.

5.3.2 Axial Pd-O coordinate interactions

There are two points in the propagation cycle where the previously-formed carbonyl group in the copolymer chain interacted with palladium from an axial site. They are both prior to insertion of either an olefin or carbon monoxide into the chain, after the Pd-O bond has been displaced from an equatorial site by the incoming molecule.

In most cases, it is straightforward to deduce which orbitals are responsible for the electron donation from the carbonyl group. The Pd-O-C bond angle is normally in the region of 120° in the plane of the >C=O bonds, so it is likely that the electron donation from an axial site to palladium is the same as that for bonding in an equatorial site: a lone pair donation from oxygen. However, the question remained as to which orbital on palladium the electrons were being donated. The most likely orbital to accept the electrons was the empty $5p_z$ orbital on palladium. This was plausible as the $5p$ orbitals were the most diffuse orbitals active in palladium complexes, and therefore suitable for the longer distance between the atoms.

A small but significant effect of this axial bond is that the complex becomes an 18-electron system instead of a 16-electron system, and it is possible that this could encourage the complex to deviate from the square plane of the equatorial ligands in order to adopt a more stable conformation around the palladium centre. It would be beyond the scope of this project to consider how the energy levels would be altered if the metal deviated from the square planar geometry, but it can be seen from the optimised structures that only olefin ligands appear to have any noticeable displacement from the square plane. Phosphorus and carbon monoxide are the least likely ligands to be displaced from the square plane as they form two sets of π-backbonds to the $4d$-orbitals in palladium, and so would stand to lose the most

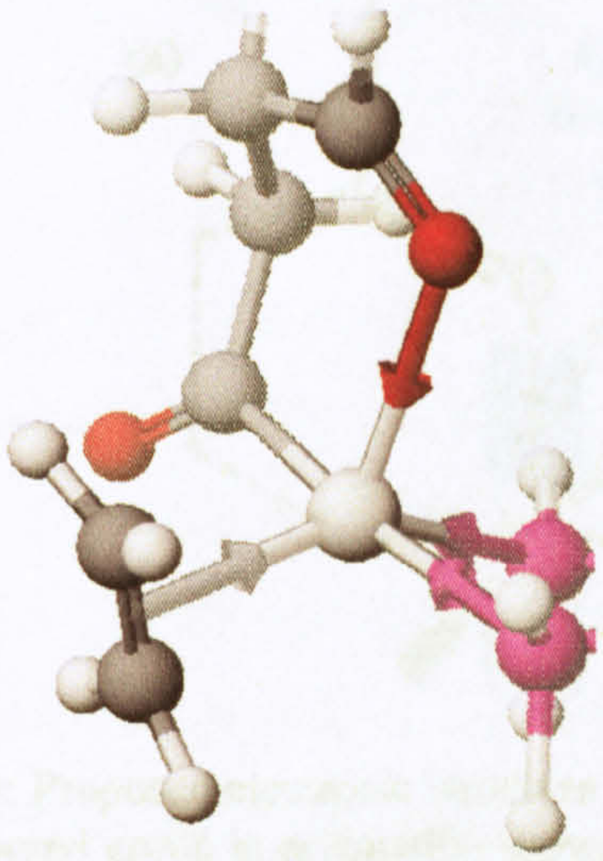


Figure 5.3.2.1: Structure of axial Pd-carbonyl interaction through Pd-O co-ordinate bond.

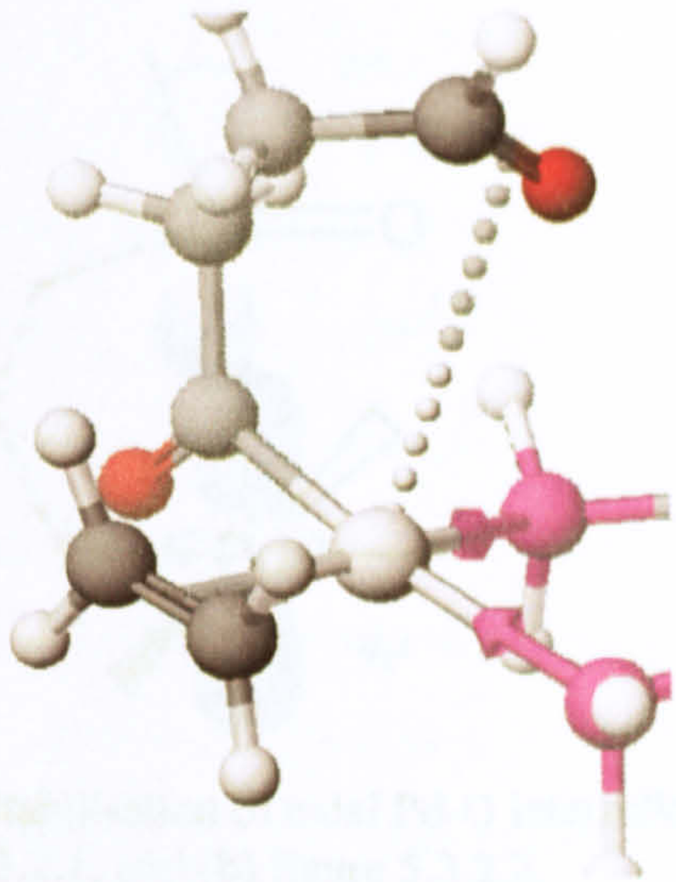


Figure 5.3.2.2: Structure of axial Pd-carbonyl interaction without Pd-O co-ordinate bond.

stability if displaced from their optimum positions. Olefins, on the other hand, only form one π–backbond and possibly are easier to displace. The Pd-acyl bond also has only one π–backbond, and the Pd-alkyl group has none, and they are not observed to be displaced from the Pd plane; however, both these groups are linked to the axially-bonded carbonyl group and it would be difficult for either of these groups to be displaced from their equatorial sites without weakening or breaking the axial Pd-carbonyl interaction in the process.

In the olefin insertion stage, there was one final puzzling effect that was difficult to explain. Prior to the olefin rotation stage, the axial Pd-carbonyl interaction quite clearly interacts through the oxygen, as one would expect, as shown in **figure 5.3.2.1**. However, as soon as the olefin starts to rotate out of its optimal geometry perpendicular to the Pd-ligand plane, the Pd-carbonyl interaction changes to the more ambiguous structure shown in **figure 5.3.2.2**. This structure remains in place when the olefin rotates into the Pd-ligand plane, and throughout the insertion process until the point where the Pd-olefin bond is broken altogether. Furthermore, by comparing the energy changes during the olefin rotation stage with and without a second carbonyl group present in the axial Pd-carbonyl site, it was estimated that changing the conformation increased the energy of the system by about 2-3 kcal/mol. There was no obvious explanation as to why altering the orientation of the olefin would cause the carbonyl group to change from one geometry to the other.

The geometry itself could be accounted for through the frontier orbitals on the carbonyl group. The π and π* orbitals are the only orbitals that extend in a significant

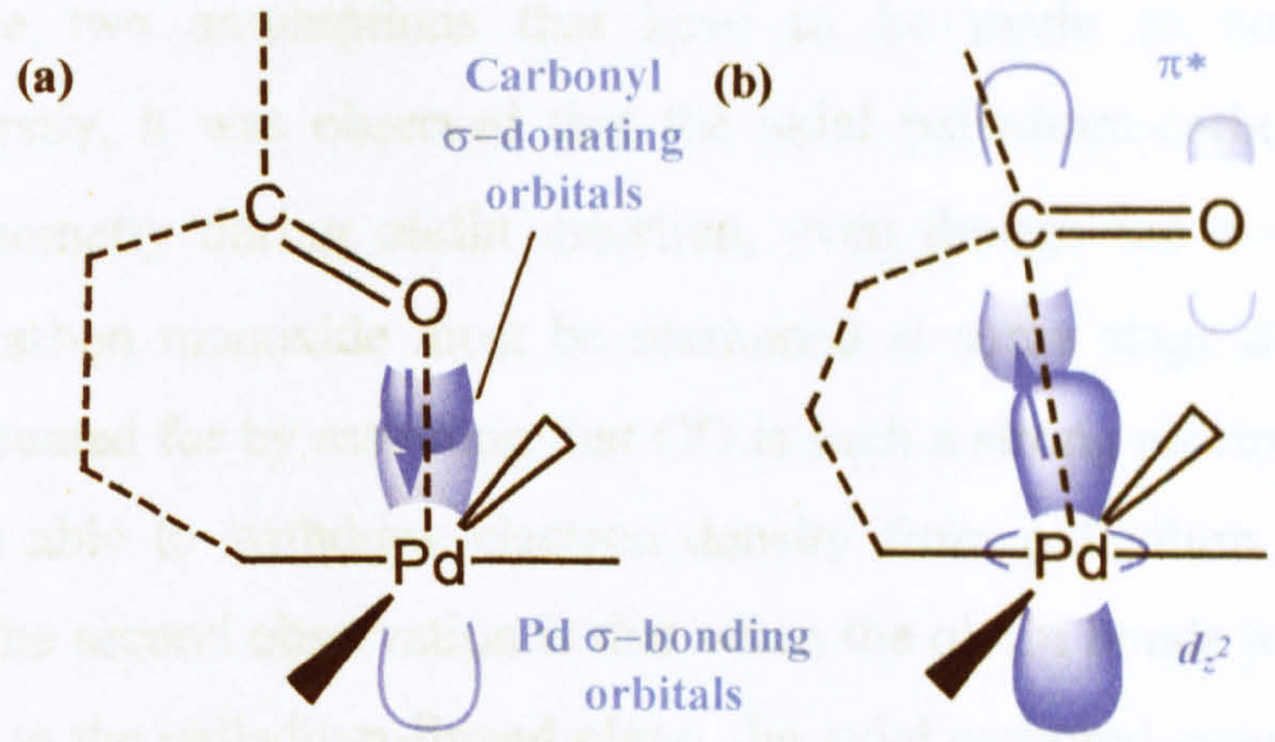


Figure 5.3.2.3: Proposed electronic structure responsible for stabilisation of axial Pd-O interaction, with axial carbonyl group in orientation shown in **(a)** figure 5.3.2.1, and **(b)** figure 5.3.2.2.

distance in the direction *perpendicular* to the >C=O plane. Normally, when the carbonyl group is bonded to palladium (either through carbon or oxygen) in an equatorial site, this does not matter as there are no atoms in this direction that the π and π* orbitals can interact with. When the carbonyl group is in an axial position, however, the lobes could conceivably interact with the $4d_{z^2}$ or $5p_z$ orbitals, as shown in **figure 5.3.2.3**, although it is not clear from the geometry which of the orbitals interact, or whether there is a combination of more than one interaction.

Why this structure should be preferred instead of the usual electron donation from an oxygen lone pair at only one specific point in the propagation cycle is a more difficult question. The chief difference between these two structures is that in figure 5.3.2.1, the carbonyl group can only donate electrons to palladium, whilst in figure 5.3.2.2, the carbonyl group can either donate or withdraw electrons, depending on how much the occupied and electron-donating π–orbitals, and unoccupied and electron-withdrawing π*–orbitals, are involved in the interactions. It is possible that the most stable conformation depends on the electron density demands of palladium. In this case, normally there would be a strong electron-withdrawing ligand (either an olefin or carbon monoxide – the acyl group or diphosphine ligands would probably not withdraw electrons strongly enough through their π–bonds to palladium to make a difference) to promote maximum electron donation from the axial carbonyl group, hence the former structure. However, when there is an olefin that is *not* in a suitable conformation to form a π–bond to palladium (such as mid-insertion into the Pd-acyl bond), this could tip the balance and make the other structure more stable.

There are two assumptions that have to be made to account for two observations. Firstly, it was observed that the axial palladium-carbonyl interaction only changes geometry during olefin insertion, even though the π–bonds between palladium and carbon monoxide must be weakened at some stage of CO insertion. This can be accounted for by assuming that CO is such a strong electron-withdrawing ligand that it is able to withdraw electron density from palladium throughout the insertion step. The second observation is that when the olefin bonds to palladium and is perpendicular to the palladium-ligand plane, the axial carbonyl group interacts with palladium though an O lone pair, but when the olefin is in the palladium-ligand plane, the carbonyl group interacts through the π/π* orbitals even though the olefin may still be withdrawing electrons though its own π–bond to palladium. If the theory, discussed in the last section, about the olefin partially bonding to the acyl group when in the coplanar geometry is correct, then it is possible that this reduces the electron-withdrawing effect from palladium, changing the way that the axial carbonyl group interacts with palladium.

The different energy barriers of the olefin rotation stage, depending on whether the axial interaction from a carbonyl group is included, can now also be accounted for through charge distribution. If the alkene is most effective at electron withdrawal when it is in the orthogonal orientation, the axial acyl carbonyl group would stabilise the complex most at this point during the olefin rotation step by donating electron density from the oxygen atom. If the reactant is stabilised in this way, it could explain the increase in the energy barrier of the following step. (It may also contribute towards the rise of the energy barrier of the entire olefin insertion stage, but there are many other variables that could influence the activation energy.)

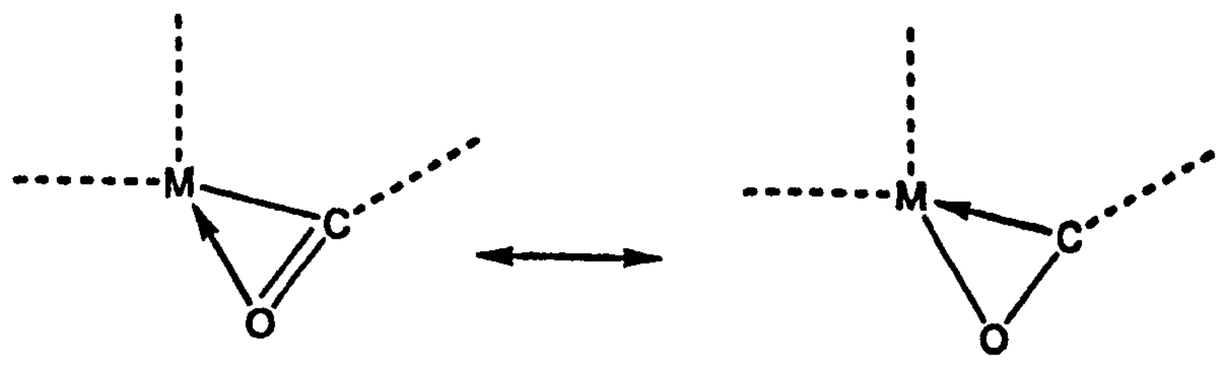
Attempts were made to verify these theories by comparing the partial charges on the palladium and carbon atoms in the olefin insertion stage both with and without a second acyl carbonyl group to form the axial interaction. However, the differences in charges were in the order of hundredths of a unit charge, and there could well have been consequential redistribution of charge around the rest of the complex Therefore, the findings did little to prove or disprove the theory. Short of undergoing a lengthy investigation of the energies of many new complexes for comparison, it seems that, for now, the reasons for this unusual behaviour can only be speculated upon.

5.3.3 Palladium-carbonyl interactions without fourth ligand

One unusual bonding structure observed in both of the initiation processes occurs after insertion of the first carbon monoxide ligand (figure 3.4.2.2), when the interaction between Pd and the acyl group does not show a clear bond between palladium and carbon. The O-C-Pd bond angle is around 90°, unlike the other structures containing the Pd-acyl bond where the bond angle is around 120°, and the Pd-C and Pd-O distances are similar. A simplistic observation is that in the former case both the carbon and oxygen atom can be considered to be bonded to palladium to complete a four co-ordinate complex around palladium, whilst in the other structures this is not needed as there is an equatorial Pd-O or Pd-olefin to act as the fourth ligand. However, it was a speculative assumption that an acyl group would account for two equatorial sites instead of one without considering how this conformation could be stabilised.

This kind of bonding between transition metals and acyl groups has been observed for over twenty years.[92,99] It was originally proposed that the structure was stabilised by the formation of a co-ordinate bond between the metal and oxygen, and further stabilised by the resonance structure shown in **scheme 5.3.3.1.** However, the bond strain of this system is unusually high. The bond angle of Pd-O=C has normally been around 120° (give or take 10°), so a Pd-O=C bond angle of 61.2° is a very large deviation from the angle one would normally expect with a Pd-O coordinate bond.

An alternative explanation lies with the *n*-orbital of the carbonyl fragment. This molecular orbital lies within the >C=O plane, and can easily be illustrated to overlap with either the $d_{x^2-y^2}$ orbital, or the σ–bonding orbitals on palladium in the direction of the O atom (in the *n*-orbital of the carbonyl group, the lobes on oxygen are thought to be the largest). It is conceivable that this structure, as shown in **figure 5.3.3**, would be sufficiently stable to overcome the bond strain produced by reducing the Pd-C-O bond angle away from the ideal 120°. The reservation with this suggestion



Scheme 5.3.3.1: Proposed stabilisation of M-acyl bonds through co-ordinate bonds and resonance structures.

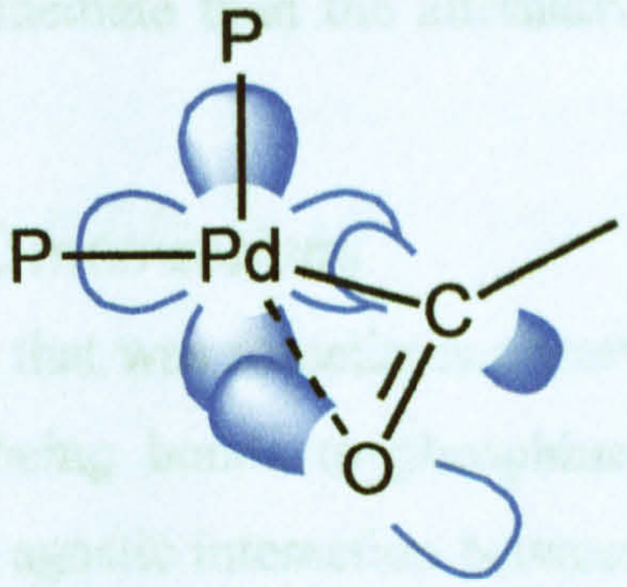
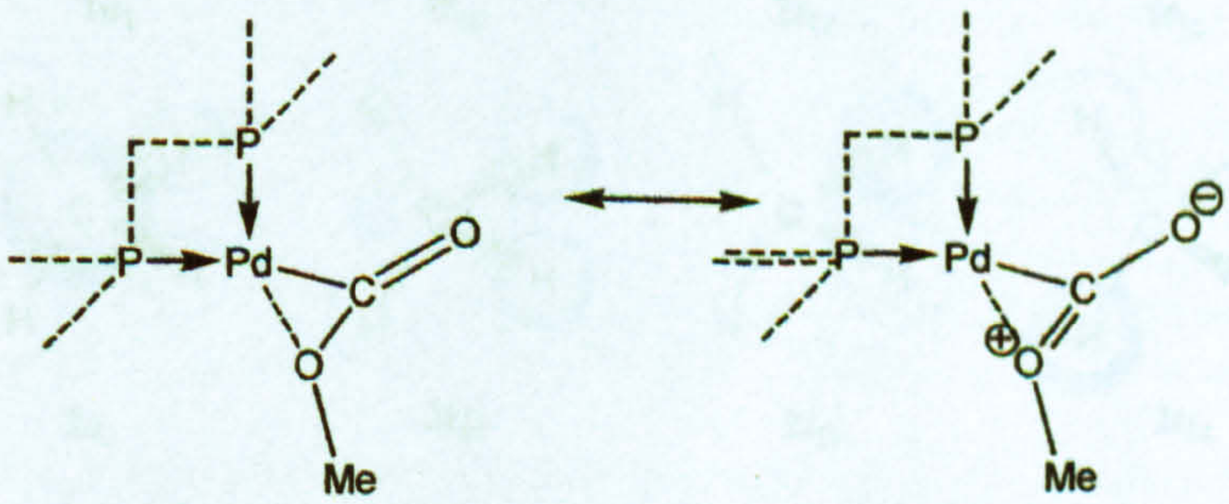


Figure 5.3.3: Bonding between *n*-orbital in carbonyl group and $d_{x^2-y^2}$ ligand in palladium. (Bonding also possible to σ–bonding orbitals on palladium in the direction of the oxygen atom).

is that the *n*-orbital of the carbonyl fragment is, strictly speaking, an antibonding orbital. One may expect the donation of electrons to the palladium atom to decrease the antibonding character, in turn strengthening the bond and decreasing the bond length, and no such decrease in bond length is observed. However, the *n*-orbital is likely to only be weakly anti-bonding, so it may not have any noticeable effect. Also, the deviation from a trigonal structure around the carbon and oxygen atoms could weaken the C=O bond, cancelling out the strengthening effect and causing a slight increase instead.

Either model can also be used to account for the intermediate observed in CO insertion into a Pd-methoxy bond in the initiation process (see figure 4.1.4.6). Whilst one would normally consider the newly-formed C-OMe bond as a single bond, it was noted that an alternate resonance structure could be drawn to treat this as a double bond, as shown in **scheme 5.3.3.2**. This theory was backed by the observation that this C-O bond length in the carboxymethyl complex of 1.34Å was significantly shorter than for 1.47Å in the methoxy group (which cannot resonate to a double-bond structure), and was not that much higher than the bond length of 1.20Å in the carbonyl group. In the right-hand resonance structure of scheme 5.3.3.2, similar O-Pd interactions can be formed to those described above. Whilst these interactions may not be a strong as those between palladium and acyl groups, it certainly does appear to



Scheme 5.3.3.2: Resonance of intermediate of CO insertion into Pd-methoxy bond.

allow a more stable intermediate than the alternative structure, an agostic Pd···H-C interaction.

5.3.4 Agostic Pd···H-C interactions

The other bonding that was sometimes observed in the absence of four strong Pd-ligand bonds (those being bonds to phosphine, acyl, alkyl, olefin, oxygen or carbon monoxide) was an agostic interaction between palladium and the atoms on the second carbon away from the palladium centre (the β-carbon atom). This kind of interaction between C-H bonds and transition metals has been known about for over twenty years, and has been backed up by X-ray crystallography, infrared spectra and NMR analysis[100], but it was desirable to account for the Pd···H-C interaction in terms of molecular orbitals.

To do this, first the molecular orbitals in CH_4 were determined. (Although CH_4 does not appear anywhere in the reaction cycle, the molecular orbitals surrounding carbon in CH_4 will be similar to those surrounding carbon in any other sp^3 environment.) One model of the orbitals is shown in **figure 5.3.4**.[75,88] (There are at least two other valid models, equally good for accounting for electron donation in the Pd···H-C agostic interaction.) The orbitals thought to be responsible for electron donation are the 1*t* orbitals. As electron density is being donated from an orbital that bonds this hydrogen to carbon this accounts for a rise in the C-H bond length. π-bonding may also be possible from the 2*t* orbitals.

However, the shape of the 1*t* orbitals is clearly not an ideal one for electron donation, compared to the σ–donating orbitals of stronger ligands. It is therefore understandable that a Pd···H-C interaction is only used as a fourth ligand when no

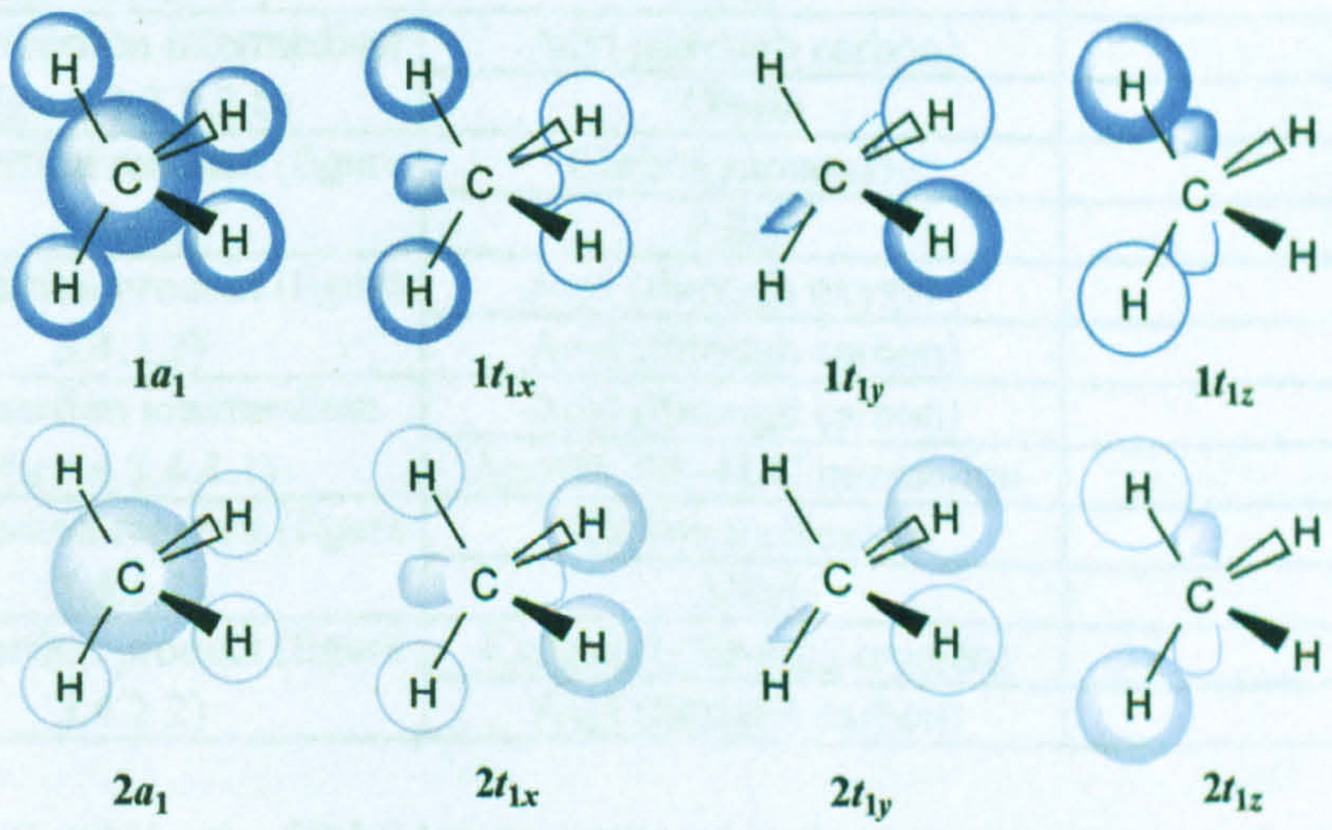


Figure 5.3.4: Molecular orbitals of CH_4 (other combinations of degenerate 1*t* and 2*t* orbitals also exist.)

other ligands are available to complete the square planar structure, and when such a structure is formed (such as the structure in figure 3.4.4.1), the activation energy required to displace this interaction for a more stable one is low.

5.3.5 Length of Pd-P bonds

The final observation to be explained were the lengths of the Pd-P bonds, which were found to vary significantly depending on which ligand was opposite the phosphorus atom. The varying distances are given in **table 5.3.5**. The following trends were observed:

- Pd-P bonds opposite alkyl groups were amongst the longer bonds at lengths of 2.41Å – 2.45 Å.
- Pd-P bonds opposite acyl groups bonding through carbon were, in the range of 2.43Å – 2.50Å, about the same length as above.
- Pd-P bonds opposite either olefins or carbon monoxide have bond lengths ranging through 2.34Å – 2.39Å, significantly lower that the above bonds.
- The Pd-P bond opposite the agostic Pd···H-C interaction had a very short bond

Structure	Group opposite P atom	Pd-P bond length
Olefin insertion reactant (figure 3.3.2.1)	Acyl (through carbon)	2.49
	Olefin	2.35
Olefin insertion product (figure 3.3.2.2)	Carbonyl (through oxygen)	2.25
	Alkyl	2.41
Olefin insertion intermediate (figure 3.3.4.2 b)	Acyl (through carbon)	2.45
	Olefin	2.34
Olefin insertion reactant (figure 3.3.5.1)	Acyl (through carbon)	2.50
	Olefin	2.39
Olefin insertion product (figure 3.3.5.3)	Carbonyl (through oxygen)	2.25
	Alkyl	2.41
Olefin insertion intermediate (figure 3.3.7.2 b)	Acyl (through carbon)	2.44
	Olefin	2.35
CO insertion reactant (figure 3.4.2.1)	Carbon monoxide	2.34
	Alkyl	2.45
CO insertion product (figure 3.4.2.2)	Acyl (through oxygen)	2.28
	Acyl (through carbon)	2.43
CO insertion intermediate (figure 3.4.4.1)	Acyl (through carbon)	2.48
	Agostic Pd···H-C interaction	2.29
CO insertion reactant (figure 3.4.5.1)	Carbon monoxide	2.35
	Alkyl	2.42
CO insertion product (figure 3.4.2.2)	Carbonyl (through oxygen)	2.27
	Acyl (through carbon)	2.48

Table 5.3.5: Bond length of Pd-P bonds compared to the ligand on the opposite (*trans*) site to the P atom.

length, at 2.29Å.

- Pd-P bonds opposite oxygen atoms (either as a co-ordinate bond from a carbonyl group or through the bonding in an acyl group described in section 5.3.5), were the shortest of all, in the range of 2.24Å – 2.28Å.

There is one single pattern that appears to emerge from all of these bond lengths, which is that phosphorus responds to the electron density demands of palladium, by the Pd-P bond shortening when groups on the opposite side are either strongly electron-withdrawing or poorly electron σ–donating. A ligand can be a strong at electron withdrawal either through strong π–back-bonding (bonds to olefins and carbon monoxide) or a highly electronegative ligand (Pd-O coordinate bonds). (It is thought the π–orbitals in acyl groups bonded to palladium through the carbon atom are too weak to make a significant difference to the electron density on palladium.) The only ligand that reduces the opposite Pd-P bond length because it is a poor σ–donor is the Pd···H-C interaction.

It was also attempted to determine a pattern from experimental data, but there were too few structures available in the Cambridge Structural Database[82] of palladium-diphosphine compounds to make many comparisons. Where palladium-diphosphine complexes had methyl groups, the Pd-P bond lengths on the opposite sites were around 2.30Å,[83] which was about 0.1Å below the Pd-P bond lengths opposite Pd-alkyl groups calculated in this project. However, methyl groups are not a reliable comparator to other alkyl groups because of their positive inductive effect. There were two structures that had an acyl group attached to palladium (on of them was the TEXPER structure shown in figure 3.3.2.3 – both structure had CO*t*-Bu groups as acyl ligand).[31] This time, the Pd-P bond lengths opposite the acyl group were very slightly under those calculated in this project, at about 2.40Å. (However, the structures available from the CSD included Pd-Cl bonds, whose effects on other bond lengths were unknown.)

If the search was extended to allow any kind of diphosphine ligand, and not just diphosphine ligands with two phenyl groups bonded to each of the phosphorus atoms, one could consider the bond lengths of Pd-P bonds opposite Pd-CO bonds. These Pd-P bond lengths were slightly higher than those calculated in this project: about 2.40Å.[85] However, the fragments in the CSD had *t*-butyl groups bonded to

phosphorus instead of phenyl groups, and the oxidation state was 0 instead of +2, either of which may have had an effect on the bond length. Overall, there was not enough experimental evidence available in the CSD to significantly support or contradict the theory proposed in this section concerning influences of *trans*-ligands on Pd-P bond length.

However, the tendency of strong ligands to weaken the metal-ligand bond on the opposite side in square planar complexes is a well-established phenomenon, known as trans-influence.[94] It has been observed, through both X-ray crystallography and infrared spectroscopy, that strong ligands such as CO and olefins cause the metal-ligand bond in the trans-position to increase in length, and in some cases, this can weaken the bond enough to be broken and control the selectivity of a reaction. Therefore, it is likely that the observed pattern in Pd-P bond-length variation in this project is a real effect and not just a by-product of computational approximations.

5.4 Summary

Consideration of how the palladium complex bonds to its ligands, the molecular orbitals that one expects to be present on all of the bonding ligands, and accounting for the bonding in terms of molecular orbitals has proved to be a useful exercise. It has helped account for a number of observations that could not be explained solely through considering the complex as a network of single, double and co-ordinate bonds.

The intermediate resulting from olefin rotation, the structure of the palladium-acyl complexes and the reduction of the Pd-P bond lengths arising from electron-withdrawing *trans*-ligands were all explained by σ– and π–bonding between the ligands and the complexes. The explanations for the existence and nature of the Pd-O axial interaction, the Pd···O interaction from acyl and methoxy groups, and the Pd···H-C interactions were a little more speculative and relied on a number of assumptions to produce a theory consistent with this model of electronic structure, but explanations were compatible with the theories. Overall, it can be concluded that the effects observed from the *ab-initio* calculations can be explained by considering the electronic structure of the complexes concerned, which significantly increases the confidence of the Gaussian results.

6 Summary

6.1 Overall conclusions

Although the entire mechanism of the copolymerisation of olefins and carbon monoxide has yet to be completed, *Gaussian* has shown itself to be capable of optimising the entire propagation cycle and two of the possible initiation mechanisms, in a reasonable amount of time, to give results that are consistent with earlier experimental and theoretical results. Patterns have also been observed that allow speculation on aspects of the mechanism that have yet to be investigated.

The propagation cycle, having had its reaction path optimised in its entirety, is summarised in section 3.8. The CO and olefin insertion steps broadly agreed with the structures optimised by Ziegler and Margl, in particular that the next carbonyl group along the chain plays an important role, forming an axial Pd-carbonyl interaction for most of the process. There were a few supplementary details on the reaction mechanisms found from doing IRC jobs. In particular, in olefin insertion, there is an early step of rotating the olefin into the palladium-ligand plane prior to insertion, whilst in CO insertion, the structure formed immediately after CO insertion is temporarily stabilised by an agostic Pd···H-C interaction before this bond is displaced by a stronger equatorial Pd-O acyl bond.

The mechanisms of adding new olefin and CO molecules to equatorial sites were optimised, having not been considered before. Previously, it had been speculated that incoming molecules would interact in an axial site to palladium before moving into an equatorial site, but there was no evidence to back up this theory. Now, it has been shown that this mechanism does indeed exist, with the equatorial Pd-O bond being simultaneously displaced into an axial position, and unless there are any unexpected alternative mechanisms, this method of adding new ligands prior to insertion into the copolymer chain appears to be the case. One interesting theory that this project addressed was that olefins cannot be directly added to an equatorial site because the palladium-oxygen bond is too strong to be displaced by such a weak ligand. It was found that this is not the case and olefins are perfectly capable of displacing a Pd-O bond without the help of any other ligands. However, CO molecules were found to be better at displacing the Pd-O bond at this stage (and there

is also the possibility of methanol doing the same). This could mean that CO promotes the stage by displacing the Pd-O bond faster than an olefin, or it could act as an inhibitor and occupy the site that the olefin then has difficultly displacing. Which of these two possibilities is the case will depend on the ease of displacing the CO ligand with an olefin, and this has yet to be considered.

The issue of an olefin displacing a Pd-O equatorial bond instead of CO after insertion of an olefin, on the other hand, raises questions about the possibility of double olefin insertion instead of CO insertion. The energies and mechanism obtained so far for double olefin insertion are summarised in section 4.2.8. The enthalpy of the double olefin insertion step is moderately higher than that for CO insertion, but double olefin insertion is further hindered by the thermodynamic unfavourability of bring an olefin into an equatorial site prior to insertion. This adds weight to the theory that palladium compounds that do allow double alkene insertion do so by weakening the Pd-O bond and so make it easier for olefins to displace the co-ordinating ketone group instead of the stronger CO.

Double CO insertion, on the other hand, also summarised in section 4.2.8, is ruled out solely because of the unfeasibility of the double CO insertion step itself. Although the effect of an axial interaction between palladium and oxygen has yet to be evaluated, the energy barrier neglecting this interaction was high enough to rule out this step, and the enthalpy of the step was highly positive. Therefore, the only residual issue, as explained above, is whether the more feasible step prior to double insertion, of adding a CO ligand into the equatorial site, assist or inhibits the propagation cycle.

Two possible mechanisms of initiation have been considered, as summarised in section 4.1.6. Of the two possibilities, it appears that the method of initiation by inserting an olefin into a Pd-H bond, to form a keto-end group, is by far the dominant mechanism. All of the stages up to insertion of the first CO into the Pd-alkyl bond have little or no activation energy and huge falls in enthalpy, whilst the only two stages in the initiation process that do have significant activation energies, being the first insertion of CO into a Pd-alkyl bond and the insertion of the first olefin into a Pd-acyl bond, have activation energies no higher than those present in the propagation cycle. In the other possible mechanism – insertion of CO into a Pd-OMe bond to form an ester end-group – the energy barrier of this step is not particularly high compared

to the energy barriers found in the propagation cycle, but it is still substantially higher than the near-zero energy barrier of the competing initiation process. This suggests that the former mechanism is indeed the dominant mechanism, but the latter mechanism cannot be ruled out and it is possible that the selectivity of the termination process may influence the initiation mechanism of the following copolymer.

Throughout all of these steps, it has been attempted to account for all of the structural characteristics through consideration of the electronic structure of the complexes. It was noted that π-back-bonding, the bond length of Pd-P bonds and possibly the geometry of Pd-carbonyl axial bonds, all play some role in the reaction mechanism. However, the most important observation was the importance of the four co-ordinate planar structure. At every point in the propagation cycle and the initiation processes, a four co-ordinate structure around the palladium centre could be accounted for, making use of agostic palladium-hydride bonds and *n*-orbitals in acyl groups where necessary, such that an equatorial site was *never* left vacant. Furthermore, the P-Pd-P bite-angle varied significantly throughout the olefin and CO stages, quite possibly to stabilise the complex to the most stable four-coordinate arrangement available, given the position of the other two chemically active ligands. The existence of an axial bond appears to be a neutral characteristic that the palladium complexes can exist with or without.

It was observed that practically every reaction mechanism observed in this project maintained a four-coordinate geometry around the palladium atom. Even when it was difficult to see how an insertion step could be accomplished without breaking the four-coordinate geometry, it was nearly always possible to find a reaction path that avoided this. The important question this poses is whether such a reaction path can be found in the termination processes. In termination by methanolysis, thought to be the dominant mechanism, an obvious reaction path can be traced that keeps a four-coordinate geometry, but it is harder to find one for termination by hydrogenation. It remains to be seen whether this is responsible for ruling out the latter mechanism, or whether an unexpected stable path can be found.

The only part of the project which has had limited success, with no obvious means of addressing the problem, was the attempt to include phenyl groups in the system. Attempting to account for the steric interactions of phenyl groups in propene insertion by performing semi-empirical calculations on a complex whose chemically

active atoms were optimised at ab-initio levels gave sporadic results, which may be good for a qualitative indication of likely regioselectivity to 1,2- or 2,1-insertion, but were too unreliable to be used for any quantitative analysis. It has been possible to optimise minima including the phenyl groups at ab-initio level, but it does seem to be exceptionally difficult to optimise transition states of this size, and there is no obvious solution of how this might be achieved without a very large amount of run-time being required.

It would be preferable to fill in the gaps rather than rely on speculation from the results obtained so far. However, this opens up a whole range of possibilities still to be explored.

6.2 Further work

The most obvious extension to this project is to complete the termination steps that need to be optimised, as well as complete the transition states of double insertion taking account of the axial palladium-oxygen interactions. These steps could be a greater challenge than the work done so far, because this involves, in most cases, optimisation of completely unknown transition states, usually with high energy barriers and the transition states may be difficult to locate. There are also side issues that are yet to be resolved, such as proving or disproving the existence of alternative reaction paths of CO and olefin insertion where the carbonyl group is interacting with the other carbonyl group (either as a ketone-ketone interaction or ketone-acyl interaction) instead of palladium through an axial interaction, and whether CO promotes or inhibits copolymerisation before the olefin insertion stage.

After this, possibly the most interesting characteristic to consider, in terms of commercial value, will be to further investigate what causes a palladium complex to start allowing double olefin insertion. By replacing the diphosphine ligand with the ligand that allows double insertion to take place, and repeating optimisation of the competing CO addition / insertion steps and double olefin addition / insertion steps, the energies can be compared to the energies of the corresponding steps using the diphosphine ligand. From this, it can be evaluated whether the reduction in energy barriers for double insertion is causes by a weakened Pd-O bond or whether other factors are responsible.

Next, there is the hypothesis to consider of whether, as the results in this project suggests, the ease of copolymerisation (as determined by the rate of copolymerisation and molecular weights) is assisted by the flexibility of the diphosphine ligands. If by varying the P-Pd-P bite angle during olefin and CO insertion did significantly stabilise the complex, then it is possible that less flexible diphosphine ligands (such as dppe and dppb) will raise the energy barrier of these steps. The reaction coordinate of these insertion steps could also be checked to see if the mobility of the P atoms is reduced. There is also the question of diphosphine ligands that stop copolymerisation altogether and instead produce monomers.

The matter of replacing a diphosphine ligand with two PH_3 ligands, which causes monomers to be produced instead of copolymers, is a little more of a puzzle. The original theory that the PH_3 ligands can adopt a *trans-* conformation now looks a little shakier, since, if vacant sites are not permitted in such complexes, there are no opportunities for PH_3 ligands to move *directly* from a *cis-* to a *trans*-position. There is also the old question of why certain insertions are allowed, where the PH_3 ligands must be in a *cis-* conformation, but others are not, and at this stage it is difficult to rule any possibilities in or out.

Finally, there is the much wider question of how the mechanism differs when olefins other then ethene are used. In propene/CO copolymerisation, the mechanism for the propagation and termination steps is thought to be different because of the wider distribution of end-groups. The question of regioselectivity is a more difficult question to answer. Some of the regioselectivity effects are likely to be down to steric interference with the acyl group and possibly a polar double bond, but the phenyl groups will have to be restored to the diphosphine ligands to consider all sources of steric hindrance. It may be necessary to reconsider the use of ONIOM for these purposes, provided that great care is taken to ensure the accuracy of the calculations is not compromised. Styrene/CO copolymerisation will also be of interest because of the possibility that the conjugation of the π-bonds affect the reaction mechanism and how this affects the bond to palladium. However, adding six extra carbon atoms to the system for each phenyl group (which must be considered at ab-initio level because of their scope for influencing the chemical reaction) would make it a lot more difficult to find a reaction path. There is also the scope for considering *stereo*selectivity, although

this will be a complicated process and one would need to consider the different ways of adding an olefin such as propene or styrene to an equatorial site.

Overall, the study of olefin / carbon monoxide copolymerisation has evolved into a project with a lot of scope for further investigation. The results produced so far are reasonably consistent with the available experimental and other theoretical results, but provide a fair amount of supplementary information to experimental inorganic chemists on the reaction mechanism. In addition to confirming steps whose mechanisms have already been optimised, it has been possible to use these observations to speculate about the mechanisms of the unexplored stages, and if these stages are explored too, perhaps it will be possible to speculate further. Nevertheless, there are still many questions that optimising the remaining steps could answer. By completing this reaction mechanism, this project can further the goal of making it an easy matter to predict the properties and reaction mechanisms of any sort of transition metal complex.

References

1: H. S. Brown, P. A Westbrook, United States Patent H983 (1989)

2: C. Bianchi, A. Meli, *Coord. Chem. Rev,.* **225**, p. 35 (2002)

3: A. S. Abu-Surrah, B. Rieger, *Top. Catal,.* 7, p. 165 (1999)

4: A. Somazzi, F. Garbassi, *Prog. Polym. Sci.*, **22**, p. 1547 (1997)

5: E. Drent, P. H. M. Budzelaar, *Chem. Rev.*, **96**, p. 663 (1996)

6: T. M. Shryne, H. V. Holler, U.S. Pat. 3,984,388, *Chem Abstr.*, **46**, p. 6143 (1952)

7: P. Margl, T. Ziegler, *J. Am. Chem. Soc.*, **118**, p. 7338 (1996)

8: P. Margl, T. Ziegler, *Organometallics,* **15**, p. 5519 (1996)

9: R. Van Asslet, E. G. C. Gielens, E. R. Rulke, K. Vrieze, C. J. Elsevier, *J. Am. Chem Soc.*, **116**, p. 977 (1994)

10: H-K. Luo, Y. Kou, X-W. Wang, D-G. Li, *J. Mol. Catal.*, **151**, p.91 (2000)

11: W. P. Mul, H. Oosterbeck, G. A. Betel, G-J. Kramer, E. Drent, *Angew. Chem. Int. Ed. Engl,* **39**, p. 1848 (2000)

12: J. S. Brumbaugh, R. R. Whittle, M. Parvez, A. Sen, *Organometallics,* **9**, p. 1735 (1990)

13: S. Schultz, J. Ledford, J. M. DeSimone, M. Brookhart, *J. Am. Chem. Soc.*, **122**, p. 6351 (2000)

14: e.g. J. S. Brumbaugh, A. Sen, *J. Am Chem Soc.*, **110**, p. 803

15: e.g. (a) B. A. Markies, D. Kruis, M. H. P. Rietveld, K. A. N. Verkerk, J. Boersma, H. Kooijman, M. Lakin, A. L. Spek, G. Van Koten, *J. Am. Chem. Soc.*, **117**, p. 5263 (1995); (b) J. Brumbaugh, R. R. Whittle, M. Parvez, A. Sen, *Organometallics,* **9**, p. 1735 (1990)

16: (a) J-T. Chen, A. Sen, *J. Am. Chem. Soc.*, **106**, p. 1506 (1984), (b) A. Sen, J-T. Chen, W. M. Vetter, R. Whittle, *J. Am. Chem. Soc.*, **109**, p. 148 (1987)

17: A. Sen. *Acc. Chem. Res.*, **26**, p. 303 (1993)

18: A. Sen, T-W. Lai, *J. Am Chem Soc.*, **104**, p. 3520 (1982)

19: F. C. Rix, M. Brookhart, *J. Am. Chem. Soc.*, **117**, p. 1137 (1995)

20: E. Drent, *Pure Appl. Chem.*, **62**, p. 661 (1990)

21: E. Drent, J. A. M. Broeckhoven, M. J. Doyle *J. Organonmet. Chem.*, **417** p. 235 (1991)

22: E. Drent, R. van Dijk, R. van Ginkel, B. van Oort, R. I. Pugh, *Chem. Commun.*, **9**, p. 964 (2002)

23: (a) M. M. Brubaker, US Patent No. 2,495,286 (1950); (b) M. M. Brubaker, D. D. Coffman, H. H. Hoehn, *J. Am. Chem. Soc.*, **74** p. 1509 (1952)

24: A. S. Abu-Surrah, B. Rieger, *J. Mol. Catal.*, **128**, p. 239 (1998)

25: Z. Jiang, G. M. Dahlen, K. Houseknecht, A. Sen, *Macromolecules,* **25** p. 2999 (1992)

26: F. C. Rix, M. Brookhart, *J. Am. Chem. Soc.*, **117**, p. 1137 (1995)

27: J. Schwarz, E. Herdtweck, W. A. Herrman, *Organometallics,* **19**, p. 3154 (2000)

28: R. A. M. Robertson, D. J Cole-Hamilton, *Co-ord. Chem. Rev,* **.225** p. 67 (2002)

29: A.S. Abu-Surrah, R. Wursche, B. Rieger, G. Eckert, W. Pechhold, *Macromolecules,* **29**, p. 4806 (1996)

30: F. Y. Xu, A. X. Zhao, J. C. W. Chien, *Makromol Chem.*, **194** (9), p. 2579 (1993)

31: Y. Koide, S. G. Bott, A. R. Baron, *Organometallics* **15**, p. 2213 (1996)

32: K. R. Dunbar, J-S. Sun, *J Chem. Soc. Chem. Common.* P. 3154 (1994)

33: W. Clegg, G. R. Eastham, M. R. J. Elsegood, R. P. Tooze, X. L. Wang, K. Whinston, *Chem. Commun.*, P. 1877 (1999)

34: A. Sen, T. Lai, *J. Am. Chem. Soc.*, **104** p. 3520 (1982), T-W. Lai, A. Sen, *Organometallics*, **3** p. 866 (1984)

35: (a) A. Sommazzi, S. Margherita, G Lugli, F. Garbassi, F. Calderazzo, D. B. Dell'Amico, US Patent No. 5314856 (1994); (b) A. Sommazzi, S. Margherita, G Lugli, F. Garbassi, F. Calderazzo, D. B. Dell'Amico, US Patent No. 5324701 (1994); (c) A. Sommazzi, F. Garbassi, G. Mestroni, B. Milani, US Patent No. 5310871 (1994); (d) A. Sommazzi, F. Garbassi, G. Mestroni, B. Milani, L. Vicentini, It. Patent no MIA002368

36: M. Svensson, T. Matsubara, K. Morokuma, *Organometallics*, **15** p. 5568 (1996)

37: A. Batistini, G. Consilglio, U. W. Suter, *Angew. Chem. Int. Ed. Engl*, **31** p. 303 (1992)

38: (a) J. A. Van Doorn, P. K. Wong, O. Sudmeijer, Eur. Patent Application 376,364; (b) P. W. N. M. Van Leeuwen, C. F. Roosbeek, P. K. Wong, Eur. Patent Application 393,710

39: P. K. Wong, Eur. Patent Application 384,517;

40: S. Bronco, C. Consiglio, *Macro. Chem. Phys.*, **197** p. 355 (1996)

41: K Nozaki, T. Hiyama, *J. Organomet. Chem.*, **576** p. 248 (1999)

42: A. Batistini, G. Consilglio, *Organometallics*, **11**, p. 1766 (1992)

43: (a) A. Sen, Z. Jiang, *Macromolecules*, **26**, p. 911 (1993); (b). M. Barsacchi, G. Consiglio, L. Medici, G. Petrucci, U. W.Suter, *Angew. Chemie Int. Ed. Engl.* **30** p. 989 (1991)

44: M. Brookhart, F. C. Rix, J. M. DeSimone, J. C. Barborak, *J. Am. Chem. Soc.* **114**, p. 5894 (1992)

45: A. S. Abu-Surrah, R. Wursche, B. Reiger, *Marcomol. Chem. Phys.*, **198**, p. 1197 (1997)

46: E. A. Klop, B. J. Lommerts, J. Veurink, J. Aerts, R. R. Van Puijenbroek, *J. Poly. Sci., Part B, Polm. Phys.*, **33**, p. 315 (1995)

47: T. Zielger, *J. Chem. Soc. Dalton*, p. 642 (2002)

48: S. Niu, M. B. Hall, *Chem. Rev.*, **100**, p. 353 (2000)

49: A. Dedieu, *Chem. Rev.*, **100**, p. 543 (2000)

50: P.W. Atkins, R.S.Friedman, *Molecular Quantum Mechanics*, Oxford University Press, Third Edition (1997)

51: James B. Foresman, Æleen Frisch, *Exploring Chemistry With Electronic Structure Methods*, Gaussian Inc., Second Edition

52: Technical notes from http://www.gaussian.com web-pages

53: W. Kohn, L. J. Sham, Phys. Rev. 140, p. A1133 (1965)

54: (a) A.D. Becke, *J. Chem. Phys.*, **98** p. 1372 (1993), (b) P. J. Stephens, J. F. Devlin, C. F. Chabalowski, M. J. Frisch, *J. Phys. Chem.* **98**, p. 11623 (1994)

55: R. J. Meier, *Farad. Diss.*, **124** p. 405 (2003)

56: S. Niu, M. B. Hall, *J. Phys.Chem., A* **101** p. 1360 (1997)

57: K. E. Frankcombe, K. J. Cavell, B. F. Yates, *J. Phys. Chem.*, **99** p. 14316-14322 (1995)

58: I. R. Levine, *Quantum Chemistry*, Prentice Hall, New Jersey, Fifth Edition (2000)

59: Y. Fan, M. B. Hall, *J. Chem. Soc. Dalton*, p. 713 (2002)

60: C. Peng, H. B. Schlegel, *Israel J. Chem.*, **33** p. 449 (1993)

61: G. te Velde, F. M. Bickelhaupt, E. J. Baerends, C. Fonseca Guerra, S. J. A. van Gisbergen, J. G. Snijders, T. Ziegler, *J. Comput. Chem*, **22** p. 931 (2001)

62: J. Li, T. Ziegler, *Inorg. Chem.* **34**, p. 3245 (1995)

63: P. J. Hay, W. R. Wadt, *J. Chem. Phys.*, **82**, p. 270 (1985), W. R. Wadt, P. J. Hay, *J. Chem. Phys.*, **82**, p. 284 (1985), P. J. Hay, W. R. Wadt, *J. Chem. Phys.* **82**, p. 299 (1985)

64: (a) T. H. Dunning Jr. and P. J. Hay, in Modern Theoretical Chemistry, Ed. H. F. Schaefer III, Vol. 3 (Plenum, New York, 1976) 1-28. (b) M. Dolg, H. Stoll, H. Preuss, R.M. Pitzer, J. Phys. Chem. 97 p. 5852 (1993)

65: L. Deng, T. K. Woo, P. M. Margl, T. Ziegler, *J. Am. Chem. Soc.*, **119**, p. 6177 (1997)

66: L. Perrin , L. Maron and O. Eisenstein, *Farad. Diss.*, **124** p. 25 (2003)

67: C. R. Landis, J. Uddin, *J. Chem. Soc. Dalton,* p. 729 (2002)

68: J. Tomasi, *Chem. Rev.*, **94**, p. 2027 (1994)

69: T. Visentin, A. Dedieu, E. Kochanski, L. Padel, *J. Mol. Struct.*, **459** p. 201 (1999)

70: Gaussian 94, Revision E.1, M. J. Frisch, G. W. Trucks, H. B. Schlegel, P. M. W. Gill, B. G. Johnson, M. A. Robb, J. R. Cheeseman, T. Keith, G. A. Petersson, J. A. Montgomery, K. Raghavachari, M. A. Al-Laham, V. G. Zakrzewski, J. V. Ortiz, J. B. Foresman, J. Cioslowski, B. B. Stefanov, A. Nanayakkara, M. Challacombe, C. Y. Peng, P. Y. Ayala, W. Chen, M. W. Wong, J. L. Andres, E. S. Replogle, R. Gomperts, R. L. Martin, D. J. Fox, J. S. Binkley, D. J. Defrees, J. Baker, J. P. Stewart, M. Head-Gordon, C. Gonzalez, and J. A. Pople, Gaussian, Inc., Pittsburgh PA, (1995)

71: Gaussian 98, Revision A.9, M. J. Frisch, G. W. Trucks, H. B. Schlegel, G. E. Scuseria, M. A. Robb, J. R. Cheeseman, V. G. Zakrzewski, J. A. Montgomery, Jr., R. E. Stratmann, J. C. Burant, S. Dapprich, J. M. Millam, A. D. Daniels, K. N. Kudin, M. C. Strain, O. Farkas, J. Tomasi, V. Barone, M. Cossi, R. Cammi, B. Mennucci, C. Pomelli, C. Adamo, S. Clifford, J. Ochterski, G. A. Petersson, P. Y. Ayala, Q. Cui, K. Morokuma, D. K. Malick, A. D. Rabuck, K. Raghavachari, J. B. Foresman, J. Cioslowski, J. V. Ortiz, A. G. Baboul, B. B. Stefanov, G. Liu, A. Liashenko, P. Piskorz, I. Komaromi, R. Gomperts, R. L. Martin, D. J. Fox, T. Keith, M. A. Al-Laham, C. Y. Peng, A. Nanayakkara, M. Challacombe, P. M. W. Gill, B. Johnson, W. Chen, M. W. Wong, J. L. Andres, C. Gonzalez, M. Head-Gordon, E. S. Replogle, and J. A. Pople, Gaussian, Inc., Pittsburgh PA (1998)

72: M.W. Schmidt, K.K. Baldridge, J.H Jensen, S. Koseki, S.M.S Gordon, K.A. Nguyen. T.L Windus, S.T. Eldbert, *Quantum Chem. Program Exch. Bull.*, 10, p. 52 (1990)

73: E. J. Baerends, J. A. Autschbach, A. Brces, C. Bo, P. M. Boerrigter, L,. Cavallo, D. P. Chong, L. Deng, R. M. Dickinson, D. E. Ellis, L. Fan, T. H. Fischer, C. Fonseca Guerra, S. J. A. van Gisbergen, J. A. Groeneveld, O. V. Gritsenko, M. Grning, F. E. Harrie, P. van der Hoek, J. Jacobsen, G. van Kessel, F. Kootstra, E. van Lenthe, V. P. Osinga, S. Patchkovskii, P. H. T. Philipsen, D. Post, G. C. Pye, W. Raveneck, P. Ros, P. R. T. Schipper, G. Schreckenbach, J. G. Snijders, M. Sola, M. Swart, D. Swerhone, G. te Velde, P. Vernoojis, L. Versluis, T. Ziegler, *ADF2002.02*, Vrije Universitiet, Amsterdam 2000, http://www.scm.com

74: M.C. Payne, M.P. Teter, D.C.Allan, J.D. Joannopoulous, *Rev. Mod. Phys.*, **64**, p. 1045

75: CAChe, Oxford Molecular Ltd. / Fujitsu Ltd. (2001)

76: CAChe user manual, Oxford Molecular Ltd. / Fujitsu Ltd. (2001)

77: (a) H. Hagelin, M. Svensson, B. Akermark, *Organometallics* **18** p.4574 (1999); (b) M. Mohr, J. P. McNamara, H. Wang, S. A. Rajeev, J. Ge, C. A. Morgado, I. H. Hillier, *Farad. Diss.*, **124** p. 413 (2003)

78: Jmol, Jmol development team, http://jmol.sourceforge.net/

79: Basis set obtained from http://www.emsl.pnl.gov/forms/basisform.html

80: (a) P. C. Harihara, J. A. Pople, Theoretica Chimica Acta, 28, p. 213(1973); (b) M. M. Francl, W. J. Petro, W. J. Hehre, J. S. Binkley, M. S. Gordon, D. J. DeFrees and J. A. Pople, J. Chem. Phys. 77, p. 3654 (1982)

81: N. Godbout, D. R. Salahub, J. Andzelm, E. Wimmer, *Can. J. Chem.*, **70**, p. 560 (1992)

82: Cambridge Structural Database: D. A. Fletcher, R. F. McMeeking and D. J. Parkin, *J Chem. Inf. Comput. Sci.*, **36**, p. 746-749 (1996)

83: A. S. Abu-Surrah, T. Debaerdemakaer, W. Huhn, B. Rieger, M. Klinga, T. Repo, M. Leskela, *Acta Crystallogr. Sect. C: Cryst. Struct. Commun.* **56** p. e42 (2000)

84: P. Dierkes, P. W. N. M. van Leeuwan, *J Chem. Soc. Dalton Trans.*, p. 1519 (1999)

85: R. Trebbe, R. Goddard, A. Rufinska, K. Seevogel, K-R. Porschke Organometallics, **18**, p. 2466 (1999)

86: (a) M-H. Prosenc, C. Janiak, H-H. Brintzinger, *Organmetallics,* **11** p. 4036 (1992); (b)C. Janiak *J. Organometallic Chem.*, **452** p. 63 (1993)

87 : D. W Dockter,. P. E. Fanwick, C. P. Kubiak, *J. Am. Chem. Soc.*, **118**, p. 4846 (1996)

88: S. A. Macgregor, G. W. Neave, *Organometallics,* **22**, p. 4547 (2003)

89: (a)V. D .Makhaev, Z .M. Dzhabieva, S. V. Konovalikhin, O. A. D'Yachenko, G. P. Belov, *Koord. Khim. (Russ.) (Coord. Chem.),* **22** p. 958 (1996); (b) V. Gramlich, G. Consiglio, *Helv. Chim. Acta,* **62** p. 1016 (1979)

90: T. A. Albright, J. K. Burdett, M-H. Whangbo, *Orbital interactions in chemistry,* Wiley Interscience, New York (1995)

91: C. Elschenbroich, A. Salzer, *Organometallics:a concise introduction,* Wienheim, Second Edition (1992)

92: G. Wilkinson (ed.), *Comprehensive Co-Ordination Chemistry Vol 2,* Pergamon Press (1987)

93: D. S. Marynick, *J. Am. Chem. Soc.* **106**, p. 4064 (1984)

94: R. H. Crabtree, *The Organometallic Chemistry of the Transition Metals*, John Wily & Sons, Inc. (1988)

95: A. B. Gray, *Electrons and Chemical Bonding,* W. A. Benjamin (1965)

96: I. Fleming, *Frontier Orbitals & Organic Chemical Reactions*, John Wiley and Sons (1976)

97: D. H. Williams, I. Fleming, *Spectroscopic Methods of Organic Synthesis,* McGraw-Hill, London, Fifth Edition (1995)

98: O. Eisenstein, R. Hoffmann, A. R. Rossi , *J. Am. Chem. Soc.*, **103**, p. 5582 (1981)

99: T. J. Marks, *Science,* **217**, p. 989 (1982)

100: M. Brookhart, M. L. H. Green, *J. Organomet. Chem.*, **250**, p. 395 (1983)

List of abbrevations used in this thesis

*x-yz*G:	(e.g 3-21G, 6-31G) Basis sets, where *x* is the number of Guassians used for the basis function core electrons, and *y* and *z* are the number of Gaussians used for the two basis functions for the valence electrons. (* or ** may be added to represent polarisation functions, + or ++ may be added to represent diffuse functions.)
ADF:	Amsterdam Density Functional program. *Ab-initio* electronic structure program Alternative to Gaussian.
AM1:	Parameter set for MOPAC used in CAChe.
B3-LYP	Becke's Three-parameter / Lee-Yang-Parr method. A DFT method.
CASTEP:	Cambridge Serial Total Energy Package. *Ab-initio* electronic structure program that uses plane waves instead of basis sets.
CAChe:	Molecular structure program that uses molcular mechanics and semiemperical methods.
CO:	Carbon monoxide.
CSD:	Cambidge Structural Database.
DFT:	Density Functional Theory.
DIIS:	Direct Inversion of the Iterative Subspace. Alogorithm for optimising a moeuclar structure using estimates of force constants.
dippp:	1,3-bis(diisopropylphosphino)propane.
dppb:	1,3-bis(diphenylphosphino)butane.
dppe:	1,3-bis(diphenylphosphino)ethane.
dppp:	1,3-bis(diphenylphosphino)propane.
DZDP:	Double-zeta diffuse polarisation. Non-pseudopotential basis set that includes palladium as a supported element.
EPSRC:	Engineering and Physical Sciences Research Council.
GAMESS	General Atomic and Molecular Electronic Structure System. Free ab-initio electronic structure program.
GC-MS:	Gas Chromatography – Mass Spectrometry.
GDIIS:	Geometry Optimization using Direct Inversion of the Iterative Subspace. Alternative alogorithm to DIIS sometimes used for larger systems.
HFIPA:	Hexafluoryl-isopropyl alcohol.
HOMO:	Highest Occupied Molecular Orbital. (HOMO – n = n^{th} energy level below HOMO.)
IRC:	Intrinsic Reaction Co-ordinate. Process for determining reaction path from a transition state geometry.
Jmol:	Molecular structure viewing program.
LanL2DZ:	Basis set that uses Los Alamos pseudopotentials.
LDA:	Local Density Approximation. A DFT method.
LST:	Linear Synchronous Transit. Method of estimating transition state geometry. (Usually written as LST2 or LST3 depending on whether or not a starting transition state geometry is included in addition to reactant and product geometries.)
LUMO:	Lowest Unoccupied Molecular Orbital. (LUMO + n = n^{th} energy level above LUMO.)
MOPAC:	Molecular Orbitals Package. Set of semiempiercal methods used in CAChe and other programs.
NMR:	Nuclear Magnetic Resonance.

ONOIM: Our own n-layered integrated molecular orbital + molecular mechanics. A QM/MM method used in Gaussian.

PM3/PM5: Parameter sets for MOPAC used in CAChe.

QM/MM: Quantum mechanics / molecular mechanics. Process of optimising a mocecule using quantum mechanics for a chemically active region and molecular mechanics for the rest of the system.

QST: Quadratic Synchronous Transit. Method of optimising transition state geometry. (Usually written as QST2 or QST3 depending on whether or not a starting transition state geometry is included in addition to reactant and product geometries.)

SCF: Self Consistent Field method.

SDD: Stuttgart-Dresden basis set. Basis set that uses pseudopotentials, as used in this project.

STO-3G: Slater Type Orbital – 3 Gaussian basis set. Very small basis set used for fast qualitative calculations.

XPS: X-ray photoelectron spectroscopy.

ZPE: Zero-point energy. Energy added to structure from ground-state vibrations.